

PB87222535



中美砖结构抗震学术讨论会

会议论文集

PROCEEDINGS OF THE
US-PRC JOINT WORKSHOP
ON SEISMIC RESISTANCE OF MASONRY STRUCTURES

MAY 21-23, 1986
HARBIN, CHINA

主办单位

中国国家地震局

美国国家科学基金会

REPRODUCED BY:
U.S. Department of Commerce
National Technical Information Service
Springfield, Virginia 22161

NTIS

SPONSORED BY
STATE SEISMOLOGICAL BUREAU, PRC
NATIONAL SCIENCE FOUNDATION, USA

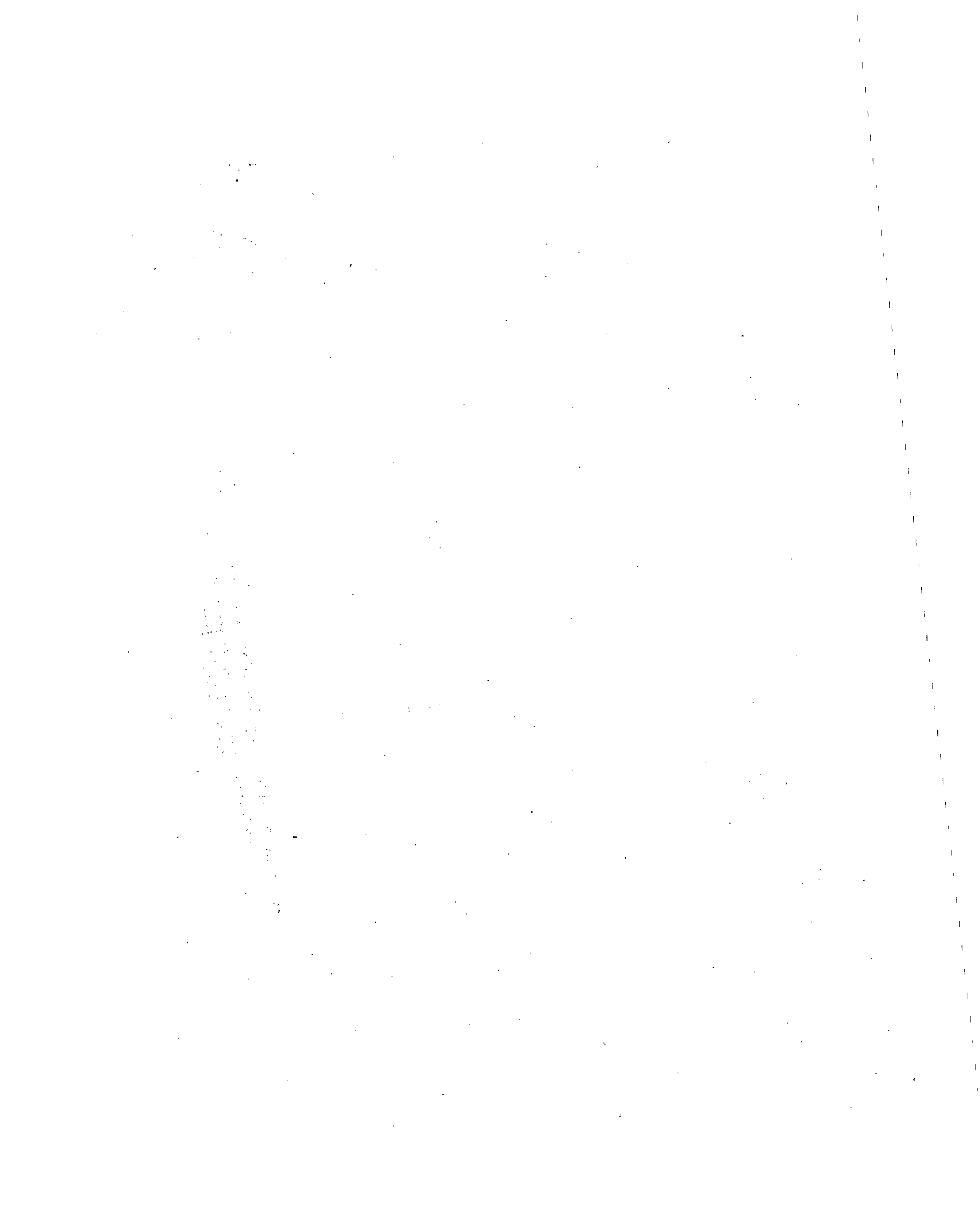
COLOR ILLUSTRATIONS REPRODUCED
IN BLACK AND WHITE

NAMES OF PERSONS IN THE PICTURE (from left to right)

- The front row:** XIE Lili, YE Yiaoxian, D. P. ABRAMS, HU Yuxian, J. C. KARIOTIS, LIU Huixian, J. E. AMRHEIN, A. A. HAMID, XIE Junfei, XU Houde, JIANG Jinren
- The second row:** GU Ping, WU Mingshu, NIU Zezhen, R. D. EWING, K. A. WOODWARD, S. W. WOODWARD, ZHANG Ruyu, J. L. NOLAND, LOU Yonglin, XIE Kelin
- The third row:** CHEN Dasheng, R. H. BROWN, CAI Changgeng, TU Jinmin, G. C. HART, L. R. JONES, J. G. TAWRESEY, A. TAWRESEY, ZHOU Fulin, WU Ruifeng, BAI Xuesong, LU Xilin, HUO Zizheng, YIN Zhiqian
- The fourth row:** QIAN Yiliang, FENG Jiangguo, CHEN Xingzhi, CHEN Rui, SHEN Jumin, GAO Yunxue, QIAN Peifeng, SONG Bingze, GAO Benli, DAI Nianzhong, LIU Dahai
- The fifth row:** LIN Mingzhou, DING Shiwen, XU Shanfan, LIU Muzhong, XIA Jingqian, LEI Tongshun, LI Yihong, YANG Wenzhong, LU Qinnian, SONG Longbo, LI Qiusheng, ZHU Bolong, YANG Liu, ZHANG Shuhua, SONG Xuerun, LIU Ji, N. M. HAWKINS, S. A. HAWKINS, CHEN Jinhua, DU Ruiming, ZHONG Wangping, ZHAO Yangang, LUO Xuehai
- The front left:** ZHANG Xiaolin, HAN Suying, QI Xiaozhai, YANG Yucheng



**Attendants at the Opening Session of the US-PRC Joint Workshop
on Seismic Resistance of Masonry Structures
Harbin May 21, 1986**



目 录 CONTENTS

Photograph of Attendants at the Opening Session	
Preface	
会议主席	1
Co-Chairmen	2
组织委员会	3
Organizing Committee	4
正式代表	5-9
Participants	5-9
列席代表	10-13
Invited Participants	10-13
Workshop Program	14-17
Author's Index	18
Final Report of Workshop	19-22
US Participant's Technical Schedule	23
Papers:	
I. DESIGN METHOD	I-1-I-6
II. BEHAVIOR OF BRICK MASONRY STRUCTURES	II-1-II-7
III. BEHAVIOR OF BRICK MASONRY STRUCTURES	III-1-III-9
IV. DANAGE PREDICTION, RELIABILITY ANALYSIS AND STRENGTHENING	IV-1-IV-11
Errta	

PREFACE

The US-PRC Workshop on Seismic Design of Masonry Structures was held at the Institute of Engineering Mechanics in Harbin, China during May 20 through 23. Twelve official participants from the United States joined 20 official participants and 29 invited participants from China to discuss and make presentations on design, construction and research pertaining to earthquake-resistant masonry structures. These Proceedings include the technical papers and summary statement presented at the workshop.

Most workshop expenses incurred in China were supported by the State Seismological Bureau. Expenses incurred for travel of the U. S. delegation to China were supported by the National Science Foundation through Grant No. ECE-8413408. Encouragement and support of NSF program directors Dr. John B. Scalzi and Dr. A. J. Eggenberger which made the workshop possible are gratefully acknowledged.

Any opinions, findings, and conclusions or recommendations expressed in this publication are those of the individual contributors and do not necessarily reflect the views of the State Seismological Bureau or the National Science Foundation.

Hu Yuxian
Daniel P. Abrams

中美砖结构抗震学术讨论会

会议主席

中方主席:

胡聿贤

国家地震局工程力学研究所
所长、教授

美方主席:

艾布拉姆斯

伊利诺大学纽马克土木工程实验室
副教授

WORKSHOP CO-CHAIRMEN

PRC CO-CHAIRMAN

HU, Yuxian
Professor & Director
Institute of Engineering Mechanics
State Seismological Bureau
9 Xuefu Road, Harbin, China

US CO-CHAIRMAN

ABRAMS, Daniel P.
Associate Professor
3148 Newmark Civil Engineering Laboratory
University of Illinois
Urbana, IL 61801, USA
217-333-0565

中美砖结构抗震学术讨论会

组织委员会

主任： 江近仁
国家地震局工程力学研究所
工业与民用建筑抗震研究室
室主任、副研究员

委员： 顾 平
国家地震局外事办公室
项目主任
钮泽葵
中国建筑科学研究院
工程抗震研究所
室主任、工程师
齐霄斋
国家地震局工程力学研究所
科研处付处长、工程师
杨玉成
国家地震局工程力学研究所
助理研究员

ORGANIZING COMMITTEE

CHAIRMAN

JIANG, Jinren
Associate Professor
Division of Earthquake Resistant
Building Constructions
Institute of Engineering Mechanics
State Seismological Bureau
9 Xuefu Road, Harbin, China

MEMBERS:

GU, Ping
Program Director
Division of Foreign Affairs
State Seismological Bureau
Beijing, China

NIU, Zezhen
Engineer & Division Head
Institute of Earthquake Engineering
China Academy of Building
Research
Beijing, China

QI, Xiaozhai
Engineer & Deputy Chief
Research Planning Division
Institute of Engineering Mechanics
State Seismological Bureau
9 Xuefu Road, Harbin, China

YANG, Yucheng
Research Associate
Institute of Engineering Mechanics
State Seismological Bureau
9 Xuefu Road, Harbin, China

LIST OF PARTICIPANTS

PARTICIPANTS FROM USA

ABRAMS, Daniel P.
Associate Professor
3148 Newmark Civil Engineering Laboratory
University of Illinois
Urbana, IL 61801, USA
217-333-0565

AMRHEIN, James E.
Executive Director
Masonry Institute of America
2550 Beverly Blvd.
Los Angeles, California 90057 USA
213-388-0472

BROWN, Russell H.
Professor and Head
Department of Civil Engineering
Clemson University
South Carolina 29631 USA
803-656-3314

EWING, Robert D.
President
Ewing and Associates
28907 Doverridge Dr.
Rancho Palos Verdes
California, 90274, USA
213-541-3795

HAMID, Ahmad A.
Associate Professor
Department of Civil Engineering
Drexel University
Philadelphia Pennsylvania, 19104, USA
215-895-2364

HART, Gary C.
Professor
Department of Civil Engineering
University of California
Los Angeles, USA
213-733-2640

代表名单

美国代表

艾布拉姆斯
美国伊利诺大学
纽马克土木工程实验室
副教授

阿姆莱因
美国砖结构研究所
执行所长

布朗
美国克莱姆森大学土木工程系
主任、教授

尤因
美国加州兰乔帕洛斯维德斯
尤因联联公司
总经理

哈米德
美国费城德雷克塞大学
土木工程系
副教授

哈特
美国洛杉矶加州大学
土木工程系
教授

HAWKINS, Neil M.
Professor and Chairman
Department of Civil Engineering, FX-10
University of Washington
Seattle 98196, USA
206-543-2390

霍金斯
美国华盛顿大学
土木工程系
主任、教授

JONES, Lindsay R.
Principal
Computech Engineering Services, Inc.
2855 Telegraph Ave., Suite 410
Berkeley, California 94705, USA
415-843-3576

琼斯
美国加州伯克利
计算机技术开发公司
经理

KARIOTIS, John C.
Kariotis and Associates
711 Mission St., Suite D
South Pasadena, California 91030 USA
213-682-2871

卡里奥蒂斯
美国帕萨迪纳
卡里奥蒂斯联谊公司
博士

NOLAND, James L.
Atkinson-Noland and Associates Inc.
2619 Spruce St.
Boulder, Colorado 80302 USA
303-444-3620

诺兰
美国博尔德
阿特金森-诺兰联谊公司
博士

TAWRESEY, John G.
Vice President
KPF Consulting Engineers
850 First Interstate Center, 999 Third Ave.
Seattle, WA 98104 USA
206-622-5822

陶里塞
美国西雅图KPF 顾问工程公司
副总经理

WOODWARD, Kyle A.
Senior Development Engineer
University of California, at San Diego
La Jolla, California 92093 USA
619-452-6801

伍德沃德
美国圣迭哥加州大学
高级发展工程师

PARTICIPANTS FROM CHINA

CHEN, Rui
Engineer
Research Department
Institute of Beijing Architectural
Design
Beijing, China

FENG, Jianguo
Senior Lecturer
Xian Institute of Metallurgy and
Construction Engineering
Xian, China

HU, Yuxian
Professor and Director
Institute of Engineering Mechanics
State Seismological Bureau
Harbin, China

HUO, Zizheng
Engineer
Shanxi Research Institute
of Building and Construction
Xian, China

JIANG, Jinren
Associate Research Professor and Head
Div. of Earthquake Resistant
Building Constructions
Institute of Engineering Mechanics
State Seismological Bureau
Harbin, China

LU, Xilin
Lecturer
Tongji University
Shanghai, China

NIU, Zezhen
Engineer and Division Head
Institute of Earthquake Engineering
China Academy of Building
Research
Beijing, China

中国代表

陈 芮
北京市建筑设计院研究所
工程师

冯建国
西安冶金建筑工程学院
高级讲师

胡聿贤
国家地震局工程力学研究所
所长、研究员

霍自正
陕西省建筑科学研究所
工程师

江近仁
国家地震局工程力学研究所
工业与民用建筑抗震研究室
室主任、副研究员

吕西林
同济大学
讲师

钮泽葵
中国建筑科学研究院
工程抗震研究所
室主任、工程师

QIAN, Peifeng
Professor
Department of Architecture Engineering
Beijing Institute of Architecture
Engineering
Beijing, China

QIAN, Yiliang
Senior Engineer
North-East Architectural
Design Institute
Shenyang, China

SHEN, Jumin
Professor & Director
Institute of Structural Engineering
Qinghua University
Beijing, China

WU, Mingshun
Associate Professor
Institute of Structure Theory
Tongji University
Shanghai, China

WU, Ruifeng
Professor
Department of Engineering Mechanics
Dalian Institute of Technology
Dalian, China

XIA, Jingqian
Associate Reserach Professor
Institute of Engineering Mechanics
State Seismological Bureau
Harbin, China

XU, Houde
Head of Division of Foreign Affairs
State Seismological Bureau
Beijing, China

XU, Shanfan
Engineer
Sichuan Institute of Building
Research
Chengdu, China

钱培风
北京建筑工程学院
建筑工程系
教授

钱义良
东北建筑设计院
高级工程师

沈聚敏
清华大学结构工程研究所
所长、教授

吴明舜
同济大学结构理论研究所
副教授

邬瑞峰
大连工学院工程力学系
教授

夏敬谦
国家地震局工程力学研究所
副研究员

许厚德
国家地震局外事办公室
主任

徐善藩
四川省建筑科学研究所
工程师

Yang Yucheng
Research associate
Institute of Engineering Mechanics
State seismological Bureau
Harbin, China

YE, Yiaoxian
Director & Senior Engineer
China Building Technology
Development Centre
Beijing, China

YIN, Zhiqian
Associate research Professor
Institute of Engineering Mechanics
State Seismological Bureau
Harbin, China

ZHANG, Ruyu
Engineer
China Northwest Building
Design Institute
Xian, China

ZHU, Bolong
Professor & Director
Institute of Structural Theory
Tongji University
Shanghai, China

杨玉成
国家地震局工程力学研究所
助理研究员

叶耀先
中国建筑技术开发中心
主任、高级工程师

尹之潜
国家地震局工程力学研究所
副研究员

张汝渝
中国建筑西北设计院
工程师

朱伯龙
同济大学结构理论研究所
所长、教授

INVITED PARTICIPANTS FROM CHINA

中国列席代表

BAI, Xuesong
Senior Engineer
Liaoning Building Design Institute
Shenyang, China

白雪松
辽宁省建筑设计院
高级工程师

CAI, Changgeng
Engineer and Vice Head
Information Section
Building Design Institute
Logistics Department of Guangzhou
Military Command of CPLA
Guangzhou, China

蔡长庚
广州军区后勤部
基建营房设计所
副主任, 工程师

CHEN, Jinghua
Engineer
Urban and Rural Construction
Department of Liaoning Province
Shenyang, China

陈金华
辽宁省城乡建设厅
工程师

CHEN, Dasheng
Associate Research Professor
Institute of Engineering Mechanics
State Seismological Bureau
Harbin, China

陈达生
国家地震局工程力学研究所
副研究员

CHEN, Xingzhi
Professor and Chairman
Department of Civil Engineering
Hunan University
Changsha, China

陈行之
湖南大学土木工程系
系主任, 教授

DAI, Nianzhong
Engineer
Chongqing Research Institute of
Architecture and Building
Chongqing, China

戴念中
重庆市建筑科学研究所
工程师

DING, Shiwen
Engineer
Institute of Engineering Mechanics
State Seismological Bureau
Harbin, China

丁世文
国家地震局工程力学研究所
工程师

DU, Ruiming
Associate Research Professor
Institute of Engineering Mechanics
State Seismological Bureau
Harbin, China

杜瑞明
国家地震局工程力学研究所
副研究员

GAO, Benli
Engineer and Head
Building Structure Office
Jiangsu Research Institute
of Architecture and Building
Nanjing, China

GAO, Yunxue
Engineer
Institute of Engineering Mechanics
State Seismological Bureau
Harbin, China

LEI, Tongshun
Engineer and Director
Beijing Building Repairing and
Construction Research Institute
Beijing, China

LI, Yihong
Engineer and Deputy Director
Beijing Building Repairing and
Construction Research Institute
Beijing, China

LIN, Mingzhou
Research Associate
Seismological Bureau of Shanghai
Shanghai, China

LIU, Dahai
Senior Engineer
China Northwest Building Design Institute
Xian, China

LIU, Ji
Professor
Harbin Architectural and Civil
Engineering Institute
Harbin, China

LIU, Muzhong
Lecturer
Department of Civil Engineering
Huachiao University
Quanzhou, China

高本立
江苏省建筑科学研究所
室主任、工程师

高云学
国家地震局工程力学研究所
工程师

雷同顺
北京市房屋修建技术研究所
所长、工程师

李毅弘
北京市房屋修建技术研究所
副所长、工程师

林命遇
上海地震局
助理研究员

刘大海
中国建筑西北设计院
高级工程师

刘季
哈尔滨建筑工程学院
教授

刘木忠
华侨大学土木工程系
讲师

LOU, Yonglin
Engineer and Head
Research Department
Building Science Research
Institute of Liaoning Province
Shenyang, China

LU, Qinnian
Research Associate
Institute of Engineering Mechanics
State Seismological Bureau
Harbin, China

SONG, Bingze
Professor and Chief Engineer
The Architectural Design and Research
Institute of Tianjin University
Tianjin, China

SONG, Longbo
Research Associate
Seismological Bureau of Jiangsu Province
Nanjing, China

SUN, Qishang
Chief Engineer
Harbin Real Estate Bureau
Harbin, China

TU, Jinming
Assistant Engineer
Gansu Building Prospecting Design Institute
Lanzhou, China

XIE, Kelin
Engineer and Deputy Director
Anhui Research Institute of
Architecture and Building
Hefei, China

YANG, Liu
Research Associate
Institute of Engineering Mechanics
State Seismological Bureau
Harbin, China

楼永林
辽宁省建筑科学研究所
室主任、工程师

陆钦年
国家地震局工程力学研究所
助理研究员

宋秉泽
天津大学建筑设计研究院
教授、总工程师

宋龙伯
江苏省地震局
助理研究员

孙启尚
哈尔滨市房地局
总工程师

屠锦敏
甘肃省建筑勘察设计院
助理工程师

解哀临
安徽省建筑科学研究所
副所长工程师

杨 柳
国家地震局工程力学研究所
助理研究员

YANG, Wenzhong
Engineer
Tangshan Urban-Rural
Construction Committee
Tangshan, China

ZHANG, Shuhua
Deputy Chief Engineer
Tangshan Institute of Building Design
Tangshan, China

ZHANG, Xiaolin
Graduate Student
The Architectural Design and Research
Institute of Tianjin University
Tianjin, China

ZHONG, Wangping
Engineer and Manager
Department of Computer
The 6th Design Institute of
Machine Industry Ministry
Zhengzhou, China

ZHOU, Fulin
Deputy Chief Engineer
The 4th Design and Research Institute
of Machine Industry Ministry
Luoyang, China

杨文忠
唐山市城乡建设委员会
工程师

张树华
唐山市建筑设计院
副总工程师

张晓临
天津大学建筑设计研究院
研究生

鍾望平
机械工业部第六设计研究院
计算机室负责人
工程师

周福霖
机械工业部第四设计研究院
副总工程师

WORKSHOP PROGRAM

Tuesday, May 20, 1986

REGISTRATION

Wednesday, May 21, 1986

OPENING SESSION (8:30 - 9:00 AM)

Chairman: HU, Yuxian
Speakers: ABRAMS, D. P. (USA Co-Chairman)
LIU, Huixian (President of CAEE)
XU, Houde (Head of Div. of Foreign Affairs, SSB)

SESSION 1: DESIGN METHODS AND OTHERS (9:15 - 12:00 AM)

Co-Chairmen: HU, Yuxian ABRAMS, D. P.

1. KARIOTIS, J. C. EWING, R. D. JOHNSON, A. W.	"Methodology for Mitigation of Earthquake Hazards in Unreinforced Brick Masonry Buildings"	I-1
2. YE, Yiaoxian	Factors Affecting Damage of Multi-story Brick Buildings and Their Strengthening Techniques	II-7
3. TAWRESEY, J. G.	"Seismic Provisions of the Uniform Building Code"	I-2
4. SHEN Jumin FENG, Shiping WENG, Yijun	"Inelastic Behavior of Reinforced Concrete Frame Subjected to Reversal Cyclic Loading"	III-9
5. AMRHEIN, J. E.	"Research and Design of Tall Slender Walls"	I-4
6. GONG, Sili	"Revision of the Chinese Seismic Design Code---Brick Structure Section" (not presented)	I-6
7. MO, Yong	"Crack and Collapse-resistant Design of Multi-story Brick Building with Large Spacious First Story in Seismic Area" (not presented)	I-3

SESSION 2: BEHAVIOR OF BRICK MASONRY STRUCTURES
(1:00 - 4:10 PM)

- Co-Chairmen: TAWRESEY, J. G. ZHU, Bolong
1. BROWN, R. H. "Structural Properties of Unreinforced Hollow Brick Masonry" II-2
YORKDALE, A. H.
 2. ZHOU, Bingzhang "An Experimental Study of Aseismic Reinforcing of Brick Buildings" II-1
CHEN, Rui
 3. BA, Rongguang "An Investigation of the Aseismic Behavior of Perforated Brick Buildings" II-3
 4. FENG, Jianguo "The Seismic Shear Strength of Masonry Wall" II-4
 5. NOLAND, J. L. "An Investigation into Methods and Materials Required to Obtain Flaw-Free Grout in Hollow Brick Masonry" II-5
KINGSLEY, G. R.
TULIN, L. G.
 6. XIA, Jingqian "Test of Aseismic Behavior of Brick Masonry Wall" II-6
DING, Shiwen
ZHOU, Sijun

Thursday, May 22, 1986

SESSION 3: BEHAVIOR OF BLOCK MASONRY STRUCTURES
(8:30 - 10:30 AM)

- Co-Chairmen: YE, Yiaoxian AMRHEIN, J. E.
1. ABRAMS, D. P. "Resistance of Concrete Masonry Building System to Lateral Force" III-1
 2. QIAN, Peifeng "Earthquake Proof Blocks with Good Thermal Performance" III-2
LO, Yongkang
GUO, Zaiyu
 3. XU, Shan-fan "Study of Seismic Behavior of Hollow Concrete Block Buildings" III-3
LIU, Dexin
 4. WOODWARD, K. A. "Shear Behavior of Unreinforced Concrete Block Walls" III-4
 5. HEGEMIER, G. A. "On Simulating the Nonlinear Planar Hysteretic Response of Reinforced Concrete and Concrete Masonry" (not presented) III-10
MARAKAMI, H.

SESSION 4: MODEL TEST OF BLOCK MASONRY BUILDING

(10:45 - 11:45 AM)

- Co-Chairmen: HAWKINS, N. M. WU, Ruifeng
1. ZHU, Bolong "A Review of Aseismic Test for Masonry Structures in China" III-5
 2. LU, Xilin "Identification for the Mathematical Models to Predict the Earthquake Response of the Unreinforced Concrete Block Masonry Building and Estimation of Its Aseismic Capacity" III-7
ZHU, Bolong.

SESSION 4: (CONTINUED)

(1:00 - 2:20 PM)

3. JONES, L. R. "An Investigation of the Seismic Behavior and Reinforcement Requirements for Single-Story Masonry House" III-6
CLOUGH, R. W.
MAYERS, R. L.
4. HAMID, A. A. "Direct Small Scale Modeling of Grouted Concrete Block Masonry" III-8
ABBOUD, B. E.
HARRIS, H. G.

SESSION 5: EVALUATION AND STRENGTHENING

(2:35 - 4:50 PM)

- Co-Chairmen: QIAN, Yiliang KARIOTIS, J. C.
1. ZHU, Bolong "Shaking Table Study of a Five-Story Unreinforced Block Masonry Model Building Strengthened with Reinforced Concrete Columns and Tie Bars" IV-11
WU, Mingshun
ZHOU, Deyuan
 2. HAWKINS, N. M. "Comparison of U. S. and Chinese Methodologies for the Seismic Evaluation and Strengthening of Existing Unreinforced Masonry Structures" IV-8
CHOU, F.
YIN, X.
 3. NIU, Zezhen "Seismic Computation of Strengthened Brick Structures" IV-9
 4. ZHONG, Yichun "Repair and Strengthening of Reinforced Concrete Columns" (not Presented) IV-10
REN, Fudong
TIAN, Jiahua

Friday, May 23, 1986

SESSION 6: DAMAGE PREDICTION AND RELIABILITY ANALYSIS
(8:30 - 12:00 AM)

- Co-Chairmen: NOLAND, J. L. SHEN, Jumin
1. YANG, Yucheng "Prediction of Damage to Brick Buildings in Cities in China" IV-2
YANG, Liu
 2. KARIOTIS, J. C "Prediction of Stability for Unreinforced Brick Masonry Walls Shaken by Earthquakes" IV-1
EWING, R. D.
JOHNSON, A. W.
 3. YIN, Zhiqian "A Method for Earthquake Damage Evaluation of Single-Story Factory Buildings" IV-3
LI, Shuzhen
 4. HART, G. C. "Reliability Concepts for Earthquake Resistant Masonry" IV-4
 5. WU, Ruifeng "Seismic Reliability of Multistory Reinforced Brick Building" IV-5
CHEN, Xizhi
XI, Xiaofeng
 6. JIANG, Jinren "Seismic Reliability Analysis of Multi-story Brick Buildings" IV-6
HONG, Feng
 7. HUO, Zizheng "Earthquake Resistant Reliability of Brick Residential Buildings" IV-7

OPENING FORUM
(1:00 - 3:00 PM)

Co-Chairmen: ABRAMS, D. P. HU, Yuxian

CLOSURE
(3:15 - 4:50 PM)

Chairman: ABRAMS, D. P.

AUTHOR INDEX

ABRAMS, D. P.	III-1
AMRHEIN, J. E.	I-4
BA, Rongguang	II-3
BROWN, R. H. YORKDALE, A. H.	II-2
FENG Jianguo	II-4
HAMID, A. A. ABBOUD, B. E., HARRIS, H. G.	III-8
HART, G. C.	IV-4
HARKINS, N. M., CHOU, F., YIN, X.	IV-8
HEGEMIER, G. A., MURAKAMI, H.	III-10
HUO, Zizheng	IV-7
JIANG, Jinren, HONG, Feng	IV-6
JONES, R. L., CLOUGH, R. W., MAYERS, R. L.	III-6
KARIOTIS, J. C., EWING, R. D., JOHNSON, A. W.	I-1
KARIOTIS, J. C., EWING, R. D., JOHNSON, A. W.	IV-1
LU, Xilin, ZHU, Bolong	III-7
MO, Yin	I-3
NIU, Zezhen	IV-9
NOLAND, J. G., KINGSLEY, G. R., TULIN, L. G.	II-5
QIAN, Peifeng, LO, Yongkang, Guo, Zaiyu	III-2
SHEN, Jumin, FENG, Shiping, WENG, Yijun	III-9
TAWRESEY, J. G.	I-2
WOODWARD, K. A.	III-4
WU, Ruifeng, CHEN, Xizhi, XI, Xiaofeng	IV-5
XIA, Jingqian, DING, Shiwen, ZHOU, Sijun	II-6
XU, Shanfan, LIU, Dexin	III-3
YANG Yucheng, YANG, Liu	IV-2
YE, Yiaoxian	II-7
YIN, Zhiqian, LI, Shuzhen	IV-3
YU, Andong, JIN, Ruichun, SHI, Yuan	I-5
ZHONG, Yichun, REN, Fudong, TIAN, Jiahua	IV-10
ZHOU, Bingzhang, CHEN, Rui	II-1
ZHU, Bolong	III-5
ZHU, Bolong, WU, Mingshun, ZHOU, Deyuan	IV-11

**FINAL REPORT
of
WORKSHOP**

**Co-Chairmen: Daniel P. Abrams
Hu Yuxian**

Introduction

There is a high potential in both the People's Republic of China and the United States of America for great loss of human life and property damage as a result of collapse of unreinforced masonry buildings during destructive earthquakes. The Tangshan Earthquake of 1976 was a clear illustration of what may occur. Among the existing buildings stock in both countries there are many masonry structures which are vulnerable to severe shaking. Unreinforced clay-unit masonry buildings comprise the principle type of construction in China today. Unreinforced and reinforced clay and concrete masonry buildings have been and will continue to be constructed in the United States. Because of differences in materials, design methods and forms of construction for each country, there is a substantial amount of information which may be transferred between engineers and researchers in each country.

The workshop has discussed six subject areas through presentations and open discussions:

1. Methods for aseismic design of new masonry construction and strengthening of existing buildings.
2. Behavior and response of brick masonry structures and measures for mitigating damage.
3. Behavior and response of block masonry structures and measures for mitigating potential damage.
4. Earthquake simulation tests of model block structures.
5. Evaluation and strengthening techniques for brick and block structures.
6. Damage prediction and reliability analysis for masonry structures.

Recommendations

All the participants from PRC and USA understand that mitigation of earthquake damage to masonry buildings and prevention of loss of life is a problem which must be solved not only in both countries, but in all other earthquake-prone regions of the world. As shown from presentations made in the workshop, research and development in this field is going on in each country. The participants agree that technical research areas of common interest which require further study include:

1. Investigations defining behavior of masonry materials and composites. Studies should include identification of strengths and deformations of masonry units, mortars and grouts.
2. Experimental studies on force-deflection relation of masonry walls and systems including consideration of flexibility of floor diaphragms.

Laboratory techniques should be improved so that the stressed condition of test walls under reversals of lateral deflection will simulate that of walls in actual structures subjected to earthquakes.

3. Analytical studies on force-deflection relations for masonry walls. Numerical models should reflect nonlinear behavior of walls with openings or without subjected to deflection reversals.

4. Research on dynamic response of masonry building systems from initial cracking through the final damage stage. Physical and numerical models which reflect nonlinear behavior of walls and systems should be improved through investigations using shaking tables and modern computational facilities.

5. Evaluation of aseismic behavior and earthquake damage prediction for existing unreinforced masonry buildings. Nondestructive test methods should be studied as well as ways to interpret their results for assessing vulnerability of existing construction. Reliability and decision analysis techniques should be utilized, which consider inherent randomness and uncertainty.

6. Development of new approaches for improving seismic behavior. Innovative methods of design and construction should result in reductions of earthquake damage and prevention of collapse, and may include development of new materials, types of masonry units and conceptual schemes using base isolation and energy dissipation devices.

7. Instrumentation of existing masonry buildings for strong shaking.

Implementations

All participants recognized that in order to implement the above mentioned recommendations, the following approaches could be taken.

(1) The now ongoing cooperative research projects between PRC and USA should pay due attention to research on topics of seismic resistance of masonry structures.

(2) Exchange of research information should be pursued. Mutual survey of damage to masonry structures in future earthquakes would provide a good opportunity for further cooperative study.

(3) All participants are encouraged to develop cooperative research projects on topics of mutual interest. There are two ways to implement the projects.

a. The project is under "PRC-US Protocol for Scientific and Technical Cooperation in Earthquake Studies", which requires submission of proposal to NSF or SSB for approval of the project.

b. The project is undertaken by individual institutions. In this case, the funds for research and exchange of personnel may be arranged as follows: The researcher's salary and international travel expenses are paid by the home institution or subsidized by the host institution; local expenses and local travel expenses are paid by the host institution.

Resolution

It is resolved that the workshop has been a good beginning of cooperative effort in research on seismic resistance of masonry structures for engineering professionals and researchers from PRC and USA. In order to carry out effectively cooperative efforts in mitigation of earthquake damage to masonry structures in both PRC and USA, as a resolution, all participants of the Workshop from both countries acknowledge the following objectives.

1. New discoveries and research results should be provided to each other as soon as possible.
2. Cooperative research proposals should be actively developed for submission to funding agencies in respective countries.
3. All researchers welcome participants from other country to join in their research projects for collaboration and to their best ability, provide cooperative research conditions.
4. Further workshops (bilateral or multiple lateral) in either country or specialty subjects related to earthquake resistance of masonry structures should be held in 2-3 years.

US Participant's Technical Travel Schedule

Sturday, May 17 -- Arrive at Shanghai

Monday, May 19 -- Visit Tongji University

Tuesday, May 20 -- Arrive at Harbin

May 21 - 23 -- US-PRC Workshop at Institute of Engineering
Mechanics, Harbin

Saturday, May 24 -- Visit IEM, Leave Harbin for Tangshan by train

Sunday May 25 -- Visit Tangshan Post-Earthquake Site

Monday, May 26 -- Leave Tangshan for Beijing by train

May 27 - May 29 -- Leave Beijing

1. The first part of the document discusses the importance of maintaining accurate records of all transactions and activities. It emphasizes that this is essential for ensuring transparency and accountability in the organization's operations.

2. The second part of the document outlines the various methods and tools used to collect and analyze data. It highlights the need for consistent and reliable data collection processes to ensure the validity of the results.

3. The third part of the document describes the different types of data that are collected and how they are used to inform decision-making. It notes that a combination of quantitative and qualitative data is often used to provide a comprehensive view of the organization's performance.

4. The fourth part of the document discusses the challenges and limitations of data collection and analysis. It identifies common issues such as data quality, bias, and incomplete information, and offers strategies to address these challenges.

5. The fifth part of the document provides a summary of the key findings and conclusions of the study. It reiterates the importance of data-driven decision-making and the need for ongoing monitoring and evaluation of the organization's performance.

6. The sixth part of the document offers recommendations for future research and practice. It suggests areas for further exploration and provides practical advice for implementing effective data collection and analysis processes.

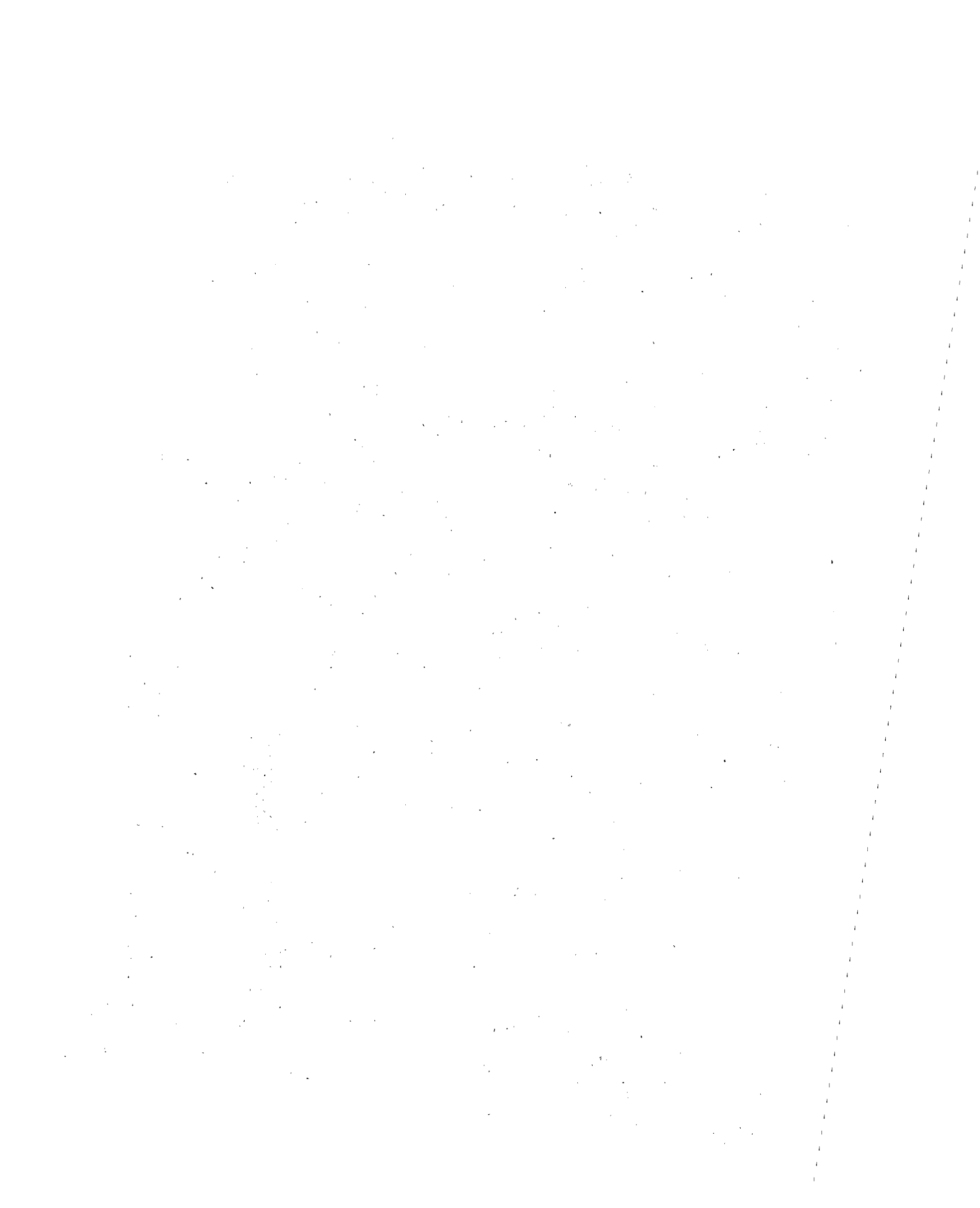
7. The seventh part of the document includes a list of references and a bibliography. It cites various academic sources and industry reports that have informed the research and analysis.

8. The eighth part of the document contains a list of appendices and supplementary materials. These include additional data, charts, and tables that provide further detail and support for the findings.

9. The ninth part of the document includes a list of figures and tables. These visual elements help to illustrate the data and make it easier to understand and interpret.

10. The tenth part of the document is a concluding statement that summarizes the overall purpose and significance of the study. It expresses the hope that the findings will be useful and informative to the organization and its stakeholders.

1 DESIGN METHOD



METHODOLOGY FOR MITIGATION
OF EARTHQUAKE HAZARDS IN UNREINFORCED
BRICK MASONRY BUILDINGS

Kariotis, J.C., Ewing, R.D., and Johnson, A.W.¹

ABSTRACT

Seismic hazards in existing unreinforced masonry buildings were investigated in order to provide a methodology to strengthen these buildings to appropriate resistance levels. The testing program was comprised of static and dynamic testing of walls and diaphragms, both in-plane and out-of-plane, and of anchorages between walls and diaphragms. In these guidelines for the analysis of existing buildings, there were several significant departures from the code provisions for new construction. Results can be used as retrofit guidelines in accordance with the three seismic hazard levels of the 1978 ATC provisions based on effective peak accelerations of 0.1, 0.2, and 0.4 g.

INTRODUCTION

Building construction using unreinforced masonry (URM) predates the development of seismic criteria that guide the design and construction of present-day buildings. A substantial number of these buildings are still being used in seismically active areas, even though investigations of earthquake damage have confirmed that this type of building has been a major contributor to loss of life during earthquakes. It has become imperative that a system of analysis methods and procedures--a methodology--be devised to determine realistic hazard mitigation requirements that will lead to cost-effective methods of retrofit for these buildings. In this way, the choice will not remain limited to either an enormous investment to make existing buildings conform to present standards for new construction or an economic loss resulting from the demolition of these buildings. Such a methodology can help meet seismic hazard mitigation goals of cities squeezed between threats to life-safety and economic constraints. This paper describes the results derived from an extensive research program and gives guidelines for its application.

The research program resulted in the publication of topical reports on various phases of the analysis and testing. The final volume, entitled The Methodology (1), provides in "guideline" form the procedures for investigating existing URM buildings for the purpose of strengthening them to resistance levels that correspond to three levels of ground shaking intensity that constitute the principal seismic hazard zones of the United States. This paper provides a summary of the procedure discussed in the Methodology volume.

¹ ABK, A Joint Venture, El Segundo, California, USA

BASIS OF THE METHODOLOGY

A review of research work on masonry showed that most of the effort has been directed toward determining the characteristics and response of reinforced masonry components to in-plane forces; and little or no effort was devoted to typical URM building response and the dynamic interaction among the building components. Accordingly, a research program was initiated that included several types of tests:

- o Dynamic testing of full-scale walls, out-of-plane
- o Static and dynamic testing of full-scale diaphragms, in-plane
- o Static and dynamic testing of walls, in-plane
- o Anchorage between walls and diaphragms

As a result of these experiments, it was determined that elastic or equivalent static procedures are not completely satisfactory to define the dynamic and highly nonlinear response of URM buildings.

The experimental data were then used in conjunction with analytical models for four related component responses and their interactions:

- o In-plane motions of endwalls and crosswalls induced by the earthquake ground motion
- o Roof and floor diaphragms subjected to in-plane motions induced by the endwalls and crosswalls
- o Walls subjected to out-of-plane motions induced by ground motion at the foundation level and by the diaphragm motion or by a pair of diaphragms
- o Anchorage between the walls and diaphragms

IN-PLANE RESPONSE OF WALLS

During an earthquake, the ground motion is transmitted from the building/foundation interface through the endwalls (in-plane response) to the floor and/or roof diaphragms that drive the walls in the out-of-plane direction. Masonry shear walls can be considered rigid relative to the diaphragm stiffness and can be modeled as a rigid block resting on a soil. Analyses performed over a realistic range of building aspect ratios and soil stiffnesses showed that the ground motion is transmitted through the endwalls with little amplification.

ROOF AND FLOOR DIAPHRAGMS SUBJECTED TO IN-PLANE MOTIONS

The dynamic response of diaphragms shows a nonlinear hysteretic behavior for ground motions of moderate and higher intensities. The analytical model developed for this type of diaphragm requires only two parameters to define the load-deformation envelope (i.e., the ultimate load capacity and the initial stiffness) and one parameter to define the degrading, unloading and reloading stiffness. For typical unreinforced masonry buildings, the diaphragm stiffness is modeled by nonlinear, hysteretic shear springs, and the sidewall mass and tributary diaphragm

mass are lumped at the nodes. Peak velocities at the top and bottom of the out-of-plane walls can be obtained from the dynamic model, as well as relative deformations between the top and bottom of the walls.

WALLS SUBJECTED TO OUT-OF-PLANE MOTIONS

The dynamic stability of fully anchored URM walls subjected to out-of-plane motions was determined from full-scale testing. The parameters that affect stability are:

- o Velocities imparted by the diaphragms to the ends of the walls.
- o Ratio of weight of wall above the story under consideration to the weight of the wall in the story under consideration.
- o Height/thickness (H/t) ratio of the wall in the story under consideration.

ANCHORAGE BETWEEN WALLS AND DIAPHRAGM

Adequate anchorage of the walls to the diaphragm is an essential part of achieving hazard mitigation in URM buildings. Anchorage forces have been developed for use in the methodology that are based on tests and nonlinear, dynamic analyses of the diaphragms. Although not a new concept, the paramount consideration of the methodology is life-safety. This is obtained by limiting building damage and by minimizing the probability of separation of the walls and parapets from the floors and roof. The collapse of parts of the gravity load-carrying system that are sensitive to relative displacement is investigated.

NEW CONCEPTS

As stated earlier, the guidelines proposed for the analysis of existing buildings are not the same as the code provisions for new construction. Significant departures are:

- o Due to the sensitivity of earthquake hazard mitigation recommendations to the intensity of ground shaking, the use of state-of-the-art documents for seismic hazard zoning is recommended.
- o Due to the nonlinear, dynamic response of unreinforced masonry buildings, the procedures for each seismic hazard zone are separately defined rather than using a factored coefficient for each seismic hazard zone.
- o The seismic response model for the buildings is a rigid block on flexible soils. This basic response model is modified for walls with a limited interstory shear capacity and ductile-like behavior.
- o The diaphragm response imparted to the out-of-plane walls is based on nonlinear, dynamic analyses that have been correlated with full-scale diaphragm tests.
- o Dynamic stability concepts for URM wall elements subjected to out-of-plane motions are utilized in lieu of requirements for an elastic resistance capacity.
- o Materials resistance capacities are based on inelastic behavior of materials.

- o All existing materials and elements in the building that are distorted by relative horizontal or interstory displacement are considered in the response model and the structural resistance model.

FIELD SURVEYS AND PRELIMINARY DESIGN

The methodology for mitigating seismic hazards in URM buildings is presented for the three seismic hazard zones described by the ATC 3-06 provisional guidelines (2). These seismic hazard zones are defined by Effective Peak Accelerations (EPA) of 0.1 g, 0.2 g, and 0.4 g.

The procedure for using the methodology begins with a five step field survey that is the same for all seismic zones: prepare preliminary framing plans for roofs and floors; prepare preliminary elevations of all walls; investigate anchorage of walls; investigate wall materials; and test existing materials. Once these preliminary steps have been accomplished, the analysis procedure begins. This is done in the following steps for 0.1 g and 0.2 g seismic zones:

- o Identify all hazardous building elements on framing plans, floor plans, and wall elevations.
- o Calculate recommended wall anchorage force at each floor above the building base and at the roof level.
- o Verify capacity of existing wall anchors.
- o Design retrofitted wall anchorage systems.
- o Design bracing systems for parapets and appendages extending above the roof anchorage level.

In addition, special investigations may be required by the methods recommended for 0.4 g seismic hazard zones for the following conditions:

- o Wall H/t ratios are in excess of historic standards and building height-plan dimension ratio exceeds 3, and the structure is founded in soft soils.
- o Diaphragm discontinuities exist adjacent to an unreinforced masonry wall.
- o The building survey has determined that parts of the vertical load-carrying system may act as a tie to a shear wall, and horizontal displacement of that part of the vertical load-carrying system relative to the shear wall will cause loss of bearing capacity.
- o The building survey has determined that major elements of the vertical load-carrying system are supported on masonry piers, and there is a probability that significant relative displacement will occur in that story.

ANALYSIS GUIDELINES

The analysis procedures for seismic hazard zone EPA = 0.4 g are more extensive, and in the following sections of this paper these procedures will be summarized.

The guidelines describe a probable response of existing building elements that is correlated to element displacements that extend into the inelastic range. Capacities of existing materials are given as yield capacities. Yield capacities of structural elements are used for design of retrofitted systems.

1. Anchorage of Wall Elements. Calculate the recommended anchorage force at each floor above the building base and at the roof level, where the anchorage force is equal to 1.0 times tributary wall weight. This includes the design of the bracing system for parapets above the roof anchorage level. If existing wall anchorages are to be used as part of the wall anchorage system, verify capacity of the embedded ends of the existing wall anchors by nondestructive testing. Qualify nondestructive testing by limited destructive testing.

For analysis of the shear anchorage of the diaphragm to the walls, a response factor is recommended that is an upper bound of dynamic amplification. This upper bound of amplification is appropriate for diaphragms that have near-elastic response.

2. Stability of Anchored Wall Elements. Allowable H/t ratios of walls for several types of buildings are given in Table 1. These H/t ratios are dependent on the presence of crosswalls and on diaphragm demand/capacity ratio and span length. Crosswalls are existing walls constructed of materials other than unreinforced masonry, or retrofitted structural elements that extend between all diaphragms at all levels of the building. Buildings with diaphragms conforming to the requirements of Figure 2 qualify as "buildings with crosswalls".

TABLE 1. ALLOWABLE HEIGHT/THICKNESS RATIO OF UNREINFORCED MASONRY WALLS WITH MINIMUM QUALITY MORTAR

	<u>Buildings with Crosswalls</u>	<u>All Other Buildings</u>
Walls of one-story buildings	20	14
First-story walls of multistory buildings	20	20
Walls in top story of multistory buildings	14	9
All other walls	20	15

Table 1 uses the plot of predicted dynamic stability shown in Figure 1. The parameters that affect stability are:

- o Input velocities imparted by the diaphragms to the ends of the walls
- o Ratio of weight of wall in the stories above the story under consideration to the weight of the wall in the story under consideration
- o H/t ratio of the wall in the story under consideration

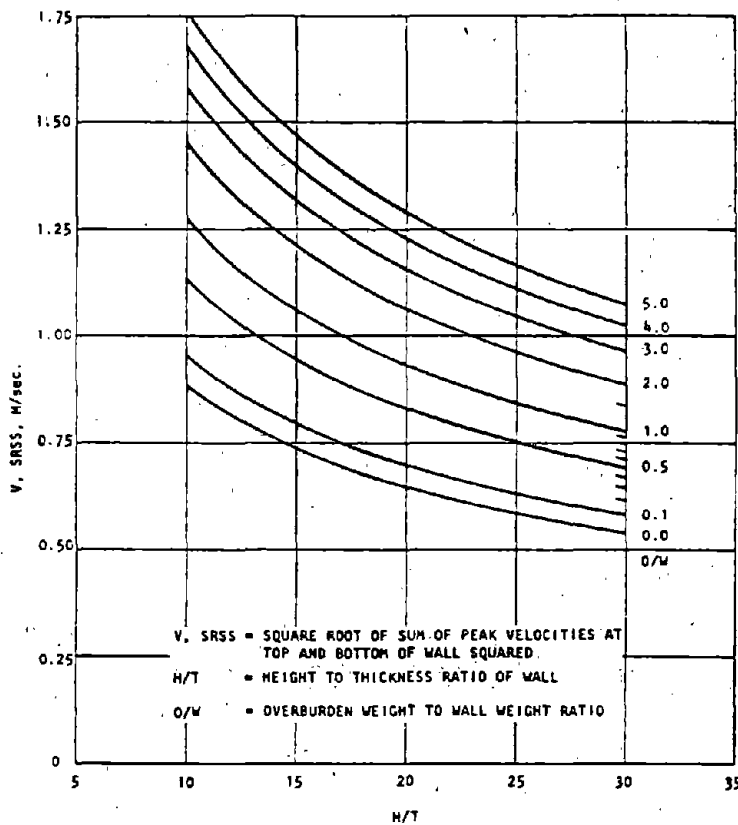


FIGURE 1. UNREINFORCED MASONRY WALL STABILITY CRITERIA
98% PROBABILITY OF SURVIVAL

Crosswalls conforming to the minimum requirements of Figure 2 may be introduced into the building to increase the acceptable H/t ratio of walls; or walls that exceed the recommended H/t ratio may be braced by supplemental members spanning between diaphragm levels.

Recommendations for design and installation of the supplemental bracing members are:

- o Design bracing members for 0.4 times the tributary wall weight.
- o Deflection of the bracing member, calculated using recommended forces, should not exceed 0.15 times the wall thickness.
- o Horizontal spacing of the vertical bracing members should not exceed one-half the unsupported height of the wall or 3 m. maximum.
- o The vertical bracing members should be anchored to the floor or roof framing independently of the recommended wall anchorage system.

3. Computation of Earthquake Response Force. Recommendations for computation of earthquake response forces are:

- o Calculate weight of building as a lumped weight at each level. Tabulate the weight computations as in-plane wall weight (W_w) and weight tributary to diaphragms (W_D), at each level, for each axis of analysis of the building.
- o For analysis of the shear connection of diaphragms to the shear walls, select C from Table 2. The shear used for design of the connection need^p not exceed ($v_u \cdot D$) of the diaphragm.

Yield capacities, v_u , in U.S. units of typical diaphragms are given in Table 3.

- o The restoring shear capacity, V_R , of any shear wall composed of piers need not exceed $0.2 W_w + 0.2 W_D/2$, and the diaphragm shear at any level need not exceed the yield capacity ($v_u \cdot D$) of the diaphragm.
- o For analysis of in-plane shear in each shear wall, when determined to be critical, use $V = 0.4 W_w + 0.4 W_D/2$. However, the diaphragm shear at any level need not exceed the yield capacity ($v_u \cdot D$) of the diaphragm.

The seismic response factors, C , of the diaphragms are given in Table 2. These factors equal or exceed the seismic zone EPA to account for diaphragm amplification of earthquake motions. However, the upper bound of response shear that can be coupled with the shear walls is the yield capacity of the diaphragm.

The building response is calculated as the hazard zone EPA times the weight of the shear wall and the diaphragm weight that can be coupled with the shear wall. The effective coupling of the diaphragm is

limited to the yield capacity of the diaphragm at any level. This procedure is not intended to give an arithmetical summation of peak element response.

TABLE 2. RESPONSE FACTOR, C_p , FOR SHEAR CONNECTION OF DIAPHRAGM

Single layer of boards with applied roofing	0.45
Double layer of boards or blocked plywood	0.8
Steel decking not detailed for lateral load resistance	0.6
Concrete filled steel decks or concrete framed systems with span/depth ratio of 2 or less	0.4

TABLE 3. YIELD CAPACITIES, v_u , OF EXISTING ROOF AND FLOOR CONSTRUCTION

<u>Description of Construction</u>	<u>Yield Capacity of Materials in lb/ft., shear</u>
Straight sheathing with roofing applied on the sheathing or a single layer of tongue and groove sheathing	300
Straight sheathing with plywood overlay	650
Unblocked plywood sheathing with roofing applied on the sheathing	400
Plywood sheathed floors or roofs with blocking at panel edges	2-1/2 x shear values listed in design codes such as Uniform Building Code
Double board systems with board edges offset	1800
Metal roof deck system designed for minimal lateral load capacity	1800
Metal roof deck systems designed for lateral load capacity	3000
Concrete filled steel decks	As determined by static yield capacity testing

4. Analysis of Horizontal Diaphragms. Recommended analysis procedures for diaphragm displacement control is based on dynamic testing and modeling. The procedure is as follows:

- o For diaphragms without crosswalls:

Calculate demand/capacity ratio

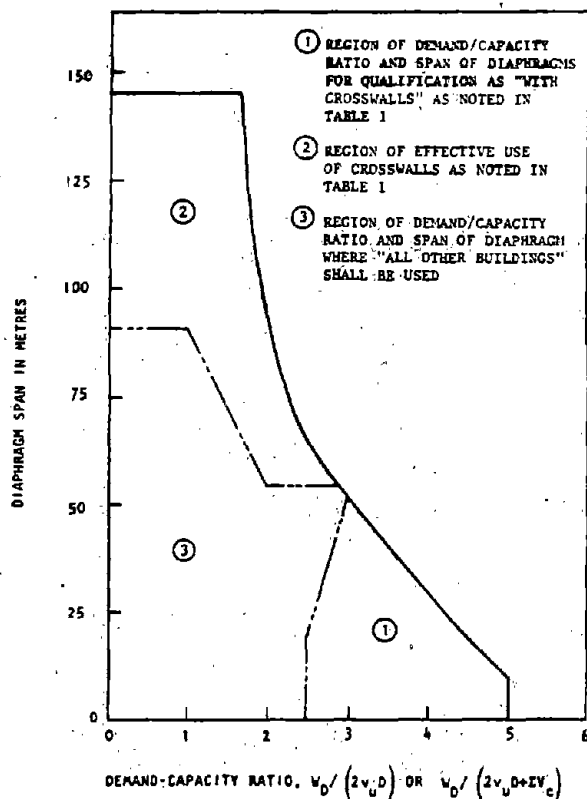
$$\frac{W_D}{2v_u \cdot D}$$

where W_D = Total weight tributary to diaphragm

v_u = Yield capacity of diaphragm (see Table 5)

D = Diaphragm depth

From Figure 2, using the demand/capacity ratio and span length, determine adequacy of existing diaphragm. If the existing diaphragm does not meet the span limitations, the diaphragm must be retrofitted to increase v_u , or crosswalls may be added to limit relative horizontal displacement.



FOOTNOTES:

- 1) Maximum spacing of crosswalls is 12 metres measured in the direction of span.
- 2) Minimum capacity of crosswalls is 30 percent of diaphragm capacity.

FIGURE 2
ACCEPTABLE SPAN FOR DIAPHRAGMS
(BASED ON DISPLACEMENT CONTROL CONCEPTS)

- o For diaphragms with crosswalls:

Calculate demand/capacity ratio:
$$\frac{W_D}{2v_u \cdot D + \Sigma V_c}$$

ΣV_c = total yield capacity of crosswalls that are spaced not to exceed that specified in Figure 2.

- o If the spacing of existing crosswalls is that specified in Figure 2 and the capacity ΣV_c exceeds 20% of W_D , the span of the diaphragm shall be unlimited.
- o For multistory buildings, V_c utilized for diaphragm analysis at any upper story shall be added to the W_D of the story below for analysis of that story.

For the special case of horizontal displacement control of an "open-front" building, the recommendation for diaphragms with shear walls at the diaphragm ends may be used (Fig. 2). To utilize Figure 2, an equivalent L_1 is calculated. The wall weight, W_w , at the open end is used to calculate L_1 :

$$L_1 = 2 \left(\frac{W_w}{W_D} \cdot L + L \right)$$

Compare demand/capacity ratio of diaphragm with an acceptable span calculated as L_1 . If acceptable crosswalls exist, calculate

$$\frac{W_D + W_w}{v_u \cdot D + \Sigma V_c} \quad \text{for entry to Figure 2.}$$

5. Analysis of In-Plane URM Elements. For shear walls that are divided into piers by door and window openings, calculate the restoring shear capacity of each pier as:

$$V_R = 0.9 PD/H$$

Where P = Axial load on pier

D = In-plane depth of pier

H = Least height of pier if opening height on sides of pier varies

For computation of restoring shear, the stability moment of a fully cracked pier system is used. Compare the total restoring shear capacity

with the minimum recommended restoring shear:

$$V_R \text{ min.} = 0.2 W_W + 0.2 W_D/2$$

Compare calculated V_R of each pier with its in-place shear capacity V , where

$$v = \frac{V_a A}{1.5}$$

Where A = Area of pier

$$V_a = 3/4 (3/4 v_t + P/A)$$

Where v_t = 20th percentile of in-plane test shear values reduced to equivalent shear at zero axial stress

$$\text{If } V_R < 0.2 W_W + 0.2 W_D/2$$

and for all piers $V_R < V$, supplement restoring shear by materials designed at yield capacity. If for any pier $V_R > V$, in-plane shear failure is probable and piers must be analyzed for shear capacity, using the following four steps:

- o Distribute response shear V to pier system using stiffness as D/H .
- o Calculate $v = 1.5 V/A$ for stiffest pier.
- o If $v > v_a$, increase shear capacity of wall with consideration of relative stiffness of existing and new materials.
- o For walls without openings and with height/length ratio ≤ 0.5 , calculate $v = V/A$.

6. Interconnection of Building Elements. A continuous load path for all response forces should be provided. However, interconnection capacity of existing materials need not be analyzed. Two design steps must be undertaken: design the tie system parallel to the shear wall for distribution of calculated response forces, and design the distribution tie system in the diaphragm for retrofitted crosswalls or shear walls.

7. Review of Vertical Load-Carrying Elements. If the building survey has determined that major elements of the vertical load-carrying system are supported on masonry piers, provide independent structural steel columns or equivalent at the face of the masonry pier. An independent foundation system is not required. If a shear wall is retrofitted into the line of bearing masonry piers, the independent support columns are not required.

SUMMARY

A useful methodology for the mitigation of seismic hazards in existing unreinforced masonry buildings has been established based on a research program that combined analytical and experimental investigations.

Several new concepts were introduced that are significant departures from the current code provisions for new construction. The results, given here in "guideline" form for the highest of the three seismic hazard levels defined by the 1978 Applied Technology Council provisions, were originally presented in a report produced by ABK, A Joint Venture, entitled The Methodology.

ACKNOWLEDGEMENT

This research was conducted by ABK, A Joint Venture, for the National Science Foundation under Contract No. NSF-C-PFR-78-19200 and Grant No. CEE-8100532. The Joint Venture ABK consists of the three firms, Agbabian Associates, S.B. Barnes & Associates, and Kariotis & Associates, all in the Los Angeles area. The principal investigators for the three firms are R.D. Ewing, A.W. Johnson, and J.C. Kariotis. Dr. J.B. Scalzi served as Technical Director of this project for the National Science Foundation and maintained scientific and technical liaison with the joint venture throughout all phases of the research program. His contributions and support are greatly appreciated.

REFERENCES

- (1) ABK, A Joint Venture. Methodology For Mitigation of Seismic Hazards in Existing Unreinforced Masonry Buildings, Vol. 8, "The Methodology," ABK-TR-08. El Segundo, CA: Agbabian Associates, June 1984.
- (2) Applied Technology Council. Tentative Provisions for the Development of Seismic Regulations for Buildings, ATC 3-06. Palo Alto, CA: ATC, 1978.

SEISMIC PROVISIONS OF THE UNIFORM BUILDING CODE

By

John G. Tawresey¹

SUMMARY

The Uniform Building Code has extensive requirements for seismic design. Recently the entire masonry design chapter, Chapter 24, was revised. Many of the new provisions affect the seismic design of masonry. Many of the provisions in the other chapters of the UBC also affect seismic design. This paper presents the major provisions for seismic design of masonry structures. A simple design example is presented.

INTRODUCTION - BUILDING CODE STANDARDS

The building codes in the USA are administered at the local levels of government. Each local level (town, city, county or township) adopts one of the model building codes as a law. Usually the local unit of government adopts the model building code without modification, but sometimes codes are modified to conform to local special requirements.

There are three model building codes in the USA, the Uniform Building Code, the Basic Building Code and the Southern Building Code. These documents are not actually codes, since to be a building code they must be adopted into law by the local unit of government. The model building codes are more correctly referred to as "standards".

The only standard with extensive seismic provisions is the Uniform Building Code (Standard). This standard is written by the International Conference of Building Officials (ICBO). ICBO is composed of the building officials from each of the local units of government that use the ICBO standard.

ICBO doesn't normally write the provisions of the standard. Typically, ICBO only votes to accept or reject the new provisions. The new provisions and changes to existing provisions are written by individuals or organizations involved in design and construction. The organizations include:

1. The structural engineers of the states of California, Washington, Oregon and Arizona.

¹ Vice President, KPFF Consulting Engineers, Seattle, Washington
President, The Masonry Society

2. The organizations representing material suppliers such as the Portland Cement Association, The National Concrete Masonry Association, The Brick Institute of America, Western States Clay Products Association, and many others.
3. The professional societies such as the American Concrete Institute (ACI), the American Society of Civil Engineers (ASCE), and The Masonry Society (TMS).

The process for review and approval of new provisions is tedious and beyond the scope of this paper. However, the process is often called the consensus process wherein before adoption, all objections must be removed. This is accomplished through a combination of revising the proposal, further review of the supporting test and research data, additional testing and political compromise.

This paper presents a summary of the seismic provisions of the 1985 Uniform Building Code. The point of view is that of a structural engineer designing a masonry structure. The sequence is that normally occurring during the design process. First, the provisions affecting the design loading are discussed, followed by a detailed review of provisions specific to masonry design and construction. A design example is presented which outlines the process used to design a four-story masonry building.

SEISMIC PROVISIONS OF THE UBC

There is no single section of the Uniform Building Code document that addresses seismic design. Often it is difficult to separate the seismic provisions from other provisions of the standard. This is because good seismic design also results in good design for other loadings. The provisions of the standard are often written to address several requirements simultaneously.

Base Shear Equation - Section 2312(d)

To begin, the UBC contains a rather involved procedure for establishing the seismic loads. In most building designs the simple base shear equation is used:

$$V = ZIKCSW \quad \text{Eq. 1}$$

Where each term is as follows:

1. "Z" is the numerical scaling factor dependent on the seismic zone or level or ground motion expected in the region where the building is to be constructed. The value of "Z" lies between 0.0 and 1.0.
2. "I" is the occupancy importance factor that depends on the building use. The value of "I" lies between 1.0 and 1.5. The value of 1.5 is used for essential facilities which must be usable following a design level earthquake.
3. "K" is the numerical scaling factor dependent on the type of building structure frame. Each different type of building structural frame has different requirements. The structural frame is defined in Section 1702 of the standard as:

"The structural frame shall be considered to be the columns (walls) and the girders, beams, trusses and spandrels having direct connections to the columns (walls) and all other members which are essential to the stability of the building as a whole. The members of floor or roof panels which have no connection to the columns (walls) shall be considered secondary members and not part of the structural frame."

The values for "K" are given in Table 23-1 of the standard. The value of "K" for most masonry structures is 1.33 since masonry buildings are usually classified as "box systems".

4. "C" is the factor that relates the magnitude of the base shear to the building dynamic characteristics. Most masonry structures have low periods, and thus the value of "C" is usually set at the maximum value of 0.12. The UBC standard provides the designer with an approximate method for the determination of the period "T" by the use of the following equation:

$$T = 0.05 h / \sqrt{D} \quad \text{Eq. 2}$$

where "h" is the height of the building in feet and "D" is the plan dimension of the building in feet in the direction of the applied load. "T" may also be determined by an elastic analysis of the structure. The elastic analysis is the preferred method, but is only used on projects large enough to justify the extra cost of design.

5. "S" is a factor relating the base shear loading to the relationship between the soil stiffness and the building stiffness. The value lies between 1.0 and 1.5. If the characteristic site period (T_s) is known, then the value of "S" is given as:

$$S = 1.0 + T/T_s - 0.5*(T/T_s)^{0.5} \quad \text{when } T/T_s \leq 1.0 \quad \text{Eq. 3}$$

$$S = 1.2 + 0.6*T/T_s - 0.3*(T/T_s)^{0.5} \quad \text{when } T/T_s > 1.0 \quad \text{Eq. 4}$$

Since most masonry structures have low periods, the first equation normally applies. The UBC limits the value of T in this equation to not less than 0.3 seconds and the value of T_s to between 0.5 seconds and 2.5 seconds. For masonry structures where the building height is less than the plan dimension, the characteristic period will be less than the 0.3 limit and the first equation applies. For rock foundations or stiff soils, the site characteristic period will be low. Therefore, the maximum value of S becomes 1.42 ($T = 0.3$ and $S = 0.5$).

6. "W" is the total dead load of the structure including partition loading (20 pounds per square foot when partition locations are subject to change), plus 25% of the floor live load in storage and warehouse occupancies and snow loading in excess of 30 pounds per square foot.

Equation 1 is used to determine the base shear for both orthogonal directions of the building. The analysis proceeds considering each direction independent of the other. It is not required to analyze the building for the resultant of the two directional forces.

The base shear loads are then distributed to the building floors using the following formula:

$$F_x = (V - F_t)W_x H_x / (\sum(W_i H_i)) \quad i = 1, N \quad \text{Eq. 3.}$$

where F_t is the force at the roof defined as:

$$F_t = 0.07TV \quad \text{Eq. 4}$$

but need not be greater than 25% of the total base shear.

Distribution of Horizontal Shear - Section 2303(b)1

Once the base shear is distributed to the roof and each floor, the analysis proceeds to distribute the forces to each element supporting the floor. The forces are distributed to each element in proportion to its rigidity, considering the rigidity of the horizontal bracing system or the horizontal diaphragm. Normally, in the case of wood diaphragms (considered flexible) the forces are distributed in proportion to the contributing area without consideration of the stiffness of the walls. For concrete or similar diaphragms (considered rigid) the forces distribute in proportion to the stiffness of the walls. The stiffness of the walls can be expressed as a function of their height and length.

Accidental Torsion - Section 2312(e)4

In addition to the distribution of the base shear, first to the floors and then to the elements supporting the floors, a specified torsional force must also be applied. The specified torsion is the larger of that resulting from the story shear acting with an eccentricity of 5% of the maximum building dimension, or an eccentricity equal to the distance between the center of mass and the center of rigidity. The torsional force is then distributed to the supporting elements in proportion to their rigidities in the same fashion as the shear was distributed. However, the resulting shear forces cannot be used to reduce the shear force on the supporting element.

Load Combinations - Section 2303(f)

The UBC specifies the loads that must be combined with seismic loads. There are two loading conditions, as follows:

1. Dead load plus floor live load plus seismic.
2. Dead load plus floor live load plus snow plus seismic.

When the floor live load results in lower stresses (relief of overturning forces) the floor live load should not be included. Moreover, it is common practice to use 90% of the dead load in these cases as an additional conservatism.

Stress Increase - Section 2303(d)

The allowable stresses for "working stress design" may be increased by one-third when considering earthquake (seismic) forces either acting alone or in combination with vertical loads. This one-third increase has been justified as a short duration stress increase.

Reinforced Masonry or Concrete - Section 2312(j)2B

The UBC requires all concrete and masonry buildings in Seismic Zones No. 2, 3, and 4 to be reinforced. Both horizontal and vertical reinforcing is required. In masonry structures, the following minimum reinforcing is required:

1. In Zone 2, vertical #4 bars (area equal to .2 sq. in) are required at four foot on center, at the edge of each opening and at the element corners.

In addition, horizontal #4 bars are required at the bottom and top of wall openings, at connections to floors and roofs, at the bottom and top of the wall and at ten foot maximum separation.

For stack bond masonry, the minimum area of horizontal reinforcement is $0.0007bt$ where "t" is the specified thickness of the wall and "b" is the bar spacing.

2. In Seismic Zones 3 and 4, there is the additional requirement that the area of vertical and horizontal reinforcement must exceed $0.002bt$, with the area in any one direction to be not less than $0.0007bt$. Additionally, the horizontal reinforcement spacing cannot exceed four foot.

The seismic steel requirements are often referred to as arbitrary steel since there is no rational basis for the values specified. However, actual performance in earthquakes has demonstrated good behavior at these levels. Additionally, recent testing at the University of California at Berkeley has shown that these levels of reinforcing provide high levels of ductility and energy absorption.

It should be noted that UBC Section 2312(j)2B also requires that reinforcing be placed not less than two foot on center when the masonry is used on buildings relying on a moment-resisting space frame to resist seismic forces. Thus the standard masonry infill panel used on concrete or steel moment frames must have reinforcement spaced at two foot or less in both directions.

Lateral Support of Masonry - Section 2312(j)3

In Seismic Zones 2, 3, and 4 the anchoring of masonry walls to horizontal wood diaphragms cannot be accomplished through the use of nails placed perpendicular to the longitudinal grain of the wood, or rely on the resistance of wood in cross-grain bending or tension. The provision was added to the UBC as a result of experience with failures in actual earthquakes. Moreover in Section 2310, connections between walls and horizontal diaphragms must be designed for 200 pounds per lineal foot, or the design load, whichever is greater.

Masonry walls may be supported laterally by wood horizontal diaphragms provided the wood diaphragms do not resist forces by rotation. Vertical wood diaphragms may not be used to support masonry. However, these restrictions do not apply to buildings of one story in height.

Chapter 24 Masonry

The UBC contains design and construction provisions for each material in separate chapters. Masonry provisions are contained in Chapter 24. Because masonry must be reinforced in earthquake sensitive areas, many of the require

ments of this chapter that address reinforced masonry may be considered seismic provisions. The most important of these are the construction requirements.

Construction, Grouted Masonry - Section 2404(f)

All reinforcing must be embedded in mortar or grout. Grout is not concrete. Grout is a mixture of cement, hydrated lime, sand and sometimes pea gravel aggregate to which is added sufficient water to assure placement and hydration. Grout is typically placed with slumps in the range from 8 to 11. If this material acted like concrete, then its strength would be very low. But, because grout is placed in the masonry unit and the masonry unit acts like a sponge to remove the water, very high strengths are achieved in actual practice.

The masonry units commonly used in seismic regions are hollow clay brick and hollow concrete block. The units typically have two or more cells which line up in running bond to form a continuous vertical cell the full height of the wall. The reinforcement is placed in the cell after the wall has been constructed to a specified height, often up to sixteen feet. After the reinforcement is placed in the cell, the cell is grouted.

Horizontal reinforcing is commonly placed in units with a channel sliced through the cross webs. The reinforcement is placed during the construction of the wall and grouted when the top of the wall is grouted (the grout flows horizontally in the bond beam channel) or the bond beam is grouted after the horizontal reinforcement is placed and the vertical cells which will contain reinforcement are blocked leaving the cell clear for grouting the vertical reinforcement.

The UBC limits the height of grout pour by the size of the cell in the masonry units. Table I herein presents the limitations. For grout pours in excess of twelve inches, it is required to mechanically vibrate the grout after the initial loss of water and before initial set.

Additionally, the code requires the placement of steel within specified tolerances. It must be placed within 1/2-inch for flexural members with d less than 8 inches, within 1-inch for d less than 24 inches and within 1-1/4 inches for d greater than 24 inches. Longitudinal reinforcement must be placed within 2 inches.

Material Limitations - Section 2407(h)

The UBC restricts the use of certain materials in seismically sensitive areas. There are no restrictions for Seismic Zone 0 and 1. In Seismic Zone 2, Type O mortar, masonry cement, plastic cement, nonload-bearing masonry units, and glass block cannot be used as part of the structural frame (see the above definition for the structural frame). In Seismic Zones 3 and 4 the same restrictions apply with the additional limitation that type N mortar cannot be used as part of the structural frame.

Design Strength Limitations - Section 2407(h)

There are three methods used to determine the strength of masonry. The first relies on a prism test specific to the project being designed. The second relies on 30 prior tests of similar materials. The third relies on the strength of the masonry unit and the proportions of the mortar. Whenever the third method is used

and the project is located in Seismic Zones 3 or 4, the strengths specified are limited to 1500 psi for concrete masonry and 2600 psi for brick masonry.

Dimension Limitations - Section 2407(h)

Bearing walls in Seismic Zones 3 and 4 must be at least 6 inches in nominal thickness except that 4 inch high strength load bearing construction is allowed under certain conditions. Column dimensions are limited to 12 inches nominal unless half the allowable stress is used, in which case the smallest allowed nominal dimension is 8 inches.

Flexural Modes of Failure - Section 2407(h)4K

In Seismic Zones 3 and 4, the UBC requires the designer to increase the design shear stress in shear walls by a factor of 1.5, without a corresponding increase in the associated moment. The designer, therefore, is required to increase the margin of safety for the shear mode of failure, while maintaining the same margin of safety for the flexural mode of failure. The more ductile flexural mode of failure is thereby encouraged.

Reinforcement Special Requirements - Section 2407(h)

Whenever shear reinforcement (usually horizontal) is used in shear walls to resist the design loads, it is required that the shear wall be specially inspected in accordance with Sections 306 and 2405. Among other requirements these sections require prism testing, site observation during mortar and grout mixing, and site observation of the placement of units, reinforcing and grout. This provision increases the factors of safety by improving the quality of materials and workmanship.

It is also required that shear reinforcement be terminated by a standard hook or with an extension of proper embedment length beyond the reinforcing at the end of the wall. The hook or extension may turn up, down, or be horizontal.

DESIGN EXAMPLE

Figures 1 through 7 present a design example. The building is a four-story, six-inch load bearing, reinforced, brick structure. The design example is for Seismic Zone 4.

CONCLUSION

The major provisions of the Uniform Building Code for masonry design for areas of high seismic risk were presented. A design example was presented to demonstrate their use in general practice by the structural engineer. There are many other provisions in the Uniform Building Code that are related to seismic design and the designer should not consider the material presented here to be comprehensive.

TABLE NO. 24-H -- GROUTING LIMITATIONS

Grout Type	Grout Pour ⁴ Maximum Height M(Ft)	Least Clear Dimensions ³			Clean- Outs Required ²
		Width of Grout Space, MM(In) ¹	Cell Dimensions MM(In)	Cell Dimensions MM(In)	
Fine	.3(1)	19.1(3/4)	38.1x50.8(1-1/2x2)	38.1x50.8(1-1/2x2)	No
Fine	1.5(5)	38.1(1-1/2)	38.1x50.8(1-1/2x2)	38.1x50.8(1-1/2x2)	No
Fine	2.4(8)	38.1(1-1/2)	38.1x76.2(1-1/2x3)	38.1x76.2(1-1/2x3)	Yes
Fine	3.7(12)	38.1(1-1/2)	44.5x76.2(1-3/4x3)	44.5x76.2(1-3/4x3)	Yes
Fine	7.3(24)	50.8(2)	76.2x76.2(3x3)	76.2x76.2(3x3)	Yes
Coarse	.3(1)	38.1(1-1/2)	38.1x76.2(1-1/2x3)	38.1x76.2(1-1/2x3)	No
Coarse	1.5(5)	50.8(2)	63.5x76.2(2-1/2x3)	63.5x76.2(2-1/2x3)	No
Coarse	2.4(8)	50.8(2)	76.2x76.2(3x3)	76.2x76.2(3x3)	Yes
Coarse	3.7(12)	63.5(2-1/2)	76.2x76.2(3x3)	76.2x76.2(3x3)	Yes
Coarse	7.3(24)	76.2(3)	76.2x101.6(3x4)	76.2x101.6(3x4)	Yes

¹ Grout space width shall be increased by the horizontal projection of the diameters of the horizontal bars within the cross section of the grout space.

² Clean-outs may be omitted if approved provisions are made to keep the grout space clean prior to grouting.

³ The clear dimension is the cell or grout space width less mortar projections.

⁴ For grout pours over 1.5M (5 feet) high, see 2404(f)1.

Table 1 - UBC Table 24-H

TABLE NO. 24-H -- GROUTING LIMITATIONS

Grout Type	Grout Pour ⁴ Maximum Height M(Ft)	Least Clear Dimensions ³			Clean- Outs Required ²
		Width of Grout Space, MM(In) ¹	Cell Dimensions MM(In)	Cell Dimensions MM(In)	
Fine	.3(1)	19.1(3/4)	38.1x50.8(1-1/2x2)	38.1x50.8(1-1/2x2)	No
Fine	1.5(5)	38.1(1-1/2)	38.1x50.8(1-1/2x2)	38.1x50.8(1-1/2x2)	No
Fine	2.4(8)	38.1(1-1/2)	38.1x76.2(1-1/2x3)	38.1x76.2(1-1/2x3)	Yes
Fine	3.7(12)	38.1(1-1/2)	44.5x76.2(1-3/4x3)	44.5x76.2(1-3/4x3)	Yes
Fine	7.3(24)	50.8(2)	76.2x76.2(3x3)	76.2x76.2(3x3)	Yes
Coarse	.3(1)	38.1(1-1/2)	38.1x76.2(1-1/2x3)	38.1x76.2(1-1/2x3)	No
Coarse	1.5(5)	50.8(2)	63.5x76.2(2-1/2x3)	63.5x76.2(2-1/2x3)	No
Coarse	2.4(8)	50.8(2)	76.2x76.2(3x3)	76.2x76.2(3x3)	Yes
Coarse	3.7(12)	63.5(2-1/2)	76.2x76.2(3x3)	76.2x76.2(3x3)	Yes
Coarse	7.3(24)	76.2(3)	76.2x101.6(3x4)	76.2x101.6(3x4)	Yes

¹ Grout space width shall be increased by the horizontal projection of the diameters of the horizontal bars within the cross section of the grout space.

² Clean-outs may be omitted if approved provisions are made to keep the grout space clean prior to grouting.

³ The clear dimension is the cell or grout space width less mortar projections.

⁴ For grout pours over 1.5M (5 feet) high, see 2404(f)1.

Figure 2 - UBC Table 24-H

kpff
consulting engineers
washington

PROJECT	FOUR STORY RESIDENCE	BY	JGT	DATE	12/1/85	NO. OF SHEETS	1 OF 7
LOCATION		DATE		DESIGNED		CHECKED	
CLASS		DATE					

	GIVEN:
	BUILDING GEOMETRY:
	ZONE 4
	STIFF SOIL
	BECK MANNET:
	$F_{all} = 4000 \text{ PSI}$
	6" WALLS
	DL =
	FLOORS = 100 PSF
	ROOF = 100 PSF
SEISMIC DESIGN N-S DIRECTION	
$V = ZIKCSW$	
$Z = 1.0$	ZONE 4
$I = 1.0$	RESIDENTIAL
$K = 1.33$	BOX SYSTEM
$C = 1/5\sqrt{T}, T = .05W/\sqrt{D} = .05 \times 36/\sqrt{36} = .30$	
$= .12$	
$S = 1.0 + 3/5 - (2/5)^2$	
$= 1.42$	EQ. 3
$CS = .17, CS_{max} = .14$	MAX. CS = .14
$V = 1.0 \cdot 1.0 \cdot 1.33 \cdot 1.4 \cdot W = .186W$	

kpff consulting engineers 1400 K Street, N.W. Washington, D.C. 20004	project FOUR STORY RESIDENCE	date 12/1/85	sheet no 2 OF 7
	location	checked	job no
	client	date	
WEIGHT			
FLOORS			
$3 \times 36 \times 45 \times 100 = 486^k$			
ROOF			
$36 \times 45 \times 100 = 162^k$			
WALLS			
$[2(13\frac{1}{2} + 9 + 9) + 18 + 18 + 36] \cdot 3.5 \times 60 \text{ PSF}$			135 FT OF WALL
$= 255.1^k$			
PARTITIONS			
(ASSUME 20 psf)			
$3 \times 36 \times 45 \times 20 = 97.2^k$			
TOTAL 1000.3^k			
SEISMIC FORCE N-S			
$V = .186 \times 1000.3^k = 186.1^k$			BASE SHEAR
DISTRIBUTION TO FLOORS:			
$F_b = .07TV = .07 \times .30 \times 186.1^k = 3.9^k$			EQ. 6
$F_x = (V - F_b) \frac{w_x h_x}{\sum_{i=1}^n w_i h_i}$			EQ. 5

kpff

consulting engineers
north, washington

PROJECT: FOUR STOREY RESIDENCE	DATE: JGT	NO: 30P7
LOCATION:	DATE: 12/1/86	
CLIENT:	CHECKED:	
	DATE:	

► DISTRIBUTION TO FLOORS -

	W _w	h _w	W _w h _w	F _w	TOTAL
ROOF	198.9	36'	7,142	60.5 ÷ 3.9	= 64.2
FL3	267.3	27'	7,217		= 60.9
FL2	267.3	18'	4,811		= 40.6
FL1	267.3	9'	2,406		= 20.3
	✓ 1000.3		21,576		186 KW

► DISTRIBUTION TO N-S WALLS
(FLOOR DIAPHRAGM ASSUMED RIGID)

WALL NO.	W _w	R	%	%
			TO WALL	
1	110'	.25	10.8	1) $R = \frac{1}{[(W/L)^2 + 3(W/L)]}$ 2) $\% = R/SR \times 100$
2	110'	.25	10.8	
3	110'	.25	10.8	
4	110'	.25	10.8	
5	.25	1.31	56.8	
		2.31	100%	

► ACCIDENTAL TORSION

CENTER OF MASS - E-W

FLOORS	486K × 22.5	= 10,935 K FT
ROOF	162K × 22.5	= 3645 K FT
WALLS	34K × 0	= 0
	34K × 4.5	= 153 K FT
	68K × 22.5	= 1530 K FT
	51K × 38.25	= 1951 K FT
	68K × 45	= 3062 K FT

kpff
consulting engineers
san diego, california

PROJECT: FOUR STORY RESIDENCE	BY: JLT	DATE: 12/1/85	SHEET NO.: 4 OF 7
LOCATION:	DATE:	DESIGNED:	CHECKED:
OWNER:	DATE:	DESIGNED:	CHECKED:

ACCIDENTAL TORSION - CENTER OF MASS (CONT.)

PARTICANS

$97.2 \times 22.5 = 2187 \text{ K FT}$

$\sqrt{1000.2} = 23463 \text{ K FT}$

C of M, $\bar{x} = 23.45 \text{ FT}$

CENTER OF RIGIDITY

WALL No.	R	R · X
①	.25	0
②	.25	0
③	.25	5.62
④	.25	5.62
⑤	1.31	58.95
	<u>2.31</u>	<u>70.19</u>

C of R, $\bar{x}_r = 30.38$

ECCENTRICITY

MIN. = $.05 \times 45 = 2.25'$
ACTUAL = $(30.38 - 23.45) = 6.93' \leftarrow$

TORSION DISTRIBUTION

WALL No.	R _x	d _x	R _x d _x	R _y d _y	$\frac{R_x d_x}{\sum R_x d_x}$
①	.25	30.38	7.59	230.7	.0098
②	.25	30.38	7.59	230.7	.0098
③	.25	7.88	1.97	15.5	.0026
④	.25	7.88	1.97	15.5	.0026
⑤	1.31	-19.62	-19.15	280.0	-.0248
			<u>20.70</u>	<u>772.9</u>	<u>0</u>

kpff

consulting engineers
1000 Washington

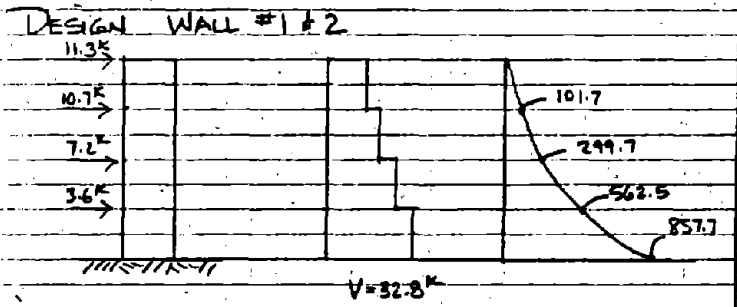
PROJECT FOUR STORY RESIDENCE

DATE 12/1/85

5 OF 7

WALL FORCES WALLS No. 1 & 2

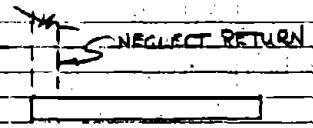
LEVEL	Fx	TORSION		TOTAL
		T _{FT}	Vt	
R	6.93	444.9	4.36	11.3 ^K
FL3	6.57	422.0	4.13	10.7 ^K
FL2	4.38	281.3	2.76	7.2 ^K
FL1	2.19	140.7	1.38	3.6 ^K



DEAD LOAD @ LEVEL 0

WALL $36 \times 9 \times 60 = 19.4^K$
 FLOORS $\left(\frac{22.5}{2}\right) \times \left(\frac{36}{2}\right) \times 100 = 60.7^K$
 ROOF 20.2^K
100.3^K

DESIGN 90% -
 $P_{DL} = 90.3^K$
 $M = 857.7^K \cdot FT$



kpff

consulting engineers
san diego, california

FOUR STORY RESIDENCE

12/85

12/85

6007

$$M/Pd = 857.7 / 90.3 \times (9-1) = 1.18 > .17$$

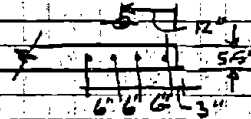
CRACKED

$$A_s \approx M / 22200 \times 1.33 \times 96$$

$$= 3.35 \text{ IN (WITHOUT DEAD LOAD RELIEF)}$$

$$\text{T12Y } A_s = 2.4 \quad (4) \#7$$

$$d = 9-12" = 96"$$



$$K^2 + (2nc + 2 \frac{E_m}{E_s})K - (2nc + 2 \frac{E_m}{E_s}) = 0$$

$$E_m = P / E_m b d \quad E_m = 1000 \text{ lb/in}$$

$$\frac{E_m}{E_s} = n c (1 - K/3) / (M/Pd + K/3 - 1)$$

$$n c = 29 E^6 / 4 E^6 \times (2.4) / 5.5 \times 96 = .0330$$

$$\text{T12Y } K = .3$$

$$\textcircled{1} \quad E_m/E_s = .1061 \quad K = .406 \quad \text{T12Y } K = .38$$

$$\textcircled{2} \quad E_m/E_s = .0940 \quad K = .392 \quad \text{T12Y } K = .37$$

$$\textcircled{3} \quad E_m/E_s = .0926 \quad K = .391 \quad \text{OK } j = .8697$$

$$M_u = 240 \times 24,000 \times 1.33 \times .8697 \times 96 + 90,300 \times 96/2$$

1/3 STRESS INC.

$$= 894.2 \text{ K-FT} > 857 \text{ K-FT OK}$$

$$M_u = \frac{(5.5 \times 96^2 / 2) \times .8697 \times .391 \times 1759}{90,300 \times 96/2}$$

F3 = .33 f_m
+ 1/3 INC.

$$= 902.4 \text{ K-FT} > 857 \text{ K-FT OK}$$

kpff

consulting engineers
1000 Washington

PROJECT	FOUR STORY RESIDENCE	DATE	JGT	NO. OF	7 OF 7
SECTION		DATE	12/1/05		
DATE		CHECKED			
		DATE			

SHEAR - GROUT SOLID

$$V_{DESIGN} = 1.5V$$

$$= 1.5 \times 32.8 = 49.2^k$$

$$v = \frac{V}{b_d d}$$

$$= \frac{49,200}{5.5 \times .87x}$$

$$= 107.11 \text{ PSI}$$

$$\frac{M}{Vd} = \frac{857.7^k \text{ FT}}{49.2 \times 96/12} = 2.18 > 1.0$$

$$F_{cr} = 1.5 \sqrt{4000} \times 1.33 = 126.5 \text{ PSI}$$

$$\text{MAX } 75 \text{ PSI} \times 1.33 = 100 \text{ PSI}$$

M.S. - 7% OK?

$$A_r = \frac{SV}{F_s d}$$

$$= .26$$

CHOOSE S = 12" O.C. (SEE PLAN)

$$F_s = 24,000 \text{ PSI}$$

$$d = 96$$

$$V = 49,200 \text{ LBS}$$

USE #5 @ 12" O.C.

SECTION 2407(h)

1/3 STRESS INCREASE

CRACK- AND COLLAPSE-RESISTANT DESIGN OF MULTISTORY BRICK BUILDING WITH LARGE SPACIOUS FIRST STORY IN SEISMIC AREA

Mo Yong*

SUMMARY

This paper recommended that an earthquake-proof structural program of the first story should be rationally selected in the seismic area for a five- or six-storied brick building with a large spacious first story, that rigid ratio of the second story to the first one should be controlled, and that the crack- and collapse-resistant design should be made in accordance with two criteria of "no cracking under the slight earthquake and no collapsing under the heavy one".

Under the slight earthquake, it is necessary for the crack-resistant design to be made, and for the sections of structural members to be selected; Under the heavy earthquake, it is necessary for the collapse-resistant design to be made, and for the equivalent strength of the first story to be checked; And under the basic intensity of earthquake, it is necessary for the structural design to be made, with the emphasis on strengthening earthquake-proof structural measures of the first and second stories.

For the sake of easy design, the design steps and block-diagram are given in the late of the paper.

I. DETERMINATION OF DESIGN BASIC PRINCIPLES

Structural characteristics of the multistoried brick building with a large spacious first story are as follows:

The first story is more spacious, and different structural systems and different building materials will be respectively used for the first story and above the first one. That is not very favourable for resistance to earthquake of the building. It is, therefore, very necessary to select and draw up a basic principle of design, which will ensure earthquake-proof safety for the type of structure.

After summing up experiences and lessons of the serious disasters caused by all previous heavy earthquakes for the mankind, the scholars at home and abroad unanimously thought that it would be appropriate to adopt two design basic principles of "no cracking under the slight earthquake and no collapsing under the heavy earthquake" in the earthquake-proof design for the building structures (1). Although China Current Stan-

* Chief Engineer, Gansu Building Prospecting Design Institute, Lanzhou, China

standard TJ11-78 has covered the principle of "no cracking under the slight earthquake", it has not yet covered the specific and definite stipulations for "no collapsing under the heavy earthquake". The author thought that it would be proper for two design basic principles of "no cracking under the slight earthquake and no collapsing under the heavy earthquake" to be adopted in the earthquake-proof design of the multistoried brick building with a large spacious first story in the seismic area.

II. SELECTION OF STRUCTURAL PROGRAMS

The investigation of Tangshan earthquake disaster showed that the disaster suffered by the multistoried brick buildings with large spacious first stories being frame or internal frame structures was considerable serious. A phenomenon of seriously deformed concentration occurred in the first story. The frame-columns or the brick piers were subjected to a higher shear force or axial force. With the result that the bending, crush and excess elasto-plastic deformation occurred, the structure was led to a serious damage, even to collapse.

The earthquake disasters suffered by the multistoried brick buildings with flexible first stories in other countries were also as similar as the said above.

Actually, the main reasons are: the first story of the building is more spacious, the upper structure is rigid and the bottom one is flexible, the rigidity will change unexpectedly, the top is heavy and the toe is light. For such a serious disaster due to the earthquake, it is not satisfactory for this building to take general structural measures. The structural program has to be rationally selected. The reinforced concrete structure of frame-shear walls used for the first story and the brick structure with structural columns used for the upper structure will be a better structural program of the five-or six-storied brick building with a large spacious first story in the seismic areas of China.

The reasons are as follows:

1. A certain number of shear walls set in the first story can avoid the upper structure to be rigid and the bottom one to be flexible, and also avoid the rigidity to be suddenly changed. Thus, the concentration of deformation of the first story under the action of earthquake will be eliminated and the weak story will be turned into a non-weak one so as to avoid the serious disaster of earthquake and ensure earthquake-proof safety of the whole building.

2. As a result of the elastic modulus of concrete being great different from that of brick walls, the quantity of shear walls required to control the rigid ratio of the first story to the second one is limited. Therefore, it will still ensure the first story to have a given large space, which can meet the needs for the first story used as the shop, restaurant, garage, etc.

III. CONTROL RIGID RATIO OF THE FIRST STORY TO THE SECOND ONE

How to control rigid ratio of the second story of the brick structure to the spacious first story is the key of changing such a weak first story into a non-weak one. The author thought that it would be necessary to control rigid ratio of the second story to the first one in order to prevent the first story from forming a weak one and suddenly changing the rigidity, otherwise the earthquake disaster would be more serious.

The rigid ratio should be less than 2, and more than 0.5. It is close to 1 as possible. i.e.

$$0.5 < \gamma = K_2 / K_1 < 2 \quad \dots\dots\dots (1)$$

$$\gamma \approx 1 \text{ as possible} \quad \dots\dots\dots (2)$$

In consideration of shear deformation, shear rigidities K_1, K_2 of the first and second stories are respectively:

$$K_1 = \frac{G_1 A_{w1}}{\mu H_1} \quad \dots\dots\dots (3)$$

$$K_2 = \frac{V_0 G_2 A_{w2}}{\mu H_2} \quad \dots\dots\dots (4)$$

where G_1 and G_2 are respectively the shear elastic modulus of concrete of the first story and that of the brick masonry of the second one,

V_0 is an increasing coefficient of earthquake-proof capacity due to the structural columns added to the brick structure of the second story,

A_{w1} is the sum of net total area of shear walls in the first story (The area of column sections, considered as a safe reserve, is negligible.),

A_{w2} is the sum of net area of brick walls in the second story.

IV. DETERMINATION OF HEAVY AND SLIGHT EARTHQUAKE INTENSITIES AND SIMPLIFICATION OF CRACK-RESISTANT DESIGN UNDER THE SLIGHT EARTHQUAKE INTENSITY

The earthquake intensity is random. It is a main current tendency to study the randomness of the earthquake action with a probability method. Taking the slight earthquake intensity as a usual intensity and the heavy earthquake intensity as a rare one, in accordance with the Reference (2), the result of analyzing earthquake risk suffered by 43 cities and towns in China and the characteristics of the brick structure showed that for the multistoried brick building with a large spacious first story, it is proper for the slight earthquake intensity to be taken 1 degree lower than the basic intensity and for the heavy earthquake intensity to be taken 1 degree higher than the basic intensity.

For the multistoried brick building with a large spacious first story, through comparison and analysis we know that the crack-resistant design made with two methods under the slight earthquake intensity corresponds to the earthquake-proof design made with the method stipulated in the Standard under the basic intensity. For the sake of simplifying the calculation, the basic intensity will be directly taken as the design intensity, and the earthquake-proof calculation can be made with the method stipulated in the Standard ($C = 0.45$).

V. CRACK-RESISTANT DESIGN

1. CRACK-RESISTANT DESIGN ABOVE THE FIRST STORY OF BRICK BUILDING

There are now two methods described respectively in China Current Standard and in the Reference (3), which have been used for the crack-resistant design of brick houses above the first story. Based on the statistic analysis and check for the earthquake-proof strength of over 400 brick buildings during 6 heavy earthquakes in Tangshan, Haicheng, etc. of China, Mr. Yang Yucheng and others of Engineering Mechanics Research Institute proposed the main parameters of crack-resistant design for the multistoried brick buildings. Main characteristics of the method are as follows:

The parameters of crack-resistant design have been obtained from failure probability of the brick walls. These data are reliable;

The integral earthquake-proof capacity of the brick building can be measured by checking the earthquake-proof strength between its stories;

The criteria discriminating different earthquake disasters under different intensities have been given.

In view of some characteristics as above, the author thought that the method described in the Reference (3) should be pre-
 cedently adopted in the crack-resistant design for the brick
 houses above the first story. Based on comprehensive policy
 decision of economy and safety in the statistic analysis of
 a large number of earthquake disasters, when checking average
 earthquake-proof strength of the stories with the method des-
 cribed in the Reference (3), the load coefficient K_0 for de-
 signing earthquake will take the values given in Table 1.

Table 1. Values of Load Coefficient K_0 for Designing Earthquake

Design Intensity	7	8	9
K_0	0.19	0.28	0.36

The method stipulated in the Standard will be also used for
 the brick houses above the first story in order to adopt the
 same method in the earthquake-proof calculation of upper and
 bottom structures. On the basis of the investigation and sta-
 tistic analysis of earthquake disasters, a preventive cri-
 terion of resisting 7-degree earthquake intensity is somewhat
 low, that of resisting 9-degree earthquake intensity is some-
 what high and that of resisting only 8-degree earthquake in-
 tensity is moderate in design of the multistoried brick build-
 ings with the method stipulated in the Standard. When the me-
 thod stipulated in the Standard is used, the earthquake load
 can be adjusted based on earthquake disasters. The expression
 is as follows:

$$Q_i = \eta C \alpha_{max} \sum_i W \dots\dots\dots (5)$$

$$(i = 2, 3 \dots n)$$

where η is adjustment coefficient of earthquake di-
 saster (see Table 2).

Table 2. Values of Adjustment Coefficient of Earthquake
 Disaster

Design Intensity	7	8	9
η	1.28	0.94	0.68

2. CRACK-RESISTANT DESIGN OF FRAME-SHEAR STRUCTURE
FOR THE FIRST STORY

In crack-resistant design of the frame-shear structure for the first story, it is necessary to solve the calculation of two external forces such as the earthquake shear force of the first story and overturning moment of earthquake, and to solve their distribution in the earthquake-proof structural members.

These problems as above are described respectively with the method stipulated in the Standard.

2.1 EARTHQUAKE SHEAR FORCE OF THE FIRST STORY

The earthquake shear force of the first story is related to the rigid ratio of the second story to the first one.

For $\gamma \leq 1$, it is not possible to exist any concentration of deformation, and the earthquake shear force has no amplifying effect;

For $\gamma > 1$, the earthquake shear force has an amplifying effect.

The amplifying value is $\Omega = \sqrt{\gamma}$ (6)

Then,
$$Q_1 = \Omega Q_0 = \Omega \sum_{i=1}^n P_i = \Omega C \alpha_{\max} W \dots (7)$$

(Note: For $\gamma \leq 1$, $\Omega = 1$.)

2.2 EARTHQUAKE OVERTURNING MOMENT OF THE FIRST STORY

Characteristics of the multistoried brick building with a large spacious first story are :

The earthquake-proof brick walls on and above the second story are used as vertical bearing members. It is, therefore, necessary to calculate not only the earthquake shear force of the members but the additional axial force produced in the walls and columns by the overturning moment caused by the earthquake load of every story above the first story.

The overturning moment which is directly transmitted from the brick walls above the first story to the frame or frame-shear walls on j axis is:

$$M_j = \sum_{i=2}^n P_{ij} (H_i - H_1) \dots \dots \dots (8)$$

where P_{ij} is the earthquake load of the brick walls of every story acting on j axis of i story,

H_i and H_1 are respectively the height from outside ground level to i floor and to the floor on the top of the first story.

2.3. DISTRIBUTION OF EARTHQUAKE SHEAR FORCE OF THE FIRST STORY

The distribution of earthquake shear force will be dependent upon rigidity of the floor on the top of the first story. As a result of the cast-in-place floor, which is thicker, used as the floor on the top of the first story, all measures of increasing rigidity will be taken as precast slabs used.

Therefore, the floor on the top of the first story can be considered as a rigid floor. For individual members of resistance to the lateral force, such as walls, columns, etc. of the first story, the earthquake shear force should be distributed according to their rigidity of side sway.

2.4. DISTRIBUTION OF EARTHQUAKE OVERTURNING MOMENT OF THE FIRST STORY

How to distribute the earthquake overturning moment acting on the first story in the individual earthquake-proof members of the first story, that is a problem required to be approached.

As mentioned above, the earthquake shear force should be distributed according to the side sway rigidity of individual earthquake-proof members owing to have a rigid floor on the top of the first story. The principle is also same for distribution of the earthquake overturning moment. But the problem depends on whether side walls of the first story can form two pieces of vertical rigid walls.

From analysis of the actual arrangement, for two large doors opened on two side walls, which foundations are mostly isolated foundations. It is difficult for the side walls to form vertical rigid walls. Therefore, the overturning moment is still mainly transmitted from the brick walls above the first story to each frame or frame-shear wall, and it is determined by the equation (8). In order to simplify the calculation, it may be considered that the total overturning moment is approximately distributed in accordance with the sectional area of brick walls on each lateral axis of the second story.

VI. COLLAPSE-RESISTANT DESIGN

1. COLLAPSE-RESISTANT DESIGN OF BRICK HOUSES ABOVE THE FIRST STORY

As a consequence of the brick masonry being a brittle structure, it is necessary to check the equivalent strength under the heavy earthquake intensity in collapse-resistant design of brick houses above the first story.

Before there is no specific calculation method to check collapse-resistant equivalent strength in China Current Standard, the method described in the Reference (3) will be tentatively used.

Statistics of the collapse probability for a lot of brick buildings in Tangshan, Haicheng, etc. of China was described in the Reference (3). When the buildings suffered from the heavy earthquake effect which intensity is 2 degrees higher than the design intensity, collapse would not generally occur (3). The author carried out the collapse-resistant calculation for some six-storied brick buildings in the seismic area of eight-degree intensity in Lanzhou District. The calculation result showed that all these buildings were able to resist the intensity little less than 10 degrees. And the collapse-resistant design was made in accordance with the heavy earthquake intensity.

As mentioned above, in case the heavy earthquake intensity which is taken is 1 degree higher than the design intensity and 1 degree lower than the collapse-resistant intensity calculated actually, the collapse-resistant capacity is more enough. It may be, therefore, considered when the multistoried brick building with a large spacious first story meets the needs of resistance to crack, it can also meet the needs of resistance to collapse.

2. COLLAPSE-RESISTANT DESIGN OF FRAME-SHEAR STRUCTURE FOR THE FIRST STORY

During the collapse-resistant design of frame-shear structure for the first story, it is at first necessary to analyze and determine two problems. Firstly, the ultimate deformation or ultimate strength will be checked; Secondly, the strength is an ultimate bending strength or an ultimate shear one if it is checked.

It is well known that for the reinforced concrete frame structure which is a flexible one, the elasto-plastic deformation should be calculated and the value of ultimate deformation should be checked under the action of heavy earthquake so that it is proper to prevent the structure from collapsing. But for a large spacious first story of the multistoried brick building, it is necessary to take another consideration.



The author carried out preliminary calculation of elastic-plastic deformation for 8 six-storied buildings with frame-shear structures of the first stories under 9-degree heavy earthquake in the area of 8-degree earthquake intensity of Lanzhou. The calculation result showed that the value of relative deformation for the first story is in the range of $1/300-1/500$, much less than the ultimate value $1/100$. That is due to the frame-shear structure as a medium rigid one, the rigidity of shear walls being higher and the selection of sections of the shear walls mainly according to the strength rather than the control of the rigidity under the slight earthquake. For the multistoried brick building with a large spacious first story, it is, therefore, necessary to check the ultimate strength of the first story, not to check the ultimate deformation.

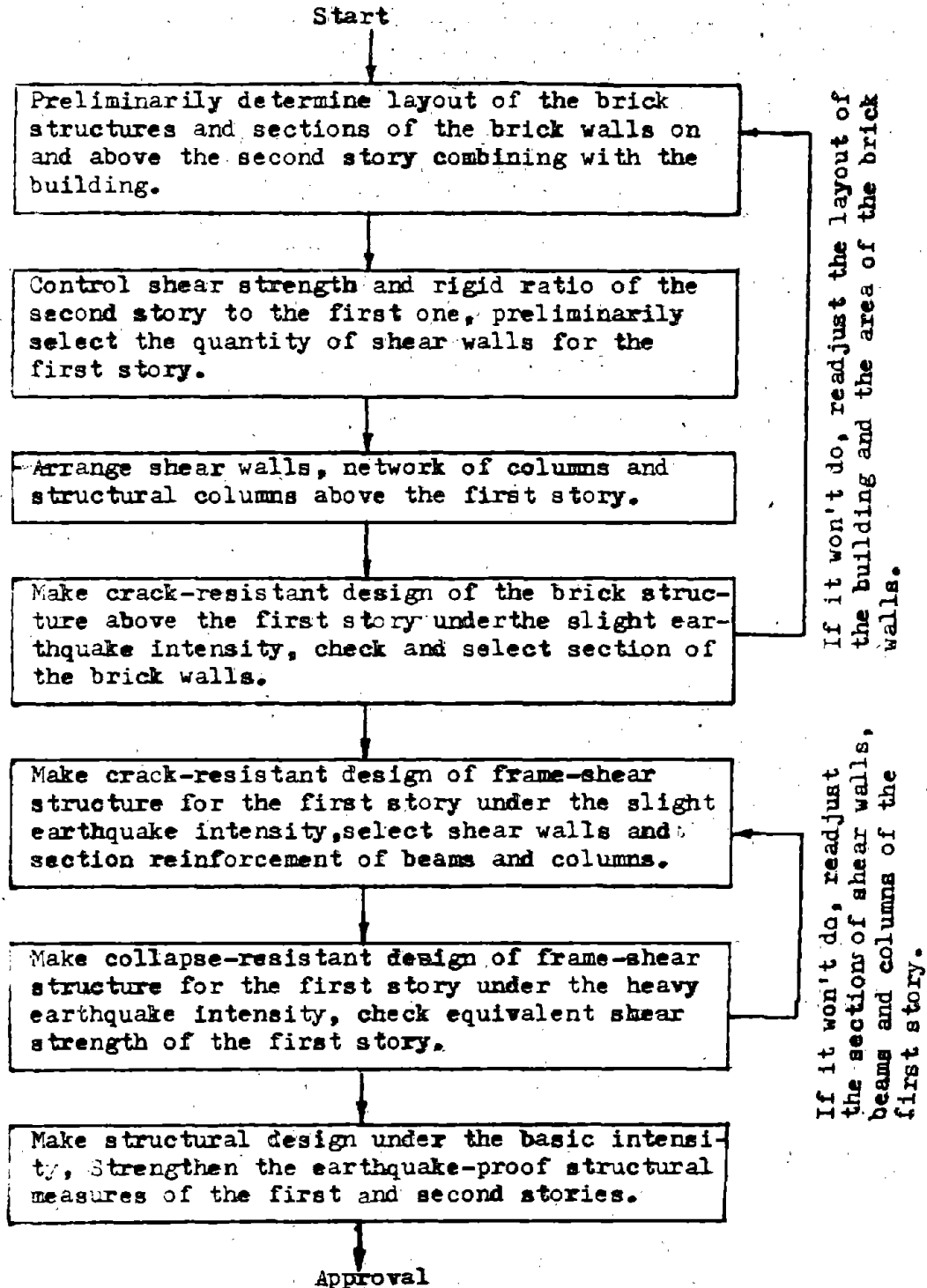
During checking the ultimate strength, it is necessary to check the ultimate shear strength. The reasons are two: The first is that the shear-span ratio of shear walls for the frame-shear structure of the first story is generally small and mainly sheared. The second is that all the shear walls for the first story of the brick building are those with side frames.

The test and analysis in the Reference (4) showed that the rupture of side-frame shear walls were mostly sheared failure. The check of ultimate shear strength of the shear walls is referred in the Reference (4).

VII. DESIGN STEPS AND BLOCK-DIAGRAM

For the design steps of the multistoried brick building with a large spacious first story (see the Block-Diagram of the Design).

Block-Diagram of Earthquake-Proof Design for the Multistoried Brick Building with a Large Spacious First Story



REFERENCES

1. Wei Yulian, etc. " On the Basic Principles of Earthquake-Proof Design for Building Structures, " published in " Building Structure Journal ", Issue VI, 1984.
2. Yang Yucheng, etc. " Probability of Earthquake Disasters for the Multistoried Brick Buildings, " published in " Developments of Seismic Engineering ", Issue IV, 1984.
3. Yang Yucheng, etc. " Seismic Damage, Crack- and Collapse-Resistant Design of the Multistoried Brick Buildings, " published by Earthquake Publishing House.
4. Shanghai Civil Architectural Design Institute and Beijing Architectural Design institute, " Analysis of Ultimate Strength of Shear Walls with Side Frames ".

RESEARCH AND DESIGN OF TALL, SLENDER WALLS

by James E. Amrhein,^I S.E.

SUMMARY

For many years, the design and construction of load-bearing masonry walls were limited to a height/thickness ratio of 25. This conservative limitation was recognized by the Structural Engineers Association of California and, accordingly, they organized and conducted a research program to demonstrate the performance of tall, slender walls subjected to both vertical and lateral loads.

The research program consisted of 32 specimens, 22 of which were masonry and 10 of tilt-up concrete.

After the results were obtained and analyzed, design parameters based on strength design were established limiting both the lateral deflection of the wall and the vertical load on the wall.

This paper describes the test program, the test results, design methods, and gives a design example for a 6" concrete masonry wall.

THE SLENDER WALL RESEARCH PROGRAM

The Uniform Building Code* h/t limitation of 25 was imposed due to lack of experimental data and an attempt to limit flexural stresses under wind load (see page 110 of Reference 4). It also was considered a restraint against possible buckling of the walls under vertical and lateral loads.

The Structural Engineers Association of Southern California (SEAOSC) and the American Concrete Institute-Southern California Chapter (ACI-SC) recognized the limitation due to this unnecessary h/t code restriction. They conducted a research program from 1980-1983 to demonstrate that load-bearing masonry walls can be built and be structurally safe when they exceeded the slenderness ratio of 25.

^I Executive Director, Masonry Institute of America, Los Angeles, Calif.

* Published by the International Conference of Building Officials (ICBO), Whittier, California

Test Specimens

There were a total of 32 test specimens built, consisting of ten concrete block, six clay brick, four clay block, and 12 concrete tilt-up panels. All test panels except one were 24'8" high and 4'0" wide. The masonry panels were reinforced with five #4 bars and the concrete panels with four #4 bars of ASTM* A615 Grade 60 steel. All masonry walls were solid grouted.

The clay masonry walls were 3.5", 5.5", 7.5" and 9.6" thick for respective h/t ratios of 57, 52, 38 and 30. The concrete masonry walls were 5-5/8", 7-5/8" and 10'5/8" thick for h/t ratios of 51, 38 and 30. Note that all of these h/t ratios exceed the allowable limit of the 1982 Uniform Building Code (UBC), therefore they are considered by definition tall, slender walls.

The materials for the hollow concrete masonry, hollow brick and solid brick panels conformed to the requirements of ASTM C90, C652, and C62.

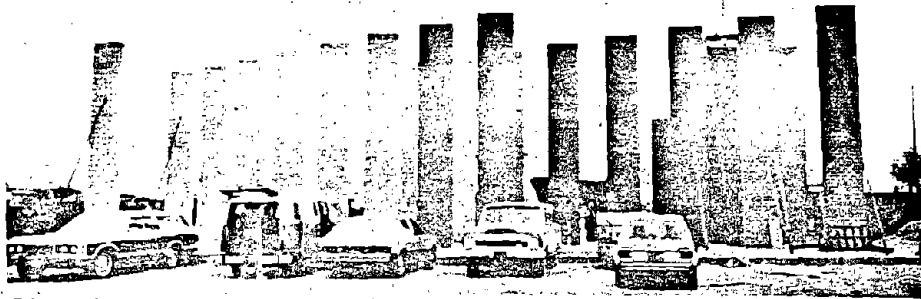


Fig. 1 -- Masonry panels in place ready to be tested

Loading on Panels

Panels were loaded to simulate a typical roof load, using an eccentric vertical load applied to a steel angle ledger. Lateral pressure was applied through an air bag for its full height and width.

Lateral Loading. To simulate the lateral loads on a panel due to wind or earthquake, an air bag was placed between the test frame and the wall. The reaction of the test frame allowed the air bag to expand and load the wall laterally. The lateral load was applied through air pressure and incremental loadings and deflection readings were taken.

The loading frame (Fig. 2) allowed the eccentric vertical load and the lateral load to be applied simultaneously to the panel. The vertical load was provided by water-filled drums, as shown.

*ASTM, American Society for Testing and Materials, Philadelphia, Pa.

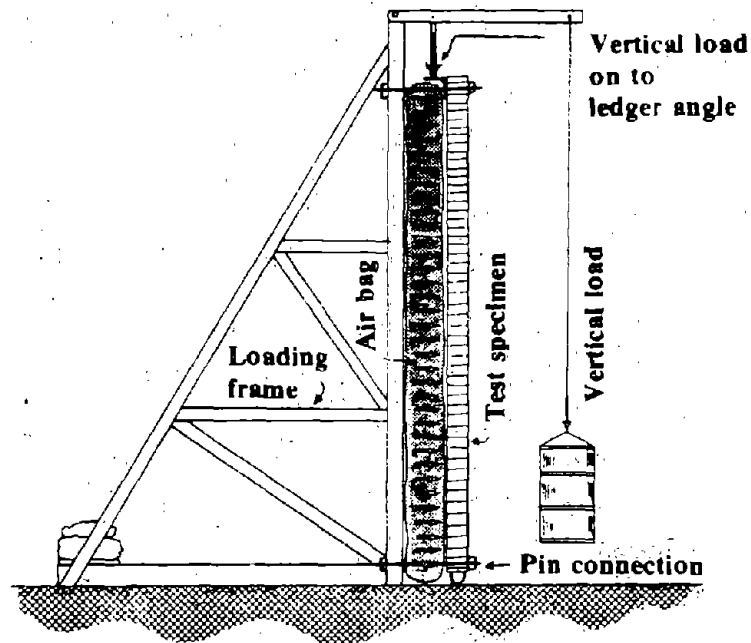


Fig. 2 -- Loading frame and wall specimen setup

Vertical Loading. Vertical load to simulate floor and roof loads was applied to a ledger angle with an eccentricity of three inches plus half the thickness of the panel. This vertical load was induced by means of two drums of water and the load was magnified through lever action (Fig. 3). The load could be varied by changing the amount of water in the drums. This simple mechanism permitted various loads to be applied.

The typical roof load of 320 lb/ft is characteristic of wood roof on a commercial building in California. A roof load of 860 lb/ft was used on seven tests to simulate heavier roof systems. This eccentric vertical roof load increases the PA effect, which was considered in wall buckling.

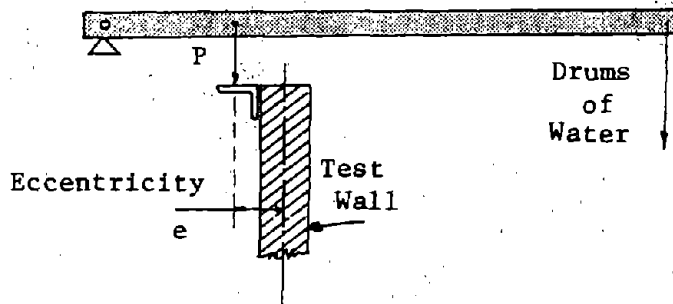
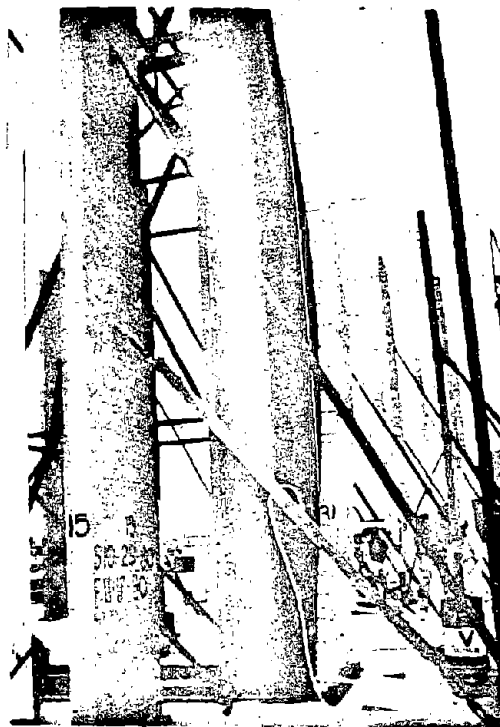


Fig. 3 -- Application of vertical load

Fig. 4 -- Panel #31
8" CMU deflected 17.5".



Typical Test Results

The load-deflection curves for the specimens followed a typical pattern. The wall under initial loading remained uncracked with a very steep load-deflection line. As the first cracks formed and the reinforcing steel (which was located in the center of the panel thickness) received tension stress, the load-deflection curve slope changed. As the load increased, the steel was stressed up to its yield strength. When the reinforcing steel was yielding, it continued to increase in strain (elongate) with a slight additional load and the slope of the load-deflection curve flattened.

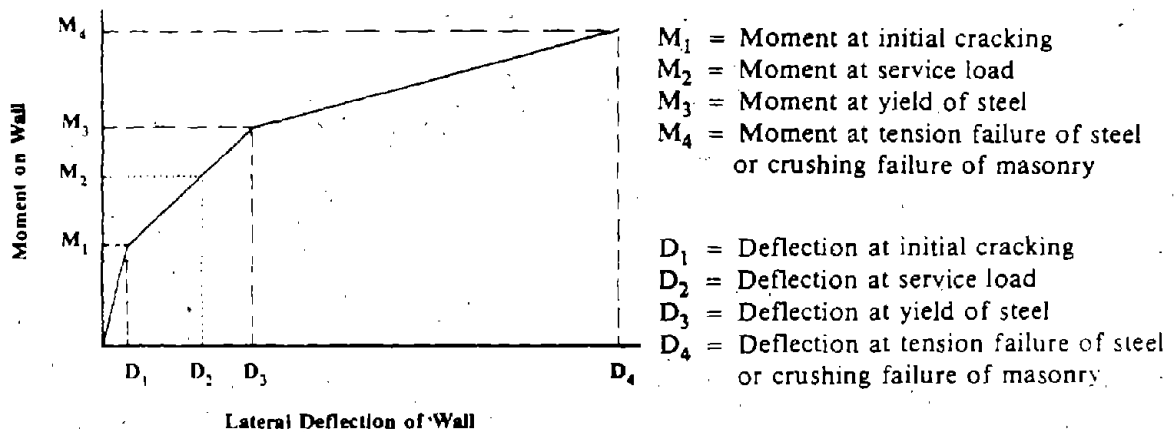


Fig. 5 -- Typical pattern of load-deflection curve

SLENDER WALL TEST RESULTS

Wall No. and Type	Thick-ness, t, in.	f' or f _m , psi	Av. Ratio	Vert. Load, plf	Lat. Load at f _y , psf	Defl. at Yield, in.	Max. Lat. Defl., in.	Lat. Load at Max. defl., psf	
CMU	1	9.63	2460	30	320	94	5.5	17.1	100
	2	9.63	2460	30	860	82	5.5	0.0	88
	3	9.63	2460	30	860	73	6.2	19.0	100
	4	7.63	2595	38	860	75	6.5	11.2	92
	5	7.63	2595	38	860	75	7.5	10.3	82
	6	7.63	2595	38	320	71	5.8	14.8	118
	7	5.63	3185	51.2	320	46	9.0	17.7	62
	8	5.63	3185	51.2	320	38	---	15.9	40
	9	5.63	3185	51.2	320	46	9.8	11.0	50
Br	10	9.6	3060	30.3	320	94	---	15.6	50
	11	9.6	3060	30.3	320	89	9.3	16.8	162
	12	9.6	3060	30.3	320	74	9.0	14.6	90
	13	7.50	3440	38.4	320	40	12.0	19.6	60
	14	7.50	3440	38.4	320	54	14.0	15.9	68
	15	7.50	3440	38.4	320	66	10.5	14.8	79
HBr	16	5.50	6243	52.4	320	57	8.0	19.3	87
	17	5.50	6243	52.4	320	48	8.2	18.2	36
	18	5.50	6243	52.4	320	55	7.9	11.1	61
Con	19	9.50	4000	30.3	320	87	7.3	9.9	55
	20	9.50	4000	30.3	320	83	5.3	7.0	83
	21	9.50	4000	30.3	320	63	7.5	12.3	89
	22	7.25	4000	39.7	320	57	5.4	12.2	64
	23	7.25	4000	39.7	320	52	7.4	11.8	61
	24	7.25	4000	39.7	860	57	7.6	11.8	65
	25	5.75	4000	52.4	860	51	8.1	13.2	59
	26	5.75	4000	52.4	860	42	7.2	11.1	44
	27	5.75	4000	52.4	320	42	8.5	12.4	44
	28	4.75	4000	60.6	320	32	11.6	13.0	34
	29	4.75	4000	60.6	320	34	12.6	19.2	40
	30	4.75	4000	60.6	320	34	13.1	15.2	36

NOTE: CMU = Concrete Masonry Unit
 Br = Two-wythe Brick
 HBr = Hollow Brick
 Con = Concrete

ADDITIONAL TEST WALLS

CMU 31	7.63	2960	38	860	55	16.8"	17.5"	129
HBr 32	5.5"	6000	52	225	47	10.0"	17.0"	56

CONCLUSIONS OF THE RESEARCH PROGRAM

1. Buckling. There was no evidence of elastic and inelastic lateral instability (buckling) for the load ranges tested, which were primarily loads with axial loads less than 1/10 of the short column axial capacity.
2. Pe Moment Effect. The significance of the eccentric moment from the applied simulated light framing roof load was small.
3. PΔ Moment Effect. The significance of the PΔ moment was most pronounced in the thinner panels but did not produce lateral instability in the load ranges tested. Panel weight was the largest component of secondary moments. Secondary moments accounted for approximately 20 percent of the total moment at yield of the reinforcement.

4. Load Deflection. Load deflection characteristics of the panels can be approximated by three straight lines representing the uncracked stage, the cracked stage, and the post yielding stage (Fig. 5). The intersection points of these lines are a function of the moment capacity of the wall section at yielding of the reinforcement. The lines represent the uncracked to cracked to yield deflection to failure stages.

5. EI Value: Tests showed that the produce of the cracked transformed section moment of inertia and the code modulus of elasticity was useful in predicting midspan deflection of the panel at yield level.

6. Residual Deflection. The panels exhibited adequate strength at and beyond the yield point and the rebound indicated that a midpoint permanent deflection can be expected for panels loaded to the yield level of the reinforcement.

7. No h/t Limitation. The tests demonstrated that there was no validity for fixed height-to-thickness limits, but revealed the need for deflection control to limit potential residual deflection in walls after being subjected to service loads.

DESIGN OF TALL, SLENDER WALLS

The design of load-bearing reinforced masonry tall, slender walls is based on the results of the research program, basic static theory, and strength concepts.

There is no limitation for the slenderness (h/t) ratio except as limited by maximum lateral deflection and strength of the wall.

The design shall be based on forces and moments determined by analysis. The procedure considers the effects of axial load and deflection in the calculation of required moments.

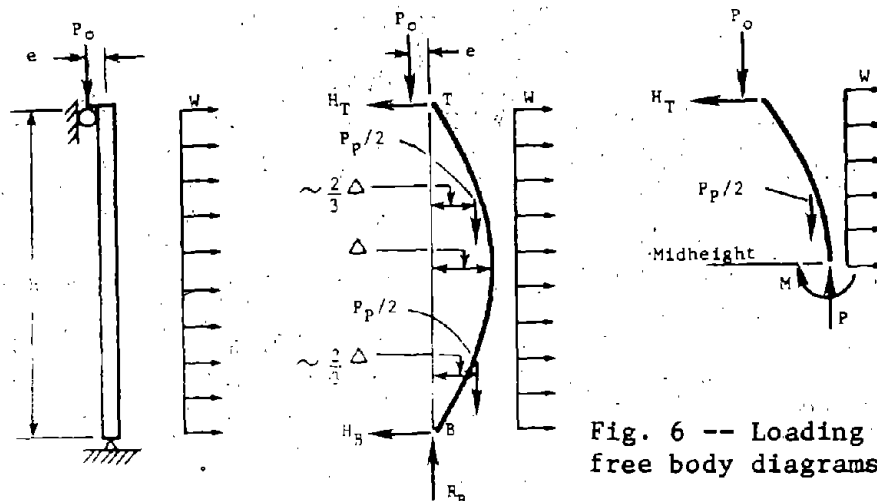


Fig. 6 -- Loading and free body diagrams of wall

Parameters of Design

For the first time, two conditions of design have been imposed on wall design. These are serviceability and ultimate strength.

Serviceability. Due to unfactored service loads, which are the actual code loads for design, including the $P\Delta$ effect, the lateral deflection of the walls is limited.

Maximum lateral deflection = $0.01h$ (SEAOSC & ACI-SC recommendations)
= $0.007h$ (approved by ICBO)

This value will be less than deflection at nominal or yield strength of the wall. Thus this maximum allowable deflection will be within the elastic limit and the wall should rebound without permanent set.

Strength Design. For factored loads (that is loads increased by the UBC load factors) the walls shall have a ductile strength and be stronger than the moments and loads imposed on them.

The strength of the wall is determined based on a limitation on the amount of steel used and thus ensures a ductile condition at yield strength. This will prevent the possibility of a brittle failure.

Maximum Vertical Load

The design procedure is limited to walls in which the vertical load stress at the location of maximum moment does not exceed $0.04 f_m$ thus

$$\frac{P_w + P_o}{A_g} \leq 0.04 f_m$$

where

P_o = Load from tributary floor or roof area

P_w = Weight of wall tributary to section under consideration

f_m = Ultimate compressive masonry stress and shall not exceed 6000 psi

A_g = Gross area of wall = bt

Maximum and Minimum Reinforcement

The maximum reinforcement shall not exceed the following ratio, p_g , of reinforcement area of the gross masonry area; $p_g = A_s / bt$

f_y	p_g
40,000 psi	0.0060
60,000 psi	0.0040

Although the steel ratio p_g is based on gross cross-sectional area it applied only to steel assumed to resist tension forces. Therefore if steel is used on each face, consider only the amount of steel on one face as being limited to the p_g ratio.

The minimum reinforcement shall not be less than the sum of steel area in both directions of 0.002 bt with the minimum steel area in either direction of 0.0007 bt.

Moment and Deflection Calculations

Generally, the moment and deflection calculations shown herein are based on simple support conditions at top and bottom, however, for other support, fixity and continuity conditions, the moments and deflections may be calculated using principles of mechanics.

Strength Design

Load Factors. The strength of the cross-section shall not be less than that required from the application of factored loads. The factored loads are based on $U = 1.4D + 1.7L$ or
 $U = 0.75 (1.4D + 1.7L + 1.87E)$ or
 $U = 0.75 (1.4D + 1.7L + 1.7W)$ or
 $U = 0.9D + 1.43E$ or
 $U = 0.9D + 1.3W$

where

- D = Dead loads or related internal moment and forces
- E = Load effects of earthquakes or related internal moments and forces
- L = Live loads or related internal moments and forces
- U = Required strength to resist factored loads or related internal moments and forces
- W = Wind load or related internal moments and forces

Required Moment and Load Capacity. The minimum required moment and axial load is generally determined at the mid-height of the wall as being the location of the most critical values and is used for design.

The required minimum moment strength, M_u , is computed as follows:

$$M_u = \frac{w_u h^2}{8} + P_{ou} \left(\frac{e}{2} \right) + (P_{wu} + P_{ou}) \Delta_u$$

Design Strength of Cross-Section of Wall

The design strength, ϕM_n , provided by the reinforced masonry wall cross-section in terms of axial force and moment is computed as the nominal moment strength, M_n , multiplied by strength reduction factor, ϕ , i.e. $M_u < \phi M_n$

where

- M_u = Minimum required moment capacity
- M_n = Nominal moment strength for cross-section
subjected to combined flexural and axial loads
- ϕ = 0.8 for construction with special inspection
- ϕ = 0.5 for construction without special inspection

Deflection Design

The mid-height deflection, Δ_s , under service lateral and vertical loads (without load factors) must not exceed

$$\Delta_s = 0.01h \quad (\text{SEAOSC - ACI-SC recommendation})$$

$$\Delta_s = 0.007h \quad (\text{ICBO Technical Report No. 4189})$$

The deflection, Δ_s , at mid-height is computed as follows:

Deflection when the service moment does not exceed the cracking moment:

$$M_s < M_{cr} \qquad \Delta_s = \frac{5 M_s h^2}{48 E_m I_g}$$

Deflection when the service moment exceeds the cracking moment, i.e.

$$M_{cr} < M_s < M_n \qquad \Delta_s = \frac{5 M_{cr} h^2}{48 E_m I_g} + \frac{5 (M_s - M_{cr}) h^2}{48 E_m I_{cr}}$$

where

- h = Height of wall between supports, simple supports
- M_s = Service moment at the mid-height of the wall
including $P\Delta$ effects
- E_m = Modulus of elasticity of masonry = 1000 f'_m ;
3,000,000 psi maximum
- I_g = Gross moment of inertia of cross-section, usually

$$I_g = \frac{bt^3}{12}$$

I_{cr} = Cracked moment of inertia of cross-section

$$I_{cr} = nA_{se} (d - c)^2 + \frac{bc^3}{3}$$

M_{cr} = Cracking moment strength of the masonry wall

M_n = Nominal moment strength of the masonry wall

The cracking moment strength of the wall is $M_{cr} = S_m f_r$

where

S_m = Section modulus of gross cross-section $S_m = \frac{bt^2}{6}$
 f_r = Modulus of rupture of the masonry wall

Values for f_r for determining deflection are:

2.5 $\sqrt{f'_m}$ for hollow brick and concrete block masonry

2.0 $\sqrt{f'_m}$ for two-wythe brick masonry

Design of a Tall Slender Wall —

1. CONCRETE MASONRY WALL ; SOLID CROUTED;
SEISMIC ZONE II NO SPECIAL INSPECTION
REQUIRED.
A 6" CMU WALL IS 18' BETWEEN POINTS OF
LATERAL SUPPORT OF THE ROOF LEDGER AND THE
FLOOR.

WT OF WALL = 58 PSF ; WIND LOAD = 15 PSF
 $f'_m = 1,500$ PSI ; $f_y = 60,000$ PSI ;
NO SPECIAL INSPECTION REQUIRED $\phi = 0.9$;
ROOF LOAD $P_0 = 400$ PIF ON A 4' x 12' LEDGER
PARAPET : 2.5'

DETERMINE THE SIZE & SPACING OF VERTICAL
REINFORCING , $d = \frac{t}{2}$

SOLUTION : PD METHOD

1. LOADS

- a. WEIGHT OF WALL = 58 PSF
WEIGHT AT MID-HEIGHT
 $P_w = 58 \left(2.5 + \frac{18}{2} \right) = 667$ PIF
ROOF LOAD = $P_0 = 400$ PIF

CHECK AXIAL LOAD LIMITATION
 $\frac{P_u}{A_g} = \frac{P_w + P_0}{12 \times 563} = 15.8$ PSI
 $0.04 f'_m = 2.4 \times 1500 = 60$ PSI
15.8 PSI < 60 PSI

- b. LATERAL LOAD
SEISMIC LOAD = $F_p = Z I C_p W$
FOR SEISMIC ZONE II ; $Z = 1.00$
 $F_p = 1 \times 1 \times 0.3 \times 58$
 $= 17.4$ PSF ← GOVERNS
WIND LOAD = 15 PSF

c. FACTORED LOADS

ULTIMATE LOAD = $0.9D + 1.43E$

FACTORED WALL LOAD
 $P_{wu} = 0.9 \times 667 = 600$ PIF
FACTORED ROOF LOAD
 $P_{ou} = 0.9 \times 400 = 360$ PIF
FACTORED VERTICAL LOADS
 $P_u = P_{ou} + P_{wu}$
 $= 360 + 600 = 960$ PIF

FACTORED SEISMIC LOAD
 $W_u = 1.43 \times 17.4 = 24.9$ PSF

2. ASSUME VERTICAL STEEL REINFORCING
= 6 BARS @ 24" O.C.

$A_s = 0.44 \times \frac{12}{24} = 0.22$ sq. in./ft.

a. GROSS STEEL RATIO

$$\frac{A_s}{bt} = \rho_g = \frac{0.22}{12 \times 563} = 0.0033 \approx 0.0032 \text{ MAX.}$$

b. STRUCTURAL STEEL RATIO

$$\frac{A_s}{bt/2} = \rho = \frac{0.22}{12 \times 281} = 0.0066$$

3. a. MODULUS OF ELASTICITY E_m

$$E_m = 1000 f'_m = 1000 \times 1500 = 1,500,000 \text{ PSI}$$

b. MODULAR RATIO n

$$n = \frac{E_s}{E_m} = \frac{29,000,000}{1,500,000} = 19.33$$

c. MODULUS OF RUPTURE f_r

$$f_r = 2.5 \sqrt{f'_m} = 2.5 \sqrt{1500} = 96.8 \text{ PSI}$$

d. GROSS MOMENT OF INERTIA I_g

$$I_g = \frac{bt^3}{12} = \frac{12 \times 563^3}{12} = 178.5 \text{ in}^4$$

4. MOMENT AT CRACKING M_{cr}

$$M_{cr} = \frac{2 I_g f_r}{t} = \frac{2 \times 178.5 \times 96.8}{563} = 6.138 \text{ in. lbs}$$

5. a. CRACKED MOMENT OF INERTIA

$$I_{cr} = n A_{se} (d - c)^2 + \frac{1}{3} bc^3$$

$$A_{se} = \frac{P_u + A_s f_y}{f_y} = \frac{960 + 0.22 \times 60000}{60000} = 0.236$$

b. DEPTH OF RECTANGULAR STRESS BLOCK a

$$a = \frac{P_u + A_s f_y}{0.85 f'_m b} = \frac{960 + 0.22 \times 60,000}{0.85 \times 1500 \times 12} = 0.926''$$

c. DISTANCE TO NEUTRAL AXIS c

$$c = \frac{a}{\beta_1} = \frac{0.926}{0.85} = 1.089''$$

Design of a Tall Slender Wall — Cont.

A. CRACKED MOMENT OF INERTIA

$$I_{cr} = n A_{sc} (d - c)^2 + \frac{bc^3}{3}$$

$$= 19.3 \times 0.236 (2.02 - 1.089)^2 + \frac{12 \times 1.089^3}{3}$$

$$= 13.65 + 5.17$$

$$= 18.82 \text{ in}^4$$

G. ECCENTRICITY OF LEDGER ROOF LOAD

USE 4" x 12" LEDGER; ACTUAL THICKNESS = 3.5

$$e = 3.5 + \frac{t}{2}$$

$$= 3.5 + \frac{3.62}{2} = 6.32"$$

I. CALCULATE MID-HEIGHT MOMENT AND LATERAL

DEFLECTION DUE TO SERVICE LOADS BY ITERATION METHOD

a. FIRST ITERATION ; ASSUME $\Delta_s = 0"$

$$M_{u1} = \frac{wL^2}{8} + P_o \left(\frac{e}{2} \right) + (P_o + P_w) \Delta_s$$

$$= \frac{17.4 \times 18^2 \times 12}{8} + 400 \left(\frac{6.32}{2} \right) + (400 + 667) \times 0$$

$$= 8,456.4 + 1,264 + 0$$

$$= 9,720 \text{ in. lbs.}$$

$$\Delta_{s1} = \frac{5 M_{cr} h^2}{48 E_m I_g} + \frac{5 (M_u - M_{cr}) h^2}{48 E_m I_{cr}}$$

$$= \frac{5 \times 6138 \times (18 \times 12)^2}{48 \times 1,500,000 \times 178.5} + \frac{5 (9720 - 6138) (18 \times 12)^2}{48 \times 1,500,000 \times 18.82}$$

$$= 0.11 + 0.62 = 0.73"$$

b. SECOND ITERATION ; $\Delta_s = 0.729"$

$$M_{u2} = 8,456 + 1,264 + (400 + 667) \times 0.729$$

$$= 10,498 \text{ in. lbs.}$$

$$\Delta_{s2} = 0.11 + \frac{5 (10498 - 6138) (18 \times 12)^2}{48 \times 1,500,000 \times 18.82}$$

$$= 0.11 + 0.73 = 0.84"$$

$$\text{CHECK CONVERGENCE : } \frac{M_{u2} - M_{u1}}{M_{u2}} = \frac{10498 - 9720}{10498}$$

$$= 7.4\% > 5\% \text{ ALLOWABLE } \therefore \text{N.G.}$$

c. THIRD ITERATION ; $\Delta_s = 0.865"$

$$M_{u3} = 8,456 + 1,264 + (1067) \times 0.865$$

$$= 10,640 \text{ in. lbs.}$$

$$\Delta_{s3} = 0.11 + \frac{5 (10640 - 6138) (18 \times 12)^2}{48 \times 1,500,000 \times 18.82}$$

$$= 0.11 + 0.77 = 0.88"$$

d. CONVERGENCE

$$\frac{M_{u3} - M_{u2}}{M_{u3}} = \frac{10640 - 10498}{10640} = 0.0133$$

$$= 1.33\% \text{ WITHIN } 5\% \text{ O.K.}$$

B. CHECK LATERAL DEFLECTION ALLOWANCE

AT SERVICE LOAD.

$$\text{ALLOWABLE } \Delta_s = 0.007 h$$

$$= 0.007 \times 18 \times 12 = 1.51"$$

$$\text{ACTUAL } \Delta_s = 0.88 < 1.51" \text{ O.K.}$$

$$\text{OR } \frac{h}{\Delta_s} = \frac{18 \times 12}{0.88} = 245 > 143 \text{ O.K.}$$

THE SERVICE LOAD DEFLECTION OF 0.88" IS LESS

THAN THE MAXIMUM ALLOWABLE DEFLECTION,

1.51" ; THEREFORE THE DEFLECTION CRITERIA

IS SATISFIED.

J. STRENGTH CALCULATIONS

CALCULATE MID-HEIGHT MOMENT UNDER FACTORED LOADS.

$$M_u = \frac{w_u L^2}{8} + P_{ou} \left(\frac{e}{2} \right) + (P_{ou} + P_{wu}) \Delta_u$$

a. FIRST ITERATION ; ASSUME $\Delta_u = 0"$

$$M_{u1} = \frac{24.9 \times 18^2 \times 12}{8} + 360 \left(\frac{6.32}{2} \right) + (360 + 600) \times 0$$

$$= 12,100 + 1,138 + 0$$

$$= 13,238 \text{ in. lbs.}$$

$$\Delta_{u1} = \frac{5 M_{cr} h^2}{48 E_m I_g} + \frac{5 (M_u - M_{cr}) h^2}{48 E_m I_{cr}}$$

$$= \frac{5 \times 6138 (18 \times 12)^2}{48 \times 1,500,000 \times 178.5} + \frac{5 (13,238 - 6138) (18 \times 12)^2}{48 \times 1,500,000 \times 18.82}$$

$$= 0.11 + 1.22 = 1.33"$$

b. SECOND ITERATION ; $\Delta_u = 1.33"$

$$M_{u2} = 12,100 + 1,138 + 960 (1.33)$$

$$= 14,515 \text{ in. lbs.}$$

$$\Delta_{u2} = 0.11 + \frac{5 (14,515 - 6138) (18 \times 12)^2}{48 \times 1,500,000 \times 18.82}$$

$$= 0.11 + 1.44$$

$$= 1.55"$$

c. THIRD ITERATION ; $\Delta_u = 1.55"$

$$M_{u3} = 12,100 + 1,138 + 960 (1.55)$$

$$= 14,726 \text{ in. lbs.}$$

d. CONVERGENCE

$$\frac{\Delta_{u3} - \Delta_{u2}}{\Delta_{u3}} = \frac{1.59 - 1.55}{1.59}$$

$$= 0.025 = 2.5\%$$

SATISFACTORY ; LESS THAN 5%

K. DETERMINE NOMINAL STRENGTH OF WALL, M_n

$$M_n = A_{sc} f_y \left(d - \frac{a}{2} \right)$$

$$= 0.236 \times 60,000 \left(2.02 - \frac{0.926}{2} \right)$$

$$= 33,375 \text{ in. lbs.}$$

$$\phi M_n = 0.5 \times 33,375$$

$$= 16,687 \text{ in. lbs.}$$

$$\phi M_n > M_u$$

$$16,687 > 14,726 \text{ O.K.}$$

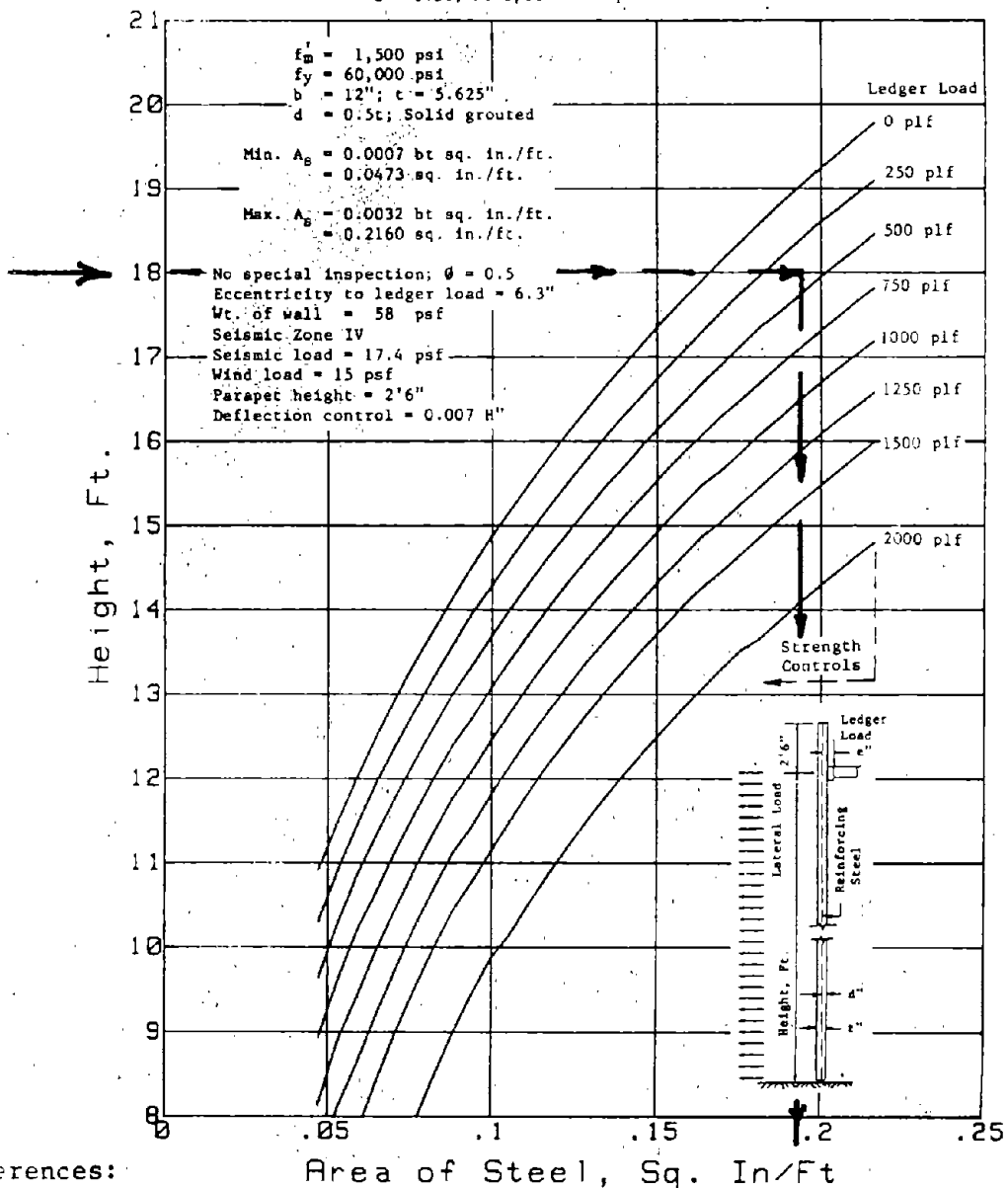
THE CAPACITY OF THE SECTION, $\phi M_n = 16,687 \text{ in. lbs.}$

IS GREATER THAN THE ULTIMATE MOMENT, $M_u = 14,726 \text{ in. lbs.}$

THEREFORE SECTION IS ADEQUATE FOR STRENGTH

6" CONCRETE MASONRY UNITS; $f_m = 1,500$ psi

$d = 0.5t$; No Special Inspection



References:

1. 1985 edition Uniform Building Code, International Conference of Building Officials, Whittier, Calif.
2. SEAOSC-ACI/SC Task Committee on Slender Walls, Los Angeles, Calif. Test Report on Slender Walls
3. Amrhein & Lee, 1984, Design of Reinforced Masonry Tall Slender Walls Western States Clay Products Assoc., San Francisco, Calif.
4. Amrhein, 1984, Reinforced Masonry Engineering Handbook, 4th edition Masonry Institute of America, Los Angeles, Calif.
5. Amrhein & Lee, 1985, Tall Slender Masonry Walls - Estimating Curves Masonry Institute of America, Los Angeles, Calif.

THE DYNAMIC PROPERTIES AND ASEISMIC DESIGN OF
JINLING HOTEL AND SHANGHAI GUEST HOTEL

YU Andong* JIN Ruichun** SHI Yuan*

SUMMARY

In the original dynamic analysis of Jinling Hotel the calculated natural periods are wrong. The result based on experimental formulas, simplified formula and FEM program SAP V are all in agreement with that obtained from surveying.

It is shown by the surveying and results of SAP V that the original dynamic design of Shanghai Guest Hotel is reasonable and reliable. The dynamic characteristics measured from the actual structure is close to the value adopted in the design.

The choosing of parameters in dynamic design and simplified method is discussed.

INTRODUCTION

Jinling Hotel and Shanghai Guest Hotel are the highest hotels in Nanjing and Shanghai, respectively. The structural system of Jinling Hotel is frame-tube of 109.85m high (Fig.1). Shanghai Guest Hotel is frame-shear wall structure and 88m in height (Fig.2).

Jinling Hotel was designed by the Palmer and Turner Architects and Engineers, Hongkong. In its aseismic design, intensity 7 was taken into account. Shanghai Guest Hotel was designed by the Shanghai Civil Building Design Institute. The authors, as staff of Tongji University, were involved in the aseismic design. Considering the safety problem

*. Institute of Structure Theory Tongji University
Shanghai, China

**.. Computer Centro Tongji University Shanghai, China

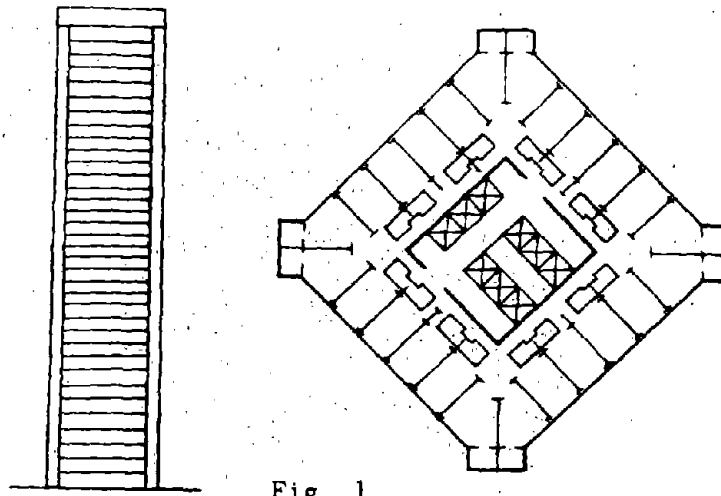


Fig. 1

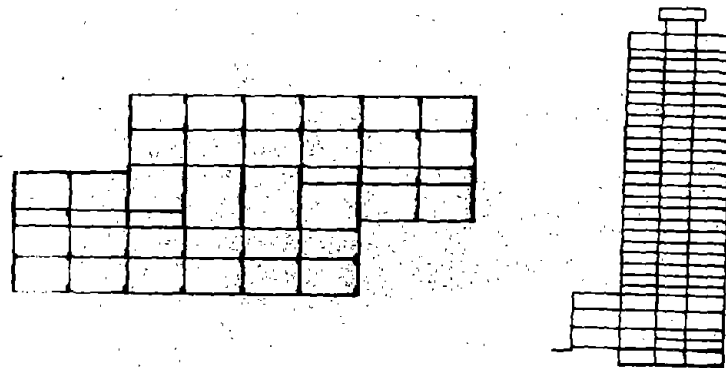


Fig. 2

of this important building, intensity 7 was also taken into account.

After these two buildings had been constructed, surveyings with surrounding excitation was carried out by the Institute of Structural Theory of Tongji University in 1983. The 1st - 4th natural modes, periods and corresponding damping ratios are obtained in the surveyings.

In this paper, the results of surveying and aseismic design of both tall buildings are compared. The aseismic design of those buildings are evaluated, then the method for choosing the dynamic properties in aseismic design is discussed.

DISCUSSION ON THE ASEISMIC DESIGN OF JINLING HOTEL

According to the document on the static and dynamic analyses of Jinling Hotel provided by Palmer and Turner, beside the dynamic analysis, the static analysis is in accordance with Chinese, New Zealand and SEACO (California) Codes. But there are some problems in the design. It seems rather surprising that the natural period of this tall building is 7.877 sec. as a result of dynamic analysis. It is unusual and disagrees with the result of static analysis.

1. The Aseismic Design of Palmer and Turner Architects and Engineers

(1) Dynamic Analysis:

Response spectrum analysis was carried out using spectrums in El-centro earthquake (18.5.1940/NS) and Osaka earthquake (27.3.1963/EW). The peak value of ground acceleration was assumed to be 50 cm/sec² and damping factor of 10% was used. For design purposes, if the ground acceleration increases, the results should increase linearly. Masses computed from the structural dead load plus $\frac{1}{2}$ superimposed load were lumped at each floor level. The computed fundamental periods are as shown in Table 1.

Table 1

Mode	1	2	3	4	5
Natural frequency	0.7966	2.787	5.779	9.405	13.76
Period	7.887	2.255	1.087	0.668	0.456

It is obvious that the designers regarded the natural frequency as cyclic frequency (cycles/sec), so that

$$T_1 = \frac{2\pi}{\omega} = \frac{6.282}{0.7966} = 7.887$$

This result is in contradiction with experience of tall buildings of 30 ~ 40 stories. For example, the fundamental periods of Baiyun Guest Hotel in Guangzhou (33 stories) are $T_1 = 1.440$, $T_2 = 0.350$ in lateral direction and $T_1 = 0.835$, $T_2 = 0.273$ in longitudinal. In "Earthquake Engineering" by L. Wiegel, a 41-storied tall building, as discussed by M. Newmark, has the period $T_1 = 2.3$.

The designers of Jinling Hotel themselves also admitted "the calculated fundamental period of the tower is high". In January 1984, one month after the dynamic analysis, they used the Rayleigh's method to calculate the fundamental period and obtain $T_1 = 3.5$.

(2) Static Analysis

In the static analysis, Chinese Code (TJ11-78), New Zealand Code (NZSS1900, 1965) and California Code (SEACO, 1966) were used. The results are as shown in Table 2.

Table 2

Code	Formula	T_1 (sec)	Q_0	Q_0 for design
TJ11-78	$T = 0.45 + 0.0011H^2/D$	0.87	0.0322W	0.04W
NZSS1900, 1965	$T_1 = 0.32 \sqrt{D}$	0.91	0.05W	0.04W
SEACO, 1966	$T = 0.05 h n / \sqrt{D}$	1.77	0.041W	0.04W

They adopted $Q_0 = 0.04W$ to determine the maximum lateral force at the base. Then in the "Tower Block Seismic Analysis", this datum was also applied in frame and shear wall design.

2. Surveying:

The results of surveying with surrounding excitation in March, 1983 are summarized in Tables 3 and 4, which were recorded by RTP-500B and processed by 7T08S.

Table 3 Natural frequency and period

Mode		1	2	3	4
N-S	f	0.6832	2.5864	5.2704	7.1248
	T	1.464	0.387	0.189	0.140
E-W	f	0.6832	2.5376	5.1240	
	T	1.464	0.394	0.195	
Rotation	f	1.1712	3.5624		
	T	0.854	0.281		

Table 4 Damping ratio (%)

Mode	1	2	3	4
Flexure	5.85	2.88	1.79	1.43
Rotation	2.08	1.37		

The transfer function and mode are as shown in Figs 3 and 4.

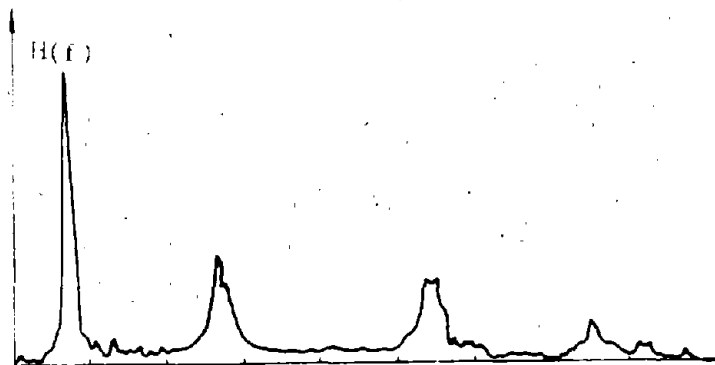


Fig. 3

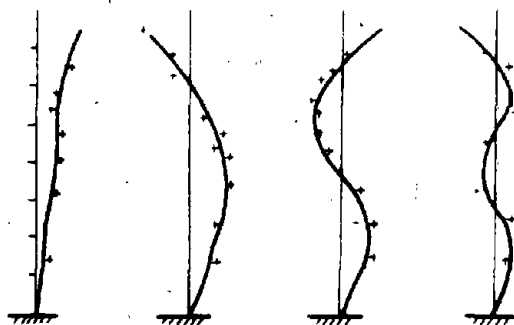


Fig. 4

3. Discussion

(1) Experiential formula

Based on surveyings, a lot of experiential formulas for determining the natural period of tall building exist. Usually, the results from these formulas are shorter than the actual period. Many data acquired in San Fernando Earthquake show that the period of buildings increased 1.1~2.0 time during the Seism and 1.0~1.4 time after the Seism.

By choosing ten experiential formulas applicable to Jinling Hotel, the results are as shown in Table 5.

Note	Formula	T ₁
1 Los Angelos	0.108 H/√B	2.114
2 Los Angelos	0.09 H/√B	1.76
3 California 1974	0.05 H/√B	0.978
4 Romania	0.075 N	2.775
5 Beijing	0.01156 H	1.2698
6 Shanghai	0.47+0.166 H/√B	1.047
7 Japan	0.07 H/√B	1.37
8 China	0.054 N	1.998
9 China	0.042 N	1.554
10 China(for chimney)	0.45+0.0011 H ² /D	0.87
	mean value	1.573

(2) Simplified formula

The simplified formula for determining the natural period of flexural vibration of cantilever beam is

$$T_1 = 1.78 H^2 \sqrt{\frac{q}{gEI}}$$

where: H: height of the building;
g: weight per unit height;
E: Young's modulus of concrete;
I: inertial momentum

The stiffness of tubes at four corners is only taken into account in the column 1 of table 6.

W	1	2
DL + $\frac{1}{3}$ LL	1.470	1.976
DL + $\frac{1}{2}$ LL	1.508	2.016

Result T₁ = 1.47 is reasonable.

(3) SAPV

The computer program SAP V is used to check the above results

obtained experiential formulas and simplified formula. $DL + \frac{1}{3} LL$ is used and the corner tube is taken into account. Major computed results are shown in Table 7.

Table 7

Mode	1	2	3	4	5
Frequency (HZ)	0.6965	4.378	12.34	24.30	40.18
Period (sec)	1.436	0.228	0.081	0.041	0.025

(4) comparison

If we regard the natural frequency as f in the dynamic analysis of the building, then we have Table 8.

Table 8

Mode		1	2	3	4	5
Design	f	0.7966	2.787	5.779	9.405	13.76
(Modified)	T	1.2553	0.3588	0.1730	0.1063	0.076
Surveying	f	0.6832	2.5864	5.2704	7.1248	
	T	1.464	0.3876	0.189	0.140	
SAP V	f	0.6965	4.378	12.34	24.30	40.18
	T	1.436	0.228	0.081	0.041	0.023
Experiential formula	f	0.6357				
	T	1.573				
Simplified formula	f	0.6803				
	T	1.470				

All the five values of T_1 are close to each other. The results of mode 2 ~ mode 5 from SAP V are not so good because the model is over-simplified.

It may be concluded that $T_1 = 7.887$ is wrong, but the aseismic character of Jinling Hotel is still reliable, since

- (i) The structural detail of Jinling Hotel designed by Palmer and Turner is only based on their static analysis.
- (ii) $Q_0 = 0.04 W$ leads to $T_1 = 0.87$, so a larger earthquake loading is adopted. In the design spectrum, Q_0 is constant at $T_1 = 1.47$ and less than $0.04 W$.

- (iii) The damping ratio in surveying is 7% and it is 10% in design. It has no problem because the damping ratio will increase in the nonlinear range.

DISCUSSION ON THE ASEISMIC DESIGN OF SHANGHAI GUEST HOTEL

1. Aseismic Design

A member-story model analysis on the dynamic responses of tall buildings subjected to earthquake excitation was presented by the authors and their collaborators. There the authors have also derived: (i) the inelastic and geometrically nonlinear stiffness matrix of a member with two rigid zones at its ends, using one-component model of a member and considering axial, shear and bending deformations; (ii) the spatial stiffness matrix with three degrees of freedom for every floor corresponding to two components of displacements and one of rotation considering the interaction of shear walls and frames; and (iii) the concept of transition stiffness pertaining to the turning points of hysteresis loops. According to the model mentioned above, a program MS was developed and applied in the design.

When the dimensions of structural stiffness are only one dimension, then:

$$\begin{bmatrix} MO \\ OJ \end{bmatrix} \begin{Bmatrix} \ddot{U} \\ \ddot{\theta} \end{Bmatrix} + \begin{bmatrix} C_{xx} & C_{x\theta} \\ C_{\theta x} & C_{\theta\theta} \end{bmatrix} \begin{Bmatrix} \dot{U} \\ \dot{\theta} \end{Bmatrix} + \begin{bmatrix} W_{xx} & W_{x\theta} \\ W_{\theta x} & W_{\theta\theta} \end{bmatrix} \begin{Bmatrix} U \\ \theta \end{Bmatrix} = - \begin{bmatrix} MO \\ OJ \end{bmatrix} \begin{Bmatrix} \ddot{U}_\theta \\ 0 \end{Bmatrix}$$

where:

$$W_{xx} = \sum_{\alpha} K_{\alpha} \cos^2 \phi$$

$$W_{x\theta} = \sum_{\alpha} K_{\alpha} \cos \phi_{\alpha} (\gamma_{x\alpha} \sin \phi_{\alpha} - \gamma_{y\alpha} \cos \phi_{\alpha}) = W_{\theta x}$$

$$W_{\theta\theta} = \sum_{\alpha} K_{\alpha} (\gamma_{x\alpha} \sin \phi_{\alpha} - \gamma_{y\alpha} \cos \phi_{\alpha})^2$$

in which: K_{α} is the lateral stiffness matrix of α th lateral load resisting element and is formed by stiffness matrix of a single member, K_{GM} . The stiffness matrix of single member with rigid

arms at it's ends is derived and the matrix considers both the elastoplastic and $P-\Delta$ effects. As every member of the tall building is very large, so it is rather difficult to deal with the turning points of hysteresis loops synchronously. Those points transiting from elastic state to plastic state must be made much account and treated by the concept of transition stiffness.

By using the MS system programs, the dynamic analysis of Shanghai Guest Hotel was made by authors and collaborators. In the analysis the four earthquake waves were imported, and they are El-Centro, 1940 NS; Taft 1952, EW; Tianjin, 1976 and Haichen, 1975, while the maximum ground acceleration was taken to be 100 gal. The displacement history curves (at the top of building) of the elastic dynamic response are shown in Fig.5.

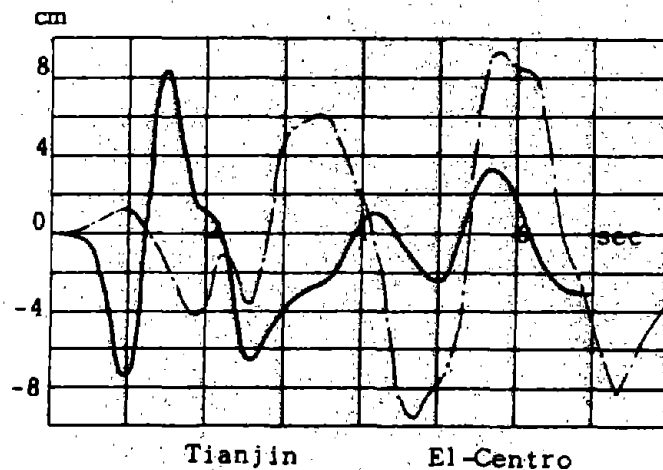


Fig. 5

The elastoplastic dynamic analysis was also made for another project of this building and it results in the displacement history curves in Fig.6.

The program with member-story model may offer a series of "data for story" as the maximum interstory drift δ_{max} , maximum absolute acceleration $(\ddot{U} + \ddot{U}_e)_{max}$ etc. Herein the "maximum" means the maximum value during the whole range of the time history. Some examples are shown in Fig.7 and Table 9.

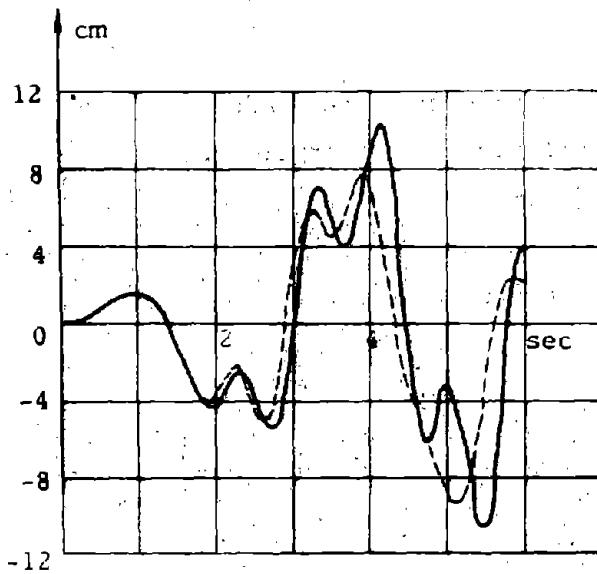


Fig. 6

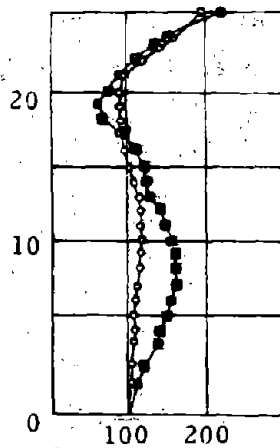


Fig. 7a ($\bar{U} + \bar{U}_e$)

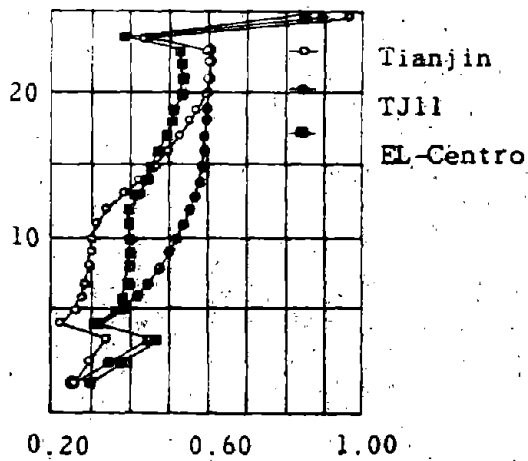


Fig. 7b δ_{max}

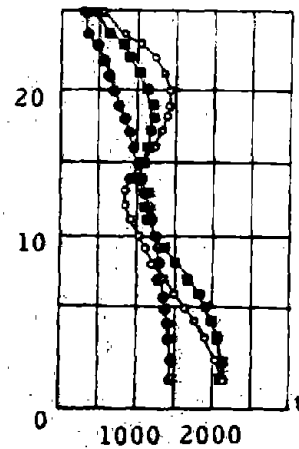


Fig. 7c Q

Table 9

input	TJ11-78	Tianjin	El-Centro
U_{max}	13.08	8.37	9.58
δ_{max}	0.965	0.962	0.851
$(\bar{U} + \bar{U}_e)_{max}$		202	167

The member-story model can supply the "data for member" too. Some moments and shear forces in coupled walls and coupling beams are obtained and can serve for the design purpose directly. Few examples

are shown in Fig.8. In the design of Shanghai Guest Hotel, those data have been used.

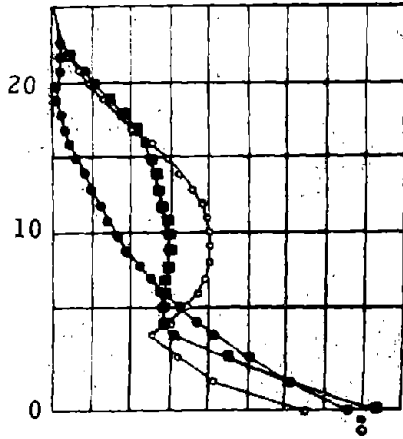


Fig. 8a M_w

$\times 10^3 t-m$

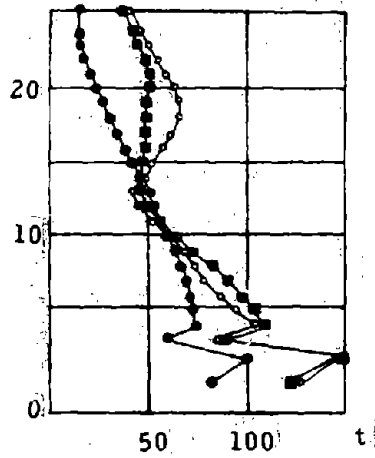


Fig. 8b Q_L

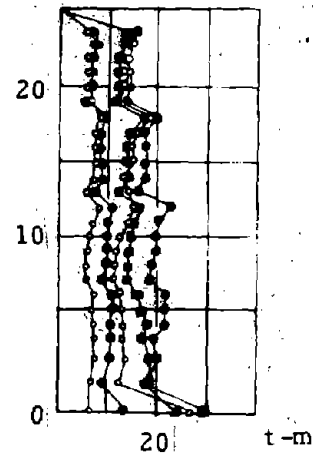


Fig. 8c M_C

2. Surveying

The results of surveying with surrounding excitation, May, 1983 are shown in Tables 10 and 11.

Table 10 Natural frequency and period

Mode		1	2	3
N-S	f	0.684	3.333	
	T	1.46	0.30	
E-W	f	0.926	3.704	6.667
	T	1.08	0.27	0.15
Rotation	f	1.176	4.348	
	T	0.85	0.23	

Table 11 Damping ratio (%)

Mode	1	2	3	4
Flexure	5.85	2.88	1.79	1.43
Rotation	2.08	1.37		

3. Analysis

SAP V is used to analyse the structural system of Shanghai Hotel. The fundamental natural periods (NS) are shown in Table 12.

Table 12

SAP V		1	2	3	4	5
S-N	f	0.7526	4.067	11.06	21.58	36.18
	T	1.329	0.2459	0.0904	0.0463	0.0276

$T_1 = 1.329$ is close to $T_1 = 1.46$ obtained from surveying.

Although $T_1 = 1.329$ is smaller than $T_1 = 2.0$ which is used in the design, it seems reasonable. The non-linear behavior of the structural system during earthquake is considered, E is reduced by a coefficient. However, E is not reduced for SAP V. The results can compare with data of surveying. It may be noticed from these two examples that in design T_1 can be taken as 1.4 times of the value obtained from surveying or the linear elastic analysis.

The comparison between the two response histories obtained

from two programmes in which El-Centro earthquake wave as input. It is as shown in Fig.9.

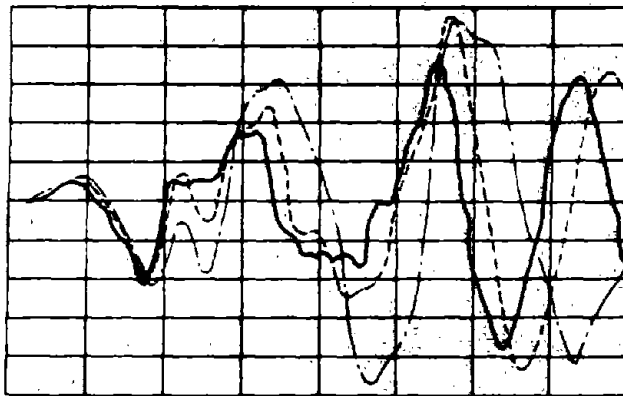


Fig. 9

It can be noticed that (i) E was reduced when SAP V was used and $T = 1.89$, it was close to the value obtained from MS program; (ii) The response histories between two results had some difference partly, because the different structural model had been used. The storey model had a larger error at the range where the influence of higher vibration mode was stronger. But (iii) the maximum value of displacement and its instant were close to each other.

PARAMETERS IN ASEISMIC DESIGN

This analysis has also confirmed that the simplified computing method for the natural periods is applicable, provided the rigidity of the structure is properly chosen. When the system is in its elastic stage, e.g. in surveying a smaller load (e.g. $\frac{1}{3}L$) and nonreduced Young's modulus should be adopted, while in aseismic design it should be on the contrary.

The damping ratio reduces when ω increases. The Reilaght form of damping, which is often used in the dynamic analysis of structures, is

$$[C] = a [M] + [K]$$

From the definition of the damping ratio,

$$\xi_i = \frac{(\phi_i)^T (C) (\phi_i)}{2 \omega_i M_i}$$

where ω_i and ϕ_i are circular frequency and mode of vibration.

$$M_i = (\phi_i)^T (M) (\phi_i)$$

Hence,

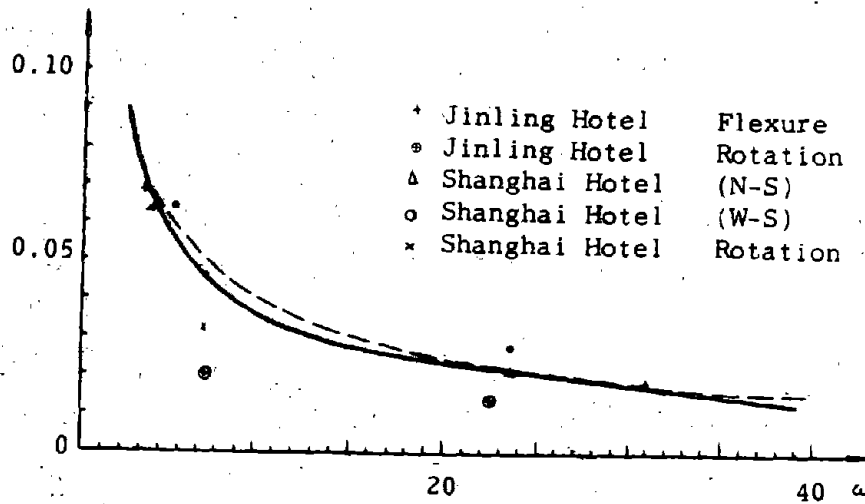
$$\xi_i = \frac{1}{2} \left(\frac{a}{\omega_i} + b \omega_i \right)$$

The relation of ξ to ω given in [7] is as shown in Fig. 10, so the following experimental formula is suggested:

$$\xi = 0.25/\omega + 0.0005\omega, \quad a = 0.50, \quad b = 0.0009.$$

Therefore, if b is small, then the effect of $[K]$ is negligible, that is,

$$[C] = a[M]$$



In fact, ξ increases when $[K]$ decreases. A test on a single frame [9] obtains the results shown in Table 13.

Table 13

Specimen	Before Loading	Cracking	Yielding
K 2-1	0,027	0,034	0,055
K 3-1	0.016	0,043	0,061

Although the data in Table 13 are limited, the tendency suggests

that b should not be taken as a constant and it should be a decreasing coefficient with an increasing $[K]$ when it is not negligible.

Both the detailed analysis and simplified calculation are worthwhile to continue to study, since the comparison between these two can indicate the applicability of simplified methods. The surveying and analysis of dynamic characteristics also provide the valuable information for the reliability of the existing design as well as the guidance for the choosing of parameters in dynamic design.

ACKNOWLEDGEMENT

The authors are grateful to Gu Jayang, Zhuang Meizheng, Huan Yunqiao, Sun Yeyang, Jian Lusheng for their help and would like to thank prof. Zhu Bolong for his direction.

REFERENCES

- [1] M.F. Gierson: Two Nonlinear Beams with Definition of Ductility, ASCE Vol. 95 No. ST2 Feb. 1969
- [2] Palmer and Turner Architects and Engineers: Jinling Hotel, Static and Dynamic Analysis, Hongkong Job No. 1253, Dec. 1979, Jan. 1980
- [3] Sun Yeyang, Yu Andong, Jin Ruichun, Jiang Lusheng, The Use of a Combined Member-Story Model for Analysing Earthquake Responses of Tall Buildings, Journal of Tongji University, No. 1, 1980
- [4] Sun Yeyang, Yu Andong, Jin Ruichun, Jiang Lusheng, Earthquake Responses of Shanghai Guest Hotel by Use of the Combined Member-Story Model, Journal of Tongji University, No. 2, 1981
- [5] Sun Yeyang, Yu Andong, Jin Ruichun, Non-Linear Stiffness Matrix of Single Member Considering P- Δ Effect and Inelasticity, Shanghai Mechanics, No. 4, 1980
- [6] Yu Andong, Huan Yunqiao, Discussion on Aseismic Design of Jinling

Hotel, Construction Technique, Dec. 1983

- [7] Shi Yuan, Discussion on Structural Surveying Method under Wind Load, Tongji University Report 83269
- [8] Zhu Bolog, Yu Andong, A Nonlinear Full-Range Analysis of Reinforced Concrete Rigid Frames, Journal of Tongji University, No. 3, 1983
- [9] Yu Andong, Ma Yunfeng, Investigation of Restoring Behavior Reinforced Concrete Single Frame, Tongji University Report 80273

REVISION OF THE CHINESE ASEISMIC DESIGN CODE
— BRICK STRUCTURE SECTION

Gong Sili ¹

ABSTRACT

The design philosophy, computation and certain important earthquake resistant measures for brick structures proposed in the revision of the code which is being carried out are introduced in the paper. Owing to the fact that brick structure is the main type of structures in China at present, it plays an important role either in the current code or in its revised version. Performance of brick structures in the recent earthquakes for the past two decades provides a basis for the revision of the code, which is also briefly mentioned in the paper.

INTRODUCTION

The current Chinese aseismic code (TJ 11-78) is the revised version of the TJ 11-76 code and was put into effect in 1978, soon after the occurrence of the great Tangshan earthquake, therefore majority of experience gained from the earthquake has not yet been involved in the code. Multi-storey brick structures are widely adopted as residential buildings in China. Such buildings are 5-storey buildings generally with no reinforcement in the masonry. In the Tangshan earthquake, most of them were seriously damaged or even collapsed, causing heavy casualties. Thus it is very important to incorporate the experience of the Tangshan earthquake in the revised version of the aseismic code.

At present, there is a draft for the revision of the TJ 11-78 code. Here introduced are the design specification of brick structures in the draft and the main difference between the draft and the current code.

BASIC REQUIREMENT FOR EARTHQUAKE RESISTANCE

Requirement for buildings in the current aseismic code is: "when a building is subjected to an earthquake with an intensity corresponding to the design intensity, certain damage to the building will allowed and the building can still be serviceable without repairing or with minor repairing." This is the requirement for the design intensity only, no requirement is given for intensities higher or lower than the design

¹ Senior Research Engineer, Institute of Earthquake Engineering, China Academy of Building Research, Beijing, China.

intensity. Therefore, consideration is only taken for brick buildings subjected to an earthquake of design intensity in the current code, i.e. "cracks which can be repaired are allowable". While draft of the revised version states: "buildings will be intact in minor earthquakes and will not collapse in major earthquakes". Thus, three levels of earthquake resistance are proposed:

First Level. When subjected to earthquakes of intensity lower than the local basic intensity, buildings will have no damage and normal service requirements should be met.

Second Level. When subjected to earthquakes of intensity equal to the local basic intensity, certain extent of damage to buildings is allowed, but not causing danger to human life and equipment for production, and can still be serviceable without repairing or with minor repairing.

Third Level. When subjected to earthquakes of intensity higher than the local basic intensity which scarcely occur, collapse or serious damage to buildings which will affect safe of human life should be avoided, i.e. requirement for the safe of human life should be met.

Based on the statistic analysis of historic earthquakes occurred in more than 60 cities in China, there are some relationship between the above levels and basic intensities approximately.

Intensity, exceeding probability of which is about 10% within 50 years, corresponds to the basic intensity given in the current Chinese Seismic Intensity Zoning Map. Such intensity will be taken as the Second Level intensity.

Intensity, exceeding probability of which is about 62.3% (i.e. the expectancy of intensity) within 50 years and which is about $1\frac{1}{2}$ grade lower than the basic intensity will be taken as the First Level intensity, i.e. intensity of earthquakes often occurred.

Intensity, the exceeding probability of which is about 2% and which is about 1 grade higher than the basic intensity, will be taken as the Third Level intensity.

For brick structures, it is of significance to use ground motion acceleration corresponding to the First Level intensity in strength checking the cross section of the structure. Such checking will guarantee building structures, when subjected to earthquakes commonly occurred, to be in an elastic state and no repair or strengthening is required.

For Second and Third Level of earthquake resistance, no strength and deformation checking is stipulated in the draft. Under the action of an earthquake of higher level intensity, earthquake-resistance of brick structure is guaranteed mainly by aseismic measures.

CALCULATION OF SEISMIC ACTION

It is stipulated in the draft of the revised version that, for structures in different conditions, different methods of calculations for seismic action should be adopted, such as equivalent lateral force method, modal analysis, time history analysis, etc. for brick structures, equivalent lateral force method should be unanimously adopted, i.e.

Overall horizontal seismic action of structure:

$$F_a = \alpha_1 G_{eq}$$

Horizontal seismic action of lumped mass i

$$F_i = \frac{G_i H_i}{\sum_{r=1}^n G_r H_r} F_Q (1 - \delta_n) \quad (i = 1, 2, \dots, n)$$

for brick structure, $\alpha_1 = \alpha_{max}$.

Table 1

Intensity	7	8	9
max	0.09	0.18	0.36

where δ_n — additional seismic effect coefficient on the top (see Table 2)

Table 2

Type of site soil	δ_n
I	$0.08T_1 + 0.07$
II	$0.08T_1 + 0.01$
III - IV	$0.08T_1 - 0.02$

G_{eq} — equivalent total gravity load of the structure, G_{eq} is taken equal to $0.85G$.

G — effective total gravity load for producing the seismic effect, $G = \sum_{r=1}^n G_r$.

Design and Checking of Cross-Section

Following equation is adopted in the draft for calculating the

combination of seismic effect and other load effect..

$$S = \gamma_G C_G G_K + \gamma_{E1} C_{E1} E_{1K} + \gamma_{E2} C_{E2} E_{2K} + \sum_{i=1}^n \psi_{Ci} \gamma_{Qi} C_{Qi} \cdot Q_{ik}$$

where G_K — standard value for permanent load;
 E_{1K} — standard value for horizontal seismic action;
 E_{2K} — standard value for vertical seismic action;
 Q_{ik} — standard value for the i th variable load;
 ψ_{Ci} — a coefficient for the combination value for the i th variable load;
 $C_G, C_{E1}, C_{E2}, C_{ai}$ — effect coefficients.

Expression for Design and Checking of Cross-Section

$$S \leq R/\gamma_R$$

where R — resistance of member section;
 γ_R — aseismic regulated coefficient for resistance; for unreinforced aseismic wall, $\gamma_R = 2$; for aseismic wall with constructional column, $\gamma_R = 1.8$.

For the design of brick structure cross-section, the above formula is expressed as

$$Q \leq \frac{f_{tp} \cdot A}{\xi \gamma_R} \sqrt{1 + \frac{\sigma_c}{f_{tp}}}$$

where Q — design seismic shear force subjected by aseismic wall;
 ξ — inhomogeneous coefficient of shear stress in the cross-section;
 σ_c — average compressive stress;
 f_{tp} — principal tension stress of brick masonry.

For brick buildings, effect of vertical seismic load is not considered in the new revised code. No checking is need also for the earthquake resistance of foundation.

GENERAL REQUIREMENT OF THE ASEISMIC MEASURES FOR BRICK BUILDINGS

As mentioned before, brick structure is a kind of structure made by brittle material. It's deformability and energy absorbability are very small. Strength and earthquake-resistance of such structure in the elastic state can only be estimated through calculation when subjected

to minor earthquake. Once cracked, i.e. subjected to earthquake of basic intensity or higher than basic intensity, it is difficult to estimate the earthquake-resistance of brick structure through calculation.

Under the action of an earthquake of higher intensity, earthquake-resistance of brick structure can be guaranteed mainly by aseismic measures. In summary, these measures are principally:

- Adoption of regular configuration
- Adoption of appropriate aseismic structural layout; to use transversal wall or both of transversal and longitudinal wall as aseismic wall.
- Limitation of the space between aseismic walls
- Limitation of the overall height of building
- Strengthening the bonding and deformability of building materials, such as limitation of the minimum strength of mortar, addition of transversal and vertical reinforcements in the brick masonry.
- Strengthening integrity of brick structure, e.g. bricklaying in the connection of transversal and longitudinal wall must be overlapped, layout of spandrel beam at each storey and layout of R.C. constructional column in the connection of transversal and longitudinal wall.
- Prevention of local weakening, such as flue inside a building.
- Strengthening of associated members (parapet, canopy), strengthening of the anchorage of the cornice and the main structure.

These measures are developed based on the experience of strong earthquakes.

Limitation of the Overall Height of Building

For brick structures in seismic region, limitation of overall height of building is a key measure for earthquake-resistance, the purpose of which is to prevent buildings from serious damage or collapse. It is shown by the damage of the recent strong earthquakes in China that, for the unreinforced engineered brick structures (or unreinforced by constructional columns), three-storey buildings would not collapse in earthquakes of intensity IX, five-storey buildings would not collapse in earthquakes of intensity VIII; while in earthquakes of intensity VII, buildings with storeys more than five would not collapse generally.

Based on this concept and on account of safety appropriately, limitation of the height of brick buildings has been specified in the current aseismic design code, and such limitation will be relaxed, if the effect of constructional columns is considered.

Limitation of building height
in the current code

Table 3

Type of walls		Intensity		
		VII	VIII	IX
24cm and more than 24 cm solid wall	Without constructional columns	19m (6 storeys)	13m (4 storeys)	10m (3 storeys)
	With constructional columns	25m (8 storeys)	19m (6 storeys)	16m (5 storeys)

Limitation of the height of multi-storey brick buildings in the new revised code (draft)

Table 4

Type of walls		Intensity		
		VII	VIII	IX
24cm and more than 24 cm solid wall	Without constructional columns	12m (4 storeys)	9m (3 storeys)	6m (2 storeys)
	With constructional columns	21m (7 storeys)	18m (6 storeys)	12m (4 storeys)

From the above two tables, limitation of building height in the new revised code is more rigorous than that in the current code. This is because, in the new revised code, the fact that buildings would not collapse seriously when subjected to earthquakes of intensity higher than the local basic intensity will be taken into account, for example, in the region of basic intensity VIII, no. of storeys of brick buildings without constructional columns is limited to 3. If earthquake of intensity IX would occur, no collapse would have occurred to such buildings, based on the performance of recent major earthquakes.

R.C. CONSTRUCTIONAL COLUMN

It is specified in the current code that, at the connection of inner and outer wall of multi-storey brick buildings, R.C. constructional column should be erected, based on the experience of the Tangshan earthquake. During the earthquake, brick buildings without any reinforcement seriously collapsed, causing heavy casualties. But, in some accidental cases, no collapse occurred in brick buildings designed with R.C. columns, although damage was suffered, thus proving safety of human beings. This experience has been involved into current code (TJ 11-78), taking as a

provision.

Views on the above provision have been unified after the current code was effective for several years. But different views on the function of construction column specified in the code exist. Some considered such column as structural column, thus enlarging its cross-section to bear loads. Of course, it is not necessary.

Constructional column is not required in the code to suffer (axial) loads but considered as a kind of vertical constraint member of walls, such as spandrel beam which is a kind of constraint member in the horizontal plane. Both constraint members improve integrity of brick buildings.

Therefore, the main purpose of constructional column is to prevent collapsing after cracking of the resistant wall. Thus, no requirement for the design of cross-section and structural analysis of constructional column is specified in the current code and its revised version. Only the basic cross-section dimension and amount of reinforcement for constructional column are specified.

In the new revised version, it is proposed that the cross-section of constructional column may not be too large, and its amount of reinforcement may be too large also, based on the fact that its function is only to constrain the masonry. The min. cross-section of constructional column is restricted to 12 x 24 cm in the revised version while 18 x 24 cm is required in the current code. But 40% of longitudinal reinforcing bars is still specified for constructional column in the revised version, according to the requirement in construction.

Since no structural analysis is required for constructional column in the new revised code, so limitation of overall height of brick buildings is specified as in Table 4.

Strengthened with constructional columns, earthquake-resistance of brick building can be raised 10-15%, based on experimental study. This has not been reflected in the current code, but is considered in the new revised version.

MULTI-STOREY BRICK BUILDINGS WITH R.C. FRAME AND BRICK SHEAR
WALLS IN THE 1ST FLOOR (TYPE 1) AND FRAMED MULTI-STOREY
BRICK BUILDINGS WITHOUT OUTER R.C. COLUMNS (TYPE 2)

These structures are made of two kinds of materials, i.e. R.C. and bricks, and are unfavourable for earthquake conventionally. But owing to their requirement for special use, economics and convenience for construction, they are widely used both in cities and towns.

Type 1 brick building is a kind of structure with R.C. frame of larger span in the 1st floor for commercial use and brick shear walls as lateral resisting members. Above the 1st floor, common brick structure

is adopted. The R.C. part of Type 1 building is designed based on R.C. structure with brick shear walls while the other part is designed according to the requirement for multi-storey brick buildings. But the limitation of overall height of Type 1 building is more rigorous than that of common multi-storey brick buildings.

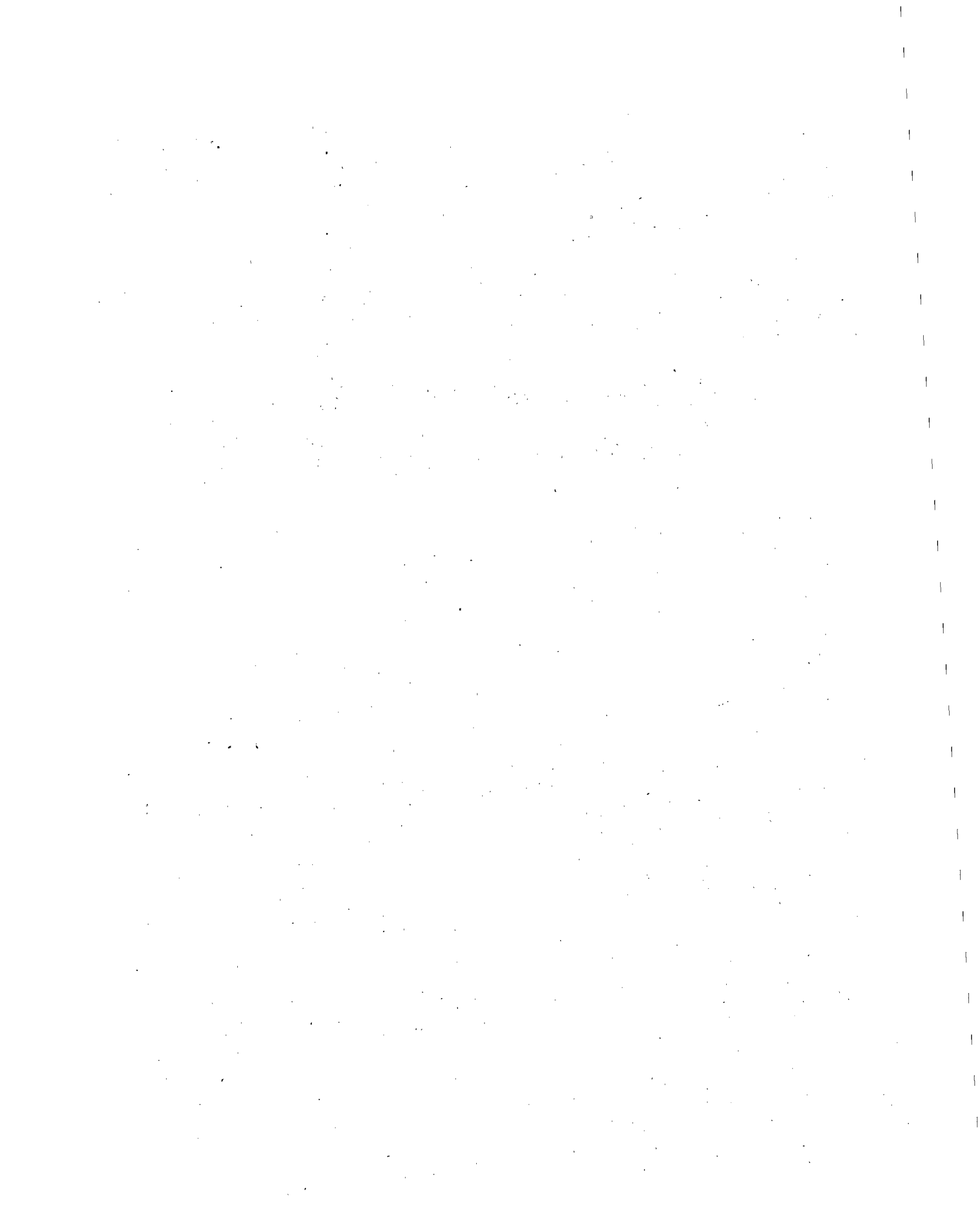
Type 2 brick building is a kind of structure with outer brick wall as lateral force resisting wall, and inner R.C. frame consisting R.C. beams and columns. The inner span of Type 2 brick building is relatively large, so this kind of buildings are often used as commercial buildings, multi-storey plant for light industry, library and office buildings, etc. Based on the field survey after the Tangshan earthquake, this kind of building were seriously damaged more than the others, thus, in the new revised code, restrictions for Type 2 buildings are more rigorous than those of common multi-storey brick buildings, such as limitation of overall height, more constructional columns are needed and control of the interval of transversal walls.

Earthquake damage to Type 2 buildings were very complicated. Damage to the top storey was often more serious than the lower storeys. The cause and mechanism for the damage are not yet known. In the new revised code, the seismic load on the upper storey has been increased appropriately for compensation of the above drawback.

CONCLUSION

Brick building is one kind of structures widely used in Chinese cities and villages. A lot of data on its performance during recent strong earthquake in China have been collected and cumulated, which can be taken as a basis in the revision of the seismic code. In the draft of the new revised code, such building plays an important role. But the behaviour of brick buildings post elastic working stage is not yet known, thus some problems not yet to be solved are not involved in the new code. Therefore, further investigation has to be carried on.

II BEHAVIOR OF BRICK MASONRY STRUCTURES



AN EXPERIMENTAL STUDY OF
ASEISMIC REINFORCING OF BRICK BUILDINGS

Zhou Bing-zhang^I and Chen Rui^{II}

ABSTRACT

In order to investigate the aseismic role of reinforced concrete columns attached on the exterior surface of the exterior wall, tests of 14 single walls and 2 building models (1/4 scale) have been done.

To investigate the reinforcing role of netting with a layer of mortar on the original brick wall, 33 single walls have been tested. The tests show: The two methods are effective.

INTRODUCTION

The 1976 Tangshan earthquake is one of the most destructive earthquakes quite rare in Chinese history. An earthquake with centre focussed exactly on a century-old industrial city of 1.06 million people is the only instance known to us. The tremendous toll it took of life and property is a shock to many.

In our attempts to sum up and analyse the experiences and lessons we learn from it calmly, we realize that one of the important factors that accounted for the enormous loss of life and property to people is that the entire city and its suburbs comprise buildings whose load-bearing structures were all of brick construction not aseismatic. Under the impact of a high intensity earthquake, 85-100% of these masonry buildings were seriously destroyed and collapsed. This is the direct cause for the death and injury of many people and the loss of much property.

China has a vast territory with a seismic area of over one-third. In building up cities and towns in the past, brick was the major material for laying load-bearing structures of countless buildings which are found throughout the country. Brick-laid structures are in themselves low in both tensile and shear strength and poor in aseismic performance. Thus, they form a kind of construction destroyed the most in successive earthquakes. In view of this, to find some measure to reinforce ma-

I Director, Senior Research Engineer, II Research Engineer,
The Research Department of the Beijing Architectural Design
Institute, China

sonry buildings and improve their aseismic performance is of paramount importance.

The Tangshan earthquake taught us that in order to prevent such a disaster from recurring in other cities, the crucial point lies in carrying out the aseismic reinforcing of the large amount of brick buildings in seismic regions in a planned way in batches and in stages so as to promote their ability to withstand earthquakes. The main objective of such a move is to prevent their collapse in case of encountering high intensity earthquakes (magnitude surpassing that designed for). Of course, during ordinary ones (of designed intensity) reinforced buildings should not be damaged above norm.

Through the macroscopic earthquake damage survey, two relatively better methods of reinforcing brick buildings are derived: One is to erect reinforced concrete columns on the exterior surface of the exterior wall with pull rods or girts to strengthen the connection of interior and exterior wall bodies to serve as restraints to aseismic transverse walls from shattering and falling down after their damage, thereby, utilising the force of friction of broken brick walls and the additional reinforced concrete construction columns to resist the horizontal shear of earthquakes. At the same time, vertical load is borne by the wall body broken into four large pieces (a common condition), thereby, preventing the load-bearing wall body from collapse. The second is to affix a netting or two on one or both sides of original brick wall that is of insufficient shear strength or already impaired, and then plaster the reinforcement with high grade cement mortar. These two methods have been proved by tests done on single walls and monolithic models to be effective.

I. An experimental study on aseismic reinforcement by erecting reinforced concrete construction columns externally on the exterior wall

In order to investigate the aseismic role of reinforced concrete columns attached on the exterior surface of the wall body of buildings, tests have been done on 14 single wall bodies and two blocks of building models. Two kinds of mortar have been used for bonding bricks to study the effect of such columns on wall bodies of different strength.

1. Specimens and tests

Single wall specimens: 2m x 63cm; in 4 groups. (see fig.1 and tab.1)

The two 4-story monolithic model test specimens are made after the 76 housing standard residence designed by Beijing Architectural Design Institute with geometrical dimensions one-fourth

of the actual size. Model I has columns attached externally, while model II goes without. Its height is 3 meters with layout plan dimensions as shown in figure 2.

A girt is built for every storey. Bars used for it are $2\phi 6$ and are anchored in the columns. Between the column and the wall, two pull bars are provided for each storey.

The construction structures of the additional column and the girt as well as the wall body are shown in figure 3.

Loading: A vertical load of compression stress 3.5kg/cm^2 is applied on the top of the single wall body, and horizontal loading is applied at the ends of the concrete beam atop the test specimen.

Horizontal loads are repeatedly applied at every layer in the direction of the transverse wall of the monolithic model. A reverse triangle appears along the vertical distribution.(Fig.4). Dynamic and static vibration excitation tests of the model are carried out. Such methods as the pulsation, the tension-release and the vibration starter excitation have been employed. Finally, dynamic damage tests have been done with vibration starters placed on the tops of the models.

2. Results and analysis

Wall bodies bonded by mortar above #10 and strengthened with additional reinforced concrete columns and pull rods have gone up 56 % in load-bearing capacity under test conditions described here, while that of those using mortar prepared from #5 grade cement and lime in the ratio of 1:3 for bonding has only gone up 23 %. Obviously, the results are quite different. Table 2 shows the load-bearing capacity of the test specimens.

Comparison of load-bearing capacity of monolithic models I and II: Models I and II are damaged at 8.93 and 5.81 tons respectively. After adding construction columns to each, the load-bearing capacity is raised by 54 %. With single wall bodies and models not reinforced, they will rapidly be destroyed once cracks appear. But after being reinforced by exterior construction columns, wall bodies are restrained by them, thereby, strengthening the integrity of the construction. As such, after the cracking of wall bodies, the force received by the additional construction columns increases until the steel bars "flow". The concrete on the columns cracks or is shattered. Only then test specimens reach the limit of their load-bearing capacity.

Stress of steel bars: To measure the stress of steel bars at the bottom of the concrete column of the single wall body and at the middle of pull rods: Under the action of horizontal loads, the test specimen, Yz1, like the suspension arm components and

the steel bars of loaded side columns, are all subjected to tension, while those at the other end are subjected to compression. But with test specimen, Yz2, the common action of wall columns is rather poor as the grade of mortar used for it is relatively low.

The strain variation characteristics of additional construction steel bars of the model: (1) Prior to the cracking of the wall body, the strain of bars basically presents a linear relationship. After cracking, it will develop into a non-linear one with respect to the variation of loading; (2) Strain decreases with the increase of the height of course. The strain of a column along course height is basically of the same sign; and (3) When the construction approaches destruction, the wall and the column are detached at the base which is subjected to tension, and steel bars have almost or already yielded.

Characteristics of cracking and damage: Cracks mainly occur at the first storey. After horizontal loading of model II has reached 5.21 tons, destruction and collapse due to brittleness suddenly take place during the process of dynamic agitated vibration. However, although model I undergoes repeated static and dynamic tests showing signs of wall body damage, cracking of additional columns occurs with concrete broken and detached from them, and even a number of steel bars at the base have snapped, still the structural model does not collapse in spite of the serious cracking. These phenomena are shown in Fig.5.

Deformation and ductility: From the load deformation hysteresis loop, it can be seen (Fig.6) that at the initial stage of cyclic loading, the growth of deformation is small. After the cracking of the wall body, deformation grows more rapidly. The area encircled by the hysteresis loop of model II is smaller than that of model I. This reflects that it has a relatively larger energy absorption capacity, i.e., after the addition of the exterior construction columns, the aseismic performance of the structure is raised. On the basis of load displacement relationship, make a sketch showing the rigidity and deformation variation of models I and II like figure 7.

When finding the ductility factor, it is necessary to find the displacement of the yield point of the idealised elastoplasticity system based on conditions like the energy absorption phase, etc. The ductility factors of the two models are found to be $u_I = 3.43$ and $u_{II} = 1.8$, i.e., the ductility factor of model I is 1.91 times that of model II.

Dynamic characteristics: See table 3 for the dynamic characteristics of the models at different stages of work.

From the table it can be seen that the self-vibration fre-

quency of models with columns is slightly higher than that of those without. This shows that after the addition of columns, rigidity is raised somewhat. From results of actual determinations, we note that the frequency of a model decreases markedly with the increase of both load and degree of severity of the damage. After the cracking of brick walls, the rigidity of the model is immediately lowered, damping increased and frequency diminished. The self-vibration periodicity of the destructive stage, when compared with that of the elastic stage, has prolonged 2.3 fold approximately. Specific damping determined at the elastic stage is about 0.07 which is increased at the destructive stage. The dynamic destruction process of the model approaching collapse as revealed by dynamic tests is like this: When seen from the deformation at the time of collapse, maximum displacement at the apex prior to the collapse of model II is 2.5cm, whereas, model I is still standing when it is 3.5cm; when seen from the prolongation of vibration time, model II collapses within a few seconds from the commencement of vibration agitation to resonance; when seen from the characteristics of destruction, the collapse of models without columns reveals the destruction characteristics of brittle structures; whereas, with models with columns, their structure can still support them although their wall bodies are terribly shattered - thanks to the restrictive effect of the construction columns and the girts.

3. The discussion of calculation of the exterior reinforced concrete construction columns

Reinforcement of buildings to withstand ordinary earthquakes calls for erecting columns with respect to structure. The method of calculation proposed here is based on test results and may serve for reference. The working formula for shear strength is:

$$P \leq \alpha_1 \frac{RA}{\xi} + 0.07 \sum bh_0 R_a \times 0.9 + \alpha_2 \sum A R_g \quad \text{--- (1)}$$

in the formula, α_1 - consider the factor of whether the masonry envelope is monolithic or not at the time of reinforcing. If monolithic, then $\alpha_1 = 1$; in working out, 0.9 may be taken when reduction of strength is envisaged, and 0.4 is taken for wall bodies bonded with mortar below #10.

$$R_\tau = R_j \sqrt{1 + \frac{\sigma_0}{R_j}}$$

R_j : Strength of main tensile stress of brick masonry envelope (kg/cm²)

σ_0 : Average compression stress of masonry envelope (kg/cm²)

ξ - Non-uniform factor of shear stress of section, take 1.5 for rectangle

A - Area of wall cross section

- b - Width of concrete column
- h - Effective height of concrete column profile
- R_0 - Anti-compression strength of concrete core
- α_2^m - Take 0.25 as the factor of steel bars in working condition
- A - Tensile strength of column steel bars; take $\frac{8}{6}$ 2400kg/cm² for that of #3 bar.

II. The experimental study of using plastered steel netting to reinforce wall bodies

Comparative tests have been done on 33 single wall bodies under the action of lateral force, and a comparison has been made of their bearing capacity and destruction characteristics before and after reinforcement. In the tests, variable factors like the following have been considered:

Prior to reinforcement, wall bodies are either intact or damaged;

Wall bodies are to be reinforced either on one or on both sides;

Wall body thickness to be either 12 or 24 cm;

Reinforcement layers at the point of flooring are wholly or partially continuous; the influence of vertical pressure, σ_0 , within the wall bodies, etc. The conditions for the test specimens are seen in table 4.

1. Making test specimens and conditions of tests

#100 machine-made bricks were used for wall bodies of test specimens, and #10 mixed mortar for bonding. Wall thickness was either 12 or 24 cm. The dimensions of these specimens are given in Fig.8.

The specimens were rendered with #100 cement mortar to give a reinforced layer of about 3 cm thick. $\phi 6$ steel bars were used for the reinforcement netting with bars arranged vertically and horizontally and spaced at 20 and 25 cm. $\phi 6$ bars used for linking are set at 50 cm intervals in a quincuncial fashion.

Loading: Average pressure σ_0 for the masonry envelope is 3.5 kg/cm² which corresponds roughly to the compression stress of the second floor of a 5-storey residence. Then apply lateral force repeatedly in one or two directions at the end of the concrete beam atop the wall body.

2. Test results and their analysis

See table 5 for experimental destruction load values. From

the table it can be seen that no matter whether the wall body is damaged or not, the method of reinforcement with bar netting rendered with a layer of mortar will promote bearing capacity. If wall bodies are not damaged (or has been restored), it will be raised much more after reinforcement. A comparison of the load-bearing capacity of group I test specimens before and after reinforcement shows an increase of 2.03 fold. Wall bodies that are intact like those of group III show a 2.84 fold increase when both sides of the wall are reinforced. If this is done on one side, the increase is only 1.65 fold.

When the plastered layers at the lower part and the steel netting of the test specimen are partially broken, the weakest part along the bottom layer of the specimen will be destroyed, thereby, lowering the load-bearing capacity. From a comparison of a few groups of test specimens, it is possible to analyse the influence of the vertical compression stress σ_0 : Compare groups IX and I before the specimens are reinforced - $\sigma_0 = 0$. Comparing this with $\sigma_0 = 3.5$, we see that destruction load is lowered by almost 7.6 tons. Also make a comparison of the reinforced wall body, group VII, with the test specimens, group IV. When $\sigma_0 = 0$ is increased to 3.5 kg/cm^2 , the load-bearing capacity shows a 9.9 ton increase.

Under the action of horizontal loading, the cracks that resulted are shown in Fig.9.

3. The discussion of calculation methods

On the basis of wall body tests, an investigation is made on shear strength of walls reinforced with a layer of steel netting plastered with mortar. With the understanding that brick walls, mortar-reinforced netting layers and reinforced steel are severally able to withstand earthquake loads in common, the following formula is proposed:

$$KQ \leq m_0 \frac{RCA_0}{\xi} + m_s \frac{R}{R_s} RTA_s + m_s R \frac{A}{S} \frac{S}{S_g} B \quad \text{-----}(2)$$

in the formula, K - When components are shear-resistant, the safety factor to have is $2.3 \times 0.8 = 1.84$

Q - Seismic shear borne by wall body

m_0 - The integral factor of wall body at reinforcement (when wall body has through cracks, $m_0 = 0$; when it is integral, m_0 takes 0.9)

m_s - Factor for reinforcement and working condition; Choose from 0.5-0.9 according to different working conditions.

R_s - Compression strength of cement mortar

- R - Compression strength of masonry
- A_g - Planar area of mortar reinforcement layer
- m_g - Take 0.45 as factor for working condition of bars
- A_g - Area of a piece of transverse steel section (when one face of wall is being reinforced)
- R_g - Tensile strength of steel bars
- B - Actual length of reinforced wall
- S - Mesh spacing of reinforced netting (horizontal bars and vertical ones equidistantly arranged)

III. Conclusion

Through tests made on single wall bodies and monolithic building models, the following points are clarified:

1. Erecting reinforced concrete structural columns on the exterior wall to reinforce multi-storey brick buildings will promote shear strength of wall bodies. When the grade of masonry mortar is above #10, bearing capacity may be raised some 50%. But this is not appreciable with wall bodies bonded with lime mortar of low grade even though they are also reinforced.

2. After reinforcement is made by erecting an exterior construction column, ductility and deformation capacity of the structure is increased: the ductility factor of the monolithic model is raised by 1.91 times, deformation capacity by 2.15 fold. The ductility factors μ for both single walls and test models may reach 3 - 4.

3. As the exterior column and the wall body are closely bonded, it strengthens the integrity of the structure, restrains the shattering and collapsing of the wall body after its damage and has a conspicuous effect in preventing it from falling over.

4. Reinforcing wall bodies by reinforced netting plastered with cement mortar raises their capacity to withstand horizontal loads. The upgrading of their load-bearing capacity is related to whether or not the original wall bodies are damaged. Those that are intact, bearing capacity will be raised 1.3 fold roughly after reinforcement, while that for damaged ones will go up 55%. Other factors involved include vertical pressure σ_0 , the passing of the reinforcement layer through the flooring or not, the rate of matching bars used and the height to width ratio.

5. The two methods described above are applicable to the reinforcing of brick walls. The former aims primarily at preventing t

the collapse of brick buildings, and the latter in promoting the shear strength of wall bodies. Therefore, both methods may also be used in combination.

Units participating in the above tests include:

Aseismic Group of the Beijing Earthquake Brigade, Aseismic Research Institute of the China Architectural Research Academy, the Engineering Mechanics Institute of Academia Sinica, the Department of Civil Engineering of Tsinghua University, Beijing No.1 and No.5 Construction Companies, and the Housing Administration Bureau of Beijing Municipality. Members of this Institute who also took part in the work are Fang Jishan, Kang Suxing, Kiu Yinsheng, Wen Guodong, Guan Qixun and Shou Guang.

Table 1

Specimen No.	Qty.	Specimen feature	Bar for column	Grade of cement for column (kg/cm ²)	Grade of cement for mortar (kg/cm ²)
Yz ₀	5	without column	/	/	10
Yz ₁	3	with col.	4φ8	225	16.9
Yz ₂	3	with col.	4φ8	260	5.2
Yz ₃	3	without column	/	/	5.2

Table 2

Specimen No.	Destruction load value (aver.) T	Specific value		Structural feature	Mortar grade No. (kg/cm ²)
		Pyz ₁ /Pyz ₀	Pyz ₂ /Pyz ₃		
Yz ₀	9.14	/	/	No column	10
Yz ₁	14.3	1.56	/	With cols.	16.9
Yz ₂	6.8	/	1.23	With cols.	5.2
Yz ₃	5.5	/	/	No column	5.2

Table 3

Work stage Mod. No.	Elastic stage			Elastoplastic stage			Destructive stage			Collapsing stage	
	Puls- ation	Tens- ion	Reson- ance	Puls- ation	Tens- ion	Reson- ance	Puls- ation	Tens- ion	Reson- ance	Resonance	
Mod. II	Freq.	25.0	20	17.6		18.6	16.2			10.8	Abrupt fall
	Spec. Damp.		0.067	0.068		0.083	0.086			0.10	
Mod. I	Freq.	23.4	23	19		20	16	12.8	10	10	2 - 3
	Spec. damp.		0.076	0.08		0.10	0.11		0.12	0.068	

Note: Frequency unit - Hertz

Table 4

Specimen group	Qty.	Wall thick. (cm)	Steel netting for reinforcement	1 or 2 sides reinf.	Wall cond. before reinf.	Reinf. layer cont. or not at flooring	Remarks
I	5	12	6-20 squares	Both	Damaged	lower part continuous	$\sigma_0 = 3.5 \text{ kg/cm}^2$
II	5	12	" "	Single	Not damaged	" "	" "
III	5	12	" "	Both	" "	" "	" "
IV	1	12	" "	Both	" "	Most bars at lower pt. of reinf'd layer snapped	" "
V	4	24	6-25 squares	"	" "	lower part continuous	" "
VI	5	24	" "	"	Damaged	" "	Among them, VI-5 without steel bars
VII	2	12	6-20 squares	"	Not damaged	Most bars at lower pt. of reinf'd layer snapped	$\sigma_0 = 0$
VIII	3	12	" "	"	" "	lower part continuous	"
IX	3	12	Not reinforced	/	/	/	"

Table 5

No.	Wall thick.	Reinf. features	Destruction load (T)		Aver. value (T)		Spec. value Q_1/Q_0	Remarks		
			Before reinf.	After reinf.	Q_0	Q_1				
I - 1	12 cm	Damaged, both sides reinf'd	12.6	24.6	9.14	27.65	Δ	$\sigma_0 = 3.5\text{kg/cm}^2$		
- 2			8.9	24.5						
- 3			6.3	30.3						
- 4			9.0	31.2						
- 5			8.9	/						
II - 1	12 cm	Single side reinf'd		/	9.14	24.2	Δ	" "		
- 2				23.1						
- 3				25.5						
- 4				23.7						
- 5				24.5						
III - 1	12 cm	Both sides reinf'd		32.5	9.14	35.1	Δ	" "		
- 2				/						
- 3				37.7						
- 4				35.2						
- 5				/						
IV - 1	12 cm	Reinf'd layer broken		19.2		19.2	2.06	" "		
V - 1	24 cm	Intact, Both sides reinf'd		39	14.80	34.25	Δ	" "		
- 2				/					35	
- 3				36.5					40	
- 4				29.5					25.5	
VI - 1	24 cm	Damaged, Both sides reinf'd	15	14	20.5	/	14.8	23.4	Δ	VI-5 rendered with #180 mortar but without bars
- 2			14	13.5	21.0	20.5				
- 3			15.3	14.8	21.8	26.5				
- 4			15.2	17.0	/	/				
- 5			15.5	14.4	/	28.2				
VII - 1	12 cm	Reinf'd layer broken		8.6		9.3	6	$\sigma_0 = 0$		
- 2				10						
VIII - 1	12 cm	Both sides reinf'd		15.4		16.4	10.6	" "		
- 2				/						
- 3				17.4						
IX - 1	12 cm	Wall not reinf'd	/			1.55		" "		
- 2				1.3						
- 3				1.8						

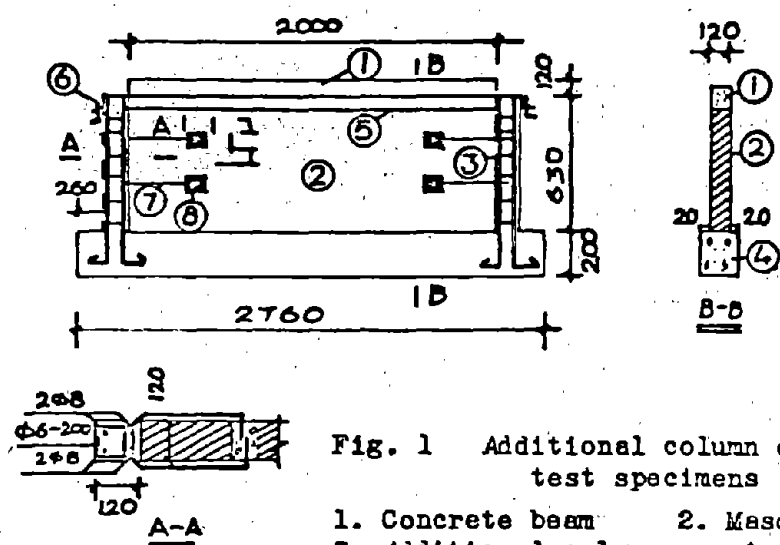


Fig. 1 Additional column of single wall test specimens

- | | |
|------------------------|--------------------------------|
| 1. Concrete beam | 2. Masonry envelope |
| 3. Additional column | 4. Reinforced concrete base |
| 5. $\phi 12$ pull bar | 6. Angle steel |
| 7. $2\phi 8$ pull bars | 8. Fine stone concrete filling |

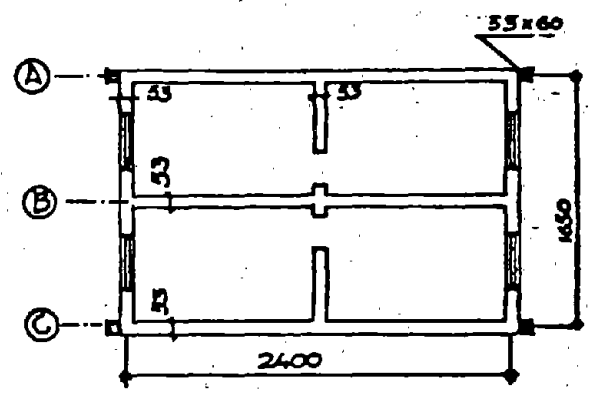


Fig. 2 General layout

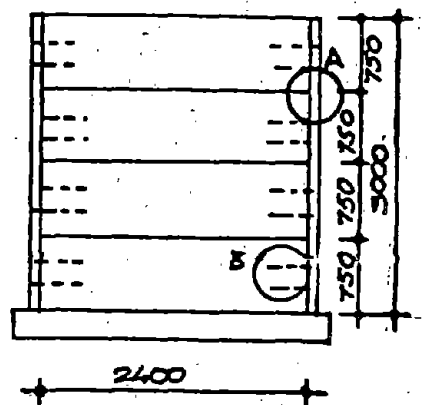


Fig. 3 Connection of model and wall

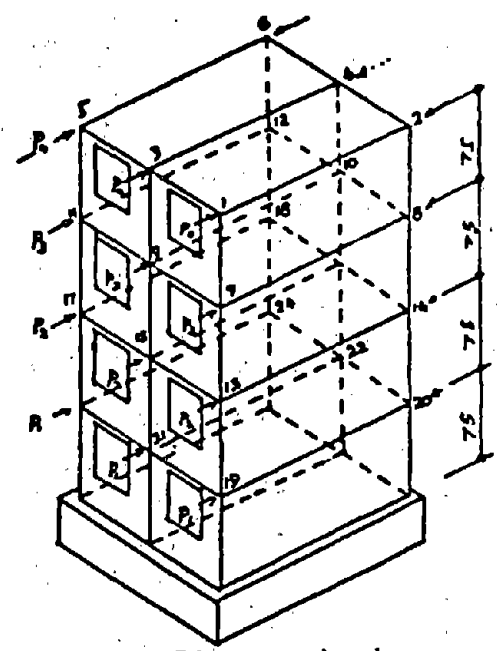


Fig. 4 Diagram showing horizontal load distribution of model

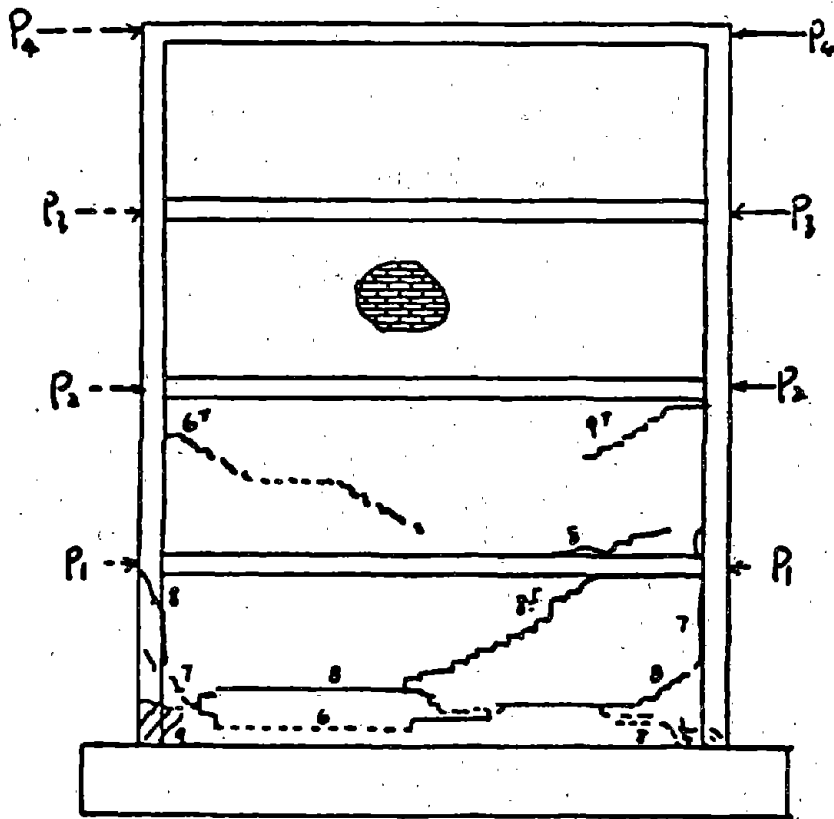


Fig. 5a Model I.
Cracks on the
east wall

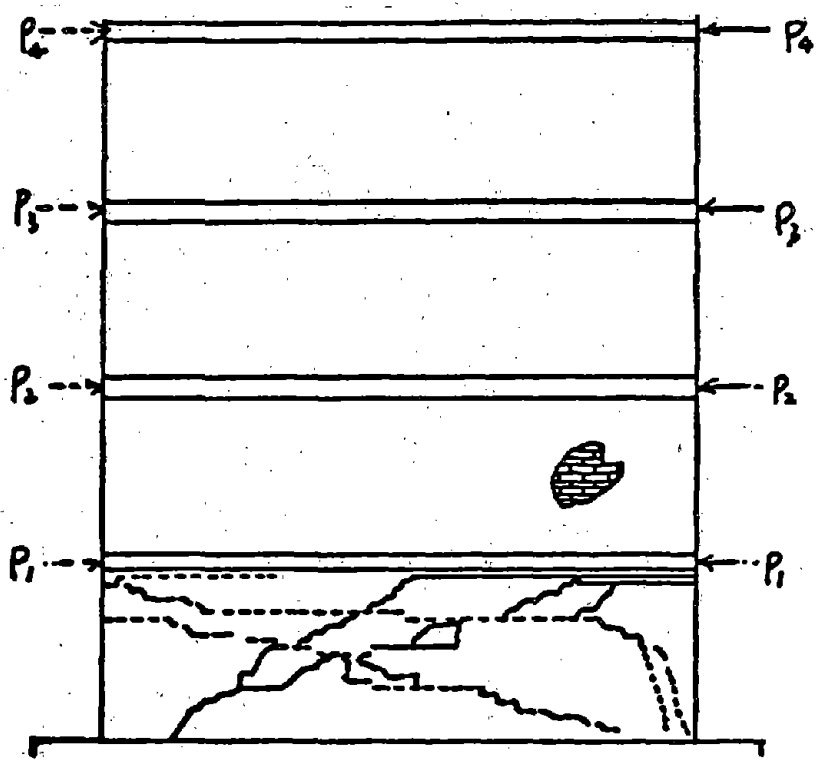


Fig. 5b Model II.
Cracks on the
east wall

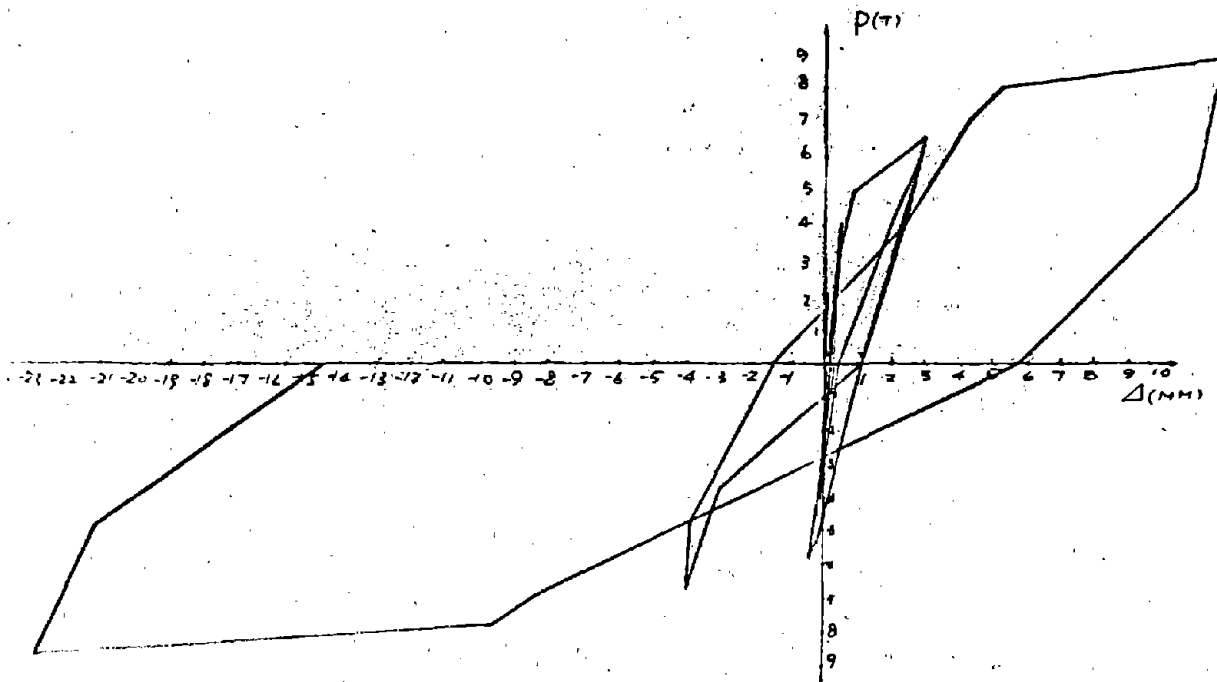


Fig. 6a Model I. Hysteresis loop of top storey of west wall

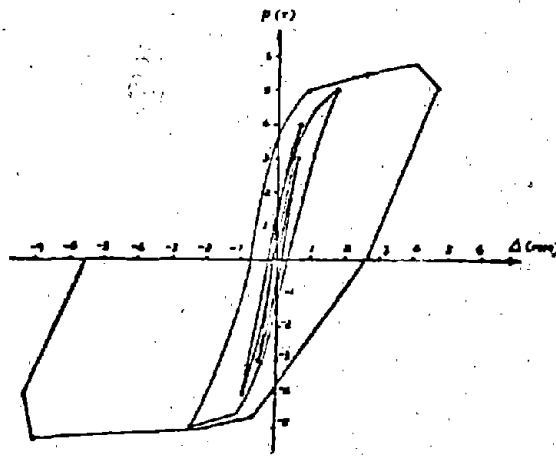


Fig. 6b. Model II. Hysteresis loop of the top storey of west wall

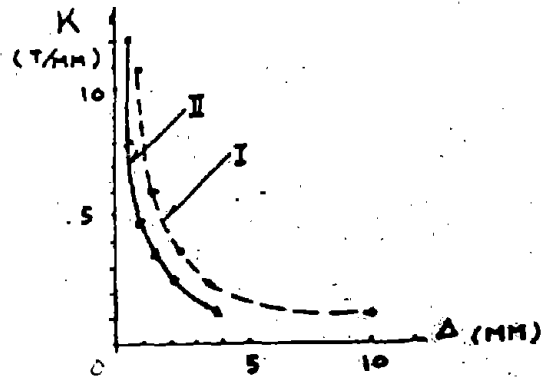


Fig. 7

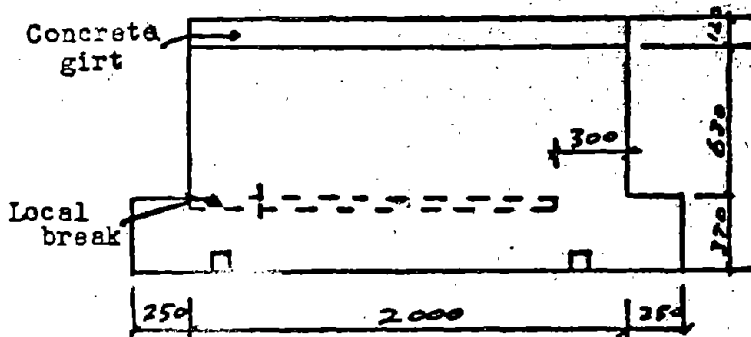


Fig 8

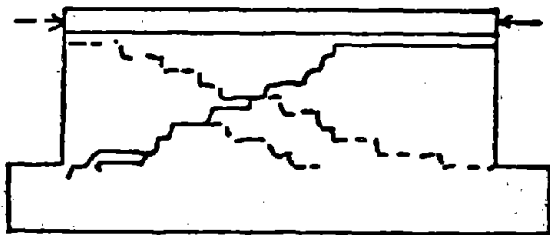


Fig. 9a Fissures of wall body not yet reinforced

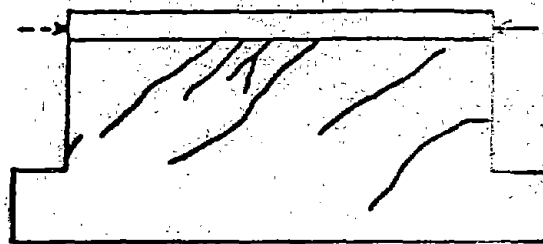


Fig. 9b Fissures of wall body after reinforcement

STRUCTURAL PROPERTIES OF UNREINFORCED HOLLOW BRICK MASONRY

Russell H. Brown¹ and Alan H. Yorkdale²

SUMMARY

A testing program was conducted by the Brick Institute of America for the purpose of developing hollow brick masonry design specifications. The four-phase program included the testing of prisms in compression, walls under eccentric compression, wall panels under shear, and walls and prisms under transverse loading. Wall thicknesses of 4, 6, 8, and 10 in. were included. Mortar types included Type M, S, N, and organically modified high-bond mortars. Not included in the program were grouted or reinforced masonry.

INTRODUCTION

Recent development of the hollow brick unit represents a potential breakthrough for loadbearing clay masonry structures. The development of a standard specification for hollow brick by the American Society for Testing and Materials, ASTM C 652, provides the manufacturer and specifier with guidance in producing and specifying high-quality units. At present, design with such units is limited to empirical and semiempirical methods rather than the rational approach developed for solid brick masonry.

Hollow brick consists of structural clay units with cores or cells having a total area of from 25 to 40% of the bearing area. Cells are sufficiently large to permit reinforcing and grouting thus making single-wythe vertically reinforced brick masonry walls possible. The units are more economical to manufacture and ship than their solid counterparts since they require less material for a given wall thickness, have lower shipping weight per unit of wall thickness, and require less energy for firing since the face shell and web thicknesses are generally less than those of solid units.

¹Professor and Head, Department of Civil Engineering,
Clemson University, Clemson, South Carolina, USA.

²Vice President of Engineering and Research, Brick
Institute of America, Reston, Virginia, USA.

Although hollow brick units are generally larger than solid brick, the exposed face shells have approximately the same height to width ratio, and it is difficult to distinguish a wall constructed of hollow brick from one made of solid brick. Hollow brick walls require less mortar per unit volume of the wall and generally can be constructed faster because of the larger wall area covered by each unit.

The hollow brick unit has many of the benefits of the hollow concrete masonry unit in addition to having the appearance of a brick wall. Walls can be constructed in running bond or stack bond, using a face shell bedding or full bedding, and grouting as many cells as required for structural considerations. Since the cells align vertically, reinforcing can be placed vertically and encased with grout producing a single-wythe vertically reinforced brick wall.

MATERIALS

Hollow Brick Units

The four types of brick used throughout the test program are shown in Fig. 1 and their compressive strengths in Table I. A single manufacturer supplied all of the hollow brick units for the initial phase of the test program. They were manufactured from the same clay in the same plant and same kiln using the same manufacturing process.

Mortar

With the exception of the organically-modified mortar, all mortars were mixtures of Portland cement, lime, and sand in accordance with BIA Specification M1-72. The organically-modified mortar was Sarabond mixed in accordance with manufacturer's recommendations. All mortar was batched by weight and properly mixed throughout the test program. Samples for determination of flow and for mortar cubes were taken immediately upon discharge prior to addition of retempering water.

TEST PROGRAM

Scope of Test Program

The test program was conducted in four phases - prism testing, wall compressive testing, shear testing, and flexural testing. More detailed results of each phase are available from the Brick Institute of America [1, 2, 3, 4]. Yorkdale (1976) has also previously reported some of the data.

Prism Phase The scope of the prism phase included compression testing according to ASTM E 447, four thicknesses of unit (4, 6, 8, and 10 in.), four slenderness ratios ($b/t = 2, 3, 4, \text{ and } 5$), four mortar types (Type N, S, M, and HB), and of both face shell bedding and full

bedding. Five replications of each combination of variables resulted in the testing of 640 compressive prisms. All were constructed in stack bond and single wythe in thickness.

Wall Compression Phase The wall compression phase included compression testing according to ASTM C 72, two wall thicknesses (6 and 8 in.), four slenderness ratios (approximately 10, 15, 20, 30), three maximum end eccentricities ($e/t = 0, 1/6, 1/3$), and four curvature conditions ($e_1/e_2 = -1, -1/2, 0, \text{ and } +1$). Type S Portland cement-lime mortar and full bedding of face shells and all cross webs were used. Three replications of each combination of variables resulted in a total of 119 wall specimens. Additionally, five compressive prisms were tested.

Shear Phase The shear test program included diagonal tension testing according to ASTM E 519, including the effect of superimposed compressive loads normal to the bed joints. Four stress levels (0, 167, 335, and 500 psi) based on net bedded areas were tested. Types M, S, and N Portland cement-lime mortars were used. Five replications of each test resulted in 60 shear tests. Additionally, five compressive prisms were tested.

Flexural Phase Flexural testing included flexural testing of walls according to ASTM E 72, including the determination of the effect of superimposed vertical compressive loads (0, 75, 100 and 125 psi) on the flexural strength normal to the bed joints. Three types of Portland cement-lime mortars (M, S, and N), and, with one exception, five replications of each combination of variable resulted in testing of 58 wall specimens. Five flexural prisms were also tested in accordance with ASTM E 518-74.

Instrumentation

Test specimens were instrumented with dial gages. The resulting data permitted the determination of axial deformation, flexural deformation, shear deformation, and lateral deflection.

Testing Equipment and Procedure

Most of the tests were performed in a one-million pound capacity hydraulic testing machine. Specimens were capped with high-strength gypsum capping compound prior to placement in the testing machine. Instrumented specimens were loaded in increments small enough to permit sufficient data points to define load-deformation characteristics. Instrumentation was removed at a load of approximately 75% of the anticipated maximum load.

TEST RESULTS

Prism Phase

Compressive strengths of prisms and mortar cubes and moduli of elasticity of prisms are summarized in Table II. Modes of failure for all prisms regardless of h/t was splitting of end cross webs. Secant moduli of elasticity (E_m) based on net bedded area compressive strength at stress levels of $0.20 f'_m$ ranged from 1800 to 3450 ksi, with a mean of 2470 ksi and 15% coefficient of variation. The average ratio of modulus of elasticity to prism compressive strength was 480 with a 21% coefficient of variation.

Comparison of prisms with face shell bedding and full bedding indicated no significant difference in net bedded area compressive strength. There was no direct correlation between compressive strength of mortar cubes and prism compressive strength. The higher strength mortars did produce higher strength prisms, but the coefficients of variation of these ratios were too high to establish a meaningful relationship.

Wall Compression Phase

The results of the wall compression phase are presented in Tables III-VI. Fig. 2 shows typical net area compressive stress vs. average compressive strain for a typical series of wall specimens. Fig. 3 is a deflection profile of a wall loaded in double curvature.

Included with test results in Tables III-VI are allowable wall loads calculated according to the BIA Standard [6] except that net areas rather than gross areas were used. Factors of safety, ratios of ultimate test load to calculated allowable load, are also presented. They ranged from a low of 4.86 to a high of 11.6 with 18% coefficient of variation. Also calculated are the probabilities that the ultimate load will exceed the allowable load based on the assumption that the test data were distributed according to Student's t distribution [7]. The worst case had a failure probability of 1 chance in 60.

Evaluation of the factors of safety for the different variables tested indicates that the procedure used to calculate allowable load (P) properly accounts for eccentricity, slenderness, curvature, and prism compressive strength. Hollow walls were found to be less sensitive to eccentricity and to slenderness than solid walls. The more efficient shape of the hollow brick cross section (higher radius of gyration) permits the walls more eccentricity and slenderness than solid walls. Hollow walls were affected by curvature in about the same manner as solid walls. The effect of prism compressive strength was

not established since only one series of five prisms was made for the entire group of 90 8-in. walls, and five prisms for the 29 6-in. walls.

Stress strain curves for the walls revealed that the axial stiffness did not vary significantly with eccentricity or curvature conditions as shown by the constant slope of the test data (Fig. 2).

The deflection profile for double curvature ($e_1/e_2 = -1$) shown in Fig. 3 illustrate that deflection is not symmetric as expected. Hence double curvature does not benefit a wall as much as theoretically might be expected. Hatzinikolas et al. [8] observed that masonry walls loaded in double curvature buckled in the first mode.

Shear Phase

Results of shear testing are shown in Table VII. Shear stress vs. shear strain curves for a single series are shown in Fig. 4. Fig. 5 shows the relationship between shear strength and superimposed normal stress.

The mode of failure was essentially tensile splitting along the vertical diagonal. Most specimens with 0 or 167 psi normal stress failed in the mortar joints in a zigzag pattern from top to bottom, regardless of mortar type. Specimens with higher levels of normal stress failed both in the mortar joints and by splitting of the units.

Higher strength mortars resulted in higher shear strengths, especially with lower normal stresses. Modulus of rigidity also increased with mortar compressive strength, with the ratio G/f'_m averaging 132 with a coefficient of variation of 9.24%.

The variability of the shear strength results was remarkably low compared to the scatter ordinarily observed in diagonal tension testing of brittle materials. The highest observed coefficient of variation for any group of five specimens was 11.7%. The average coefficient of variation of all groups of five specimens was 8%. Higher normal stresses resulted in reduced scatter of test results.

The factors of safety shown in Table VII (ratio of experimental shear strength to allowable shear stress permitted by the BIA Code [6]) ranged from 3.6 to 6.3. More importantly, the probability of a shear failure (allowable shear stress exceeding ultimate shear stress) based on Student's *t* distribution [7] was very low. The highest failure probability was 1/833. All specimens having superimposed compressive stress had failure probabilities less than 1/1500.

The direction of the measured shear strength for the entire experimental program was in the plane of the wall. Shear stresses

resulting in out-of-plane loading such as wind load might result in different ultimate shear strengths. The elastic distribution of shear stress in an "I" shaped cross section results in significantly higher shear stresses in the web portion. The use of face shell bedding to resist out-of-plane shear loads may result in reduced shear strengths.

Flexural Phase

Results of the flexural or transverse loading phase are presented in Table VIII. Fig. 6 shows a typical load-deflection curve for one of the wall specimens. Since all of the walls could not be loaded to failure due to airbag pressure limitations, a definition of failure was adopted for the purpose of comparing specimens. The lateral load at a 0.01 in. offset deflection parallel to the linear portion of the load-deflection curve was selected as the basis of comparison for all axially-loaded walls. The walls which were not axially loaded were loaded to failure and actual ultimate strengths were used. A typical construction of the 0.01 in. offset strength is shown in Fig. 6.

The typical mode of failure was abrupt tensile failure in a horizontal bed joint at or near midspan. The initial onset of cracking was difficult to observe and probably occurred before it was noticed. Specimens which could not be laterally loaded to failure had the normal wall load reduced with lateral load held constant until failure occurred.

The effect of mortar type on flexural strength appeared to depend on the superimposed compressive load. For walls having 0 and 75 psi superimposed compressive stress levels, the highest bond strength was developed using Type S mortar. At higher compressive stress levels, Type M mortar was slightly superior, followed by Type S and finally Type N.

The effect of superimposed compressive load was to increase the calculated flexural tensile stress at 0.01 in. offset deflection. The secondary bending moment produced by the axial load is small compared to the bending moment imposed by the lateral load, at least in the elastic range. As the walls' stiffness reduced in the inelastic range (Fig. 6), the buckling load substantially diminished and the secondary moment caused by wall slenderness was calculated to be as much as 9% of the primary moment.

Moduli of elasticity (E) in flexure were calculated from load-deflection data using a linear regression analysis for those points which appeared to be in a linear range. Correlation coefficients averaged 0.996, an indication that the straight line fit the data very well. The average value of E in flexure for all

specimens was 1.84×10^6 psi with coefficient of variation of 11.25%. Elastic modulus did not appear to have a strong correlation with compressive stress level or mortar type.

The ratio of experimental flexural tensile strength to allowable flexural tensile stress perpendicular to bed joints (Table VIII) ranged from a low of 2.17 for 0 normal stress to a high of 4.68 for maximum normal stress. The average safety factor increased with normal compressive stress. Probabilities of failure could not be calculated since actual failure stress levels were not obtained in most cases due to airbag pressure limitations.

SUMMARY AND CONCLUSIONS

A four-phase experimental testing program was performed by the Brick Institute of America to evaluate the structural performance of hollow brick masonry. Extensive test results are presented for compressive prisms, eccentrically-loaded walls, walls loaded in shear, and walls loaded in flexure. Moduli of elasticity in compression, in flexure, and in shear are presented. Mortar type, wall thickness, and face shell vs. full mortar bedding are all considered. Test results are compared to allowable loads calculated from the BIA Standard [6] for solid brick masonry. Some of the major observations are as follows:

1. Secant modulus of elasticity based on net bedded area compressive strength at a stress level of $0.20 f'_m$ was $480 f'_m$ with 21% coefficient of variation.
2. There was little difference in prism strength for face shell bedding compared to full bedding when strengths were based on net bedded area.
3. Hollow brick prisms were less sensitive to slenderness ratio than solid brick prisms.
4. Higher compressive strength mortars resulted in only slightly higher prism compressive strengths.
5. The procedure presented in the BIA Standard [6] for the design of solid load-bearing brick walls appears to properly account for eccentricity, slenderness, end curvature conditions, and prism compressive strengths when applied to hollow brick masonry walls.

6. Factors of safety for wall compressive strength ranged from 4.86 to 11.62, and the highest probability of failure was about 1 chance in 60.
7. The use of the BIA Code [6] for allowable shear stress results in factors of safety of from 3.6 to 6.3 and failure probabilities below 1 chance in 800.
8. The effect of mortar type on flexural strength was not uniform and depended on the level of axial compressive stress. Axial compressive stress generally increases flexural tensile strength. Modulus of elasticity in flexure averaged 1.84×10^6 with coefficient of variation of 11.25%.
9. Factors of safety based on allowable flexural stresses in the BIA Code [6] ranged from 2.17 to 4.68 and increased with increased normal compressive stress.

REFERENCES

- [1] "Compression Prism Strength Tests of Hollow Brick Masonry," Research Report No. 20, Brick Institute of America, McLean, VA, 1979.
- [2] "Wall Compressive Strength Tests of Hollow Brick Masonry," Research Report No. 21, Brick Institute of America, McLean, VA, 1979.
- [3] "Shear Strength Tests of Hollow Brick Masonry," Research Report No. 22, Brick Institute of America, McLean, VA, 1979.
- [4] "Flexural Strength Tests of Hollow Brick Masonry," Research Report No. 23, Brick Institute of America, McLean, VA, 1979.
- [5] Yorkdale, Alan H., "Structural Research and Investigation for the Development of a Rational Engineering Design Standard for Hollow Brick Masonry," Proceedings of the 4th International Brick Masonry Conference, Brugge, Belgium, Published by Groupment National de l'Industrie de la Terre Cuite, April, 1976, p. 4.d.4.
- [6] "Recommended Practice for Engineered Brick Masonry," Brick Institute of America, McLean, VA, November, 1969.
- [7] Benjamin, J. R., and Cornell, C. A., Probability, Statistics, and Decision for Engineers, McGraw-Hill, New York, N.Y., 1970, p. 295.
- [8] Hatzinikolas, M., Longworth, J., and Warwaruk, J., "Buckling of Plain Masonry Walls with Initial Double Curvature," Proceedings of the North American Masonry Conference, Boulder, Colorado, Aug., 1978, Paper No. 87.

Table I
Physical Properties of Hollow Brick Units

Units ^a						Compressive Strength					
Actual Dimensions					Gross Area		Net Area				
t	h		Area	Area	Radius	Machine	f _b ^b	x	f _b ^b	x	v ^d
in.	in.	in.	sq. in.	sq. in.	of Gyration	Load	psi	psi	psi	psi	%
3.5	3.5	11.63	40.70	27.27 (67%)	3.25	442.5	10,870		16,230		
						416.8	10,240		15,280		
						458.9	11,280	10,750	16,830	16,040	3.9
						444.8	10,930		16,310		
						423.7	10,410		15,540		
5.63	3.63	11.63	65.48	45.83 (70%)	1.90	423.7	6,470		9,250		
						440.2	6,720		9,610		
						477.6	7,290	6,630	10,420	9,470	6.3
						402.7	6,150		8,790		
						426.1	6,510		9,300		
7.63	3.63	11.63	88.74	54.13 (61%)	2.59	458.9	5,170		8,480		
						475.2	5,350		8,780		
						496.2	5,590	5,520	9,170	9,060	5.3
						491.6	5,540		9,080		
						529.1	5,960		9,770		
9.60	3.63	11.63	111.65	69.22 (62%)	3.14	692.8	6,210		10,010		
						678.2	6,070		9,800		
						600.3	5,380	5,790	8,670	9,330	6.1
						614.9	5,510		8,880		
						644.1	5,570		9,310		

^aDimensions are averages of 5 specimens.

^bTested in accordance with ASTM Standard Methods, C 67-66.

^cFigures in parentheses are the percentages of gross area in the plane of loading.

^dCoefficient of variation.

Table II
Compressive Strength of 8-in. Hollow Brick Prisms

Mortar Type	Prisms Mortar Bedding	Net Area in. ²	h/t	Compressive Strength, f_m^a			Mortar Strength ^b psi	Secant Modulus ^c of Elasticity, E_m psi x 10 ⁶
				Gross Area psi	Net Area psi	ν %		
N	FB	54.4	2	2590	4230	9.4	1370	1.89
			3	2540	4160	4.7	1370	
			4	2650	4330	7.5	1370	
			5	2280	3730	7.6	1430	
			5	2280	3730	7.6	1430	
	FS	32.6	2	1700	4650	8.2	1370	2.04
			3	1704	4650	10.2	1370	
			4	1790	4890	10.5	1430	
			5	1320	3600	11.6	1430	
			5	1320	3600	11.6	1430	
S	FB	54.4	2	3120	5090	4.5	3295	2.41
			3	3380	5520	5.7	2295	
			4	2970	4850	6.7	2295	
			5	3360	5490	4.4	1725	
			5	3360	5490	4.4	1725	
	FS	32.6	2	2230	6080	9.8	2295	2.60
			3	2110	5750	5.0	2295	
			4	1960	5350	7.9	1725	
			5	1840	5010	7.3	1725	
			5	1840	5010	7.3	1725	
M	FB	54.4	2	4090	6690	2.7	3350	2.64
			3	3810	6230	4.1	3350	
			4	3720	6080	9.3	3035	
			5	3310	5400	26.0	3035	
			5	3310	5400	26.0	3035	
	FS	32.6	2	2420	6610	6.9	3350	2.94
			3	2270	6180	5.6	3350	
			4	2290	6240	3.4	3035	
			5	2070	5660	5.4	3035	
			5	2070	5660	5.4	3035	
HB	FB	54.4	2	4250	6950	3.6	6125	2.40
			3	3650	5960	5.3	6125	
			4	3640	5940	3.7	6875	
			5	3740	6110	2.2	6875	
			5	3740	6110	2.2	6875	
	FS	32.6	2	2790	7610	7.1	6125	2.90
			3	2310	6310	7.4	6125	
			4	2430	6630	4.6	6875	
			5	2300	6270	6.1	6075	
			5	2300	6270	6.1	6075	

^aAverage of 5 specimens.

^bAverage of 3 2-in. cubes.

^cAt 0.20 f'_m .

Table III
Compressive Strength of Hollow Brick Walls With
Hinged Ends Top and Bottom (Case I, $e_1/e_2 = -1$)

Test Specimens				Test Results			Comparisons		
h	t	h/t	e_2	Average ^b Ultimate Load P_u kips	Average ^b Ultimate Stress Net Area psi	v %	Relative ^c Strength	P_u/P_d	Probability $P_u > P$
40	7.6	5.3	0 ^a	-	-	-	1.00	-	-
71	7.6	9.34	t/6	305.2	2766	3.7	1.02	6.66	.999
			t/3	233.3	2112	9.4	0.78	6.43	.995
119	7.6	15.7	t/6	316.8	2871	4.3	1.06	7.80	.998
			t/3	274.4	2650	11.5	0.98	8.52	.991
167	7.6	22.0	t/6	243.3	2205	8.7	0.81	6.97	.995
			t/3	207.0	1876	-	0.69	7.50	-
167	5.6	29.8	t/6	219.3	2480	5.7	0.68	7.43	.997
			t/3	185.3	2095	-	0.58	7.92	-

^aCompressive prisms, tested with axial load, both ends fixed.

^bAverage of 3 specimens.

^cRatio of average ultimate stress to average f'_m of 2706 psi for 8 in. walls and 3630 psi for 6 in. walls.

^dAllowable load P from Section 4.7.8.1 of BIA Standard [6] using net area.

Table IV
Compressive Strength of Hollow Brick Walls With
Hinge at Top and Fixed at Bottom (Case II, $e_1/e_2 = -1/2$)

Test Specimens				Test Results			Comparisons		
h in.	t in.	h/t	e	Average ^b	Average ^b	v %	Relative ^c Strength	P _u /P ^d	Probability P _u > P
				Ultimate Load P _u kips	Ultimate Stress Net Area psi				
40	7.6	5.3	0 ^a	-	-	-	1.00	-	-
			0	289.9	2627	5.1	0.97	4.86	.997
68	7.6	8.9	t/6	297.9	2700	4.7	1.00	6.77	.998
			t/3	219.3	1988	6.8	0.73	6.83	.996
			0	361.4	3275	3.0	1.21	7.06	.998
116	7.6	15.3	t/6	322.4	2922	4.0	1.08	8.55	.999
			t/3	257.2	2331	5.9	0.86	9.35	.997
			0	331.5	3004	3.7	1.11	7.76	.999
164	7.6	21.6	t/6	252.2	2285	8.4	0.84	8.03	.999
			t/3	195.3	1770	10.2	0.74	8.53	.993
			0	290.1	3281	2.6	0.90	8.36	.999
164	5.6	29.3	t/6	241.6	2733	-	0.75	9.44	-
			t/3	146.0	1652	5.8	0.46	7.81	.997

^aCompressive prisms, tested with axial load, both ends fixed.

^bAverage of 3 specimens.

^cRatio of average ultimate stress to average f'_m of 2706 psi for 8 in. walls and 3630 psi for 6 in walls.

^dAllowable load P from Section 4.7.8.1 of BIA Standard [6] using net area.

TABLE V
Compressive Strength of Hollow Brick Walls With
Hinged Ends Top and Bottom (Case III, $e_1/e_2 = 0$)

Test Specimens				Test Results			Comparisons		
h in.	t in.	h/t	e	Average ^b Ultimate Load P _u kips	Average ^b Ultimate Stress Net Area psi	v %	Relative ^c Strength	P _u /P ^d	Probability P _u > P
40	7.6	5.3	0 ^a	-	-	-	1.00	-	-
			0	325.5	2950	3.2	1.09	5.40	.999
71	7.6	9.34	t/6	283.6	2570	4.1	0.95	6.70	.999
			t/3	233.2	2113	4.0	0.73	8.36	.999
			0	350.2	3174	3.0	1.17	7.50	.999
119	7.6	15.7	t/6	286.1	2593	6.9	0.96	8.64	.996
			t/3	253.4	2297	4.5	0.85	11.62	.998
			0	299.0	2710	6.8	1.00	8.15	.996
167	7.6	22.0	t/6	222.2	2014	6.6	0.74	8.55	.996
			t/3	180.4	1635	8.4	0.60	10.55	.995
			0	230.0	2602	5.5	0.72	8.85	.997
167	5.6	29.8	t/6	155.1	1754	4.6	0.48	8.43	.998
			t/3	86.0	942	4.9	0.27	7.11	.998

^aCompressive prisms, tested with axial load, both ends fixed.

^bAverage of 3 specimens.

^cRatio of average ultimate stress to average f'_m of 2706 psi for 8 in. walls and 3630 psi for 6 in walls.

^dAllowable load P from Section 4.7.8.1 of BIA Standard [6] using net area.

Table VI
Compressive Strength of Hollow Brick Walls With
Hinged Ends Top and Bottom (Case IV, $e_1/e_2 = +1$)

Test Specimens				Test Results			Comparisons		
h	t	h/t	e	Average ^b Ultimate Load P _u kips	Average ^b Ultimate Stress Net Area psi	v %	Relative ^c Strength	P _u /P ^d	Probability P _u > P
40	7.6	5.3	0 ^a	-	-	-	1.00	-	-
71	7.6	9.34	t/6	280.4	2541	3.1	0.92	8.59	.999
			t/3	149.3	1353	16.8	0.50	9.33	.983
119	7.6	15.7	t/6	252.9	2292	0.8	0.85	11.34	.999
			t/3	75.1	681	1.7	0.25	6.77	.999
167	7.6	22.0	t/6	188.1	1705	5.9	0.63	- ^e	-
			t/3	44.2	400	8.0	0.15	-	-
167	5.6	29.8	t/6	96.9	1096	5.6	0.30	-	-
			t/3	25.9	293	14.0	0.08	-	-

^aCompressive prisms, tested with axial load, both ends fixed.

^bAverage of 3 specimens.

^cRatio of average ultimate stress to average f'_m of 2706 psi for 8 in. walls and 3630 psi for 6 in. walls.

^dAllowable load P from Section 4.7.8.1 of BIA Standard [6] using net area.

^eMaximum slenderness ratio permitted in BIA Standard [6] $e_1/e_2 = +1$ is 20.

Table VII
Shear Strength, v'_m , of 8-inch Hollow Brick Masonry Walls

Superimposed Compressive Stress psi net area	Mortar Type	Average Ultimate Load ^a kips	Average v' net area psi	Coeffi- cient of Variation %	Mortar Com- pressive Strength ^b psi	Allow- able Shear Stress ^c psi	Ratio of Ultimate Shear Stress to Allowable Shear Stress	Failure Probability ^d %
0	M	65.0	209.0	11.7	1980	33	6.3	0.11
	S	49.4	159.0	10.7	1108	30	5.3	0.08
	N	32.9	106.0	10.5	918	29	3.7	0.12
167	M	79.4	255.0	4.9	2358	66	3.9	Less than 0.7
	S	71.7	230.0	6.6	1071	63	3.6	Less than 0.7
	N	62.2	199.0	7.4	895	56	3.6	Less than 0.7
335	M	105.5	339.0	5.5	2859	80	4.2	Less than 0.7
	S	107.8	346.0	8.7	1915	80	4.3	Less than 0.7
	N	86.6	278.0	6.8	933	56	5.0	Less than 0.7
500	M	134.4	431.0	8.9	2762	80	5.4	Less than 0.7
	S	127.3	408.0	5.0	1524	80	5.1	Less than 0.7
	N	104.5	336.0	5.3	890	56	6.0	Less than 0.7

^aAverage of 5 specimens.

^bAverage of 15 2-in. cubes.

^cCalculated from Section 4.7.12.3 of the BIA Code [6].

^dProbability that allowable shear stress will exceed shear capacity.

Table VIII
Transverse Strength of 8 Inch Hollow Brick Walls

Wall Specimens		Test Results ^a								
Mortar Type	Normal Stress, f_m , psi	Lateral Load at 0.01 in. Offset Deflection, psi	Tensile Stress at 0.01 in. Offset Deflection, psi	Maximum Lateral Load, psi	Maximum Tensile Stress, f'_t , psi	Maximum Midspan Deflection, in.	Modulus of Elasticity in Bending, $\text{psi} \times 10^6$	Ratio of Experimental to Allowable ^d , f'_t/f_t		
M	0	-	-	92	78	20	.0085	1.57	2.17	
S	0	-	-	103	87	10	.0084	1.91	2.42	
N	0	-	-	83	70	14	.0069	1.96	2.50	
M	75	184	80	210	102	12	.063	1.57	2.83	
S	75	205	98	228	117	-	.050	1.95	3.25	
N	75	196	90	231	120	-	.054	1.70	4.29	
M	100	240	102	254	114	-	.058	2.19	3.16	
S	100	230	94	262	121	-	.054	1.92	3.36	
N	100	220	85	262	121	-	.062	1.78	4.32	
M	125	280	111	299	127	-	.046	2.14	3.53	
S	125	235	73	308	135	-	.086	1.67	3.75	
N	125	230	69	304	131	-	.074	1.69	4.68	

^aValues given are the average of 5 tests except the M mortar series with $f_m = 75$ psi in which there were 3 tests.

^bCalculated from the Equation $f_t = M/S - f_m$ where M is the bending moment produced by the lateral load on a one ft. width over a span of 7.5 ft. The section modulus is 100.0 in. per ft. of width.

^cCoefficient of Variation is not shown for those specimens which were loaded to a predetermined lateral pressure and unloaded.

^dFrom Table 3 of the BIA Code [6].

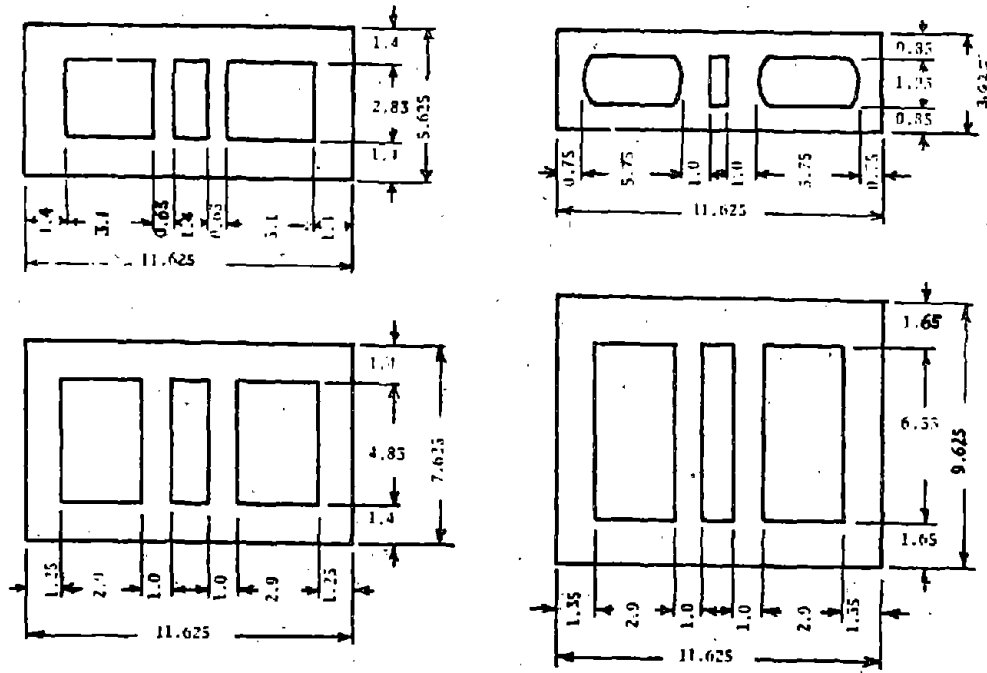


FIGURE 1 GEOMETRIC PROPERTIES OF HOLLOW BRICK UNITS

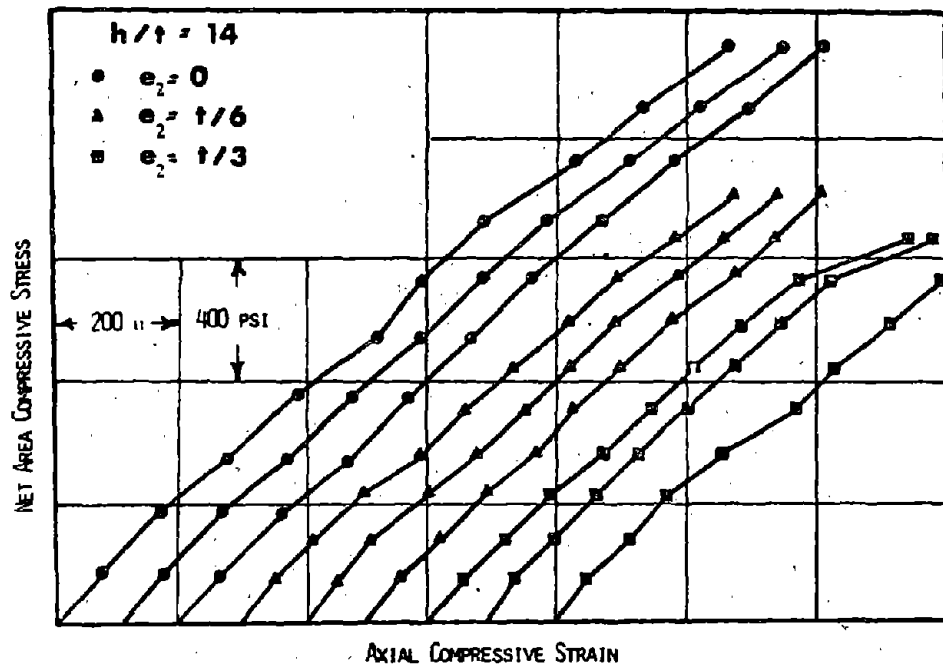


FIGURE 2 TYPICAL STRESS-STRAIN CURVES FOR HALLS IN COMPRESSION

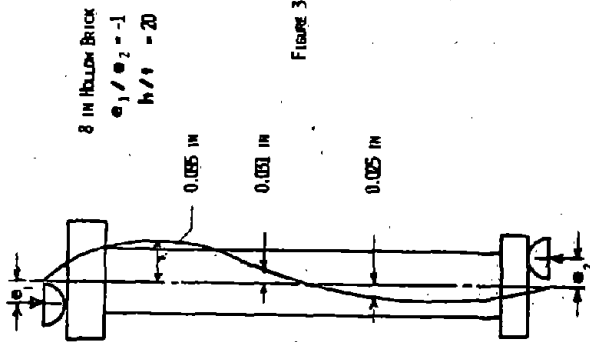


FIGURE 3 DEFLECTION PROFILE OF WALL IN DOUBLE CURVATURE

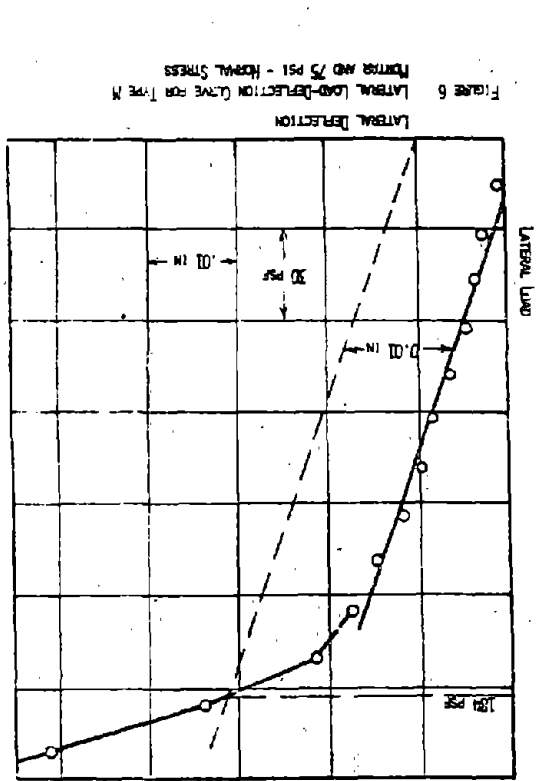


FIGURE 6 LATERAL LOAD-DEFLECTION CURVE FOR TYPE M MORTAR AND 75 PSI - NORMAL STRESS

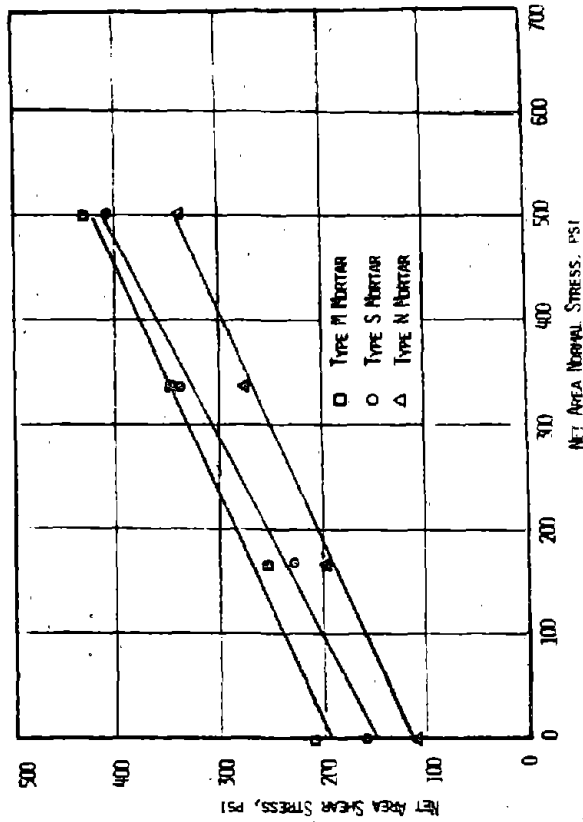


FIGURE 5 RELATIONSHIP BETWEEN SHEAR STRENGTH AND NORMAL COMPRESSIVE STRESS

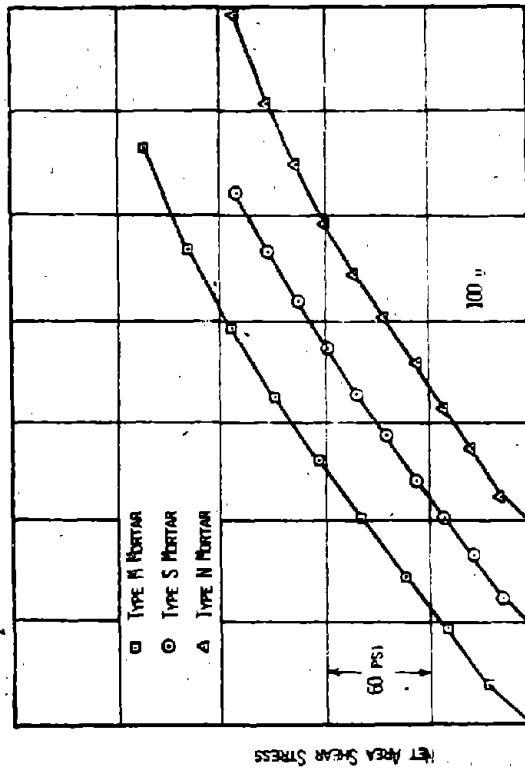


FIGURE 4 SHEAR STRESS-STRAIN CURVE FOR NORMAL STRESS OF 167 PSI

AN INVESTIGATION OF THE ASEISMATIC BEHAVIOR
OF PERFORATED BRICK BUILDINGS

Ba Rongguang ¹

ABSTRACT

This paper presents the work done in research of the aseismatic characteristics of reinforced perforated brick structures. Experiments are conducted for the determination of shear strength on a large number of specimens. Emphasis is placed on the effect of such factors as static stress, shear-span ratio, flange, amount of reinforcement under the condition of unrestricted flexural strength. Also given is an unified method for the determination of shear strength of reinforced and unreinforced wall units. It is believed that this method yield results of closer agreement with those by nonlinear analyses and experiments than by most current approaches.

1. Introduction

Traditional Chinese houses are usually of the unreinforced masonry type, using common clay bricks as the main building material. In order to reduce dead load and consequently to improve their earthquake-resistant capability, the author proposes the adoption of a type of perforated bricks (see Fig. 1). which permit the placing of all-important vertical reinforcements.

In Fig. 1, KP1 is the standard unit which combined with the non-standard units KJ1, KJ2, and KJ3 makes it possible to insert vertical bars at wall junctions and at door or window edges, and this material was used extensively in dwelling house up to about six storey in most

moderate earthquake areas. These buildings will be referred to as "perforated brick bearing system with vertical reinforcements".

The author is responsible for the research program "A Study of Perforated Brick Dwelling Buildings in Seismic Regions" whose objective is to propose methods of improving the aseismatic behavior of masonry construction by suitable reinforcing and to suggest appropriate criteria for design purposes. To meet this requirement, an considerable amount of analytical work has been

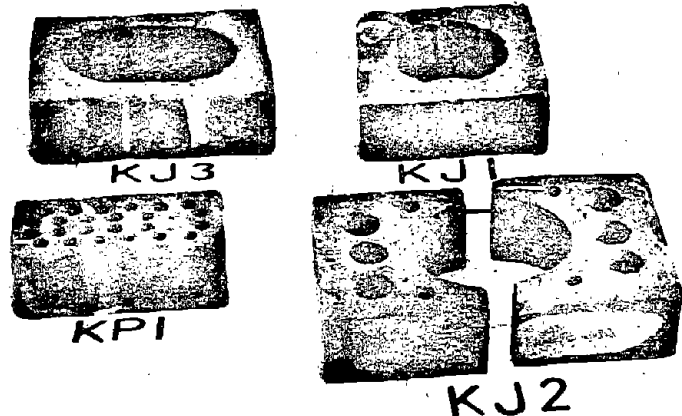


Fig. 1

¹ Structural engineer, China Northwest Building Design Institute.

carried out besides exhaustive experiments concerning the production of the new material and relevant construction methods.

In both experimental and theoretical work, attention is always aimed at the determination of reliable values of shearing strength, because it is well known that shear failure is the principal failure mode of masonry structures under lateral load. Shearing strength experiments have been conducted on 528 block specimens, among which 335 are of perforated bricks and 193 of the solid type. For wall specimens, 14 large-size units and 159 small-size units have been tested, besides using one single-storey model (With door or window openings) and another similar five-storey unit. The effects of wall flange and the variation of shear strength with the number of storeys have also been studied.

As a supplement to experimental work and for the sake of verification and comparison, it is deemed necessary to employ nonlinear finite element techniques for theoretical analyses."

2. Brief Description of Experiments

All test specimens are built as uniformly in quality as possible by maintaining a continuous and controlled output of mortar. Lateral loads are applied alternatively in following manner: in load-wise steps before appearance of diagonal cracks and in displacement-wise steps after. Generally for each applied load, three cycles are considered sufficient.

Generally three identical specimens are being tested for each item.

The main experimental works on the three types of specimens include, P- Δ curves, reinforcement strain or P- ϵ curves, tri-directional strain of wall surface, etc. The developments of cracking is observed and recorded in detail. The main properties of the specimens are showed in Tables 1, 2 and Fig.2.

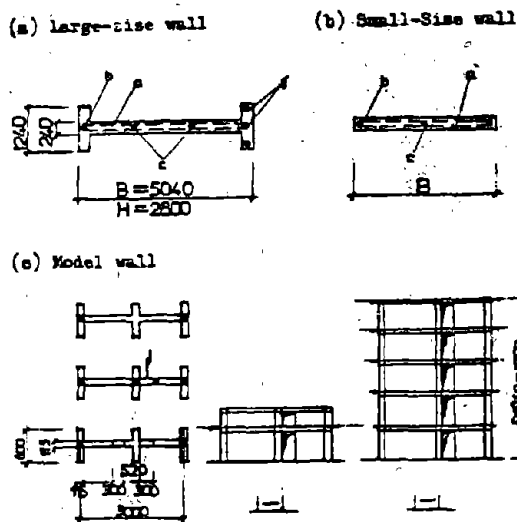


Fig.2 Simple Figure of specimens

Note: (1) The section of reinforced concrete in b.c.f. are #160.

(2) The section of reinforced concrete in Fig.2(a) is 240 x 240

3. Experimental Results and Analyses

3.1 Shear strength

The shear strength (along mortar joints) is regarded in this country as the basic aseismatic design criterion for masonry structures. From the results of experiments on 528 test specimens, the following results are obtained:

In the construction of perforated

Description of wall units

Table 1

Type of specimen	Mark	Sectional shape	No. of specimens		Normal stress σ_c (Kg/cm ²)	Design mortar grade R ₂ (Kg/cm ²)	Reinforcement		Steel percentage (in area)			
			Unreinforced	Reinforced			No. of types	Feature of type				
Large size	BQ-1,2	I		2	3.5	75	1	g	a: 0.05, 0.07,			
	PGQ-1,2,11	I		3			1	b	0.12, 0.21			
	PGQ-3	I		1			1	f	b: 0.035, 0.084			
	PGQ-4	I		1			1	ab	0.108, 0.149			
	PGQ-5	I		1			1	abc	c: 0.04, 0.084			
	PGQ-9,10	F		2			1	b	0.108			
	PGQ-6,7,8	Rectangular		3			1	b	e: 0.109, 0.187			
	BQ-1	I	1							f: 0.078		
Small unit	B-I(125 x 40)	Rectangular	9		2 - 6.5	25, 50, 100	10	a, b, c, ac, ab, bc, abc, e				
	C-I(175 x 50)		4		2.5	"						
	D-I(225 x 70)		24	37	2 - 6.5	"						
	E-I(225 x 90)		4		3.5, 5	50						
	F-I(225 x 110)		11		3.5 - 6	25, 50, 100						
	F-I(350 x 110)		3		5	50						
	G-I(175 x 140)		3		5, 6.5	50						
	A-I(225 x 130)		15	10	2 - 8	50, 100			4	e, ac, ab, abc		
	I-I(175 x 140)		4	4	2 - 6.5	50			3	a, b, ab		
	I-I(225 x 140)		6	4	2 - 6.5	25, 50, 100			3	a, b, ab		
	J-I(225 x 150)		3		3.5, 5	50						
	K-I(225 x 180)			18	5 - 8	50			7	b, ab, abc, e, bc		
												g: 0.075

Note: a, b, c, f and g denote types of reinforcement. For instance, e shows reinforcement in 150 x 110(mm) R.C. belt at mid-height of wall.

brick masonry, some part of the mortar is forced into the holes and, when hardened, acts as "keys". This explains the slightly higher R_j value of perforated bricks, and we can regard a 10% increase as being conservative. Furthermore, the reduction of weight for perforated masonry buildings over the conventional type is about 16%. Taking all the above-mentioned factors into consideration, the perforated brick buildings can be regarded as possessing an overall aseismatic strength 25% higher than those of solid brick construction.

Description of Model Units

Table 2

Type	Specimen Mark	Opening	Reinforcement
5-storied (Single-storied)	NS-1 (NS-01)	None	None
	NS-2 (NS-02)	None	ends of wall (steel content 0.112%)
	NS-3 (NS-03)	Single row	ends of wall (steel content 0.112%)
	NS-4 (NS-04)	Single row	ends of wall and door edges (steel content 0.224%)
	NS-5 (NS-05)	Double row	ends of wall (steel content 0.112%)

Note: Normal stress σ_n of single-storied unit set at same value of that for bottom story of corresponding five-storied specimen.

3.2 Factors chiefly influencing shear strength.

3.2.1 Normal stress σ_n .

Statistical results of experiments on 18 specimens of identical dimensions and mortar strengths are given below:

σ_n (kg/cm ²)	2	3.5	5	6.5
Q_p (ultimate lateral load in tons)	13.8	19.07	23.4	25.5

Which shows that the effect of normal stress on shear strength is not negligible.

3.2.2 shear-span ratio Z

For single-storied units, Z is defined as

$$Z = \frac{H}{Q \cdot Bd} = \frac{H}{Md}$$

where M and Q are respectively the moment and shear sustained by the specimen, and Bd its effective width which is reduced to B in the case of a rectangular section.

A total of 16 specimens of $B=225$ and $R_2=50$ are divided into 5 groups D, F, A, J and G, and are tested under constant normal stress $\sigma_n=5\text{kg/cm}^2$ and Z -values 0.3111, 0.4889, 0.5778, 0.6667 and 0.8 respectively. Results are shown in Table 4. To compensate for the lack of experimental data corresponding to Z -values $\sigma_n=2, 3.5$ and 6.5 , non-linear analyses are carried out for $\sigma_n=2, 3.5, 5$ and 6.5 , and the analytical results are also listed in Table 3.

Both experimental and computed results, which agree with each other fairly closely, indicate that the effect of shear-span ratio on shear strength should not be overlooked. According to TJ11-78, with σ_n between 3.5, 5 and 6.5 the term "ratio" in Table 3 remains pra-

critical constant for given Z, but with $\sigma=2$ this term becomes smaller than corresponding values with σ between 3.5 and 6.5. This indicates the necessity of introducing a further reduction factor varying as Z.

3.2.3 Wall Flange

Experimental results for large-size wall units of I, T and rectangular sections (see Fig. 2 and Table 2) are shown below:

Values in parentheses are analytical results. It may be seen that for flange width $b=124$ the Q_p values for I-shaped and T-shaped sections are respectively 17.5% and 10% higher than those for rectangular sections. For larger values of effective flange-widths, i.e., larger values of B_d , even more marked differences may be expected.

Experimental and Theoretical Results

Table 3

Method	σ	Item	Z				
			0.3111	0.4889	0.5778	0.6667	0.800
Experimental	5	Q_p	25.36	21.4	20.25	18.45	17.10
		Ratio	1.150	0.971	0.919	0.837	0.776
Analytical	2	Q_p	15.96	15.223	13.636	11.889	9.394
		Ratio	0.973	0.873	0.782	0.682	0.539
	3.5	Q_p	20.516	18.618	16.678	15.410	13.691
		Ratio	1.096	0.995	0.891	0.823	0.732
	5	Q_p	23.455	21.493	19.392	17.861	15.868
		Ratio	1.064	0.975	0.880	0.810	0.720
	6.5	Q_p	25.803	23.351	21.589	19.895	17.686
		Ratio	1.074	0.972	0.899	0.828	0.736

Note: "Ratio" denotes the ratio of experimental or theoretical result between that given by $B_r = R_d \sqrt{1 + \frac{\sigma}{R_d}}$ according to seismic code EI11-78.

Section Item	I	T	Rectangle
	Q_p (T)	83.2(82.26)	77.91(75.41)
Ratio	1.175	1.100	1.00

3.2.4 Number of storeys

The experimental and computed results of five corresponding pairs of 5-storied and single-storied model units are shown in Table 4.

It is apparent from Table 4 that:

(1) The reduction of Q_p values for 5-storied units as compared to single-storied units is quite considerable, the reduction factor being 0.465 for experiments and 0.515 for analyses (the slightly lower experimental values are probably due to warping during loading and construction defects).

(2) The bending strength of single-storied units is much higher than its shear strength, so that no apparent bending cracks have been observed. The contrary is true for the case of 5-storied units. This fully demonstrates that with large values of Z and with insufficient strength against bending, the shear strength can be greatly reduced owing to premature horizontal cracks.

(3) It is suggested that some sort of requirement be provided for cases of H/B exceeding 1.5.

3.2.5 Reinforcement

From tests on nearly 100 wall units with various amounts and arrangements of reinforcement, the conclusion is reached that reinforcement is the most effective means of improving the structure's aseismic behavior by increased ductility and limiting of crack development. Results of tests indicate that for low reinforcement and without restricted bending stresses, the following points should preferably be borne in mind.

(1) Horizontal reinforcement appears to be quite effective in improving the shear strength. This is verified by the fact that wall

unit PGQ-5 gives no sign of shear failure before bearing of two layers of horizontal bars. But this is only true when the wall unit possesses sufficient bending strength or when the (effective) shear-span ratio is relatively small. As Z exceeds 0.6, horizontal cracks appear at the wall bottom and thus it is advisable to provide vertical reinforcement of type b or g to ensure the full shear strength of wall combined with type a reinforcement.

(2) Type e consists of a horizontal R.C belt that is much more rigid and stronger than masonry. This type of reinforcement is effective only when an ample b or g type of reinforcement or a sufficient bending strength is provided, otherwise detrimental effects such as slipping at the base may occur. As a matter of fact, the only test that results in collapse is with type e reinforcement only.

(3) Reinforcements of type b, g and f are most effective in resisting bending, and their stresses increase with increase of Z , sometimes reaching yield-point. These reinforcements prevent the opening of horizontal cracks and at the same time ensure the full development of shear strength. As soon as initial cracking occurs, these reinforcements start to act as "keys" and sustain the greater part of tensile or compressive stresses. Vertical reinforcement c in the middle of wall is subjected to low tension or compression, but its "keying" action is obviously more effective and thus tends to provide more shear strength than that of type b (g,f). Type f reinforcement is useful in resisting both longitudinal and transverse earthquake forces.

(4) The most effective means of improving earthquake-resistance is by combining type a, b and c, but the components cannot develop their useful effects at the same time. Under experimental conditions, an increase of 30-60% in shear strength is obtained.

Experimental and computed Results of Model Units

Table 4

Specimen	Experimental (T)			Computed (T)			Q _e /Q _y
	Q _y	Q _e	Ratio	Q _y	Q _e	Ratio	
VB-1		> 8		(6.34)	10.4	0.450	
VB-2	12(8)	13	0.496	(8.95)	14.3	0.584	0.912
VB-3	8(6)	10.8	0.495	(6.66)	11.3	0.490	0.957
VB-4	10(6)	12.2	0.439	(6.89)	13.4	0.526	0.910
VB-5	8(4)	8	0.428	(6.00)	10.1	0.516	0.794
VB-01	-	26.1	1	(10.6)	22.7	1	1.151
VB-02	75	26.2	1	(11.2)	24.4	1	1.073
VB-03	11	21.8	1	(7.68)	23.0	1	0.946
VB-04	11	27.8	1	(10.2)	25.5	1	1.090
VB-05	11	18.7	1	(6.32)	19.5	1	0.954

Note: 1. Ratio denote VB-1/VB-01.

2. Q_e denotes load at initial crackings values due to shear in parentheses are loads at initial cracking due to bending.

It should be noted that: although vertical reinforcements are not as effective as horizontal reinforcements in resisting shear, but it has the advantage of providing greater ductility.

The combination of types a, b and c has the maximum capability of energy dissipation, providing ductility and reducing cracks (see Fig. 3). Risk of collapse after the state nominally regarded as failure is also lessened.

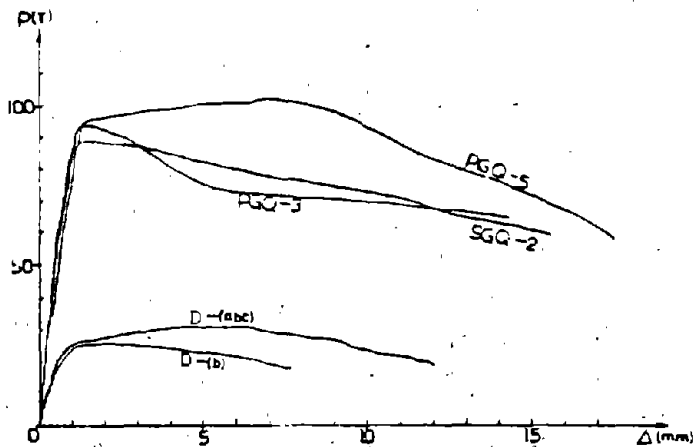


Fig. 3

4. Proposed Method for Calculating Shear Strength

From earthquakes damage surveys, the diagonal cracks observed on various wall location are results that can be attributed to principal tensile stresses. Under cyclic loading tests, diagonal cracking (usually accompanied by horizontal cracks with small Z-value) are also produced, thus implying the presence of critical stress state causing cracking and failure along the cracked surface. According to calculations for Z ranging from 0.2 to 0.8, and by observing the stresses along cracked surfaces and the area enveloped by the maximum stresses (i.e the maximum shear Q_{max} along the surfaces), the following conclusions may be drawn:

- (1) Principal tensile stress is the critical factor, and it increases with larger values of Z.
- (2) The maximum principal tensile stress occurs at the side of loading near the wall center where initial shear cracks appear.

The author proposes a unified formula of calculating the shear strength of both unreinforced and reinforced wall-units in the terms of principal tensile stress as given below ($Z \leq 1$):

$$Q_p = \frac{\eta A_c R_T}{\xi} + 0.06 R_a A_h + m_1 \sum_{i=1}^3 m_i R_g A_{g_i} \dots \dots \dots (1)$$

in which

- Q_p --- Ultimate shear strength of wall unit.
- A_c --- effective horizontal sectional area (effective flange area included) of masonry of wall unit.

$$R_T = R_j \sqrt{1 + \frac{\sigma_c}{R_j}} ;$$

ξ --- coefficient of shear stress variation, being 1.2 for rectangular section and $1.2 \left(\frac{A}{B \cdot t} \right)^{\frac{1}{2}}$ for arbitrary section.

A and t --- effective horizontal sectional area and thickness of wall respectively.

η --- coefficient of influence of Z on shear strength being $\eta = 1.22 - 0.71Z$ when $\sigma_c \geq 3.5$.

$$\text{and } (1.22 - 0.71Z) \left\{ 1 + [0.065 + 0.28(Z - 0.311)^3] \right. \\ \left. - (\sigma_c - 3.5) \right\} \text{ when } \sigma_c < 3.5 \dots \dots \dots (2)$$

- Ah and Ra --- sectional area of R.C. core and axial compressive strength respectively.
- l ---- index number (1-3) for reinforcement types a(e), b(s,f) and c respectively.
- Ag & Rg --- sectional area and tensile strength of reinforcements respectively.
- m₁ --- coefficient of efficiency for combined reinforcements, being 0.9 for combination of a (e), b(f) and c, and 1.0 for all other cases.
- m_g --- coefficient of strength participation of reinforcement in shear, being 0.2 for type b, 0.4 for type c, 1.0 for type a with abc combination, and 0.6 for all other cases. For number of layers 2-6. m_g should be multiplied by a reduction coefficient of 0.9-0.7.

A comparison of values of η computed by the proposed method and those obtained by various other means is shown in table 5.

Calculated and experimental results of ultimate shear strength Q_p for large-size wall units and model specimens are listed in table 6. as results for small size wall-units are too numerous to be given separately.

It can be seen that:

(1) The shear strengths calculated according to the proposed method agree closely to those from experiments, the deviations being on the conservative side.

(2) For specimens having small values or large Z values, the proposed method provides greater measure of safety and closer agreement with experiments.

Comparison of Values of η for Different Method

Table 5

Method	σ_c	Z				
		0.311	0.489	0.578	0.667	0.800
Experimental	5	1	0.844	0.799	0.728	0.675
Analytical	2	0.903	0.810	0.725	0.633	0.500
	>3.5	1	0.875	0.827	0.761	0.677
Proposed	2	0.903	0.780	0.711	0.629	0.488
Formula	>3.5	1	0.873	0.810	0.746	0.652
U.S. Code (2)		1	0.882	0.823	0.763	0.675
U.S.S.A Code (3)	2	0.733	0.547	0.492	0.448	0.395
	3-5	0.854	0.707	0.631	0.592	0.530
	5	0.924	0.794	0.738	0.676	0.613
	6.5	0.978	0.852	0.808	0.765	0.687

5. Some tentative conclusions

(1) The shear strength of perforated brick masonry proves to be 10% higher than that of solid brick construction. Building of such construction are better suited for seismic regions.

(2) The influence of static normal stress, shear-span ratio and flanges of wall-units are considerable in their shear strength and should not overlooked.

(3) The proposed method of shear determination takes into account many factors traditionally ignored and is based on the results of an exhaustive study by analytical and experimental work. The results given by this method appear to be reasonable and safe to use in design.

(4) For buildings with height-width ratio H/B exceeding 1.5 provisions are given for bending strength in design.

(5) The most effective means of improving shear strength is by horizontal reinforcement, that for improving bending strength is by vertical reinforcement. Better over all aseismatic performance can be expected by using mesh-type reinforcement abc.

Experimental and Computed Results of Q_p (T)

Table 6

Type of Specimen	Specimen Number	Experimental Value	Calculated Result by Proposed method (TJ11-78)	Percentage of difference
large size	SGQ-1*	76		
	SGQ-2	85.5	91.14	6.59
	PGQ-1	81.0	88.66	3.28
	PGQ-2	82.5	86.37	4.69
	PGQ-3	92.5	87.95	4.92
	PGQ-4	88.3	93.70	6.12
	PGQ-5	99.9	101	1.01
	PGQ-6	57.13	55.26	3.27
	PGQ-7	58.13	55.26	4.94
	PGQ-8	70.83	71.77	1.33
	PGQ-9	77.01	79.91	3.77
	PGQ-10	78.81	79.91	1.39
PGQ-11	83.20	88.21	6.02	
	SR-1	80.35	80.27	0.10
model	WB-1	8	8.45 (9.60)	5.62 (20)
	WB-2	13	13.27 (14.07)	2.08 (16.23)
	WB-3	10.8	11.46 (10.38)	6.11 (-3.89)
	WB-4	12.2	13.56 (10.38)	11.15 (-14.92)
	WB-5	8	10.10 (9.38)	26.25 (17.25)
	WB-01	26.1	25.27 (9.60)	41.49 (-76.39)
	WB-02	26.2	20.04 (14.07)	23.51 (-46.3)
	WB-03	21.8	17.03 (10.38)	21.88 (-52.39)
	WB-04	27.8	21.44 (10.38)	22.88 (-62.66)
	WB-05	18.65	15.43 (9.38)	20.87 (-49.71)

Acknowledgment

This study is conducted throughout under the guidance of chief Engineer Sun Guodong without whose invaluable suggestion and patient scrutiny the task cannot be fulfilled. The author also wish to express his gratitude to lecturer Feng Jianguo of Xian Metallurgical Building Institute, Prof. Wu Ruifeng and Lecturer Xi Xiaofeng of Daliang Institute of Technology, Engineers Bai Fenggeng, Fu Shuling and Zhu Bing for their whole-hearted collaboration and

untiring efforts. Thanks are also extended to the many workers of the Chinese Building Science Academy and the Building Research Institute of Sichuan Province for their support in carrying out the experiments.

References

- (1) Wu Ruifeng, Lu Hexiang, Xi Xiaofeng: Inelastic Analysis on the Cracking Development of Masonry Walls with Localized Vertical Reinforcements, Journal of the Daliang Institute of Technology, Vol. I, 1979
- (2) Robert R. Schneider, Walter L. Dicker "Reinforced Masonry Design" 1980
- (3) Госстрой СССР, Каменные и армокаменные конструкции СНиП (II-22-81) , 1983

THE SEISMIC SHEAR STRENGTH OF MASONRY WALL

Feng Jianguo¹

SUMMARY

This paper discusses shear strength of brick masonry walls under cyclic horizontal load. Eighty-six specimens of unreinforced masonry walls have been tested. The results show that the shear strength is significantly affected by the aspect ratio of the wall as well as mortar strength and vertical compression.

On the basis of test data, statistical analysis of orthogonal table and calculations by elastic-plastic finite element method, the seismic shear strength formula including three factors (R_s , σ_v , $\frac{h}{b}$) is proposed. Calculated value by suggested formula are compared with the test data and they are shown in good agreement.

INTRODUCTION

As to the expression for shear strength, exists two different opinions in China and abroad. One is the square root type (expression of tensile principal stress). The other is linear type (expression of shear-friction).

The square root type formula is proposed by Turnsek et. al. in 1971. He supposed that the wall be a homogeneous elastic body; diagonal cracking take place around the centre of wall, when the acting tensile principal stress exceeds the tensile strength of masonry wall.

$$\tau \leq R_s \sqrt{1 + \frac{\sigma_v}{R_s}} \quad (1)$$

1. Senior Lecturer

Dept. of Xi'an Institute of Metallurgy and
Construction Engineering

Where R_e -the tensile strength of masonry,

R_c -the compressive strength of masonry.

The linear type formula is proposed by Inha et. al. in 1970. He supposed that the masonry be considered as a plastic-friction hardening materials; horizontal shear sliding take place along the cracking of masonry. On the basis of Coulomb-Mohr's strength, is given

$$\tau \leq R_j + f\sigma \quad (2)$$

Where R_j -pseudo- cohesion;

σ -actual compression;

f - pseudo-friction coefficient, (0.3-0.8. Hendry 1981).

Either square root or linear expression, contains only two factors: The shear strength of mortar R ; and vertical compressive stress σ . A great deal tests in China and abroad have shown that the shear strength of wall is also relate to the aspect ratio h/b (height to length). The reasonable formula must contain three factors. The expression of relationships as follow:

$$\tau \leq f (R_j \sigma \frac{h}{b}) \quad (3)$$

On the basis of this expression, the experimental study is carried out.

DESCRIPTION OF TEST

Specimens are designed according to three factors, the level of each factor is decided by actuality: $R_j=0.2-0.4$ Mpa; $\sigma=0.2-0.6$ Mpa; $\frac{h}{b}=0.6-1.6$ (for fixed ends; for cantilever's multiply 0.5). The specimens organized by orthogonal table $L_{27}(3^{13})$. At least two or three of the same condition specimen must be made. Other specimens were used to investigate the influence of single factor, here only versus it's own level. Eighty-six specimens have been made in all.

The dimensions of specimens are decided by piers and transverse wall in multi-story masonry building. All specimens had a thickness of 240^{mm} , length of $1250-3500^{\text{mm}}$, height of $400-1500^{\text{mm}}$.

Specimens are made up of perforated brick, whose technical standard is "kp-1". Strength of brick is larger than 10 Mpa. Design strength of mortar 2.5-10 Mpa.

Test specimen and test apparatus for fixed ends and cantilever are shown in Fig.1. The vertical loading add to the design value at first, after steadness, add the cyclic horizontal loading: At the begining under the control by load, the load increments are 20-30kN. Untill the ultimate strength is reached, change to the control by lateral deflections, the deflection increment is one or half displacement of ultimate loading.

At the top of centr line on wall, set up a displacement guide, the signals continuously recorded by x-y function recorder.

THE MAIN RESULTS OF TEST

The cracking processes of all of test walls under reversing actions were approximately similar on the whole. In the curve of lateral load-deflection, exist four stages and five character points as shown in Fig.2. From statistics of test data we obtained the point of elastic limit $p_e/p_u=0.42$ (coefficient of variation $c_v=0.14$); the point of horizontal flexible cracking p_m , whose value is determined by aspect ratio h/b , the point of diagonal cracking $p_y/p_u=0.88$ ($c_v=0.02$), the point of ultimate loading p_u , the point work loading $p_w/p_u=0.91$ ($c_v=0.03$).

Load versus deflection envelopes for specimens are shown in Fig.3. The deflection is that, at top of the specimen, the evelope for each curve was obtained by passing lines through peak point of each new maximum loading cycle. The lateral load-deflection curve is taken from the mean value of envelopes of load vesus deflection on

two directions. It's show in Fig.3.

Since the ultimate loading point is more clear than any one, we take following values to evaluate the characteristic of lateral resistance: The ultimate lateral loading p_u ; The distortion (deflection angle δ/h) at ultimate loading and strain energy (area of load-deflection diagram) at ultimate loading.

ANALYSIS OF INFLUENCE FACTORS FOR LATERAL RESISTANCE

The influence factor for lateral ultimate resistance were mortar strength (or bond strength) R_j , compressive stress σ_c and aspect ratio h/b , as listed above. In order to obtain the influence of one factor, the other two are fixed. The following conclusions are based on the results of these tests.

As shown in Fig.4(a) with the increasing of the mortar strength, the lateral resistance is increased, the distortion is decreased; the strain energy almost remain the same.

As shown in Fig.4 (b), with the increasing of the compressive stress σ_c , all of the lateral resistance, distortion and strain energy are increased.

As shown in Fig.4 (c), with the increasing of aspect ratio h/b , all of the lateral strength, distorting, strain energy are decreased.

The normal tests were progressed according to orthogonal table $L_{27} (3^{13})$. By means of analysis of variance deviation for orthogonal table, the test results as shown in table 1. are obtained. From table 1. conclusions are as follow:

(1) All of the three factors appear considerably remarkable, any one cannot be neglected in formula;

(2) The interactions for either factor appear very small and can be neglected;

(3) The random errors also very small, it indicates that, the test is progressing successfully;

(4) The degrees of influence by factor are σ , R_j , h/b in order, the degrees for the last two are equalized.

Table.1. Analysis table of variance deviation

Source of Variance Deviation	Square Sum	Degree of Freedom	Stand Deviation	Statistical Quantity	Safety Limit	Statistical Judge
A(b/h)	57.49	2	28.75	47.9	F _{0.01}	Outstanding
B(R _j)	74.01	2	37.01	60.7	(2.20)	"
C(σ)	250.84	2	125.42	205.6	=5.85	"
A B	2.52	4				
A C	1.96	4	0.61			
B C	6.81	4				
Error	0.89	3				
Totil Square Sum	394.52	26				

Using the method of elastic-plastic finite element. The shear strength for testing wall is calculated under $R_j=0.2-0.4$ Mpa, $\sigma=0.2-0.6$ Mpa, $h/b=0.61-1.6$. The calculation results by computer is shown in Fig.5. It yet indicates that, the aspect ratio h/b cannot be neglected.

THE SESIMIC SHEAR STRENGTH OF MASONRY WALL

From analysis of factors for lateral resistance we can see that, reasonable formula must contains three factors: R_j , σ , and h/b . In practice, the masonry wall bears the combined effect of shear, compression and bending stress in earthquake.

The tests indicated that, testing wall has different kinds of critical state under defferent loading terms. Under crack loading, the critical state has type of rocking mode. Under ultimate loading the critical state has a type of sliding mode.

In the case of rocking mode, the wall remains entire

yet, rocked somewhat small angles. At the top and bottom of wall have a segment of horizontal crack in opposite direction. In this condition, wall resists external forces as a strut or arch. The critical cracking state is shown in Fig.6. It means that, the wall bears tensile principle stress, under the crack loading.

In the case of sliding mode, the masonry wall has been separated into two parts--up and down trilateral or polygonal blocks by diagonal cracks depending upon aspect ratio in one direction, the wall have somewhat returned. The critical sliding state is shown in Fig.7. It means that, the wall bears shear-friction between the up and down blocks under ultimate loading.

Tests also show that, the up and down blocks move with respect to each other in horizontal direction under cycle actions in ultimate loading terms. The crack section of wall presents a step-shaped type. Considering that, the head joints of masonry cannot be fully filled with mortar in workships, let the bed joints of masonry subjected to the total lateral force on step section. From the step section cut out an infinitely small element, according to the theory of Coulomb-Mohr, the strength condition on the face of element is.

$$\tau \leq R_y + f \sigma_y \quad (4)$$

Where τ - Nominal shear stress defined $\tau = p/A$,

R_y - Strength of grip after crack, let $R_y = \alpha_z R_s$

σ_y - The compressive stress.

The compressive stress σ_y must contain direct compressive stress σ_c and normal stress of bending moment σ_m , which come from eccentricity of acting load. Since the σ_m can be replaced by product of nominal shear stress τ and aspect ratio h/b , then

$$\sigma_y = \sigma_c + \alpha \frac{h}{b} \tau \quad (5)$$

Substituting it in expression (4), and the constants replaced by $\alpha_1, \alpha_2, \alpha_3$, respectively, then the expression will be

$$\tau = \frac{1}{1 + \alpha_1 \frac{h}{b}} (\alpha_2 R_j + \alpha_3 \sigma_0) \quad (6)$$

The constants $\alpha_1, \alpha_2, \alpha_3$, are determined by test data, using the method of statistical mathematic-physic. The calculation can often be simplified if the factors $\frac{h}{b} \tau, R_j, \sigma_0, \tau$ in expression (6) can be replaced by x_1, x_2, x_3, y_t respectively.

Thus

$$y_t = \sum_{i=1}^k \alpha_i x_i \quad (t=1, 2, \dots, n) \quad (7)$$

Let the sum of error square

$$Q = \sum_{t=1}^n (y_t - \sum_{i=1}^k \alpha_i x_{ti})^2 \quad (8)$$

Estimate points α_i by letting y_t approach to minimum value $\alpha_1, \alpha_2, \dots, \alpha_n$

$$-2 \sum_{t=1}^n (y_t - \sum_{j=1}^k \alpha_j x_{tj}) x_{ij} = 0 \quad (9)$$

i.e.

$$\sum_{j=1}^k \alpha_j \left(\sum_{t=1}^n x_{tj} x_{ti} \right) = \sum_{t=1}^n y_t x_{ti} \quad (i=1, 2, \dots, k) \quad (10)$$

Then, the coefficients of regress can be found by following matrixs:

$$\{ \alpha_j \} = (L_{ij})^{-1} \{ L_{iy} \} \quad (11)$$

where

$$L_{ij} = \sum_{t=1}^n x_{ti} x_{tj}$$

$$L_{iy} = \sum_{t=1}^n x_{ti} y_t$$

On the basis of test data of orthogonal table $L_{27}(3^{13})$, the regressive coefficients can be calculated by means of list table (neglected). At last, the expression is found to be:

$$\tau = \frac{0.6}{1 + 0.31 \frac{h}{b}} (R_s + \epsilon) \quad (12)$$

The coefficient of corellation $R=0.9697$;

The coefficient of partial corellation

$$r_{xy} = 0.948 \quad r_{xy} = 0.621 \quad r_{xx} = 0.787;$$

The surplus stand deviation $S=0.0915$.

These indicate that, it is full well for practical application.

The mean value m , stand deviations σ , and coefficients of variation c_v of ratio of calculated value to test data are listed in table 2. For sake of comparison, the calculated value includes design code formulas (2)(3) besides this paper's. Test data come from above three hundred specimens, including tests of another units in China.

Table.2. comparison table of ratio for calculated value to test data

Kinds of formula	Code 3	Code 2	This paper
Specimens by carefully chosen 105	$m=1.041$ $\sigma=0.221$ $c_v=0.212$	$m=1.284$ $\sigma=0.295$ $c_v=0.23$	$m=0.979$ $\sigma=0.14$ $c_v=0.43$
Specimens by general chosen 300	$m=1.036$ $\sigma=0.25$ $c_v=0.241$	$m=1.278$ $\sigma=0.273$ $c_v=0.214$	$m=0.947$ $\sigma=0.207$ $c_v=0.219$

CONCLUSIONS

The following conclusions are based on the test results and experimental study.

(1). When mortar strength (bond strength) is increased, the lateral resistance increases, the distortion decrease, the strain energy remain constant.

(2). When the vertical compressive stress is in-

creased, all of the lateral resistance, distortion and strain energy decreased.

(3). When aspect ratio is increased, all of the lateral resistance, distortion and strain energy decrease .

(4). Analysis of variance deviation of orthogonal table indicate that, all three factors appeared considerably remarkable, any one cannot be neglected in formula.

(5). Calculation by finite element method indicate that, the lateral resistance is significantly effected by aspect ratio of wall, as well as mortar strength and vertical compression.

(6). The aseismic shear strength formula is suggested as expression (12).

REFERENCES

1. Feng Jianguo, Ba Rongguang, Fu Shulin, "Experimental Study on Shear Strength of Unreinforced Masonry Walls Under Cyclic Actions" 1985.

2. Masonry Structures Design Code (GBJ3-73).

3. Earthquake Resistant Design Code of Industrial and people's Buildings (TJ11-78).

4. T.P. Tassons "Interaction Diagramme for Reinforced and Unreinforced Masonry Walls" 1984.

5. CIB. "Symposium Wall Structure Warsonry" 1984.

6. R.L.Mayes and R.W. Clough "State of the Art in Seismic Shear strength of Masonry Walls" 1975.

7. Robert.R. Schneider "Reinforced Masonry Design" 1980.

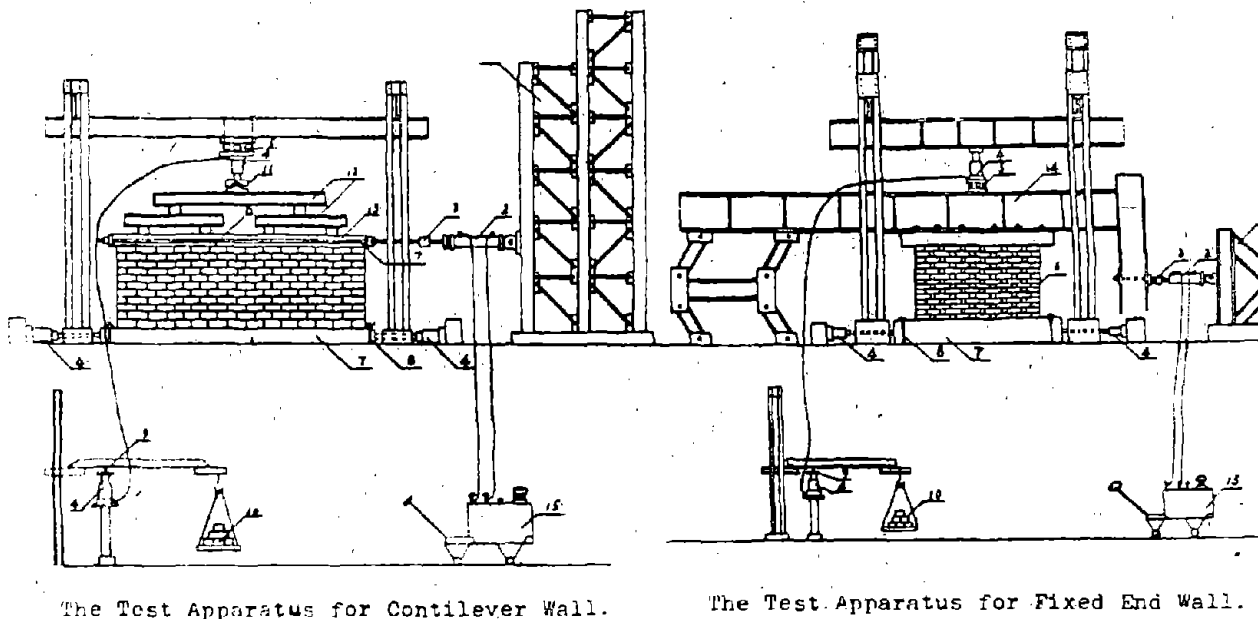


Fig.1. Specimen and Test Apparatus.

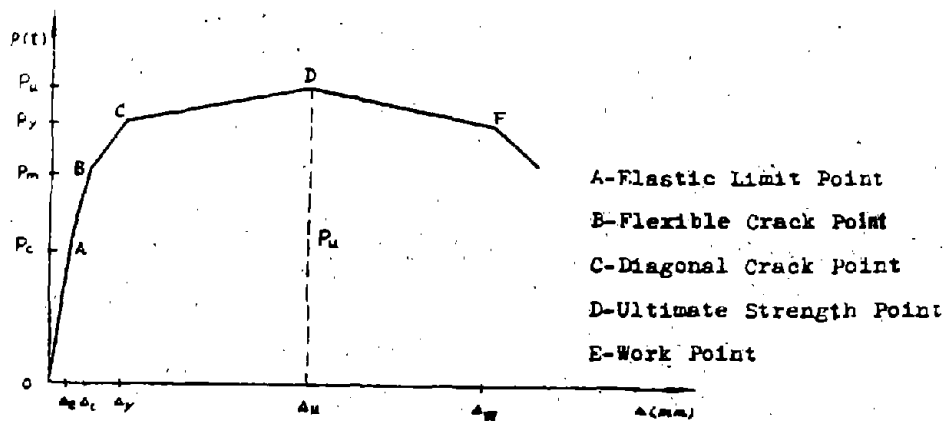


Fig.2. The Lateral Load-Deflection Curve of Testing Wall.

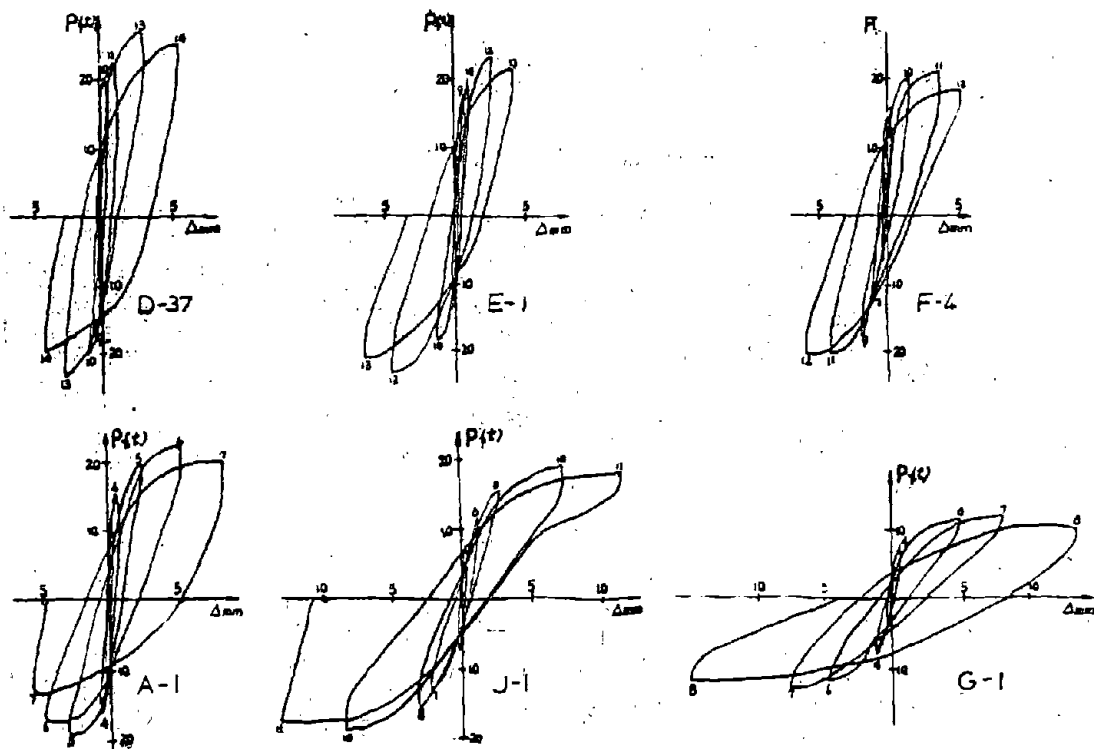


Fig.3. Load-Deflection Behaviour of Wall for Aspect Ratio
 =0.6,0.8,0.9,1.2,1.35,1.6.

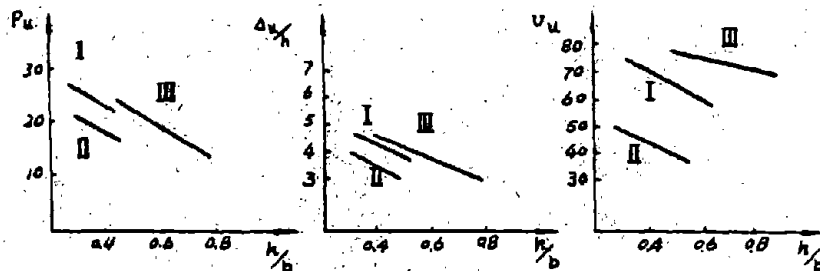


Fig.4 Lateral Resistance, Distortion and Strain Energy of Masonry.

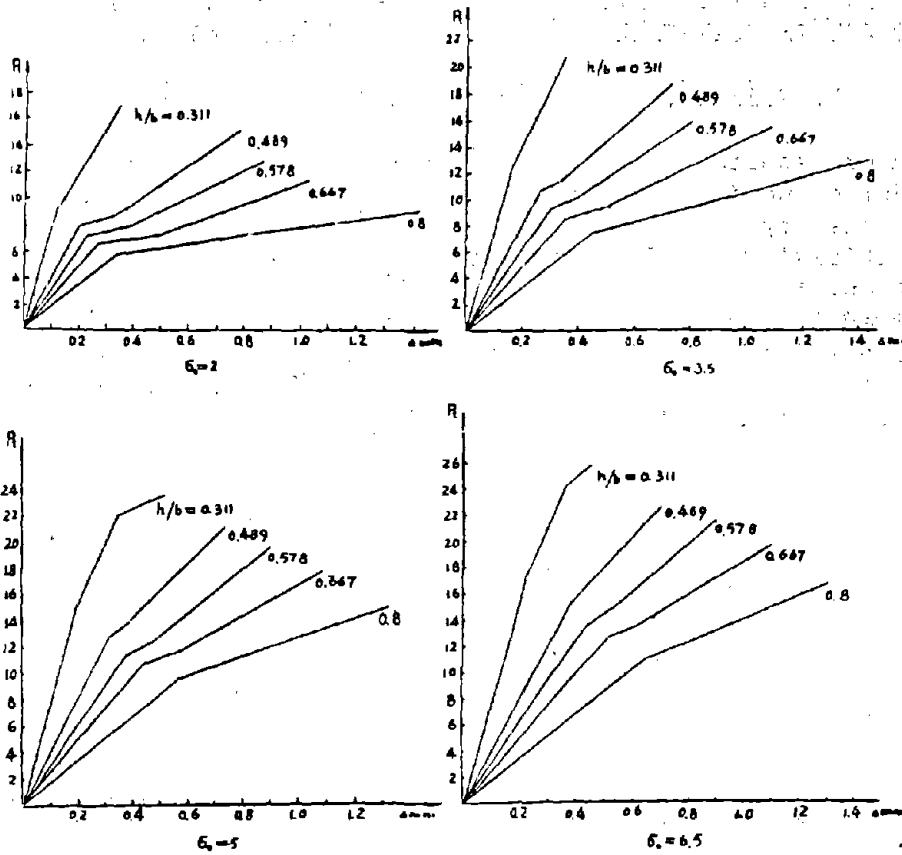


fig.5. Calculated Results By Elastic-Plastic Finite Element Method for Testing Contilever Wall.

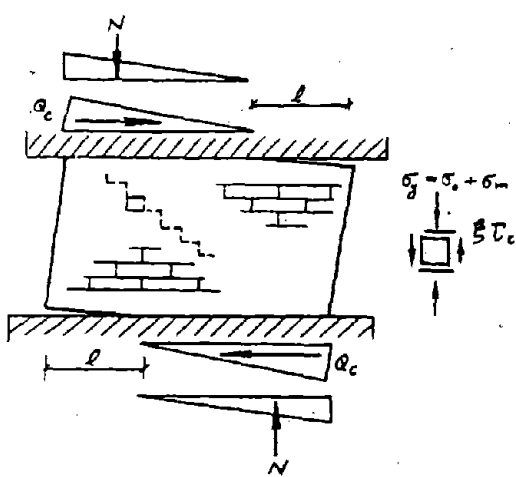


Fig.6. The Cracking State - Rocking Mode.

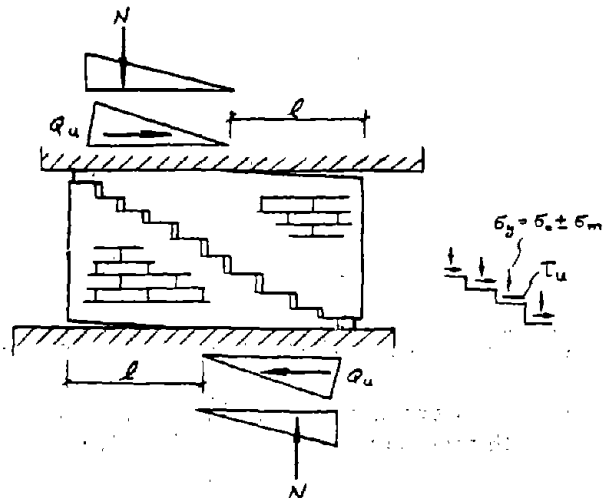


Fig.7. The Ultimate State - Sliding Mode.

AN INVESTIGATION INTO METHODS AND MATERIALS REQUIRED
TO OBTAIN FLAW-FREE GROUT IN HOLLOW BRICK MASONRY

J. L. Noland^I, G. R. Kingsley^I, L. G. Tulin^{II}

This paper reports on a research project, recently completed, in which procedures and materials necessary to obtain flaw-free grout in hollow brick masonry were evaluated. The influence of unit absorption properties, initial water content of grout, time of consolidation and reconsolidation, type of aggregate, and additives were considered. It was observed that an additive containing a plasticizer, expansive agent, water retentivity agent, and workability agent was essential and that aggregate type and time of consolidation were significant in obtaining quality grout in hollow brick masonry.

I. Atkinson-Noland & Associates, Inc., Boulder, Colorado.

II. Department of Civil, Environmental, and Architectural Engineering,
University of Colorado, Boulder.

AN INVESTIGATION INTO METHODS AND MATERIALS REQUIRED
TO OBTAIN FLAW-FREE GROUT IN HOLLOW BRICK MASONRY

J. L. Noland^I, G. R. Kingsley^I, L. G. Tulin^{II}

INTRODUCTION

Properly constructed reinforced masonry is a viable material for construction of buildings subject to lateral loads induced by seismic and wind forces. Reinforced masonry consists of masonry units and mortar with reinforcement enclosed in grout to form a material which acts as a composite to resist imposed loads. It is essential, therefore, that the grout be free of voids and cracks to be completely bonded to the reinforcement and masonry units.

Grouted, reinforced masonry, particularly grouted hollow concrete unit masonry has been used for many years in seismic-prone areas in the United States. In recent years hollow clay unit brick masonry has been introduced as an alternative. However, unless proper materials are used and proper procedures followed, grout may not bond to the masonry units and may contain voids and cracks thus inhibiting composite behavior. Further, the presence of voids and cracks in grout may permit moisture to reach the reinforcement and cause corrosion.

It has been observed on various construction projects by the first author, by others(3)(6) and in previous research (4)(5) that flaw-free grout required very careful placement procedures and even with such procedures success was not certain.

Recent research (4)(5) identified procedures and materials required to obtain flaw-free grout in hollow concrete unit (block) masonry, however, such information was not available relevant to hollow clay unit masonry.

This paper presents the results of work done to identify materials and procedures which, if used, would reasonably assure flaw-free grout in hollow clay unit masonry.

PROGRAM SCOPE

A series of experiments were conducted to evaluate the effect of various parameters upon grout quality. The parameters considered included masonry unit absorption, unit size, water content of grout, aggregate size, admixtures, and consolidation procedures as discussed.

I. Atkinson-Noland & Associates, Inc., Boulder, Colorado

II. Department of Civil, Environmental, and Architectural Engineering,
University of Colorado, Boulder.

below:

Masonry Absorptive Properties

Due to the porous nature of clay, bricks have a tendency to absorb water from the mortar or grout in contact with them. The magnitude of this effect depends on the absorption properties of the particular unit, and the properties of the mortar or grout. The result of this migration of water from grout is a reduction in the water-cement ratio of the grout, as well as significant reduction of grout volume. The units in this study were chosen to represent a wide range of absorption properties in order to determine the effect of absorption on grout properties. The absorption characteristics of each brick used are listed in Table 1.

TABLE 1. BRICK ABSORPTION PROPERTIES

Brick Type	Width		IRA	
	mm	in	kgm	gm
			m ² (min)	30in ² (min)
Buckskin	92	3-5/8	0.258	5
Buckskin	143	5-5/8	1.137	22
Copper Nugget	92	3-5/8	1.292	25
Copper Nugget	143	5-5/8	1.602	31
Copper Nugget	194	7-5/8	1.963	38
Mission Autumn Gold	194	7-5/8	1.137	22
Walnut	92	3-5/8	0.620	12
Buff	194	7-5/8	0.413	8

Unit Size

Hollow clay units with nominal widths of 102, 152, and 203 mm were chosen to represent the range of brick sizes used in construction.

Grout Water Content

The compressive strength of concrete and cement mortars depends on the quantity of water available for hydration of the cement. It is fairly easy to control this quantity in concrete. In grouted masonry,

however, the absorbent units decrease the water content of the grout, leaving an unknown quantity of water for hydration. Since different bricks absorb differing amount of water, the grout water content at the time the cement takes its initial set remains unknown even if the initial water content is tightly controlled. One of the primary objectives of this project was to determine the effect of varying initial water content on the properties of grout.

The initial water content of grout controls its pourability. Normally, water is added to grout to attain a pourable consistency. A slump of 203 mm, (8 inches), represents a reasonable lower bound for the desired consistency. The upper bound cannot be measured adequately by the slump test, but is recognized as the point just before the constituents begin to segregate. For the purposes of this study the initial water contents for the grout were chosen to represent these upper and lower bounds plus an additional intermediate point. The amount of water required for each batch was varied as required by the presence of admixture and coarse aggregate.

Aggregate

Both fine and coarse aggregates were used in this investigation in order to determine the influence of aggregate size on grout shrinkage and strength.

Admixtures

Grout admixtures were considered as a possible means to eliminate flaws and shrinkage cracks (4). Several admixtures were investigated and judged purely qualitatively by visual examination of the grouted cavities. Since water loss is the source of grout shrinkage, each admixture had some effect on the water in the grout. The admixtures chosen for investigation were lime, bentonite, super-plasticizer, fly ash, and a combination of aluminum powder, plasticizer, and a combination of ingredients known as Grout Aid.

Consolidation

A great deal of emphasis is placed on the importance of proper consolidation in the field, with particular attention paid to the practice of "reconsolidation", (i.e. a second consolidation performed after absorption has ceased but before workability is lost). Since the purpose of reconsolidation is to eliminate shrinkage cracks (4), consolidation technique was an important parameter. Consolidation methods tried were rodding and mechanical vibration. The time of the second consolidation was also varied (from 30 seconds to 60 minutes after pouring), as well as the total number of consolidations, (from 0 to 5 times in a 30 minutes period).

EVALUATION PROCEDURE

Grout was placed in the cells of 4-unit high stack-bond hollow-unit prisms. After curing, the prisms were cut vertically through the grouted cells to expose a complete grout column. Evaluation consisted of a visual examination of the grout to observe any cavities and separation of the grout from the unit.

RESULTS

The results were recorded in the form of photographs and descriptive notes indicating the effect of each variable on the quality of the grout (i.e. freedom from flaws and shrinkage cracks). Figure 1 shows an example specimen. In no combination of brick-type, grout initial water content, and consolidation technique without additives was it possible to eliminate shrinkage cracks consistently. Some important observations were made concerning the effect of reconsolidation on grout.

Specimens that were reconsolidated soon after pouring, while grout was still fluid, invariably developed shrinkage cracks. The early consolidation did eliminate air bubbles, and yielded a noticeably denser grout than in unconsolidated specimens, but continued migration of water after vibration caused significant grout shrinkage.

Specimens that were reconsolidated at later times showed a variety of results depending on the absorption characteristics of the brick and the initial water content of the grout. For bricks with low IRA's or grouts with high initial water contents, reconsolidation at any time up to about fifteen minutes had no more beneficial effect than initial consolidation. After this time, consolidation of the continually stiffening grout served only to disrupt the body of the grout, leaving voids where the vibrator had been. In the case of high IRA bricks or grouts with low initial water contents, the grout became too stiff to consolidate as early as two minutes after pouring. In many cases, shrinkage cracks still appeared when grout was vibrated in a stiff condition.



Figure 1

The use of grout admixtures to eliminate shrinkage cracks was more encouraging. While lime and fly ash improved the workability of the wet mix, they did not help to decrease shrinkage. Bentonite caused an undesirable stiffening of the grout, and as a result of the additional water required, caused an increase in the amount of shrinkage. The addition of super-plasticizer permitted a dramatic decrease in the initial water content of the grout, and resulted in grout that contained fewer shrinkage cracks than in standard grout. Grout Aid consistently reduced shrinkage cracks to a minimum, usually eliminating them entirely.

CONCLUSIONS

Some conclusions regarding the parameters studied are listed below. Conclusions are based only on the data collected in this project, and apply only to grouted hollow clay unit masonry.

1. Mechanical vibration produces a more thoroughly consolidated core than rodding.
2. There appears to be no optimum time for reconsolidation, because grout shrinkage continues after grout ceases to be fluid enough to vibrate. For hollow clay units with high rates of absorption or grouts with low water contents, the grout can become too stiff to vibrate as soon as two minutes after pouring. Thus, not only is reconsolidation unable to serve its intended purpose of eliminating grout shrinkage cracks, it could potentially destroy the integrity of a grout core if performed at the wrong time.
3. Admixtures which most successfully decreased grout shrinkage either (a) eliminated its source by permitting a decrease in initial water content without a loss of pourability, or (b) counteracted it by causing a slight expansive action in the grout. Super-plasticizers were moderately successful, and Grout Aid was extremely successful in minimizing shrinkage cracks. Admixtures that improved the water retentivity or workability of grout had little effect on grout shrinkage.
4. Hollow clay unit size and absorption properties had little effect on the size and number of shrinkage cracks in grout, however, bricks with very high IRA's caused shrinkage to occur at a quick rate, thus affecting the amount of time available for consolidation.
5. The amount of water absorbed from grout by a particular unit seems to be a function of the initial water content of the grout rather than the absorption properties of the bricks. The higher the initial water content of the grout, the more

water will be absorbed from it by the surrounding masonry, and thus more shrinkage occurred.

6. Grouts with coarse aggregates showed less shrinkage than grouts with fine aggregates.

Based upon the results of the research it appears that the quality of grout in hollow clay unit masonry may be progressively improved by:

1. use of coarse grout if permitted by the size of the grout space with mechanical vibration,
2. use of a super plastizer to reduce initial water content, with mechanical vibration,
3. use of Grout-Air with mechanical vibration.

Grout Aid and super plasticizer would not be used simultaneously. Consolidation by mechanical vibration should be done before the grout begins to stiffen particularly for option 1 above.

REFERENCES

1. HAMID, A. A., and R. G. DRYSDALE, Effect of Grouting on Strength Characteristics of Concrete Masonry, Proceedings of the North American Masonry Conference, Boulder, CO, August 1978.
2. HAMID, A. A., and R. G. DRYSDALE, Suggested Failure Criteria for Grouted Concrete Masonry Under Axial Compression, ACI Journal, October 1979.
3. HARRINGTON, R. W., Construction and Quality Control of High Lift Grouted Reinforced Masonry, Proceedings of the North American Masonry Conference, Boulder, CO, August 1978.
4. MILLER, M. E., R. O. NUNN, and G. A. HEGEMIER, The Influence of Flaws, Compaction, and Admixture on Strength Elastic Moduli of Concrete Masonry, National Science Foundation Report No. UCSD/AMES/TR-78-2, August 1978.
5. NUNN, R. O., M.E., MILLER, and G. A. HEGEMIER, Grout-Block Bond Strength in Concrete Masonry, National Science Foundation Report No. UCSD/AMES/TR-78/001, March 1978.
6. PERSON, ASCAR F., How the High Lift Grout System was Developed, Proceedings of the North American Masonry Conf., Boulder, CO 1978.
7. Uniform Building Code, Chapter 24, 1979.

TESTS OF ASEISMIC BEHAVIOUR OF BRICK MASONRY WALL

Xia Jingqian^I Ding Shiwen^{II} Zou Sijun^{II}

Summary

In the paper test results of fourteen pears of brick masonry wall under lateral cyclic loading up to failure are described. From test for the restoring characteristics of the brick masonry wall from the initial loading to the collapse four stages had been observed; elastic stage, elasto-plastic-cracking stage, failure stage under decreasing loading and slip stage under friction. The deformability of masonry wall is very low, the ultimate shearing angle and the maximum displacement are about $1/366$ and 1.9cm/m in average respectively when wall collapses. The most important factors that significantly influence upon the failure of brick masonry are the ultimate strength (deformation) and the cumulative energy of dissipation. In the paper the cumulation of the energy of dissipation, cyclic loading number versus load (displacement) relation are given.

INTRODUCTION

Brick masonry building is one of the types of structures widely used for the public buildings in China. It suffered heavy damages during strong earthquakes happened during last twenty years. Brick masonry wall is the major member for the lateral force resistance. Under earthquake loading it in general damages at first, and this often leads to the collapse of the whole building. A great deal theoretical and experimental studies have been conducted on the aseismic behaviour of brick masonry members. It should be noted that most of the past works were focused on the behaviour of the masonry wall before ultimate loading and litter attention has been given to it's behaviour after the ultimate loading. In recent years with the development of the studies on the earthquake resistance the concept of designing according to two stages has been introduced in the aseismic design in many countries. With different earthquake intensities building should has associate earthquake resistance. The buildings aren't damage under weak earthquake and are not collapse under severe earthquake, the principle has been introduced in the chinese code of aseismic design. However, There isn't a complete method for brick masonry building design

^I Associate Research Professor, ^{II} Engineering, Institute of Engineering Mechanics, State Seismological Bureau, Harbin, China.

against collapse. In order to solving this problem, It is necessary to have a well understanding about the behaviour of the brick masonry wall not only before ultimate loading but also after that as well, the mechanism of collapse and the governing parameter effecting on the collapse etc.

On the other hand, under strong earthquake buildings are generally in the nonlinear state. The damage or collapse sustained by buildings are due to, besides unadequate of the ductility (strength), more often, relatively long duration of the strong shaking, under which the cumulative damage takes place in the structure material.

In the present paper the experimental study on the restoring force characteristics of the brick masonry wall for initial loading to collapse is described, the magnitude of deformation at collapse is given. Tests have been conducted for the energy cumulation of dissipation after entering the nonlinear state of the brick wall.

The test results provided the basis for the reliability analysis in the aseismic design of the building.

SPECIMENS AND TEST PROCEDURE

The dimensions of the specimens tested were determined on basis of the size of piers and transversal walls and the capacity of the test equipment. The dimensions of the specimen and the mechanical behaviour of the material used are listed in Tab.1.

The tests were performed on a pseudo-static machine. There were RC beams on the top and bottom of the tested wall. The bottom beam was fixed on the platform, while the top one was connected with the four-link mechanism (see Fig.1), through which the top boundary condition-moving horizontally without rotation under lateral loading is ensured.

During test the amplitude of the horizontal cyclic loading was increased stage by stage. The increasing of the load amplitude per stage was about 1 ton before cracking. After cracking the application of the loading was controlled by displacement.

For specimens used for studying the effect of cumulation of dissipative energy, the applied load approaching the initial cracking value (ie. at which the first crack appears) for specimens No.4, 9 and 10 was maintained without change and cycled with frequency of 0.05HZ until specimen failed. The amplitude of the cyclicloading assumed the value of the predicted ultimate load for specimens No.3, 6, 11, 12, 13, and 14 and the median value between the predicted ultimate load and initial cracking load for specimens No.5, 7 and 8. In order to simulate the actual normal stress in the walls of the base floor for a one to five-story masonry building, there were two hydraulic jacks on the top of the pier. The arrangement of the instruments is show in Fig.2. The displacement meters were used to measure the lateral translation of the top of the wall, and the strain gauges with long base to monitor the appearance of cracks.

TEST RESULTS AND ANALYSIS

a) Failure Characteristic

All specimens failed in shear. As the horizontal loading being below 40-60 percent of the ultimate shear force (P_u) the load-displacement relationship was essentially linear. With increasing the load the displacement increased more fast than the load did and the stiffness of the wall decreased significantly. When the applied load assumed 80-90 percent of the ultimate shear force inclined cracks appeared at first in the central portion of the wall, then they extended toward the corners of the wall and connected to form diagonal cracks. As soon as the applied load reached the ultimate value, the loading capacity of the wall decreased quickly and the displacement continuously increased. The wall was divided into four triangular blocks of mechanism by the extending diagonal cracks. At that time, the shear strength of the inclined cross sections of the wall was exhausted. The residual loading capacity was due to friction from vertical pressure. With increasing cycles the two lateral blocks displaced outwards and downward and rotated as well. Finally, as the lateral blocks were out of the wall plane the wall collapsed (see Fig.3). The failure pattern of the specimen was similar to that observed during earthquake.

b) The Hysteresis Envelops

The typical hysteresis curves are shown in Fig.4a¹⁰. In which Fig.10 for studying the effect of cumulative energy of dissipation. Hysteresis envelops are shown in Fig.5 in dimension-less coordinates P/P_u and Δ/Δ_u . From the hysteresis envelops four stages may be noted, they are

- 1, The linear-elastic stage associating with applied load ratio P/P_u being below about 0.5.
- 2, The elasto-plastic cracking stage associating with applied load ratio being in range of 0.5-1.0. At this stage the stiffness of the wall decreases significantly and inclined cracks appear in the central portion of the wall as load ratio assuming 0.8-0.9.
- 3, Failure stage under decreasing load which takes place after the applied load arrives at the ultimate value, the displacement increases with decreasing load.
- 4, Slip stage under friction. At this stage the loading capacity of the masonry wall is contributed due to friction between blocks formed by the extending diagonal cracks.

c) Loading Capacity and Deformability

The test results of the load-displacement relation of the specimens are summarized in Tab.1. It can be seen that the ratio of the

cracking load to the ultimate load is 0.87 on an average indicating that there is little strength potential after first inclined crack appearing. Before exceeding the ultimate load, the loading capacity decreased quickly until losing shear strength of the masonry wall. The friction force (P_f) is an important factor. The tests results show that the loading capacity of the brick masonry wall depends on the normal pressure (σ) acting on the wall, the mortar compressive strength (R) and the height-width ratio of the specimen (h/b) (as show in Fig.6-9, R_s and R_t are shear and principle tension strength of the masonry). The deformability of the wall is very low. The ultimate displacement is only about 3-5 mm. The ultimate shearing angle is $1/366$ in average. The values of the maximum slip under friction after the shear resistance in the inclined cross section was exhausted are listed in the last column of Tab.1. The displacement values (Δ_p) at the begining slip is about 7.9mm in average, the maximum displacement is about 1.9 cm/m in average when the wall collapses.

d) Behaviour of Cumulative Energy Dissipation (CED) of The Brick Masonry

For groups of specimen B-1, B-2, and B-3 the amplitudes of the applied repeated cyclic load when the tested wall approached the nonlinear state are different. Test results show that even though the load does not arrive at the ultimate value, the wall will fail due to excessive cumulation of the dissipative energy. In respect of CED and the cycle number of the load sustained by the wall before it's collapse the following preliminary viewpoints may be yielded.

1, the value (E_d) of CED for all tested specimens are presented in Tab.2, in which for specimens No.4&5 the load originally applied during test was higher than the specified value and then decreased to the associate specified value and cycled repeatedly (see Fig.10b). Thus specimens No.4 & 5 for which the wall was weakened by the extensive cracks, have relatively low CED value comparing with other specimens in the same group. Besides, for specimen No.6 the wall suffered some local damage during erection and high strength mortar has been used in repairing thus the stiffness of the wall increased and the CED value decreased slightly. Test results indicate that the CED depends on the amplitude of the applied load, the strength of the masonry wall (especially the mortar strength) and the normal stresses in the wall. Defining the CED after loading cycles N at a given load amplitude dividing by the CED associating with the initial cracking as the CED ratio (β), in Fig.11 the relationship between CED ratio and the load amplitude is presented and may be expressed as

$$\beta = 4.4(P)^{-4.09} \quad (1)$$

Where $P=P/P_u$ varying in range of 0.87 to 1.0. Expression(1) was obtained from test results of specimens NO.7 to 12 having normal stress and mortar strength not greatly different. Furthermore, we

can see that CED increases with increasing mortar strength and normal stresses by comparing specimens No.3 and No.14 with No.13.

2, The higher is the amplitude of the applied load, the less is the it's cycle number at which collapse takes place. The relation (as shown in Fig.12) between the load amplitude and its cycle number can be expressed as

$$N=2.47(P)^{-20.45} \quad (2)$$

Equ.(1) and (2) reflect the combined effect of the strength (deformation) and CED on failure of the masonry walls. With high amplitude of the applied load the main factor that influences upon the failure of the masonry wall is its strength (or deformability), with low amplitude of applied load is the CED instead, in intermediate cases, is the combination of the strength (or deformability) and CED.

e) Stiffness and Damping Ratio

Fig.13 and 14 are the illustration of the stiffness and damping ratio of the masonry wall. The equivalent stiffness of the masonry wall decreases with increase of deformation. The stiffness at cracking is about 40% of the initial value.

The damping ratio in elastic stage is about 5%, statistical analysis has shown that the following relationship between the equivalent damping ratio and the lateral deformation of wall can be expressed

$$\lambda = 0.055 + 0.009 \Delta$$

Δ -lateral deformation of wall, in mm.

CONCLUDING REMARK

From test results the following conclusion can be drawn.

1, Under horizontal cyclic loading the damage pattern of the masonry wall is in shear type, which is very similar to that observed during earthquake. From the hysteresis envelop four stages may be noted; elastic, elasto-plastic-cracking, failure under decreasing loading and slip under friction.

The shearing resistance of the masonry wall depends primarily on normal stress, strength of the masonry (especially the mortar strength) height-width ratio of the wall, and reinforcement ratio.

The deformability of the unreinforced masonry wall is very low. It's ultimate displacement and the ultimate shearing angle are about 4×10^{-3} and $1/366$ in average. The maximum slip at collapse is 1.4 cm/m .

2, As the masonry wall enters the nonlinear stage under the cyclic

loading the cumulation of the dissipation energy is one of the important factors leading to increase the damage cumulation and the failure extent. It should be considered appropriately in the earthquake resistant design of buildings.

3, The cycle number of the repeated loading which can be sustained by the wall before it's collapse depends on the load (deformation) amplitude and may be expressed as follows

$$N=2.47(P)^{-20.45}$$

The cumulative energy of dissipation relates to the amplitude of repeated loading (deformation), the strength of the masonry and the normal compression etc.

REFERENCES

- 1, R.L.Mayes, R.W.Clough "State-of-the-Art in Seismic Shear Strength of Masonry-An Evaluation and Review" 1975
- 2, R.L.Mayes, Y.Omate, R.W. Clough "Cyclic Shear Tests on Masonry Piers" Proc.of WCEE.
- 3, Zhu Bolong etc. "Experimental Study on Basic Behaviour of Brick Masonry under Reversed loading"
Journal of Tongji University, 1980, No.2
- 4, Wu Ruifeng etc. "The Failure Mechanism of Masonry Walls under Lateral and Vertical Loads" Journal of Dalian Institute of Technology, Vol.20, No.3
- 5, Xia Jingqian etc. "Experimental Study on Basic Mechanical Properties of Brick Buildings" Proceedings of US-Pro Bilateral Workshop on Earthquake Engineering. Harbin, China, 1982
- 6, M.Tomazevic etc. "The Effect of Horizontal Reinforcement on Strength and Ductility of Masonry Walls" Institute for testing and Research in Materials and Structures. Ljubljana, Yugoslavia. Report No.2, 1985

Table 2

Group No.	B-1				B-2			B-3				
	4	6	9	10	5	7	8	3	11	12	13	14
Specimen No.	29	39	47	59	17	19	21	4	1	1	1	1
Cycle number	38	52	53	70	23	40	34	12	7	12	13	11
Total number	46	105	414	374	50.5	171	108	384	45.9	131	174	237
C D E (t-mm)	7.7	10.9	9.5	7.6	4.4	6.6	8.2	5.5	4.6	3.8	8	10

- Note 1. "Cycle number" is referred to as cycles of the repeat load with specified value.
 2. "Total number" is referred to as the total cycles of the repeat load from the initial to the wall failure.

Table I

Group	Specimen No.	Specimen size (cm)	Mortar strength R_{s2} kg/cm ²	Normal stress 6 kg/cm ²	Ratio reinforcement μ %	Under initial cracking load			Under ultimate load			At beginning of slip			P_0/P_u	Δ/Δ_u	Ult. shear angle $\times 10^{-3}$	Max. slip cm/m	
						load	strength	displ.	load	strength	displ.	load	strength	displ.					
						P_c (t)	R_{s2} kg/cm ²	Δ_c (mm)	P_u (t)	R_{s2} kg/cm ²	Δ_u (mm)	P_s (t)	R_{s2} kg/cm ²	Δ (mm)					
A	1	224x145x24	23	1.25	0	6.0	1.10	2.70	7.0	1.28	4.49	3.7	0.68	10.3	0.86	0.60	3.10	2.20	
	2	224x145x24	50	2.84		14.5	2.66	3.00	17.7	3.25	4.62	8.0	1.47	6.00	0.82	0.65	3.19	1.16	
	3	224x145x24	45	2.84		12.0	2.21	2.01	14.8	2.71	3.84	9.5	1.85	10.4	0.81	0.52	2.65	1.25	
	11	112x150x24	11.3	4.20		5.1	1.90	2.30	5.8	2.14	4.49	4.2	1.56	6.85	0.88	0.51	3.00	2.70	
	12	112x150x24	11.3	4.20		5.5	2.05	2.13	5.9	2.19	2.82	4.5	1.67	8.52	0.93	0.76	1.90	2.53	
	13	112x148x24	16.4	3.20		5.5	2.05	2.48	6.2	2.31	4.56	5.4	2.01	7.60	0.89	0.54	3.10	2.12	
	14	112x148x24	18.4	5.20		6.8	2.53	2.25	7.5	2.77	3.23	5.8	2.16	5.57	0.91	0.70	2.18	1.31	
Average value															0.87	0.61	2.73	1.9	
B	4	112x148x24	21	4.20	0	5.1	1.90	0.83											
	5	112x148x24	47.6	4.20		7.0	2.60	1.76											
	6	112x148x24	20	4.20		5.9	2.2	0.86											
	7	112x148x24	12.1	4.20		6.2	2.29	2.77											
	8	112x148x24	18.9	4.20		5.3	1.97	1.83											
	9	112x148x24	11.3	4.20		5.2	1.93	2.63											
	10	112x148x24	11.3	4.20		4.5	1.69	1.77											

Note 1. The value of load(displacement) listed in the table is the average value of the push and pull loads(displacement)
 2. The strength of brick is 75kg/cm²

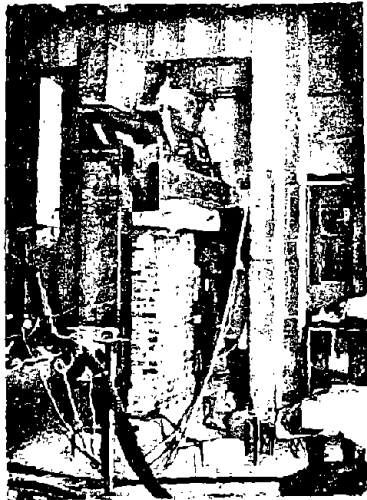
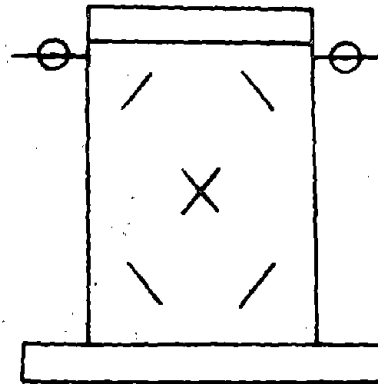


Fig.1 Test set-up

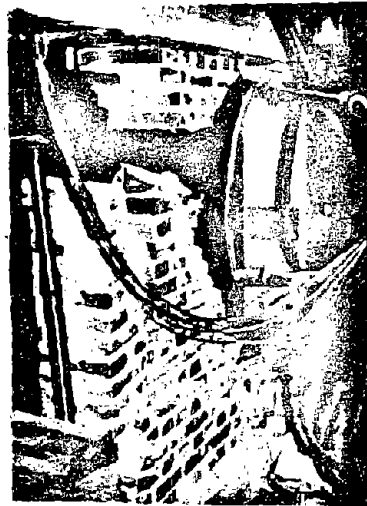


— Strain gauge
 ⊖ Displ. meter

Fig.2 Arrangement of instruments

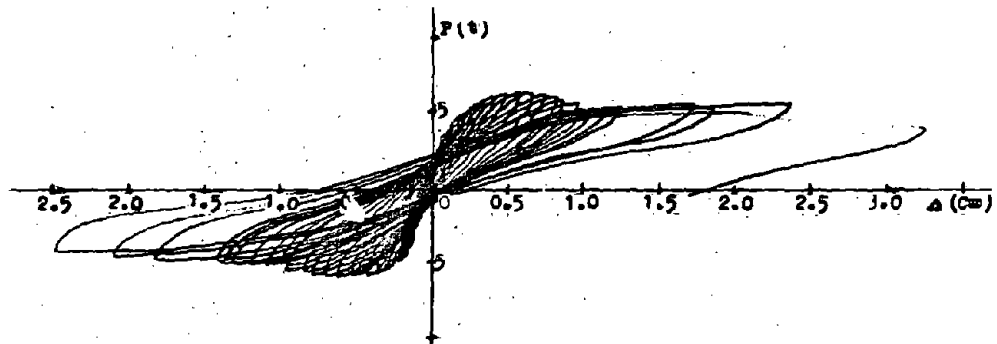


(a)



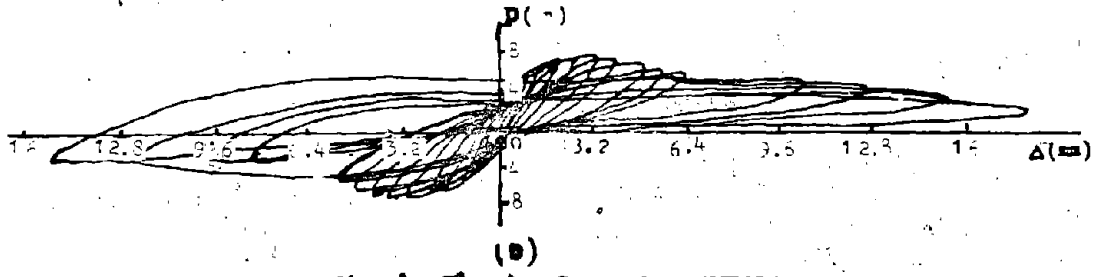
(b)

Fig.3 Crack pattern of unreinforcement wall



(a)

Fig.4 The hysteresis curves



(b)
Fig. 4 The hysteresis curves

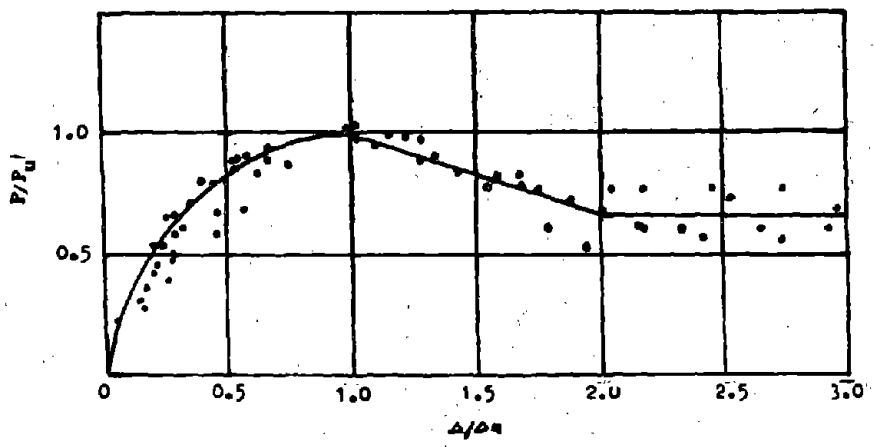


Fig. 5 Hysteresis envelop diagram

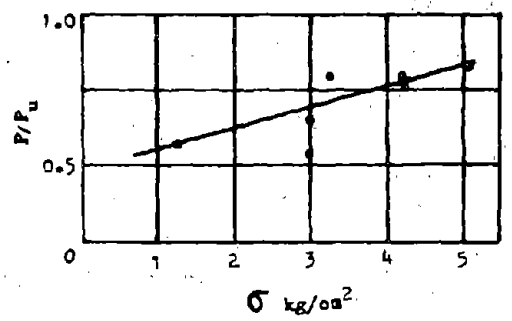


Fig. 6 Compressive stresses versus slip loading

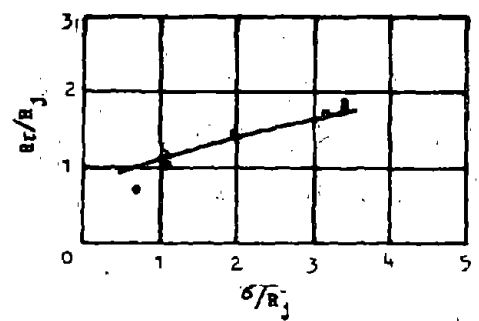


Fig. 7 Compressive stresses versus shear stresses

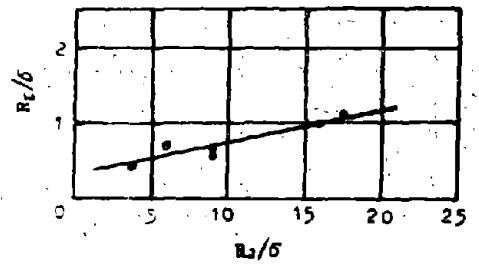


Fig. 8 Mortar stress versus shear stress

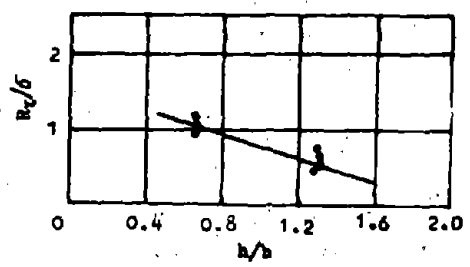


Fig. 9 High-width ratio of the wall versus shear stress

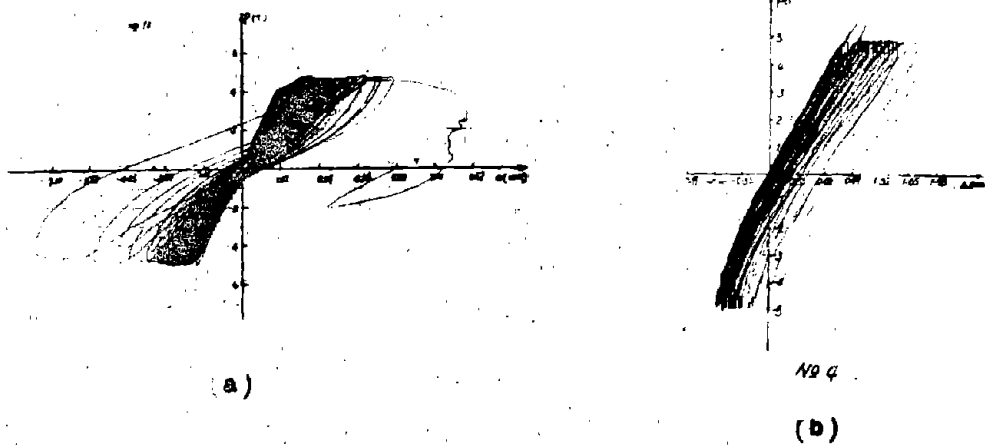


Fig.10 The hysteresis curves

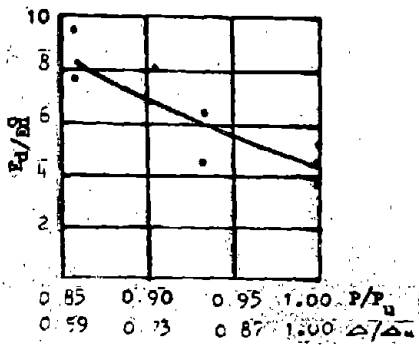


Fig.11 Dissipation energy ratio versus load(displacement) curve

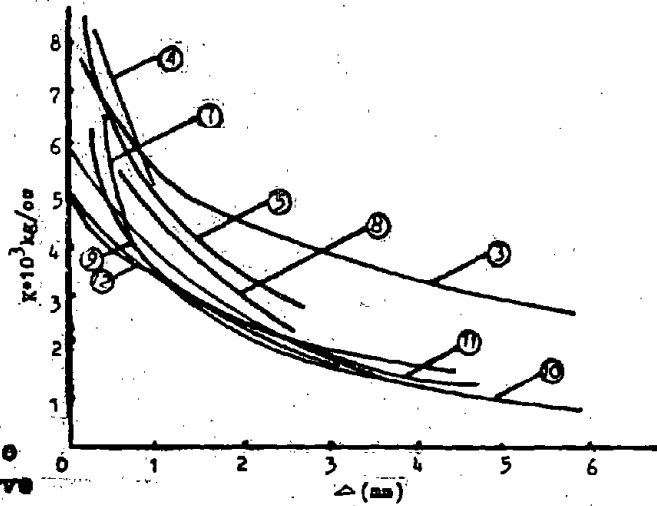


Fig.13 Stiffness degradation versus displacement

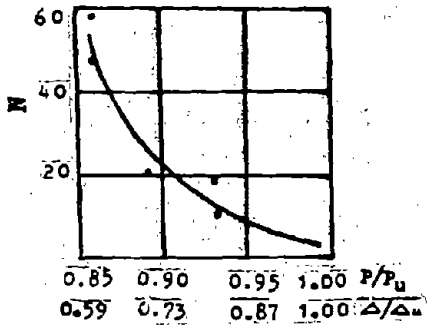


Fig.12 Cycle number versus load(displacement) ratio

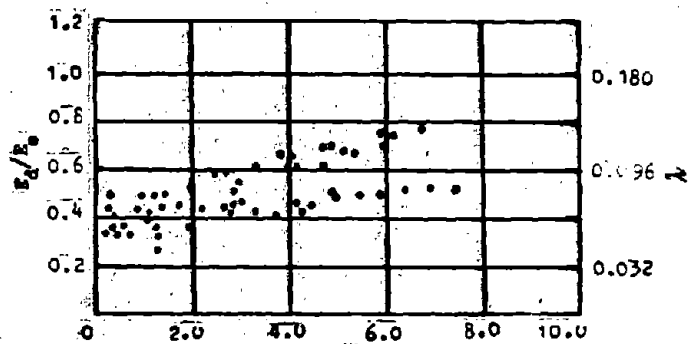


Fig.14 Energy and damping ratio versus displacement

FACTORS AFFECTING DAMAGE OF MULTISTORY BRICK BUILDINGS AND THEIR STRENGTHENING TECHNIQUES

Ye Yaoxian^I

ABSTRACT

The paper is divided into three parts. According to lessons learned from strong earthquakes which have occurred in China since 1960's, the factors affecting damage to multistory brick buildings, such as earthquake intensity, site soil condition, bearing wall system, floor structure, building configuration, building height, ring beam system, spacing of transverse bearing walls, and moderate ratio of wall cross section area to floor area, are described in the first part. The strategy and techniques of strengthening existing multistory brick masonry buildings are presented in the second part of the paper. Finally, some conclusions and comments are cited for reference.

INTRODUCTION

The strong earthquakes occurred in China and abroad show the greatest sources of life and property loss comes from highly vulnerable, poorly designed and poorly constructed buildings. It has long been recognized that unreinforced brick masonry buildings are highly vulnerable and highly hazardous. However, because of simplicity in structure, convenience in construction, cheapness in building cost, fire-proofing, heat and cold proofing, durability, and easy acquirement of materials, the unreinforced brick masonry multistory buildings are widely used in China. They are mainly used for civil and public buildings, such as housing, office buildings, school buildings and hospitals etc.

According to recent statistical figures, the investment of buildings covers nearly 70% of the total investment for construction and installation works. The housing, industrial buildings, and public buildings cover 60%, 14%, and 13% of the building construction respectively. In the coming 15 years, about 150 million square meters of urban housing and 800 million square meters of rural housing are expected to be built per year. Brick masonry bearing wall system is adopted for most of the above mentioned buildings. Therefore, identifying factors affecting damage and developing strengthening techniques are urgently needed for seismic design and seismic strengthening.

I. Director and Senior Engineer, China Building Technology Development Centre, 19 Che Gong Zhuang Street, Beijing, The People's Republic of China

FACTORS AFFECTING DAMAGE

The main factors contributing to the damage or collapse of a building have been the earthquake effects, including both physical and sociological effects, building design, and building construction quality. The physical earthquake effects depend upon many parameters, including intensity and duration and frequency content of ground motion, magnitude of an earthquake, geologic and soil condition, location and depth of focus. The sociological earthquake effects are dependent upon many factors, such as density of population, time of day of the earthquake occurrence and community preparedness for the possibility of such an event.

The design must be such as insure that the building has adequate strength, high ductility, and will remain as a unit, even while subjected to very large deformation. Up to now we can do little to diminish earthquake hazards, however, we can do much to reduce risks and thereby reduce disasters provided we design and build or strengthen the buildings so as to minimize the losses based on the knowledge of the earthquake performance of different building types during an earthquake. Therefore, the study of factors affecting damage provides an important step in seismic safety of a building.

Earthquake Intensity

The damage percentage of multistory brick buildings versus earthquake intensity is listed in Table 1, and shown in Fig.1. The statistics are based on observation of China's destructive earthquakes occurred since 1960's. It follows that:

- No damage and slight damage are found in the area with earthquake intensity of VI, VII, and VIII.
- Severe damage is mostly found in the IX intensity area.
- In the area with intensity of X and above, most of the unreinforced brick masonry buildings are expected to collapse.

Therefore, In the area with intensity IX and above, the brick building should be reinforced.

Site Condition

The site condition significantly effects on the building damage. The site is know as a wide range of strata surrounding a building. The site effect mainly caused by the differences in its geotectonic condition, soil condition and topography.

The geotectonic condition mainly means the faults. The buildings situated along both sides of the causative fault are expected to be severely damaged or collapsed. Non-causative faults have no signifi-

cant effect on building damage. Therefore, the current idea is that the causative fault zones are dangerous to a building in the point of view of earthquake resistance, and structures in or near such zones are not recommended. Fig.2 shows the relationship between intensity and distance from building site to fault based on the observed data in China's earthquakes.

As regards soil condition, earthquake studies have almost invariably shown that the intensity of a shock is directly related to the type of soil layers supporting the buildings. Buildings built on solid rock near the epicentre of an earthquake frequently fare better than more distant buildings on soft ground. Comparing with ordinary soil condition, the damage of buildings built on rock or thin covering soil is lighter than those built on thick alluvial soft soil and the soil in the bearing layer with a soft and hard distribution. The field observation and research work show that only the potential liquefied sand soil with depth less than 15-20m underground has appreciable effect on building damage.

The topography of a building site has an effect on its damage. The building built on the site with open and even topography were slightly damaged in an earthquake. The buildings on strip-shaped hill ridge, separated high hillock, and non-rock steep slope were severely damaged. And the buildings built on the site where landslides, landslips and cave-ins or settlement of ground might be occurred in earthquake were usually destroyed.

Bearing Wall System

Fig.3 shows the damage percentage distribution of 87 unreinforced brick masonry multistory buildings with different bearing wall systems based on statistical data observed in the 1975 Haicheng earthquake. It follows that the transverse bearing wall system is much better than either the longitudinal system or the longitudinal and transverse system.

Floor Structure

The reinforced concrete, wood and brick arch floor structures are commonly used for brick buildings. Fig.4 illustrates damage percentage distribution effecting different types of floor structures based on 1976 Wulumuqi and 1976 Tangshan earthquakes. Fig.5 shows collapse percentage vs. number of story for 748 brick masonry buildings with different types of reinforced concrete floor structures in Tangshan city during the 1976 event. It follows that:

- In VII intensity area, the damage percentage distribution are independent on the types of floor structure.
- In X intensity area, the buildings with wood slabs are more vulnerable than that with reinforced concrete slabs.

- For cast-in-situ reinforced concrete slabs, the collapse percentage increases with the number of building story. For prefabricated reinforced concrete floor slabs, however, there is a small change in collapse percentage.
- For the buildings with three story and above, collapse percentage for cast-in-situ R/C floor slab buildings is higher than that for R/C prefabricated floor slab buildings.

Building Configuration

The building configuration including building plan and building elevation, is an important factor affecting damage to a building. The building with round plan and less height have a good behaviour for earthquake resistance. The building with irregular plan may not worse than that with regular plan, since the different parts of the building may support each other for resistance. Therefore, for non-engineered construction, it may be beneficial to separate a building into several units of simple shape in plan by seismic joints in design for mild and moderate earthquake, since the cost for repair can be decreased. In design for strong earthquakes, however, separating a building into several units not only needs more funds but also may be disadvantageous to hold the building during an earthquake.

The buildings with simple elevation shapes have the great chance of survival and the influence of the elevation shape on building's earthquake performance is greater than that of the plan shape.

The facade outstanding parts of a building, either facade setback or penthouses, are vulnerable in an earthquake. Let W_1 and W_2 denote the lumped weights of the main building and the setback respectively. The lateral load applied to the weight W_2 can be calculated by the following formula:

$$P_2 = P_1 (1 + \sqrt{W_1/W_2}) / 2$$

Where P_1 denotes the lateral load applied to the weight W_2 as if the setback directly stands on the ground. Since W_1 is much greater than W_2 , the P_2 is much higher than P_1 . That is why the outstanding part is very apt to damage or collapse.

Building Height

The damage and collapse percentage are increased with the building height. Fig.6 shows moderate damage percentage vs. building story obtained from 1975 Wulumuqi earthquake observation. The figures 5 and 6 tell us the higher building, the greater damage percentage. Therefore, the building height of brick building should be limited.

Ring Beam System

"Tie the building together" is a very important rule for seismic design. In brick buildings, they can be made safer by joining the parts with ring beams. Almost all structural failures during an earthquake have occurred at weak connections, that is connections where the members were not properly tied together.

The earthquake's experiences show that:

- In the same intensity area, damage to buildings with ring beams is slighter than that without ring beams.
- The closer ring beams, the better performance of a building in an earthquake.
- Ring beam at roof level is more efficient than that at floor level.
- Reinforced concrete ring beams are better than reinforced brick ring beams
- For the place of ring beams, the closer to floor slab, the better performance of the building in an earthquake.

Spacing of Transverse Bearing Walls

The damage to longitudinal brick walls is closely related to the spacing of transverse bearing walls and to the type of floor and roof structure. The greater spacing of transverse bearing walls, the smaller rigidity of floor and roof structures, the severer damage to longitudinal walls. For the building with precast reinforced concrete floor and roof slab in VII intensity, when the spacing of transverse walls is greater than 16.5m, the longitudinal walls are expected to be damaged. Therefore, the spacing of transverse bearing walls should be limited.

Moderate Ratio of Wall Cross Section Area to Floor Area

Fig.7 shows the relationship between moderate ratio of wall cross section area to floor area for first floor and building damage (α_1). For 1th story, we have:

$$\alpha_1 = \left(\sum_j A_{1j}^n \cdot R_j / A_1 \right) \cdot 10^4$$

Where

- α_1 --- Moderate ratio of wall cross section area to floor area
- A_{1j}^n --- Net cross section area of jth wall in 1th story
- R_j --- Shear strengthen of mortar
- A_1 --- 1th floor area

It follows that the greater α , the better earthquake performance of a building.

STRENGTHENING STRATEGY AND TECHNIQUES

Strengthening Strategy

The existing strengthening strategy is to identify:

- Critical cities or regions where strengthening existing structures is urgently needed.
- Critical enterprises for which function loss due to earthquake damage will cause heavy life or/and property loss.
- Critical buildings, for which damage or collapse will cause serious life loss or/and property loss, and
- Effective and economic strengthening procedures.

Strengthening Techniques

Based on the research work and practical experiences from recent earthquakes, seismic strengthening techniques for various types of buildings have developed and brought into practice. Especially, most of the techniques had experience of the earthquake occurred in the recent years. The comparison of relative earthquake performance for strengthened, repaired and unstrengthened buildings shows that there is great benefit in seismic strengthening of existing buildings.

The aim, techniques, and elements of strengthening are shown in Fig.9.

CONCLUSION AND COMMENT

1. The brick buildings situated in the area with intensity VIII and above should be reinforced.
2. There are many factors affecting damage to brick buildings including earthquake intensity, site soil condition, bearing wall system, floor structure, building configuration, building height, ring beam system, spacing of transverse bearing walls, and moderate ratio of wall cross section area to floor area etc. While design and strengthening a brick building, all the above mentioned factors should be considered.
3. To strengthen existing buildings, one has to start with consideration of increasing earthquake resistant capacity of the whole building, and should never just strengthen the damaged items or even only strengthen the buildings without comprehensive analysis.

4. While strengthening a building, appropriate strengthening techniques should be selected.

REFERENCES

1. Liu Dahai and el. Earthquake Resistant Design of Buildings, 1985 (in Chinese)
2. Yang Yucheng and el., Earthquake Damage and Design of Multistory Brick Buildings, 1981 (in Chinese)
3. Ye Yaoxian, Project Progress Report, MURCEP group of China's side, First Joint Workshop, PRC-USA Joint Research Project on Risk Analysis and Seismic Safety of Existing Buildings, Beijing, China, Sept., 25-27, 1985
4. Ye Yaoxian, Earthquake Performance of Strengthened Structures, Proceedings of US-PRC Bilateral Workshop on Earthquake Engineering, Vol.I, pp. c-6-1--c-6-19, 1982, China
5. Ye Yaoxian, Performance of Building During Earthquake, Chapter 2, IAEE book "Basic Concepts of Seismic Codes", Part II "Nonengineered Construction", 1985

TABLE 1 DAMAGE PERCENTAGE VS. INTENSITY FOR BRICK BUILDINGS

Damage Category	Earthquake Intensity				
	VI	VII	VIII	IX	X
No damage	45.9	40.8	37.2	5.8	0.8
Slight damage	42.3	37.7	19.5	9.1	2.5
Moderate damage	11.2	12.2	24.8	24.7	5.6
Severe damage	0.6	8.8	18.2	53.9	13.0
Collapse	0	0.5	0.3	6.5	78.6
Total number of buildings	501	613	379	154	1187

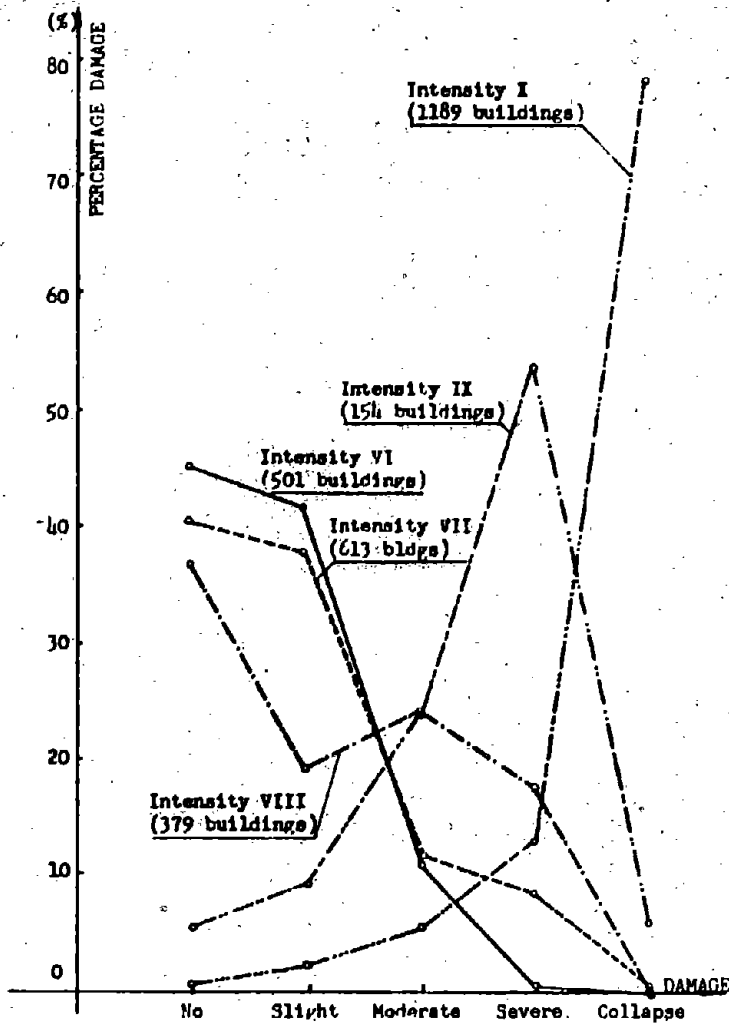


Fig.1 Damage percentage distribution for various earthquake intensity

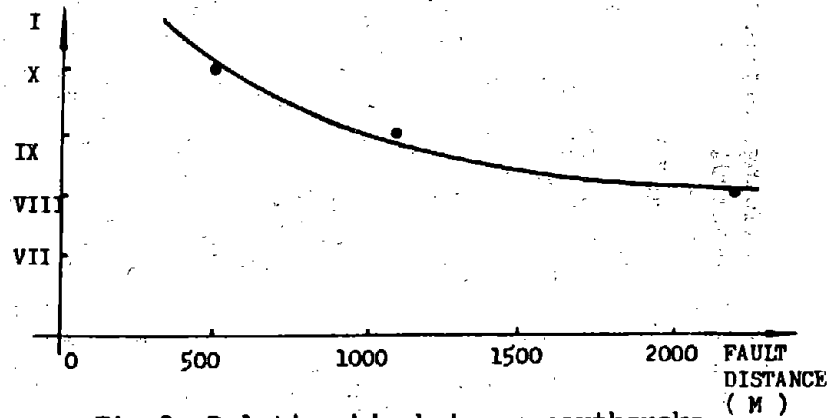


Fig.2 Relationship between earthquake intensity and fault distance

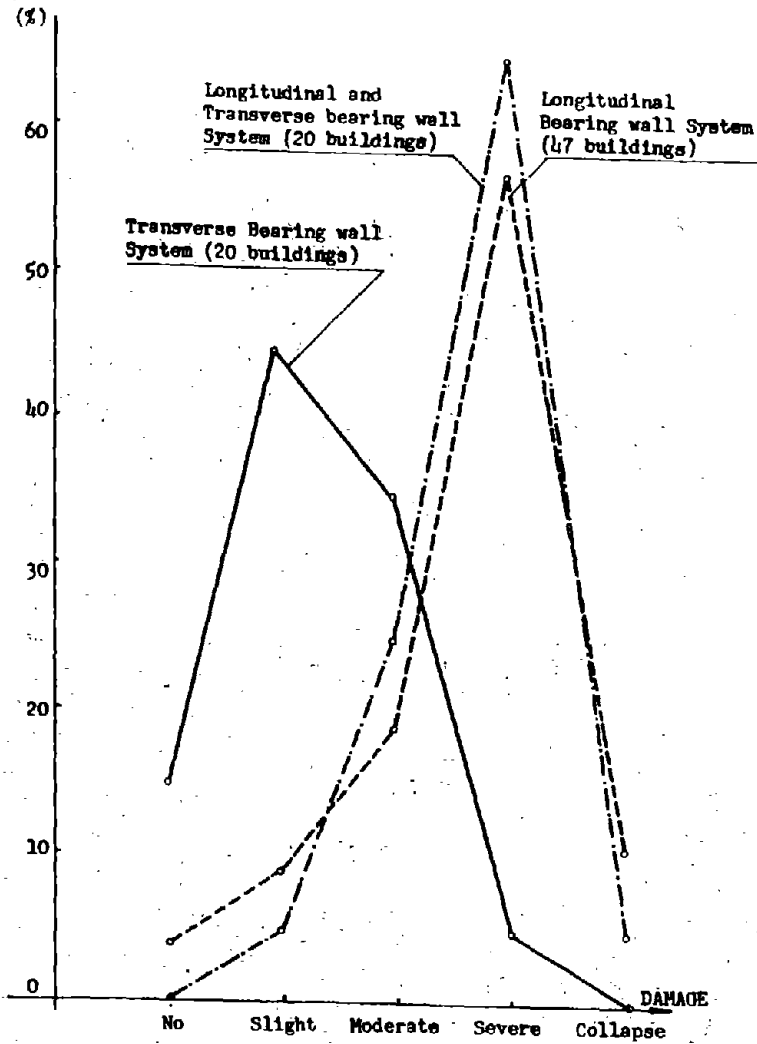


Fig.3 Damage percentage distribution of brick buildings with different bearing wall systems

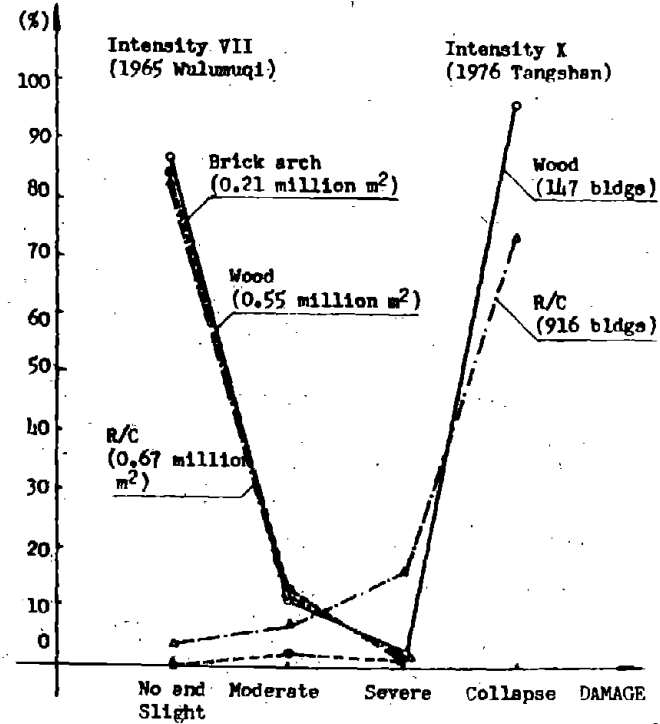


Fig.4 Damage percentage distribution effecting on floor slab category

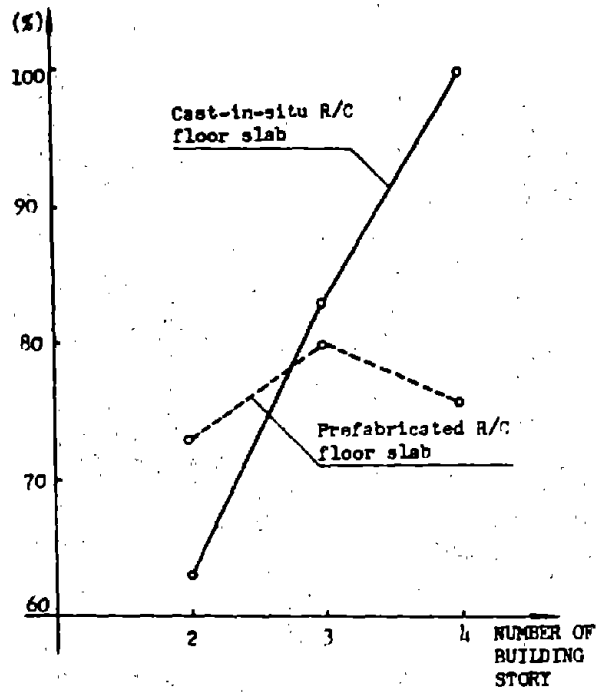


Fig.5 Collapse percentage vs. number of story of brick buildings with cast-in-situ and prefabricated R/C floor structures

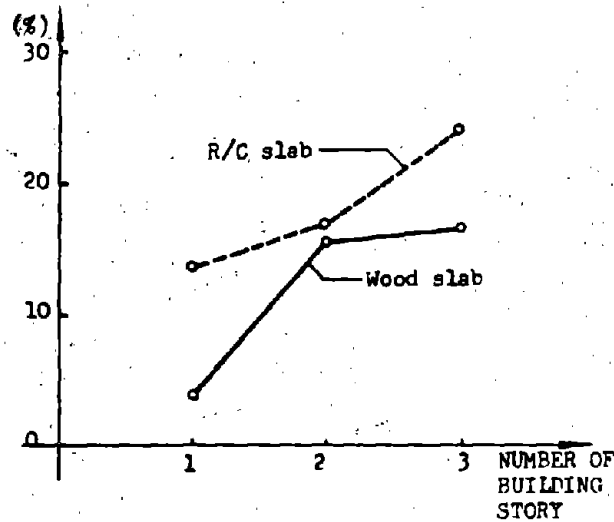


Fig.6 Moderate damage percentage vs. building story number

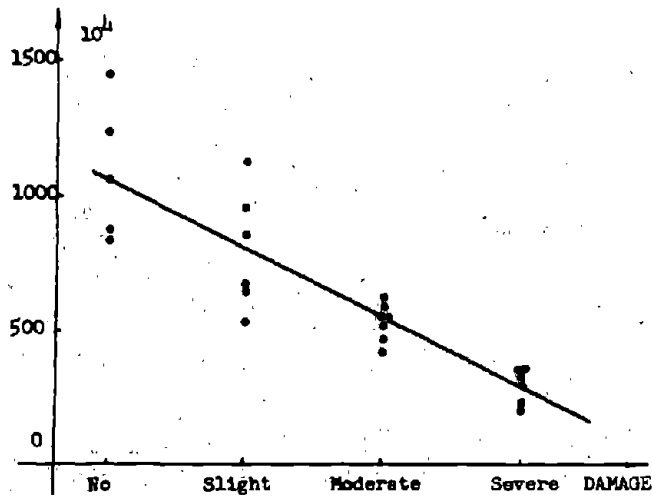


Fig.7 Relationship between moderate ratio of wall cross section area to floor area (.) and damage (intensity VII)

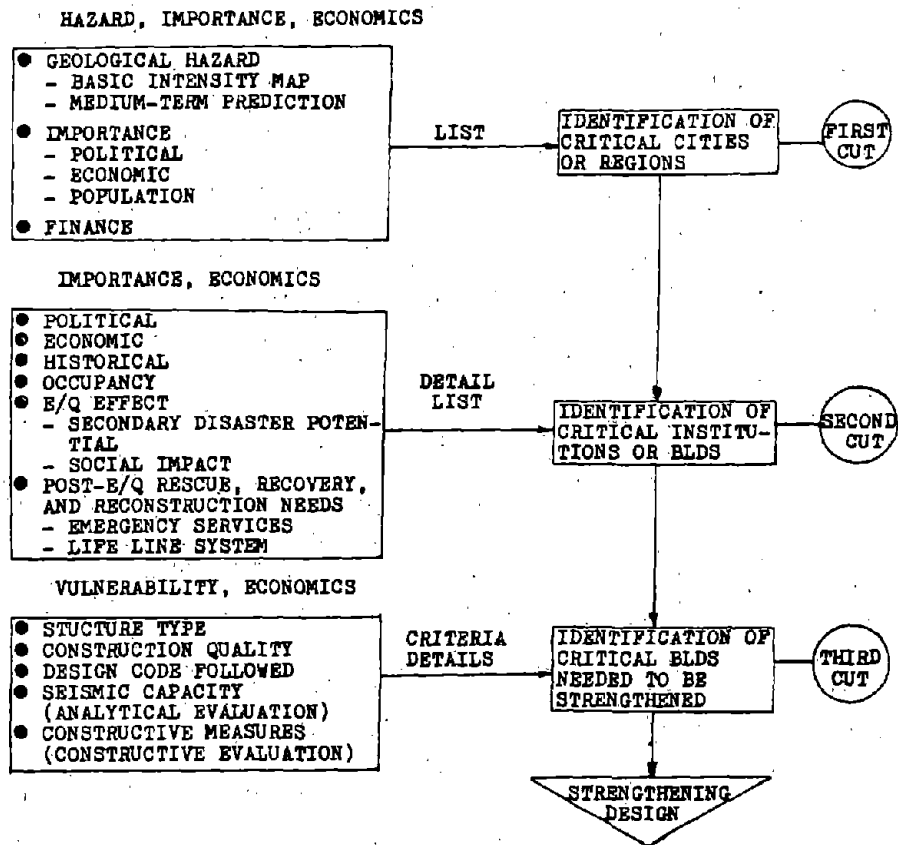


Fig.8 Flow chart of strengthening existing buildings

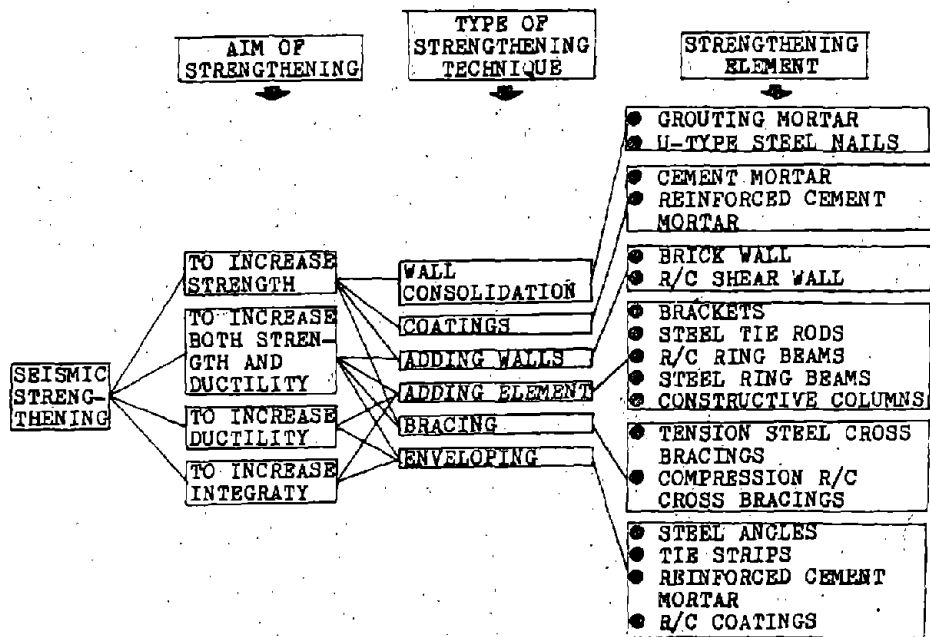


Fig.9 The aim, techniques, and elements of strengthening existing buildings

III BEHAVIOR OF BLOCK MASONRY STRUCTURES

RESISTANCE OF CONCRETE MASONRY BUILDING SYSTEMS TO LATERAL FORCE

by

Daniel P. Abrams¹

SUMMARY

A two-story test structure is constructed at full scale to study resistance of concrete masonry building systems to lateral forces. The specimen is reinforced and partially grouted in accordance with provisions of the recently revised 1985 Uniform Building Code. It is planned to subject the structure to a series of slowly applied reversals of deflection until it collapses, or suffers a severe loss of strength. In addition, low-amplitude dynamic response will be measured under ambient and forced vibrations. Results from the study will help (a) verify current building code provisions, (b) establish hysteretic force-deflection relations for response evaluations of actual buildings, and (c) examine the suitability of representing dynamic response with both numerical, and reduced-scale physical models.

INTRODUCTION

The capability of a building system to resist gravity forces is tested with the construction of every structure. However, the capacity of a system to resist lateral forces remains uncertain for nearly all buildings because severe wind or earthquake events seldom occur. Laboratory test data is available on the strength and behavior of masonry materials and subcomponents such as individual walls or piers. However, knowledge of how the entire system reacts lateral force is necessary for the safe and economical design of new construction as well as the strengthening of existing structures.

¹Associate Professor of Civil Engineering, University of Illinois at Urbana-Champaign, USA.

This paper describes a research program in which the lateral-force resistance of a reinforced concrete masonry building system is investigated. A two-story test specimen is constructed within a laboratory environment, which will be subjected to slowly applied reversals of lateral force until failure occurs. In addition, a series of low-amplitude dynamic tests will be done to study dynamic characteristics.

The research program has several objectives: each with the overall intent of understanding the response of a building system to strong lateral forces. Each objective is itemized below.

Verification of Building-Code Provisions

The first objective of the test program is to question the applicability of present building code specifications for seismic resistance. Recently developed code provisions conflict former ones, yet little if any experimental data on system response is available for verification of new or old specifications. The test structure was designed in accordance to the most recent masonry code for seismic effects, Chapter 24 of the 1985 Uniform Building Code.

Identify Hysteretic Behavior of Building System

The second objective of the test program is to identify resistance mechanisms for a typical masonry system under large-amplitude reversals of lateral deflection. Knowledge of hysteretic behavior is essential for estimation of the dynamic response of a building system to excitation due to high winds or strong ground motion. Measured force-deflection relations are also necessary to verify the accuracy of numerical models which incorporate material and component properties to compute system response.

Reference for Reduced-Scale Physical Models

The third objective is to establish a reference for developing reduced-scale models that can replicate behavior of full-scale construction. In the future, a counterpart specimen will be fabricated at one-quarter scale and forced through a similar history of lateral deflection as the large-scale specimen. Through correlations of observed damage and measured relations of base shear and top-level deflection, the validity of reduced-scale physical models may be ascertained. Modeling practices may then be altered if needed to mimic that of the prototype. Reduced-scale test structures may then be shaken at true dynamic rates using an earthquake simulator. Shaking-table testing is necessary to examine response under rapidly changing distributions of lateral force with progressive damage, and strain-rate effects.

Reference Data for Calibration of Evaluation Techniques

The fourth objective of the test program is to provide reference data for calibration of methods used to measure the strength or behavior of new and existing structures. Substudies include investigations of the reliability of test methods to estimate ultimate strength or performance under strong excitations. Such methods which will be studied include (a) the use of test prisms to reflect shear and flexural strengths of walls and systems, (b) the use of ambient vibration tests to reflect modal frequencies and shapes for large-amplitude vibrations, (c) the use of strain-gages applied at selected locations to reflect the stiffness and strength of a system, and (d) other methods of nondestructive test evaluation.

CURRENT SEISMIC CODE PROVISIONS

The most recently revised document for structural masonry is Chapter 24 of the Uniform Building Code (UBC, 1985) which represents a substantial modification from the earlier UBC specification. The test structure was designed in accordance with this document.

An alternate set of specifications was published by the Applied Technology Council (ATC, 1978, Chapters 12 and 12A). These provisions were published solely on a tentative basis and are still under review by the profession for acceptance. However, because these chapters represent the latest developments in seismic masonry construction before 1978, they are used to contrast those of the recently revised Uniform Building Code, and to help illustrate possible variances in structural designs.

A summary of selected design specifications is shown in Table 1 for the 1985 UBC and the 1978 ATC. Only those sections of each code are shown which are pertinent to the design of shear wall structures that are reinforced for flexure with conventional deformed steel bars, and for shear with joint reinforcement only. This type of construction was chosen because of the high cost of placing horizontal reinforcing bars through block and associated difficulties with horizontal grouting.

Both codes state that joint reinforcement may be used to meet minimum reinforcing requirements, however, they differ on its role in resisting shear. The ATC states that joint reinforcement "shall not be considered in the determination of the strength of the member." However, the UBC states, "The portion of the reinforcement required to resist shear shall be uniformly distributed and shall be joint reinforcing, deformed bars, or a combination thereof."

Table 1
Comparison of Code Provisions for Reinforced Walls

<u>Item</u>	<u>ATC¹</u>	<u>UBC²</u>
1. Minimum percentage of reinforcement		
For shear walls:		
vertical or horizontal	0.0015	0.0007
sum in both directions	0.0030	0.0020
For running bond if all shear taken by reinforcement:		
vertical or horizontal	0.0007	same
sum in both directions	0.0020	
2. Role of joint reinforcement in resisting shear	no	yes
3. Allowable shear stress		
Reinf. taking no shear		
For shear walls with inspection		
M/Vd > 1	$0.9*(f'_m)^{0.5} < 40\text{psi}$	$1.0*(f'_m)^{0.5} < 35\text{psi}$
M/Vd = 0	$2.0*(f'_m)^{0.5} < 50$	Equation 1.1
4. Boundary elements		
Effective width of flange for C-shaped walls	1/16 times wall height or 8 times thickness	6 times wall thickness

Notes:

1. Seismic Category "D"

2. Seismic Zones "3" and "4"

Eq. 1.1 $F_v = (1/3)*(4-M/Vd)(f'_m)^{0.5} < (80-45M/Vd) \text{ psi maximum}$

Allowable shear stresses are similar for UBC and ATC whether shear reinforcement is provided to resist all of the shear or not. However, the interpretation of the role of joint reinforcement is a key difference between code provisions. Lightly stressed walls designed by UBC may have much larger allowable shear stresses (more than double that for unreinforced in shear) because all of the shear may be assigned to joint reinforcement. For walls with amounts of shear in excess of joint-reinforcement capacity, deformed bars must be added and then both codes tend to agree.

Under the ATC, if reinforcement does not resist the entire shear (which would normally require horizontal deformed bars), then the minimum percentage of steel is limited to 0.15% in both directions. Under UBC, this value is cut in half provided that the sum in both directions is less than 0.20%. A typical design with this percentage would be No. 4 bars (0.5 inch diameter) at 16-in. spacing (every other cell) vertically, and No. 9 gage wire for joint reinforcement in every other course. With the ATC, slightly more vertical steel is required, but horizontal steel should be doubled.

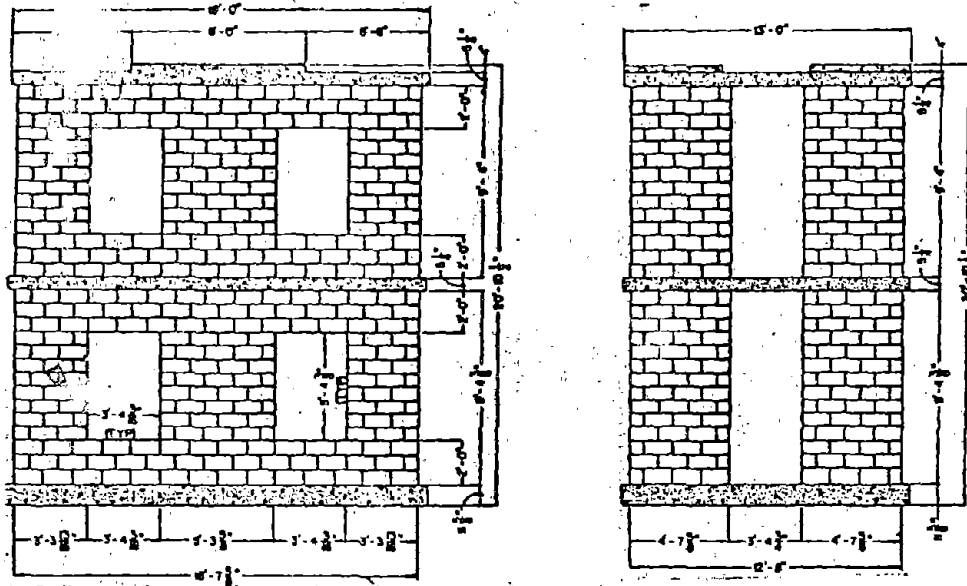
There is a difference in effective widths of compressive flanges for boundary elements. The ATC limits the width to 1/16 of the height of wall above the section under consideration. The UBC has no such limitation. For a two-story building, the width of effective flange is limited to 15 inches by ATC as contrasted with 48 inches by UBC.

SPECIMEN DESCRIPTION

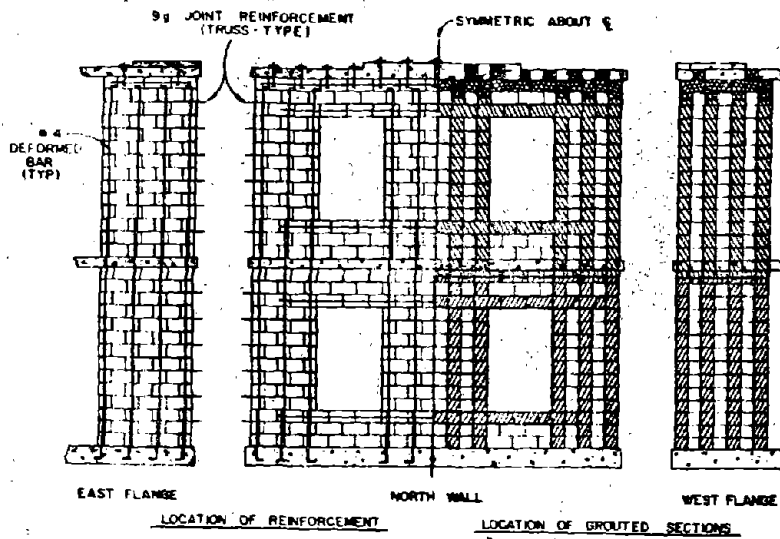
Layout and Design

A sketch and a photograph of the test specimen are shown in Figs. 1 and 2. The test structure represents the lower two stories of a three-story building. Lateral forces are applied at the second (or top) level which is approximately where the centroid of lateral force would be for the prototype.

The structure is comprised of two C-shaped walls that are connected with relatively stiff reinforced concrete slabs at each of the two levels. The precast slabs are 6.0 inches thick and tied to the walls with reinforcement and grout. The system is symmetrical about each plan axes. The webs of the walls are placed parallel to the direction of lateral force, and are perforated with window openings. The layout of openings was chosen so that the central pier would be square, and the width of the exterior piers would be one-half that of the central pier. The number of courses per story (14) was chosen to have three courses above and below the openings. The width of the flanges is three units (4'-0") which represents the UBC provision of six times the nominal wall thickness.



(a) overall dimensions



(b) reinforcement

Fig. 1 Description of Test Structure

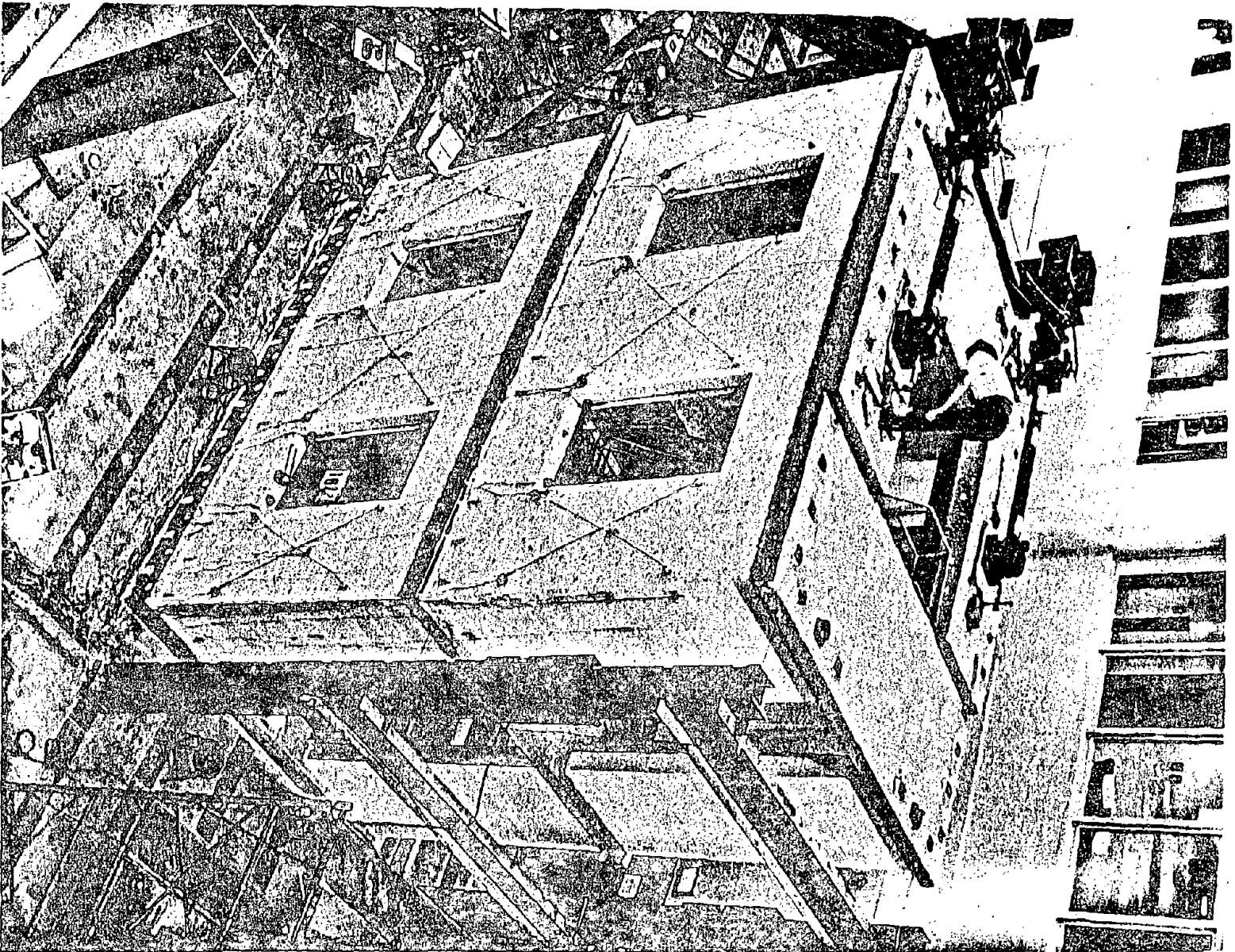


Fig. 2 Test Structure

III-1-7

Vertical reinforcement consists of No. 4 deformed reinforcing bars at 16-inch spacing, or one bar in every other cell (percentage of gross area equal to 0.125%). Horizontal reinforcement consists of one No. 2 deformed bar above and below each window opening (with an extension of 2'-0" past the opening), and No. 9 gage wire ladders in alternate bed joints. The total area of horizontal reinforcement divided by the nominal gross section is 0.112%. Bond-beam units are provided for each horizontal deformed bar.

The structure is supported on a reinforced concrete grade beam which is bolted to the test floor. Dowels project from the beam to provide a 2'-0" lap with vertical wall reinforcement. Bars run vertically through 4-in. diameter holes in the first-level slab, and extend 2'-0" from the top of the slab. Second-story bars extend to the top course which is a continuous bond beam with one No. 4 bar and filled with concrete. Bolts are embeded in this course which are used to connect the top slab.

Lateral forces are applied through the top-level slab which acts as a diaphragm in distributing forces to each wall. Keeping with the symmetry of the test specimen, hydraulic actuators are mounted to the slab at its centroid in the longitudinal direction. Steel "shoe" plates are grouted within recesses in the slab for transfer of lateral force. The slab thickness is built up to 10-inches in this region.

Fabrication

Masonry construction was done by a crew of professional masons. Block for the first story was layed in a day and a half. After lifting the first-level slab from its casting location on the test floor, and positioning it on the blockwall, vertical reinforcing bars were placed and the first story was grouted up to midheight of the top course. Two weeks later, masons returned to lay second-story block which took one day. The second story was grouted the following day up to the midheight of the second course from the top. Grout was poured from buckets by hand, and then vibrated. The second-level slab was lifted and placed on top of the walls. Concrete was placed and vibrated in the top-course bond beam through 4-inch holes in the top slab.

Materials

Concrete block, and mortar and grout materials were obtained from a local supplier. Mortar was Type S. Mortar was mixed in a paddle-type mixer which was borrowed from a masonry construction firm. Grout was mixed using the laboratory concrete mixer with 1 part cement, 3 parts sand and 1.5 parts pea gravel (3/8-inch maximum

aggregate). Water was added until the slump reached 8 to 10 inches. An expansive agent was added to the grout to compensate for shrinkage and insure good bond with reinforcement.

Sample prisms are tested as well as test cylinders of mortar. Grout samples are cast against block units and absorptive paper. Each coupon is tested in uniaxial compression. Samples of reinforcing bars are tested in uniaxial tension.

TEST APPARATUS AND EXPERIMENTAL PLAN

Force Application

Lateral forces are applied to the top-level slab using two hydraulic actuators, each with a force capacity of 110,000 lbs. or 500kN. Each ram is controlled electronically so that displacements may be varied at a uniform rate. In this manner, the test structure may be swayed back and forth, not in the precise deflection history as would occur during some particular base motion, but with sufficient variation to depict the generalized hysteretic relation between force and deflection.

Because of limitations with hydraulic flow capacity of the distribution system, and servovalves, the test specimen is deflected at static rates. Inertial forces are negligible because of the very slow accelerations, however, the test is still valid for identifying mechanisms intrinsic to the transfer of lateral force. The rams simulate the total base shear with a crude lateral-force distribution, however, the moment-to-shear ratio at the base is modeled. Once the hysteretic properties of the overall structure are defined and characterized numerically, then estimates of dynamic response during specific base excitations can be computed.

Each of the two rams are based on the same displacement history to avoid twisting about the vertical axis. Although this may not be entirely realistic, the idealization is appropriate to examine planar behavior of the two C-shaped walls. In actual construction, many walls would support a floor system much larger in area than that of the test specimen. The tendency for twisting of the floor slab would be reduced substantially from that of the test structures.

Lateral force is transferred from each ram to the test floor with a planar truss (Fig. 3). The truss consists of a vertical steel member which is a built-up section of channels and plates, and a pretensioned concrete strut member. The strut is designed to resist forces resulting from the full ram capacity while remaining in compression. In this manner, the large stiffness of uncracked

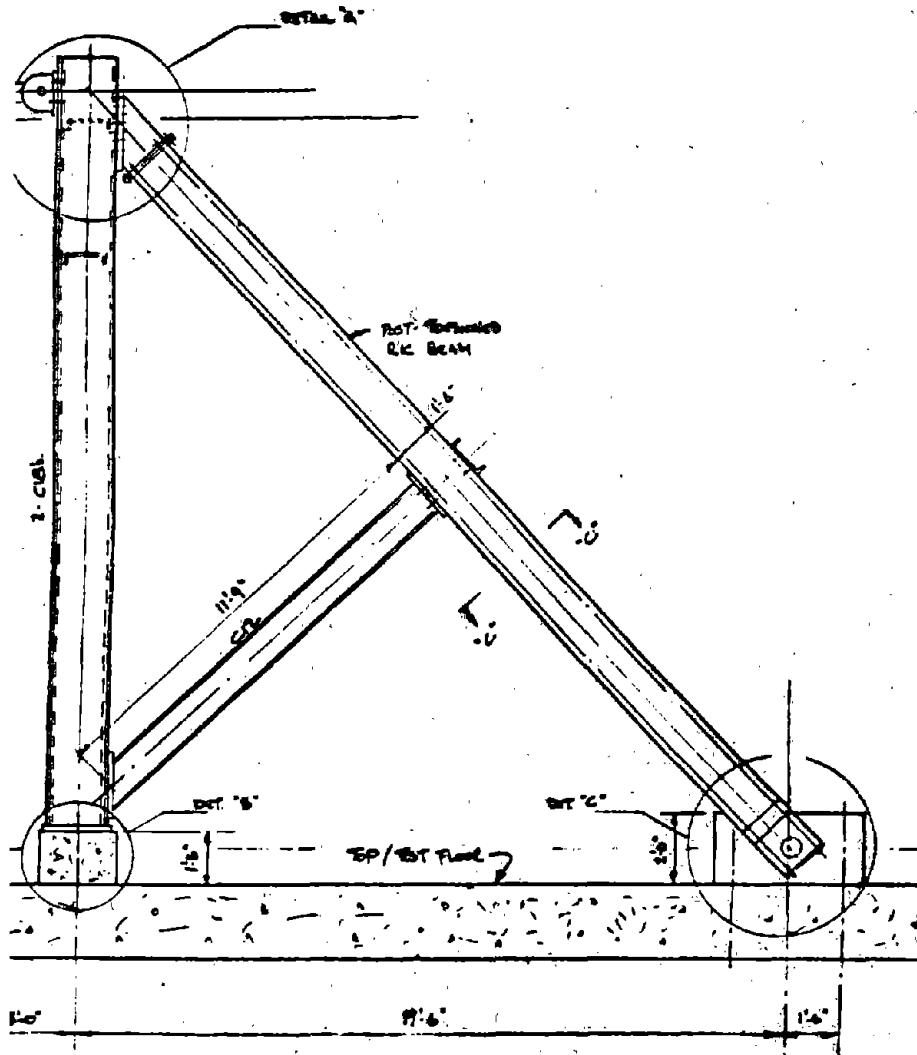


Fig. 3 Description of Reaction Truss

concrete may be relied on in addition to the large strength of the prestressing tendons. Horizontal forces between the strut and the base of the test structure are reacted by the top deck of the test floor.

Instrumentation

Lateral force is measured with load cells located on each actuator. Lateral displacements at each of the two levels is measured with electronic transducers (LVDT's) in addition to transit readings. Instruments are secured to a reference structure which is separate from the reaction structure. Force application is controlled in accordance with displacements measured from these transducers.

Axial and shear deformations of selected regions of the specimen are measured with displacement transducers, and checked with mechanical distance gages. Slip between walls and floor slabs is measured with similar instruments. Mechanical dial gages are used to augment LVDT readings. Electrical resistance strain gages are also placed at selected locations to estimate distributions of lateral force to each pier.

Voltage signals are digitized and stored on diskette using a microcomputer. Specific channels of data are reduced during the test, and plotted on video screens to monitor system response. In addition, analog signals are plotted without digitization on x-y plotters to detect sudden changes in performance of the specimen or testing system. Monitored relations include total applied force with lateral deflection at the top level, and individual ram forces with deflection.

Auxiliary Testing

Before the static force-reversal test to failure, a series of low-amplitude dynamic tests are done to explore response characteristics of the test specimen. Accelerometers are mounted on the specimen at each floor level parallel with both axes. Measured waveforms are digitized and stored on a computer for later analysis.

Firstly, acceleration readings are taken during ambient conditions within the laboratory which often includes the drive through of heavy trucks, the operation of a 20-ton overhead crane, and the operation of fork-lift trucks. Measurements are deduced using stochastic processes to reveal modal frequencies, shapes and damping factors. The validity of such methods are examined relative to response of the damaged structure.

Secondly, the specimen is impacted with a mass which is hung from the overhead crane to excite it in free vibration. Modal frequencies and shapes are determined from measurements of accelerations at the first and second levels along each plan axes. The structure is impacted at each level in an attempt to excite different modes of vibration. Results are compared with those of the smaller amplitude ambient measurements.

Thirdly, the hydraulic rams are attached and the specimen is subjected to a series of low-amplitude harmonic forces. The amplitude of the forces is one order of magnitude lower than the base-shear capacity of the structure because of flow limitations of the hydraulic power supply and distribution system. Frequencies of the force are varied across a range of expected fundamental frequencies so that the relation between dynamic magnification and input frequency may be deduced. From this plot, frequency and damping of the structure are estimated. Results are correlated with those of the first two tests.

ANTICIPATED RESPONSE

Testing of the specimen is scheduled for January of 1986. According to allowable stresses set forth by UBC, the weak element of the structure is the central pier in diagonal tension. The central pier should crack before the longitudinal reinforcement yields in tension whether shear is redistributed to the external piers or not. This is because of the larger uncertainty and safety factors associated with shear of masonry than for reinforcing steel in tension.

According to tests of individual piers (Hegemier, 1982 and Schneider) the actual shear strength of the central pier should still be less than the flexural strength of the wall. Diagonal tension cracking of the central pier should occur before yield of vertical reinforcement. However, the combined shear strength of the central and external piers should be greater than the flexural strength. If the joint reinforcement allows redistribution of shear to the external piers, the hysteretic behavior will be governed by inelasticity in the vertical reinforcement, and thus be stable and good for many cycles of reversed deflections. If the central pier cannot develop the necessary inelastic shear deformations, hysteretic behavior of the overall structure will be dominated by diagonal tension and will thus be unstable and poor. A severe loss of strength should be observed in the first or second large-amplitude cycle of response.

CONCLUDING REMARKS

A test program has been described which examines lateral-force resistance of masonry building systems. Objectives of the experimental program have been outlined. Design of the specimen has been discussed in terms of recently modified provisions of the Uniform Building Code. Descriptions of the specimen configuration, materials and construction techniques have been provided in addition to plans for testing. Expected trends in behavior have been addressed. Final results of the test program will be presented at the workshop.

ACKNOWLEDGMENTS

The research presented herein is made possible by the Illinois Masonry Institute, the Department of Civil Engineering of the University of Illinois at Urbana-Champaign, and the Campus Research Board. Appreciation is extended to the many individuals whose interest in the project has stimulated its progress.

REFERENCES

1. Uniform Building Code, Chapter 24, International Conference of Building Officials, Whittier, California, 1985 Edition.
2. Tentative Provisions for the Development of Seismic Regulations for Buildings, Applied Technology Council, ATC3-06, National Bureau of Standards Special Publication 510, 1978.
3. Hegemier, G.A., R.O. Nunn, and S.K. Ayra, "Behavior of Concrete Masonry under Biaxial Stress," Proceedings of the North American Masonry Conference, University of Colorado, Boulder, August 1978.
4. Schneider, R.R., "Shear in Concrete Masonry Piers", Civil Engineering Department, California State Polytechnic College, Pomona, California.

EARTHQUAKE PROOF BLOCKS WITH GOOD
THERMAL PERFORMANCE

Qian Peifeng¹ Lo Yongkang² Guo Zaiyu³

SUMMARY

In earthquake catastrophies, brick buildings are always destroyed by stepped fractures developed along mortar joints where shear strength is low. For buildings built of the introduced earthquake proof blocks, the fractures will not develop unless the bodies of the blocks are brocken, thus the earthquake proof capacity of the buildings is greatly increased. The earthquake proof blocks, with their excellent thermal performance, also satisfactorily settle the difficulty of heat insulation which is a common defect of the concrete blocks.

-
1. Professor, Department of Architecture Eng., Beijing Institute of Architecture Eng., China.
 - 2.3. Vice Director and Section Chief of Laboratory respectively, Department of Architecture Eng., Yunan Institute of Technology, China.

INTRODUCTION

In brick buildings, earthquakes are liable to produce stepwise slant cracks or horizontal dislocations along mortar joints where shear strength is low. In 1957, the first author of this paper designed a kind of earthquake proof bricks or blocks (for brevity called EPB-pieces) with a special shape to give more strength during earthquakes than the normal bricks. If the cracks keep going on, the seismic shear force must destroy the bodies of the earthquake proof bricks rather than the mortar joints. The former are stronger than the latter, thus buildings of this kind of bricks possess more powerful seismic proof ability. For some historic reasons, unfortunately, only the compressive strength test was carried out at that time at the Institute of Engineering Mechanics in Harbin. In 1982, a research group was set up to continue this project and then the shear strength test was done with ideal results. The Yunan Institute of Technology is in charge of this project and the second author of this paper is the project leader. The first author designed a new type of earthquake proof blocks to give better earthquake proof capacity and good thermal performance in 1984. Mr. Shung Huigao is in charge of the thermal testing work.

FORM AND SIZE OF THE EPB-PIECE

There are five kinds of the EPB-pieces.

- (1) Fundamental piece: Fig. 1(a) and (b) are the front view and top view of it. For the sake of better thermal performance and to facilitate construction, there are two round holes in the block. The vertical position of all holes is arranged uniformly in a line, to put reinforced concrete in if necessary. Except the adjusting block, all possess holes, the effects are all alike. The thickness of walls in the two experiment buildings is 20cm, if the wall thickness varies, then the width of block would vary accordingly.
- (2) A semi-piece is half of a fundamental piece but with 6mm less length (the half breadth of a mortar joint). It is used at vertical position of door or window. Fig. 2(a) and (b) are its front view and top view respectively.
- (3) Corner piece: It is used at corner of exterior wall, the front view, top view and corner planar view are shown respectively in Fig. 3 (a), (b) and (c). The

upper and lower lapping length at corner pieces is just the wall thickness. The lapping length varies accordingly with the varying of wall thickness.

- (4) T-joint piece (Fig. 4 (a) and (b)) is made from a corner piece by decreasing 150mm of its right side, which is used in T-joint and is located layerly alternating with corner piece. T-joint piece may also be used in cross joint.
- (5) Adjusting piece: Fig. 5 (a) and (b) correspond its front view and top view. It is to fulfill building modulus so as to give facility by increasing the usage of the EPB-piece. The thickness of adjusting piece changes with the change of wall thickness.

EXPERIMENT OF SHEAR RIGIDITY FOR SINGLE WALL

We apply method comparative test between EPB-pieces wall and common clay brick wall to find out the ratio r between shear strength of EPB-pieces block R_{jEPB} and of clay brick

$R_{j \text{ brick}} (r = \frac{R_{j \text{ EPB}}}{R_{j \text{ brick}}})$. Based on it, one may precede seismic proof checking calculation according to our nation's contemporary seismic proof design rules for the EPB-piece buildings.

Owing to restriction of condition, the EPB-pieces are made by 200# concrete only. There are nine single walls, made in two groups, six in first, the average length is 187 cm, with height 129 cm, thickness 23.8cm, built in 25# mortar; three in second, for base beam is fairly thick, the height is 135 cm and the other size is the same as the first time, built in 50# mortar. The brick block specimens are twelve and also made in two groups, six in first with average length 193cm, thickness 24cm built in 75# bricks and about 25# mortar; six in second with average length 190cm height 136cm built in 75# bricks and average 50# mortar. The first six specimens are in excellent building quality but not so for the second six.

The experiments proceed in four comparing groups, three specimens for each group (in the third group there are six brick specimens). The fourth group uses blocks of the first and second groups and the broken specimens to give inverse loading experiments. In plane, nine apply

LIST 1

Group order		Average initial fracture load (t)	Ratio	Average destructive load (t)	Ratio	Average shear intensity R_j (kg/cm ²)	Ratio $r = \frac{R_j \text{EPB}}{R_j \text{brick}}$
1~2	<u>EPB piece</u> <u>brick</u>	$\frac{22.2}{12.7}$	1.7	$\frac{36.6}{20.0}$	1.8	$\frac{7.9}{2.9}$	2.7
3	<u>EPB piece</u> <u>brick</u>	$\frac{16.6}{11.1}$	1.5	$\frac{25.0}{13.6}$	1.8	$\frac{5.0}{1.9}$	2.6
4	<u>EPB piece</u> <u>brick</u>	$\frac{22.3}{12.2}$	1.8	$\frac{32.6}{21.0}$	1.6	$\frac{6.5}{2.8}$	2.3
Average	<u>EPB piece</u> <u>brick</u>	$\frac{20.2}{11.9}$	1.7	$\frac{31.4}{18.3}$	1.7	$\frac{6.5}{2.6}$	2.5

Notice: the void ratio of EPB-pieces is 13%, its shear area is smaller than brick.

horizontal load, uniformly distributed vertical load and eccentric concentrated vertical load for equilibrium moment (or: for balancing overturning moment) to make specimens yielding slant shearing fracture rings in order to measure the ratio r registered in the following list:-

It is easily seen from figures in List 1 that EPB-piece block made of 200# concrete has its shear intensity R_{jEPB} stronger than that of the R_{jbrick} for a block made of 75# bricks and the same kind of mortar. The average value of r is 2.5, i.e.

$$r = \frac{R_{jEPB}}{R_{jbrick}} = 2.5$$

More experiments on the EPB-pieces made of different number of concrete are being carried out now.

COMPARISON OF EARTHQUAKE PROOF INTENSITY FOR MULTI-STORY BUILDINGS

According to the experimental results based on our national contemporary seismic proof design rules TJ11-78, calculations to seismic proof intensity of two experimental buildings, one residential building and a school building in Beijing show evidently that the buildings of EPB-pieces have increased earthquake proof resistance. One example is given in List 2. Analysis shows: in nine degree area four-storey buildings can be built with 200# concrete EPB-pieces and the wall thickness is 20cm. If the wall thickness increased to 24cm and 30cm, then five or six-storey buildings would be done. But for brick buildings, if the bottom wall has thickness 24cm plus structural columns, only three-storey buildings can be made. If four-storey buildings must be built, the bottom wall would have thickness 36cm together with supplemental structural columns, still the seismic proof ability is lower than that of EPB-piece buildings. In eight degree area adopting 200# concrete EPB-pieces, the building would be eight storied if the transverse wall is 20cm thick and longitudinal wall is 24cm thick in the bottom storey. Still two or three stories could be added if wall thickness is increased to 30cm. But for brick buildings even if structural columns are supplemented with transverse wall 36cm thick and longitudinal wall 49cm thick, the seismic proof intensity is still lower than demand.

THE PRODUCTION AND BUILDING SITUATIONS

The production and building situations of two experimental buildings made of EPB-pieces illustrate: The production of EPB-pieces is fairly straightforward, the building construction is also very simple, without trouble, and the wall builds over twice as fast as a brick wall.

LIST 2: The residential building for colleagues of Kakung Municipal Construction Committee (a four storey building with field-made R. C. floors, nine degrees, second category ground)

floor	strength of mortar	EPB-pieces with thickness 20cm and void ratio 26.2%		bricks supplemented structural columns, wall thickness 36mm	
		safety factor K	compared with the design rules "+" means increasing	safety factor K	compared with the design rules, "+" means increasing
4th	50	4.34	+117%	3.82	+91%
3rd	50	2.48	+24%	2.02	+1%
2nd	100	2.42	+21%	2.06	+3%
1st	100	2.34	+17%	1.91	-4%

ANALYTIC RESEARCH OF ECONOMIC BENEFIT

Through practice and survey of these two experimental buildings, under premise of almost equivalent seismic proof capacity (EPB-piece block are always stronger than bricks with supplemental structural columns), the

following advantages are possessed by EPB-pieces:

- (1) Increasing applicable area 8% of the building.
- (2) The weight of walls decreased about $1/4 - 1/3.5$, which is advantageous for diminishing the breadth of foundation.
- (3) Easy to build, so as the quality being guaranteed.
- (4) Less mortar being used. Accompanying the realization of machined fashioning technique, the breadth of mortar joint and thickness of mortar or wall surface will be decreased, thus the amount of mortar is use could be diminished again.
- (5) With EPB-pieces buildings could be built much higher than brick ones, thus several kinds of frame or frame-shear structures may be substituted.

A NEW TYPE OF EARTHQUAKE PROOF BLOCKS

Analysis and preliminary test prove that the lately improved earthquake proof blocks possess excellent thermal performance and better earthquake proof capacity. For example, a 27 cm thick wall of such blocks gives similar best insulation as a 36cm thick one of normal clay bricks. Now the blocks are still under improvement.

DISCUSSION

- (1) All the above experimental analysis and calculation derives from our nation's earthquake resistant regulations which are based upon the traditional viewpoint that horizontal seismic force is dominant. Qian Peifeng et al [2][3][4]... has pointed out since 1957, and it was proved further by analysing earthquake damage induced by many strong earthquakes in our country, that this traditional viewpoint is incorrect. Practically the vertical seismic force plays a leading role. For an earthquake in eight degree area, vertical seismic force may exceed own weight. Upon that viewpoint, the EPB-pieces building may give much higher seismic resistant capacity than the above calculated results.
- (2) A strong earthquake may not occur within a hundred years, thus building damage on a certain level short of falling down and injuring people should be permitted. If the consideration is to prevent cracks from

extending further after they have appeared, then the EPB-piece buildings possess higher earthquake resistant ability than the above calculated results.

- (3) The increasing of seismic resistant capacity for EPB-piece buildings mainly depends on increasing the strength of block pieces or bricks, other than strength of mortar. Thus a further step to increase the earthquake resistant capacity is to raise the strength of block piece or brick.
- (4) The EPB-pieces used in weak seismic areas also prevent slant cracks appearing in walls.

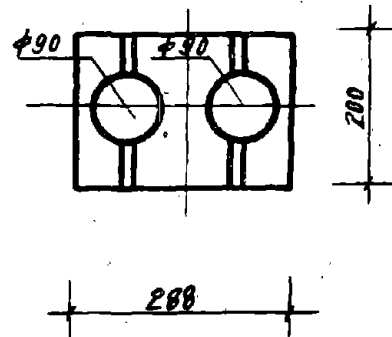
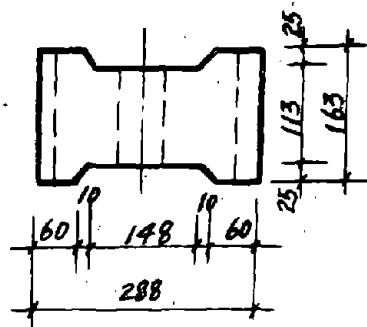


Fig. 1(a). Front standing view of fundamental block

Fig. 1(b). Plane of fundamental block

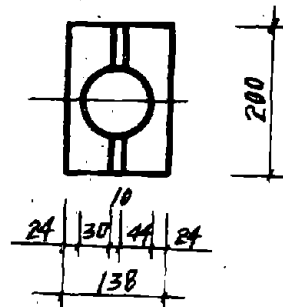
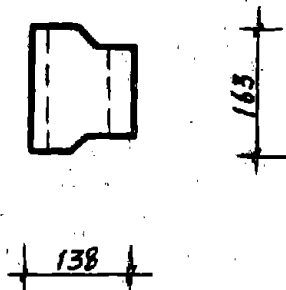


Fig. 2(a). Front standing view of semi-block

Fig. 2(b). Plane of semi-block

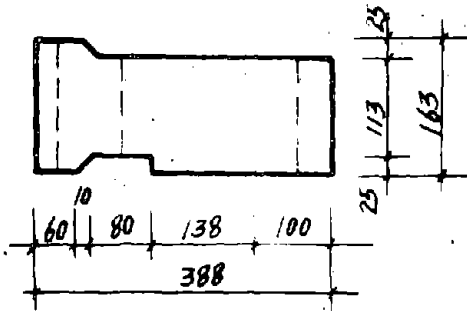


Fig. 3(a). Front standing view of turning corner block

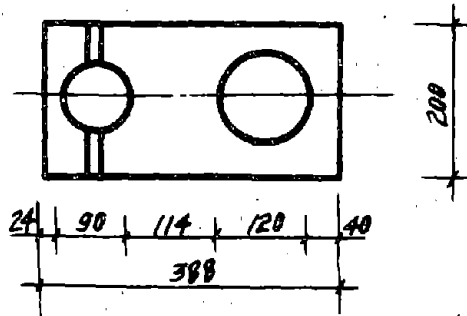


Fig. 3(b). Plane of turning corner block

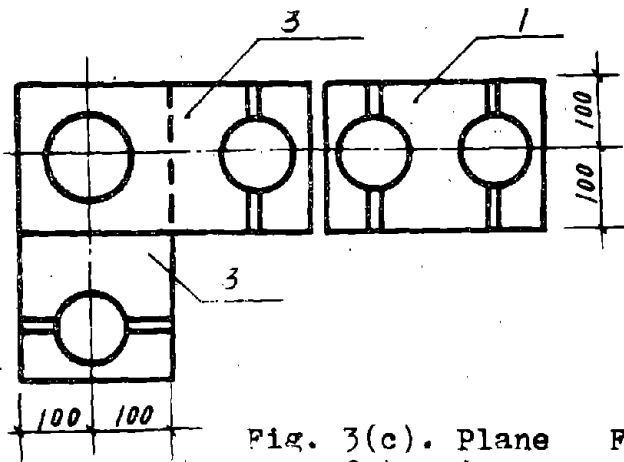


Fig. 3(c). Plane of turning corner

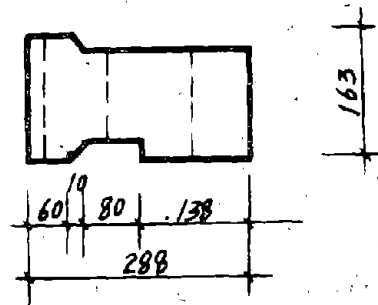


Fig. 4(a). Front standing view of T-joint block

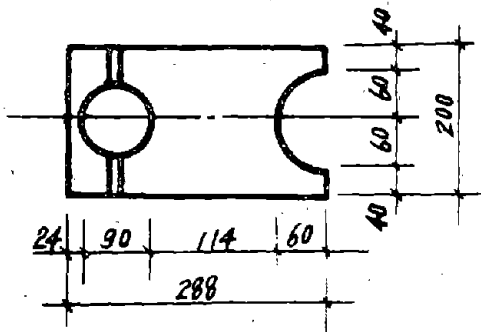


Fig. 4(b). Plane of T-joint block

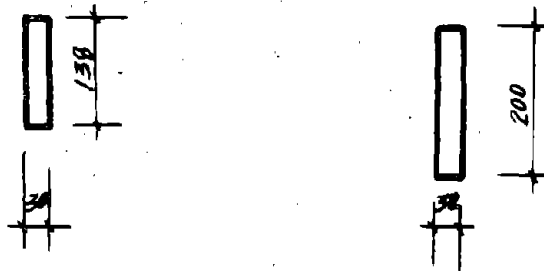


Fig. 5(a). Standing view of adjusting block

Fig. 5(b). Plane of adjusting block

REFERENCES

- (1) Present seismic resistant regulation of our country, TJ11-78.
- (2) Qian Peifeng. Several explanations to destruction of chimneys under action of earthquake force. Paper for the First National Seismic Proof Symposium, 1957.
- (3) Qian Peifeng. Collected papers on vertical seismic force and seismic proof style bricks, Yunnan Institute of Technology, 1981.
- (4) Qian Peifeng. Seismic Proof Analysis of Structures. The Seismology Publishing House, 1983.
- (5) Qian Peifeng et al. Vertical Earthquake Load on Chimneys, 7th WCEE, 1980.
- (6) Qian Peifeng. On Vertical Seismic Force. Construction Structures, No. 3, 1979.
- (7) Qian Peifeng. The Serious Effect of Vertical Seismic Force. J. Seismological Research, Vol. 6, No. 2, 1983.
- (8) Qian Peifeng. The Vertical Seismic Force and its Precautions for Earthquake Resistance of the Brick Buildings. J. Seismological Research, Vol. 4, No. 2, 1981.
- (9) Qian Peifeng. On computations for Certain Parameters of Vertical Earthquake Force on Engineering Structures, ACTA Seismologica Sinica, Vol. 5, No. 4, 1983.
- (10) Qian Peifeng. Vertical Earthquake Force, Earthquake Engineering and Engineering Vibration, Vol. 3, No. 2, 1983.
- (11) Qian Peifeng. Qian Da: Analysis of Earthquake Damage to Brick Structures. Proc. 7th International Brick Masonry Conference. 1985. 2.
- (12) Qian Peifeng. Inverse Calculations of Horizontal and Vertical Earthquake Force According to Earthquake Damages. Journal of Beijing Institute of Civil Engineering and Architecture. No. 1 1985.
- (13) Qian Da, Qian Peifeng. Analysis of The Vertical Force and the Seismic Hazard of the Multi-layered Frame-words. J. Seis. Res., Vol. 7, No. 1, 1984.

STUDY OF SEISMIC BEHAVIOR OF HOLLOW CONCRETE BLOCK BUILDINGS

Xu Shanfan^I, Liu Dexin^{II}

ABSTRACT

This paper describes the fundamental mechanical properties of masonry constructed of hollow concrete blocks, putting stress on summing up the major research achievements in pseudo-static test of block walls.

Tests show that the damages of specimens are characterized by shear friction mechanism. The shear strength of the specimen is mainly controlled by the shear strength of the through joints of the masonry, the compressive stress and the number of reinforced grout.

In order to predict shear strength and obtain practical design method, we proposed a strength formula on the basis of analysis of numerous test statistic data.

The paper also discusses the inelastic behavior of walls followed by the increase of displacement, states the restoring force characteristic model.

INTRODUCTION

As early as 1920's, 25 two-story residential buildings were constructed of hollow concrete blocks in Shanghai in China. Afterwards some three-story residential buildings and other buildings were completed in the 1950's. By the end of the 1970's, stress was put on the technology and machines for making concrete blocks and they were put into applications in the low seismic intensity regions with a large number of multi-story residential buildings erected. In Guangzhou which is located in the region of 7 seismic intensity, the completion of pilot buildings amounting to over 20,000 square metres in-

I, II Engineers of Sichuan Institute of Building Research, China.

icated a notable progress. From then on, all-round research work has been carried out. Up to now concrete masonry structures have rapidly developed in the southern provinces as well as some northern provinces in China.

This paper presents the research achievements gained by the Sichuan Institute of Building Research, attaches importance to summing up the test results of concrete block walls subjected to cyclical reversed lateral load, makes comments on the characteristics of load bearing shear walls made of blocks and gives measures dealing with construction resisting earthquake. The early achievements (apply to regions of 7 intensity) have been brought into the "Design and Construction Regulations for Buildings Constructed of Hollow Concrete Blocks (JGJ 14-82", standard of the Ministry of Urban and Rural Construction and Environmental Protection. The recent achievements (apply to regions of 7 and 8 intensity) are to be included in the "Design Code of Industrial and Civil Buildings Resisting Earthquake"; the state standard being revised.

1. BASIC MECHANICAL PROPERTY OF CONCRETE BLOCK

The main size of the blocks is 390 x 190 x 190 mm, taking other size as auxiliary to meet requirements. The porosity ranges within 40-50% and the compressive strength, based on gross section, falls into four kinds, i.e. 100 kg/cm, 75 kg/cm, 50 kg/cm and 35 kg/cm.

With regard to standard masonry, the axial compressive strength R , axial tensile strength R_1 , flexure tensile strength R_w and shear strength R_j are adopted according to Tables 1 and 2.

Table 1 Axial compressive strength of masonry $R(\text{kg/cm}^2)$

Block grade No. R_k	Mortar grade No. R_2			Mortar strength
	100	50	25	
				0
100	50	44	40	30
75	40	35	31	22
50	29	25	22	15
35	22	19	16	10

Table 2 R_1, R_w, R_j (kg/cm^2) of masonry

Category of strength	Force direction	Grade No. of mortar		
		100	50	25
Axial tensile strength R_1	Along teathed joint section	2.2	1.5	1.0
Flexure tensile strength R_w	Along through joint section	2.2	1.5	1.0
	Along teathed joint section	2.6	1.8	1.2
Shear strength R_j	Along through joint & stepped sections	2.2	1.5	1.0

Note: The principal tensile strength (R_2) is taken equal to joint shear strength R_j .

Modulus of elasticity E and shear modulus G of masonry are employed in the light of the data shown in Table 3.

Table 3 E and G of masonry

Grade No. of mortar	100	50	25
Modulus of elasticity E	800R	700R	600R
Shear modulus G	320R	280R	240R

2. OBJECTIVES AND PROCEDURE OF THE INVESTIGATION ON SEISMIC BEHAVIOR

It is desired to understand, through large number of tests, the failure mechanism and inelastic characteristics of concrete block shear wall lightly reinforced, describes the mathematical model of the wall with inelastic features so as to predict the earthquake response of concrete block buildings, thus evaluating the safety of the buildings.

As for the first series of tests, it is mainly intended to, by making use of experiences obtained from seismic damages of brick masonry houses and the relevant test results, approach the shear strength of single shear wall, propose construction measures to form the basis for working out regulations of design and construction of concrete block buildings. In the mean time, attention was paid to keep in line with the present seismic design code. For the second series of test, emphasis was given to the failure mechanism and inelastic behavior of lightly reinforced walls.

3. A BRIEF ACCOUNT OF TEST

3.1 Design of Test Specimen

The specimen was designed to typify the segment of wall between stories having an aspect ratio of 0.5-0.6.

The first series of 44 specimens were divided into two types in dimensions: 1 m high x 1.6 m wide and 1.4 m x 1.6 m. The second series of 51 specimens had dimension of 1.2 m x 2.8 m. The two series covered three types, namely, un-grouted, partially grouted and both grouted and placed with horizontal bars in courses. All grouted cells were placed with one vertical stud bar of $\phi 12$.

3.2 Loading Apparatus

Both series of tests were carried out with contraflexure loading set up. Horizontal and vertical loads were imposed by hydraulic jacks.

3.3 Load Application

The horizontal cyclical load was applied by using load controlled jack for the first series of tests in one way. As regard to second series, horizontal load was applied in a series of cyclical reversals controlled by load prior to primary crack and by displacement after crack.

Both series of experiments were imposed with a constant precompressive load.

3.4 Instrumentation

The displacement at wall top was measured by providing a displacement sensor and P- Δ curve was self-recorded by a function device.

4. FAILURE MECHANISM AND SHEAR STRENGTH

4.1 Failure Mechanism

Under the above said loading conditions, the test specimen underwent shear deformation which predominated, displaying shear failure featured by diagonal stepped cracks.

The relation between load and displacement is roughly linear prior to first crack, and the specimen displacement notably increased after primary crack and the p- Δ curve took turn. With the increase of load and displacement, the discontinuous joint cracks linked up to form major cracks, followed by secondary cracks. At the moment, the load reached limit.

The major cracks in un-grouted specimen developed apparently with less secondary cracks. The limit load was greatly raised and the blocks in corner toe were crushed when the specimen was subjected to higher compressive

stress, correspondingly, the failure of masonry was more serious. For the grouted specimen, the degree of major crossing stepped cracks was not as serious as that of cracks emerged in un-grouted specimen, but accompanied by a lot of secondary slight cracks. Only at the time of limit load appearing or after that and experienced reversal deformation, the grouted cores were cut off.

After crack, the partial assemblage of blocks slid along stepped bed joints rather than pulled apart along diagonal section. Then, a lateral load increase of 20%-30% was observed until limit load emerged. Under reversed cyclic loading, the comprehensive deterioration of masonry was of the mechanism of shear friction damage. This indicated that the appearance of primary cracks was under the elastic limit condition, characterised by losing the strength of principal stress, while the formation of major stepped diagonal cracks was under the elasto-plastic limit condition, featured by shear friction. Such a mechanism comes from the following causes:

- i. The specimen had low aspect ratio.
- ii. The bonding strength of the mortar employed was low, hence the stepped damage of masonry was unavoidable.
- iii. The specimen was subjected to a certain amount of compressive stress.

For the typical failure mode of masonry, please see Figs. 1 and 2.

4.2 Shear Strength

The shear strength of masonry serves as the main index controlling the seismic design of masonry building. Owing to the serious heterogeneity and anisotropy as well as sensitivity of quality in field, indeed, the problem of masonry strength is not one of theory but practice.

In case the condition of elastic limit is taken as design index, the heterogeneity and anisotropy are ignored on purpose for seeking way out in theory, and the following equation is derived from the stress mode at a certain point:

$$R_t = \frac{R_j}{\beta} \sqrt{1 + \frac{\sigma_0}{R_j}} \quad (4-1)$$

In the equation the undeterminable value of principal tensile intensity is replaced by the shear strength R_j of through joints of the masonry to calculate in reverse the shear strength R_t of masonry subjected to composite stress.

ses. σ_c is compressive stress.

In order to describe the condition of elasto-plastic limit, the equation which coincides with the failure mechanism of shear friction will be adopted, generally,

$$R_t = aR_s + f\sigma_c \quad (4-2)$$

where a and f are empirical co-efficients determined by test, the value of a is slightly larger than 1 and f is friction co-efficient in name, approximately 0.60. Numerous test data showed statistically the existence of the linear relation.

It is advisable to use such ultimate strength to determine the failure index, so as to apply the concept of energy dissipation of structural elements under seismic loading and echo with the method defining seismic force in current seismic code. Therefore, the seismic load estimated with elastic design method can be deducted by a factor and the requirement for ductility implied in the deduction can be satisfied by setting up proper grouted cores as well as horizontal reinforcing steel.

Experiments prove that the compressive stress greatly affects the raising of cracking strength and ultimate strength. In defining the strength formula for design purpose, we consider R_s as a strength factor independent of σ_c , and also take into account the deterioration of strength due to low cyclic fatigue of specimen. In the mean time, owing to the fact that greater ratio of axial pressure makes heavier damage of specimen and the weightlessness caused by vertical ground motion is disadvantageous to shear strength, we carefully adjusted the influence of compressive stress on strength, using lower co-efficient. As a result, it is conformable to the margin of safety and economic index obtained by traditional design practice. The formula to calculate the shear strength of masonry for design purpose is expressed as follows:

$$R_t = R_s + f\sigma_c \quad (4-3)$$

Considering that let $a=1$ after deterioration of strength, assume $f=0.35$ for making provisions against earthquake in regions of 7 intensity and assume $f=0.30$ in regions of 8 intensity. In this formula, R_t is no longer the shear stress at a point, but the average shear stress of the whole specimen. The effect of non-uniformity of shear strength is neglected. The comparison of Equation (4-1) and (4-3) is shown in Fig.3.

The wall grouted partially not only markedly raised the capacity resisting lateral force, but also improved deformation behavior. The existing Regulations (JGJ14-82) stipulates that the following formula is used to represent the effect of mortar, compressive stress and grouted core on shear strength.

$$Q = \left(\frac{R_c}{\beta} \sqrt{1 + \frac{\sigma_c}{R_c}} \right) A + 0.05 R_a A_h \quad (4-4)$$

where A is gross section area of wall; R_c is the axial compressive design strength of the concrete or grouted core; A_h is section area of the total intermediate cores placed in wall (except extreme cores); β is the co-efficient of non-uniformity of shear stress, let $\beta = 1.2$.

Further investigation demonstrated that it is advisable to express design strength of grouted wall by means of shear friction mechanism. The strength is regarded as a linear composition of R_c , σ_c and the dowel action of cores.

$$Q_u = (R_c + \eta \sigma_c) A + 0.05 \eta R_a A_h \quad (4-5)$$

where η is work factor of different cell-filling ratio ρ , $\eta = 0$ for $\rho < 15\%$; $\eta = 1.0$ for $15\% \leq \rho < 25\%$; $\eta = 1.10$ for $25\% \leq \rho < 50\%$; $\eta = 1.15$ for $\rho \geq 50\%$.

Based on the provisions made for 8 seismic intensity, the design strength calculated with formula (4-5) is about 16% higher than that calculated with formula (4-4). The statistical average value of test ultimate strength to calculated strength ratio is 1.68 according to the test results of 44 specimens of various types obtained by the Sichuan Institute of Building Research. In checking the strength of wall, in case the safety co-efficient $K=2$ is adopted in accordance with the current seismic code, implying that the strength of actual wall is at least 3 times of the checking strength.

5. INELASTIC BEHAVIOR

For the investigation of inelastic behavior, emphasis was given to the strength, deformation and hysteretic characteristics of masonry walls subjected to horizontal reversed loading and the effect of such factors as cores and compressive stress etc. on them.

For the typical skeleton curve and hysteresis curve, see Figs. 4, 5 and 6.

The relation between shear force and displacement

coincided with the hysteretic rule of trilinear restoring force characteristic model with stiffness degradation.

The skeleton curve turned apparently when the specimen cracked and it began to decline after reaching peak limit load, presenting remarkable degradation of stiffness and strength. The degradation for grouted specimen was lighter than that for un-grouted specimen. Despite that the decline of skeleton curve reflected the process of brittle rupture, the decline was gentle and the loading capacity would not be dropped sharply. The specimen showed a trend similar to ductility and was able to stand large displacement.

The hysteresis loops appeared to be slender prior to crack and was like a shuttle after crack. As for the un-grouted specimen, the hysteresis loops were still like a shuttle even limit load was reached and gradually trended towards rigid-plastic behavior, reflecting the characteristics of energy dissipation due to friction. After the grouted specimen reached limit load, the hysteresis loops became a opposite "S" from shuttle shape, showing the behavior of sliding, see rigs.7,8. Major strength deterioration seemed to occur between the first and second cycles of each deformation amplitude, the losses of strength was about 10%. Having stood large displacement, the grouted specimen was still able to keep a steady hysteresis loop.

The cracking strength Q_c and ultimate strength Q_u as well as initial stiffness K_0 rose with the increase of compressive stress σ_c , and there exists likely a linear relation between K_0 and σ_c .

With modelling of restoring force characteristics of specimen (see rig.9), it is possible to obtain a series of formula relating to characteristics parameters.

$$\text{Cracking strength } Q_c = \beta Q_u \quad (5-1)$$

Based on statistical average, $\beta=0.80$ for the un-grouted specimen; $\beta=0.75$ for the grouted specimen.

The initial stiffness was the secant stiffness at cracking point. It is possible to attain the following equation according to the shear mode of deformation and the effect of σ_c on elastic characteristics of the masonry:

$$K_0 = \lambda \frac{Et}{\left(\frac{h}{b}\right)^3 + 3\left(\frac{h}{b}\right)} \quad (5-2)$$

where E --- elastic modulus (refer to JGJ14-82)

t --- wall thickness
 λ --- co-efficient obtained statistically from
 test results, $\lambda = 0.99 + 0.27\sigma$, ($3.5 \leq \sigma \leq 7$)
 n/b --- aspect ratio of masonry.

The formula calculating the initial stiffness of grouted specimen is as follows:

$$K_{oc} = \psi K_o \quad (5-3)$$

where $\psi = 1.10 - 1.25$, the raising co-efficient decided by different cell-filling ratio.

Elasto-plastic stiffness K_1 , negative stiffness K_2 and unloading stiffness K' are obtained on the basis of test results.

For un-grouted specimen:

$$K_1 = 0.09K_o,$$

$$K_2 = -0.06K_o,$$

$$K' = \left(\frac{\Delta_c}{\Delta_m} \right)^\alpha K_o, \text{ the co-efficient of stiffness degradation } \alpha = 0.63, \text{ where } \Delta_c \text{ is cracking displacement, } \Delta_m \text{ is the displacement corresponding to unloading stiffness.}$$

For grouted specimen:

$$K_1 = 0.08K_{oc},$$

$$K_2 = -0.02K_{oc},$$

$$K' = \left(\frac{\Delta_c}{\Delta_m} \right)^\alpha K, \alpha = 0.70.$$

6. MEASURES FOR EARTHQUAKE RESISTANT CONSTRUCTION

The unreinforced or lightly reinforced masonry houses are very popular in China. Due to their poor ability resisting earthquake, it is necessary to adopt reasonable measures against seismic action, and to enhance the integrity and ductility in addition to checking strength of walls.

In the seismic regulation (JGJ14-82), the following provisions are put forward.

6.1 Spacing of Cross walls Against Earthquake

Spacing of cross wall should not exceed the data listed in Table 6.1.

Table 6.1 Maximum spacing of cross wall
resisting earthquake (m)

Type of roof and floor	Maximum spacing of cross walls	
	7 intensity region	8 intensity region
Cast-in-site concrete	15	12
prefabricated concrete	12	9
Timber	9	

6.2 Height Restriction of Building

Based on the experience of seismic damages of brick masonry structures, the overall height and the number of story of block masonry building stipulated do not exceed 19 m (6 stories) for regions of 7 seismic intensity and 16 m (5 stories) for regions of 8 intensity respectively, so as to control the total shear force on base. For the buildings with less cross walls used as schools, hospitals and so forth, the height should be reduced appropriately.

6.3 Setting up ring beams

Cast-in-site reinforced concrete ring beams are required to position on exterior wall and on interior longitudinal walls at each story, close to floor slabs or roof slabs. It is necessary to arrange ring beams on interior cross wall at each story and the cross spacing will not be more than 7 m in regions of 7 intensity and not more than 4 m in regions of 8 intensity.

6.4 Positioning grouted cores

The grouted cores, in addition to checking seismic strength, will meet the requirements stated in Table 6.4.

CONCLUSIONS

1. On the basis of failure mechanism of shear friction, we proposed, by rule of thumb and theory, a formula to predict the shear strength of masonry, which serves as a description of elasto-plastic limit. This corresponds with the concept of design seismic force determined by energy dissipation and elastic response spectrum. Though the calculated strength by the formula of shear friction is a little higher than the result obtained from formula of elastic limit theory, it possesses sufficient strength reservation proved by numerous test.

2. The bearing stress acting on wall has great effect on raising cracking strength, ultimate strength and initial stiffness of masonry. Further investigation should

be made to assess and utilize the factor.

3. It is possible to raise deformation capacity and keep loading capacity in case of large displacement of masonry by placing proper reinforced cores, which is a major means of enhancing strength as well as a necessary seismic construction in assuring appropriate ductility.

4. Based on identical test condition and reversed horizontal loading, the skeleton curve, hysteresis loops showed fairly good regularity and can act as the foundation of restoring force characteristic modelling.

Table 6.4 Requirements for positioning grouted cores

Number of story		Location of core	Constr. requirements for core
7*	8+		
3-4	J	At four corners of building and staircase	L type corner: 3 cells are filled.
5	+	Same as above and also at joint between gable wall and int. long. wall, and joint between int. cross wall and ext. long. wall for every other room.	T joint: 4 cells are filled.
6	5	Same as above except that core is placed at the joint between int. cross wall and ext. long. wall for every room.	L type corner: 5 cells are filled. T joint: 4 cells are filled. + joint: 4 cells are filled. All the cells are filled with Grade 150# concrete with 1Ø12 stud inserted in them.

* Regions of 7 seismic intensity.

+ Regions of 8 intensity.

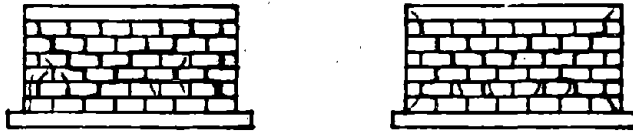


Fig. 1 Failure mode of ungrouted wall
 Fig. 2 Failure mode of grouted wall

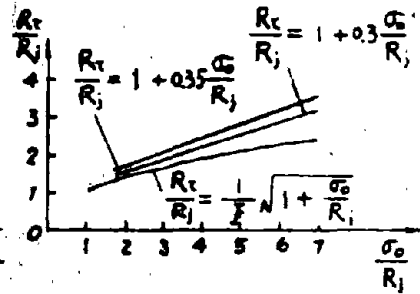


Fig. 3 Comparison of eqs. (4-1) and (4-3)

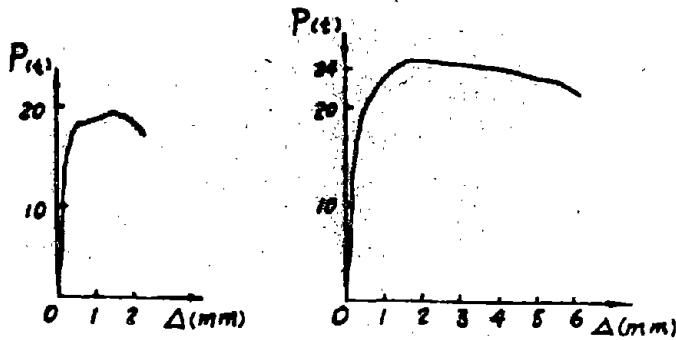


Fig. 4 Skeleton curve of ungrouted wall
 Fig. 5 Skeleton curve of grouted wall

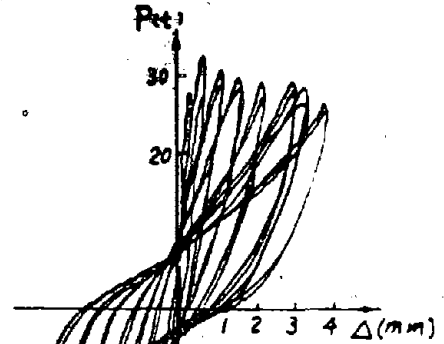


Fig. 6 Hysteresis curve of grouted wall

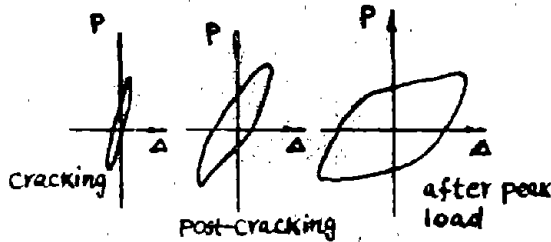


Fig. 7 Hysteresis loop of ungrouted wall

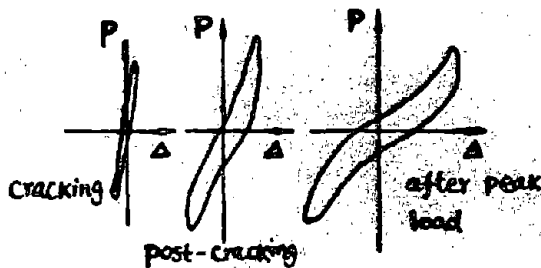


Fig. 8 Hysteresis loop of grouted wall

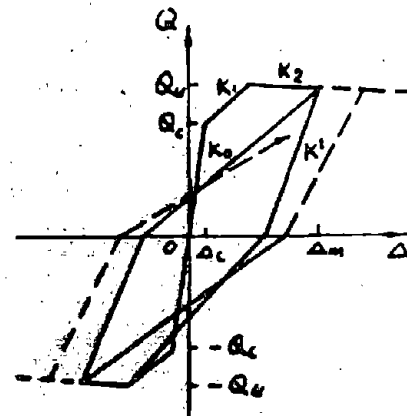


Fig. 9 Restoring force characteristic model

SHEAR BEHAVIOR OF UNREINFORCED CONCRETE BLOCK WALLS

Kyle Woodward^I

SUMMARY

An experimental investigation is described which has as its primary focus the determination of the shear resistance exhibited by unreinforced, ungrouted, hollow concrete block masonry walls. Forty-seven wall panel tests are reported. The parameters in the investigation include the amount of applied vertical compressive stress, wall aspect ratio, block strength, mortar type, and loading history. One major finding of the investigation is that the relationship between increasing amounts of applied vertical compressive stress and the resulting increased shear resistance is significant and nearly linear. Another observation is that there exists a critical diagonal tension strain which defines the onset of wall diagonal tension cracking.

INTRODUCTION

The Center for Building Technology of the National Bureau of Standards is currently undertaking a program of experimental research on the shear resistance and behavior of shear-dominated masonry walls. The parameters under study are applied vertical (axial) compressive stress, wall aspect ratio (length-to-height), block and mortar type, horizontal and vertical reinforcement, out-of-plane loadings, and loading history. This paper reviews the test program on ungrouted, unreinforced hollow concrete block masonry walls.

The investigation reported herein involves tests on forty-seven wall panels whose nominal dimensions are 8 in. thick, 64 in. high, and either 48 in., 64 in., 80 in., or 96 in., long. The walls are subjected to a vertical compressive stress in combination with in-plane lateral displacement. In addition to the variation of aspect ratio, the vertical compressive stress, block strength, and mortar type are also varied in this series of tests. The resulting data include in-plane lateral load resistance, wall displacement, and strains measured at discrete locations on the wall faces.

WALL PANEL DETAILS AND TEST SETUP

Materials

The concrete masonry units are two-core hollow block and have nominal dimensions of 8 in. x 8 in. x 16 in. The block labeled as

^I/ Senior Development Engineer, Univ. of Calif., San Diego

high strength have a gross area of 119.2 sq. in., a net solid area of 61.5 sq. in., and a gross area compressive strength of 1813 psi based on the average of six unit tests. The block labeled as low strength have a gross area of 119.8 sq. in., a net solid area of 60.4 sq. in., and a gross area compressive strength of 1304 psi based on the average of nine unit tests. The mortar is either Type S proportioned with 1 part by volume of portland cement, 3/8 part by volume of lime, and 4 parts by volume of sand or Type N proportioned with 1 part by volume of portland cement, 1 part by volume of lime, and 5 parts by volume of sand.

Details and Fabrication

A typical planar and corner wall panel are shown in fig. 1. The wall panels are constructed in running bond using face-shell bedding except for the two end cross-webs. The joints are struck flush, but not tooled. Mortar cubes and prisms are also built and later tested as companion specimens to the wall panels. The mortar cubes are 2 in. x 2 in. x 2 in. and the prisms are made by stack bonding three stretcher units.

The details of selected wall panels are listed in table 1. The wall panel identifier is a two-part mnemonic with the two parts separated by a hyphen. That part of the identifier preceding the hyphen is descriptive and has the form mABn. The m term denotes the wall length in inches while the n term specifies the approximate vertical compressive stress applied to the wall. The stress is based on the net cross-sectional area of the wall and is expressed in units of psi. The A term indicates the block strength while the B term indicates mortar strength with A and B being replaced by either H for high strength or L for low strength. The terms high and low strength are used only in a relative sense and do not imply an absolute measure. That part of the identifier following the hyphen is a construction code and provides for unique identification of each wall.

Test Setup

The test setup (fig. 2) is the NBS Tri-directional Test Facility (NBS/TTF), a permanent loading apparatus designed to test building components using three-dimensional loading histories. The NBS/TTF is a computer-controlled loading apparatus which applies forces/displacements in all six degrees of freedom at one end of a test specimen. The other end of the specimen is fixed. All of the test specimens listed in table 1 are laterally displaced while the upper crosshead maintains a zero rotation condition.

Instrumentation

In the interest of brevity, only that instrumentation which

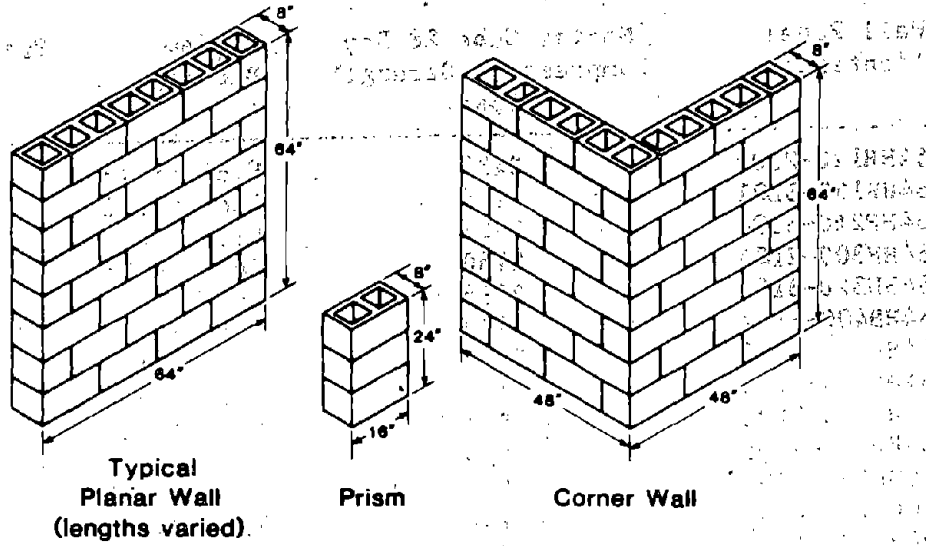


Figure 1. Typical wall panels.

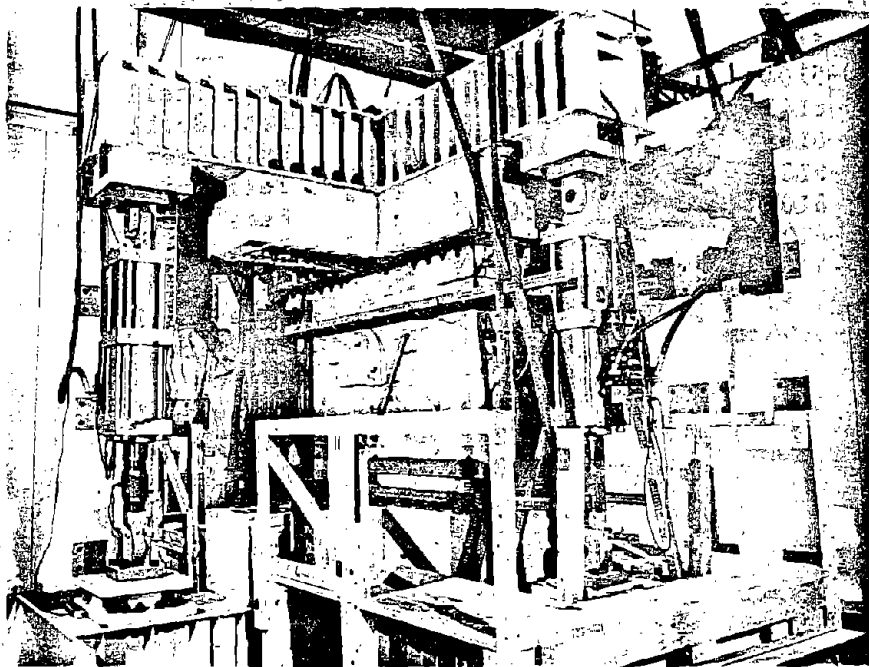


Figure 2. Test setup (NBS/TTF)

Table 1. Wall Panel Details

Wall Panel Identifier	Mortar Cube 28 Day Compressive Strength (psi)	Prism Bedding	Prism Compressive Strength (psi)
64HH120-2L04	2437	Face Shell	1839
64HH160-3L01	1825	Face Shell	1820
64HH240-3L04	2237	Face Shell	2132
64HH300-2L05	2160	Face Shell	1870
64HH320-3L03	2095	Face Shell	2091
64HH400-3L02	2139	Full Area	2810
64HH400-2L03	2232	Face Shell	2074
64HH500-2L06	2191	Face Shell	2005
48HH150-3L06	1847	Full Area	2661
48HH450-3L05	2055	Full Area	2645
80HH250-3L07	1994	Face Shell	1867
80HH400-4L01	3254	Face Shell	2050
96HH200-4L03	3076	Face Shell	1917
96HH300-4L02	2746	Full Area	2615
96HH400-4L04	2425	Full Area	2783
64HL160-5L01	1826	Face Shell	2049
64HL240-5L02	1809	---	--
64HL320-5L03	1761	---	--
64HL400-5L04	1490	Face Shell	1923
64LL170-6L07	1987	Face Shell	1522
64LL250-6L06	1841	Full Area	1955
64LL340-6L08	1591	Full Area	1983
64LL420-6L09	1505	Face Shell	1443
64LH105-6L01	2646	Face Shell	1630
64LH170-6L02	2657	Full Area	2033
64LH250-6L03	2772	Face Shell	1522
64LH340-6L04	3127	Full Area	2133
64LH420-6L05	3110	---	--
48LH170-6L10	2985	Face Shell	1447
48LH450-6L11	2892	Full Area	2094
96LH220-6L12	2700	Face Shell	1537
96LH320-6L13	2810	Full Area	2025

Note: The mortar cube stress is based on an area of 4 sq. in. The values listed are the average of at least three cube tests. Mortar cubes are removed from the molds after 24 hours and air cured in the laboratory environment until tested.

The prism stress is based on the unit net solid area. The values listed are the average of at least three prism tests.

provides data used in this paper is described. The loads imposed on the wall panels are measured by load transducers incorporated in the hydraulic actuators. The wall panel displacement (in-plane) is measured by displacement transducers mounted horizontally between the top course of the wall and an external fixed reference (fig. 3). The diagonal strain referenced in future discussion is computed from the displacement measured by a displacement transducer mounted diagonally on the wall panel (fig. 4).

TEST RESULTS

General Behavior

In general, the primary form of distress exhibited by the wall panels was a diagonal-tension type of failure as illustrated by the typical crack patterns in fig. 4. However, there were exceptions. Flexural distress in the form of horizontal flexural tension cracks in the mortar bed joints occurred if the applied vertical compressive stress was insufficient to suppress this failure mode. It should be noted that even the walls exhibiting flexural distress did, in fact, suffer a local diagonal-tension distress in a corner block and when the vertical compressive stress was increased, the primary mode of distress changed to a general diagonal-tension failure. In all of the walls tested, the final failure of the wall was the result of an inability to sustain the applied vertical compression load in combination with the imposed lateral displacement.

While the cracking pattern was relatively insensitive to the parameters studied in the test program, it appeared that the orientation of the cracking was influenced by both the level of vertical compressive stress and the wall aspect ratio. The tendency of the diagonal cracking to follow the mortar joints or to pass through the units was affected by vertical compressive stress, block strength, and mortar strength. Walls built with low strength mortar exhibited a pronounced tendency to exhibit mortar joint cracking while the walls built with the high strength mortar exhibited much more cracking through the block. Increased vertical compressive stress increased the likelihood of block cracking, especially for the high strength block and mortar combinations.

The 48 in., 64 in., and 80 in. walls tended to form a consistent corner-to-corner diagonal crack pattern which essentially separated the wall into two triangular segments. The shear transfer between the two segments took place along the diagonal crack by shear friction. The 96 in. long wall, by contrast, did not form the corner-to-corner crack. The crack pattern which formed did not separate the wall into triangular segments but, instead, included a horizontal crack in the high flexural compression region of the wall. The combination of favorable crack orientation (horizontal) and high normal compressive

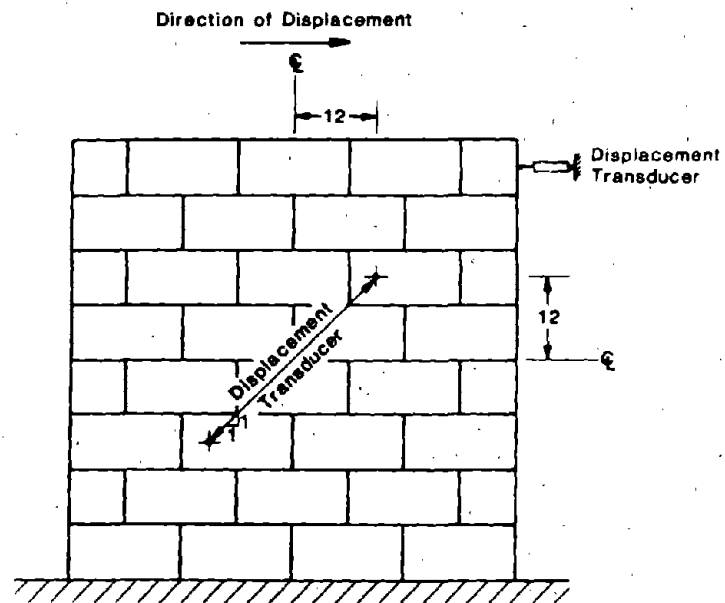


Figure 3. Instrumentation.

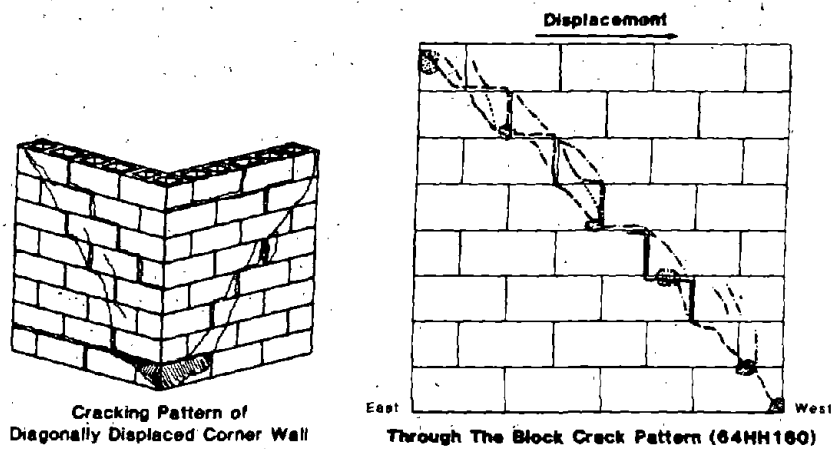


Figure 4. Typical crack patterns.

stress permitted a much more efficient shear friction mechanism to form than was possible in the shorter walls. In fact, 96 in. walls were able to resist more lateral load through the shear friction mechanism than from the diagonal-tension mechanism. First cracking was not coincident with the maximum lateral load resistance.

Loading History

The effect of cycling on the behavior and resistance of the wall panels depends strongly on the maximum displacement applied to the wall. If the cyclic displacements do not exceed the monotonic displacement at which maximum capacity is achieved, then the effect of cycling is negligible on both wall stiffness and resistance even for several hundred thousand cycles. However, excursions past the critical displacement cause severe degradation of both stiffness and resistance, even if the displacement is not incrementally increased.

Based on the five corner walls tested, there is no apparent reason to differentiate the behavior of planar walls from corner walls. When displacements are applied only along one leg of a corner wall, the effect of the outstanding leg is negligible on the cracking pattern and general wall behavior. The behavior of a corner wall subjected to simultaneous displacements along both legs is adequately predicted by evaluating each leg independently of the other. In other words, behavior could be considered in terms of resultant actions.

Shear Stress-Displacement Relationships

The shear stress versus wall displacement curves for some of the tests are shown in various combinations in figures 5 and 6. Shear stress is computed by dividing the measured in-plane lateral load by the net cross-sectional area of the wall. There appears to be a common form to the curves regardless of the variation in parameters. The effect of the applied vertical compressive stress is much more pronounced on the maximum stress achieved than on the initial stiffness of the wall. This observation excludes the gross differences in the stress-displacement relationship for the walls having flexural distress prior to diagonal tension distress. As the applied vertical compressive stress is increased, the shear stress, or conversely the wall displacement, at which the curve exhibits nonlinearity also increases. Thus, higher applied vertical compressive stresses delay the onset of nonlinear behavior. However, the applied vertical compressive stress has a negligible impact on the absolute wall displacement at which the wall reaches its maximum resistance. Therefore, the displacement which causes diagonal cracking is relatively independent of vertical stress, but the maximum resistance and initial stiffness are increased by vertical compressive stresses.

The effect of the block and mortar strengths on the initial

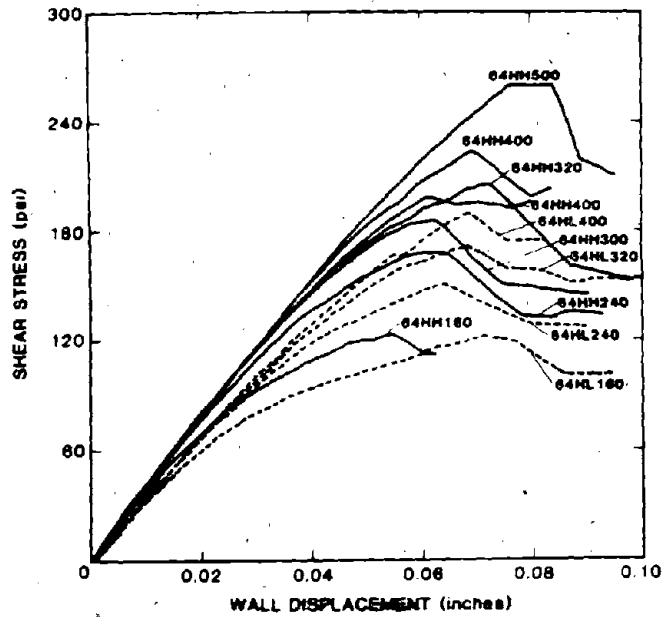


Figure 5. Stress-displacement relationships for high strength block walls.

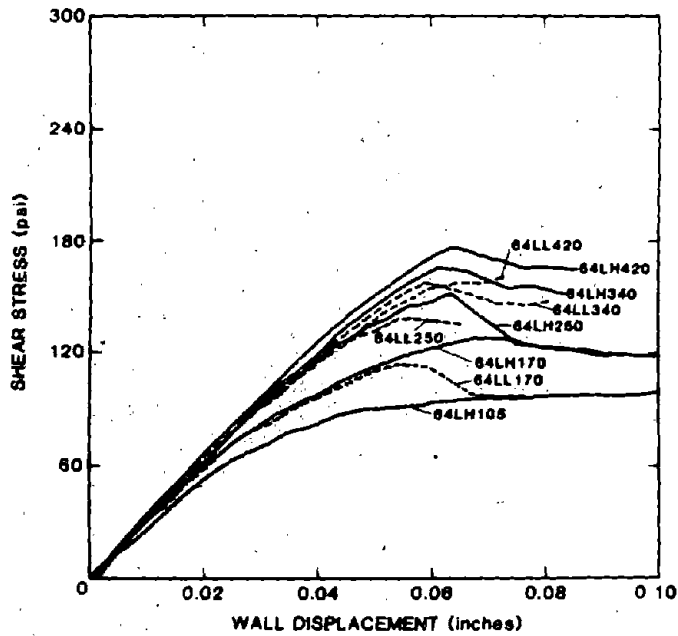


Figure 6. Stress-displacement relationships for low strength block walls.

stiffness of the walls is interactive. For example, the effect on the wall stiffness caused by varying the mortar type is significant when the walls are made with high strength block as illustrated in fig. 5. Conversely, the effect on the wall stiffness caused by varying the mortar type is negligible when the walls are made with low strength block as shown in fig. 6. The overall behavior tends to suggest that the stiffness of the wall is strongly related to its probable final crack path (mortar joint or through block) and ultimately its weakest material component.

Maximum Shear Stress Resistance

The maximum shear stresses computed from the maximum measured lateral loads along with the other pertinent data are listed in table 2 for selected wall panels. Selected maximum shear stresses for the 48 in., 64 in., and 96 in. long wall panels are plotted versus the applied vertical compressive stress in fig. 7. Clearly, there is an increase in maximum shear resistance with increased vertical compressive stress. The nature of the relationship between the shear stress and the vertical stress is affected by the wall aspect ratio and the combination of material strengths. Figure 7 illustrates the significant effect of aspect ratio, but the effect becomes pronounced only for the higher levels of vertical stress. Larger aspect ratios produce higher values of maximum shear resistance. The impact of material strengths on the maximum shear stress-applied vertical stress relationship is also shown in fig. 7. The most advantageous combination in terms of maximum resistance is, not surprisingly, high strength block and mortar. The least advantageous is the low strength block and mortar, but as with aspect ratio, the effect of material strength becomes significant only for the higher levels of applied vertical compressive stress. A regression analysis of the data plotted in fig. 10 produces an equation of the form

$$v = 70.8 + 0.313a$$

where v is the maximum shear stress and a is the applied vertical compressive stress both in units of psi. The standard error of estimate of the regression analysis is 17.4 psi and the correlation coefficient is 0.91.

Diagonal Strain

The general mode of distress exhibited by the test specimens is diagonal cracking, indicative of a diagonal tension failure. It is reasonable to expect that the diagonal tension strain should provide a reasonable predictor of the onset of wall distress. The relationships between shear stress and the diagonal wall strain computed from measured displacements are shown in fig. 8 for most of the 64 in. long wall tests. With certain exceptions, the curves in fig. 8 suggest the

Table 2. Wall Panel Maximum Shear Stresses

Wall Panel Identifier	Wall Net Cross-Sectional Area (sq. in.)	Applied Vertical Compressive Stress (psi)	Maximum Shear Stress Resistance (psi)
64HH120-2L04	246.0	122	113
64HH160-3L01	246.0	162	123
64HH240-3L04	246.0	243	167
64HH300-2L05	246.0	305	186
64HH320-3L03	246.0	325	206
64HH400-3L02	246.0	406	205
64HH400-2L03	246.0	406	227
64HH500-2L06	246.0	507	260
48HH150-3L06	184.5	163	117
48HH450-3L05	184.5	434	175
80HH250-3L07	307.5	228	178
80HH400-4L01	307.5	390	202
96HH200-4L03	369.0	217	157
96HH300-4L02	369.0	312	208
96HH400-4L04	369.0	407	251
64HL160-5L01	246.0	163	122
64HL240-5L02	246.0	243	151
64HL320-5L03	246.0	316	171
64HL400-5L04	246.0	407	190
64LL170-6L07	241.6	162	115
64LL250-6L06	241.6	246	144
64LL340-6L08	241.6	332	158
64LL420-6L09	241.6	413	174
64LH105-6L01	241.6	103	101
64LH170-6L02	241.6	161	128
64LH250-6L03	241.6	248	152
64LH340-6L04	241.6	327	166
64LH420-6L05	241.6	418	177
48LH170-6L10	181.2	165	116
48LH450-6L11	181.2	430	162
96LH220-6L12	362.4	220	163
96LH320-6L13	362.4	315	203

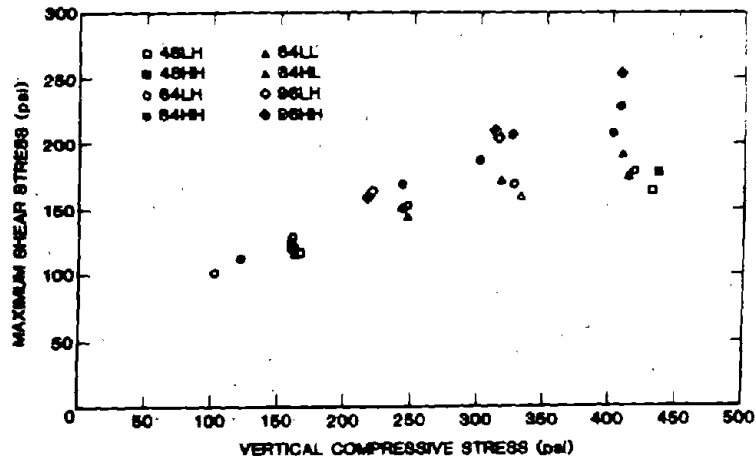


Figure 7. Shear capacity versus vertical stress.

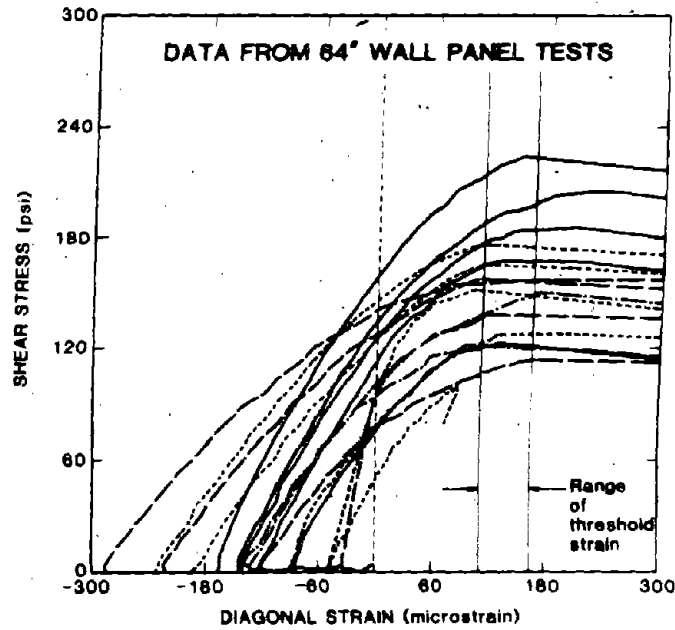


Figure 8. Shear stress versus wall diagonal strain.

existence of a common diagonal tension strain, in the range of 100-150 microstrain, at the onset of diagonal cracking. Diagonal cracking is indicated in the relationships by the sudden large increase in diagonal tension strain (displacement) with little or no increase in load resistance. The exceptions are wall tests having high vertical compressive stresses. The commonality of the threshold diagonal strain suggest a material criterion which defines the onset of diagonal cracking independent of strength and vertical compressive stress.

CONCLUSIONS

The following conclusions are based on the experimental test data obtained in the investigation described in this paper.

- * A nearly linear relationship existed between increased amounts of vertical compression and the resulting increases in maximum in-plane shear resistance of the wall panels when other parameters are held constant.
- * The lateral displacement coincident with the attainment of diagonal cracking was not significantly influenced by the amount of vertical compression applied to the wall panel, by the wall aspect ratio, or by the material strengths.
- * Tensile strain across the wall panel diagonal was the critical determinant of diagonal cracking and there appeared to exist a threshold strain of about 150 microstrain above which diagonal cracking occurred.
- * The maximum shear capacity of a wall was affected by its aspect ratio and material strengths for higher levels of applied vertical compressive stress, generally being higher for larger aspect ratio and increased material strengths.
- * There is a threshold in-plane lateral displacement below which application of repeated cycles of loading does not affect observed wall behavior. Repeated imposed displacements greater than the threshold displacement cause both stiffness and load capacity reductions.
- * Corner walls displaced along their diagonal axis have maximum resistances equal to the resultant of the in-plane resistance of each leg.

ACKNOWLEDGEMENT

The research reported herein was performed while the author was employed at the National Bureau of Standards.

A REVIEW OF ASEISMIC TEST FOR MASONRY STRUCTURES IN CHINA

Zhu Bolong¹

SUMMARY

Since Tangshan Earthquake of 1976 many research organization pay attention to study the aseismic behaviour of masonry structures. Some descriptions and discussions on pseudo-static and dynamic tests, including the test design, size and strain rate effects, constitutive relationship, model test and system identification, are presented in this paper.

INTRODUCTION

Unreinforced masonry structures are widely built in seismic area of China. During Tangshan Earthquake of July 28, 1976, the most multi-story brick buildings, brick chimneys and other industrial constructions are suffered very serious damages. Since then the Chinese aseismic research organizations, including universities and academies, pay attention to study the seismic capacity of unreinforced masonry structures and to research how to strengthen them. According to incomplete statistics about 300 wall specimens, including unstrengthened and strengthened, with and without openings or wing walls, under static cyclic loading were tested. Besides, a number of model and prototype buildings were experimental at the laboratories or on sites. In recent years, the shaking table test and strain rate effect study have more attention. In spite of the fact that the masonry material has a very low crack strength, the static tests show that it is of a certainly aseismic capacity.

STATIC TEST OF MASONRY STRUCTURES SHEAR STRENGTH FROM IDEALIZED SPECIMENS

It is well known that shear strength is one of the important factors for the aseismic capacity of masonry structures. There are two kinds of test method to determine the shear strength of masonry as shown in Fig. 1 and Fig. 2.

¹ Prof. of Civil Engineering, Chairman of Department of Structural Engineering. Director of Research Institute of Engineering Structural, Tongji University, Shanghai, China.

Wang Qinglin, et al. (Xian Institute of Metallurgy and Construction Engineering — XAIMCE) have investigated a series of prismatic (Fig. 1, H/B=3) specimens with different angle of mortar joints. From this test it is found that failure mode depends upon the angle of mortar joints (Table 1), and the maximum axial load increases with increasing θ . Many research organizations, such as: Sichuan Building Research Institute — SCBRI, Liaoning Building Research Institute — LNERI, Beijing Architecture Design Institute — BADI, et al., have tested cantilever wall specimens subjected to diagonal load (Fig. 2) to determine the average

Failure Mode

Table 1.

Angle of Mortar Joints	Failure Mode
$0 < \theta < 45$	Shear
$45^\circ < \theta < 60$	Shear - Compression
$\theta > 60^\circ$	Compression

shear strength. Test results show that the test results of wall specimens with different height-width ratio (H/B) subjected to diagonal load are not very scattered in the range of H/B=0.6 ~ 1.5.

Unreinforced Masonry Wall Tests

Test Set-up It is no any unified test set-up scheme stipulated in China up to now. Therefore, according to different study purpose the research units select their test set-up. The main set-up schemes are shown in Fig. 3.

Test scheme shown in Fig. 3a is a cantilever wall specimen subjected to vertical and horizontal loads. Owing to the fact that Fig.3a scheme is relatively close to actual stress condition, many research units (Institute of Engineering Mechanics — IEM, Chinese Academy of Building Research — CAER, Tongji University — TJU, Shanxi Building Research Institute — SXBRI, et al.) adopt it. Test set-up shown in Fig.3b provides an interstory-shear mechanical model — fixed end at top and bottom of wall and it is a special loading apparatus (SCBRI, XAIMCE, et al.). Test scheme shown in Fig. 3c (Guangxi University) is a cantilever wall specimen subjected to moment, vertical and horizontal loads. Test scheme shown in Fig. 3d (TJU) is used for pier specimen. The latter two schemes are relatively close to actual stress conditions.

Brief Summary of Test Results

From 1978 to 1983 the unreinforced walls occupied an important place in Chinese experimental work of masonry structures. The following main points can be summarized from the test results:

(a) Size Effect

For masonry structure the size of test specimen strongly influences

the average shear strength. Fig. 4 shows the relationship between the strength ratio R_T/R_j (R_T - average shear strength of masonry; R_j - pure shear strength of mortar joint) and cross section of specimen A. Besides, the height h and length l ratio of wall also strongly influences the shear strength R_T (Fig. 5 (12)) and failure mode of masonry.

(b) Normal Pressure Effect

Test results verified that the average shear strength R_T depends upon the normal compressive stress σ_0 . Fig. 6 shows the relationship between R_T/R_j and σ_0/R_j . It can be found that the test data have a certain regularity in spite of the different test set-up schemes. Besides, in Fig. 6 four line were plotted, and their formulas are given in Table 2. By the way, for Chinese residential buildings the σ_0/R_j value generally is less than 5.

Formulas of R_T

Table 2.

BJG 3-73 ⁽¹⁾	TJ-11-78 ⁽²⁾	TJU ⁽³⁾	IEM, et al.
$1 + 0.7\sigma_0/R_j$	$\sqrt{1 + \sigma_0/R_j}$	$0.4 + 0.5\sigma_0/R_j$	$0.7(1 + 0.7\sigma_0/R_j)$

(c) Aseismic Capacity

Fig. 7 shows the typical hysteresis loops of unreinforced masonry wall (TJU⁽³⁾). In spite of the fact that the cracks of masonry wall occurred due to the low tensile strength, the masonry structure has a limited aseismic capacity which is reflected by the ability of energy dissipation due to the certain deformability.

Unreinforced Masonry Building Test

In order to investigate a building subjected to the lateral load for the purpose of studying aseismic behaviour, since 1977 a number of full-scale and model buildings were tested by many Chinese research units.

Full Scale Unreinforced Masonry Building Test on Site. Eight full-scale brick or concrete block buildings were tested at Kunming, Lanzhou, Hangzhou, Harbin (IEM)⁽⁴⁾ and Shanghai⁽⁵⁾ since 1978 to 1979. The plan and profile of the latter one⁽⁶⁾ are shown in Fig. 8; besides, the crack pattern and relationship between total horizontal load and roof displacement are shown in Fig. 9.

Model Unreinforced Masonry Building Test. Four single-story (Shanghai Building Research Institute) and two two-story⁽¹²⁾ (TJU) model buildings were tested under lateral loading during 1978 - 1981. Because the model building is cheaper than full-scale, for the purpose of studying the failure mechanism it was adopted by many research units.

Brief Summary of Test Results From the full-scale and model building tests, the following view-point can be drawn:

(1) It is verified that the failure mechanism of single masonry wall specimens is close to the buildings.

(2) As shown in Fig. 9, the damage of ground floor is serious and it reduces upwards story by story.

(3) It is very difficult to say which seismic intensity can be resisted by one building after static test, but a restoring force model (For example Fig. 10⁽³⁾) can be given and it can be used in nonlinear seismic response analysis to help us to evaluate the seismic grade of masonry building.

Strengthened and Reinforced Masonry Structure

Masonry Structure Strengthened with Reinforced Concrete Columns In order to strengthen the existing masonry building in seismic area, many research organizations (Dalian Institute of Technology DLIT⁽⁷⁾, CABR⁽⁸⁾⁽⁹⁾, TJU⁽¹⁰⁾⁽¹⁶⁾, et al.) have carried out their study programs for wall specimens or model buildings strengthened with reinforced concrete columns and tie bars. Fig. 11 shows the strengthened effect of masonry wall⁽¹⁸⁾.

Masonry Structure Repaired with Reinforced Columns TJU⁽¹²⁾ has performed a program to study the damaged walls or model buildings repaired with reinforced columns without grouting the cracks of wall. Fig. 12 shows the repaired effect of the damaged walls.

Masonry Structure Strengthened with Cement Mortar Cover Reinforced by Steel Mesh. In seismic area of China the cement mortar cover reinforced by steel mesh is widely used to strengthen the walls of existing building. In generally, the cover is only 3cm in thickness and the spacing of the bars is 20 cm, but the strengthened effect is very evident, as shown in Fig. 13⁽¹⁴⁾.

Brief Summary of Test Results

(a) The reinforced concrete columns directly contribute their shearing capacity to resist the seismic load together with brick wall, and the ductility of wall is improved.

(b) The brick building strengthened with reinforced concrete column had increased in aseismic capacity more than 100% during Tangshan Earthquake, but the static test shows that the aseismic capacity has increased only to 20%. This problem should be solved by shaking table tests.

(c) The strengthening effect of cement mortar reinforced with steel mesh for brick wall is relatively evident.

DYNAMIC TEST

Strain Rate Effect

The author's research group (TJU) carried out a test of four masonry

wall specimens subjected to reversed lateral loading with different frequencies (0.1Hz, 1 Hz, 3 Hz). It is evident that the strain rate has influence on shearing strength of masonry wall as well as on the area of loops, as shown in Fig. 14.

Brick Model Building Test

Some strengthened and unstrengthened five-story brick model buildings (scale 1:8) have tested in laboratory of BADI. The building was vibrated by vibration generator, which was located on the top of roof; and the walls were subjected to cyclic loading.

Brief Summary of Dynamic Test

(a) The strain rate has strongly influence on the shear strength of masonry wall.

(b) The masonry model buildings strengthened with reinforced concrete columns can resist stronger earthquake, it is also verified by the dynamic cyclic loading.

SHAKING TABLE TEST

Brick Wall Test

The author's research group performed a program of shaking table test for masonry wall with or without openings in laboratory of Tongji University. The additional mass has a weight of 8.5t. Fig. 15 shows the partial test results of masonry wall tested on the shaking table excited by an input record of El-Centro Earthquake (1940 NS).

Concrete Block Model Building Test

Unreinforced Block Model Building Test Three five-story unreinforced concrete block model building were tested on shaking table (TJU)⁽¹⁵⁾ and three single-story brick model buildings were experimented on another one (IEM)⁽¹⁷⁾. Besides, in order to obtain the mathematic model of building from the shaking table test data, the non-linear system identification is developed⁽¹⁶⁾. Fig. 16 shows the experimental and identified results of the five-story building.

Strengthened Block Model Building Test One block model building strengthened with reinforced concrete columns was tested by author's research group (TJU) on shaking table. The test results show that the strengthened effect is evident and it can explain the additional columns how to resist the seismic loading.

EXPLOSIVE - FIELD DYNAMIC TEST

Two three-story masonry building with internal reinforced columns

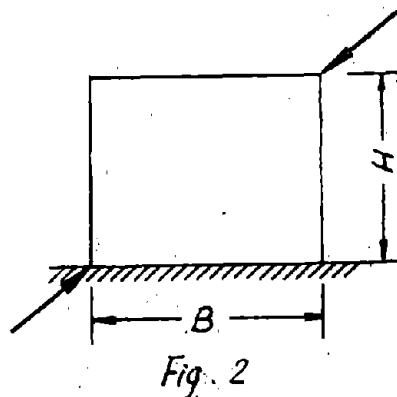
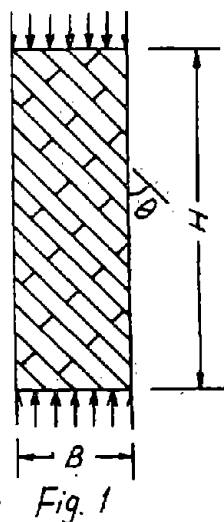
and beams were tested on the field by Prof. Zhang (ZHU)⁽¹⁰⁾ using explosive method. The distance from the explosive center to the buildings was 132m, as shown in Fig. 17. The damage is similar to that of an earthquake: the horizontal cracks appeared in the walls above and under the windows of the third floor, and the similar cracks appeared in the walls of second floor but much lighter.

REFERENCES

- (1) "Design Code of Masonry Structure (GBJ 3-73)" (in Chinese), 1973, Beijing.
- (2) "Aseismic Design Code for Industrial and Civil Buildings (TJ 11-18)" (in Chinese), 1978, Beijing.
- (3) Zhu Bolong, Wu Mingshun, Jiang Zhixian, "Experimental Study on Basic Behaviour of Brick Masonry under Reversal Loading" (in Chinese), Journal of Tongji University, 1980, No. 2.
- (4) Xia Jiangqian, et al., "Experimental Study on Basic Mechanical Properties of Brick Buildings" (in Chinese), Earthquake Engineering and Engineering Vibration, Mar., 1983.
- (5) Hua Ruju, Qin Tongyin, "Aseismic Capacity of Solid Concrete Block Masonry Residential Building" (in Chinese), Building Structure, 1980, No. 4.
- (6) Zhu Bolong, Jiang Zhixian, Wu Mingshun, "Seismic Analysis of a Five-Story Concrete Block Masonry Building", Journal of Tongji University, 1981, No. 4.
- (7) Wu Ruifeng, et al., "Test and Analysis of the Earthquake Resistant Behaviour of the Brick-Walls with Reinforced Concrete Columns" (in Chinese), Journal of Dalian Institute of Technology, 1983, No.3.
- (8) Liu Xihui, et al., "A Study of Aseismic Characteristics of Masonry Building with Reinforced Concrete Tie-Columns" (in Chinese), Journal of Building Structure, Vol. 2, No. 6.
- (9) Niu Zezhen, Du Qi et al., "A Study of Aseismic Strengthening for Multi-Story Brick Building by Additional R/C Columns, "Proc. of 8 WCEE, Vol. 1.
- (10) Zhu Bolong, Wu Mingshun, et al., "A Study on Aseismic Resistance of Repaired and Strengthened Block Masonry Buildings", Proc. of US-PRC Bileteral Workshop on Earthquake Engineering, Aug. 1982, Harbin, China.
- (11) Zhu Bolong, Jiang Zhixian, et al., "A Study on Aseismic Capacity of Brick Masonry Buildings Strengthened with Reinforced Concrete Columns and Tie Bars" (in Chinese), Proc. of US-PRC Bileteral Workshop on Earthquake Engineering, Aug. 1982, Harbin, China.
- (12) Zhu Bolong, Wu Mingshun et al., "A Study on Aseismic Behaviour of Concrete Block Masonry Buildings and Its Strengthening by Rein-

forced Concrete Columns" (in Chinese), Journal of Building Structure, 1984, No. 5.

- (13) Zhu Bolong, Jiang Zhixian, et al., "A Study on Aseismic Capacity of Brick Masonry Building Strengthened with Reinforced Concrete Columns" (in Chinese), Journal of Tongji University, 1983, No. 1.
- (14) Zhu Bolong, Wu Mingshun, et al., "A Study on Aseismic Capacity of Brick Wall Strengthened with Cement Mortar Reinforced with Steel Mesh" (in Chinese), Journal of Earthquake Engineering and Engineering Vibration, 1984, Vol. 4, No. 1.
- (15) Zhu Bolong, Lü Xilin, "Shaking Table Study of a Five-Story Unreinforced Concrete Block Masonry Model Building", Proc. of International Workshop on Earthquake Engineering, Vol. II, March, 1984, Shanghai, China.
- (16) Lü Xilin, Zhu Bolong, et al., "Identification of Nonlinear Structural Parameters of Multi-Degree-of-Freedom Systems", Proc. of International Workshop on Earthquake Engineering, Vol. II, March, 1984, Shanghai, China.
- (17) Gao Yuxue, Yang Yucheng, et al., "Experimental Research on Model Brick by Shaking Table", Proc. of International Workshop on Earthquake Engineering, Vol. II, March, 1984, Shanghai, China.
- (18) Zhang Liangduo, Na Xiangqian, "Experimental Study and Analysis of Earthquake Damage of R/C Frame Building with Exterior Brick Bearing Walls and Their Strengthening", Proc. of 8WCEE, Vol. 1.



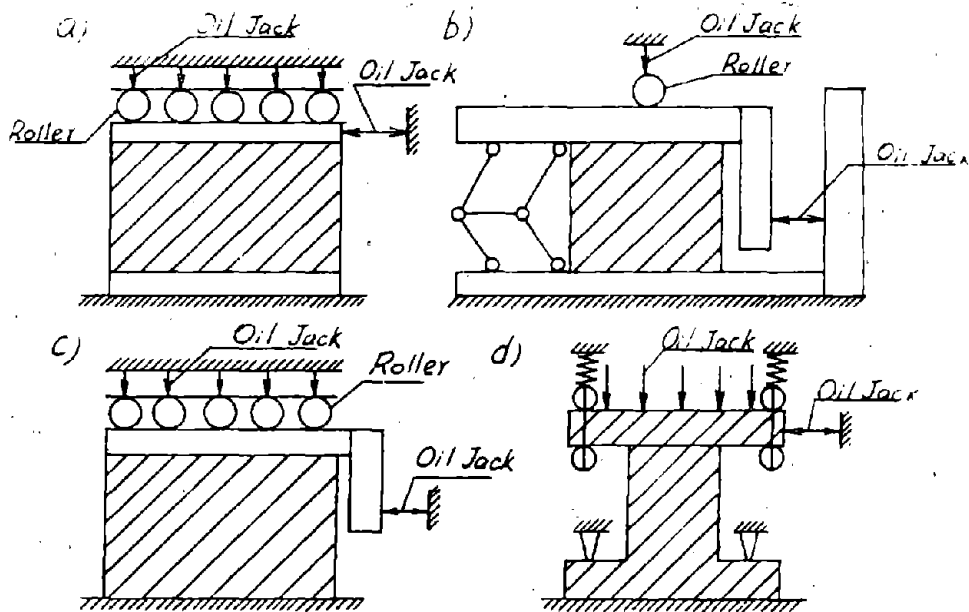


Fig. 3

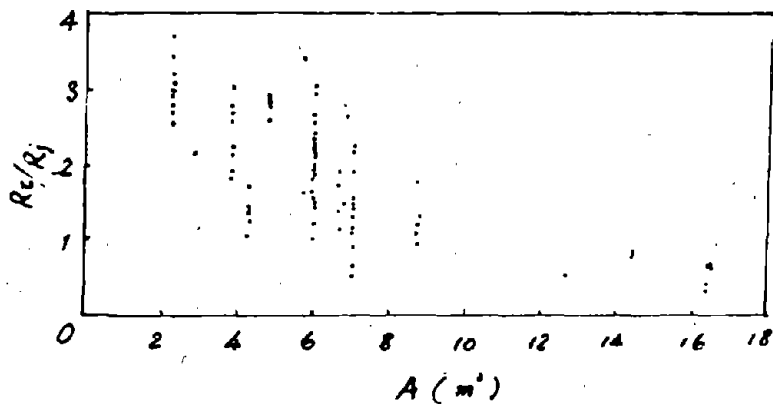


Fig. 4

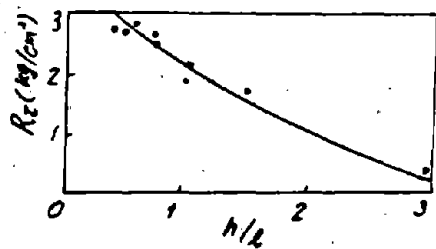
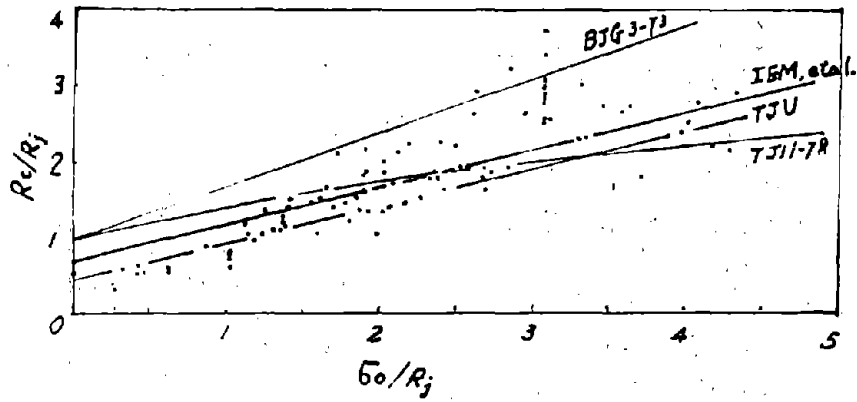


Fig. 5



BJG-3-73 $\frac{R_c}{R_j} = 1 + 0.7 \frac{\sigma_0}{R_j}$

TJ11-78 $\frac{R_c}{R_j} = \sqrt{1 + \frac{\sigma_0}{R_j}}$

IEM, et al. $\frac{R_c}{R_j} = 0.7 + 0.49 \frac{\sigma_0}{R_j}$

TJU $\frac{R_c}{R_j} = 0.4 + 0.5 \frac{\sigma_0}{R_j}$

Fig. 6

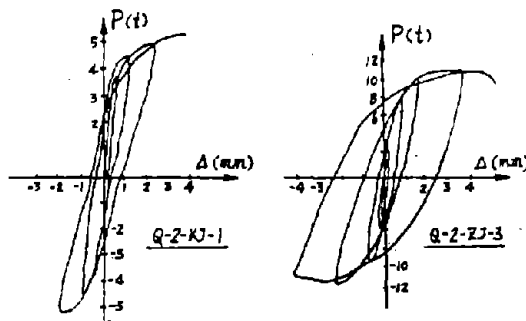


Fig. 7

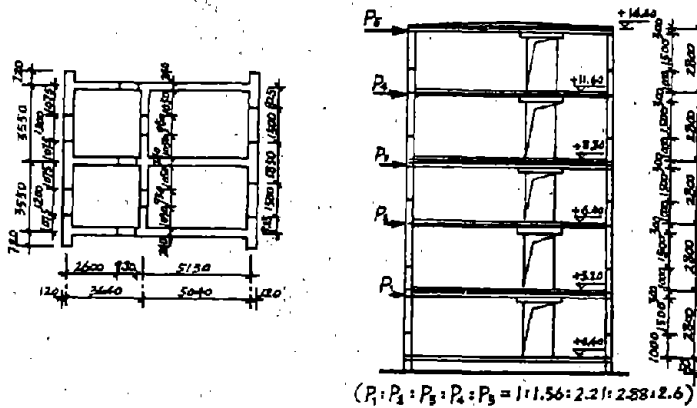


Fig. 8

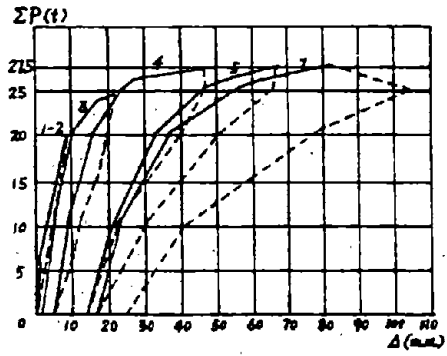
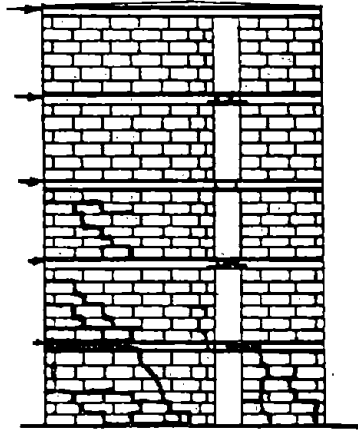


Fig. 9

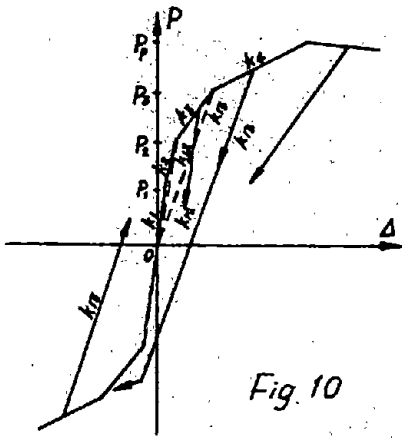


Fig. 10

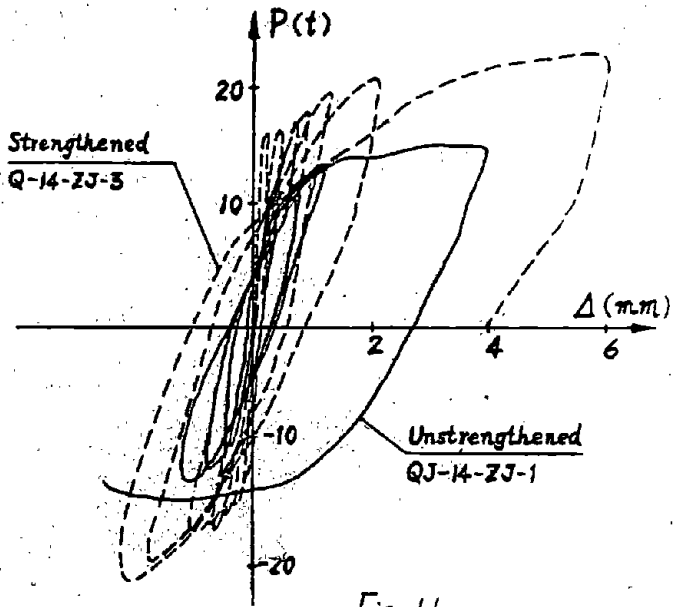


Fig. 11

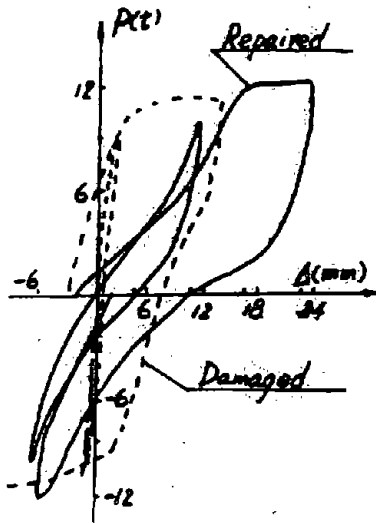


Fig. 12

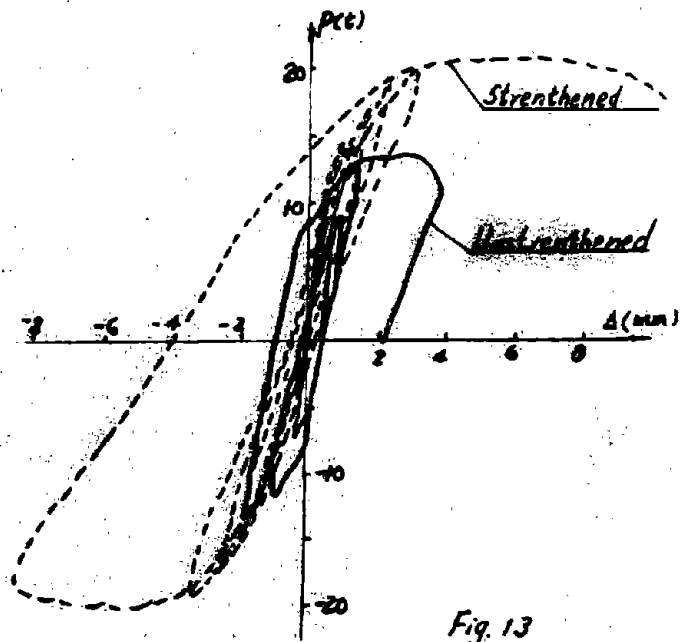


Fig. 13

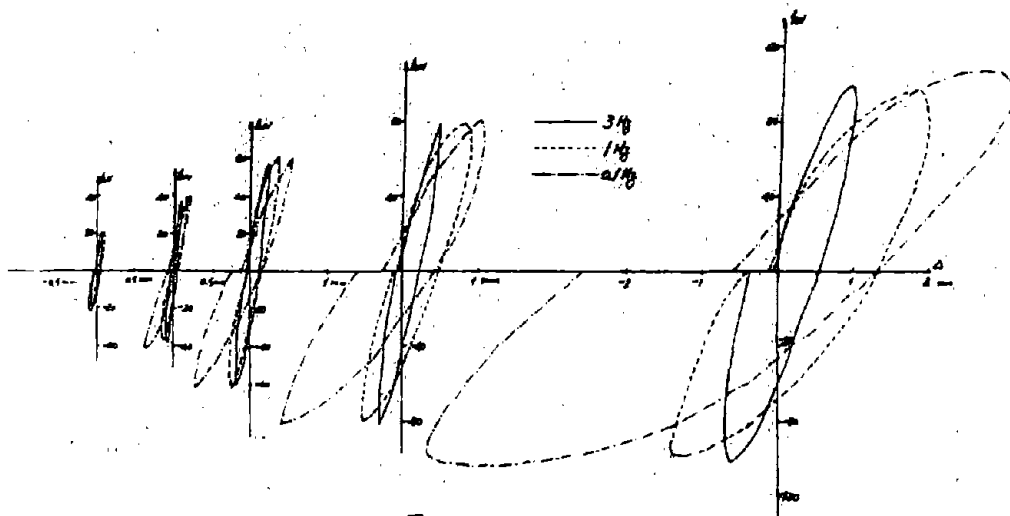


Fig. 14

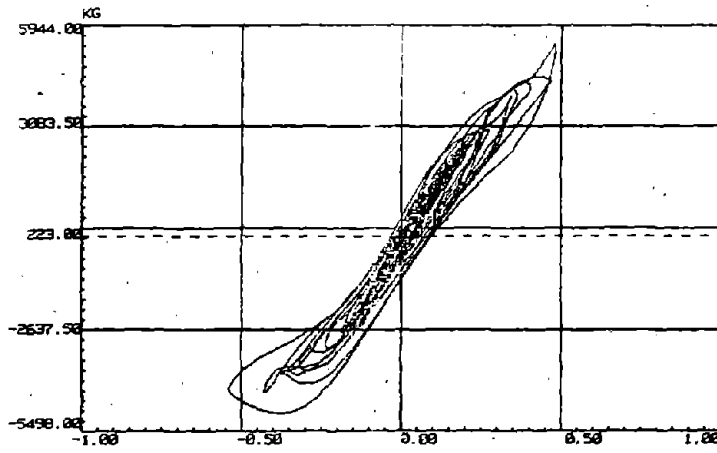


Fig. 15

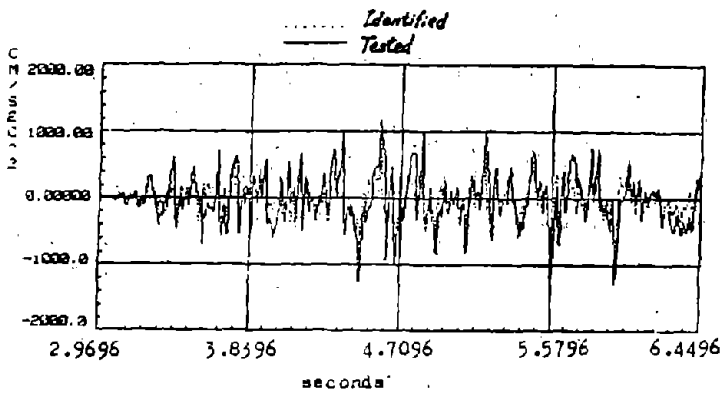


Fig. 16

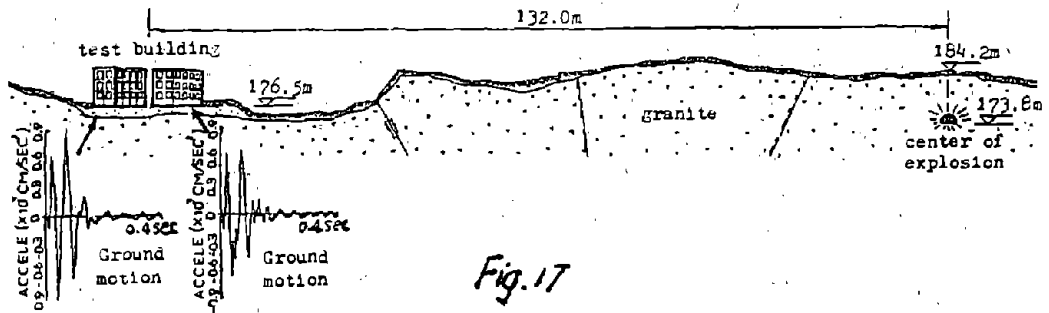


Fig. 17

**AN INVESTIGATION OF THE SEISMIC BEHAVIOR AND
REINFORCEMENT REQUIREMENTS FOR SINGLE-STORY MASONRY HOUSES**

Lindsay R. Jones⁽¹⁾, Ray W. Clough⁽²⁾, Ronald L. Mayes⁽¹⁾

SUMMARY

This paper presents the results of an investigation undertaken to determine the reinforcement requirements for single-story masonry houses located in Uniform Building Code Seismic Zone 2 areas of the United States. The investigation consisted of testing five masonry houses measuring 16 ft. (4.90 m) square in plan on a two-component shaking table capable of horizontal and vertical motions. The dynamic response of each house was measured and careful observations made. The resulting design recommendations is that no reinforcement is necessary for single-story brick or concrete block residences in Zone 2 provided minimum lengths of masonry shear resisting elements are provided. If these minimum length requirements cannot be met, then partial reinforcement is required and procedures are proposed to determine the minimum lengths of partially reinforced walls.

BACKGROUND

Seismic design requirements specified by the U.S. Department of Housing and Urban Development (HUD) are referenced to "seismic risk zones" defined by the Uniform Building Code (UBC). Changes in the UBC maps were incorporated into HUD requirements and this resulted in the requirement for partial reinforcement for masonry houses in newly specified Zone 2 areas. These requirements were considered too conservative by the construction industry in Phoenix, Arizona, one of the affected locations, and it was decided to study the question experimentally by subjecting assembled components of masonry houses to simulated earthquakes on the EERC shaking table. The primary objective was to determine the maximum earthquake intensity that could be resisted satisfactorily by an unreinforced house, and to evaluate the additional resistance provided by partial reinforcing. Results of the house and roof to wall connection tests are given in [1], [2], [3] and [4].

(1) Principal, Computech Engineering Services, Inc., Berkeley, CA

(2) Professor of Civil Engineering, University of California, Berkeley

STRUCTURES TESTED

The unique feature of the study was the testing of full scale components of typical masonry houses subjected to motions recorded in actual earthquakes. Masonry walls 8 ft. - 8 in. (2.64 m) in height and up to 16 ft. (4.90 m) long were constructed of commercially available 6 in. wide hollow concrete block or hollow clay brick units. The walls were assembled to form 16 ft. (4.90 m) square test "houses" built on strip footings. Each wall unit was connected at the top by a standard timber roof structure. Concrete slabs were bolted to the roof structure to compensate for the reduction of mass resulting from scaling the plan dimensions. The weight of the slabs were chosen so that the ratio of total roof load to total wall peripheral length was similar to that of a 40 x 50 ft. (12 x 15 m) house with a specified roof load of 20 psf (1 kN/m²).

Figures 1, 2 and 3 show the details of Houses 1, 2, 3 and 4. The first four models were designed so that transverse and in-plane response of both unreinforced and partially reinforced panels were used in a single test. All partial reinforcement consisted of vertical bars. In the fifth house a series of tests was conducted when all four wall panels were initially unreinforced; during the subsequent phase, all walls were partially reinforced with two No. 3 (10 mm) bars.

House 5 was oriented in such a way on the shaking table with respect to the horizontal axis of table motion that its masonry walls were simultaneously subjected to two horizontal (in-plane and out-of-plane) as well as to vertical input motion - Figure 4. In this way, the effect of the combined in-plane and out-of-plane action of earthquake input on the masonry walls was investigated.

The test structures were generally subjected to a series of base motions with progressively increasing intensity - Figure 5. Some tests performed on Houses 3 and 4 included both horizontal and vertical components of motion. Three earthquake motions were used derived from the 1940 El Centro, 1952 Taft and 1971 Pacoima Dam accelerograms.

All simulated earthquake records had both one horizontal and one vertical component with no time scaling; the simultaneous action of two horizontal components on the masonry walls of House 5 resulted from the orientation of the walls with respect to the one axis of horizontal table motion; walls A and B formed a 30 degree angle and walls A1 and B1 a 60 degree angle (Fig. 4).

TEST RESULTS FOR HOUSES 1, 2, 3 and 4

The specimens used in this study were typical of "box" structures which derive their lateral force resistance from "membrane" action of the walls. The major part of the lateral force developed in these tests

resulted from the concrete blocks bolted to the roof. Resistance to this force was provided by a mechanism dependent on the relative in-plane rigidity; the out-of-plane rigidity of the wall panels and the flexural stiffness of their connections to the roof were of negligible value in resisting the roof loads. The roof structure simply provided the top support for out-of-plane forces.

From this description, it is clear that the out-of-plane walls of a masonry house must have sufficient flexural strength to resist their own inertial forces when acting as vertical beams, while the in-plane walls must have the capacity to resist the inertial forces of the entire roof system plus the top half of the walls.

In general, the observed behavior was consistent with this description of box structures subjected to lateral forces. During the tests, roof displacement amplitudes were directly related to the behavior of the in-plane walls (designated as A and B in Figs. 1 to 3). Differential displacements of the two in-plane walls were accommodated by "racking" distortions of the roof; relatively little in-plane distortion was observed in the out-of-plane walls, so it may be concluded that the roof structure did not rotate as a rigid unit. This is consistent with the usual design assumption that plywood diaphragms are much more flexible in shear distortion than are masonry walls.

A significant observation made from these experiments was that typical single-story masonry houses are so rigid that they do not develop complicated seismic response mechanisms. Motions of the test structures followed the shaking table motions very closely, with distortions generally proportional to, and in phase with, the base accelerations. The peak input acceleration may therefore be cited as the dominant quantity controlling response. The most significant features of the observed response of the test structures taken as a whole may be summarized as follows:

For Unreinforced Wall Units:

1. No cracking was observed in any major unreinforced wall unit for tests with peak accelerations less than 0.2g. The lowest intensity shaking that caused cracking of a non-bearing in-plane wall occurred during tests with peak accelerations of 0.21g; the minimum intensity to cause cracking of an out-of-plane wall was 0.25g.
2. Unreinforced out-of-plane walls continued to perform satisfactorily after cracking during several tests of increased intensity. The displacements of these walls generally became excessive where accelerations exceeded 0.4g. These large displacements involved hinging at the horizontal crack line and exhibited potential instability.

3. Cracking of unreinforced in-plane walls was of two types: horizontal cracks in panels without openings, and a diagonal crack extending downward from the window corner in the wall units with window penetrations. Permanent displacements generally were associated only with the diagonal cracks and these became unacceptably large with further testing.

For Partially Reinforced Wall Units:

1. Nearly all partially reinforced wall units performed satisfactorily in all tests. None of the partially reinforced out-of-plane components developed any significant cracks during any test, including several with peak accelerations in excess of 0.5g.
2. Partially reinforced in-plane walls also performed satisfactorily although some cracked when peak accelerations exceeded 0.3g. Cracking in the pier units without window openings was associated with rigid body rocking, and included a horizontal crack due to uplift near the base of the wall. Residual cracks were easily repairable.
3. The only partially reinforced wall which exhibited unsatisfactory behavior was the window wall of House 4 (unit A in Fig. 3). A typical diagonal crack extending from the window corner to the "toe" of the wall developed during the first phase of testing when this house was unreinforced. After the addition of two undowelled bars, the wall resisted a 0.32g test without additional cracking. However, in subsequent tests with peak accelerations in the range of 0.47 to 0.68g further cracking did develop as a result of uplift at the undowelled corner.

TEST RESULTS FOR HOUSE 5

Figure 6 presents the tests that unreinforced House 5 was subjected to. House 5 was partially reinforced after the completion of the eight tests shown in this figure. The reinforcing arrangement used for the partially reinforced House is also shown in Figure 4.

Observations from the performance of unreinforced House 5:

- a. The first structural crack appeared during test No. 5 (Figure 6). This crack was at a horizontal mortar joint near the right bottom corner of loadbearing wall B. The dynamic crack opening during test No. 5 attained the value of 0.060 in. However, the permanent deformations were negligible.
- b. The dynamic house response after the formation of this first structural crack is dominated by large uplift displacements of wall B at the crack location inducing large in-plane displacements for wall B and

large out-of-plane displacements for wall A1.

- c. All walls of House 5 have been subjected to a combination of significant in-plane and out-of-plane inertial forces (Figure 6) and developed significant in-plane and out-of-plane displacement response.
- d. The first unacceptable damage for unreinforced House 5 occurred during test No. 7 (Figure 6) in the form of partial loss of support for the door lintel beam of wall B. The term "unacceptable damage" was defined as cracking or sliding permanent deformations in excess of 1/4 in. The performance of unreinforced House 5 is depicted in Figure 6; the abscissae in this figure represent the sequential test number and the ordinates the test intensity in terms of base accelerations.

Observations from the performance of partially reinforced House 5:

- a. The partially reinforced House 5 was subjected to many tests. Figure 6 provides a summary of the base motions used for ten of these tests. The observed damage of partially reinforced House 5 is well within acceptable levels even for tests of very high intensity.
- b. The large displacement, acceleration, torsional and distortional response observed during the tests of the unreinforced House 5 after the formation of the first structural crack is well controlled by the reinforcing arrangement of the partially reinforced House 5.
- c. A comparison of the earthquake performance of the partially reinforced Houses 5 and 4, (which are essentially the same except that the partial reinforcement of the loadbearing wall A of House 4 is not provided with dowels), shows that House 5 exhibited satisfactory performance, whereas for House 4 the partial reinforcement of wall A was unable to contain the damage within acceptable levels [3].

SUMMARY OF TEST RESULTS

From the previous discussion of the test results as well as from the tables and figures the following conclusions can be drawn:

- a. The first acceptable damage (in unreinforced models) is observed for two simultaneous horizontal components of effective peak acceleration of 0.24g and zero for House 4 or 0.24g and 0.14g for House 5. The corresponding input levels for the first unacceptable damage were 0.26g and zero for House 4 or 0.26g and 0.15g for House 5.
- b. These effective peak acceleration values for first damage (either acceptable or unacceptable) are higher than the expected maximum effective peak accelerations in any part of Zone 2.

- c. The simultaneous action of two horizontal components of seismic input for the Zone 2 maximum expected effective peak acceleration does not result in an increase of damage for unreinforced House 5, compared with the damage for unreinforced House 4.
- d. The observed amplification factor at the roof level has a maximum value of 2.5 for the moderately cracked house, with input effective peak acceleration just above the Zone 2 expected maximum value. This value is also representative of the partially reinforced House 5 but for EPA values well above the expected EPA for Zone 2.
- e. An amplification factor greater than 2.5 is obtained for the unreinforced house in its postcracking stage at the roof level for EPA values above the zone 2 maximum expected EPA.
- f. The amplification factor at the top of the walls is in the range between 1.0 and 1.5. The only exception is for the cracked house when the sharp spikes of the acceleration record are included.
- g. A nominal experimental shear stress value of approximately 30 psi was found for the unreinforced masonry shear walls with input EPA values just above the EPA expected for Zone 2. A value of 60 psi was found for the nominal shear stress for the partially reinforced masonry shear elements and for EPA well above the Zone 2 maximum expected EPA. These values correspond to the first (1) definition of the net cross-sectional area in Table 1. For the second definition of net cross-sectional area (2) in the same table, the corresponding values are 50 psi and 100 psi, respectively.

DESIGN RECOMMENDATIONS

Simplified design recommendations have been proposed. These are based on the earthquake performance of the five test structures and extrapolation of these results to real prototype houses. This extrapolation considered seismic input, roof loading, foundation and roof flexibility, geometry, torsional response and other loading [4].

Definition of Seismic Zoning

For the purpose of design recommendations, the UBC Zone 2 has been divided into two subzones according to the ATC-3 estimates of expected maximum effective peak acceleration (Figure 7). The maximum expected effective peak acceleration for Zone 2A is 0.1g and for Zone 2B is 0.2g.

Definition of Structural Systems and Components

For the purpose of making design recommendations, three structural systems are defined that resist the lateral forces. The distinction between

these systems is based on the use of two types of shear-resisting masonry components (unreinforced or partially reinforced).

Shear-resisting masonry components:

- a. An unreinforced shear panel is an unreinforced masonry wall element of a certain length, defined by the design recommendations, that extends from floor to ceiling without any penetrations, openings, or discontinuities.
- b. A partially reinforced shear panel is a masonry wall element of a certain length, defined by the design recommendations, that has a No. 4 vertical reinforcing bar fully grouted at each end of the panel and dowelled to the floor (No. 4 bar). All masonry, steel and parts of this panel extend from floor to ceiling without any penetrations, openings or discontinuities.

Type I: A structure with all the masonry shear resisting elements unreinforced.

Type II: A structure with a combination of unreinforced masonry and partially reinforced masonry shear resisting elements.

Type III: A structure with all masonry shear resisting elements partially reinforced. In addition, each exterior corner is provided with at least one fully-grouted reinforcing bar with a dowel connection to the foundation. Moreover, all non-shear-resisting elements are provided with a fully-grouted No. 3 or greater reinforcing bar (no dowel) at an average spacing of 8 ft. and with a maximum spacing of 12 ft.

Design Recommendations

1. All exterior walls must have a shear-resisting element that can resist the lateral seismic forces, with the specified length as determined by the procedure in the next section.
2. For Zone 2A the minimum length of an unreinforced shear-resisting elements are 6 ft. and 5 ft. respectively.
3. For Zone 2B the minimum length of an unreinforced shear-resisting element is 9 ft.; alternatively there may be two 6 ft. elements. The minimum length of a partially reinforced shear-resisting element is 5 ft.

Adequacy of the Shear-Resisting Elements

The adequacy of the shear-resisting elements can be checked by comparing the lateral load to be resisted with the shear force capacity

of these elements.

1. The lateral force (LF) can be found as the product of the roof load per wall (W) and the effective peak acceleration of the zone (EPA = 0.1g for Zone 2A and EPA = 0.2g for Zone 2B) and an amplification factor (AF).

$$LF = W * EPA * AF$$

2. The shear force resisting capacity (SFC) of the shear panels can be found as the product of the net cross-sectional area of the panel (net A) and a maximum allowable shear stress (r).

$$SFC = (\text{net A}) * r$$

Table 1 includes proposed values of the amplification factor and of the maximum nominal allowable shear stress. For the case of solid brick masonry wall, an equivalent nominal shear stress value should be used when the net cross sectional area from a section through the solid brick is considered. An unreinforced shear resisting element in excess of 9 ft. can be replaced by two shear resisting elements each with a minimum length of 6 ft. To check the total length adequacy for these two shear resisting elements, the proposed shear value must be reduced by 30 percent.

REFERENCES

- [1] Gulkan, P., R.L. Mayes, and R.W. Clough, "Shaking Table Study of Single-Story Masonry Houses - Volume 1: Test Structures 1 and 2," Earthquake Engineering Research Center Report No. UCB/EERC-79/23, September 1979.
- [2] Gulkan, P., R.L. Mayes, and R.W. Clough, "Shaking Table Study of Single-Story Masonry Houses - Volume 2: Test Structures 3 and 4," Earthquake Engineering Research Center Report No. UCB/EERC-79/24, September, 1979.
- [3] Clough, R.W., R.L. Mayes and P. Gulkan, "Shaking Table Study of Single-Story Masonry Houses - Volume 3: Conclusions and Recommendations," Earthquake Engineering Research Center Report No. UCB/EERC-79/25, September, 1979.
- [4] Manos, G.C., R.W. Clough and R.L. Mayes, "Shaking Table Study of Single-Story Masonry Houses: Dynamic Performance Under Three Component Seismic Input and Recommendations," Earthquake Engineering Research Center Report No. UCB/EERC-83/11, July 1983.
- [5] Gulkan, P., R.L. Mayes, and R.W. Clough, "Strength of Timber Roof Connections Subjected to Cyclic Loads," Earthquake Engineering Research Center Report No. UCB/EERC-78/17, September, 1978.

ACKNOWLEDGEMENTS

The investigation described in this paper was part of a research program entitled "Laboratory Studies of the Seismic Behavior of Single-Story Masonry Buildings in Seismic Zone 2 of the U.S.A.," sponsored by the Department of Housing and Urban Development under Contract No. H2387. The authors would like to acknowledge the support they have received from HUD which made the study possible. The testing of the first four houses was performed under the direct supervision of Dr. Polat Gulkan whereas Dr. George Manos was responsible for the testing of House 5. The considerable efforts of both are very gratefully acknowledged. The concrete block units were donated by the California Concrete Masonry Technical Committee, and are gratefully acknowledged. D.A. Sullivan Co. fabricated the masonry walls. Planning and implementation of the tests were carried out with the suggestions of the Applied Technology Council (ATC) Advisory Panel consisting of J. Gervasio, J. Kesler, O.C. Mann, L. Pritchard and R.L. Sharpe, and subcontractor R.D. Benson. The government technical representatives on the project were the late W.J. Werner and R. Morony. Additional coordination with the Department of HUD was provided by L. Chang and A. Gerich. W.L. Dickey, consulting engineer, was present during all experiments and offered numerous helpful suggestions and background information. Student assistants P. Buscovich and T. Nearn did the laboratory work, D. Steere implemented the data acquisition setup in addition to running the earthquake simulator, and the personnel of the Structural Research Laboratory headed by I. Van Asten contributed to every phase of the experimental work. Initial phases of the study were done under the supervision of Y. Omote and R. Hendrickson.

TABLE 1 : PROPOSED AMPLIFICATION FACTORS AND MAXIMUM ALLOWABLE SHEAR STRESS

Structural System		Unreinforced Shear Element		Partially Reinforced Shear Element	
Type I	Amplif. Factor	2.5		--	
	Shear Stress (psi)	15 ⁽¹⁾	22 ⁽²⁾	--	
Type II	Amplif. Factor	2.5		1.67	
	Shear Stress (psi)	15 ⁽¹⁾	22 ⁽²⁾	35 ⁽¹⁾	45 ⁽²⁾
Type III	Amplif. Factor	--		1.67	
	Shear Stress (psi)	--		35 ⁽¹⁾	45 ⁽²⁾

- NOTES: 1. Based at the net cross sectional area through the hollow concrete block of the masonry wall.
 2. Based at the net cross sectional area of the horizontal mortar joint of the masonry wall.

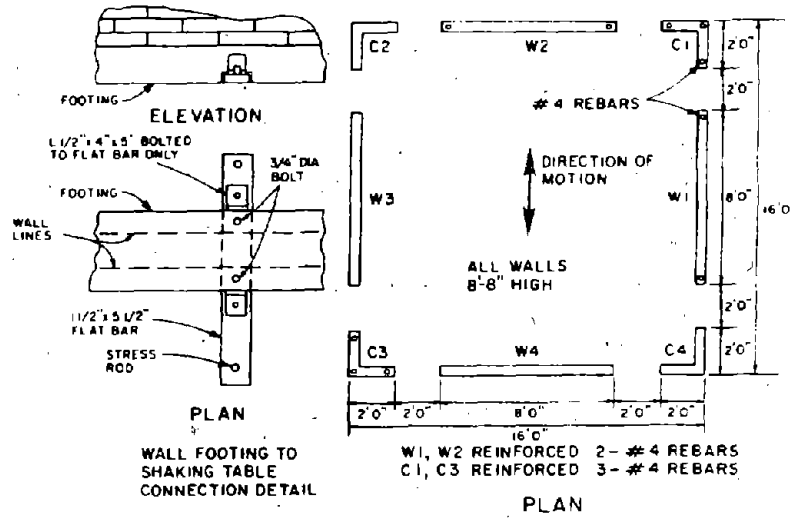


FIGURE 1 : HOUSE 1

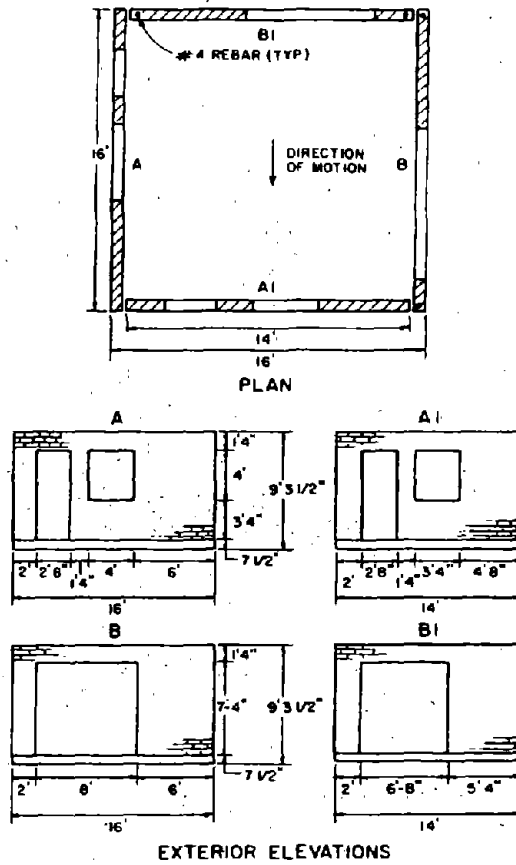


FIGURE 2 : HOUSE 2 AND 3

III-6-11

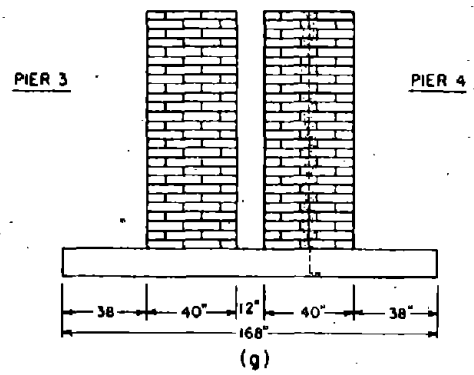
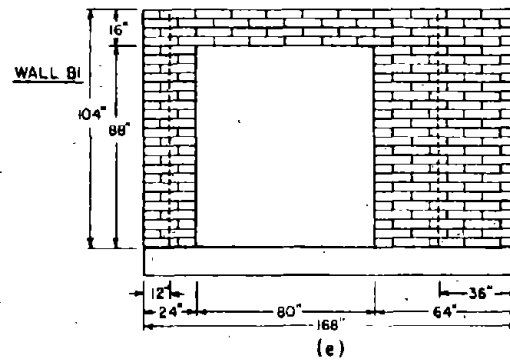
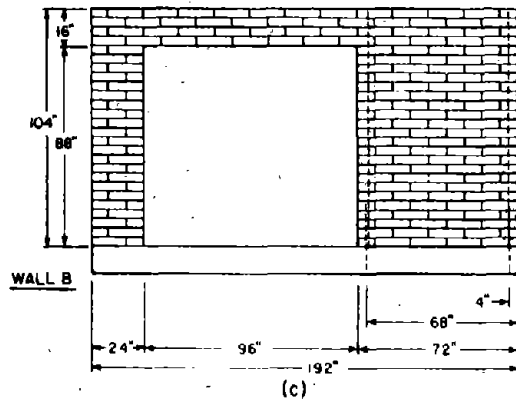
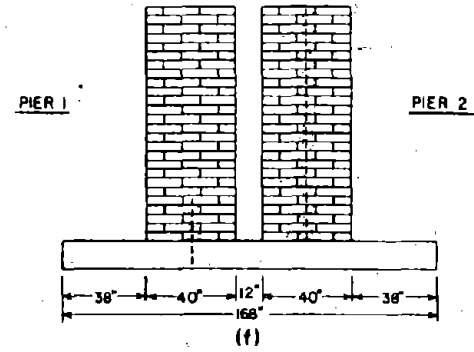
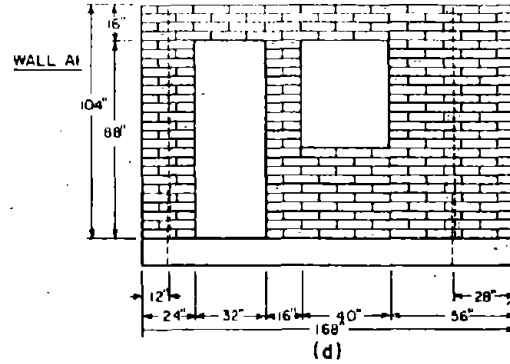
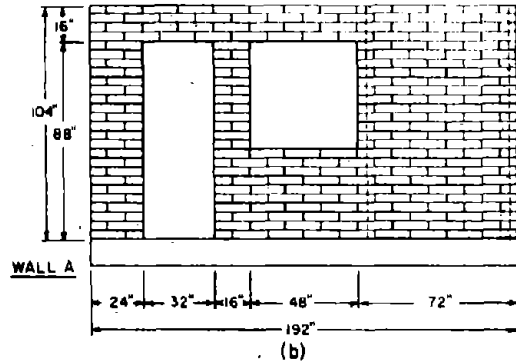
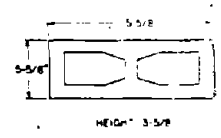
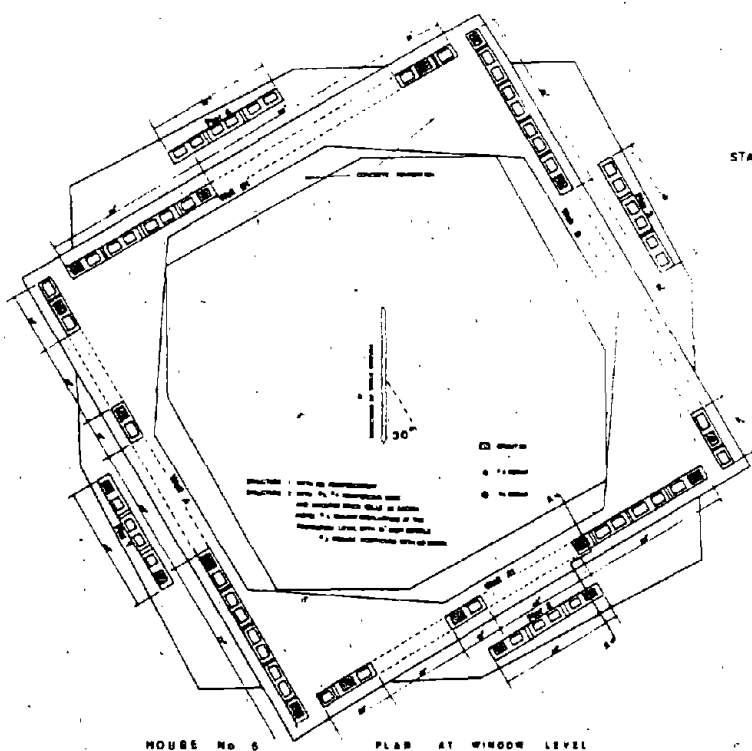


FIGURE 3 : HOUSE 4



STANDARD CONCRETE BLOCK UNIT FOR HOUSE 5

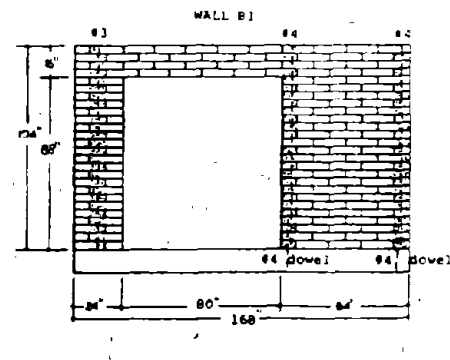
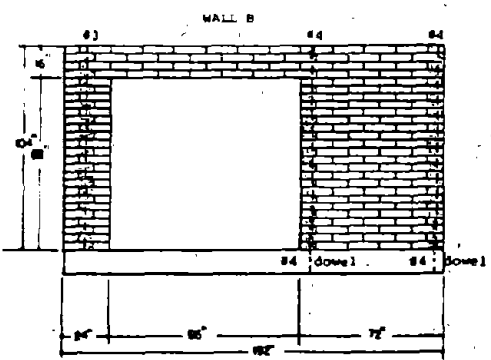
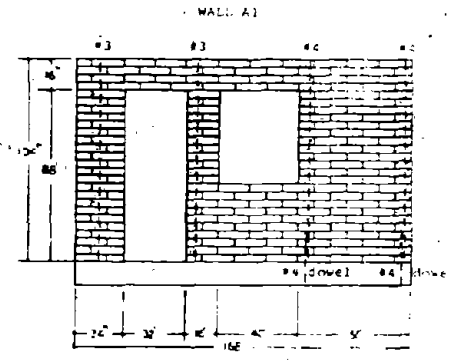
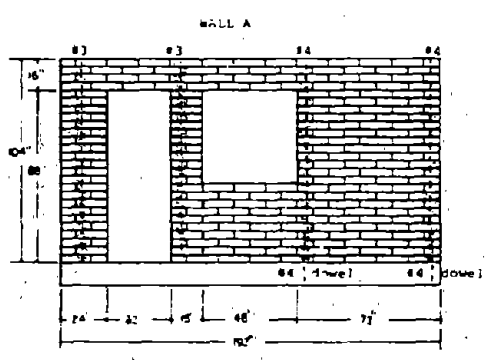
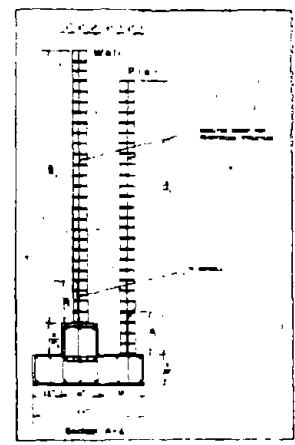


FIGURE 4 : HOUSE 5 WITH PARTIAL REINFORCEMENT

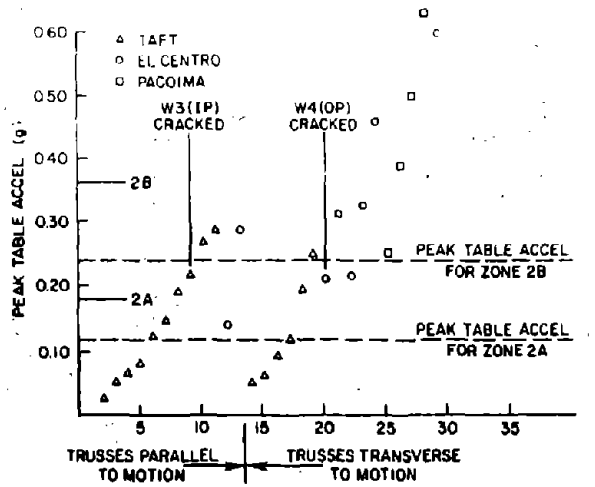


FIGURE 5.1 : SEQUENCE OF TESTS FOR HOUSE 1

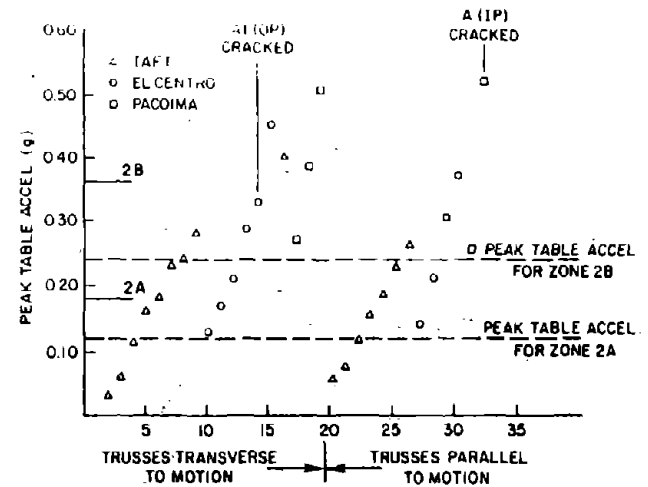


FIGURE 5.2 : SEQUENCE OF TESTS FOR HOUSE 2

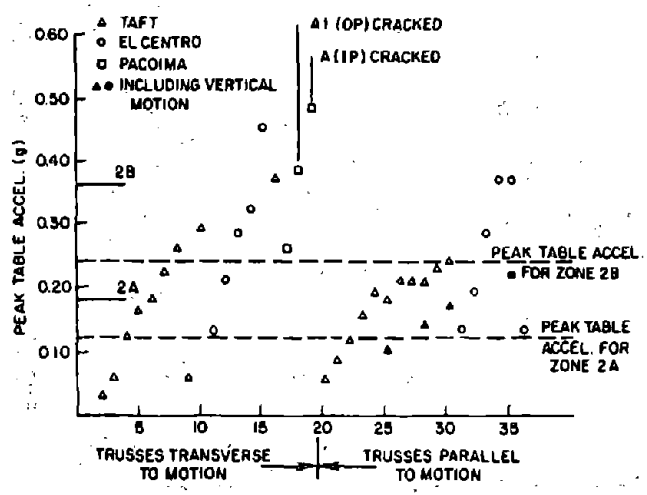


FIGURE 5.3 : SEQUENCE OF TESTS FOR HOUSE 3

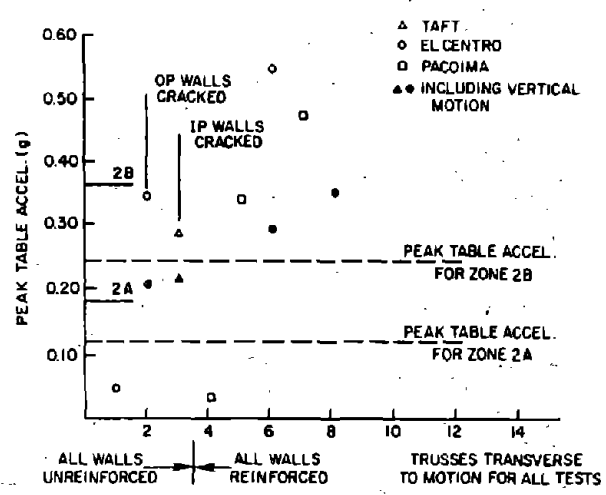


FIGURE 5.4 : SEQUENCE OF TESTS FOR HOUSE 4

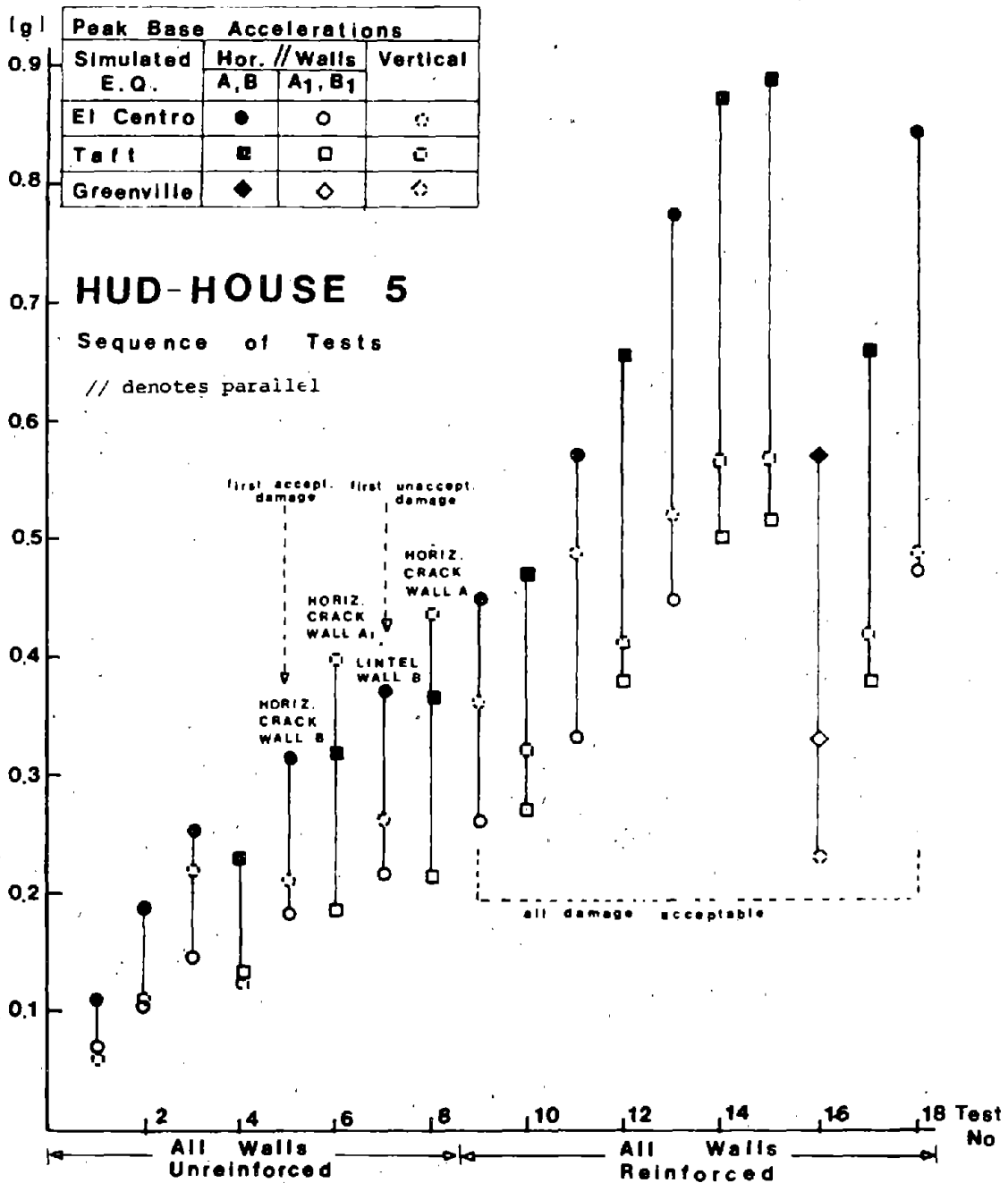


FIGURE 6 : SEQUENCE OF TESTS FOR UNREINFORCED AND PARTIALLY REINFORCED HOUSE 5

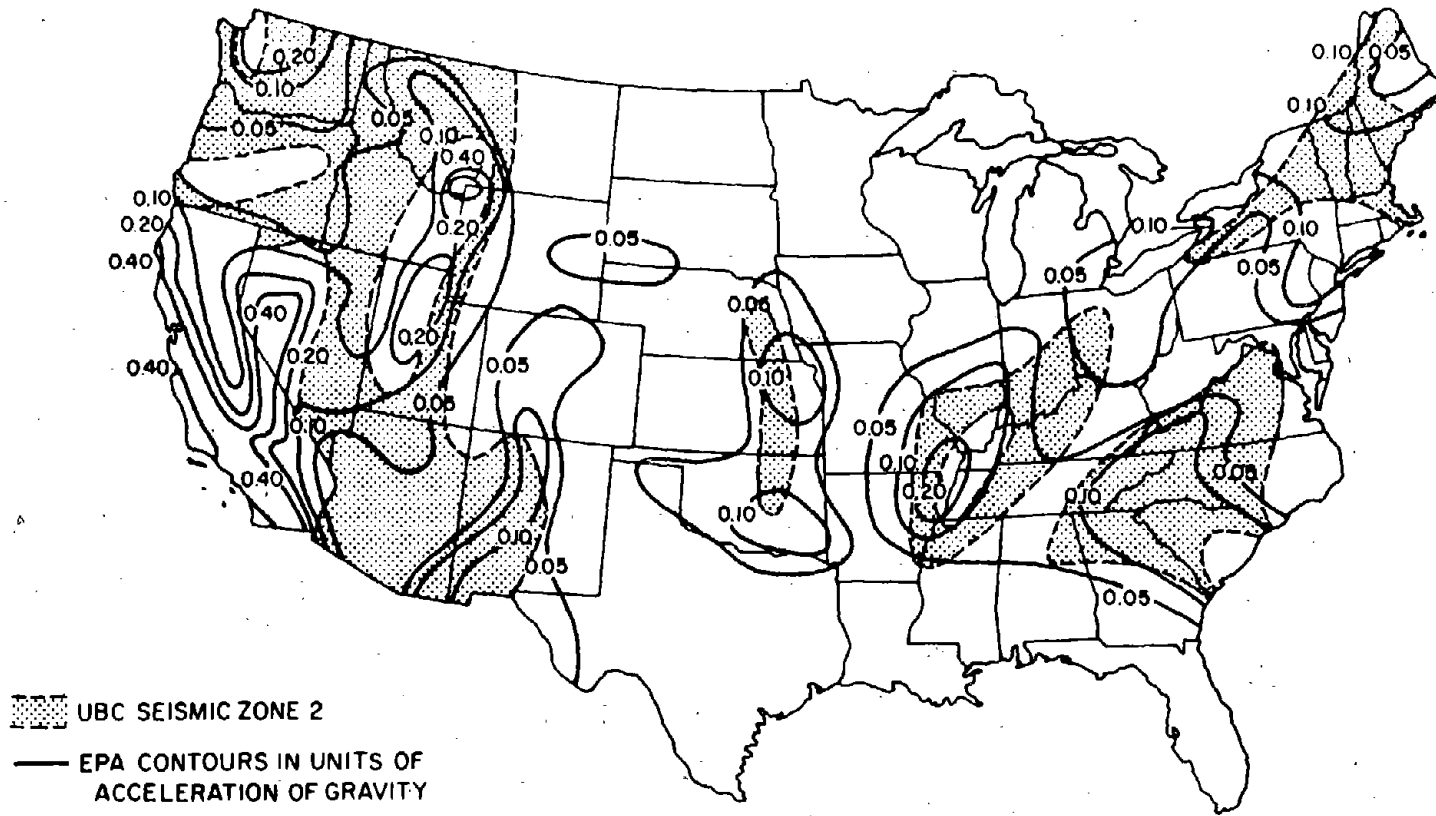


FIGURE 7 : COMPARISON OF UBC SEISMIC ZONE 3 AND THE CONTOUR MAP OF EFFECTIVE PEAK ACCELERATIONS

IDENTIFICATION FOR THE MATHEMATICAL MODELS
TO PREDICT THE EARTHQUAKE RESPONSES OF THE
UNREINFORCED CONCRETE BLOCK MASONRY BUILDING
AND ESTIMATION OF ITS ASEISMIC CAPACITY

Lü Xilin¹

Zhu Bolong²

SUMMARY

Based on shaking table experiments and nonlinear system identification, the mathematical models of unreinforced concrete block masonry building were developed to predict the nonlinear earthquake response of the building, and the aseismic capacity of the building was estimated. This paper covers four areas as follows:

1. Prediction of aseismic capacity of prototype building from small-scale model building test on shaking table.
2. Presentation and verification of an iterative process for the identification of nonlinear mathematical models of shear building.
3. Confirmation of a "semi-degrading tri-linear" model of restoring force for the analysis of cracking building, by using shaking table experiments and system identification.
4. Development and formulation of a "shear-slip" restoring force model for the nonlinear identification of the model building during failure stage.

SHAKING TABLE EXPERIMENTS OF FIVE-STORY UNREINFORCED
CONCRETE BLOCK MASONRY BUILDING

In order to study the aseismic behavior of masonry structure and to identify the nonlinear mathematical models of the building during strong earthquake, three model buildings which are on the scale of one-fourth of the prototype building were tested on shaking table in Tongji University. The plan and profile of the test building are shown in Fig. 1 and Fig. 2. The model building and loading procedure basically satisfied the similitude requirements. An artificial earthquake accelerogram corresponding to the third category of soil condition of Chinese "Aseismic Design Code for industrial and Civil Building" was used as input data with the compressed duration according to the time scale of each model building. Accelerations at every floor and roof displacement were measured during test procedure.

¹ Dr. of Engineering, Tongji University, Shanghai, China.

² Prof. of Civil Engineering, Tongji University, Shanghai, China.

The strength of mortar, normal stress of wall and input peak acceleration are shown in Table 1.

Table 1.

Mechanical Properties of Model Buildings and Loading Steps

Model building	Strength of mortar at 1st story (MPa)	Strength of mortar at roof level (MPa)	Normal stress of wall at 1st story (MPa)	Normal stress of wall at roof level (MPa)	ΔT (s) Time interval	T(s) Duration	Amplitude cm/s ²	Failure condition
(I)	0.811	1.092	0.223	0.026	0.0058	3.48	196 546 706 1200	uncrack crack crack slip
(II)	2.903	2.892	0.231	0.336	0.0062	6.20	155 466 880 1780	uncrack crack crack slip
(III)	2,903	1.143	0.319	0.0471	0.0074	7.40	108 686 900	uncrack crack slip

The test results of three model buildings are as follows:

1. When the model buildings were subjected to 0.11-0.2g peak acceleration, the response of the buildings was linear, and the deformation of buildings was very small.

2. When the model buildings were excited at peak acceleration of 0.47-0.88g, the horizontal and stepped diagonal cracks appeared in the lateral walls of the first and second story, as is shown in Fig. 3 (model building III). Up to this peak value, the longitudinal walls were without visible cracks.

3. When the model buildings were excited by 0.9-1.78g peak acceleration at the first run, the walls of the first story of model building I, II and fifth story of model building III slipped apparently, and partial masonry of the external lateral wall crushed seriously. The time history of roof displacement for model building I is shown in Fig. 4. The crack pattern of walls for model building II is shown in Fig. 5.

4. When the excitations were repeated at 0.9-1.78g five or seven times, the model buildings collapsed completely, which is similar to the damage during actual earthquake.

ANALYSIS OF ASEISMIC BEHAVIOR OF UNREINFORCED
CONCRETE BLOCK MASONRY BUILDING

By analyzing the crack procedure, distribution of inertia force

and deformation of the model buildings tested on shaking table, the following comments can be drawn for the aseismic behavior of masonry building.

1. The deformation of masonry structure under seismic loading is shear type, which can be verified by shaking table experiments and earthquake damages on the spot.

2. The difference between the experimental results of distribution of inertia force along the height of the building and the theoretical results of that calculated by Chinese "Code" is small in the linear stage, but very large in the cracking stage, as shown in Fig. 6. The main difference is that the calculated results overestimate the inertia force of upper part of the building, and underestimate that of lower part of the building. When the buildings crush and the walls slip, the calculated results can not present the actual distribution of the inertia force along the height of the building, as shown in Fig. 7. If the static horizontal forces are applied according to the distribution calculated by Chinese "Code", the large tensile stress may appear in the bottom of the building, which does not agree with the results of shaking table test and earthquake damages on the spot.

3. The coefficient of structural effect defined by the ratio of the base shear of nonlinear response and that of linear response is not a constant, and it changes with the intensity of input acceleration.

4. The peak value of acceleration A_p for prototype building may be estimated from the small-scale model test on shaking table by using the following expression:

$$A_p = \frac{A_m \cdot C_x \cdot C_t}{C_t \cdot C_t \cdot K_s} \quad (1)$$

where A_m is the peak acceleration applied to model building, C_x , C_t and C_t are the scaling parameters of displacement, time and shear strength respectively, and K_s is the coefficient of size effect. The results estimated by the above-mentioned expression are shown in Table 2.

From the relationship listed in Table 2 and shaking table tests,

Comparison of Aseismic Capacity of Model and Prototype Building Table 2.

model building	C_x	C_t	C_t	A_m (gal)	A_p (gal)
(I)	4	3.448	0.997	196	64
				546	179
				706	232
				1200	394
(II)	4	3.226	0.566	155	34
				466	101
				880	191
				1780	387
(III)	4	2.702	0.506	108	30
				686	190
			0.736	900	363

the following conclusions can be summarized:

1. When the prototype building meets an earthquake corresponding to Chinese intensity 7, the horizontal and diagonal cracks will appear in the walls of the first and second story.

2. When the prototype building meets an earthquake corresponding to Chinese intensity 8, it will suffer relatively serious damages.

3. When the prototype building meets an earthquake with the intensity of 360gal peak acceleration, the walls at the first story or the fifth story will collapse and crush apparently.

But all the above conclusions only correspond to the condition of one direction excitation.

IDENTIFICATION OF NONLINEAR STRUCTURAL PARAMETERS OF MULTI-DEGREE-OF-FREEDOM SYSTEM

System identification technique has been introduced to the earthquake engineering since 1970. Now the linear identification for MDOF system has been solved by some investigators, but nonlinear identification for MDOF system is being studied. In this section, based on linear system identification and nonlinear earthquake response analysis, a new method of iteration is developed to identify the parameters in the nonlinear MDOF system. In this method, all the parameters of restoring force model of structure are divided into linear and nonlinear groups, then they can be identified in batches. The modified Simplex algorithm is used in the optimization of nonlinear parameters.

The main steps of nonlinear system identification are given as follows:

1. To set up the restoring force model for each story of the structure, and to assume the initial parameters $\{\beta\}^{(0)}$, which should describe the models appropriately.

2. To put the restoring force models with initial parameters⁽⁰⁾ into equation

$$(M) \{\ddot{x}\} + (C) \{\dot{x}\} + (K) \{x\} = - (M)\{I\} \ddot{x}_g \quad (2)$$

and to calculate the nonlinear response $\{\bar{x}(\bar{\beta}, t)\}$, $\{\dot{\bar{x}}(\bar{\beta}, t)\}$, $\{x(\bar{\beta}, t)\}$ which must have some error comparing with $\{\ddot{y}(t)\}$, $\{\dot{y}(t)\}$, $\{y(t)\}$.

3. To calculate the error function $\phi(\bar{\beta})$:

$$\phi(\bar{\beta}) = \sum_{i=1}^N \frac{1}{T} \int_0^T \{ (\ddot{x}_i(\bar{\beta}, t) - \ddot{y}_i(t))^2 + W_a (\dot{x}_i(\bar{\beta}, t) - \dot{y}_i(t))^2 + W_b (x_i(\bar{\beta}, t) - y_i(t))^2 \} dt \quad (3)$$

where $x_i(\bar{\beta}, t)$, $\dot{x}_i(\bar{\beta}, t)$ and $\ddot{x}_i(\bar{\beta}, t)$ are the response quantities calculated from the model using initial parameters $\{\beta\}^{(0)}$ and excitation \ddot{x}_g ; y_i , \dot{y}_i , \ddot{y}_i are the response quantities either from the structure subjected to the same excitation or from the measured output data;

W_a and W_b are positive scalar weighting factors; the value of T may be the full duration of the acceleration or only a portion of it.

4. Based on the optimization method to check whether the iteration procedure of identification satisfies the criteria of convergence or not. If it is unsatisfied, then to form a new set of parameters $\{\beta\}^{(1)}$ and return to step 2.

During repeating the above steps, because of a great number of parameters in the nonlinear restoring force models of MDOF system, it needs a long time for iteration, even the procedure of iteration may not converge. In order to solve this problem, the parameters of restoring force may be identified in batches. It means that all the parameters of restoring force model can be divided into two groups: (1) linear parameters which are the first stiffness K_1 (Fig. 10); (2) nonlinear parameters which consist of cracking and yielding points (P_z and P_y) as well as the second and third stiffness (K_2 and K_3), and these two groups can be identified one by one. Firstly, because the earthquake response of a structure in the initial time period is relatively small and the structure vibrates in the elastic stage, the initial small response can be used to identify the first stiffness of restoring force model. Secondly, on the basis of the known first stiffness of restoring force model, the other parameters can be identified by using the earthquake response of whole duration.

In order to verify the above-mentioned method, a three lumped mass system was selected as an example to identify the nonlinear parameters. The parameters of this example are shown in Table 3, and the acceleration time history at roof level is shown in Fig. 8. It can be found that there is a good agreement between the true and identified parameters, which means that the method developed above is feasible.

Table 3.

(Unit: kg, cm, sec.)

The Parameters of Example

Number of story	Mass	Type	True value	Before iteration		After iteration	
				Initial value	Deviation (%)	Final value	Tolerance (%)
1	50	First stiffness	20800	16640	20.000	10785	0.070
		Second stiffness	14144	16640	17.647	13792	2.488
		Third stiffness	1144	1479	29.180	1112	2.836
		Cracking point	2080	1664	20.000	2095	0.729
		Yielding point	4160	3328	20.000	3966	4.650
2	50	First stiffness	20800	16640	20.000	20751	0.235
		Second stiffness	14476	17638	21.840	14276	1.383
		Third stiffness	1188	1618	36.240	1174	1.154
		Cracking point	1976	1264	36.000	1950	1.300
		Yielding point	3952	2529	36.000	3692	6.571
3	20	First stiffness	20800	16640	20.000	20771	0.139
		Second stiffness	14809	17804	20.220	14604	1.382
		Third stiffness	Not Enter the Third Stiffness				
		Cracking point	1872	1198	36.000	1852	1.071
		Yielding point	Not Exceed the Yielding Point				

IDENTIFICATION FOR THE NONLINEAR MATHEMATICAL MODELS OF MASONRY BUILDING

The mathematical models of masonry building in every deformation stage are obtained by using shaking table experiments and system identification, the results obtained here can be used to predict the seismic response of masonry structure.

The identified results of three model buildings are as follows:

1. In uncracking stage, the mathematical model of shear type can be used to predict the linear earthquake response of masonry building. The identified and measured acceleration responses of model building III are shown in Fig. 9.

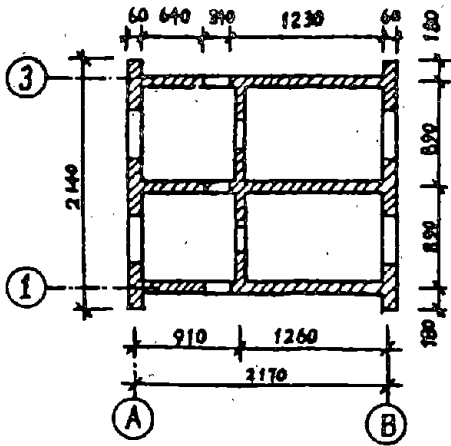
2. In the cracking stage, the restoring force model of interstory is "semi-degrading tri-linear" type as shown in Fig. 10, which is similar to the model obtained by static test but with different parameters. So it is reasonable to use the shear type model as a whole and the "semi-degrading trilinear" restoring force model to predict the nonlinear earthquake response of concrete block masonry building. The time history of acceleration at roof level of model building I subjected to the peak value of 0.55g is shown in Fig. 11.

3. In the failure stage, the "semi-degrading tri-linear" restoring force model can not predict the nonlinear earthquake response of concrete block masonry building, as shown in Fig. 12. In this stage, the restoring force model of interstory is "shear-slip" type (see Fig. 13) which is a new concept for the design of concrete block masonry building. By using this new model the nonlinear earthquake response can be predicted more accurately than by using the other models, as shown in Fig. 14 which is the acceleration time history of model building I subjected to the peak value of 1.2g.

4. The damping ratios of masonry structure change very apparently with the deformation of the structure. In the uncracking stage, $\xi_1 = 0.047 \sim 0.05$, $\xi_2 = 0.0497 \sim 0.053$; after cracking, the damping ratios are increased greatly: $\xi_1 = 0.194 \sim 0.198$, $\xi_2 = 0.323 \sim 0.358$; in the failure stage, $\xi_1 = 0.296 \sim 0.303$, $\xi_2 = 0.4 \sim 0.52$. These damping ratios can be used to predict the nonlinear earthquake response of masonry structure.

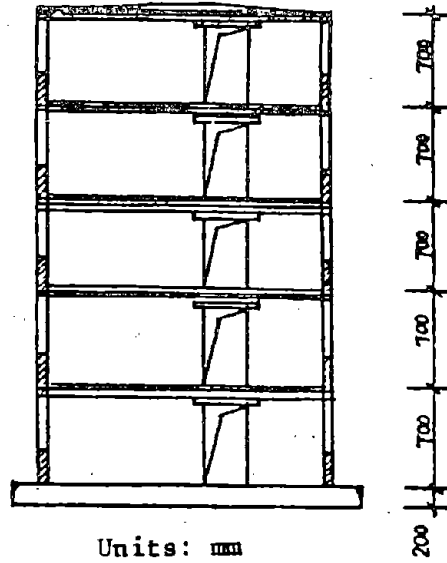
REFERENCES

1. Zhu Bolong, Lü Xilin, Shaking Table Study of a Five-story Unreinforced Concrete Block Masonry Model Building, Proc. of International Workshop on E.E., Vol.2, March, 1984, Shanghai, China.
2. Lü Xilin, Zhu Bolong, Lu Weimin, Identification of Nonlinear Structural Parameters of Multi-Degree-of-Freedom Systems, Proc. of International Workshop on E.E., Vol.2, March, 1984, Shanghai, China.
3. Zhu Bolong, Lü Xilin, Earthquake Simulation on an Unreinforced Masonry Building, "Closed Loop" The Magazine of Simulation Technology, Feb.1985.



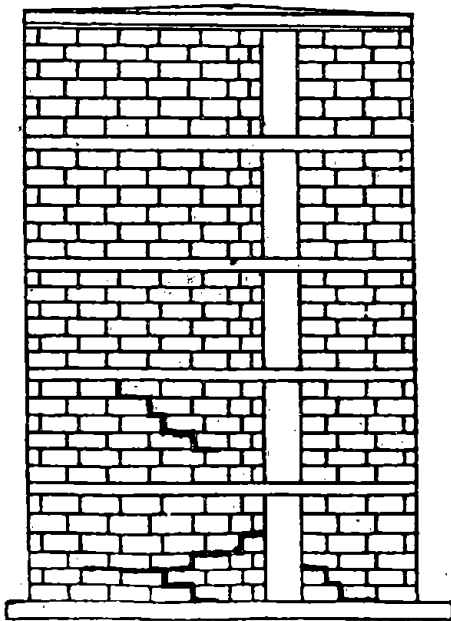
Units: mm

Fig. 1

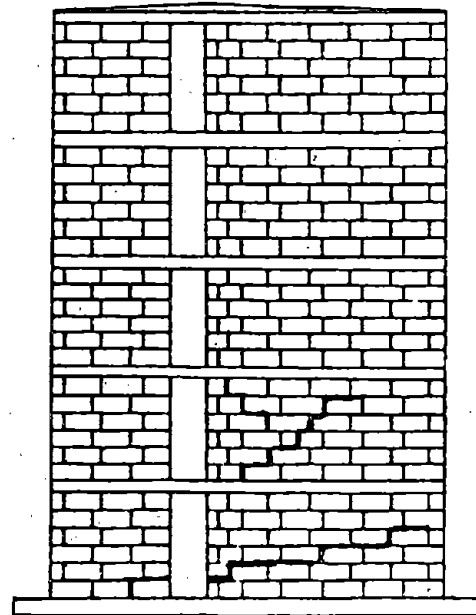


Units: mm

Fig. 2



Axis No. 3



Axis No. 1

Fig. 3

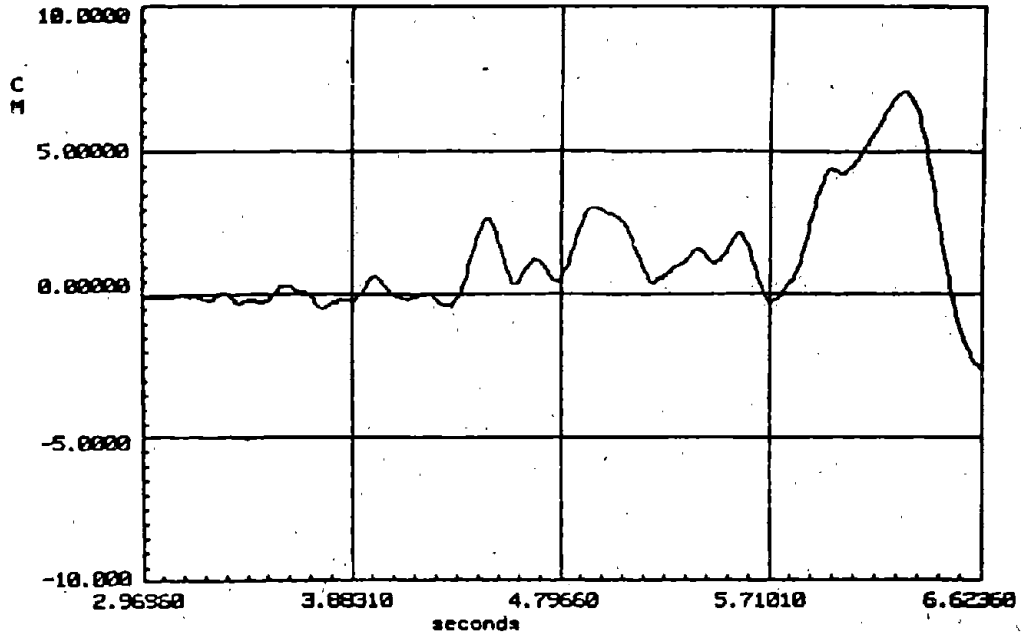


Fig. 4 (Model Building I)

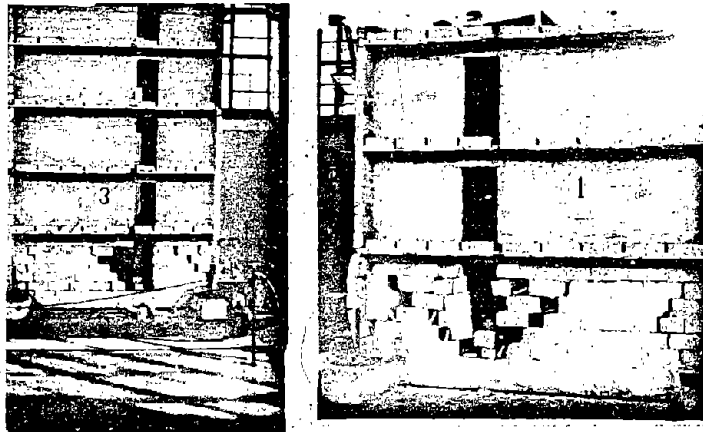


Fig. 5

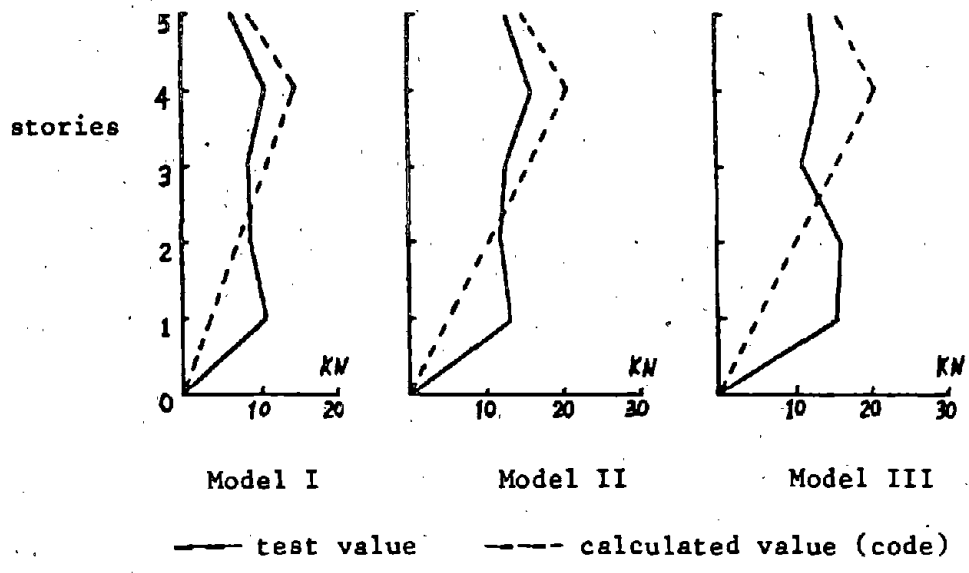


Fig. 6 (Cracking Stage)

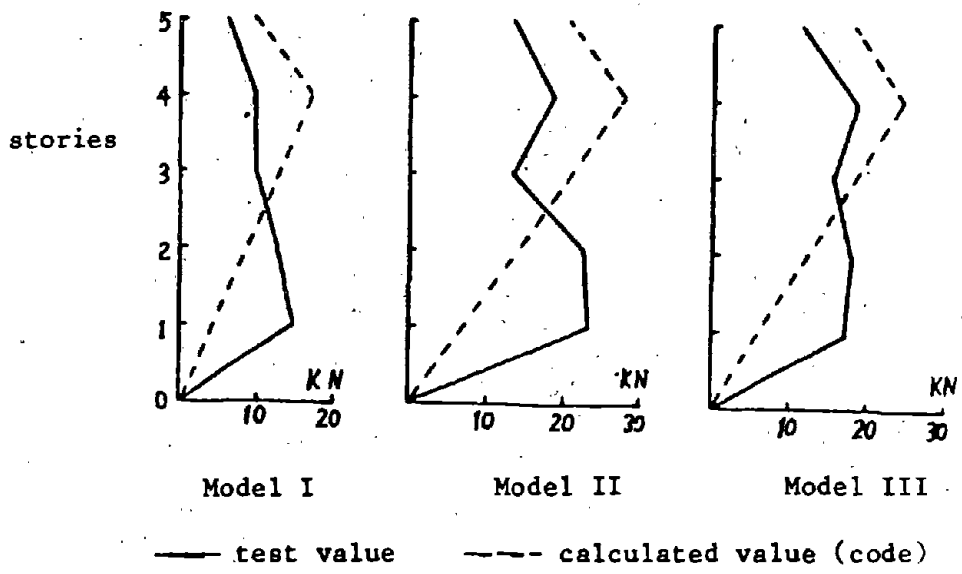


Fig. 7 (Failure Stage)

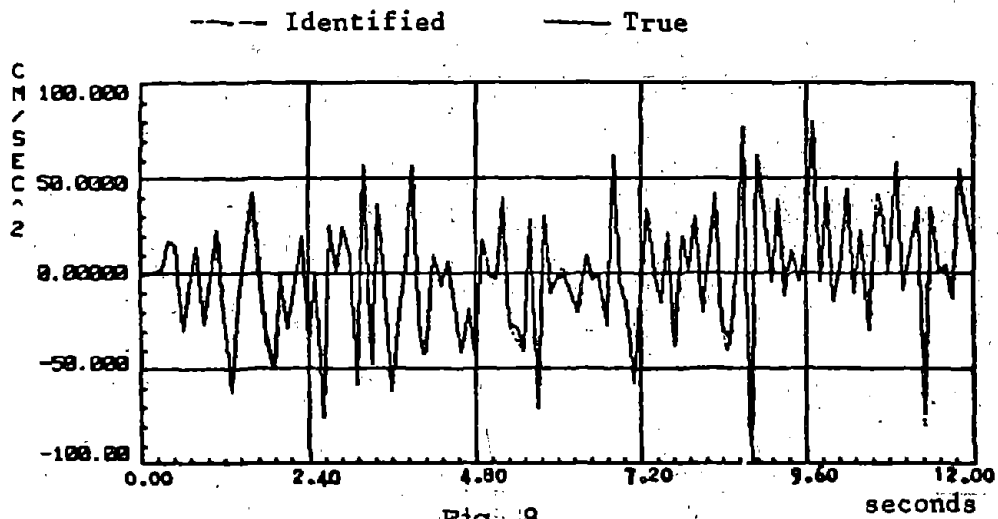


Fig. 8

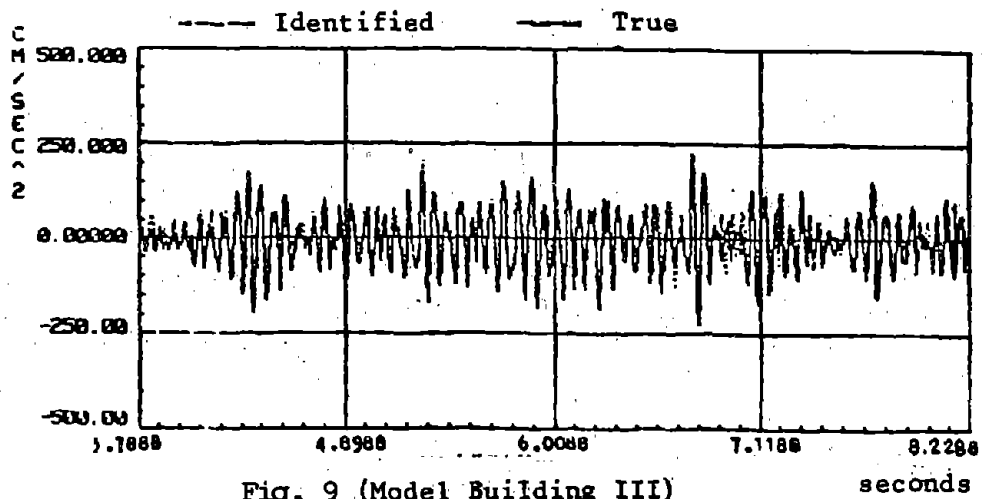


Fig. 9 (Model Building III)

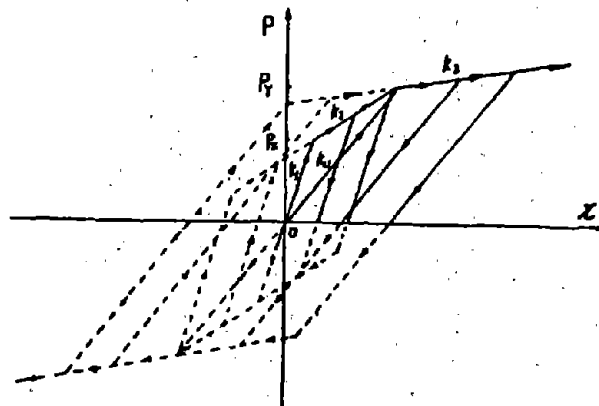


Fig. 10

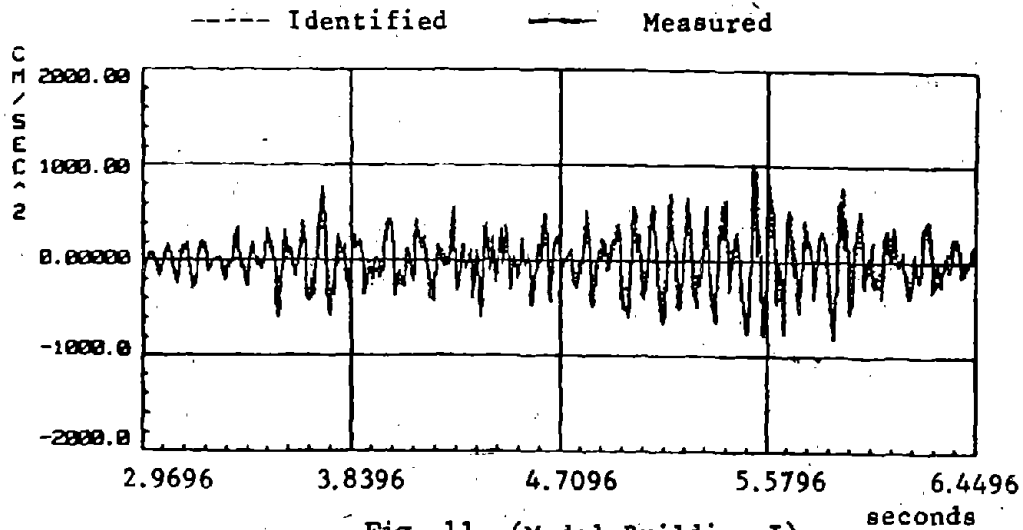


Fig. 11 (Model Building I)

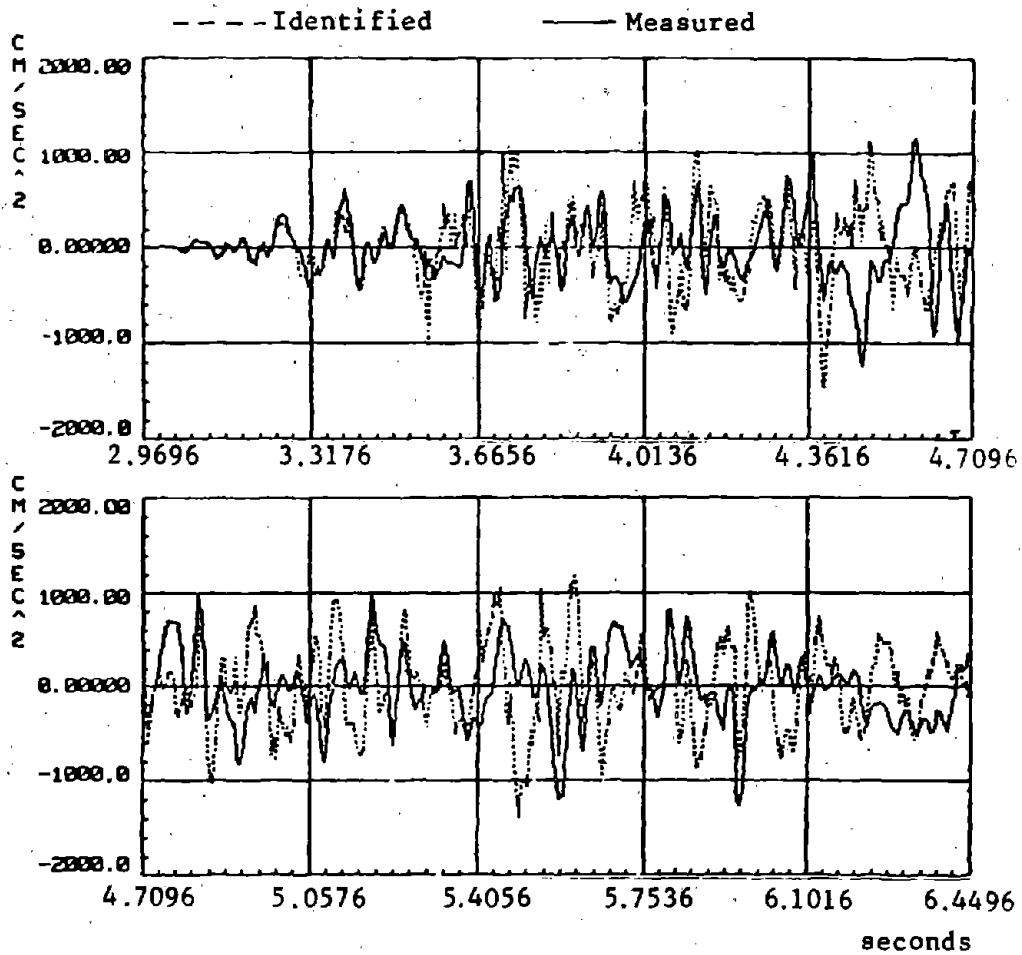


Fig. 12 (Model Building I)

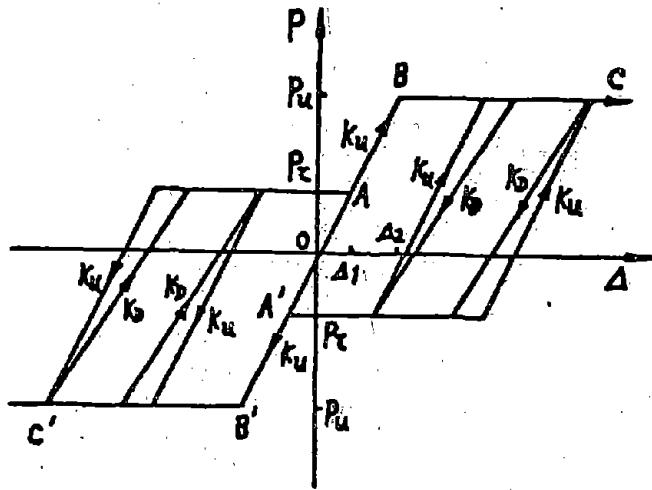


Fig. 13

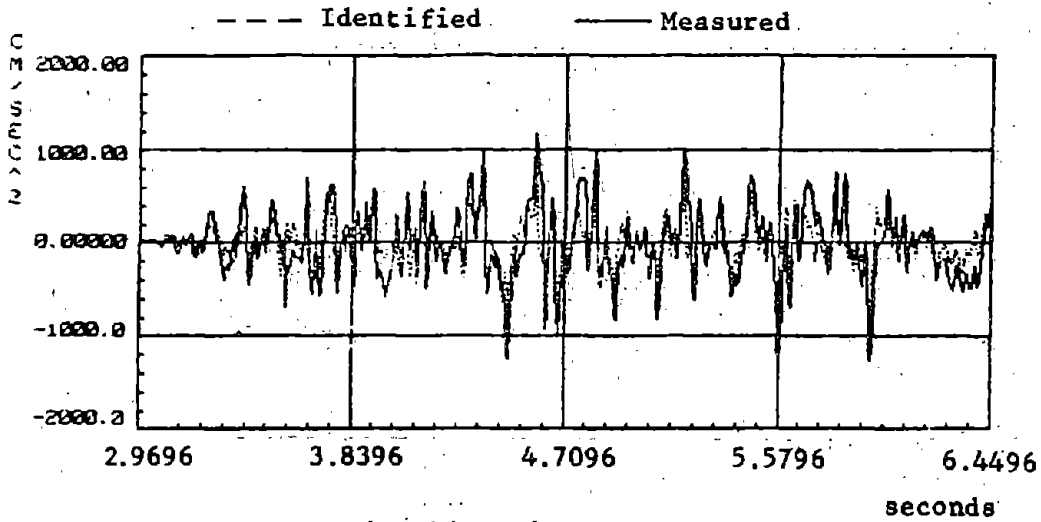


Fig. 14 (Model Building I)

DIRECT SMALL SCALE MODELING OF GROUTED CONCRETE BLOCK MASONRY*

Ahmad A. Hamid¹, Bechara E. Abboud² and Harry G. Harris³

SUMMARY

A better understanding of the complex behavior of masonry structures is necessary to embrace the more appropriate concept of limit states design. Due to the prohibitive cost of full scale testing of masonry systems, particularly under dynamic loading, a more economical method utilizing direct modeling techniques is proposed. This paper describes the first phase of an ongoing comprehensive small scale test program of concrete masonry at Drexel University since 1982. Information about the scale effect and the model properties of the blocks, mortar and grout were obtained. Model specimens duplicating prototype test specimens were tested under axial compression, shear and in-plane splitting tension. The study includes the effects of different deformation and geometric characteristics of the units, mortar and grout. Correlations between model results and available prototype tests have been performed. The results indicate that direct modeling is feasible and is capable of predicting the behavior of concrete masonry. Phase two of the program will include direct modeling of reinforced masonry walls.

INTRODUCTION

The widespread use of reinforced masonry structures in the past decade substantiates an urge for experimental studies to evaluate their complex behavior under different types of loading, especially under seismic loading. However, due to the high cost of full scale testing, only a limited number of experimental studies have been performed to evaluate basic strength under monotonic static loading. These studies did not fully utilize the performance

^{1,2,3}Associate Professor, Graduate Student and Professor, respectively, Department of Civil Engineering, Drexel University, Philadelphia, PA, U.S.A.

*Previously presented in The First Joint Technical Coordination Committee on Masonry Research Meeting, Tokyo, Japan, August 1985.

characteristics of masonry systems. Therefore, a more economical method is needed to study the complete structural behavior of masonry structures under any type of loading. With this objective in mind, a direct small scale modeling technique is proposed as an economical alternative to full scale testing. This has been successfully applied to linear and nonlinear problems of reinforced and prestressed concrete structures at the Structural Model Laboratory of Drexel University [1,2,3].

The methodology for direct small scale modeling of hollow concrete masonry was developed at Drexel University in the late seventies by Harris and Becica [4,5]. A follow up study was conducted by Hamid and Abboud [6] in 1983 to further evaluate the feasibility of small scale modeling for concrete masonry and to include grouted construction. The results were very encouraging and as a result, a comprehensive test program has been developed at Drexel University to evaluate, in detail, the use of small scale models for unreinforced and reinforced concrete block masonry.

This paper presents the results from the first phase of the program which deals with basic strength and deformational characteristics of grouted concrete masonry assemblages. The second phase of the program will include direct modeling of reinforced masonry walls.

OBJECTIVE AND SCOPE

It is the objective of this study to evaluate the use of direct modeling of grouted concrete block masonry under axial compression, shear along the bed joints and splitting tension of different orientations from the bed joint direction. The experimental study includes the effect of unit properties and mortar and grout strengths on the deformational and strength characteristics of the assemblages. The validity and adequacy of the small scale modeling in determining the strength and deformational characteristics of masonry are investigated by direct correlations with prototype tests of specimens having similar properties.

MODELING TECHNIQUE

The approach adopted in this study was to achieve "true" modeling; that is, to produce models which can predict the elastic as well as the inelastic behavior including failure. This necessitates obeying all similitude requirements for geometry, materials, and loading [3]. Using the theory of dimensional analysis [3], the similitude requirements can be derived for masonry (see Table 1). A more extensive discussion of the similitude requirements for masonry can be found in Refs. 3 and 5.

The geometric relationship between the model and prototype is provided by the scale factor. In this study a scale factor of four was used. The choice of this scale factor is primarily based upon two important considerations: (a) The Masonry Laboratory at Drexel University houses a masonry block-making machine that provides units having 1/4 the nominal size of the prototype 8x8x16-in. (200x200x400 mm) nominal blocks, and (b) an early study [5] at Drexel University indicated that the usage of scale factors greater than four would probably result in problems in the fabrication of joints. This has an added significance in view of the importance of mortar joints in affecting the overall masonry behavior [6].

EXPERIMENTAL PROGRAM

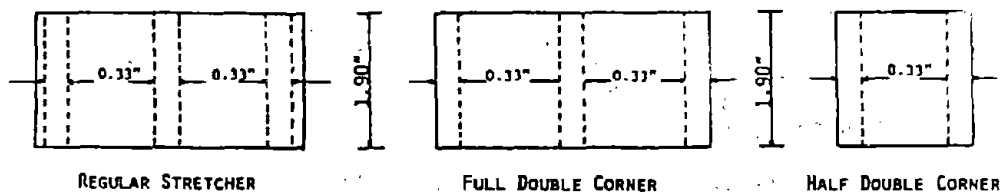
Materials

The constituent materials selected for the masonry model are scaled-down materials satisfying the similitude requirements for direct modeling [6].

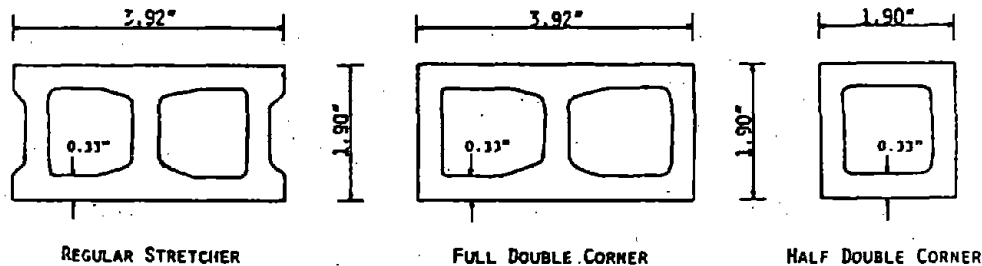
1. Model Masonry Units - Three different quarter scale configurations of hollow concrete masonry units shown in Fig. 1 were used throughout the test program. These quarter scale blocks represent full scale, nominal 8 inch (200 mm) blocks. The model block units were manufactured in-house using a block making machine at the Masonry Laboratory of Drexel University. They were

Table 1 - Prediction and design equations for direct modeling of masonry under static loading.

Equations	Description
(a) <u>Prediction</u>	
$\epsilon_m = \epsilon_p$	strain in model is the same as in prototype
$\sigma_m = \sigma_p$	stress in model is the same as in prototype
$\delta_m = \delta_p/S_L$	deflection, where $S_L = L_p/L_m$ is the length scale
$M_m = M_p/S_L^2$	bending moment per unit length
$P_m = P_p/S_L$	compression load per unit length
(b) <u>Design</u>	
$t_m = t_p/S_L$	thickness
$A_m = A_p/S_L^2$	area
$E_m = E_p$	Young's modulus
$(f'_{cm})_m = (f'_{cm})_p$	compressive strength
$(f'_{tn})_m = (f'_{tn})_p$	tensile strength normal to bed joints
$(f'_{tp})_m = (f'_{tp})_p$	tensile strength parallel to bed joints
$(f'_s)_m = (f'_s)_p$	shear strength of bed joints
$\nu_m = \nu_p$	Poisson's ratio



A) TYPICAL ELEVATIONS



B) TYPICAL CROSS-SECTIONS

Fig. 1 - Configurations of Model Masonry Blocks

moist-cured for 28 days. The physical properties of the model blocks were obtained in accordance with ASTM C140 and ASTM C67 [7] and are listed in Table 2. Figure 2 shows stress-strain relationship of model blocks.

2. Model Masonry Mortar - The model masonry mortar used throughout the experimental program consisted basically of cementitious material (Portland cement and lime) and local Delaware Valley masonry sand and with enough water to provide a workable mix. To assure a properly scaled down joint thickness of 3/8 inch (10 mm), as is commonly used, particle sizes greater than a U.S. No. 30 sieve were excluded from the masonry sand. The properties and proportions of the three mortar mixes used are summarized in Table 3. For each mortar mix three 2 inch (51 mm) mortar cubes were used during the construction of the assemblages as control specimens to obtain the compressive strength of mortar. These control specimens were air cured under the same conditions as the assemblages and tested at approximately the same age as the corresponding specimens.

3. Model Masonry Grout - The cement, lime and sand used for model masonry mortar were the same for model masonry grout. Three different types of grout were used throughout the experimental study. Their proportions and physical properties are listed in Table 3. For quality control, block molded prisms with the dimensions 1x1x2-in. (25.4x25.4x50.8 mm) were cast during grouting of the assemblages. They were air cured under the same conditions as the assemblages. These were tested under axial compression and splitting tension at the same age as the corresponding specimens [6].

Test Specimens

For axial compression, two groups of specimens (A and B) were constructed to duplicate full scale specimens [8,9]. Group A contains 28 three half-block prisms (Fig. 3) duplicating full scale prisms tested by Drysdale and Hamid [8] to study the effects of strength parameters such as mortar and grout strength

Table 2 - Properties of Model Blocks^a

Model Masonry Unit	Gross Area (in. ²)	Percent Solid	Compressive Strength			Tensile Strength	
			Individual (psi)	Mean (psi)	C.O.V. (%)	Splitting Tension, (psi)	Flexural Tension, (psi)
Regular Stretcher	7.50	53	3380 3250 3810	3480	8		620
Full Double Corner	7.50	52	3730 3270 4050	3680	11		
Half Double Corner	3.60	57	3220 3470 3620	3440	6	530	

^a 1 psi = 6.89 kN/m²; 1 in. = 25.4 mm.

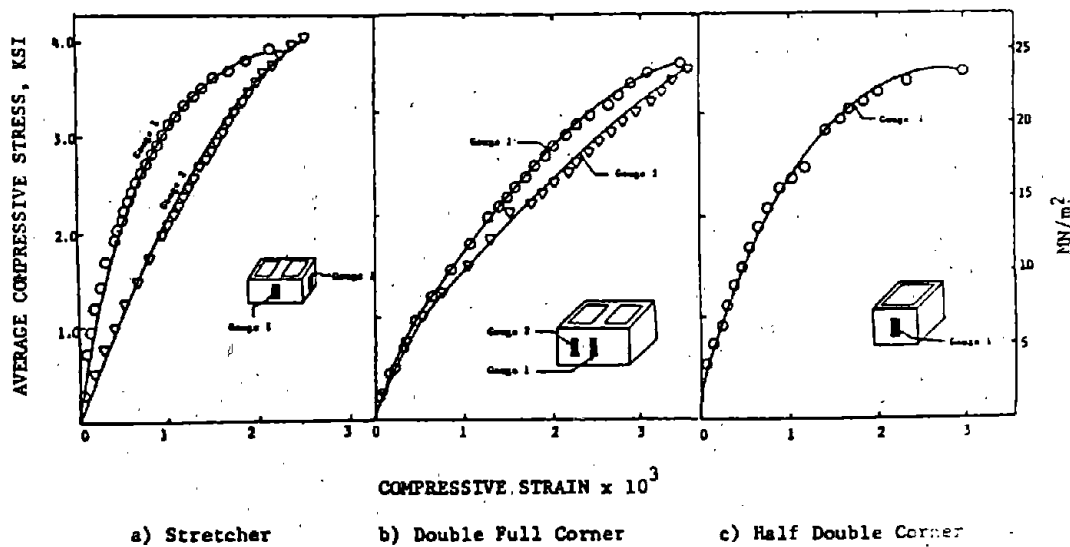


Fig. 2 - Stress-Strain Curves for Model Blocks

Table 3 - Properties of Model Mortar and Grout^a

	Type	Proportions (by weight)				Compressive Strength (psi)
		Cement	Lime	Sand	Water	
Mortar	S1	1	0.2	3.9	1.0	1720 ^b
	S2	1	0.2	4.0	1.0	1330
	N	1	0.2	4.5	1.3	860
Grout	GN	1	5.0	1.5	1480 ^c
	GN	1	0.04	3.0	1.0	3340
	GS	1	2.2	0.8	4880

^a - psi = 6.89 KN/m²; 1 in. = 25.4 mm.

^b - Compressive strength of 2 in. (50.8 mm) cubes.

^c - Compressive strength of 1x1x2-in. (25.4x25.4x50.8 mm) block molded prisms.

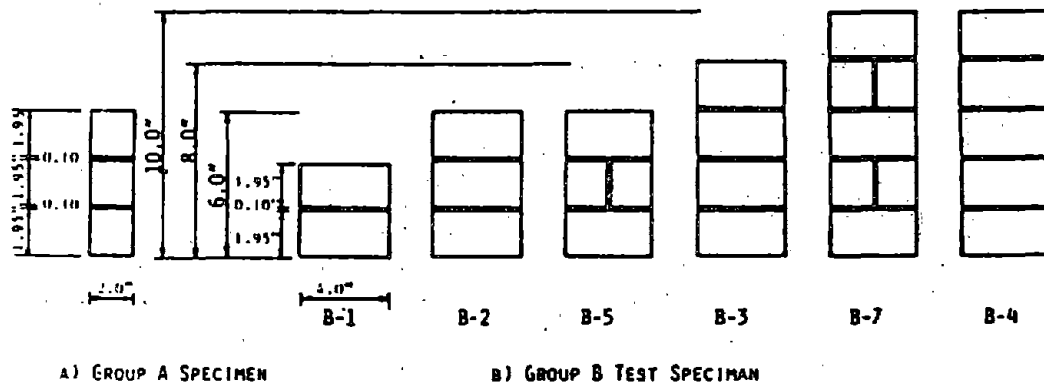


Fig. 3 - Test Specimens for Axial Compression

on masonry compressive strength, f'_m . In Group B, 21 prisms with different heights and shapes (Fig. 3) were built to mirror full-scale prisms tested under axial compression by Hegener et al [9]. This group of specimens was aimed at investigating the effects of geometric parameters such as number of courses, number of mortar joints, and bond patterns on masonry compressive strength.

The four unit assemblage shown in Fig. 4 was adapted as the shear specimens. This arrangement duplicated the full scale shear specimens tested by Hamid et al [10]. This group of specimens was designed to investigate the effect of grout strength on the shear strength of block masonry bed joints.

For in-plane splitting tension grouted model masonry specimens were constructed in running bond with full bed joints which duplicate the full scale specimens tested by Drysdale et al [11]. They were two units long by four units high on the full and double corner model units as shown in Fig. 5. A hexagonal shape was adopted for specimens to be tested under a loading plane oriented at 45 degrees from the bed joint direction. The square shape was used for the other specimens tested under loading of 0 and 90 degrees from the bed joints. The effect of grout strength on the tension capacity of the model assemblages was studied for different load orientations.

TEST RESULTS

Axial Compression

The failure mode for prisms having three-courses or more was a typical tensile splitting as shown in Fig. 6. For two-course prisms (Fig. 6) a shear mode of failure was observed due to end platen restraint [9]. Prototype results [8,9] indicate similar modes of failure. The similarity between model and prototype mode of failure indicates that the direct modeling technique is feasible to predict masonry behavior.

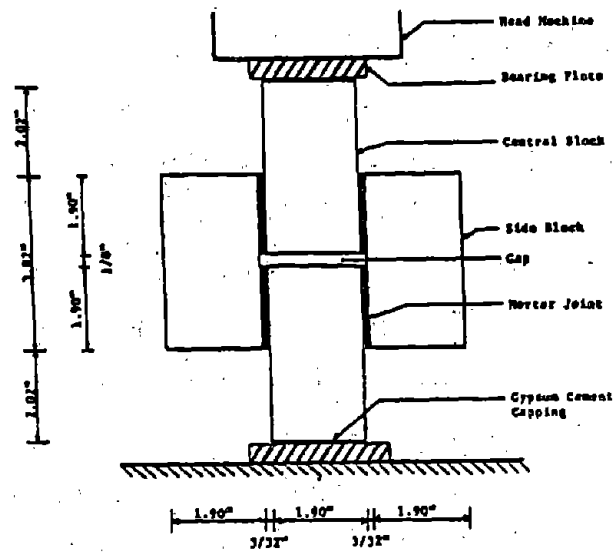


Fig. 4 - Shear Test Set-Up

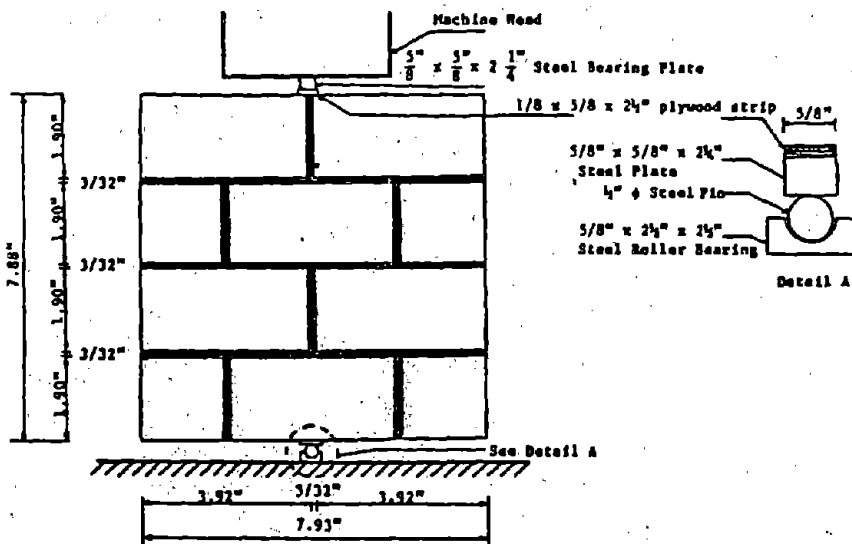


Fig. 5 - Splitting Tension Test Set-Up

Table 4 - Summary of Compression Test Results
(Group A specimens)^a

Mortar Type	Grout Type	Mortar Strength ^b	Strength ^c	Compressive Strength of Prisms		
				Individual, psi	Mean, psi	COV, %
S1	GN	2010	3310	2530 2070 2450	2570	14
S2	GN	1730	3300	2630 2520 2730	2630	4
N	GN	1120	3300	2530 2740 2540	2600	5
S1	GS	2020	4880	3580 3040 3100	3240	9
S1	GW	2020	1480	1980 1550 2180	1900	17

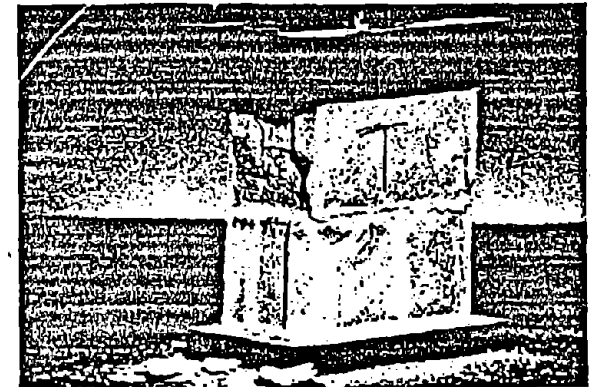
^a 1 psi = 6.89 kN/m²

^b Compressive strength of air-cured 2-in. (51 mm) mortar cubes corrected by a factor of 1.3 to account for size effect [4].

^c Unconfined compressive strength of block molded grout prism.



a) Splitting Mode of Failure



b) Shear Mode of Failure




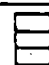

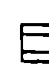

Fig. 6 - Failure Modes of Axially loaded Prisms

The results are summarized in Table 4 (Group A specimens) and Table 5 (Group B specimens) for model prisms under axial compression. Figure 7 shows stress-strain relationships for tested model prisms with those for prototype prisms. As can be seen, the elastic modulus and compressive strength of prisms with types S and N mortars were similar indicating the insignificant aspect of mortar type on assemblage modulus of elasticity under working loads. As the stress level increased, the effect of mortar type becomes significant. Prisms with type N mortar showed higher deformations compared to those for type S mortar. Similar behavior was observed for prototype prisms [8], particularly moduli of elasticity, indicating the feasibility of direct modeling in predicting the behavior under axial compression.

Figure 8 shows that the compressive strength of grout has an appreciable effect on prism strength. As can be seen, the contribution of grouting is more significant for model prisms than it is for prototype prisms. It has to be noted that the geometry of the model grout cores is not identical to that of the prototype. Full scale units have a flared shape which is not the case for model units. As a result, the critical cross section of the model grout core is larger than it should be, causing an overestimation of the contribution of grouting.

Figure 9 shows the effect of height-to-thickness ratio (h/t) ratio on prism compressive strength. As can be seen, increasing the h/t ratio decreased prism compressive strength. The lower the h/t ratio, the higher are the confining stresses. These stresses artificially increase prism compressive strength [8]. It has to be noted that model results agree with prototype results [9] in predicting the effect of prism geometry on compressive strength. Again, model prisms yielded higher strength values compared to prototype prisms, which is similar to what was observed previously with half-block prisms (Group A).

Table 5 - Summary of Test Specimens (Group B Specimens)^a

Series	h/t Ratio	Number of Courses	Mortar strength ^c (psi)	Grout strength, (psi)	Configura-tion	Compressive Strength		
						Individual (psi)	Mean, (psi)	COV (%)
B1	2	2	2450	3380	 full mortar bed	2880 2990 2760	2880	3.9
B2	3	3	2450	3380	 full mortar bed	2610 2550 2870	2680	6.4
B3	4	4	2450	3380	 full mortar bed	2610 2610 2680	2650	1.4
B4	5	5	2450	3380	 full mortar bed	2610 2250 2680	2500	9.1
B5	3	3	2450	3380	 face-shell mortar bed	2920 2750 2650	2770	4.9
B6	2	3	2450	3380	 cut, full mortar bed	2340 2800 2580	2570	8.9
B7	5	5	2450	3380	 face-shell mortar bed	2440 2370 2410	2410	1.5

^a 1 psi = 6.89 kN/m²

^b h/t = height of prism/least lateral dimension.

^c Compressive strength of air-cured 2-in. (51 mm) mortar cubes corrected by a factor of 1.3 to account for size effect [4].

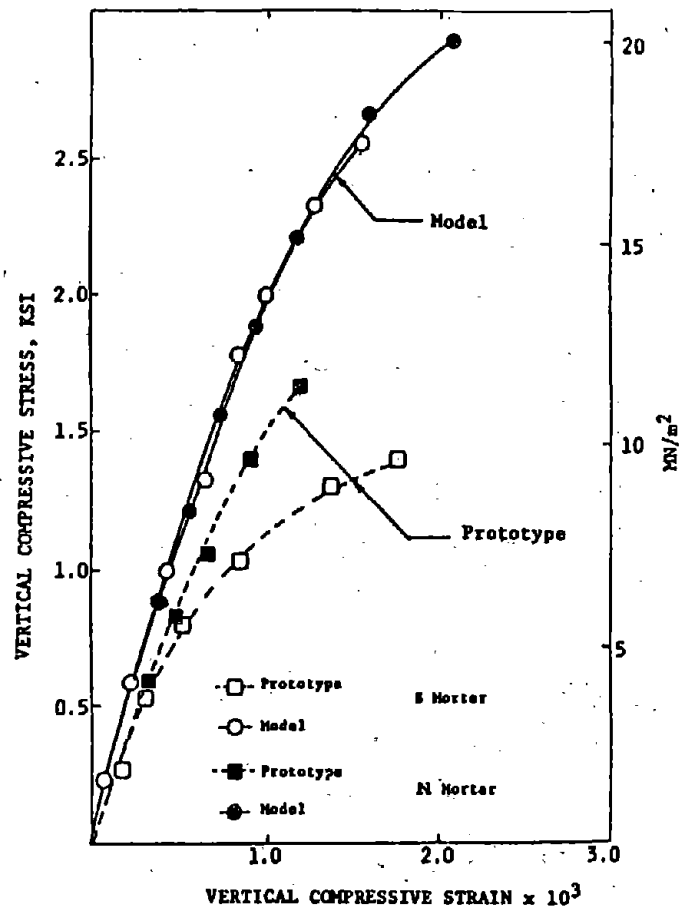


Fig. 7 - Stress Strain Curves for Group A Specimens Under Axial Compression

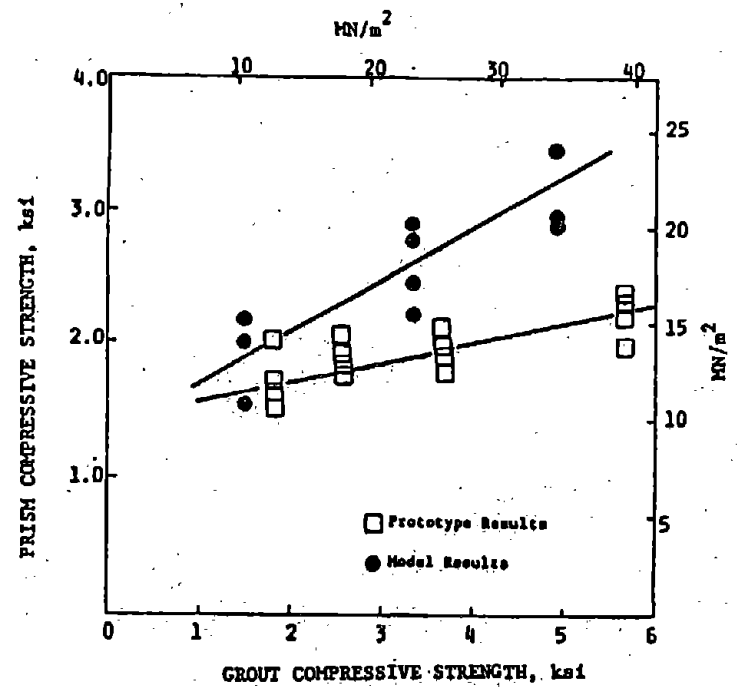


Fig. 8 - Effect of Grout Strength on Prism Compressive Strength

Comparing the results of Groups B2 and B6, Table 5, indicates the effect of number of courses on the compressive strength of prisms. The results showed that the compressive strength of prisms with $h/t = 3$ (three courses) was approximately the same as that for prisms with $h/t = 2$ (three courses with half blocks top and bottom). This indicates that prism compressive strength is a function of the number of courses and not of the h/t ratio. This conclusion agrees with Hegemier et al [9] prototype test results.

The effect of bond type on compressive strength can be studied by comparing the results of Groups B2 and B4 with Groups B5 and B7, respectively (Table 5). The results indicate that there is no significant effect of bond type on compressive strength of masonry prisms. This observation agrees with Hamid [12] and Hegemier et al [9] prototype test results.

Joint Shear

The mode of failure of the shear specimens was a shear failure of the bed joints as shown in Fig. 10. The failure was initiated by mortar debonding, followed by diagonal tensile failure of the grout cores. The model failure duplicated very well the failure modes of prototype specimens recorded by Hamid et al [10]. Table 6 summarizes the shear test results. Figure 11 shows the variation of shear strength of model masonry joints with grout compressive strength. As can be seen, grouting substantially increased the average shear strength of the model masonry joints, with higher grout strength resulting in higher shear strength. It is to be noted however, that the results of model specimens are higher than those of the prototype. The unflared shape of model units allows larger cross-sectional shear area of the grout at the mortar joints, thereby overestimating the shear strength.

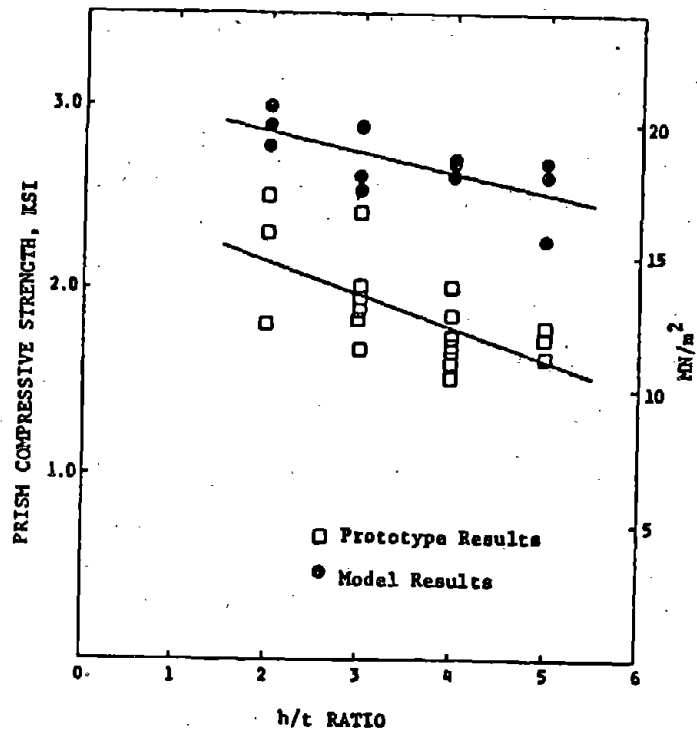


Fig. 9 - Effect of h/t Ratio on Prism Compressive Strength

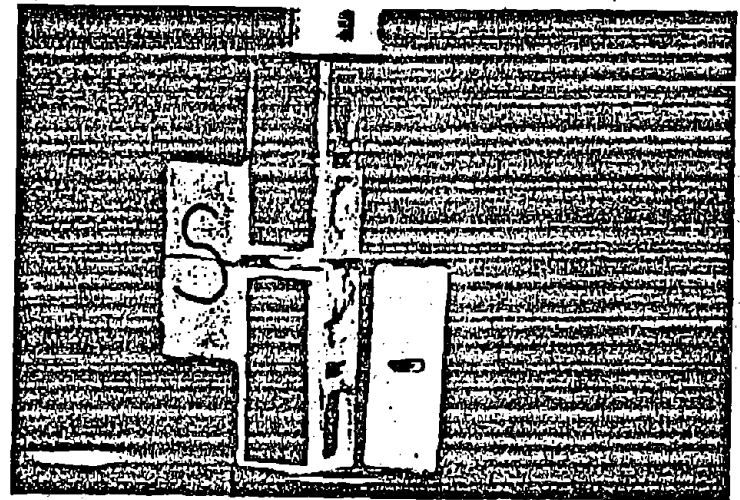


Fig. 10 - Failure Mode of Shear Specimens

Table 6 - Summary of Shear Test Results^a

Mortar Strength ^b (psi)	Grout Strength		Assemblage Shear Strength		
	compression ^c	tension ^d	Individual (psi)	Mean (psi)	C.O.V. (%)
2170	1360	210	177	194	8.8
			210		
			194		
2170	3700	390	203	200	2.5
			201		
			203		
			194		
2170	4850	640	266	256	5.9
			238		
			263		

a- 1 psi = 6.89 KN/m²

b- Average compressive strength of air cured 2 in. (51 mm) mortar cubes corrected by a factor of 1.3 to account for size effect.

c- Equivalent cylinder strength of block molded prisms [4].

d- Splitting tensile strength of grout prisms.

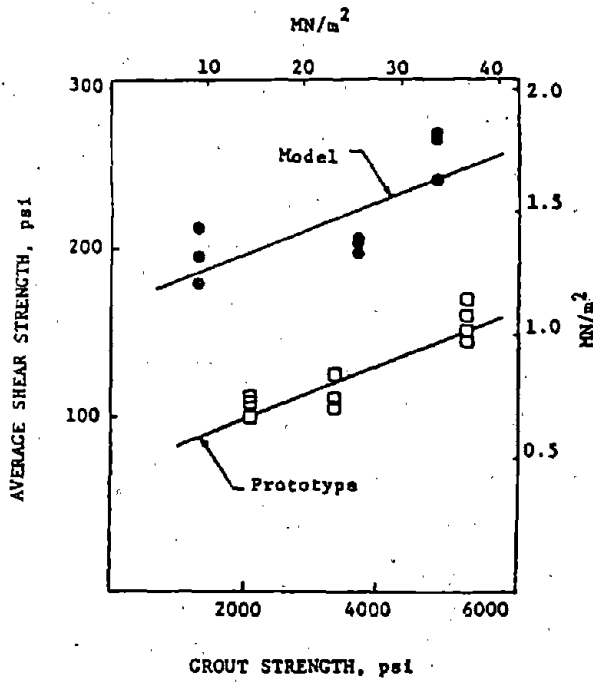
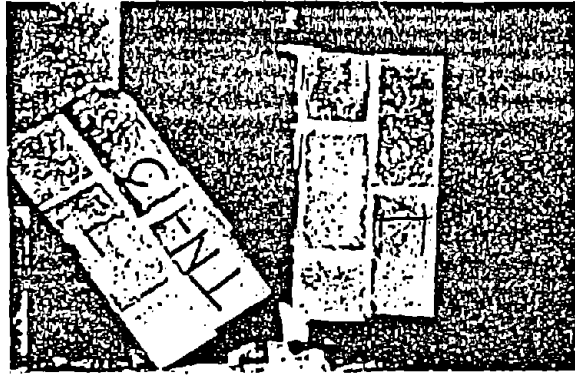


Fig. 11 - Effect of Grout Strength on the Joint Shear Capacity

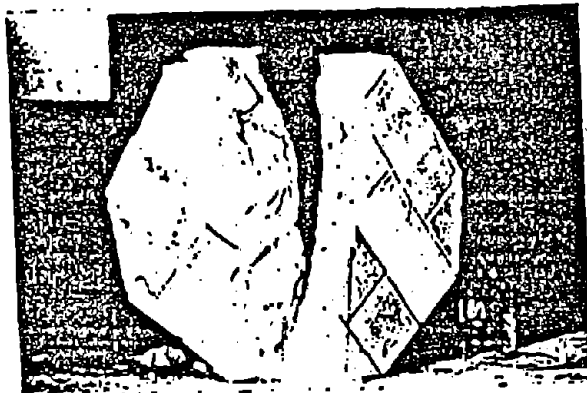
In-Plane Splitting

The failure mode for model splitting specimens was characterized, in general, as a splitting mode of failure along the line between the load points, due to the induced transverse tensile stresses. The failure plane for all panels with $\theta = 90$ degrees (angle between principal tensile stresses and bed joint, $\alpha = 0$ degree) passed through the intercepted blocks' face shells and along the mortar-block interfaces of the head joints, in a direct line between the load point as shown in Fig. 12. The failure plane left the center web and grout core intact. For $\theta = 45$ degrees ($\alpha = 45$ degrees) the fracture crack partially followed the mortar block interfaces in a zigzag plane of failure as shown in Fig. 12. In this case, it was a mixed shear-tension mode of failure. Similar modes and planes of failure were observed for prototype splitting specimens tested by Drysdale et al [11]. This indicates the feasibility of direct modeling in predicating the complex behavior of masonry panels under in-plane splitting tension.

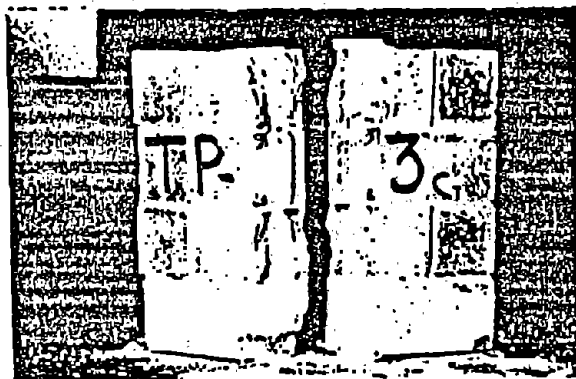
A summary of the splitting test results is presented in Table 7 and plotted in Fig. 13. Based on the results shown in Fig. 13, it is evident that the tensile strength of masonry specimens was significantly affected by the grout strength and the stress orientation with the bed joints. The grout has a maximum contribution when the principal tensile stresses were normal to the bed joint ($\alpha = 90$ degrees), since the grouted cores contributed by their tensile strength, which is much higher than the tension bond strength of the mortar. Also, note that the maximum tensile capacity of grouted specimens was achieved at $\alpha = 45$ degrees. This was due to the significant contributions of the tensile strength of the block and the grout. Similar prototype behavior was reported by Drysdale et al [11]. It is to be noted however, that model specimens revealed higher tensile strengths. This is mainly attributed to imperfection in geometry of model units and size effect which tends to cause higher strength and stiffness [3,6].



(a) $\theta = 0^\circ$



(b) $\theta = 45^\circ$



(c) $\theta = 90^\circ$

Fig. 12 - Failure Modes of Tension Specimens

III-8-18

Table 7 - Summary of Splitting Test Results*

Mortar Type	Grout Type	Tensile Strength, $\alpha = 0^\circ$			Tensile Strength, $\alpha = 45^\circ$			Tensile Strength, $\alpha = 90^\circ$		
		Individual (psi)	Mean (psi)	C.O.V. (%)	Individual (psi)	Mean (psi)	C.O.V. (%)	Individual (psi)	Mean (psi)	C.O.V. (%)
S1	GN	201	189	7.4	233	220	14.5	213	214	9.3
		192			243			194		
		174			184			234		
S1	GW	-	-	-	192	200	15.0	165	176	6.3
		-			234			186		
		-			175			177		
S1	GS	-	-	-	330	280	16.7	250	250	2.0
		-			237			245		
		-			272			255		

* 1 psi = 6.89 KN/m²

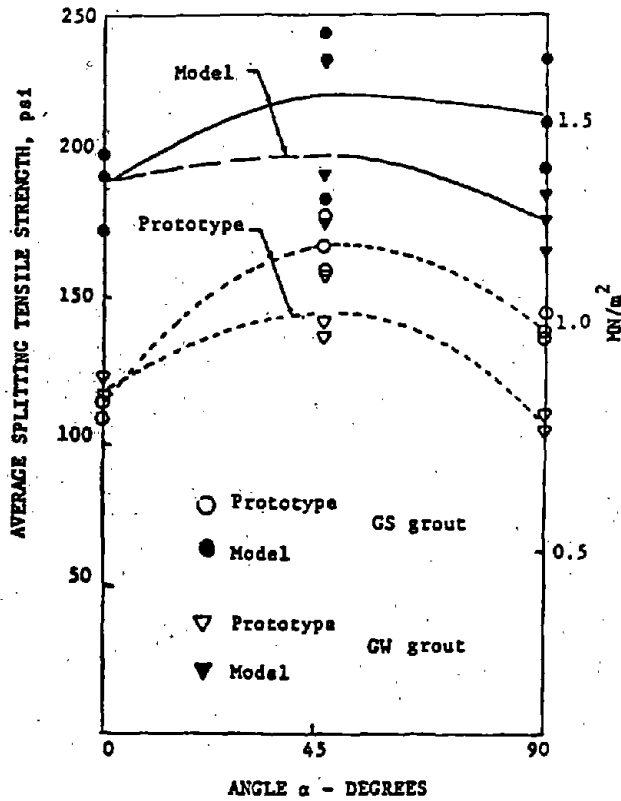


Fig. 13 - Effects of Load Orientation and Type of Grout on Masonry Tensile strength

CORRELATIONS BETWEEN MODEL AND PROTOTYPE RESULTS

As discussed in previous sections and shown in Figs. 7-9,11 and 13 the failure modes and the general trend of model masonry results compare favorably with prototype test results. Small scale model specimens provide higher strength values compared to similar prototype specimens. This is attributed to a multitude of geometric and strength parameters of the constituent materials [6,13]. Differences in model and prototype block geometry and size effect are the two main parameters affecting the degree of correlation between model and prototype results.

CONCLUSIONS

The present study concludes that direct modeling is feasible and capable of predicting the complex behavior of block masonry assemblages. The 1/4 scale masonry units do not resemble the exact geometry of prototype units, causing deviations in the strength results from prototype results. Also, the effect of the aggregate size on the behavior of the constituent materials under multi-axial stresses could be significant in direct modeling. The effects of block geometry and aggregate size on model results are currently under investigation at Drexel University.

It is the authors' opinion that with a more refined scaling of the different geometric characteristics of the model units and the proper assessment of the effect of aggregate size a better correlation between model and prototype masonry can be achieved.

ACKNOWLEDGMENT

The work presented is a part of a more comprehensive test program conducted in the Department of Civil Engineering, Drexel University to study the use of direct modeling in unreinforced and reinforced masonry structures under different loading conditions. This program is supported in part through funds

provided by Drexel University under its Faculty Development Mini-Grant Program. The financial support of the Graduate School at Drexel University is gratefully acknowledged.

REFERENCES

1. Harris, H.G. and Muskivitch, J.C., Nature and Mechanism of Progressive Collapse in Industrialized Buildings, Report 1, "Study of Joints and Sub-Assemblies-Validation of the Small Scale Direct Modeling Techniques", Department of Civil Engineering, Drexel University, Philadelphia, PA, October 1977, p. 165.
2. Muskivitch, J.C. and Harris, H.G., Nature and Mechanism of Progressive Collapse in Industrialized Buildings, Report 2, "Behavior of Precast Concrete Large Panel Buildings Under Simulated Progressive Collapse Conditions, Department of Civil Engineering, Drexel University, Philadelphia, PA, January 1979, p. 207.
3. Sabnis, G.M., Harris, H.G., White, R.N., and Mirza, M.S., Structural Modeling and Experimental Techniques, Prentice-Hall, Inc., Englewood Cliffs, NJ, 1983, p. 585.
4. Harris, H.G. and Becica, I.J., "Direct Small Scale Modeling of Concrete Masonry," Proceedings EMD-ASCE, Advances in Civil Engineering Mechanics, May 23-25, 1977, pp. 101-104.
5. Becica, I.J. and Harris, H.G., "Evaluation of Techniques in the Direct Modeling of Concrete Masonry Structures," Structural Models Laboratory Report No. M77-1, Department of Civil Engineering, Drexel University, Philadelphia, PA, June 1977, p. 96.
6. Hamid, A. and Abboud, B., "Direct Scale Modeling of Concrete Block Masonry Under In-Plane Loading", Report No. MS1/84, Department of Civil Engineering, Drexel University, 1984, pp. 98.
7. American Society for Testing and Materials, 1982 Annual Standards, Part 16, 1982.
8. Drysdale, R. and Hamid, A., "Behavior of Concrete Block Masonry Under Axial Compression," ACI Journal Proceedings, Vol. 76, No. 6, June 1979, pp. 707-772.
9. Hegemier, G., Krishnamoorthy, G., Nunn, R., and Moortly, T., "Prism Tests for the Compression Strength of Concrete Masonry," Proceedings of the North American Masonry Conference, Boulder, CO, Aug. 1978, pp. 18.1-18.17.
10. Hamid, A.A., Drysdale, R.G. and Heidebrecht, A.C., "Shear Strength of Concrete Masonry Joints," Journal of the Structural Division, ASCE, Vol. 105, No. ST7, Proc. Paper 14670, July 1979, pp. 1227-1240.

11. Drysdale, R.G., Hamid, A.A. and Heidebrecht, A.C., "Tensile Strength of Concrete Masonry," Journal of the Structural Division, ASCE, Vol. 105, No. ST7, Proc. Paper 14669, July, 1979, pp. 1261-1276.
12. Hamid, A., "Behavioral Characteristics of Concrete Masonry", Ph.D. Thesis, McMaster University, Hamilton, Ontario, Canada, 1978.
13. Hamid, A., Abboud, B. and Harris, H., "Direct Modeling of Concrete Block Masonry Under Axial Compression, ASTM STP 871, Masonry: Research Applications and Problems", Grogan/Conway, Editors, Philadelphia, 1985.

INELASTIC BEHAVIOR OF REINFORCED CONCRETE FRAME
SUBJECTED TO REVERSED CYCLIC LOADING

Shen Ju-min^I Feng Shi-ping^{II} Weng Yi-jun^{II}

SUMMARY

Three frame models which have two stories and two bays are tested. The post-yield behavior such as strength, deformation, stiffness and energy dissipation of those models under reversed cyclic loading is discussed. It is shown that the p- Δ effect and slippage of bars in beam-column joint have serious influence upon the load-carry capacity and the deformability of frame structures and can't be neglected. A generalized method for full-range analysis of reinforced concrete frame is proposed. The element stiffness equation, taking into account the cracked and yield regions and also the slippage of bars in the joint, is developed. The full-range analyses of three experimental models are made. The analytical results are in good agreement with experimental results.

Outline of Experimental Investigation

The configuration and the reinforcement of the frame models are shown in Fig.1. The foundation of the frame is fixed on the loading floor. Three frame models are designed to have the same overall dimensions and member size. They are divided into two types, one (FI type) has two strong column-weak beam models denoted by FR-1 and FR-2, another has only one weak column-strong beam model denoted by FR-3. In order to certify to the condition of strong column, at a joint the ultimate strengths of the columns are higher than those of the beams. For the models FR-1 and FR-2 the column-to-beam flexure strength ratios at the joints E_{Mc}/E_{Mb} are 2.0-3.5. Although the reinforcement and the scale of model FR-2 are the same as that of the model FR-1, the stirrup space in the bottom of columns of the first story in the model FR-2 is closer than that of the model FR-1. It is expected to investigate the influence of closed stirrup space on the strength and deformation of the frame when the plastic hinges have been formed in the columns. The model FR-3 is a weak column-strong beam type and its column-to-beam flexure strength ratios at the joint E_{Mc}/E_{Mb} are 0.42-0.78.

-
- I. Professor of Civil Engineering, Tsinghua University, Beijing, China.
II. Lecturer of Civil Engineering, Tsinghua University, Beijing, China.

The material characteristics are shown in Tab.1 The sketch of loading equipments is shown in Fig.2. Three vertical loads are applied to the top of second story columns by hydraulic jacks and are kept constant during the test. These jacks can move freely in the horizontal direction when the top of the frame model is displaced. The lateral load which simulates the earthquake load, is applied at the 2/3 height of second story on a distributed beam.

During the test the measured signals include load, displacement, rotation, reinforcement strain, slippage of bars in the joint and shear deformation of the joint core. All measured signals are recorded by computer.

General Behavior

The hysteresis loops of horizontal load H and top displacement Δ_1 of the model FR-2, which is FI type and has closed stirrup space in the columns at the first story, are shown in Fig.3. Obviously, the hysteresis loop behavior of reinforced concrete frame structure is similar to that of a member. The plastic hinge distribution of the models is shown in Fig.4. During the test the beam-column joints in the all models have not any significant cracking, that was expected in the model design.

The envelopes of the hysteresis loops of the horizontal load H and the top displacement Δ_2 for the models FR-1 and FR-3 are shown in Fig.5. It is indicated that there is no obvious yield point of the envelope in the frame structures. The nominal yield point is defined in accordance with General Yield Moment Method and is referred as D in Fig.6. The nominal yield load and corresponding yield displacement of the models are shown in Tab.2. Tab.2 also shows the maximum load and corresponding ultimate displacement. Evidently, although the models FR-1 and FR-2 have almost the same condition, due to the closed stirrup space in the columns of the model FR-2, the ultimate displacement and the ductility ratio in the model FR-2 increase 19.8% and 24.2% respectively. It is useful to delay the concrete damage in the region of plastic hinge of the column for the model FR-2. The closed stirrup space improves the deformability of the column. The deformability of the model FR-3 is poorer than that of the models of type FI, though the ductility ratio of the model FR-3 also reaches 2.78 due to the result of the yield displacement being very small. On the other hand, the load-carry capacity of the model FR-3 decreases rapidly after the load reaches the maximum value. Therefore, it is reasonable to consider simultaneously strength, deformability and energy dissipation to evaluate the seismic behavior of the reinforced concrete structures.

P-Δ Effect

Due to the vertical axial force in the column the p-Δ effect brings about an additional moment on the columns and thus reduces the load-carry capacity and deformability of the structure. The influence of the p-Δ effect increases with increasing horizontal displacement.

Fig.5 shows the p-Δ effect of the models FR-1 and FR-3, where H is the measured lateral force and H_e is the lateral force without consideration of the p-Δ effect. It is shown that the p-Δ effect has little influence before yield loading which is corresponding about 90% ultimate load. The influence of the p-Δ effect gradually increases with increasing deformation. Especially, in the descending range the p-Δ effect obviously increases.

The envelope of the shear Q—story drift is shown in Fig.7. In Fig.7 the equivalent shear Q_e is obtained by inconsideration of the p-Δ effect. From the comparison of the shear-drift curve, it can be seen that the p-Δ effect on the first story is about (1.2-1.8) times larger than that of the second story of the frame structure of FI type. However, the p-Δ effect almost concentrates on the first story of the frame structure of FII type. Even though the total p-Δ effect of two collapse types of the frame structure is similar, the frame structure of FII collapse type is more dangerous than that of FI type. The deformation of the frame structure of FII collapse type almost concentrates on the damage story.

Fig.8 shows the comparison of two hysteresis loops between H-Δ₁ and H_e-Δ₂ of the model FR-2. It is indicated that the p-Δ effect has less influence on the unloading and reloading state and is not significant on the energy dissipation of the frame structure.

Energy Dissipation

For the evaluation of the structural energy dissipation, a usual procedure is to measure area covered by the load-displacement curve. Fig.9 shows a complete hysteresis loop and a corresponding triangular area. If the areas of the hysteresis loop and triangular are denoted by E₁ and E₂ respectively, the ability of the energy dissipation can be expressed as following:

$$e = E_1 / E_2$$

The behavior of the energy dissipation of the models at some stages is shown in Tab.3. The absolute value E₁ of the energy dissipation of the model FR-2 is larger than that of the model FR-1 because of the closed stirrup space in the columns of the model FR-2. On the other hand, the ability of the energy dissipation of FI type model is much larger than that of FII type model. It is very beneficial that the earthquake resistant frame

structures should be designed for strong column-weak beam type.

For the models FR-2 and FR-3 a normalized hysteresis loop is shown in Fig.10. From Tab.3 and Fig.10, it can be seen that the energy dissipation of FR-2 model is greatly different from that of FR-3 model, but the difference between their relative ratios e is little. Therefore, the relative ratio e can not always correctly evaluate the behavior of the structural energy dissipation.

The contribution of energy dissipation of each story is shown in Fig.11. It is indicated that for the FI type frame structure the first and second story absorb 60% and 40% of the total strain energy respectively, but for the FII type frame structure the total energy dissipation almost concentrates on the first story where the failure of structure takes place. So the strong column-weak beam type frame displays distinctly much better behavior of distribution of deformation and energy dissipation.

Slippage of Bars in Joint

The experimental results show that the slippage of bars in the joint is inevitable and is very large especially after yielding. Fig.12 shows the hysteresis curve of the slippage rotation which is caused by the slippage of bars in the joint. It is indicated that the slippage rotation increases as the structural displacement increases, and the slippage rotation at the end of the beam is more serious than that at the end of the column. The deformation at the end of the structural member is shown in Fig.13. The total rotation measured in the plastic hinge zone at the end of the member can be obtained:

$$\theta = \theta_s + \theta_p$$

where θ_s --- the rotation due to the slippage of bars in the joint,

θ_p --- the elasto-plastic rotation of the plastic hinge zone at the end of the member.

The proportion of the slippage rotation is

$$\alpha_\theta = \theta_s / \theta$$

The relationship of the relative ratio α_θ and the load cyclic number n can be shown in Fig.14. The additional rotation due to the slippage of bars in the joint has a large proportion in the total rotation of the plastic hinge zone. This value is about (20-40)% either in the elastic state or in the plastic state. As a result, if the additional rotation due to the slippage of bars in the joint does not be taken into account, the calculated rotation at the end of the member is much less than the actual rotation and the calculated internal forces and deformations will not correspond with the actual reality.

Theoretical Analysis Results

According to the experimental results, it is known that the horizontal load H and the displacement Δ of the reinforced concrete structures have the relationship as shown in Fig.15. Evidently, in the descending range BC the structure presents a state of instable equilibrium. Therefore it is significant to use the concept of structural stability in discussing the ultimate load-carry capacity and full-range analysis.

A corollary from the minimum total potential is as following^[1]:

Corollary If the second variation V_p of the total potential is equal to or less than zero for at least one compatible perturbation, then the equilibrium is instable.

As far as a structure with multiple-linear physical relationship is concerned, the total potential is:

$$V_p = \frac{1}{2} \{\Delta\}^T [K] \{\Delta\} - \{\Delta\}^T (\{P\} - \{P\}_I)$$

where $[k]$ ---- global stiffness matrix only relating to current linear stiffness branch.

$\{\Delta\}$, $\{P\}$, $\{P\}_I$ ---- nodal deformation, load and initial load respectively.

If the carrying load of the structure is in an instable state in the loading direction, its V_p corresponding to the deformation of the load direction is:

$$\delta^2 V_p = \{\delta x\}^T [K_{xx} - K_{xe} K_{ee}^{-1} K_{ex}] \{\delta x\} \leq 0$$

According to the property of a real quadratic form, a mathematical criterion for predicting the ultimate load-carry capacity of the structure can be obtained.

Criterion As far as a structure subjected to load is concerned, its global stiffness matrix corresponding to deformation of loading direction is shown as following:

$$[K]^* = [K_{xx} - K_{xe} K_{ee}^{-1} K_{ex}]$$

When one of the eigenvalues of the matrix $[k]^*$ is equal to or less than zero at first time, then the ultimate load-carry capacity of the structure is reached.

In accordance with the experimental results^[2], the stiffness matrix of the member with flexure and axial force can be obtained.

In analysis the structural member may be modelled as an elasto-plastic element with nonlinear spring which represents the slippage rotation at the end of the member. The element model, deformation shape and curvature distribution along the length of the member are shown in Fig.16.

The restoring force models of the cross-section of the member and the slippage rotation spring at the end of the member are shown in Fig.17.

A computer program which can be used for the nonlinear full-

range analysis of the reinforced concrete frame structure under reversed cyclic loading is made.

The analytical and experimental results of the ultimate load-carry capacity and corresponding displacement of three models are shown in Tab.4. The envelope curves of the horizontal load H vers the displacement Δ for the models are shown in Fig.18. In the figures the solid line and dash line represent the measured and calculated results respectively. Fig.19 shows the calculated hysteresis loops for the models FR-2 and FR-3. In Fig.19 the corresponding measured hysteresis loops are also shown. From above comparison between the calculated and measured results, it is shown that the calculated complete curves and hysteresis loops are in good agreement with that from the experiment except the descending branch of the complete curve in the model FR-3.

Conclusions

- 1) The $p-\Delta$ effect has little influence on the structural behavior before yield. This effect, however, plays an important role in the state of large deformation, especially at the ultimate state and in the descending range of the displacement curve and so, it can not be ignored.
- 2) The slippage of bars in the joint significantly influences the behavior of structural deformation before and after yielding. It should be considered.
- 3) The load-carry capacity, deformability, energy dissipation and internal force distribution of FI type structure are more reasonable than those of FII type structure, therefore, FI type structure should be designed as far as possible.
- 4) The proposed generalized method for the full-range analysis of reinforced concrete frame structure is useful and powerful. The results of the computation and experiment are in good agreement.

References

- [1] Feng Shi-ping and Shen Ju-min, Elasto-Plastic Analysis of Reinforced Concrete Frame Structure, Technical Report, Research Laboratory of Earthquake and Blast Resistant Engineering, Tsinghua University, 1984.
- [2] Shen Ju-min, Weng Yi-jun and Feng Shi-ping, Behavior of Reinforced Concrete Members With Flexure and Axial Force Under Cyclic Loading, Technical Reports TR-3, Research Laboratory of Earthquake and Blast Resistant Engineering, Tsinghua University, 1981.

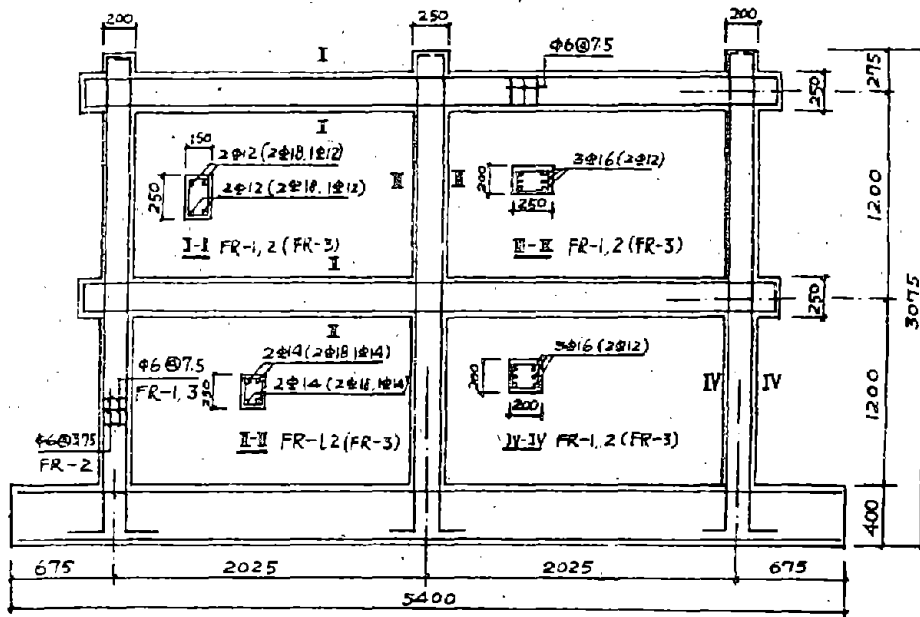


Fig. 1 configuration and reinforcement of models

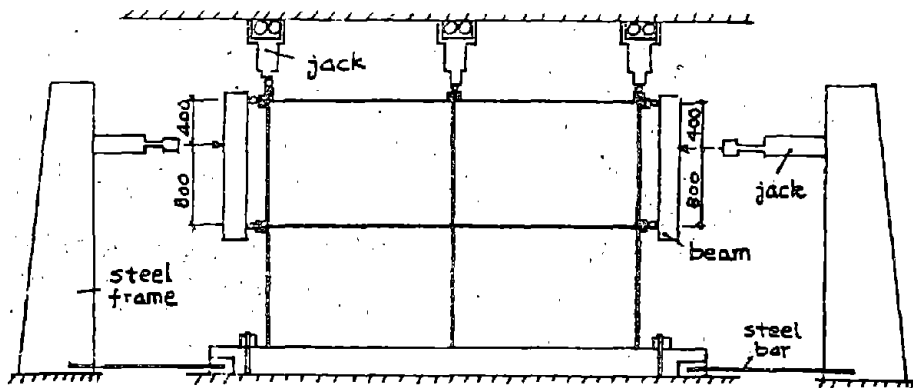


Fig. 2 outline of test equipment

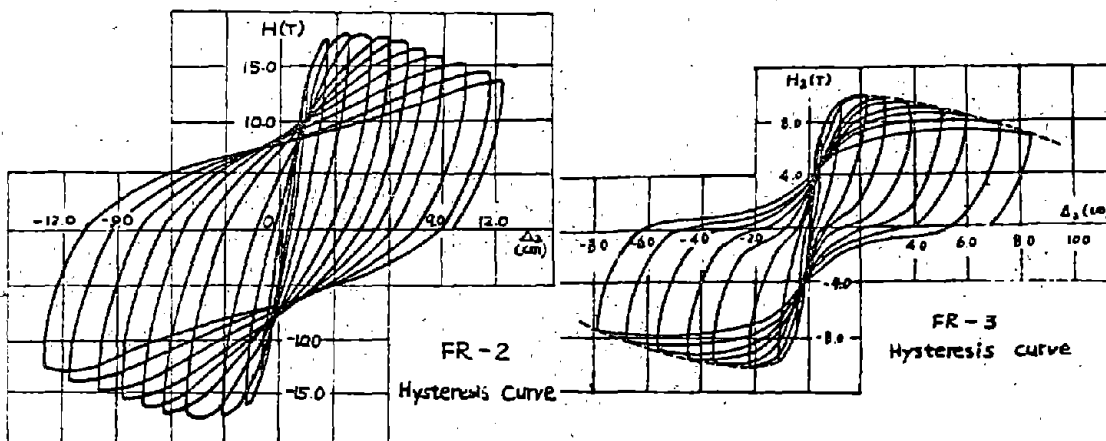


Fig. 3

Tab. 1

Model	R (kg/cm ²)	vertical force		reinforcement	
		exterior column	interior column	diameter	σ_y (kg/cm ²)
FR-1	211.9	10600	21100	$\Phi 12$	3703
FR-2	230.4	11500	23100	$\Phi 14$	3960
				$\Phi 16$	3750
FR-3	309.4	12500	25000	$\Phi 18$	4137

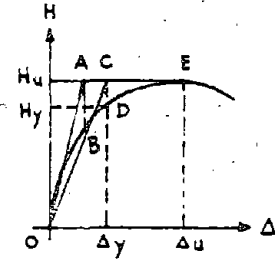


Fig. 6

Tab. 2

Model	yield point		ultimate point		H_y/H_u	$\beta_{\Delta} = \frac{\Delta_u}{\Delta_y}$
	H_y	Δ_y	H_u	Δ_u		
FR-1	13.50	1.644	16.66	4.067	0.810	2.48
FR-2	15.00	1.582	17.79	4.873	0.843	3.08
FR-3	12.60	0.840	15.13	2.346	0.832	2.79

Tab. 4

Model		FR-1	FR-2	FR-3
H_u (t)	Theo.	17.69	18.09	14.49
	Meas.	16.66	17.79	15.13
	Error	0.06	0.02	0.04
Δ_u (cm)	Theo.	4.228	4.500	1.578
	Meas.	4.067	4.873	2.346
	Error	0.04	0.08	0.32

Tab. 3

Model	yield 0.9 H_u			ultimate H_u			descending 2 Δ_u		
	E_1	E_2	E_1/E_2	E_1	E_2	E_1/E_2	E_1	E_2	E_1/E_2
FR-1	27.57	41.26	0.668	68.97	69.10	0.998	244.1	170.56	1.431
FR-2	29.56	39.92	0.741	122.53	92.47	1.325	297.4	145.4	2.045
FR-3	14.03	19.37	0.724	35.34	35.46	0.997	101.1	67.76	1.492

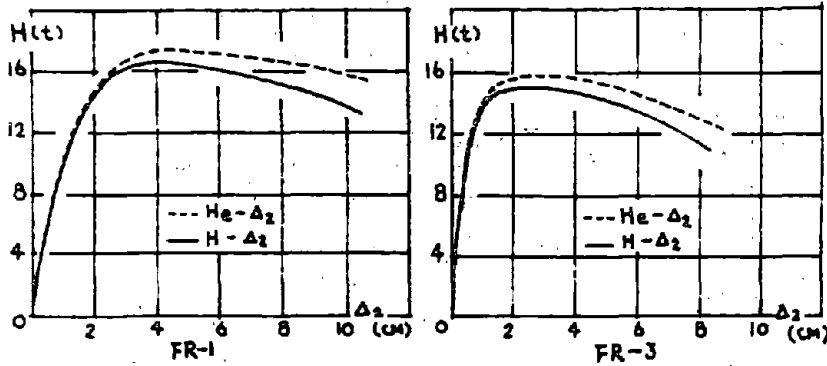


Fig. 5

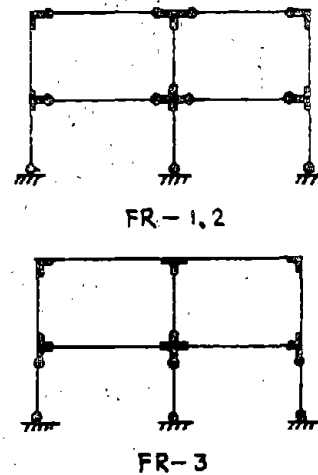


Fig. 4

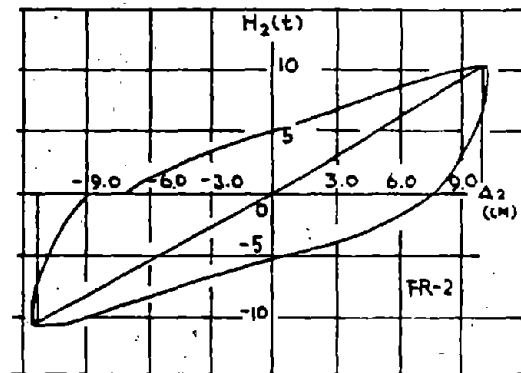
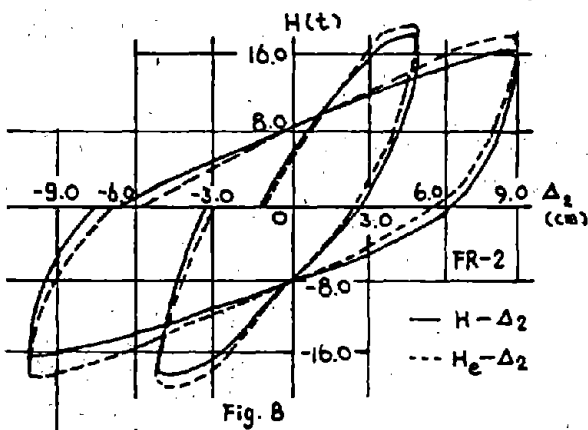
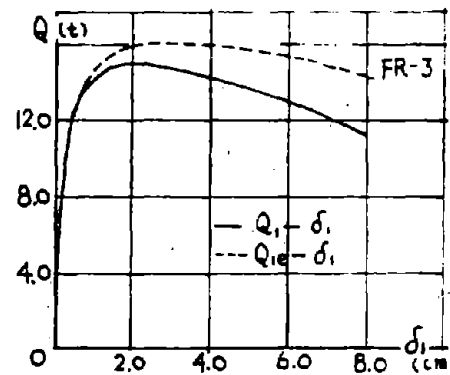
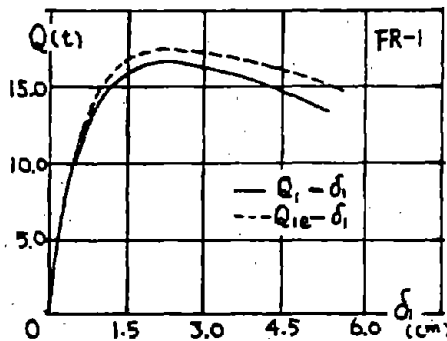
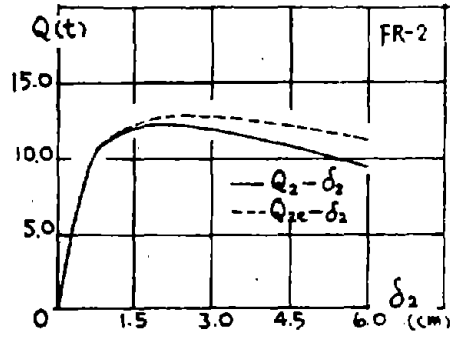
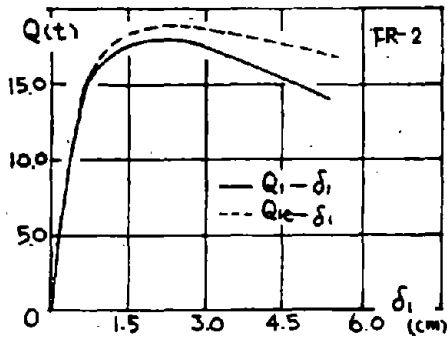


Fig. 8

Fig. 9

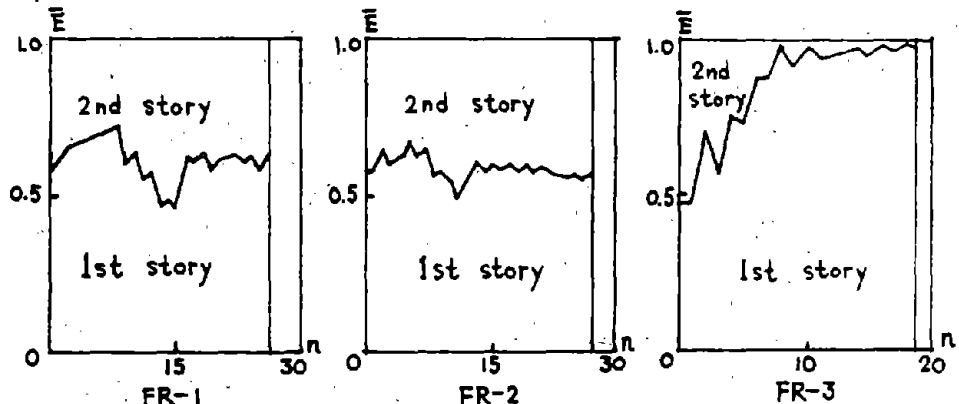


Fig. 11

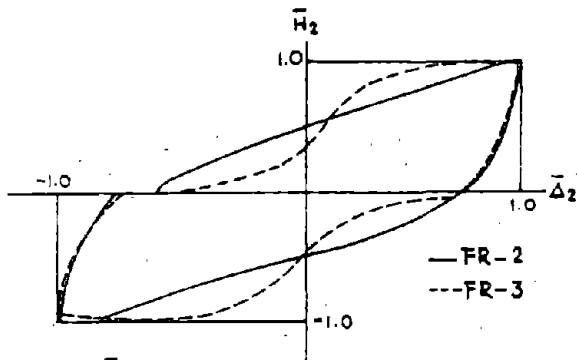


Fig. 10

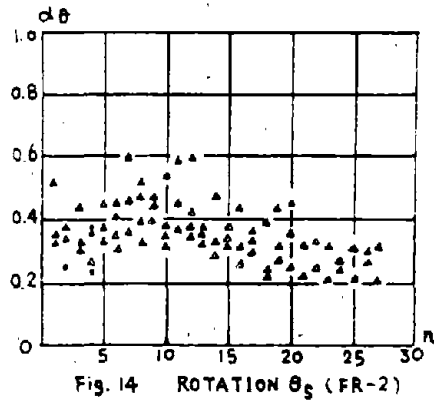


Fig. 14 ROTATION θ_s (FR-2)

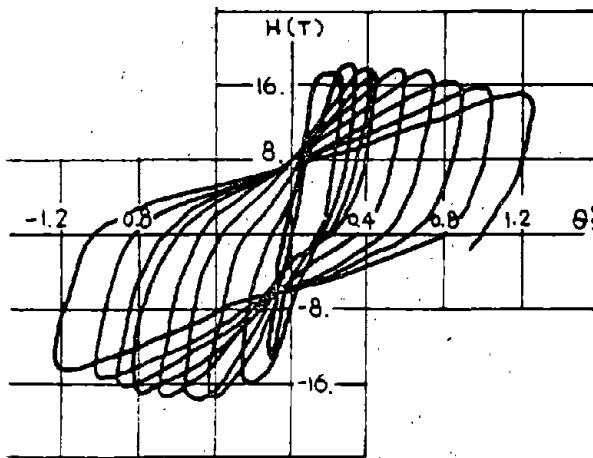
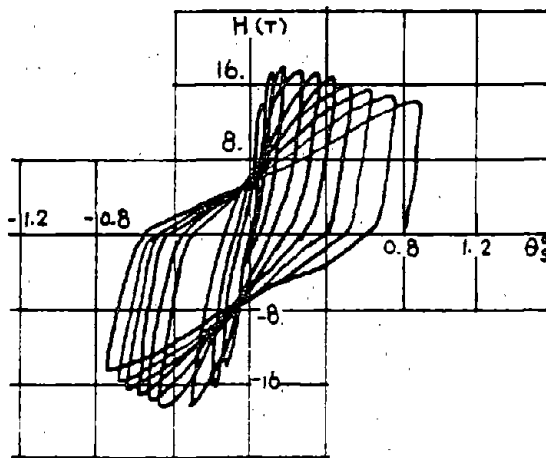


Fig. 12 (a) Slippage rotation of beam



(b) Slippage rotation of column

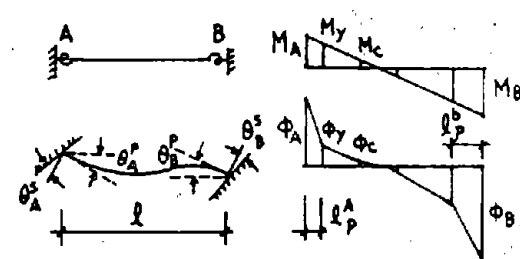
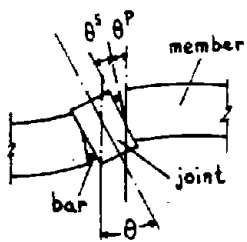


Fig. 16

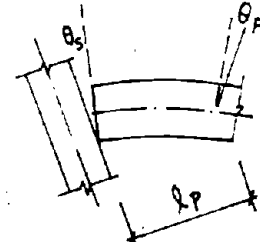


Fig. 13

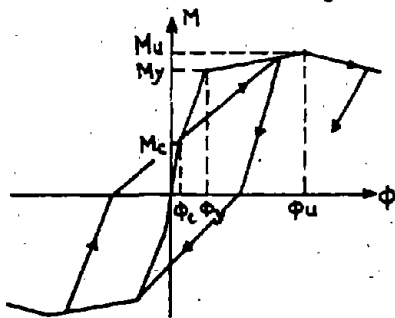


Fig. 17 (a)

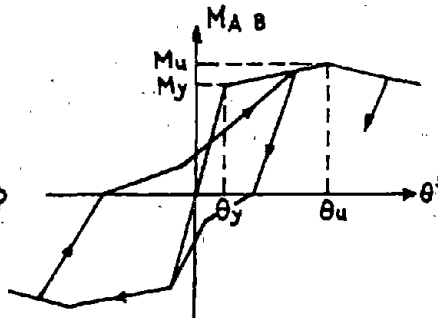


Fig. 17 (b)

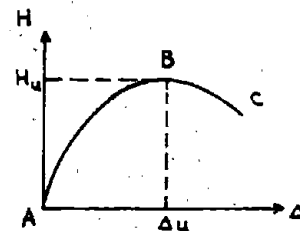


Fig. 15

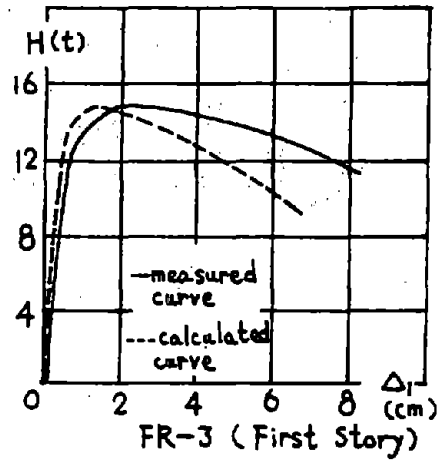
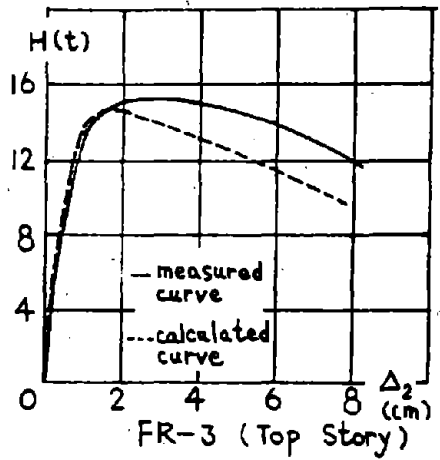
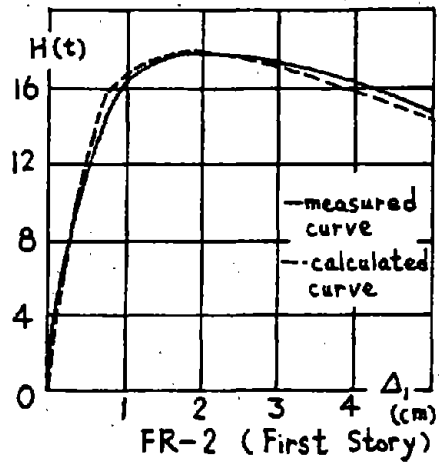
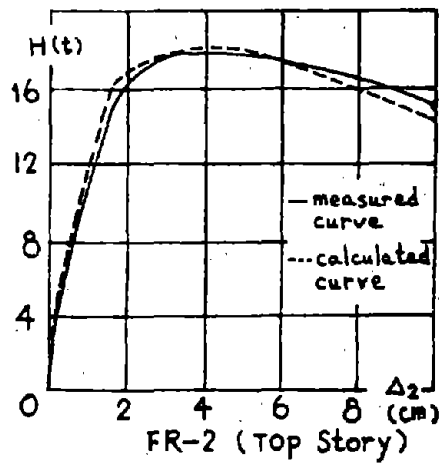


Fig. 18

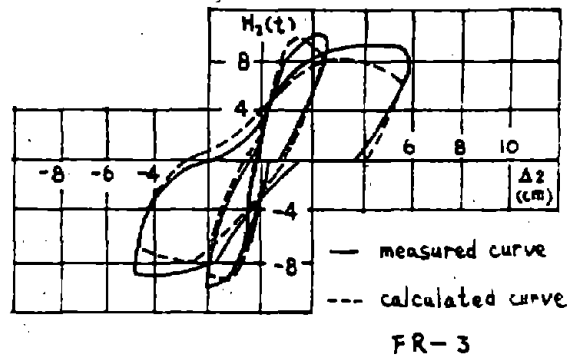
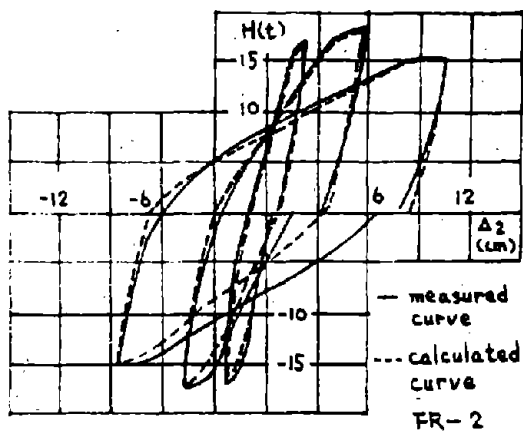


Fig. 19

On Simulating the Nonlinear Planar Hysteretic Response
of Reinforced Concrete and Concrete Masonry.

G. A. Hegemier^I and H. Murakami^{II}

ABSTRACT

This paper concerns a nonlinear model for reinforced concrete with applications also to reinforced concrete masonry. The presentation focuses upon planar response. The theoretical framework is nonphenomenological in the sense that the global equations are synthesized from the properties of the constituents and constituent interfaces, and the component geometry. The model is cast in the form of a binary mixture which resembles the overlay of two continua: steel and concrete. Validation studies reveal good agreement between simulations and experimental data for both monotonic and hysteretic deformation histories.

INTRODUCTION

The nonlinear response of structural composites such as reinforced concrete and reinforced concrete masonry is dominated by complex interactions between the steel and concrete masonry. Such interactions have a major effect on structural characteristics such as stiffness, strength, damping, and ductility. Consequently, it is necessary that a model reflect these phenomena. Further, in an effort to minimize the number and type of tests necessary to define model parameters, it is desirable that the model be nonphenomenological, i.e., that the global properties be synthesized from the properties of the steel and concrete masonry, the steel-concrete/masonry interface physics, and the steel geometry.

In this paper a candidate model is discussed that satisfies the foregoing requirements. The theoretical formulation is validated, in part, by detailed comparisons between numerical simulations and experimental data. These validations concern two primary steel-concrete interaction mechanisms: (1) The steel-concrete bond problem and (2) the steel-concrete dowel problem. Problem (1) plays a dominant role in the bending and the nonlinear stretching of reinforced concrete beams, plates, and shells. Problem (2) plays a major role in the transverse shear deformation of reinforced concrete beams, and the transverse and in-plane shear deformation of reinforced concrete plates and shells.

^IConsultant, S-CUBED, A Division of Maxwell Laboratories, Inc., P. O. Box 1620, La Jolla, CA 92038-1620, and Professor of Applied Mechanics, Department of AMES, University of California, San Diego, La Jolla, California 92038.

^{II}Assistant Professor of Applied Mechanics, Department of AMES, University of California, San Diego, La Jolla, California 92038.

The discussion to follow is devoted primarily to reinforced concrete. However, some applications render the model applicable also to reinforced concrete masonry. One such case, which involves fully grouted masonry, is treated herein.

THEORETICAL

A large class of theoretical modeling problems concerning the constitutive description of structural composites such as reinforced concrete/concrete masonry fall into the general category of "homogenization". The term, as used here, implies construction of the macro-constitutive relations via micromechanical considerations together with appropriate smoothing or averaging operations. The final result may, on the macroscale, be an "equivalent" single-phase, multi-phase, or non-local continuum.

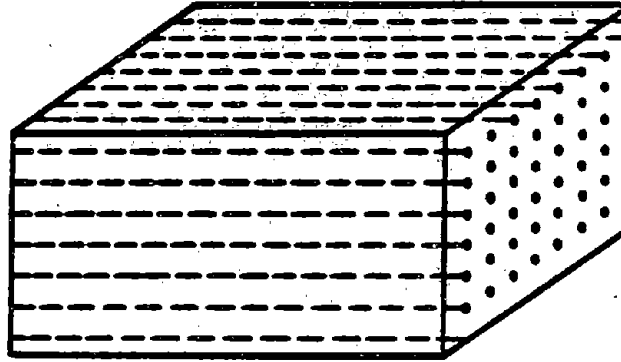
As use of the prefixes "micro" and "macro" above imply, homogenization typically enters the picture when one wishes to determine the response of a continuum for which two widely differing length scales can be identified. The large scale, or macroscale, is determined by the specimen geometry and/or the loading condition; the small scale, or microscale, is determined by material heterogeneity. In the case of reinforced concrete, the typical steel spacing constitutes the appropriate microscale. For concrete masonry, an additional microscale related to the block geometry may be necessary.

The homogenization problem is parameterized by the small ratio of the two length scales, ϵ . The fundamental problem is to determine the "proper" macroscopic response equation as $\epsilon \rightarrow 0$. Once obtained, it is natural to introduce asymptotic (small ϵ) notions into the analysis to determine a physically meaningful sequence of equations ordered in powers of ϵ . The higher order equations are intended to provide additional simulation capability on the macroscale.

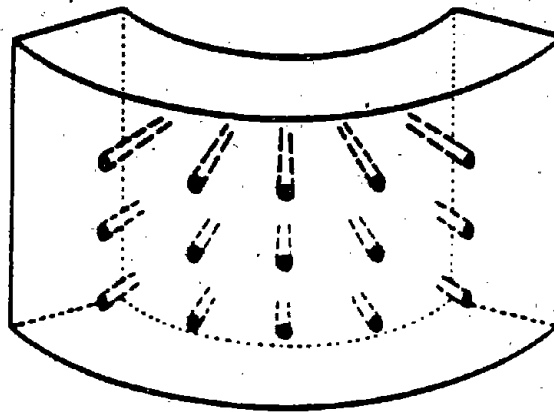
Using homogenization concepts, a nonlinear model of reinforced concrete with a "dense" unidirectional steel layout has been constructed. Typical such meshes are depicted in Fig. 1. The construction technique was based upon the use of multivariable asymptotic expansions, a variational principle and certain smoothing operations. The resulting model has been cast in the form of a binary mixture which resembles an overlay of two continua: steel and concrete; these continua interact via body forces which are functionals of the relative global displacements of the continua. A complete mathematical description of the model and the construction procedure can be found in "Development of Advanced Constitutive Model for Reinforced Concrete," (Hegemier, et al., 1984). For brevity, remarks in this paper are focused primarily upon comparisons between theoretical simulations and experimental data in an effort to demonstrate the simulation capability of the model.

STEEL-CONCRETE BOND PROBLEM

The steel-concrete bond problem concerns the manner in which normal forces are transferred across cracks in reinforced concrete, and the stiffness degradation that occurs due to progressive



(a) Rectilinear



(b) Curvilinear

Figure 1. Unidirectional Dense Steel Arrays

cracking. The phenomena considered include bond slip and degradation, concrete cracking, and yielding of the rebar. In the literature, problems of this type fall into the category of "tension stiffening".

Consider the problem of predicting the global response of a unidirectionally reinforced concrete specimen where a state of global uniaxial stress is applied in the steel direction, Fig. 2. For small deformations, the theory developed in Hegemier, et al., (1984) which is valid for multiaxial stress states and large deformations, reduces to the elementary relations:

$$N_{11,1}^{(1p)} + P_1 = 0 \quad , \quad N_{11,1}^{(2p)} - P_1 = 0 \quad , \quad (1)$$

$$\dot{N}_{11}^{(ap)} = n^{(a)} \dot{N}_{11}^{(a)} = n^{(a)} E_{ep}^{(a)} \dot{U}_{1,1} \quad , \quad (2)$$

$$\dot{P}_1 = K_{ep} (\dot{U}_1^{(1)} - \dot{U}_1^{(2)}) = K_{ep} [\dot{U}_1] \quad . \quad (3)$$

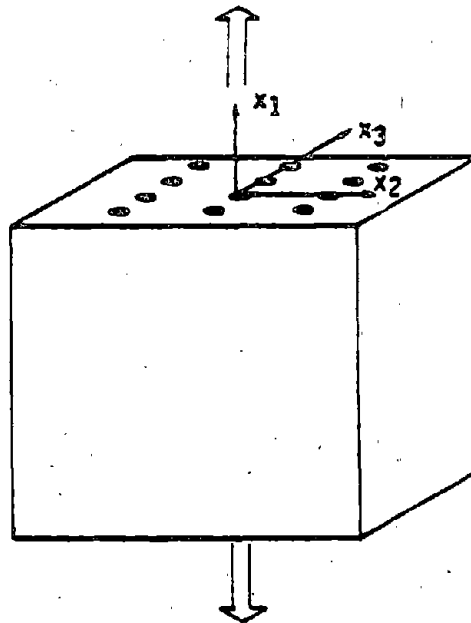


Figure 2. Global Uniaxial Loading

In the above, $\alpha = 1, 2$ refer to steel, concrete, respectively; $U^{(\alpha)}$, $N^{(\alpha)}$ denote axial displacement and axial stress (averages), respectively; $E_{ep}^{(\alpha)}$ and K_{ep} are tangent moduli; $n^{(\alpha)}$ denotes volume fraction of material α ; and $(\cdot)_{,1} = \partial(\cdot)/\partial x_1$, $(\cdot)^{\cdot} = \partial(\cdot)/\partial t$ where t represents time.

Relations (1) are the equilibrium equations for each material; the latter interact via the interaction body force P_1 which reflects interface shear transfer between the concrete and steel. Equation (3) shows that this interaction term depends upon the relative displacement history. Equations (2) represent the global constitutive relations for each material.

For the elastic response regime, the tangent moduli are determined, through a micromechanical analysis, to have the form:

$$E_{ep}^{(\alpha)} = (\lambda + 2\mu)^{(\alpha)} - \lambda^{(\alpha)2} / (\lambda + \mu)^{(\alpha)} \equiv E^{(\alpha)}, \quad (4)$$

$$K_{ep}^{-1} = \frac{\epsilon^2}{8} \left\{ \frac{1}{\mu^{(1)}} - \frac{[2+n^{(2)} + (2\ell n n^{(1)})/n^{(2)}]}{n^{(2)} \mu^{(2)}} \right\} \equiv K^{-1} \quad (5)$$

where $\lambda^{(\alpha)}$, $\mu^{(\alpha)}$ denote Lamé constants of material α . Equation (5) implies that no slip occurs between steel and concrete.

When steel-concrete slip occurs, Equation (5) must be generalized. For monotonic global deformation, a simple elastic-perfectly plastic model is sufficient. For hysteretic deformation, detailed

studies (Hageman, 1983) of steel-concrete pull-out specimens have guided the construction of an elementary bond-slip model which is depicted in terms of the interaction term P_1 in Fig. 3. For a wide range of concretes, the following selection of parameters is appropriate: $P_{cr} = 2\sqrt{n}^{(1)}(\sigma_{rx})_{cr}/\epsilon$, $-P_G = P_F = 0.8 P_{cr}$, $P_{IJ} = 0.2 P_{cr}$, $P_{DE} = -P_{GH} = 0.1 P_{cr}$. The model shown in Fig. 3 is easily placed in analytical incremental form. The description involves two parameters, K as defined by (5) and $(\sigma_{rx})_{cr}$ which represents a critical steel-concrete interface shear stress.

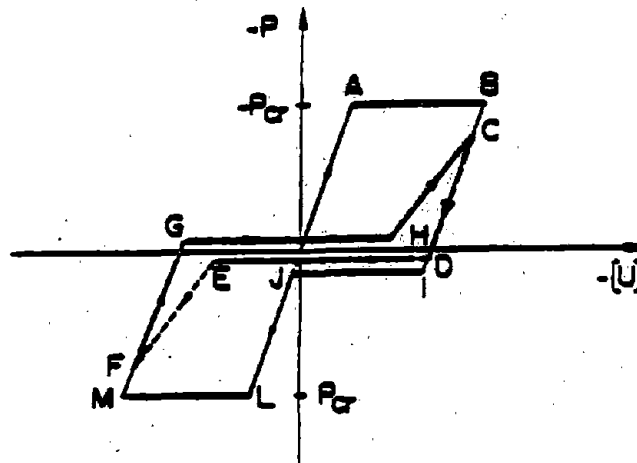


Figure 3. Bond-slip Model

Global inelastic material behavior can, within the context of the problem under consideration, take place via cracking of the concrete or yielding of the rebar. Typical global tangent moduli for these phenomena are shown in Fig. 4.

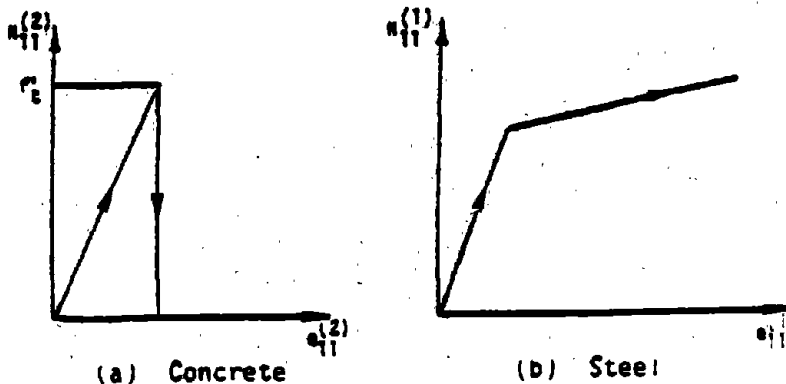


Figure 4. Behavior of constituents for monotonic extension example.

Consider now monotonic extension. For this case, an analytical solution of the foregoing model has been obtained (Hegemier, Murakami, et al., 1986). With reference to Fig. 5, the analysis reduces to the consideration of a typical "cell". Fig. 5(a) is the starting condition; in Fig. 5(b) the concrete has reached the tensile strength; the crack location is flaw-dominated and for convenience is placed at the specimen center; thereafter the theory predicts the appropriate crack location as deformation increases, Figs. 5(b)-5(d). The mathematical boundary conditions and cracking sequence are shown in Figs. 5(e)-5(h). Figure 6 shows the various response stages predicted theoretically; these consist of elastic response with no cracking, debonding, or slip (I), progressive cracking with debonding and slip (II), and slip only (III). Figure 7 shows a typical comparison between theory and experiment (scaled specimens, Somoyaji, 1979). Agreement is observed to be good (stress drops were not clearly observed since the tests were conducted under load-control). The quantities $(\epsilon_e)_{cr}$, $(\sigma_e)_{cr}$, E_m in Figs. 6 and 7 denote average strain, stress at first concrete cracking and mixture modulus; here $\sigma_e = n^{(1)}N_{11}^{(1)} + n^{(2)}N_{11}^{(2)}$ and $E_m = n^{(1)}E^{(1)} + n^{(2)}E^{(2)}$.

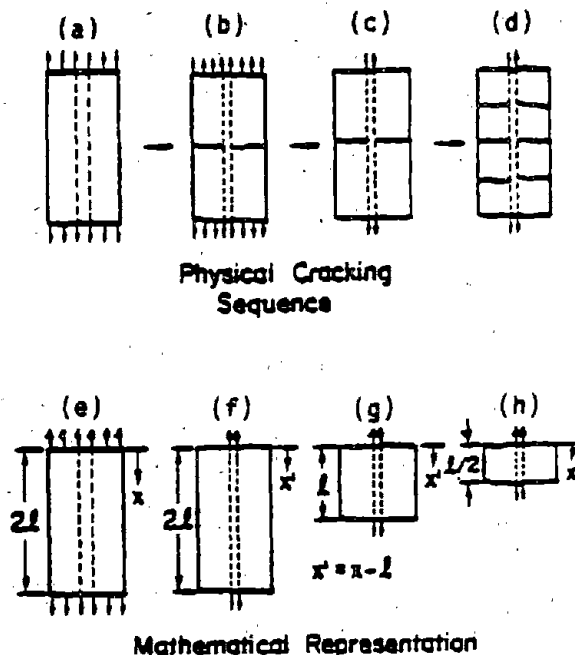


Figure 5. Cracking Sequence Assumed

A more critical test of the model concerns hysteretic deformation. A comparison of cyclic tension-compression test data by Hegemier, et al. (1978) on full-scale reinforced concrete masonry specimens and simulated test data is illustrated in Fig. 8 for test panel No. 87. Shown here is the entire load-unload-reload history of the specimen as given by the experiment (Fig. 8(a)) and as given by the simulation (Fig. 8(b)). In Fig. 9, the envelop of the experimental data has been superposed on the simulated data to illustrate

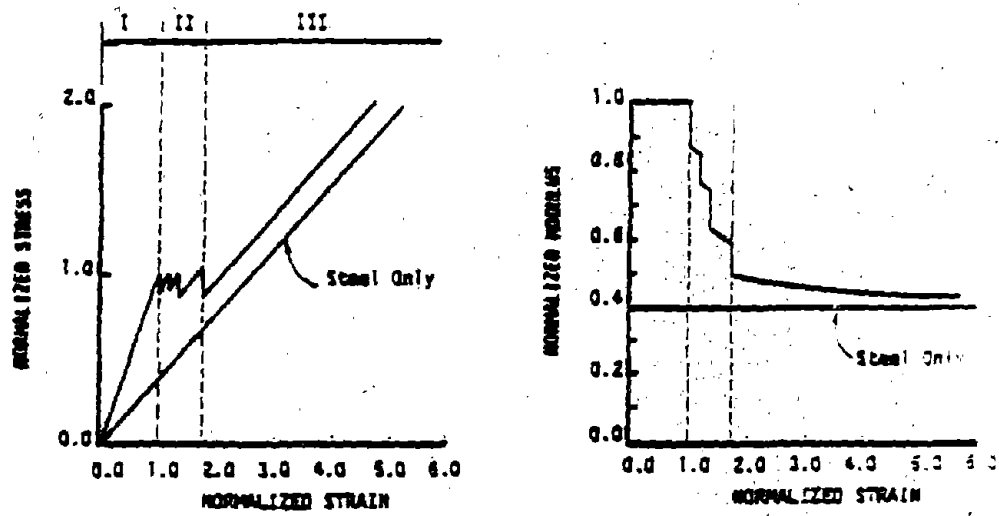


Figure 6. Stages of Response Predicted Theoretically.

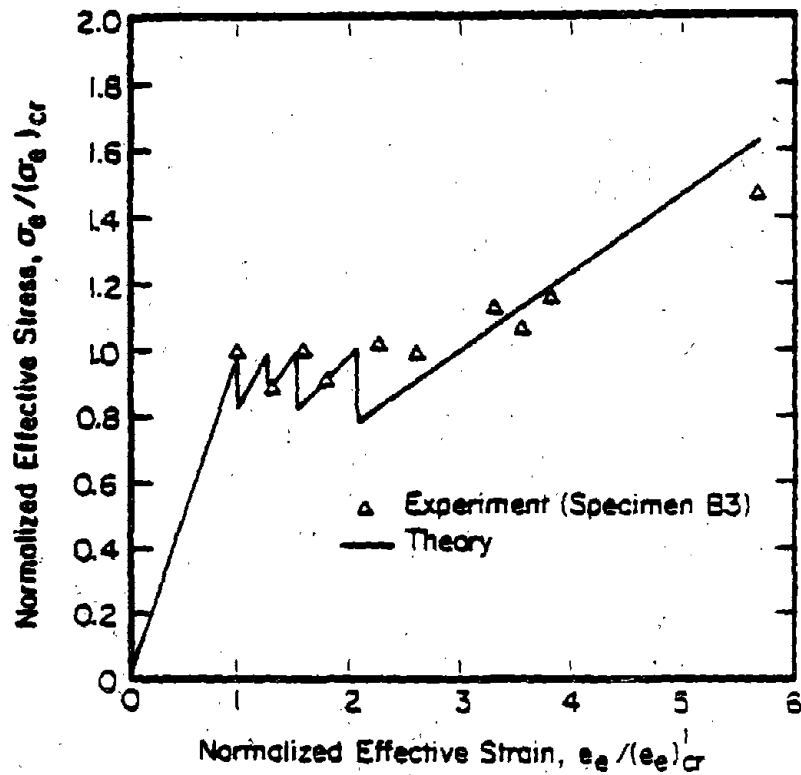


Figure 7. Comparison of Test and Simulation: Tension Specimen B3 from Somayaji (1979).

model accuracy. The agreement is generally excellent. Figure 10 gives a closer look at the experimental and simulated response for the

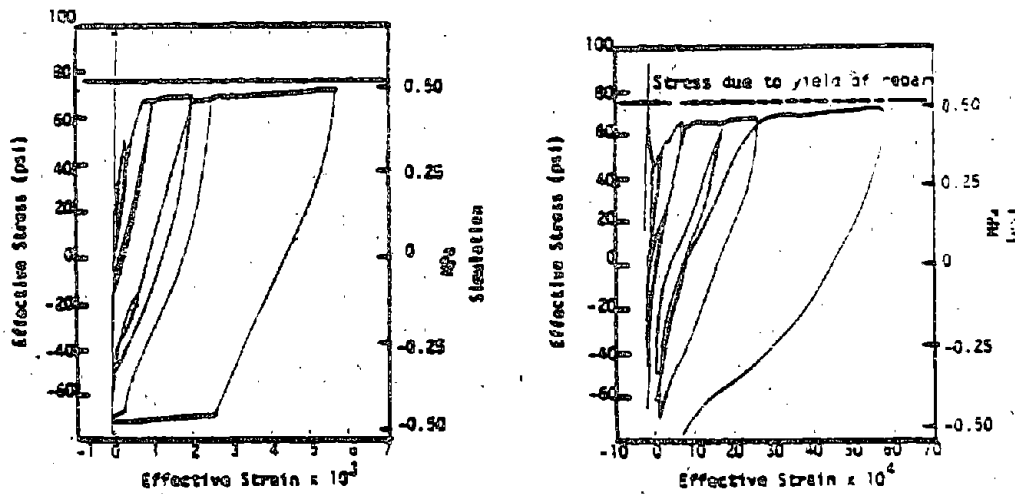


Figure 8. Comparison of Test and Simulation.

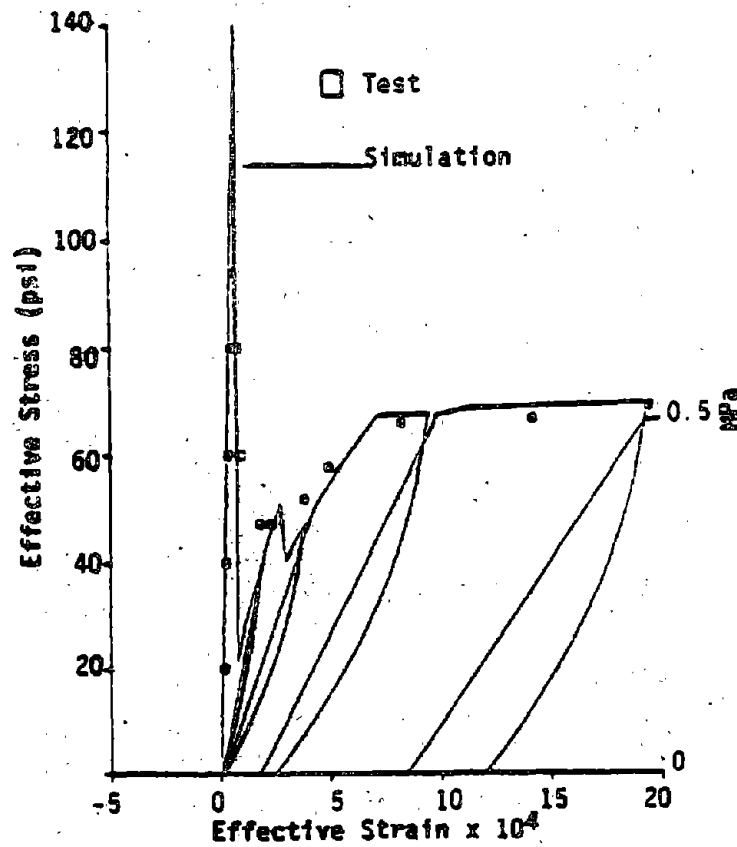


Figure 9. Comparison of Test and Simulation

first and second cycles of Fig. 8. The overall agreement is good although the experimental data indicates crack closure (i.e., steepening of the stress-strain curve) at larger strains than does the

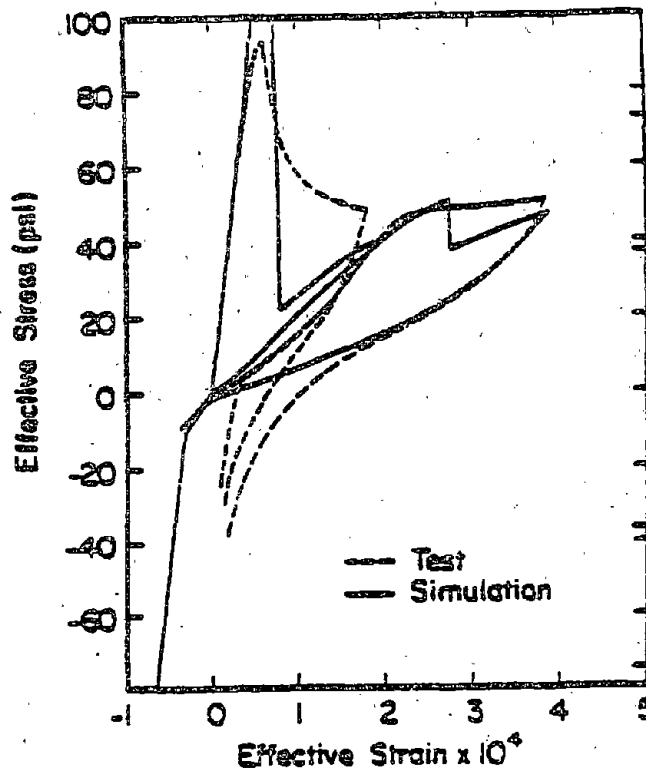


Figure 10. Comparison of Test and Simulation: σ_e - e_e Curves for First Two Cycles.

simulation. Possibly this difference is due to a mismatch of the asperities of the actual crack surfaces during reloading in compression. Hysteresis damping is apparent in the simulated response as well as the test data. The extent of this damping in both cases is clearly shown in Fig. 11 in the reproduction of the third, fourth and fifth deformation cycles. Although the shapes of the hysteresis loops are not identical, the enclosed areas, which are a measure of the damping, are similar. Finally, the tangent stiffness degradation as a result of progressive damage was determined by measuring the average slope of the unload-reload curves. Excellent agreement between theory and experiment for the tangent stiffness degradation is shown in Fig. 12.

At this point, a remark is in order concerning the above concrete masonry specimen. Concrete masonry is a composite consisting of block, grout, mortar and steel. For the purpose of simulating a fully grouted specimen under extension, it was assumed that, following the first macrocrack, only the grout cores plus steel contributed significantly to the global structural response. Thus, in tension the "cell" geometry corresponds to the grout core dimensions. In compression, on the other hand, the entire specimen cross-section was activated.

STEEL-CONCRETE DOWEL PROBLEM:

The dowel problem concerns the manner in which shear forces are transferred across cracks in reinforced specimens. Three distinct modes of shear transfer exist at a crack: (1) Interface shear

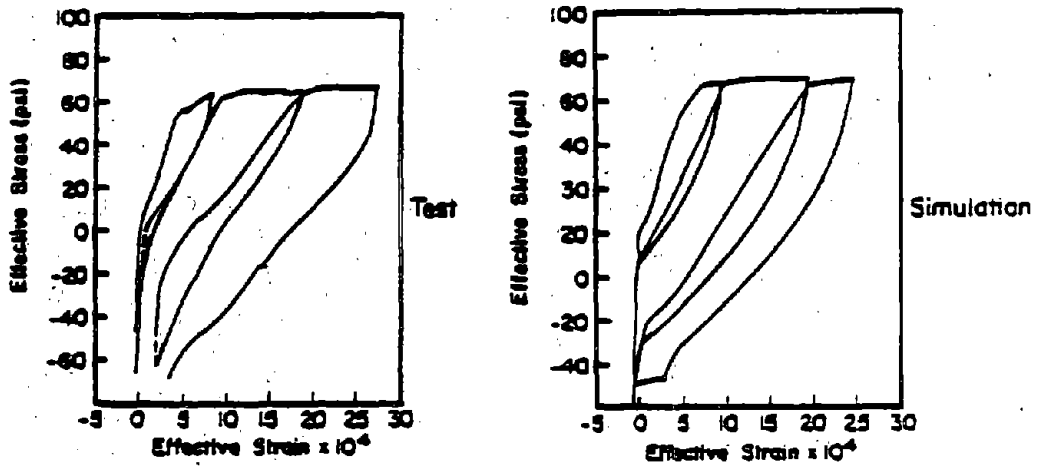


Figure 11. Comparison of Test and Simulation: $\sigma_e - e_e$ Curves for Third, fourth and Fifth Cycles.

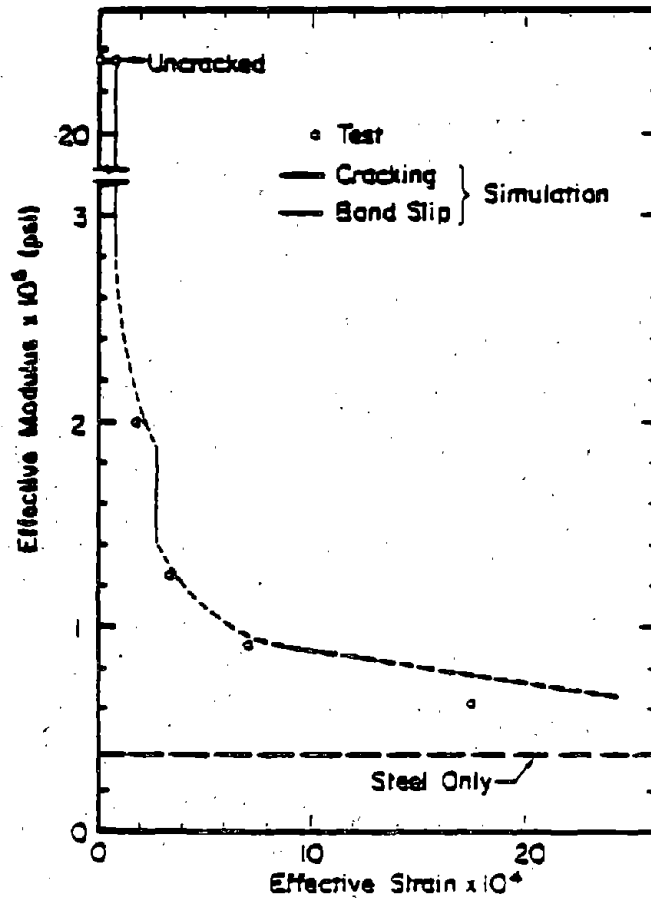


Figure 12. Comparison of Test and Simulation: Tangent Stiffness Degradation Due to Cracking and Debonding.

transfer (IST) on the rough surfaces of the crack; (2) dowel action (DA) in the reinforcement crossing the crack; and (3) components of axial forces in the reinforcing bars inclined to the crack direction. IST includes the effective frictional and bearing forces generated at a slightly open crack as the protruding particles on each side of the cracked surface come into contact. DA is induced by the shear and bending deformations experienced by the reinforcement when shear displacements are applied to the crack. Where the dowel transverse displacements become sufficiently large, axial forces in the rebars crossing the crack contribute to effective shear resistance. The example to follow focuses upon a single preexisting crack in the absence of IST with rebar initially normal to the crack surface.

The dowel problem is illustrated in Fig. 13 for the case of reinforced concrete. Of interest here is the prediction of the global shear force or stress across the crack plane for a prescribed relative

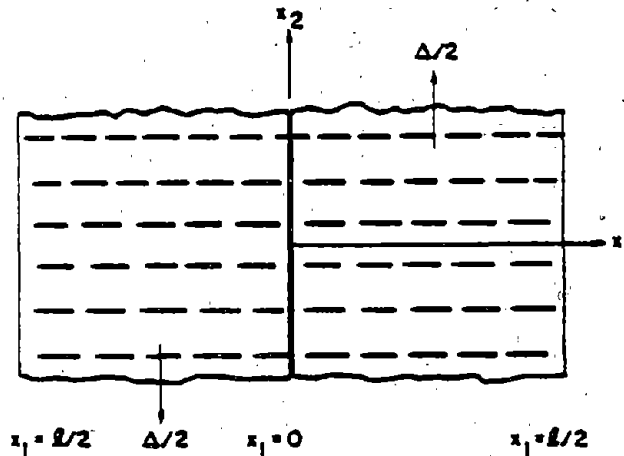


Figure 13. The Dowel Problem

displacement of the concrete. To eliminate IST, it will be assumed that the crack surface is smooth and lubricated; thus the contact shear stress between concrete segments is assumed to be negligible. Under this condition, together with the assumed prescription of the average global concrete displacements, the theory developed in Hegemier, et al., (1984) reduces to

$$N_{11,1}^{(1p)} + P_1 = 0 \quad (6)$$

$$N_{12,1}^{(1p)} + (N_{11}^{(1p)} U_{2,1}^{(1)})_{,1} + P_2 = 0 \quad (7)$$

$$M_{11,1}^{(1p)} - N_{12}^{(1p)} = 0 \quad (8)$$

$$\dot{N}_{11}^{(1p)} = n^{(1)} A E_{ep}^{(1)} (\dot{U}_{1,1}^{(1)} + \dot{U}_{2,1}^{(1)} U_{2,1}^{(1)}) \quad (9)$$

$$-\dot{N}_{12}^{(1p)} = n^{(1)} A_u^{(1)} (\dot{U}_{2,1}^{(1)} + \dot{S}_1^{(1)}) , \quad (10)$$

$$\dot{M}_{11}^{(1p)} = \frac{\pi d^{(1)4}}{64} \epsilon_{ep}^{(1)} \dot{S}_{1,1}^{(1)} \quad (11)$$

$$\dot{P}_1 = \beta_1 [\dot{U}_1] \quad (12)$$

$$\dot{P}_2 = \beta_2 [\dot{U}_2] \quad (13)$$

where $[U_1] = [U_1^{(2)} - U_1^{(1)}]$, $d^{(1)}$ is the diameter of the rebar, and A represents a certain "cell" area. In the above, $N_{ij}^{(1p)}$ is the partial stress associated with the steel, P_i is an interaction body force in the i th direction, and $M_{ij}^{(1p)}$ is a weighted stress average, i.e., a moment. Equations (6) to (8) are equilibrium relations while (9) to (11) are constitutive equations. An assumption of moderate rotations of the steel is implicit in these relations. Based in part on micromechanical considerations, the models shown in Figs. 3 and 14 were utilized to represent the interaction relations (12) and (13). The boundary conditions of the problem depicted in Fig. 12 correspond to

$$U_2^{(1)} = U_2^{(2)} = M_{11}^{(1p)} = 0 \text{ at } x_1 = 0 \quad (14)$$

$$N_{11}^{(1p)} = N_{12}^{(1p)} = M_{11}^{(1p)} = 0 \text{ at } x_1 = l/2 \quad (15)$$

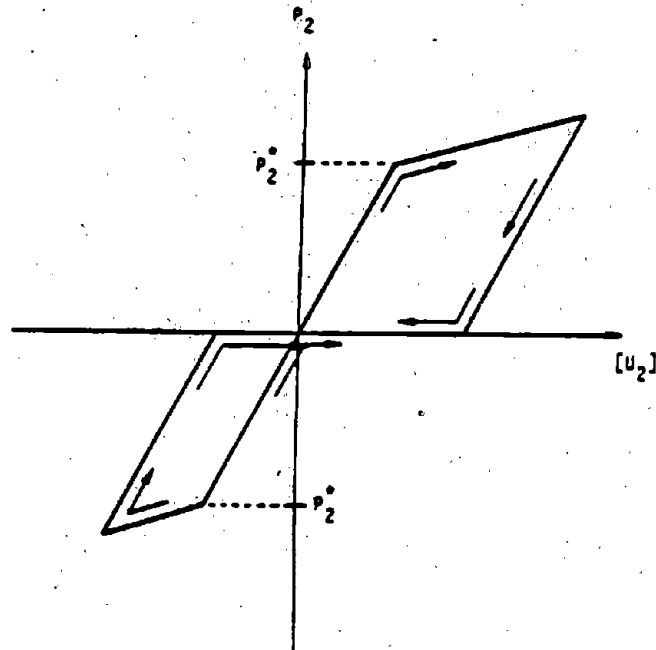


Figure 14. Interaction Term P_2 for Dowel Problem.

With use of the above model, a simulation of the monotonic dowel tests by Pauley, et al. (1974) was performed. The test specimen and setup are illustrated in Figs. 15 and 16; wax was used to lubricate the joint surface. A comparison of theoretical and experimental results are shown in Fig. 16 for three different steel volume fractions. Agreement is observed to be good. The "shear stress" in Fig. 17 is based on the specimen area.

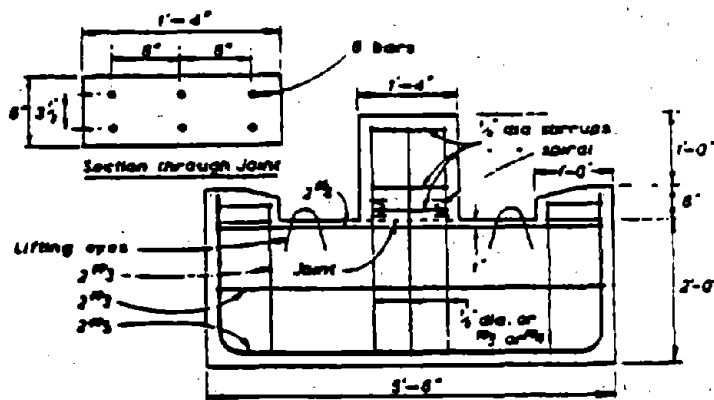


Figure 15. Details of test specimens, Pauley et al. (1974).

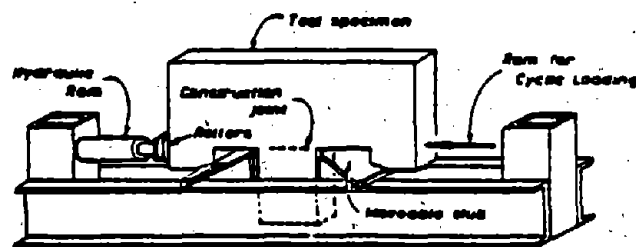


Figure 16. The Test Set Up, Pauley, et al. (1974).

A more critical test of the model simulation capability is represented by the cyclic experiments of Jimenez, et al. [7]. The specimen and test setup are illustrated in Fig. 18. Thin brass sheets were used to lubricate the joint surface. A typical simulation versus experiment is shown in Fig. 19. The agreement is observed to be good considering the complexity of the response.

Conclusion

An advanced nonlinear model for reinforced concrete has been developed for dense unidirectional steel layouts. For some

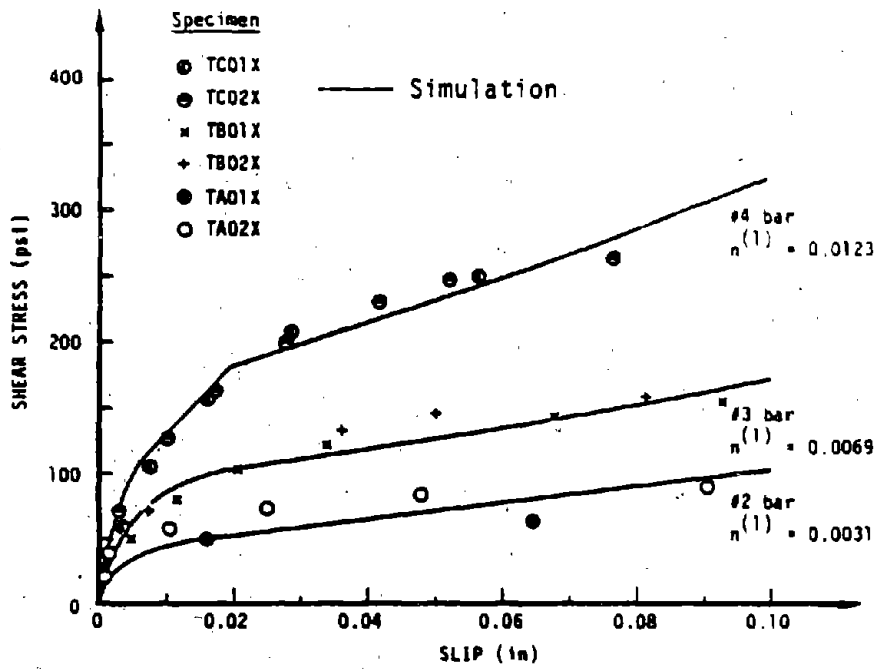


Figure 17. Load-slip Relationship for the dowel Test by Paulay, et al. (1974).

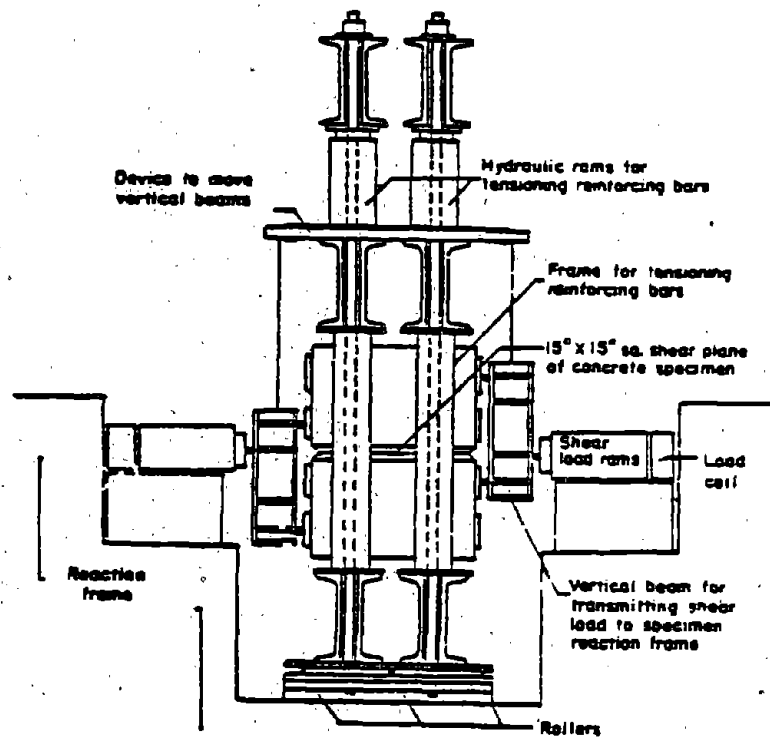


Figure 18. Test Set Up, Jimenez, et al. (1978).

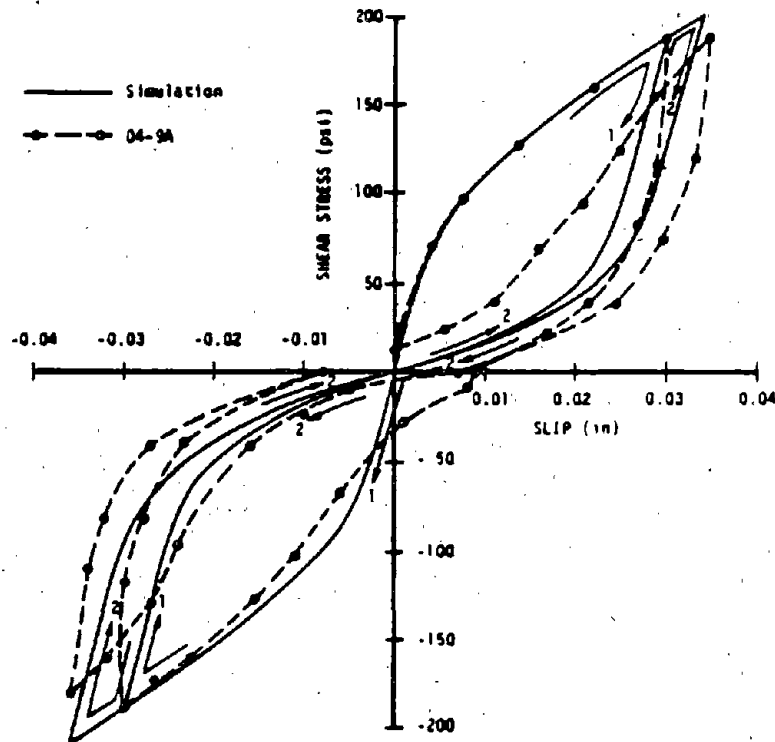


Figure 19. Load-Slip Relation for the Dowel Test by Jiminez, et al. (1978).

applications, the theory is also applicable to problems involving reinforced concrete masonry. The description takes the form of a binary mixture of concrete and steel. Validation tests performed to-date indicate that the model correctly simulates progressive concrete cracking, steel-concrete bond degradation and slip, and steel-concrete dowel action. Current efforts are focused upon extensions to include more general steel layouts and inclusion of a more accurate plain concrete model.

ACKNOWLEDGEMENT

This research was sponsored by the Air Force Office of Scientific Research (AFSC) under Contract F49620-84-G-0029 to S-CUBED, A Division of Maxwell Laboratories, Inc., San Diego, California.

REFERENCES

Hageman, L. J., "A Mixture Theory with Microstructure Applied to the Debonding, Cracking and Hysteretic Response of Axially Reinforced Concrete", Ph.D. Dissertation, University of California, San Diego, 1983.

- Hegemier, G. A., H. Murakami, and L. J. Hageman, "On Tension Stiffening in Reinforced Concrete," Mechanics of Materials, Vol. 5, 1986.
- Hegemier, G. A., H. E. Read and H. Murakami, Development of Advanced Constitutive Model for Reinforced Concrete, Report SSS-R-84-6684, S-CUBED, La Jolla, CA., April 1984.
- Hegemier, G. A., R. O. Nunn and S.K. Arya, Behavior of Concrete Masonry under Biaxial Stress," Proc. North American Masonry Conference, University of Colorado, Boulder, Colorado, August 1978.
- Jimenez-Perez, R., P. Gergely and R. N. White, "Shear Transfer Across Cracks in Reinforced Concrete," Report No. 78-4, Department of Structural Engineering, Cornell University, Ithaca, New York, August 1978 (NTIS PB-288 885/RC).
- Paulay, T., R. Park and M. H. Phillips, "Horizontal Construction Joints in Cast-In-Place Reinforced Concrete," ACI SP-42, Shear in Reinforced Concrete, Vol. 2, 1974.
- Somayaji, S., "Composite Response, Bond Stress-slip Relationships and Cracking in Ferrocement and Reinforced Concrete," Ph.D. Dissertation, University of Illinois, Chicago Circle, 1979.

**IV DAMAGE PREDICTION,
RELIABILITY ANALYSIS AND
STRENGTHENING**

STRENGTHENING
RELIABILITY ANALYSIS AND
DAMAGE PREDICTION.

PREDICTIONS OF STABILITY FOR UNREINFORCED BRICK MASONRY WALLS SHAKEN BY EARTHQUAKES

J.C. Kariotis, R.D. Ewing, and A.W. Johnson¹

SUMMARY

Full scale dynamic testing of unreinforced brick masonry walls shaken in the out-of-plane direction confirmed dynamic stability concepts. The dynamic stability prediction technique uses an experimentally-based statistical model that incorporates seismic spectral intensities as part of the input into the selection of stable wall height-thickness ratios. Earthquake response of horizontal elements such as floors and roofs was shown to be critical to the prediction of the dynamic stability of unreinforced walls, as well as the elevation locations of the walls in the building. The results of the research program were introduced into earthquake hazard reduction ordinances that are now in effect in the Pacific Coast seismic hazard zone of the United States.

INTRODUCTION

Building construction using unreinforced masonry (URM) predates the development of seismic criteria that guide the design and construction of present-day buildings. A substantial number of these URM buildings are still being used in areas considered seismically active, even though investigations of earthquake damage have confirmed that this type of building has been a major contributor to personal injury or loss of life during relatively high intensity earthquakes.

In 1977, the National Science Foundation (NSF) initiated a multi-phased program for the mitigation of seismic hazards, which resulted in a study to develop a methodology for the mitigation of seismic hazards in existing URM buildings. A key observation taken from these damage reports is that some structures sustained more damage than others, and the researchers were led to assume that the interaction among the building components was a vital issue in explaining and predicting URM building damage. Accordingly, a study of typical URM building response was conducted and three related component responses and their interactions were identified for further study; namely:

¹Co-Principal Investigators; ABK, a Joint Venture, El Segundo, CA, USA

- Horizontal diaphragms
- URM walls subjected to out-of-plane motions
- Anchorage between the URM walls and the diaphragms

The topic of this paper, stability of URM walls shaken by earthquakes, has received little or no attention in prior research. In-plane strength of URM walls can be estimated by common design procedures, but survival of URM walls shaken out-of-plane, when anchored to floor and roof systems cannot be rationalized by computations using strength concepts. Determination of the probability of stability of the anchored URM walls at the building exterior is the single most significant part of an earthquake hazard reduction program. Separation and collapse of the URM walls at the building exterior contribute to the majority of threat to life during an earthquake. Anchorage of the URM walls is a straightforward partial solution. Determination of stability of the URM walls between anchorage levels needs analytical methods previously not known. As part of the overall research program, an analytical and experimental investigation into the response of URM walls shaken out-of-plane was undertaken.

CONCEPTS OF DYNAMIC STABILITY

Unreinforced masonry walls survive moderate to strong ground shaking by mechanisms not related to usual seismic design provisions. Masonry walls in seismic zones are typically designed for out-of-plane lateral forces by prescribing a minimum moment capacity. This moment capacity is provided by either reinforcement or the tensile capacity of the masonry assemblage. The analysis or design of unreinforced walls, without tensile capacity, for out-of-plane stability when shaken by earthquake motions, is termed in this paper as analysis of dynamic stability. Dynamic testing of URM walls confirmed that fully cracked URM walls will remain stable and continue to support superimposed loads during moderate to strong shaking. The intensity of shaking included motions that are appropriate for the highest hazard zone in the United States (ABK-TR-02, 1981).

The stability of a fully-cracked URM wall, shaken by less than critical ground motion intensities, is maintained by gravity load moments applied at the cracked surfaces as shown in Figure 1. The approximate gravity load moments on the cracked surfaces $(0 + W_1)e_1$ and $(0 + W_1 + W_2)e_2$, do not have to equal at any point in time the horizontal inertial moments caused by dynamic horizontal displacement of the URM wall. These moments limit the dynamic horizontal excursions of the two rotating blocks. When the center of gravity of the vertical loads above a cracked surface lies within the wall thickness dimension "t", the gravity load moments provide a restoring moment that closes the crack upon reversal of the earthquake displacement motions.

Figure 1 presents a simplified force system to indicate the principles of dynamic stability. Shear forces transferring horizontal forces between the rotating blocks may occur at the center crack. Gravity loads W_1 , W_2 , and O are modified by vertical accelerations caused by a component of the ground motion as well as vertical accelerations resulting from the upward displacement of the wall segments, relative to the base. These upward displacements are caused by geometric relationships of the displaced and rotated wall segments. The test apparatus did not include input of vertical time histories that would be appropriate in combination with horizontal time histories. The probability of modification of dynamic stability predictions by vertical ground motions is discussed in the recommendations of this paper.

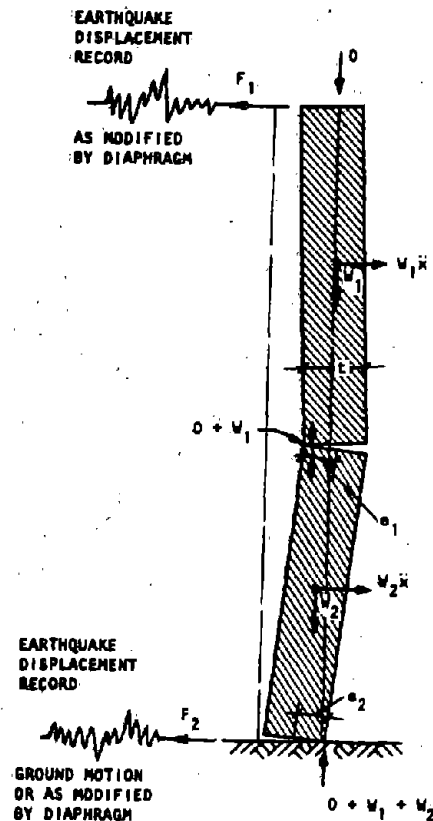


Figure 1. Dynamic Stability Force Model

The concept of control of structural displacements of yielding elements is inherent in all seismic design provisions, and a yield capacity of the lateral load resisting system is prescribed by design provisions. This prescribed capacity is less than calculated elastic structural response, but can effectively limit the magnitude of relative inelastic displacement.

DYNAMIC TESTING PROGRAM

URM wall specimens were fabricated adjacent to the test apparatus using common masonry material and mortars. The specimens were 1.8 m wide and 3.0 m to 4.9 m high. The height-to-thickness ratios (H/T) ranged from 14 to 25. The materials included three wythe common brick and grouted and ungrouted clay and concrete blocks. Four specimens were reinforced by a retrofit technique that consisted of the application of a wire mesh and plaster to the brick wall surfaces by hand plastering techniques.

The URM wall specimens were installed in a test fixture that allowed the base and top of the wall to be moved independently in the out-of-plane direction by servocontrolled hydraulic actuators. The walls were fabricated on a concrete filled, metal base with two attachment lugs for the hydraulic actuators. When the wall was installed in the test fixture the base rested on a low-friction roller-supported base plate that allowed the base of the wall to be displaced without rotation by the two hydraulic servoactuators. A mechanical header with one attachment lug was installed on the top of the wall that allowed the top of the wall to be displaced by one hydraulic servoactuator; however, the top of the wall was free to rotate. The mechanical header was guided by a pantograph linkage system that allowed the top of the wall to move in the vertical direction without restraint. In addition, the mechanical header was fitted with two vertical rods that supported an overburden mass to simulate additional wall or parapet mass above the wall section being tested. The overburden mass was suspended from the header a few inches above the laboratory floor so that its fall at the time of wall collapse would be controlled.

The basic instrumentation for the measurement of the dynamic responses and forcing functions consisted of load cells, accelerometers, and displacement sensors. The displacements were measured using string potentiometers. The displacement sensors, including feedback deflection sensors, were mounted to a stable reference frame that was independent of the frame for the forcing system. The data from each instrument was recorded on magnetic tape in digital form. The raw source data tapes were interpreted and written on new tapes, using a standard format with some data compression, for use in data presentation and interpretation. Additional data recording was taken in the form of still and motion pictures as well as observer notes and test logs. The detailed data, photographic coverage and observer notes are given in ABK-TR-04 (1981).

The kinematic motions used in the test program were based on actual earthquake ground motion records that correspond to seven major geographical regions of the United States (ABK-TR-02, 1981). The ground motion records were scaled so as to cover the full range of

seismicity from an Effective Peak Acceleration (EPA) of 0.1 g to 0.4 g. These ground motions were input to the nonlinear, dynamic analysis model of a typical URM building described earlier to obtain diaphragm/wall response motions. The model accounted for the nonlinear response of the diaphragm, including both stiff and flexible diaphragms, and the dynamic inertial effect of the URM walls. The motion sets were assembled in pairs from these dynamic motions to simulate the kinematic environment at the base and top of the URM walls for both ground level wall elements and elevated level wall elements.

The pairs of motions were selected to include the following parameters:

- Paired motions with small phase shift
- Paired motions with substantial phase shift
- Paired identical input motions.
- Increasing spectral intensity of these paired motions

The selected motions represented the full range of ground shaking intensities (EPA) that corresponds to the contours of current hazard zoning maps (Applied Technical Council, 1978). The paired motions with small phase shift can represent the kinematic environment of single story walls supported at the top by stiff roof diaphragms, walls at the midheight of buildings with similar stiffness floor diaphragms, or walls at the uppermost story of buildings with diaphragms constructed of modern materials. The paired motions with substantial phase shift represent the kinematic environment of URM walls in single story buildings with undesigned and flexible roof diaphragms, or walls at the uppermost story of a building with undesigned diaphragms. The paired identical input motions represent the kinematic environment of URM walls that are attached to diaphragms coupled by crosswalls that control relative diaphragm displacement.

The order of dynamic test motions was first based on the assumption that the collapse of the URM test specimen would be related to:

- Increasing spectral intensity (EPA)
- Large relative displacement of the wall ends
- Increasing spectral velocity of input motions

The order of dynamic motions were revised, after the first tests established that input velocities, simultaneous in time, were the critical dynamic input factors.

The URM specimens were installed in the test apparatus with a test overburden. Three overburden weights were used for each group of test specimens. The ratio of overburden weight to test specimen weight (O/W) varied from 0.13 to 5.1. The specimens were shaken by increasing intensity paired motions until collapse occurred or the excitation capacity of the apparatus was reached. Specimens with O/W

ratios above 3.8 and H/T ratios of 15.7 and 21.3 survived input velocities of 1 m/s and 0.7 m/s respectively. All specimens were fully cracked at several bed joints by prior test sequences. The bed joints that opened appeared to be related to the input end motions and were not always at the previously cracked bed joints.

The observations and interpretation of the test program confirmed that understanding of the complete response model of the URM building is necessary for prediction of stability of URM walls. The amplification of ground motions by the in-plane URM walls and the floor and roofs, both in their elastic capacity and inelastic response range, must be considered and categorized for each seismic hazard zone.

PREDICTION OF DYNAMIC STABILITY

Experimental studies of in-plane dynamic stability of URM wall piers have indicated that the stability moments caused by dynamic displacements on cracked surfaces have a linear relationship to the rotation on the cracked surface for small rotations. The relationship is nonlinear for moderate to large rotations. For the out-of-plane motions the restoring gravity moment shown in Figure 1 has a declining branch due to the rotational geometry that is similar to a degrading hysteretic moment-rotation relation. However, unloading moment-rotation paths trace the loading moment-rotation relation. Kinetic energy is lost from the system by loss of momentum on cracking closing. Mathematical duplication of this behavior is difficult and can be done only for a generalized masonry model. For this reason, statistical studies are extensively used. Statistical studies are used for parametric studies in many phases of earthquake hazard reduction research. Earthquake input motions are described on the basis of probability. Modification of the input earthquake motions by horizontal elements is based on probability values of the stiffness properties and the yield capacities of diaphragms. Apparent damping (energy adsorption) of URM walls is generalized and presently can only be given a probable value for the variety of masonry assemblages that may be subjected to dynamic motions. The recommendations for acceptable risk of collapse of URM walls need to consider probability combinations that are equivalent to those incorporated into current seismic design recommendations.

Statistical studies and analyses of the test data concluded that the key parameters that determined dynamic stability of the URM walls were:

- The square root of the sum of the squared input velocities at the ends of the URM wall (SRSS)
- The overburden to wall weight (O/W) ratio of the wall
- The wall height to wall thickness (H/T) ratio of the wall

Plots of these parameters are presented in Figure 2 for a 98% probability of survival of the URM wall. For interpretation of the test data, the parameters were plotted for 50% and 86% probability of survival. A few "wrong-side" test results were observed and the relative displacement-time plots of the cracked wall specimens were examined. The plotting of the instrumentation data indicated that the theoretical upper bound of displacement of the center of the wall relative to its ends can be momentarily exceeded. The exceedance can be explained by recognition that dynamic displacement of the ends of the wall can reduce the relative center displacement before the center of the wall drifts into instability. The observed collapse of the unstable URM wall specimens was not sudden but can be characterized as a slow drift into the instability during reversal of the dynamic motions of the ends of the walls. The collapse was generally related to single pulses of input velocity. Cyclic input of velocities of less than critical values would cause large cyclic cracked excursions of the center of the wall without instability.

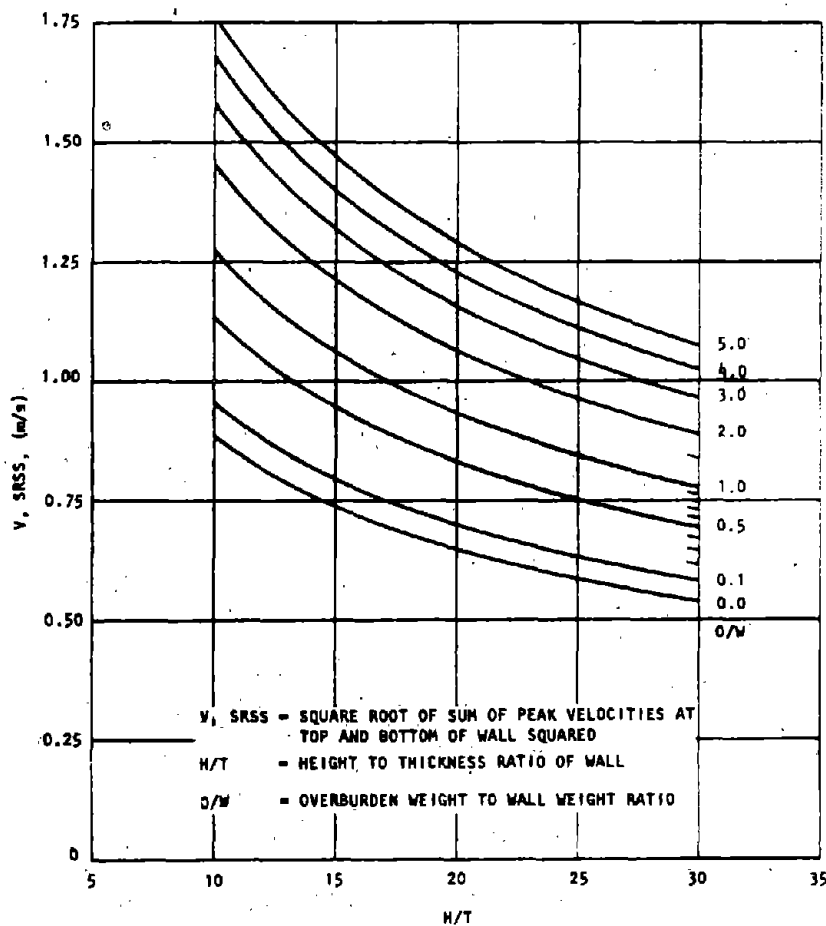


Figure 2. Unreinforced Masonry Wall Stability Criteria

The prediction of input velocity to the ends of the wall is the single parameter that depends on the URM building response model. A parallel dynamic test program for typical diaphragms was conducted to provide data for this parameter (ABK-TR-03, 1981). Interpretation of this data (ABK-TR-05, 1984), and integration of this data into the developed methodology (ABK-TR-08, 1984), recognized the influence of crosswalls on the modification of input motions by the diaphragm. A crosswall is defined as an element with elastoplastic load-displacement characteristics that interconnects the diaphragm with the ground between the diaphragm ends. These crosswalls are generally interior partitions that extend between diaphragm levels.

Development of mathematical models for time-history studies of the elastic and inelastic responses of diaphragms indicated that the hazard analysis of the diaphragm response should not utilize usual demand-capacity relationships based on probable elastic response and elastic load capacities. A plot of acceptable relative displacement control parameters (Figure 3) was developed for seismic hazard zones

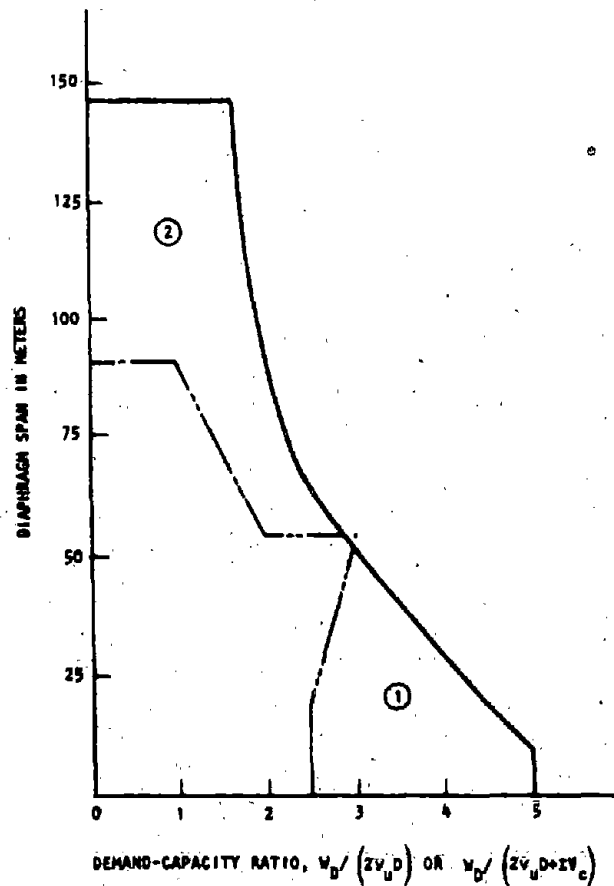


Figure 3. Acceptable Span for Diaphragms
(Based on Displacement Control Concepts)

of EPA = 0.4 g. This recommendation recognizes that crosswalls may be used for displacement control by use of the calculation of the demand-capacity ratio as

$$\frac{W_D}{2 v_u D + \sum V_c}$$

where

W_D = Total weight tributary to the diaphragm

v_u = Yield capacity of the diaphragm

D = Diaphragm depth

V_c = Total yield capacity of crosswalls

Studies of the amplification of the seismic hazard design velocities determined that diaphragms with large demand-capacity ratios (in excess of 2.5 for spans of 18 meters or more and 3.0 for a span of 54 meters maximum, region 1 of Figure 3) have a limited amplification of input velocities. For region (1) of Figure 3, the predicted amplification of the diaphragm may be taken as not greater than 1-3/4 times the design ground motion velocities. In region 2, time-history studies based on recorded ground motion scaled to an EPA of 0.4 g determined that crosswalls with a yield capacity of not less than 30% of the diaphragm capacity, $v_u \cdot D$, and spaced not more than 12 meters along the diaphragm length can also limit the diaphragm amplification factor to 1-3/4. These recommendations are fully described in the commentary in ABK-TR-08 (1984) and ABK-TR-06 (1984).

Figure 3 and the described crosswall criteria for limiting amplification of design ground motions is only applicable to a seismic hazard zone of EPA = 0.4 g. The dynamic testing and its interpretation indicates that dynamic instability of anchored URM walls with H/T ratios that are common to existing buildings is improbable in lesser EPA hazard zones. An exception to this is described for the seismic hazard zone of EPA = 0.2 g in ABK-TR-08 (1984), which describes a method of determination of acceptable H/T ratios.

RECOMMENDATIONS FOR USE OF DYNAMIC STABILITY CONCEPTS

The methodology, ABK-TR-08 (1984), recommends an upper limit of acceptable H/T ratios for URM walls in the seismic hazard zone of EPA = 0.4 g. Table 1 uses descriptive terms to define the relationship of the wall to the parameters that affect the prediction of dynamic stability. These parameters are:

- Overburden-Wall Weight (O/W) ratios
- SRSS of the input velocities to the top and bottom of the wall
- Height-thickness (H/T) ratios

Table 1. Allowable Height/Thickness Ratios of URM Walls with Minimum Quality Mortar

	Building with Crosswalls	All Other Buildings
Walls of one-story building	20	14
First story walls of multi-story buildings	20	20
Walls in top story of multi-story buildings	14	9
All other walls	20	15

These recommended allowable H/T ratios are related to Figure 2 by categorization of stability parameters as:

- $O/W = 0$ for single and top story walls
- $O/W = 0.5$ for all other walls
- Design ground motion for EPA = 0.4 g is 0.3 m/sec
- Amplification of design ground motions at the upper (roof) level is 2
- Amplification of design ground motion at floor levels is 2-1/4
- Peak velocities are assumed to be in phase
- Plots of dynamic stability using a 98% probability of survival were used to determine allowable H/T ratios

The effects of vertical ground motion were not considered to have a significant influence on the dynamic stability predictions for URM walls. If the soils under a URM building are modeled as an elastoplastic compression only medium, the recorded free-field vertical ground motions are modified and acceleration peaks are attenuated. The frequency band of vertical motions is not in the critical frequency band of horizontal ground motions. The effect of high frequency vertical motions on the restoring moments, Figure 1, does not result in a bias of increasing or reducing the restoring moments, due to the significantly lower frequency of instability excursions, especially as the relative excursion of the center part of the wall approaches instability. The design diaphragm excitation also assumed the URM shear walls were rigid bodies to transmit ground excitation to the diaphragm ends. For solid URM walls on property lines this assumption is valid, but modification of peak horizontal ground motion values by inelastic shear coupling in the soil medium is probable. The probability of vertical ground motion influencing the prediction of dynamic stability of URM walls shaken in their out-of-plane direction is smaller than the probability introduced by categorization of the critical parameters that were used for preparation of Table 1.

ACKNOWLEDGEMENT

This research was conducted by ABK, A Joint Venture, for the National Science Foundation under Contract No. NSF-C-PFR-78-19200 and Grant No. CEE-8100532. The Joint Venture, ABK, consists of three firms, Agbabian ASSociates, S.B. Barnes & Associates, and Kariotis & Associates, all in the Los Angeles area. The principal investigators for the three firms are R.D. Ewing, A.W. Johnson, and J.C. Kariotis, respectively. Dr. J.B. Scalzi served as Technical Director of this project for the National Science Foundation and maintained scientific and technical liaison with the joint venture throughout all phases of the research program. His contributions and support are greatly appreciated.

REFERENCES

1. ABK, A Joint Venture, Methodology for Mitigation of Seismic Hazards in Existing Unreinforced Masonry Buildings: Seismic Input, ABK-TR-02, El Segundo, California, USA, 1981.
2. ABK, A Joint Venture, Methodology for Mitigation of Seismic Hazards in Existing Unreinforced Masonry Buildings: Diaphragm Testing, ABK-TR-03, El Segundo, California, USA, 1981.
3. ABK, A Joint Venture, Methodology for Mitigation of Seismic Hazards in Existing Unreinforced Masonry Buildings: Wall Testing Out-of-Plane, ABK-TR-04, El Segundo, California, USA, 1981.
4. ABK, A Joint Venture, Methodology for Mitigation of Seismic Hazards in Existing Unreinforced Masonry Buildings: Interpretation of Diaphragm Tests, ABK-TR-05, El Segundo, California, USA, 1984.
5. ABK, A Joint Venture, Methodology for Mitigation of Seismic Hazards in Existing Unreinforced Masonry Buildings: Interpretation of Wall Tests, Out-of-Plane, ABK-TR-06, El Segundo, California, USA, 1984.
6. ABK, A Joint Venture, Methodology for Mitigation of Seismic Hazards in Existing Unreinforced Masonry Buildings: The Methodology ABK-TR-08, El Segundo, California, USA, 1984.
7. Applied Technology Council (ATC), Tentative Provisions for the Development of Seismic Regulations for Buildings, ATC 3-06, Palo Alto, California, USA, 1978.

PREDICTION OF DAMAGE TO BRICK BUILDINGS IN CITIES IN CHINA

Yang Yucheng, Yang Liu

SUMMARY

Based on the reference (5) and (6), a method of predicting damage to brick buildings in the whole city is developed further. Macroscopic prediction of damage, prediction of damage probability and prediction of high risk region and high risk type of building is included in this paper.

Probability of damage to multistory brick buildings designed according to current seismic code is predicted for different intensity in this paper, and it is pointed out that brick building satisfied basic design requirement of seismic code will mostly be slight or medium damage when intensity of potential earthquake is design intensity, but collapse will scarcely occur when intensity of potential earthquake is one grade higher than design intensity.

INTRODUCTION

In the 1960s-70s, the economic loss and people casualty in cities amount to nearly 85% and 90% of the total separately during earthquakes in China. Most of the buildings are brick construction in these cities, and hence, damage and collapse of brick buildings caused a huge disaster. Only in the City of Tangshan, 933 multistory brick buildings had collapsed and number tens of thousands of people had died during that earthquake. At present and even before 2000 brick buildings will be still the most important type of building in Chinese cities. Therefore, earthquake damage and damage prediction of brick building is matter of great importance for mitigation of earthquake disaster in cities.

For brick building, earthquake damage survey, test and measurement of model or prototype, aseismic design and aseismic evaluation, prediction of damage and study on countermeasure of mitigation of disaster has been paid great attention all along at IEM. After Tangshan Earthquake, we made up systematic summation about

* Institute of Engineering Mechanics, State Seismological Bureau, Harbin, China.

appearances of damage and aseismic experiences of multistory brick building (Ref.1,2) and through statistical analysis of earthquake damage to over 7000 multistory brick building undergone attack of different earthquake intensity and contrasting relationships between damage with strength in over 70000 wall pieces from almost 1000 floors of more than 400 buildings (Ref.3,4) a method of damage prediction of existing multistory brick building and had been developed (Ref.5,6). Afterwards potential damage to buildings had been predicted one by one in a zone of about two square kilometres in Anyang City, Henan Province in 1980 (Ref.7;8,9). At present the method has been Applied in more than ten cities to damage prediction or aseismic design(Ref.10).

In order to suit the needs of urban planning of against earthquake and prevent disaster, a study on prediction of damage to existing brick buildings and other types of building of the whole city is carrying out. The method of prediction damage and predicting damage probability of multistory brick building designed according to seismic code is illustrated in this paper.

The study is a section of PRC-US cooperation project "Risk Analysis and Seismic Safety of Existing Structures", and sponsored by the Join Seismological Science Foundation.

SOME KEY LINKS IN SEISMIC RISK MITIGATION OF EXISTING BUILDING

Under normal conditions, the scheme of seismic risk mitigation of existing building consists of four key links, see Fig.1. Damage prediction is middle link in the block chart of seismic risk mitigation. Both first and second links consider possibility of potential seismic event and its influence degree. But so far as present science level, uncertainty of predicting seismic event on time, space and intensity is far more than that of predicting damage to existing building for given site and intensity. Therefore for potential various intensity to predict different damages to existing building is required. Afterwards, the cost and benefits analysis on different countermeasures against earthquake and prevent disaster is conducted for policymaker's decision.

According to the block chart, damage prediction is restricted by the link both front and back and so two requirements are considered.

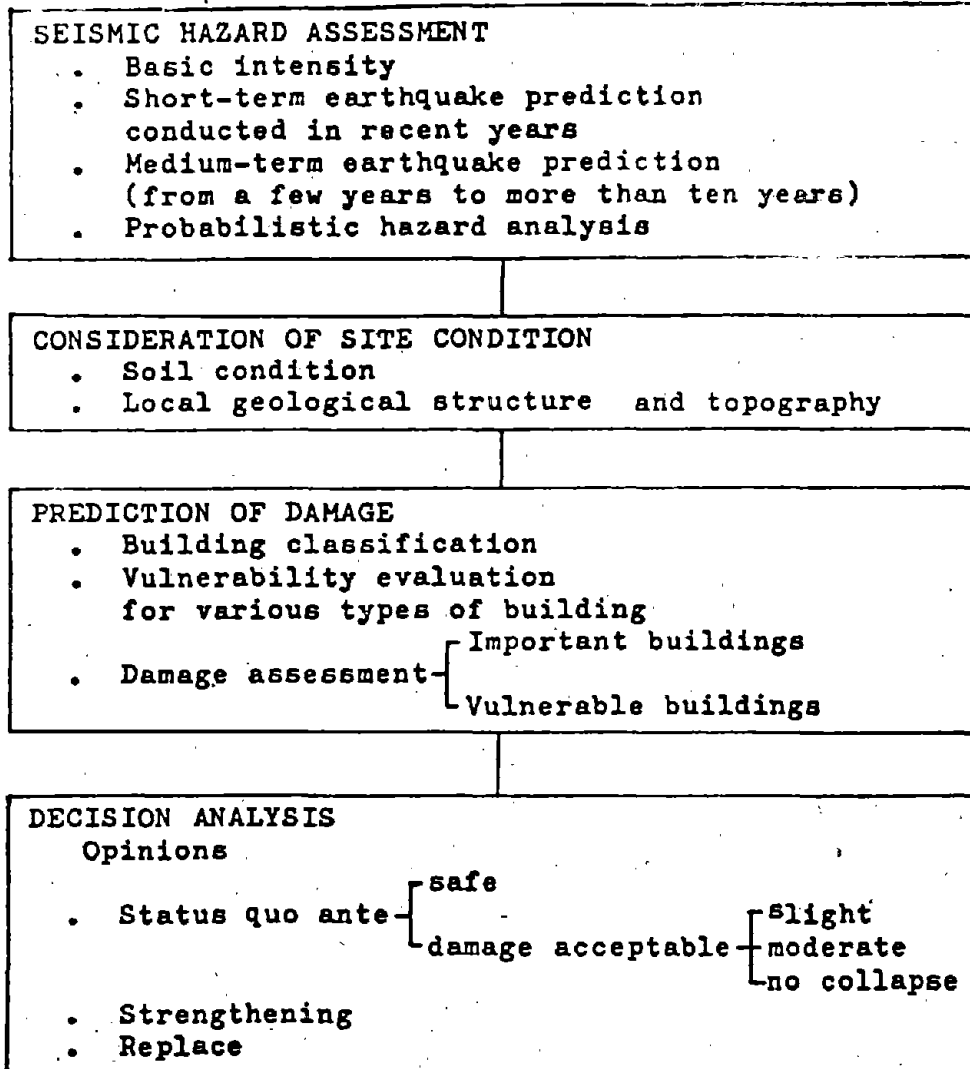


Fig.1 Scheme of seismic risk mitigation of existing buildings

(1) Due to the earthquake generating probability is very little but its uncertainty is great, consequently it is needful to predict damage to existing buildings for not only basic intensity but also lower intensity with greater probability and potential maximum intensity. In other words, in the whole city the result of damage prediction of existing building is a damage matrix which includes intensities, damage degree and probability or percentage and a set of map of predicting damage distribution in connection with site condition. That is necessary to decision analysis on seismic risk mitigation in the whole city.

(2) Sometimes it is probable that effect of different site condition on damage to building is evidenter than effect of different

buildings themselves, and so the site condition is considered seriously in prediction damage to existing buildings, particularly when we make use of past earthquake data and experiences. For example, if earthquake data of Tianjin City during Tangshan Earthquake and that of Yingkou City during Haicheng Earthquake are provided to Dalian, Yantai, Xiamen and other coastal city, it must pay attention that difference of some site condition are very great in these cities. Besides Mexico city, Tianjin city and Yingkou city are different in view of earthquake damage in the whole city, although they are all on soft ground. Therefore according to different site condition, to divide a city into some areas is required for damage prediction in the whole city.

BASIC IDEA ON DAMAGE PREDICTION OF EXISTING BUILDING IN CITY

In the whole city the prediction of earthquake damage to existing buildings includes two essential contents (classification of building and assessment of aseismic behaviour), in addition deals with three questions (estimation of casualty, economic loss and social impact). They make use of the research of seismic hazard analysis and microzonation. Result of prediction is used as identification of high risk region and high risk type of building, and as estimation of the total direct loss caused by damage to buildings for future potential earthquake. Outline of basic idea of damage prediction of existing building in the whole city is shown in Fig.2.

A lot of brick buildings may be divided into four major categories: multistory brick building, industrial brick building, large-span brick buildings and single story brick dwelling.

Predicting methods of various categories of brick building were considered, specially, the predicting method of multistory brick building has been applying extensively. Predicting damages to existing brick buildings groups were obtained according to statistical data of considerable macroscopic damages during destructive earthquakes in the 1960s-70s or to predict damage to buildings one by one in the last years. In order to suit the needs of damage prediction of considerable brick buildings in cities, at present, a method that classification and search by computer — sampling survey and discrimination by predictor — synthetical identification by computer is developing in the interest of predicting damage to existing building in the whole city for future potential earthquake.

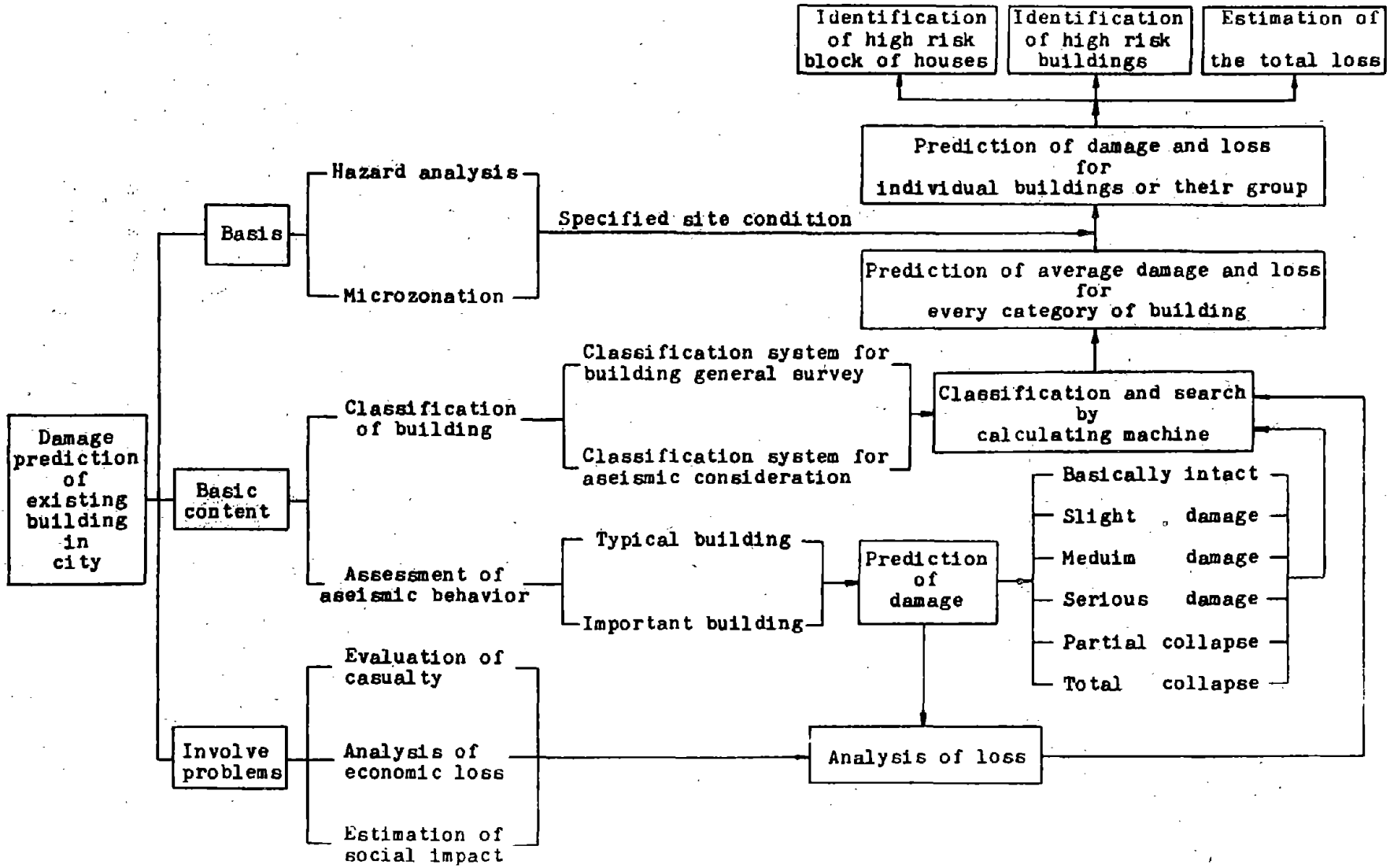


Fig.2 Block diagram for prediction of damage to existing buildings in the whole city

MACROSCOPIC PREDICTION OF DAMAGE DEGREE OF EXISTING BRICK BUILDING

Macroscopic qualitative prediction of damage degree of existing brick building for different intensities is approximately as follows:

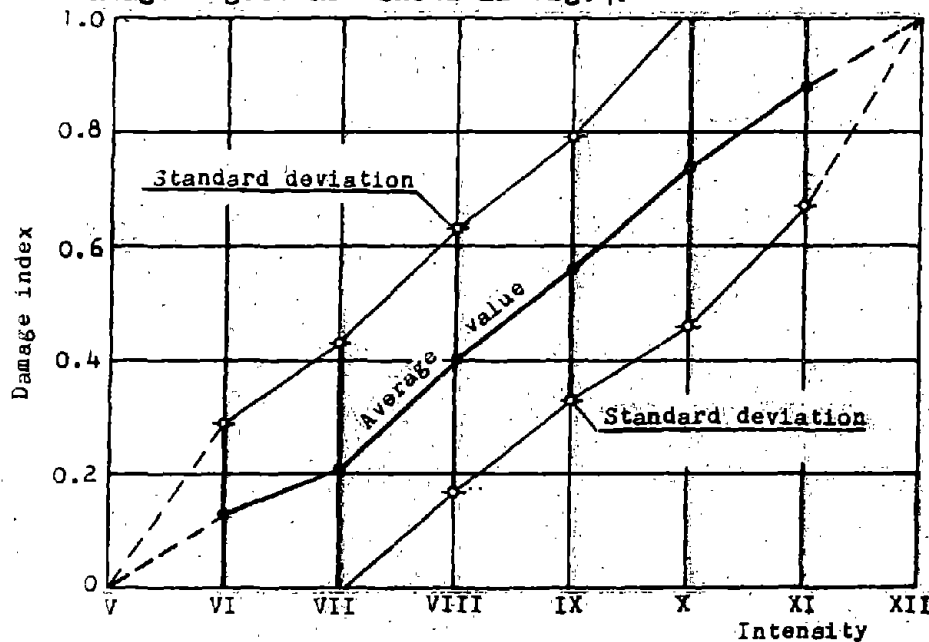
intensity VII — minority of buildings medium damaged, but majority of buildings basically intact or slightly damaged

intensity VIII — about half of buildings damaged and a few buildings collapsed

intensity IX — majority of buildings damaged, but minority collapsed and no damaged

intensity X — majority of buildings collapsed

In order to work out of urban planning of against earthquake and prevent disaster, macroscopic quantitative predicting damage to brick building in the whole city or a area where a few buildings is designed according to aseismic code may roughly adopt statistical data in past earthquake damage to various type of brick buildings. Such as according to statistical data of multistory brick building (more than 7000 buildings in 49 cities and towns or area) during six earthquakes, for various intensities average damage degree that be referred to as damage index is shown in Fig.3 and percentage of different damage degree are shown in Fig.4.



Note: Relation between the index and degree of damage

0 — basically intact	0.2 — Slight damage
0.4 — Medium damage	0.6 — Serious damage
0.8 — Partial collapse	1.0 — Total collapse

Fig.3 The damage index of multistory brick buildings for different intensity

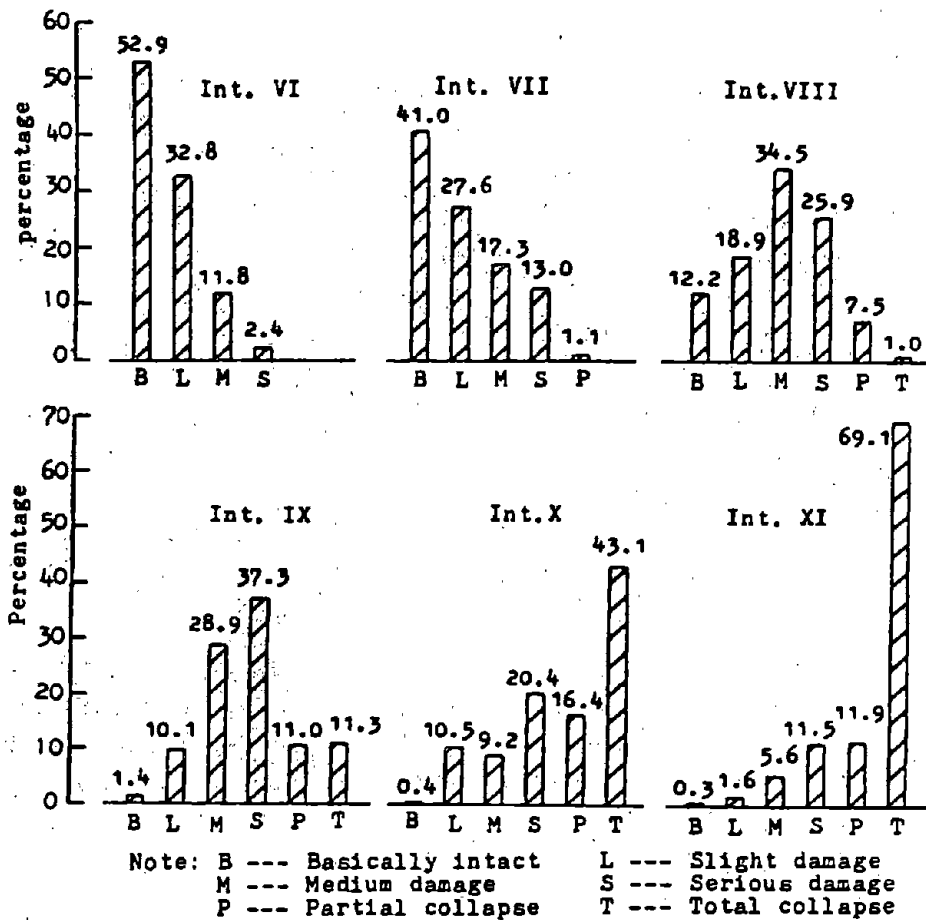


Fig.4 The damage distribution percentage of multistory brick buildings

If predicting damage make use of the two figures, the extent for multistory brick building will be controlled during future potential earthquake. But it must be admitted that variation from mean damage would be very big in the figures. Standard deviation of the predicting damages is one grade of damage degree in Fig.3 that is to say, namely average damage degree for intensity VIII is medium damage ($I=0.40$), upper limit of damage degree exceeds serious damage ($I=0.4+0.23=0.63$), lower limit is less than slight damage ($I=0.4-0.23=0.17$). So such it is required that predictor have abundant experiences of engineering and knowledge earthquake damage as well as ability to judge deviation degree of macroscopic damage from average index for the city or area. Fig.4 also shows that distribution of damage degree is very wide for intensity VIII, IX which damage to brick building will be probable from basically intact to collapse. Of course two things account for the occurrence, on the one hand evaluation of intensity is treated as a average of damage, on the other hand difference of buildings themselves is a essential

factor for different damage on identical site. In all cases, distinguishing damage degree of different existing buildings is exactly the basic task of damage prediction. In order to prediction of damage to existing building in a specified city, a rational classification of buildings is required, as a consequence, predicting average damage degree of subcategory of building so that the variation of the damages becomes as small as possible. To make macroscopic quantitative prediction of damage to multistory brick building, if the buildings are redivided into some subcategories, the variation of average damage index of each subcategory will reduce obviously. detailed level of classification depends on purpose and demand of prediction. In any wise, effect of site condition on damage degree must be estimate enough.

PREDICTION OF DAMAGE PROBABILITY OF BRICK BUILDING

Considerable earthquake experiences indicate that earthquake damage to rigid brick building depends mainly on strength of wall. According to statistical relationships between strength of wall with earthquake damage during past earthquakes, the aseismic coefficient K_{ij} of the j th brick wall element on the i th floor and the average aseismic coefficient K_i of brick walls on the i th floor is used as a main criterion for the predicting cracked and collapsed of such building. The method of prediction damage that is considered as a definite discrimination criterion had been developed and applied, see reference (5), (6), (7), (8) and (9). For the good of macroscopic prediction and probability analysis, the relationship of aseismic strength to damaged (cracked or collapsed) probability for multistory brick building is drawn in Fig. 5 and Fig. 6 respectively. In the two figures, the deviation that average damage index of samples calculating aseismic coefficient from the total average damage index of all samples for various intensity in Fig. 3 had been considered. The regulative coefficient of the damage probability is 1.05 for intensity IX and 0.89 for intensity X. To predict probability of damage to existing or being designed multistory brick building may make use of Fig. 5 and Fig. 6. In the former case with definitive discriminating criterion, the damage probability is 30%, 40% and 50% for intensity VII, VIII and IX respectively in Fig. 5, and the collapse probability is all about 50% for intensity VIII, IX and X respectively in Fig. 6.

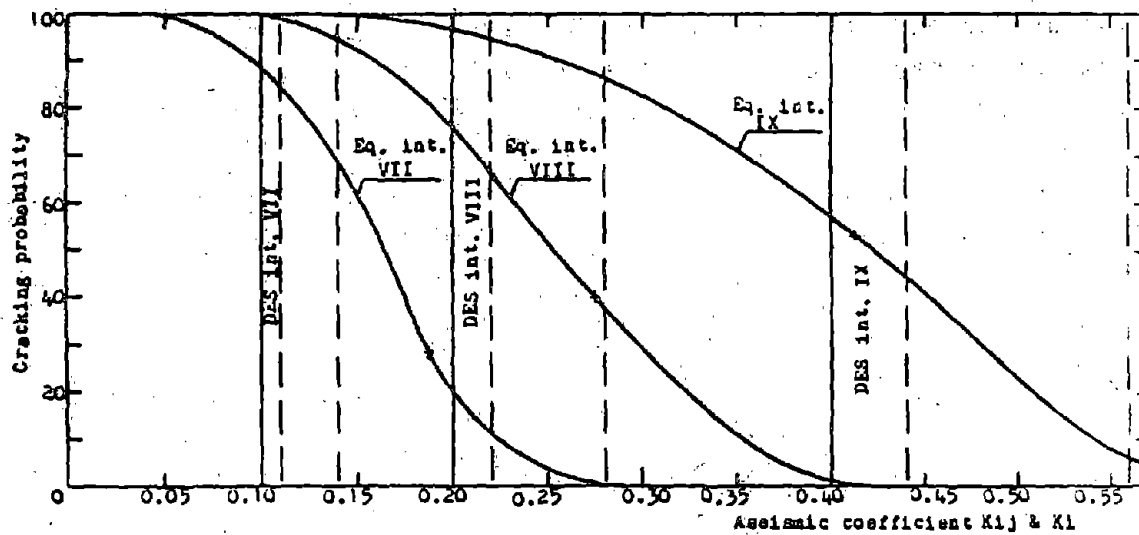


Fig. 5 The damage (cracking) probability of multistory brick buildings for different earthquake intensity

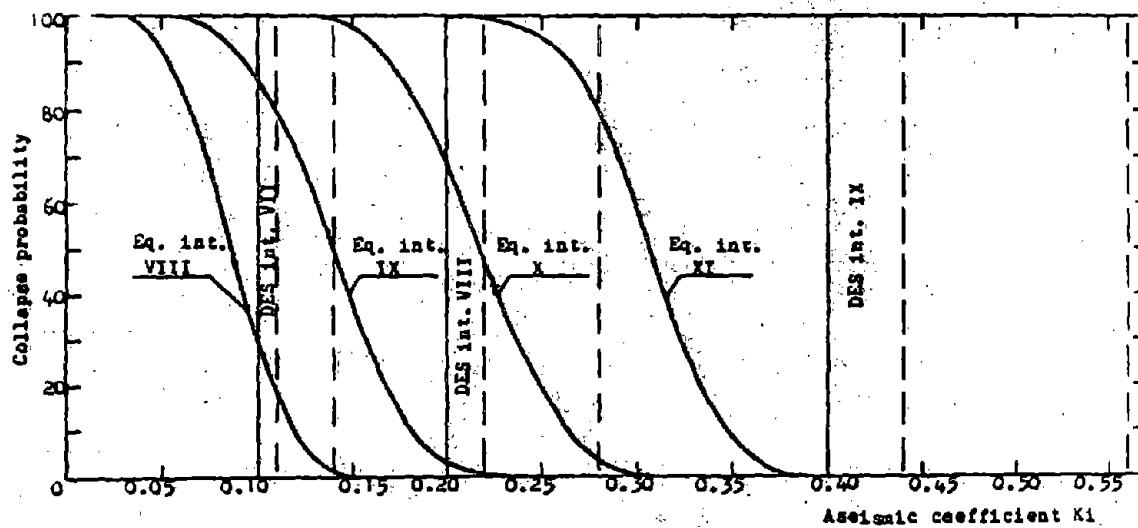


Fig. 6 The collapse probability of multistory brick buildings for different earthquake intensity

For example, predicting damage probability of brick building designing according to current aseismic code (TJ11-78) will be dealt with below. The limit values of aseismic coefficient of the weakest wall element of brick building for different intensity are marked in Fig.5 and Fig.6. For intensity VII, VIII, and IX they are 0.1, 0.2 and 0.4 respectively. Simultaneously the extent of average aseismic coefficient of brick walls on the weakest floor is marked too. In general, the coefficient of the weakest wall element is about 0.7—0.9 times of the average aseismic coefficient of the floor namely:

$$K_i = \frac{m}{\sum_{j=1}^m \frac{1}{K_{ij}}} = (1.1 \text{—} 1.4)(K_{ij})_{\min}$$

where m is number of wall element on the i th floor in transversal or longitudinal direction. For multistory brick building provided the lowest strength level by aseismic code, the damage probabilities that are found up from Fig.5 and Fig.6 are listed in Tab.1. If so the damage probability of multistory brick building satisfied with aseismic code is not greater than that value. When multistory brick building with R.C. constructive columns and other measures is built according to aseismic code, predicting damage probabilities, 3-story and 6-story residence is used as example, are listed in Tab.2. Here both ratios between area of transversal wall or longitudinal wall and area of floor of the building are all 0.0722, grade of mortar of wall masonry in every floor is listed in the table too. In 6-story brick residence for design intensity VIII, R.C. constructive columns are installed at corners of exterior wall and conjunction between interior and exterior walls, strengthening coefficient of the constructive column is taken 1.1 and 1.3 for cracked (slightly or medium damaged) resistance and seriously damaged or collapsed resistance respectively. The damage probabilities of Liaoning province 78-2-I-type and Beijing 80-2-type 6-story residence for design intensity VII and VIII respectively, if built on second type of soil, are listed in Tab.2 too.

Aforementioned results of predicting damage indicate that most of multistory brick building satisfied with lower limit of aseismic code, when subjected to a earthquake of design intensity, will cracks at weak wall elements. In other words, for such buildings designed according to the aseismic code, majority is not intact but medium damage or slight damage, and needs repairing. However when subjected

to a earthquake intensity is one grade higher than design intensity. in general, such buildings will not collapse; when that is one grade lower than design intensity, such buildings will be seldom cracked.

For model multistory brick buildings the aseismic coefficient is listed in Tab.3, where the original data of model buildings see reference (2), (12) and (13). According to such coefficient, predicting damage probability to list in Tab.1 and 2 was found up on Fig.3 and Fig.4.

Tab.1 Predicting limited value of damage probability of multistory brick buildings designed according to aseismic code(take no account of R.C. column)

Prediction intensity	Degree of damage	Design intensity		
		VII	VIII	IX
VII	Slight damage	88	20	0
	Medium damage	69- 84	1-11	0
	Serious damage	7-32	0	0
VIII	Slight damage	99	76	2
	Medinm damage	95-98	37-67	0
	Serious damage	60-83	0-7	0
	Collapse	1-17	0	0
IX	Slight damage	100	97	57
	Medium damage	99-100	86-94	6-44
	Serious damage	93-98	36-67	0
	Collapse	48-79	0-1	0
X	Collapse	99-100	3-47	0
XI	Collapse	100	80-99	0

Note: Slight damage — Cracking of wall element with minimum aseismic strength
 Medium damage — Cracking of more than half wall elements in minimum aseismic strength floor
 Serious damage— According to a criterion in reference (6) Tab.2

Tab.2 Prediction of damage probability of some model multistory brick buildings designed according to aseismic code

Prediction intensity	Degree of damage	Design intensity						
		VII			VIII			IX
		3-story	6-story	liaoning 78-2-1	3-story	6-story	Beijing 80-2	3-story
VII	Slight damage	27	72	87	13	20	/	0
	Medium damage	2	30	64	0	1	23	0
	Serious damage	0	2	7	0	0	0	0
VIII	Slight damage	80	96	99	69	76	/	20
	Medium damage	45	82	93	29	38	78	0
	Serious damage	5	45	60	0	0	10	0
	Partial collapse	0	0	<1	0	0	0	0
	Total collapse	0	0	0	0	0	0	0
IX	Slight damage	98	100	100	95	97	/	77
	Medium damage	88	98	99	82	86	97	39
	Serious damage	65	89	93	41	44	70	3
	Partial collapse	0	8	41	0	0	<1	0
	Total collapse	0	4	3	0	0	0	0
X	Partial collapse	9	80	98	<1	0	37	0
	Total collapse	3	73	68	0	0	2	0
XI	Partial collapse	91	100	100	58	23	98	0
	Total collapse	80	100	100	38	12	76	0
Mortar grade	6-floor		25	25		50	50	
	5-floor		25	25		50	50	
	4-floor		25	25		50	50	
	3-floor	25	50	50	25	100	75	50
	2-floor	25	50	50	25	100	100	75
	1-floor	25	50	50	50	100	100	100

IV-2-12

Tab.3 The aseismic coefficient of predicting damage to multistory brick buildings

Design intensity	Model building	Predicting degree of damage				
		Slight damage	Medium damage	Serious damage	Partial collapse	Total collapse
		(K _i) _{min}	(K _i) _{min}	(K _i) _{min} /0.6 or (K _i)/(.7—.9)	non-bearing (K _i) _{min}	bearing (K _i) _{min}
VII	TJ11-78	0.10	0.11-0.14	0.183-0.233	0.11-0.14	0.11-0.14
	3-story	0.189	0.264	0.376	0.264	0.281
	6-story	0.132	0.185	0.266	0.185	0.196
	Liaoning 78-2-1	0.104	0.145	0.233	0.145	0.201
VIII	TJ11-78	0.20	0.22-0.28	0.367-0.467	0.22-0.28	0.22-0.28
	3-story	0.215	0.301	0.450	0.301	0.315
	6-story	0.199	0.278	0.439	0.329	0.343
	Beijing 80-2		0.195	0.356	0.230	0.285
IX	TJ11-78	0.40	0.44-0.56	0.733-0.933	0.44-0.56	0.44-0.56
	3-story	0.326	0.457	0.601	0.456	0.471

PREDICTION OF HIGH RISK REGION AND HIGH RISK TYPE OF BUILDING

At present, predicting high risk region and high risk type of existing building in the whole city are developing. According to block chart (Fig.2) predicting process is roughly as follows.

1. Set up Data Bank of Existing Buildings On the basis of data of general survey of buildings and/or of appropriate supplement, some informations of building related to damage prediction are inputted into computer. The informations are not more than following fifteen items: (1) ordinal number of building, (2) the number of block of houses, (3) location of the building at state coordinate system, (4) the number of story, (5) built age, (6) building area, (7) architectural construction, (8) present use, (9) quality of building, (10) unfavourable factor, (11) strengthening measure, (12) the number of person in building by day, (13) the number of person in building at night, (14) worth of building at present, (15) worth of property in building.

2. Classification and Search by Computer According to (4), (5), (6), (7) and (8) items in data bank, in the whole city all buildings are classified by computer and the total amount of detailed categories, its code name, area of building, the number of person, worth and property for every gategory of building are listed.

3. Mergeing Categories of Building by Computer Based on experience, predictor determines some plans of classification and instructs computer to merge categories. Then new code name and the number of the categories of building are re-listed. Predictor selects one or some plans of classification of existing buildings for prediction.

4. Sampling Survey and Predicting Damage to Individual Building Predictor surveies various category of building by sampling, assesses aseismic behavior of sampling buildings and predicts damage to individual building. Predicting results are inputted into data bank of computer.

5. Predicting Average Damage to Various Category Building Taking second type of soil or a soil distributed the most extensively in the city as the base of site condition, average damage index of various category of building for potential different intensity is outputted.

6. Predicting Damage to Individual Building or/and Building Group
Based on the research result of seismic hazard analysis and microzonation as well as (9), (10) and (11) items in data bank, damage to individual building for various category is predicted. Then damage to building group is predicted block by block and category by category.

7. Identification of High Risk Block of Houses and High Risk Category of Building On the basis of one or some predicting plans and through comparison of damage degrees among blocks of houses and among categories of building, high risk region (one or some block of houses) and high risk type (one or some category of building) will be identified in the whole city.

CONCLUSION

According to predicting information of The Ministry of Urban and Rural Construction and Environmental Protection(Ref.14), clay brick make up 93.22% of the total volume of product of various wall material for 1985, 76.4% for 1986-1990 and 50% for 1991-2000. Therefore brick building will be still the most main type of construction at present and in future half a century in chinese cities.

Both the earthquake experiences in the last twenty years and present study on damage prediction all indicate that aseismic behavior of existing and future newly built brick building is better than that of building built before thirty years, but failure probability of potential damage or collapse is very great yet. Therefore in future half a century earthquake damage to brick buildings with their disastrous results will still become one of the most serious natural hazards in city. In order to mitigation of seismic disaster, the aseismic behavior of brick building will be needs further increased and improved in China.

REFERENCES

- (1) Yang Yucheng, et al., The Summary of Damage to Multistory Brick Buildings in the Tangshan Earthquake and Engineering Analysis, IEM report No. 78-025, 1978.

- (2) Yang Yucheng, Yang Liu, Gao Yunxue, Earthquake Damage to Multi-story Brick Buildings and Their Design for Anti-cracking and Anti-collapse, Seismological Press. 1981.
- (3) Yang Yucheng, Yang Liu, Empirical Relationship Between Damage to Multistory Brick Building and Strength of walls During the Tangshan Earthquake, 7WCEE, Vol.6, pp501-508, 1980.
- (4) Yang Yucheng, et al., The Probability of Damage to Multistory Brick Buildings, Recent Development in Earthquake Engineering, No.4, 1984.
- (5) Yang Yucheng, et al., Method of Damage Prediction for Existing Multistory Brick Buildings and Its Reliability, Earthquake Engineering and Engineering Vibration, Vol. 2, No. 3, 1982.
- (6) Yang Yucheng, et al., Prediction of Earthquake Damage to Existing Brick Buildings in China, 8WCEE, Vol.1, PP401-408, 1984.
- (7) Yang Yucheng, et al., Prediction of Earthquake Damage to Existing Buildings in Anyang, Henan Province, A Collection of Papers of International Symposium on Continential Seismicity and Earthquake Prediction, Seismological Press, PP 828-838.
- (8) Yang Yucheng, et al., Prediction of Earthquake Damage to Multistory Brick Building in Beiguan Zone of Anyang City, North China Earthquake Sciences, Vol.1, No.3, 1983.
- (9) Yang Yucheng, et al., Prediction of Earthquake Damage to Existing Buildings in Anyang Zone of Yubei, Earthquake Engineering and Engineering Vibration, Vol. 5, No. 3, 1985.
- (10) Yang Yucheng, A General Account of Development in Research on Earthquake Damage Prediction in China, World Information on Earthquake Engineering, No. 4, 1985.
- (11) Aseismic Design Code for Industrial and Civil Buildings (TJ11-78)
- (12) Chen Jinhua, Yang Liu, et al., Assessment of Aseismic Behavior and Damage Prediction of Typical Multistoty Brick Residence in Three Cities in Liaoning Province, Proceedings of National Conference on Earthquake Engineering, 1984.
- (13) Gao Xiaowang, Zhou Bingzhang, et al., Reliability Analysis for Earthquake Resistance of Multistory Brick Buildings, Institute of Earthquake Engineering, Chinese Academy of Building Research, report, 1984.
- (14) Predicting Information on Construction Industry for "The Seventh Five-Year" and Later Ten Years, Construction Technic, No.2, 1986.

A METHOD FOR EARTHQUAKE DAMAGE EVALUATION
OF SINGLE-STORY FACTORY BUILDINGS

Yin Zhi Qian^I, Li Shu Zhen^{II}, Yang Shu Wen^{III}

ABSTRACT

In this paper, according to experience of Haichang and Tangshan earthquakes, the following problems were studied.

- (1) Classification method of buildings damaged from earthquakes.
- (2) Parameters of influence on earthquake damage to R. C. single-story factory building and relation between the parameters and damage ranks.
- (3) Calculating method of earthquake damage ranks of a existing R. C. single-story factory building.

I. INTRODUCTION

Human casualties and economical loss during an earthquake are caused mainly by collapse of buildings. Therefore, to prevent collapse of buildings and to lay down program for prevention disaster in a city are main measures for alleviating earthquake disaster. Both to improve aseismic design of newly-built buildings and to strengthen existing buildings in earthquake zones are important steps for preventing collapse of buildings. So it is necessary to assess aseismic capacity of existing buildings.

In the past few years, most of the factory buildings suffered earthquake damage were not designed for earthquake resistance. There are a number of such factory buildings in earthquake zones as yet in China. In order to provide scientific basis for aseismic strengthening of existing buildings and to take urban precaution against disaster program, the aseismic capacity of those buildings should be assessed. In this study, a method for calculating damage level of existing single-story R. C. factory building is developed based on earthquake damage data Fig. 1 of Haichang and Tangshan earthquakes.

II. CLASSIFICATION METHOD OF DAMAGE OF BUILDING

To date, the available method for evaluating structural damage may generally be divided into two kinds. The first kind of method belongs to experiential, in which a relation is given between intensity and damage level of buildings based on historical data from earthquake damage. The second kind of method belongs to theoretical,

I. Associate Res. Pro. II. Research Associate III. Engineer,
Institute of Engineering Mechanics, State Seismological Bureau.

in which a relation is established between ground motion and damage level of building based on calculated response of building by forecasted ground motion, whatever method is used, it is necessary to define the damage of buildings. Generally, there are three types of definition for damage of building. The first one is numerical, the second one is given in terms of repair costs and the third one is verbal. The verbal classification for damage of building usually used in China is to classify the damage into five ranks as following; (1) collapse, (2) severe damage, (3) moderate damage, (4) slight damage and (5) no damage. Similar classification has been used in this paper, and a numeral called damage index is bestowed on each damage rank. but here the term "destruction" is used instead of collapse, because the meaning of "collapse" is not clear as sometimes both the roof of building to fall down and the whole building to collapse are called collapse. "destruction" is defined as that the building has lost its function and can not be repaired.

In this study, a factory building is divided into three parts, i. e. structural members (such as columns), non-structural members (such as cladding walls) and roof system. The damage for each part is classified into five ranks, just the same as the buildings. When the damage rank of a factory building is judged, it is necessary to judge damage ranks of the three parts at first according to the table 1 and table 2, and then a damage index is bestowed on each damage rank. Due to the structural members, the non-structural members and roof system have different effect on factory building, a weight factor is bestowed on damage index of each kinds of members. then the damage index of a factory building takes the weighted sum of the damage index of these members as follows.

$$D_s = 0.45D_c + 0.30D_w + 0.25D_r \quad (1)$$

Where D_s — damage index of a factory building,
 D_c — damage index of the columns,
 D_w — damage index of the cladding walls,
 D_r — damage index of the roof system.

Classification of damage rank of factory buildings, columns, cladding walls and roof system with the corresponding damage indexes are listed in table 2. When the damage rank of a factory building is judged on a earthquake spot, the values of D_c , D_w and D_r in equation (1) must take the standard values in table 2. The damage rank of the factory building is determined according to D_s calculated from equation (1).

Example; Suppose a factory building suffered the attack of a 8 earthquake motion, and damaged, as follows, the columns are moderate damage, the cladding walls are severe damage and the roof system is

Damage Grade of Members

Table 1.

Members Grade	Damage state of R. C. members	Damage state of brick walls	Damage state of brick columns	Damage state of roof system and floor slabs
I	At the location of break; Reinforcements were bended. Core concrete were crushed Remarkable vertical and/or horizontal deformation occurred or have been broken off.	Many remarkable cracks occurred and nearly broken into pieces or have been collapsed.	Bricks at side were crushed and brick pieces fell down or have been toppled over.	Roof slabs (or floor slabs) fell or moved. trusses fell or inclined brace failed.
II	Surface layer of members fell apart and clear cracks occurred inside. Reinforcements were revealed and bended slightly.	Remarkable cracks or severe inclination occurred.	Bricks were crushed locally at side of column.	Roof slabs (or floor slabs) moved. Clear deformation occurred on braces
III	Clear cracks occurred on surface of members and reinforcements were revealed.	Clear cracks occurred.	Horizontal cracks occurred.	Roof slabs become less crowded. Visible deformation occurred on brace.
IV	Visible cracks occurred on surface of members.	Visible cracks occurred.	Visible cracks occurred.	Visible cracks occurred on roof slabs (or floor slabs).

slight damage. From table 2 the damage index of each member can be obtained as $D_0 = 0.4$, $D_V = 0.7$ and $D_R = 0.2$. Then we obtain the damage index of the factory building $D = 0.44^R$ from equation (1) and it is defined from table 2 that this building belongs to moderate damaged rank.

Rank of Damage of Building and Damage Index

Table 2.

Rank	Damage phenomena	Damage index	
		Standard value(D)	Limite of index
Destruction	Most of members was damage for grade I and II as defined in table 1. The building was close to collapse or had been collapsed. The function of design had been lost and the building can not be repaired.	1	$.85 < D \leq 1.0$
Severe damage	Most of member was damage for grade II and a few members for grade I. They are difficult to repair.	0.7	$.55 < D \leq .85$
Moderate damage	Some members were damage for grade III and few members for grade II which can be renewed its original design function.	0.4	$.3 < D \leq .55$
Slight damage	Some members were damage for grade IV and few members for grade III.	0.2	$.1 < D \leq .3$
No damage	Members were not damage or few members were damage for grade IV.	0.0	$0 \leq D \leq .1$

III. PARAMETERS OF INFLUENCE ON DAMAGE OF FACTORY BUILDING

Earthquake damage to a single-story R. C. factory building consists of three parts, as mentioned above. The first part comes from the damage of R. C. columns, the second part from that of cladding walls and the third part from that of room system. The parameters of influence on damage of the three parts will be discussed below.

1. RELATION BETWEEN DAMAGE AND BENDING INDEX OF COLUMNS

Frame is the main member of a single-story factory building for earthquake resistance. The cross section of columns is assumed to be

rectangular. Then the maximum earthquake stresses in columns depends on the bending index λ , defined as

$$\lambda_1 = \frac{WH_c}{b_c h^2} \quad (2)$$

Where W — weight loading on the top of column(kg),
 H_c — distance from low-boom to calculated section(cm),
 b_c — width of section of the column(cm),
 h — height of section of the column(cm).

If there are more than one roof supported on different height of a column. the bending index of column will be taken as

$$\lambda_1 = \frac{\sum W_i H_{oi}}{b_c h^2} \quad (3)$$

Where W_i — weight of the i th roof loading on the column,
 H_{oi} — distance from low-boom of the i th truss to calculating section.

The bending indexes were calculated based on more than 200 samples suffered attack from Haichang or Tangshan earthquake. Most of the calculated factory buildings are of two to four spans, and a few buildings are of one span or more than five spans. one frame was calculated in each factory building. Generally, the maximum earthquake stresses occurred at the foot or variable cross-section of columns. So the bending index of such sections were calculated. the values of total 750 λ_1 were obtained. The maximum λ_1 in each factory building is connected with the damage of columns as shown in Figs 2, 3 and 4. It may be seen from these figures that the larger the λ_1 is, the heavier the damage of column is, and the minor the earthquake intensity is, the larger the λ_1 is for the same damage level. This result shows that λ_1 is an important parameter to mark the aseismic capacity of a single-story factory building. Fig. 5 shows the relation between mean values of λ_1 and damage ranks. In addition, the strength of concrete is also an important parameter that influence the damage of columns. The relation between these parameters and damage index of column may express as follows

$$D_c = \beta_0 + \beta_1 R^{-1} + \beta_2 \lambda_1 \quad (4)$$

Where R is the strength of concrete,
 β_0 , β_1 , and β_2 are the coefficients of regression.

Based on the data mentioned above a regression analysis was completed and the results were obtained as follows.

$$\begin{aligned}
D_c &= 31.9R^{-1} + 0.004\lambda_1 - 0.457, \quad \text{for intensity VII.} \\
D_c &= 86.9R^{-1} + 0.004\lambda_1 - 0.52, \quad \text{for intensity VIII.} \\
D_c &= 68.0R^{-1} + 0.005\lambda_1 - 0.49, \quad \text{for intensity IX.} \\
D_c &= 164.4R^{-1} + 0.008\lambda_1 - 0.886, \quad \text{for intensity X.}
\end{aligned}
\tag{5}$$

2. RELATION BETWEEN DAMAGE AND HEIGHT INDEX OF CLADDING WALLS.

Cladding walls are not a load-bearing member in which only the constitution measures of earthquake resistance were taken. In past earthquakes the damage ratio of cladding walls is high. The data of earthquake damage indicate that the height-to-thick ratio and the number of spandrel beam have significant influence on earthquake damage to cladding wall. Here, a wall height index was defined as

$$\lambda_2 = \frac{H_w}{b_w \sqrt{S + 1}}
\tag{6}$$

Where H_w — the height of wall,
 b_w — the thick of wall,
 S — number of spandrel beams over the height of wall.

Figs 6, 7, 8, and 9 show the relation between λ_2 and damage of cladding walls based on the data of earthquake damage mentioned above. Fig. 10 shows the relation between the mean value of λ_2 and the damage ranks. It may be seen from these figures that the higher the wall is and the fewer the spandrel beam is, the heavier the damage is. So the relation between λ_2 and damage index may be expressed as follows.

$$D_w = \alpha_0 + \alpha_1 \lambda_2
\tag{7}$$

Where α_0 and α_1 are coefficients of regression.

Based on the data mentioned above, a regression analysis leads to the results as follows.

$$\begin{aligned}
D_w &= 0.036 \lambda_2 - 0.44, \quad \text{for intensity VII.} \\
D_w &= 0.037 \lambda_2 - 0.384, \quad \text{for intensity VIII.} \\
D_w &= 0.047 \lambda_2 - 0.499, \quad \text{for intensity IX.} \\
D_w &= 0.046 \lambda_2 - 0.352, \quad \text{for intensity X.}
\end{aligned}
\tag{8}$$

3. EARTHQUAKE DAMAGE TO ROOF SYSTEM

The earthquake damage ratio of the roof systems is also high in single-story factory buildings, especially for roof system with large prefabricated concrete slabs^[3]. Fig. 11 shows the earthquake damage ratio of the roof system of single-story factory buildings in Tangshan earthquake. The main causes for damage of roof system are (1) weak or no connection between large prefabricated concrete slabs and the trusses. So the relative displacement and sliding occurred between the trusses and roof slabs resulting in falling of the roof slabs, (2) poor integrity of bracings between trusses. when the building undergoes longitudinal vibration, the bracings lost its stability resulting in tilt of trusses or falling of roof system and (3) weak connection between the trusses and columns. The causes (1) and (3) are due to the poor quality of construction, the cause (2) is mainly due to the inadequacy of design. The influence of them on the earthquake damage can not be expressed by mathematical formula. However, according to the condition of existing buildings and experience of earthquake damage, the buildings can be classified into several cases (say four cases) and give a damage index to each case. as follows.

(i). When the quality of construction of the roof system is good and the bracing system is sound, the damage index may take a numeral as shown in table 3 for various intensities.

table 3.

intensity	7	8	9	10
damage index (D_r)	0	0.05	0.20	0.35

(ii). When the quality of construction of the roof system is good but the integrity of bracing system is poor, the damage index may take a numeral as shown in table 4 for various intensities.

table 4.

intensity	7	8	9	10
damage index (D_r)	0.05	0.15	0.35	0.45

(iii). When the quality of construction of the roof system is poor and the bracing system is sound, the damage index may take a numeral as shown table 5.

table 5.

intensity	7	8	9	10
damage index (D_r)	0.10	0.20	0.40	0.55

(iv). When the quality of construction of the roof system is poor and the integrity of bracing system is poor, the damage index may take a numeral as shown in table 6.

table 6.

intensity	7	8	9	10
damage index (D_r)	0.15	0.30	0.55	0.85

Here, the quality of construction of the roof system means whether the quality of connection between trusses and roof slabs, and between trusses and columns are good or poor. The integrity of bracing system means whether the design and construction of it is good or poor.

IV. DAMAGE INDEX OF FACTORY BUILDING

The damage indexes of column and cladding wall may be calculated from equations (5) and (8) and the damage index of the roof system may be taken from table 3-6. substituting the equations (5) and (8) into equation (1), the expressions for damage index of factory building is obtained;

$$\begin{aligned}
 D_s &= 14R^{-1} + 0.0018\lambda_1 + 0.011\lambda_2 - 0.338 + 0.25D_r, \text{ for intensity VII.} \\
 D_s &= 39R^{-1} + 0.002\lambda_1 + 0.011\lambda_2 - 0.349 + 0.25D_r, \text{ for intensity VIII.} \\
 D_s &= 31R^{-1} + 0.0023\lambda_1 + 0.014\lambda_2 - 0.370 + 0.25D_r, \text{ for intensity IX.} \\
 D_s &= 74R^{-1} + 0.0036\lambda_1 + 0.014\lambda_2 - 0.504 + 0.25D_r, \text{ for intensity X.}
 \end{aligned}
 \tag{9}$$

Where R — strength of concrete,
 λ_1 — bending index of column,
 λ_2 — height index of wall,
 D_r — damage index of roof system.

Knowing the geometric sizes of cladding walls and columns and the strength of concrete of the columns, the damage index of the factory

building can be calculated from equation (9), and then the damage rank of the factory building can be determined from table 2. In order to check the error of equation (9), 25 examples of factory building that suffered attack from Tangshan or Haichang earthquake were examined. Among them six buildings are in area of intensity X, one building is in area of intensity IX and eighteen buildings are in area of intensity VIII. The examined results are shown in Fig. 12. The points drawn on the 45 line are what the calculation agree with the macroscopic investigation. From Fig. 12 it may be seen that calculated results from equation (9) agree basically with macroscopic results. The merits of this method are simplicity and easy to know well.

REFERENCES

1. A.C.Boisonnade, H.C.Shah, Earthquake damage and loss estimation review of available methods. Proceedings of US-PRC Bilateral workshop on Earthquake Engineering, Harbin, China, 1982.
2. J.T.P.Yao, Damage assessment and reliability of existing buildings. Proceedings of The US-PRC Workshop on Seismic Analysis and Design of Reinforced Concrete Structures. 1981.
3. Yin Zhi Qian, Xiao Guang Xian, Li Shu Zhen, The damage phenomena and earthquake response analysis of single-story factory buildings in Haichang and Tangshan earthquakes. Earthquake Engineering and Engineering Vibration, 1980.

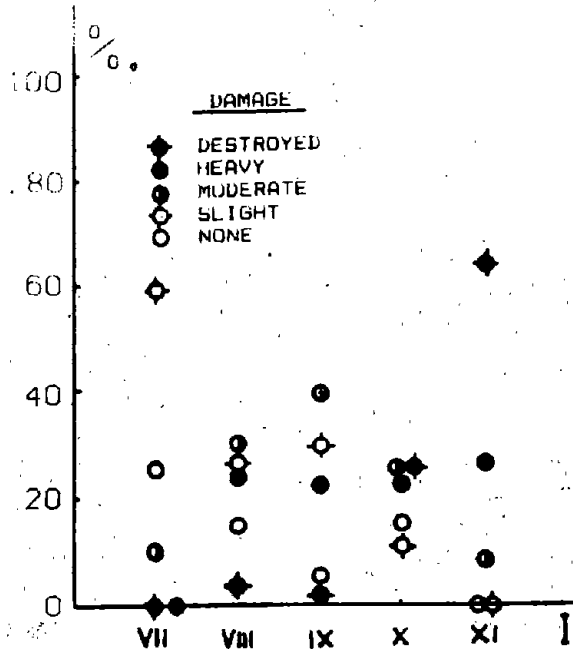


Fig. 1 Damage ratio of single-story factory buildings related to intensity.

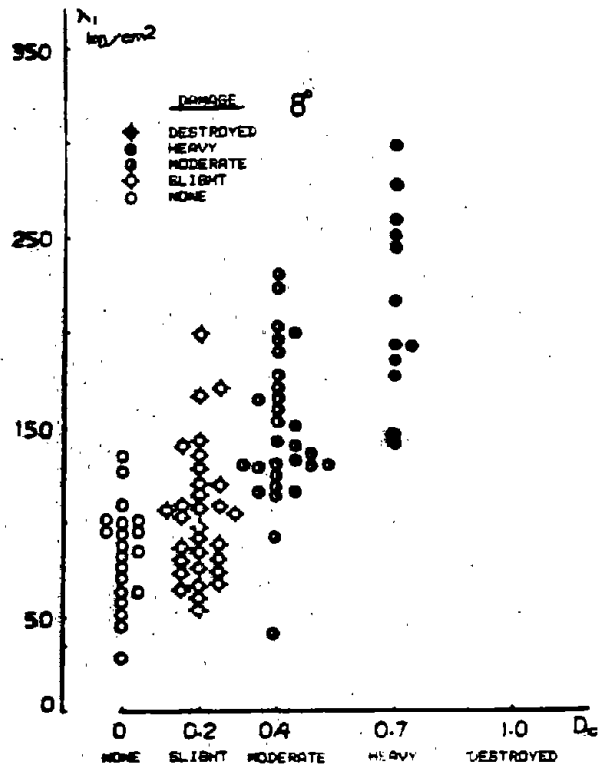


Fig. 2 Relation between λ_1 and damage rank.

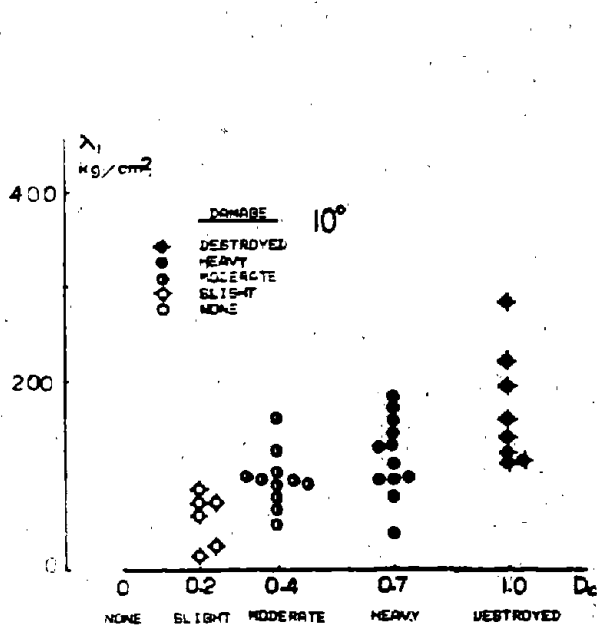


Fig. 3 Relation between λ_1 and damage rank.

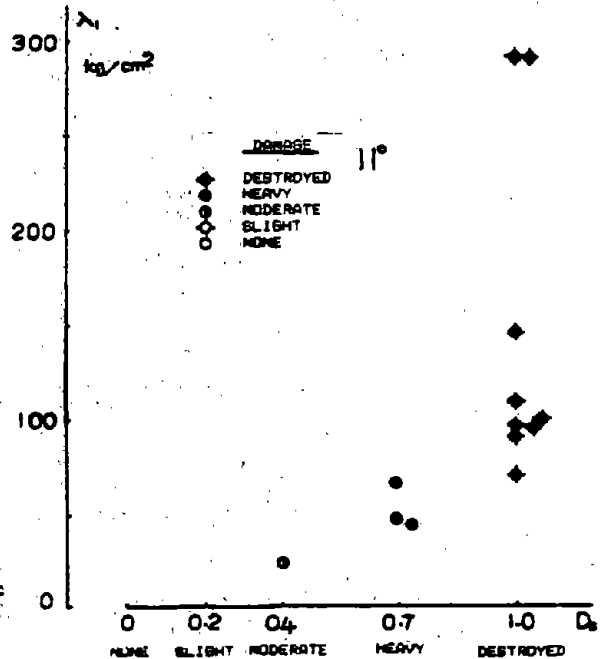


Fig. 4 Relation between λ_1 and damage rank.

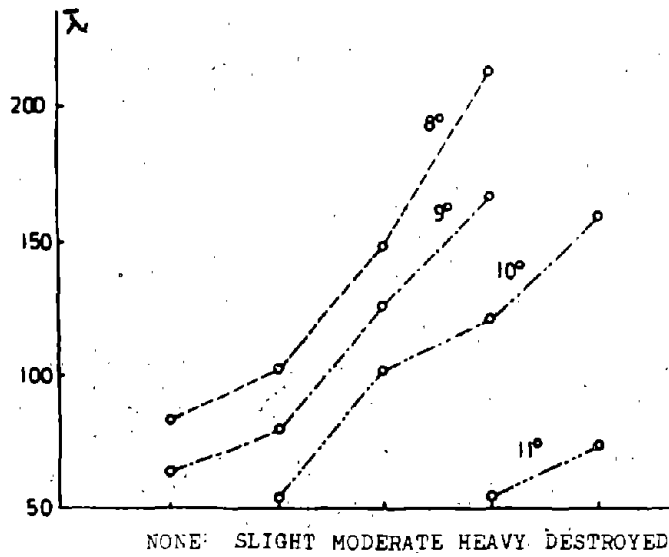


Fig.5 Relation between average of λ_1 and damage rank.

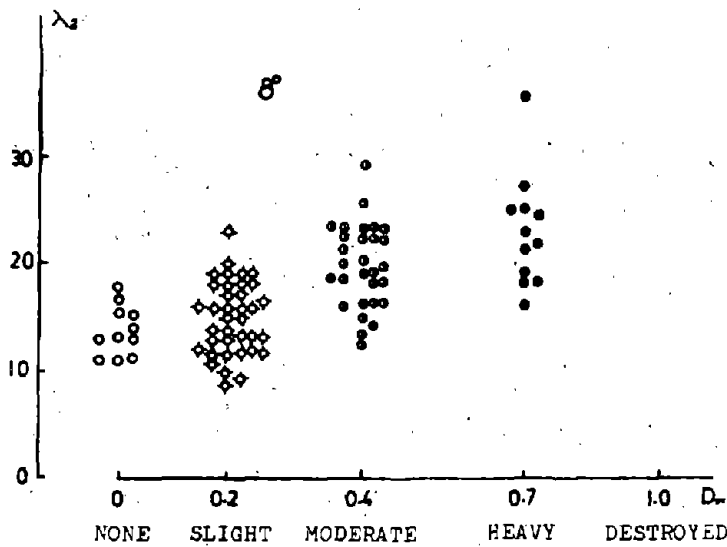


Fig.6 Relation between λ_2 damage rank.

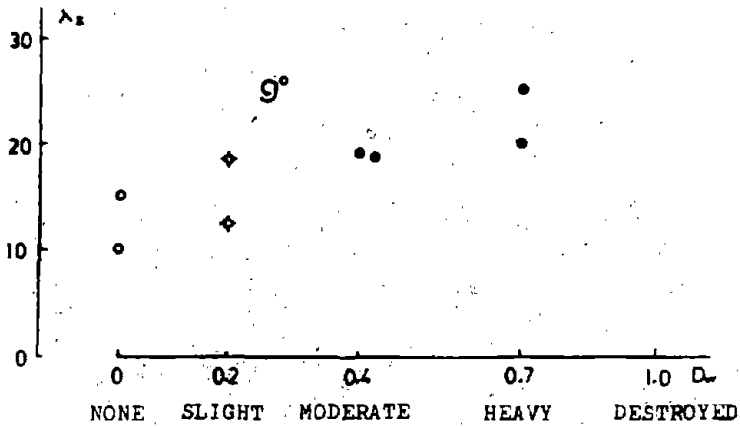


Fig.7 Relation between λ_2 and damage rank.

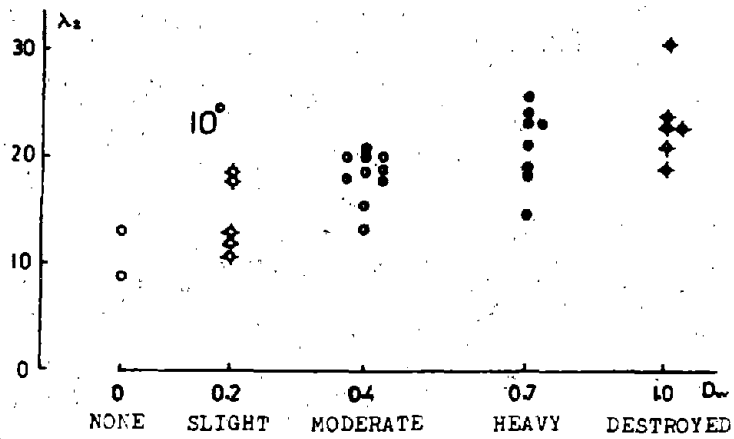


Fig.8 Relation between λ_2 and damage rank.

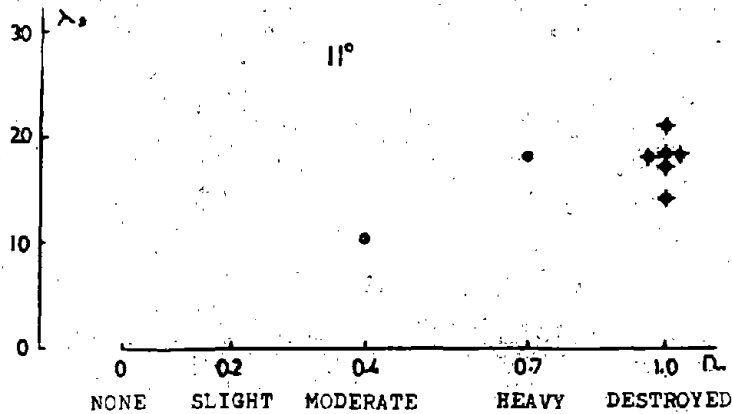


Fig.9 Relation between λ_2 and damage rank.

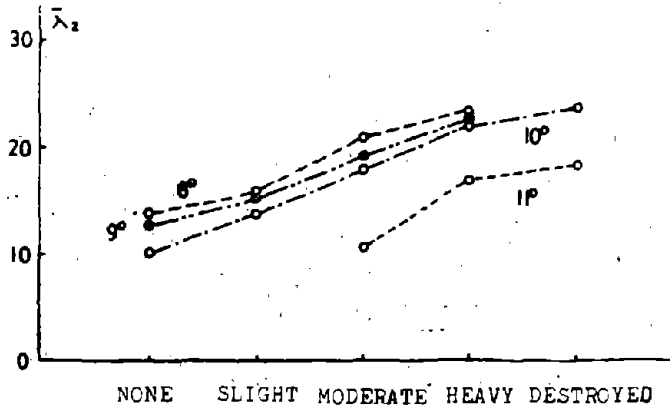


Fig.10 Relation between average of λ_2 and damage rank.

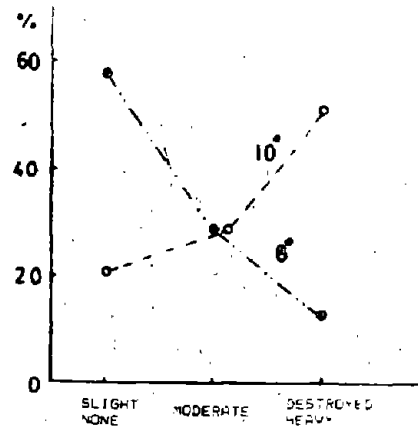


Fig.11 damage ratio of roof system.

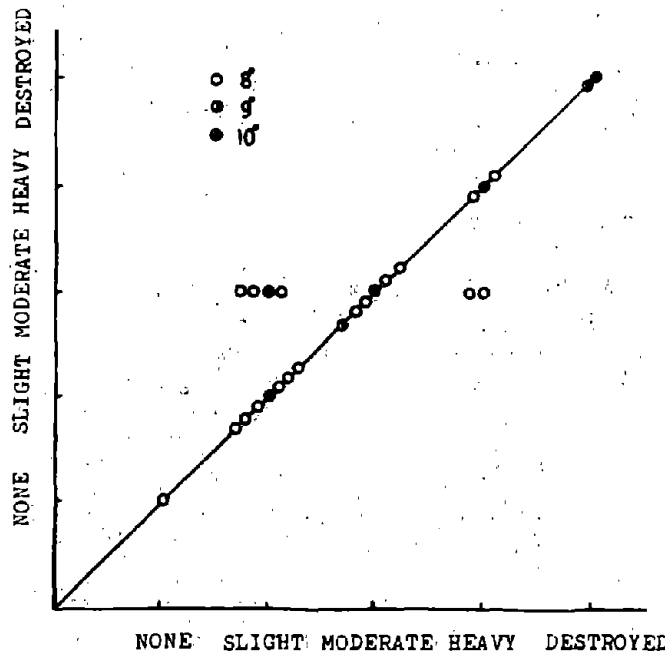


Fig.12 Comparison between calculated damage rank and damage rank of macroscopic investigation.

RELIABILITY CONCEPTS FOR EARTHQUAKE RESISTANT MASONRY

by

Gary C. Hart(I)

SUMMARY

The rational development earthquake resistant design criteria must utilize the concepts of reliability theory to define failure modes, quantify test data and analytical models, and establish design values for parameters that satisfy reasonable levels of safety and economy. This paper provides an indication of how reliability theory can be used in this development.

INTRODUCTION

An essential concept in structural design is to produce a structural system with sufficient capacity to resist the effects of the anticipated loads imposed on it during the life of the structure. Although this is a very straightforward concept, problems occur when one attempts to establish the magnitude of the "anticipated loads" for which the structure must be provided with "sufficient capacity" to resist. It appears, then, that there are two fundamental problems which must be resolved so that safe buildings may be constructed at economical costs: What are the anticipated loads, and how should the capacity of a structural member or system be established.

There is uncertainty associated with most aspects of the structural design and construction process. For example, structural engineers cannot establish with certainty the maximum loads to which a structure will be subjected during its life. Reinforcing steel is not placed exactly as shown on the construction documents. Structural engineers must design buildings in the face of this uncertainty and must do so with a final level of safety that is acceptable to society.

(I) Professor, Civil Engineering Department, University of California, Los Angeles and Principal, Englekirk and Hart, Inc., Los Angeles, California, USA

The incorporation of uncertainty in structural problems suggests the use of probability theory. It is clear, however, that it is not reasonable within today's level of practice to expect the designer to attempt to quantify the level of each source of uncertainty. Therefore, the development in the last decade of the probability-based limit state design (PBLSD) approach has been intended to be the rational vehicle for satisfying the requirements of practicality and the probabilistic aspects of the design process.

The PBLSD method used the design equation

$$(\text{Design resistance}) > (\text{effect of design loads}) \quad (1)$$

In the development of the right- and left-hand sides of Equation (1), uncertainty and probabilistic concepts are explicitly incorporated into the design process. LIMIT STATES must be identified by the structural engineer as a part of the process of designing the structural system. The design format of the PBLSD method takes the form

$$\phi R_n > \sum_{i=1}^n \lambda_i Q_i \quad (2)$$

where ϕ = strength reduction factor

R_n = calculated nominal capacity computed according to a prescribed formulation in the material specification using specified material strength and dimensions

λ_i = load factor

Q_i = service loads

The right-hand side of Equation (2) represents the summation of factored service loads specified by the appropriate building code for dead, live, wind, seismic, and other relevant loads. The specified load factors are intended to account for unfavorable variations inherent in the randomness and uncertainty associated with the true loads on a structure. The load factors are derived from a probabilistic study of the distribution of these service loads in such a way as to maintain consistent levels of safety.

The left-hand side of Equation (2) represents the computed NOMINAL CAPACITY OF A LIMIT STATE multiplied by a STRENGTH REDUCTION FACTOR. The nominal capacity of a limit state of a concrete masonry component is established using test data and the principles of mechanics. The value of the strength reduction

factor is a function of many items, including the building material, the limit state under consideration, the consequence of a particular type of failure, and the possible modeling errors.

Limit state refers to a situation in which a structural element or a structural system no longer satisfies its intended design objective. Designers typically consider two types of limit states: ultimate limit states and serviceability limit states. A limit state related to structural collapse is a strength limit state. A serviceability limit state relates to functional utility.

Limit state design requires that the designer explicitly consider possible limit states in a member or the limit states in an entire system. For example, such consideration might involve determining the load at which a wall under combined loading would fail in flexure and ascertaining that it is less than the load that will produce an undesirable compressive failure in the masonry. Most material specifications that employ the strength design method are formulated to produce the more ductile modes of failure, but it remains for the designer to step back and consider how a particular system might fail during an overload condition or because of an understrength condition in one construction material.

The specification of both the load and strength reduction factors depends on the level of structural reliability deemed sufficient by those responsible for specifying these factors. This determination indirectly represents a determination by society as a whole as to what is adequate structural performance. The estimate of reliability is defined by the RELIABILITY INDEX, β .

STRUCTURAL RELIABILITY

If one considers the shear wall it may be seen that the nominal design strength of this member may be calculated using the appropriate limit state equations. This design strength is considered to be a deterministic quantity in that the equation gives the designer but one value of moment capacity for a given set of dimensions, area of reinforcement steel, and material strengths. This number, however, does not represent the value of the actual moment strength, and until the member is loaded to failure, only statements of a probabilistic nature can be made regarding the beam's true strength. Similarly, only probabilistic statements may be made regarding the actual loads that might be imposed on the shear wall during its design life.

The structural engineer must, however, make predictions regarding the anticipated loads which the member will experience as well as attempting to establish the capacity of the member for a given limit state. Probability is useful in making these predictions,

in that probabilistic methods explicitly recognize that all predictions of the future have some level of uncertainty associated with them. These methods model reality by recognizing the observed scatter, randomness and uncertainty present in actual designs, and quantify it using probability theory.

If failure is described by the condition where the capacity of the member or system, R , is equal to or exceeded by the specified load effect, U , then failure occurs when R minus U is less than or equal to zero that is,

$$F = R - U \quad (3)$$

where F is the safety margin.

Thus, failure occurs when $F \leq 0$.

A failure condition requires two separate events to occur before the member is judged to have failed because failure is a function of both capacity and load. Consequently, failure occurs when a member of moderately low strength is loaded with a very high level of load or a very low strength member is loaded with a moderately high load. As a result, it may be seen that the occurrence of an extremely high load does not necessarily represent a failure condition unless combined with a member of sufficiently low capacity.

The variability of the data about the mean value of the safety margin, F , is quantified by the standard deviation, s_F . The standard deviation represents a measure of the spread of the data. A given value of F may be described by how many standard deviations it is away from the mean. Thus, the mean of F is zero standard deviations from the mean, while an extreme value of F might be three or four standard deviations (above or below) the mean. It is assumed that for a given value of F , the greater the number of standard deviations it is above or below the mean, the lower the probability that such a value of F will occur. The more unlikely it is that a value of F will be less than or equal to zero, the more unlikely it is that the member under consideration will fail. It thus possesses greater reliability.

If the values of F and s_F are known, it is possible to define another term which gives an indication of the reliability of a particular element or structural system. The reliability index, β , is defined as

$$\beta = \bar{F}/s_F \quad (4)$$

The above definition of reliability index is not appropriate when F is a nonlinear function of the random variables in R and U . Therefore, a more general definition, referred to as the Hasofer-Lind definition, is used for nonlinear function.

The reliability index has two fundamental advantages over conventional methods of reliability analysis. It allows the strength of building components to be viewed on a material by material basis, and it provides for and encourages the characterization of strength to be done independently of load factors. In addition, it enables one to address safety and reliability without directly quantifying the probability of component or system failure.

The advantage of the last observation may be more clearly understood if one considers that the load and resistance effects leading to structural failure occur at the extreme ends the PDFs describing R and U . The probability of failure is very sensitive to the PDF used to describe the distribution of the values of resistance and load effects because of the influence of the values at the extremes. The selection of different PDFs may result in changes in the probability of failure by several orders of magnitude. By avoiding the explicit specification of the probability of failure and relying on the reliability index, a more robust estimate of structural reliability may be obtained. It has been shown that most designs are not particularly sensitive to the actual probability of failure, and that measures of reliability not heavily dependent on the extreme tails of the PDFs describing the structural system should be used. The reliability index is such a measure.

The reliability index is a measure of structural reliability. The greater the value of β , the greater the structural reliability, and the smaller the probability of failure. Typical values of β present in current masonry, concrete, and steel design codes, are shown in Table 1. It may be seen that the reliability index is much larger in masonry components than it is in the equivalent steel or concrete element. Additional research is required to assess the impact of strength design concepts on masonry structures, but it appears at this time that these values of β are too conservative. For example, it has been found that a value of $\beta=3.0$ is consistent with average current practice for load combinations involving dead and live or dead plus snow loads, while $\beta=2.5$ and 1.75 were representative for combinations describing wind and seismic loads, respectively. Therefore, current masonry β values are too large.

TABLE 1
TYPICAL VALUES OF THE RELIABILITY INDEX, β ,
FROM CURRENT DESIGN CODES

	Masonry	Reinforced Concrete	Steel (Ultimate)
Beams	7.5-8.5	2.6-3.8	2.7-4.6
Columns	6.0-7.5	2.6-4.3	1.9-3.0

LOAD FACTORS

There are several problems that make the development of a unified set of load factors a difficult task. Current design criteria for the different materials result in different values of β . An important parameter in the variation of β is the ratio of live load to dead load, L/D. Within a particular material specification, different magnitudes of L/D also result in varying values of the reliability index. The random (probabilistic) nature of all loads, in particular live, seismic, and wind loads, creates additional problems in deriving a single set of load factors and loading combinations. The National Bureau of Standards (NBS) has recently completed a study of this problem and has proposed a new set of load factors and loading combinations which have been adopted as part of ANSI A58.1.

The total load on a member or structural system is broken up into permanent (dead) loads, sustained (live) loads, and loads of short duration (seismic or wind). The maximum total load will probably occur at some point that does not represent the combination of the maximum values of the individual loads. The time interval over which the load is monitored for the maximum combination is typically assumed to be the building design life, which, in the NBS study, was taken to be 50 years.

Now, if the probability distribution of each load type and an estimate of its mean and standard deviation are known, the different loading combinations may be simulated and the strength of various members computed. If the calculated strength is compared to the actual tested strength, the reliability of the section may be computed. The probability distributions used in the derivation of the NBS load factors are shown in Table 2.

TABLE 2
LOAD PARAMETERS

Load	PDF
Dead	Normal
Live	Type I extreme value
Wind	Type I extreme value
Snow	Type II extreme value
Earthquake	Type II extreme value

It is clear that for each material, load combination, and structural component (i.e., column, wall, beam), different values of β will be found. The basic idea is to identify a target value of β for a set of loading combinations and establish the load factors which will allow the value of β to remain as constant as possible under those conditions.

Assume that it is desired that β be equal to 3.0 for load combinations involving dead plus live load or dead plus snow load for all materials and structural components and β be equal to 2.5 and 1.75 for load combinations involving wind and seismic loads, respectively. Then it follows that the load factors can be derived, and those obtained in the NBS study are

$$U = 1.4D \quad (5a)$$

$$= 1.2D + 1.6L \quad (5b)$$

$$= 1.2D + 1.6S + (0.5L \text{ or } 0.8W) \quad (5c)$$

$$= 1.2D + 1.3W + 0.5L \quad (5d)$$

$$= 1.2D + 1.5E + (0.5L \text{ or } 0.2S) \quad (5e)$$

$$= 0.9D - (1.3W \text{ or } 1.5E) \quad (5f)$$

STRENGTH REDUCTION FACTORS

The strength reduction factor, ϕ , on the left-hand side of Equation (2) is an attempt to account for the variations in the actual loading and the in-situ capacity of the member from that calculated using the analysis and design equations. If the designer had the ability to establish the exact capacity of a structural section, it would be straightforward to compare the calculated resistance with the anticipated maximum load effects. If the capacity were greater than the demand, the section would be considered adequate. Unfortunately, just as a structural engineer does not have the ability to establish with certainty

the maximum design loads, neither is it possible to determine the exact capacity of a section for each limit state under consideration

SUMMARY

One challenge we face in the future is to define more relevant failure modes and to develop, on a rational basis, values for the strength reduction factors. This involves a team effort from experimentalists, analytical modeling persons and engineers interested in reliability theory.

SEISMIC RELIABILITY OF MULTI-STOREY
REINFORCED BRICK BUILDING

Wu Ruifeng * Chen Xizhi **

Xi Xiaofeng ** Xie Mingyu **

Summary

In this paper a method for prediction of seismic reliability of multi-storey building with a storey displacement criterion is proposed. By using of the Second-moment method the cracking and collapse probabilities of a hollow brick-wall building of 8 storey with consideration of elasticity of foundation are calculated. The effect of soil-structure interaction of this kind of buildings is specially discussed.

I. INTRODUCTION

The earthquake actions on structures and strength of materials are random, therefore the structural reliability, based on the theory of probability, is a rather reasonable method to assess the safety of a structure, but which component is the major factor of the principal

* Professor, Dept. of Engineering Mechanics, Dalian Institute of Technology, Dalian, China.

**Associate Professor, Dept. of Engineering Mechanics, Dalian Institute of Technology, Dalian, China.

criterion of damage in the analysis of reliability is still a problem. We consider that the decisive factor of collapse of a building is its deformations. The collapse of a building occurs only in case of its deflections reach a certain quantity. It is the best illustration that many serious damaged buildings still stand without collapse after the earthquake. Cracking of a wall must be also connected with deformation, and so the corresponding various deformation values are the reasonable index of cracking and collapse of buildings [1,2].

How to determine the values of deformation corresponding to cracking of wall and collapse of building is a difficult problem. The dependable way is making numerous tests to obtain necessary data. It is known that the test on whole building is not only expensively, but also very difficult. Besides, we can't make such large amount of tests to contain various kinds of buildings. Therefore a computational method for determining these values of deformations is needed. But as we know, there are not effective elasto-plastic analytical method for masonry building as a spatial structure and not enough informations of seismic experimental data about whole building to give out these values of deformations.

Arranging reinforced concrete constructional columns or heart columns, horizontal and vertical steels in wall can increase its deformable ability. The reinforced wall can be treated as a elasto-plastic element, such that, the deformation criterion for prediction of cracking and collapse of walls has based on a reasonable foundation and has practical significance.

In recent years, in china a lot of experimental and theoretical research works on brick-walls with constructional columns, heart columns and various type of reinforced steel [3-5] had been completed. For lack of experimental data and analytical method of whole building, the authors of this paper propose to utilize the test data and analytical method of a single wall to determine the deformation values, corresponding to cracking and collapse of the wall. It is a conservative approximation. At the same time, an estimation of spatical effect

of building can be made on the basis of computations and some informations from model test. This estimation will be used as a reference when the allowable failure probability is established.

We know that the responses of a building subjected to various earthquake input with same peak value of acceleration are different. In this paper, the elasto-plastic responses of a building is calculated by means of step-by-step integration method for various accelerogram of earthquake with same peak value, the elasto-plastic response of a building is calculated^[6], and the statistical values are obtained. If the number of accelerogram of earthquake used is enough, a good result can be expected.

In general, the soil-structure interaction for masonry building is not considered, but the interactive action is exist. Especially, for soil of II and III categories the effect of soil-structure interaction is apparently, and according to^[7] a study about this effect is discussed.

II. PROBABILITY OF FAILURE AND RELIABILITY

By using of the Second-moment method the practical distributions of random variable can be considered. Assume that the building is in failure when any story of it is cracked or collapsed.

Based on verification of experimental data of walls and dynamical response of deformation, the lognormal distribution and type I of extreme distribution can be accepted for failure of walls and storey displacement due to dynamic response respectively.

III. DETERMINATION OF \bar{u} AND u

\bar{u} and u are the given cracking or collapse displacements and displacement between stories of dynamic response under earthquake respectively. The determination of \bar{u} and u is to find the statistical value $m_{\bar{u}}$, $\sigma_{\bar{u}}$ and m_u , σ_u .

The characteristics of the accelerogram of earthquake is the major influence on the random variable u . Dynamic responses of a given structure differ widely for various accelerograms of earthquake with same peak value. It is not possible to use the real or experimental dynamic response of a building in order to receive the observational samples of u . We propose that instead of using the real earthquake response the dynamic analysis of a building under various accelerogram of earthquake with same peak values is used to calculate the maximum storey displacements. The maximum story displacement responses corresponding to various accelerograms of earthquake are adopted as observational samples, and from which the m_u and σ_u are obtained. As a general rule the more accelerogram of earthquake are used the more reliable statistical value is expected. Herein, a uncertainty due to the error of calculations arrived, which can be neglected at present time.

The mechanical properties of wall materials, geometric character, stress state and working quality etc. are influence on random variable \bar{u} . Currently, to utilize the experimental results of a large amount of reinforced brick-walls is a realizable way. Of courses, we can not test all walls in various combination of mortar strength, vertical loads, different height-width ratios etc. In this paper, the approximately formulas [5] verified by many testing data are used to find the stiffnesses and displacements of every region in hysteresis loops. Based on the known reinforced wall testing results and revised coefficients for given walls to find out the observational samples and mean values $m_{\bar{u}}$ and deviation $\sigma_{\bar{u}}$. In doing so, some errors and uncertainty will be produced which will be neglected in this paper.

IV. ILLUSTRATION

A horizontal and vertical reinforced hollow brick-wall building of 8 storey with transverse shearing walls is subject to ground accelerations of 0.2g and 0.4g respectively. To find out the cracking and collapse reliability of the building, the parameters of the house are shown in table 1.

Table 1. Parameters of the building

story No. Parameters	1	2	3	4	5	6	7	8
stiffness K_1 (MN/M)	13435	13435	11320	10436	10436	10436	9559	9559
stiffness K_2 (MN/M)	498	498	498	98	98	98	98	98
weight (KN)	4234	4234	4234	4234	4234	4234	4234	3675
Height (M)	2.8	2.8	2.8	2.8	2.8	2.8	2.8	2.9

It is assumed that floors in its plane are rigid, the modes of vibration are shear modes, the hysteresis loops of story shear forces and shear displacements are simplified in a two linear stiffness degrading model.

20 accelerograms of earthquake and 10 seconds are used to obtain the dynamic response. The 8-storey building simplified to a system of 8 lumped masses. Elasto-plastic dynamic analyses are performed for rigid and elastic foundation. All of the peak values of acceleration is readjusted to 0.2g and 0.4g respectively. Based on the testing results of 15 single walls with various combinations of reinforcements

and revised coefficients for different size of walls and designed vertical load the m_u and σ_u are obtained. All of these results are listed in table 2-3.

Table 2 Displacement response $u(10^{-4})^*$

storey	Rigid Foundation				Elastic Foundation			
	0.2g		0.4g		0.2g		0.4g	
	m	σ	m	σ	m	σ	m	σ
1	3.093	0.715	7.811	4.264	1.547	0.626	3.479	2.586
2	2.902	0.680	5.503	1.699	1.375	0.548	2.763	1.117
3	2.658	0.624	4.625	1.008	1.195	0.470	2.390	0.930
4	2.794	0.647	5.481	2.729	1.195	0.464	2.395	0.928
5	2.548	0.683	4.500	1.038	1.044	0.401	2.094	0.806
6	1.977	0.448	3.417	0.533	0.782	0.298	1.570	0.601
7	1.457	0.328	2.540	0.421	0.561	0.212	1.126	0.429
8	0.669	0.149	1.181	0.210	0.262	0.099	0.526	0.200

* All the values are divided by the storey height

Table 3. Failure displacements u of stories (10^{-4})

storey	cracking displacement		Limited displacement	
	m	σ	m	σ
1	10.53	3.58	5.029	1.461
2	10.60	3.61	5.127	1.489
3	10.70	3.65	5.177	1.505
4	10.92	3.72	5.280	1.534
5	11.14	3.80	5.388	1.566
6	11.37	3.88	5.499	1.599
7	11.49	3.92	5.557	1.616
8	11.61	3.96	5.617	1.632

Table 4. Failure Probability

storey	0.2g				0.4g			
	Cracking		Collapse		Cracking		Collapse	
	Rigid Foundation	Elastic Foundation	R.F.	E.F.	R.F.	E.F.	R.F.	E.F.
1	1.63×10^{-3}	5.83×10^{-5}	$< 10^{-7}$	$< 10^{-7}$	29.2×10^{-2}	4.59×10^{-2}	1.8×10^{-4}	1.0×10^{-6}
2	1.0×10^{-3}	1.81×10^{-5}	$< 10^{-7}$	$< 10^{-7}$	7.28×10^{-2}	3.63×10^{-3}	1.53×10^{-4}	$< 10^{-7}$
3	4.65×10^{-3}	4.2×10^{-6}	$< 10^{-7}$	$< 10^{-7}$	2.02×10^{-2}	1.2×10^{-3}	3.02×10^{-7}	$< 10^{-7}$
4	5.6×10^{-4}	3.1×10^{-6}	$< 10^{-7}$	$< 10^{-7}$	10.28×10^{-2}	1.05×10^{-3}	2.6×10^{-6}	$< 10^{-7}$
5	2.1×10^{-4}	5.59×10^{-7}	$< 10^{-7}$	$< 10^{-7}$	1.45×10^{-2}	3.37×10^{-4}	$< 10^{-7}$	$< 10^{-7}$
6	2.0×10^{-5}	$< 10^{-7}$	$< 10^{-7}$	$< 10^{-7}$	8.05×10^{-4}	2.56×10^{-5}	$< 10^{-7}$	$< 10^{-7}$
7	4.7×10^{-7}	$< 10^{-7}$	$< 10^{-7}$	$< 10^{-7}$	5.01×10^{-5}	8.87×10^{-7}	$< 10^{-7}$	$< 10^{-7}$
8	$< 10^{-7}$	$< 10^{-7}$	$< 10^{-7}$	$< 10^{-7}$	$< 10^{-7}$	$< 10^{-7}$	$< 10^{-7}$	$< 10^{-7}$
Max.	1.63×10^{-3}	5.83×10^{-5}	$< 10^{-7}$	$< 10^{-7}$	29.2×10^{-2}	4.59×10^{-2}	1.8×10^{-4}	$< 10^{-7}$

* Wave velocity and thickness of foundation medium are assumed 250m/s and 60M respectively.

The failure probability is listed in table 4. From table 4 it is shown that comparison with current code TJ 11-78 the height of reinforced hollow brick-wall building could be raised about 2 stories.

V. THE EFFECT OF SOIL-STRUCTURE INTERACTION

In general the interaction effect between soil and structure is not considered in seismic design, but from table 4 we can see that the effect is significant in cases of II and III category foundation soil for a building of 8 storey. In order to investigate the influence of elasticity of this foundation medium on natural frequency, first, let us consider the effect on the given building of 8 storey the result is shown in Fig.1.

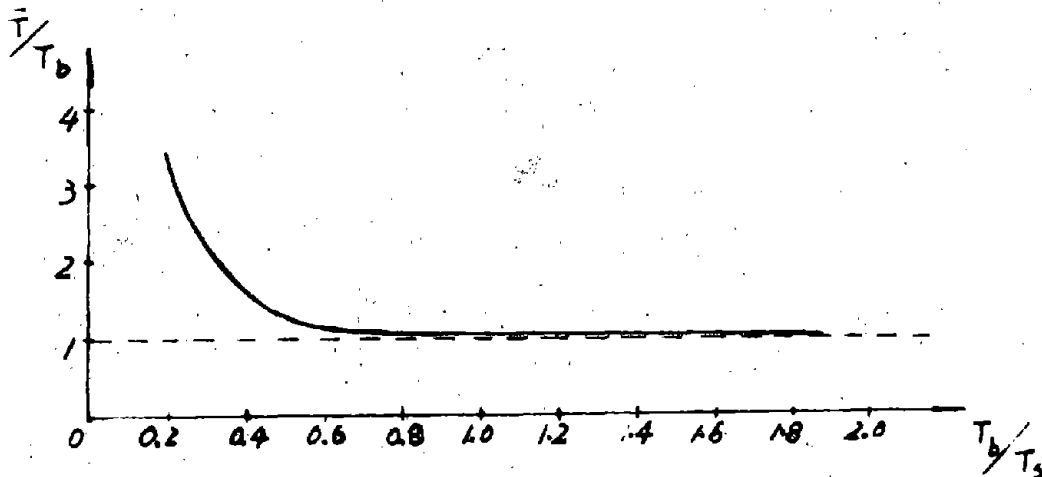


Fig. 1. Effect of soil-structure interaction on natural frequency.

From Fig.1 we can see that when $T_b/T_s < 0.6$ the consideration of interaction become necessary, where T_s , T_b and \bar{T} are natural frequencies of foundation soil, building on rigid foundation and system of building with elastic foundation soil respectively. In the analysis

the T_s is taken to equal 0.96 sec., i.e., the consideration of interaction is necessary when $T_b < 0.6$ sec., but this is in the range of natural frequency of masonry buildings. In the given example, from table 2 we can see that the storey displacements are decreased when the elasticity of foundation soil is taken into account. But, due to deformation of foundation the relative to ground displacement of the top of the building may be larger than those of rigid foundation. It must be considered when the limit height of brick-wall building is determined.

By the way, we should like to note that the spatial effect enlarge the stiffness of building and herein this effect is not considered.

VI. CONCLUSION

1. Based on the method of Second-order moment and story displacement criterion the failure probability can be obtained, from which a more reasonable limit height of masonry building can be determined.

2. The soil-structure interaction and spatial effect of building are two problems, which must be further investigated. But, in general, their effects make the building in safety side, therefore it may be considered when allowable failure probability should be determined.

References

1. Wu R.F., Gu H.X., Seismic Reliability of Multi-storey Brick Wall Buildings with constructional columns. Proceeding of National Symposium on Earthquake Engineering, 1984, March, Shanghai.
2. Yin Z.Q., et al, Reliability and Displacement Control Design of Seismic Structure, Earthquake Engineering and Engineering Vibration,

1982, No.2.

3. Peng J.G., et al, Experimental Study Report of Lateral Strength of Plain and Reinforced Masonry Walls, XiAH Institute of Metallurgical Architecture, Test Report, 1984.
4. Wu P.F., Lu H.X., Xi X.F., Elasto-plastic Analysis and Crack Growth Analysis of Reinforced Masonry Shear Wall, Journal of DIT, 1979, No.1.
5. Wu R.F, Lu H.X., Xi X.F., Zhang H.X., Zhou B.Z., Wen G.D., Test and Analysis of Brick-walls with Reinforced Concrete Columns under Lateral Cyclic Loading, Proceedings of US-PRC Bilateral Workshop on Earthquake Engineering, vol.1, 1982, Harbin.
6. Lin J.H., Ding D.M., Tian Y.S., Analysis of Elasto-Plastic Earthquake Response of Series Multi-Degree-of-Freedom System, Journal of DIT, 1979, No.2.
7. Fan M., Xie M.Y., Wu R.F. Nonlinear Seismic Response Analysis of Soil-File-Structure Interaction Systems, Earthquake Engineering and Engineering Vibration, 1985, No. 3.
8. Ang A. H-S., State-of-art of Structural Reliability and Reliability Based Design, Earthquake Engineering or Foreign Country, 1982, No. 1

SEISMIC RELIABILITY ANALYSIS OF MULTI-STORY BRICK BUILDINGS

Jinren Jiang * Feng Hong **

ABSTRACT

A method for assessing failure probability of multi-story brick buildings subjected to seismic loading is described. In order to analyze the stochastic seismic response of hysteretic brick buildings by equivalent linearization, the effective parameters of a simple brick structure with restoring force model proposed are determined from inelastic response spectra. A two parameter damage criterion model is obtained based on test data of brick wall. The structural failure probability is evaluated on the basis of two parameter damage criterion.

INTRODUCTION

Multi-story brick building is a widely used type of structure in industrial and civil buildings in China. It is known from the experience of large earthquakes that the aseismic capacity of such structures is very poor and some degree of damage is unavoidable when subjected to high intensity earthquake motion. In order to assess or predict the earthquake damage of such building in a specified period, a method for analyzing the seismic reliability or failure probability of such building is necessary. This method must include the uncertainty of occurrence of earthquake, the randomness of earthquake ground motion, the inelastic and nonlinear behavior of structure and the hysteretic characteristics and uncertainty of the structural resistance.

A method for analyzing the seismic reliability of multi-story brick buildings, which includes all of the above factors but in a simplified way, is proposed. For illustration, the method is applied to a 3-story building designed according to Chinese Aseismic Code (1).

STRUCTURAL MODEL AND EQUIVALENT PARAMETERS

Multi-story brick buildings subjected to earthquake motions can be modeled in sufficient accuracy as hysteretic multi-degree-of-freedom shear beam system. It has been shown (2) that for a nonlinear MDF system subjected to stationary random base motion, if the behavior of its nonlinear members depends only on the relative coordinate between the masses (such as shear beam system), the equivalent system can be achieved by simply replacing each nonlinear member by an elastic member with

* Associate Professor, Institute of Engineering Mechanics, State Seismological Bureau, China.

** Research Assistant, Centre for Earthquake Monitoring and Research in Northeast, SSB, China.

equivalent parameters, determined as for a SDF system. Therefore, in order to obtain the equivalent MDF system, the equivalent parameters of a simple hysteretic brick structure must be determined. The equation of motion of such structure is

$$m\ddot{z} + 2\zeta\sqrt{kmi}\dot{z} + kz = -ma \quad (1)$$

where; z is the hysteretic part of the restoring force. According to test data, a restoring force model is proposed as follows (Fig.1).

$$\dot{z} = \dot{u} - (k/(2\eta_a Q))(|\dot{u}|z + \dot{u}|z|) \quad (2)$$

in which k is the initial stiffness; Q is the ultimate strength; η_a is the parameter governing the degradation of strength.

$$\eta_a = \begin{cases} 1 & u_m \leq \alpha u_y \\ \frac{(\beta u_y - u_m) - (\alpha u_y - u_m)Q_1/Q}{(\beta - \alpha)u_y} & u_y < u_m < \beta u_y \\ Q_1/Q & u_m \geq \beta u_y \end{cases} \quad (3)$$

where; Q_1 is the frictional strength due to normal stress, u_m is the maximum displacement, u_y is the nominal yield displacement, α and β are parameters and here take values of 4.5 and 7.5 respectively.

The equivalent parameters of the simple brick structure with such restoring force can be determined from inelastic response spectra (3). An ensemble of ten earthquake accelerograms are chosen to calculate the inelastic response spectra. The peak acceleration of each accelerogram is adjusted so that the mean squared difference between the response spectrum of the earthquake and the Chinese code design response spectrum for site II and intensity VIII (1) in the period range of 0.1 - 4.0 sec. to be minimized.

The average inelastic response spectra over the ensemble of accelerograms for ductility ratio μ of 0.5, 1.0, 2.0, 4.0, 6.0 and 8.0 and the elastic response spectra for various damping are obtained. Fig.2 shows the average inelastic response spectra for ductility ratio of 8.0 and the 0.16 damped average elastic response spectra. It can be seen that the spectrum for $\mu = 8.0$ would lie almost exactly on the 0.16 damped elastic spectrum if that spectrum is shifted in period by a factor of 2.0. This fact indicates that it is possible to replace a nonlinear system by an equivalent linear system which will give nearly the same peak response as the nonlinear system over a range of periods.

Let $SD_n(T_1, \zeta, \mu)$ be the average spectral displacement of the hysteretic system and $SD_e(\alpha T_1, \zeta_e)$ be the average spectral displacement of a linear system with period αT_1 and damping ζ_e .

The difference between these two spectral displacements may be measured as

$$E_1 = (SD_e(\alpha T_1, \zeta_e) - SD_n(T_1, \zeta, \mu)) / SD_n(T_1, \zeta, \mu) \quad (4)$$

The mean squared difference can be expressed as

$$\varepsilon^2 = \frac{1}{N} \sum_{i=1}^N \varepsilon_i^2 \quad (5)$$

where, $N = 12$ is the number of period. The optimum equivalent parameters $T_e / T = c$ and ζ_e are obtained from the condition that the spectral difference attains its minimum.

Fig. 3 and 4 show $T_e / T - 1$ and $\zeta_e - \zeta$ versus μ respectively. The least square fit to the data points leads to the equivalent period

$$T_e = T(1 + 0.1858 \mu^{0.8187}) \quad (6)$$

or the equivalent stiffness

$$K_e = K(1 + 0.1858 \mu^{0.8187})^{-2} \quad (7)$$

and the equivalent damping

$$\zeta_e = \zeta + 0.06641 \mu^{0.3607} \quad (8)$$

STOCHASTIC SEISMIC RESPONSE ANALYSIS

The earthquake ground motions may be modeled as a filtered Gaussian process with zero mean and a specified power spectra density function. The mean square acceleration of the process can be expressed as

$$\sigma_n^2(t) = \psi(t) \sigma_a^2 \quad (9)$$

in which, σ_a is the mean square acceleration of a stationary Gaussian process. When the process is specified by the widely used Kanai-Tajimi spectrum, σ_a^2 is expressed as

$$\sigma_a^2 = \int_{-\infty}^{\infty} S(\omega) d\omega = \frac{S_0 \omega_g \pi}{4 \zeta_g} (1 + 4 \zeta_g^2) \quad (10)$$

in which ω_g and ζ_g are spectral parameters, representing the natural frequency and damping of the ground filter; S_0 is the spectral intensity of white noise process.

$\psi(t)$ is the envelop function defined as

$$\psi(t) = \begin{cases} (t / t_1)^2 & 0 \leq t \leq t_1 \\ 1 & t_1 < t < t_2 \\ e^{-c(t - t_2)} & t_2 \leq t \end{cases} \quad (11)$$

in which t_1 , t_2 and c are parameters.

For simplification, and considering that what we are interested in are the maximum displacement and accumulated energy dissipation rather than the response process, the nonstationary process may be replaced by an equivalent stationary process, the duration τ of which is given by that of the intensity in excess of 50% of the peak value and its mean square acceleration $\bar{\sigma}_n^2$ is taken as the time average over τ of $\sigma_n^2(t)$, i.e.

$$\bar{\sigma}_n^2 = \frac{1}{\tau} \int_{\frac{t_1}{2}}^{\tau + \frac{t_1}{2}} \psi(t) \sigma_a^2 dt = M a \quad (12)$$

$$M = \left(-\frac{17}{24}t_1 + t_2 + \frac{3}{4}c \right) / \tau \quad (13)$$

$$= -t_1/2 + t_2/2 + \ln 4/c \quad (14)$$

The spectral intensity S_0 can be determined from the maximum ground acceleration \bar{a}_{\max} by using the following relationship

$$\bar{a}_{\max} = r\bar{\sigma}_n = rM\sigma_a \quad (15)$$

in which r is the peak factor.

The parameters of earthquake loading and their coefficients of variation are listed in Table 1 (4).

The essence of the response to the filtered Gaussian excitation may be described for a SDF system. The equation of motion can be written as

$$\ddot{u} + 2\zeta_e \omega_e \dot{u} + \omega_e^2 u - 2\zeta_g \omega_g \dot{u}_g - \omega_g^2 u = 0 \quad (16)$$

$$\ddot{u}_g + 2\zeta_g \omega_g \dot{u}_g + \omega_g^2 u_g = -f(t) \quad (17)$$

in which $f(t)$ is the white noise excitation. Introducing vector $\{Y\}$ ($y_1 = u$, $y_2 = \dot{u}$, $y_3 = u_g$, $y_4 = \dot{u}_g$), eqs (16) and (17) can be written as

$$\frac{d}{dt}\{Y\} + [a]\{Y\} = \{F(t)\} \quad (18)$$

Let $[S]$ be the covariance matrix of $\{Y\}$ with the element $s_{ij} = E\{y_i y_j\}$ for the stationary excitation it can be shown that $[S]$ satisfy the following matrix equation

$$[G][S] + [S][G]^T = [B] \quad (19)$$

in which $[G]$ is the matrix of the structural system parameters, $[B]$ is the excitation matrix with $b_{44} = 2\pi S$, and other elements equal to zero. For MDF system, the same matrix equation as eq. (19) can be obtained. The solution of eq. (19) must be obtained iteratively. An effective solution of the matrix equation has been given by Bartels and Stewart (5).

Knowing the root mean square displacement σ_u , the mean value \bar{u}_m and root mean square value σ_{u_m} of the maximum displacement are easy to obtain as follows

$$\bar{u}_m = p\sigma_u, \quad p = \sqrt{2 \ln v \tau} + \frac{0.5772}{\sqrt{2 \ln v \tau}} \quad (20)$$

$$\sigma_{u_m} = q\sigma_u, \quad q = \frac{\pi}{\sqrt{6}} \frac{1}{\sqrt{2 \ln v \tau}} \quad (21)$$

in which v is the expected zero-crossing rate.

The mean value \bar{E} and root mean square value σ_E of the accumulated energy dissipation can be computed from the following equations (4)

$$\bar{E} = 2\zeta_e \omega_e m \sigma_u^2 \tau \quad (22)$$

$$\sigma_E = \bar{E} \delta \quad (23)$$

with

$$\delta = \left[\frac{2}{\zeta_e \omega_e \tau} + \frac{1}{(\zeta_e \omega_e \tau)^2} (e^{-2\zeta_e \omega_e \tau} - 1) \right]^{\frac{1}{2}} \quad (24)$$

DAMAGE CRITERION

In order to evaluate the failure probability of structure, a criterion to accurately assess the structural damage is necessary. Recently a two parameter damage criterion has been proposed for R/C structures. According to the test data at IGM, a brick structure under earthquake loadings is damaged by a combination of maximum response and number of loading cycles as for a R/C structure. Consistent with this behavior, the maximum deformation δ_m and the accumulated energy dissipation $\int dE$ are chosen as damage-controlling variables. Based on the test restoring force curve data of 45 brick wall specimens, it is found that the damage index is expressed as a nonlinear function of δ_m

and $\int dE$ as follows.

$$r^* = \left[\left(\frac{\delta_m}{u_y} \right)^2 + 3.67 \left(\frac{\int dE}{Qu_y} \right)^{1.12} \right]^{\frac{1}{2}} \quad (25)$$

in which dE is the incremental absorbed hysteretic energy and $\int dE$ is the accumulative energy dissipation.

The damage index contains two parameters u_y and Q . The Q is determined from eq.28; $u_y = Q/K$ with K determined from eq.30.

The damage index r^* follows Weibull distribution (Fig.5)

$$F(r^*) = 1 - \exp\left(-\frac{r^{*2.73}}{2080}\right) \quad (26)$$

with the mean value and mean square value equal to 14.61 and 33.34 respectively.

It should be noted that the failure defined here corresponds to the generally defined moderate to serious earthquake damage to brick buildings.

STRUCTURAL PARAMETERS AND THEIR UNCERTAINTIES

For shear beam model, the model parameters are the story mass, strength, stiffness and viscous damp ratio, which can be expressed as follows.

The story mass

$$m = \begin{cases} (W_D + W_L)/g & \text{for floor} \\ (W_D + W_S)/g & \text{for roof} \end{cases} \quad (27)$$

in which W_D is the story dead loads; W_L is the story live loads (permanent live loads W_{Lp} plus temporary live loads W_{Lt}); W_S is the snow load on the roof.

The story ultimate strength

$$Q = 0.71A(R_j + f\sigma) \quad (28)$$

in which A is the cross-section area of story wall in the direction considered; f is the friction coefficient along the wall, assumed to be 0.7; σ is the normal stress in the wall; R_j is the shear strength along step section of the wall and may be expressed as

$$R_j = 0.4\sqrt{R_2}(R_2 - 1)/R_2 \quad (29)$$

in which R_2 is the strength of mortar.

The story initial stiffness

$$K = \frac{(0.77 + 0.23)Eb}{h/l[3(1 + \nu) + (h/l)^2]} \quad (30)$$

in which ν is the Poisson ratio and can be assumed to be 0.13; h , l , and b are the height, length and width of the wall; E is the modulus of elasticity and may be expressed as

$$E = \begin{cases} 333.3R & R \leq 15 \text{ kg/cm}^2 \\ 1000(1 - 10/R) & R > 15 \text{ kg/cm}^2 \end{cases} \quad (31)$$

in which R is the compressive strength of the wall and may be expressed as

$$R = (0.1\sqrt{R_1} + 0.2\sqrt{R_2})\sqrt{R_1 + 60} \quad (32)$$

in which R_1 is the strength of brick.

The coefficients of variation of model parameters can be expressed as

$$\Omega_p = \sqrt{\delta_p^2 + \Delta_p^2} \quad (33)$$

in which δ_p is the inherent variability of the parameter and Δ_p is the uncertainty due to error of estimation. δ_p can be obtained from the predicting formula, if the coefficients of variation of its basic variables are known. The coefficients of variation of the related basic variables and predicting formulas are listed in Table 2 (4).

RELIABILITY ANALYSIS

In the following, estimation of failure probability of structure on the basis of two-parameter criterion is given. The failure probability of structure in a specified period T may be expressed as

$$P_f = \int_a \alpha(R < S/a) \cdot \beta(a) da \\ = \sum_{i=1}^N \alpha(R < S/a - 1.6\sigma) \beta(1.6\sigma - \frac{4\sigma}{2} < a < 1.6\sigma + \frac{4\sigma}{2}) \quad (34)$$

in which $\alpha(R < S/a)$ is the conditional failure probability of the structure, being given the peak acceleration of ground motion, a ; $\beta(a)da$ is the probability of occurrence of the acceleration of ground motion with intensity between a and $a+da$; $1/a$ is the discretization of acceleration of ground motion. $\beta(\cdot)$ is obtained from the hazard analysis results.

$$\alpha(\cdot) = \int_0^{\infty} f_B(x/a-1/a) F_R(x) dx \quad (35)$$

in which $F_R(x)$ is the probability distribution function of the structural resistance and is expressed by eq.26; $f_B(\cdot)$ is the probability density function of the load effects which must be expressed in terms of the damage index in consistent with the resistance. From the first order approximation the mean value of the load effect can be expressed as

$$\bar{S} = \left[\left(\frac{u_m}{u_y} \right)^2 + 3.67 \left(\frac{\bar{\epsilon}}{Qu_y} \right)^{1.12} \right]^{\frac{1}{2}} \quad (36)$$

The variance of the load effect comes from the randomness of earthquake loading, uncertainties of parameters and error of model. From the first order approximation the three parts of variance can be expressed as follows respectively

$$\text{Var1}[S] = \left(\frac{\partial S}{\partial u_m} \right)^2 \sigma_{u_m}^2 + \left(\frac{\partial S}{\partial \epsilon} \right)^2 \sigma_{\epsilon}^2 + 2\rho_{u,\epsilon} \left(\frac{\partial S}{\partial u_m} \right) \left(\frac{\partial S}{\partial \epsilon} \right) \sigma_{u_m} \sigma_{\epsilon} \quad (37)$$

$$\text{Var2}[S] = \sum_i \sum_j \left(\frac{\partial S}{\partial p_i} \right) \left(\frac{\partial S}{\partial p_j} \right) \rho_{ij} \sigma_{p_i} \sigma_{p_j} \quad (38)$$

$$\text{Var3}[S] = \left(\frac{\partial S}{\partial u_m} \right)^2 (\delta_1 \bar{u}_m)^2 + \left(\frac{\partial S}{\partial \epsilon} \right)^2 (\delta_2 \bar{\epsilon})^2 + 2\rho_{1,2} \left(\frac{\partial S}{\partial u_m} \right) \left(\frac{\partial S}{\partial \epsilon} \right) (\delta_1 \bar{u}_m) (\delta_2 \bar{\epsilon}) \quad (39)$$

in the above equations the partial derivatives take values at the mean value; $(\partial S / \partial p_i)$ is the sensitivity coefficient corresponding to parameter p_i and may be determined by central finite difference; ρ are correlation coefficients; δ_1 and δ_2 are the coefficients of variation of u_m and ϵ due to model error and are assumed here to be 0.22 and 0.20 respectively.

The probability distribution of load effect can reasonably be assumed to be Gumbel Type I distribution. When the conditional failure probability is large, its value is not sensitive to the type of distribution of load effect.

EXAMPLE APPLICATION

As an example application of the method outlined above, a 3-story

brick building designed according to the Chinese Seismic Code (1) for intensity VIII on intermediate soil site is analyzed. The structural parameters and their coefficient of variation are listed in Table 3. The value of \ddot{a}_{max} corresponding to intensity VIII is assumed to be 250 cm/sec².

Fig.6 shows the mean value of damage index in each of the three stories for four ground acceleration levels of 62.5, 125, 250 and 500 cm/sec². It is seen that for the four acceleration levels the maximum damage index all occurred in the first story. Therefore the seismic reliability of the first story of the building is analyzed. The mean value, root mean square value and coefficient of variation of the damage index in the first story are listed in Table 4 along with the percentage contribution of the randomness of earthquake, uncertainties of structural parameters and error of model to the variance of damage index. The conditional failure probabilities of the first story for the four acceleration levels are 0.9088×10^{-5} , 0.9112×10^{-3} , 0.5210×10^{-1} and 0.5079 respectively. Using the seismic hazard curve for a site in Beijing shown in Fig.7, it is obtained that the failure probability of the first story of the 3-story brick building in 50 years of lifetime is 2.18 %.

CONCLUSIONS

A method for assessing failure probability of multi-story brick buildings subjected to earthquake loading on the basis of two-parameter damage criterion is given. The method includes the randomness of earthquake, the inelastic behavior of structure, the hysteretic characteristics of the structural resistance, the uncertainties of the structural parameters and the error of the model. For practical purposes, however, simplifications had to be made. Therefore the method should be validated using damage data of brick buildings from past earthquake. Moreover, the computation of the response uncertainty is complicated and the approach to its simplification needs to find.

REFERENCES

1. The Aseismic Design Code for Industrial And Civil Buildings (TJ 11-78), 1979 (in Chinese).
2. Spanos, P-T. D. and Iwan, W. D., "On the Existence and Uniqueness of Solutions Generated by Equivalent Linearization," Int. J. Non-linear Mech., V.13, N.2, 1978.
3. Iwan, W. D., "Estimating Inelastic Response Spectra from Elastic Spectra," EESD, V.8, N.4, 1980.
4. Jiang, J. R. and F. Hong, "Reliability Analysis of Multi-story Brick Buildings Subjected to Seismic Load," Earthquake Engineering

and Engineering Vibration, V.5, N.4, 1985 (in Chinese)

5. Bartels, R. H. and Stewart, G. W., "Solution of the Matrix Equation $AX + XB = C$," Algorithm 432 in Communications of the ACM, V.15, N.9, 1972.

Table 1

site condition	soft	inter-mediate	hard (rock)
t_1	1.5	1.0	0.5
t_2	11.5	8.0	6.0
c	0.4	0.6	0.8
τ	14.2	9.8	7.5
Cov(τ)	0.9	0.9	1.0
μ	0.8659	0.8707	0.8798
ω_g	10.9	16.5	16.9
ζ_g	0.96	0.80	0.94
Cov(ω_g)		0.425	0.398
Cov(ζ_g)		0.426	0.391
r	3.2	3.0	3.0

Table 2

δW_D	0.07
δW_{LP}	0.46-0.32
δW_S	0.71
δW_{Lt}	0.69-0.54
δR_2	0.3
δR_1	0.25
Δ_m	0.1
Δ_Q	0.24
Δ_K	0.24
Δ_z	0.26

Table 3

story	K (T/cm)	Cov. K	Q (T)	Cov. Q	μ T·sec ² /cm	Cov. μ	ζ	Cov. ζ
1	7152	0.36	860.4	0.26	0.5223	0.12	0.05	0.26
2	6104	0.36	700.8	0.26	0.5223	0.12	0.05	0.26
3	5054	0.36	541.2	0.27	0.3257	0.12	0.05	0.26

Table 4

a_{max} cm/sec ²	62.5	125	250	500
Contribution to damage index:				
Randomness of earthquakes	58.2	59.7	66.8	47.8
Uncertainties of structural parameters	34.9	33.8	26.2	47.3
Error of model	6.9	6.5	7.0	4.9
Damage index:				
Mean value	0.7776	1.697	3.951	11.102
RMS value	0.3913	0.8679	1.953	6.864
Cov.	0.5032	0.5114	0.4943	0.6183

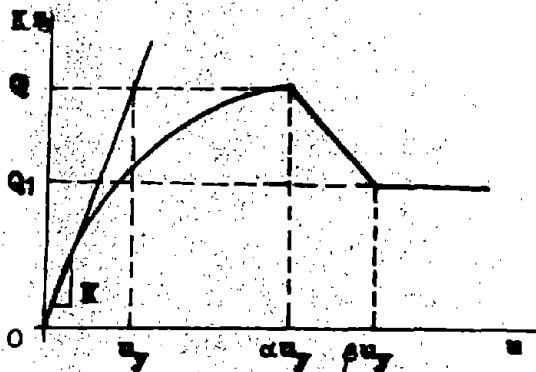


Fig. 1

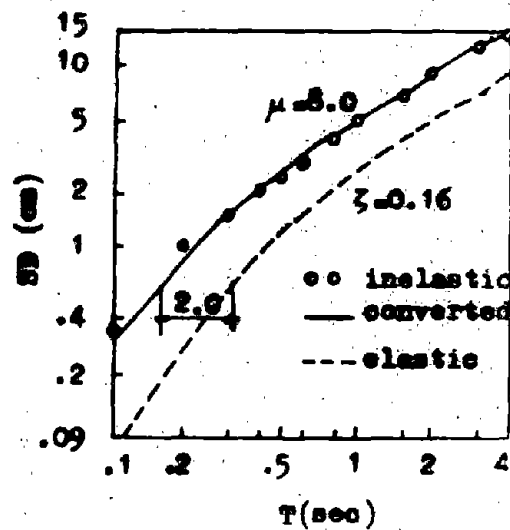


Fig. 2

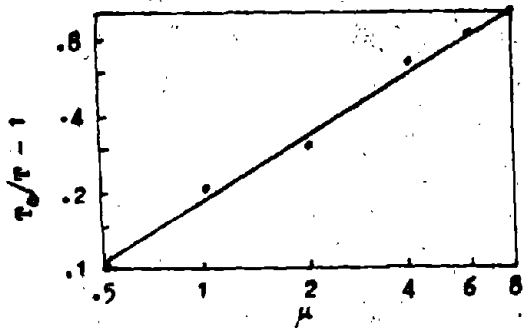


Fig. 3 Equivalent period versus nominal ductility ratio

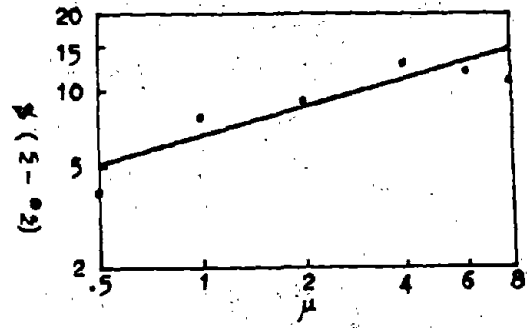


Fig. 4 Equivalent damping versus nominal ductility ratio

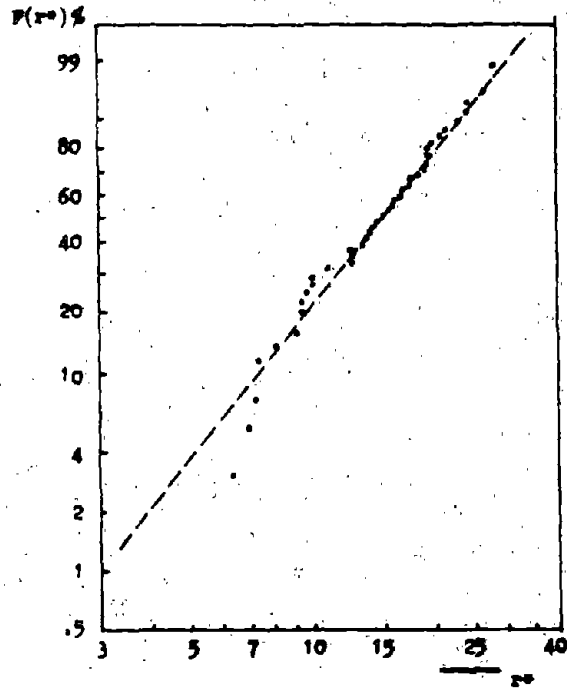


Fig. 5 Damage index on Weibull probability paper

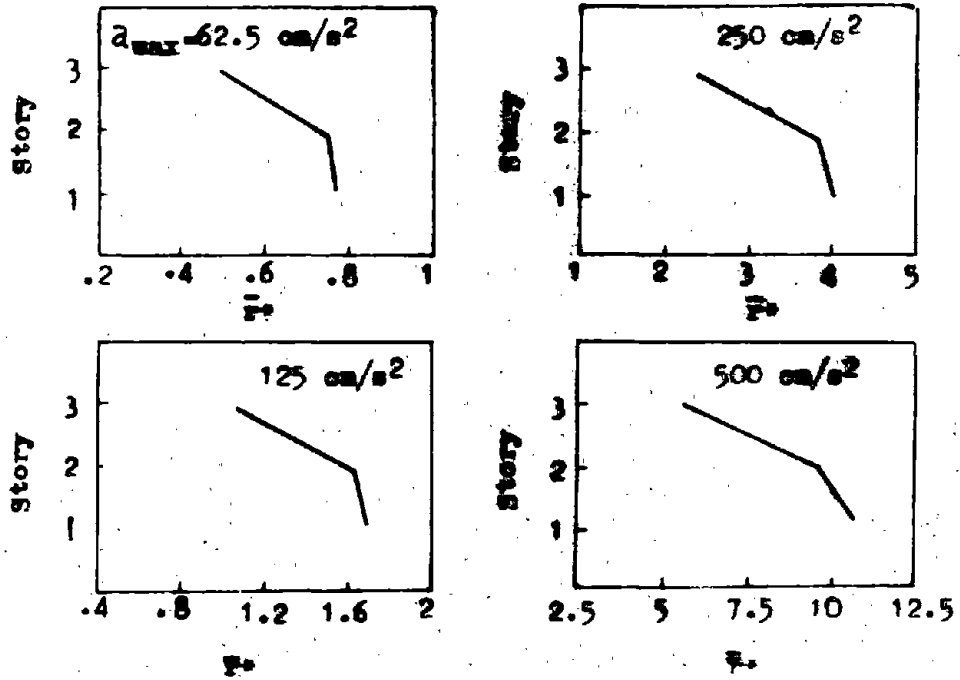


Fig.6 Mean value of damage index \bar{r}_d for the 3-story building

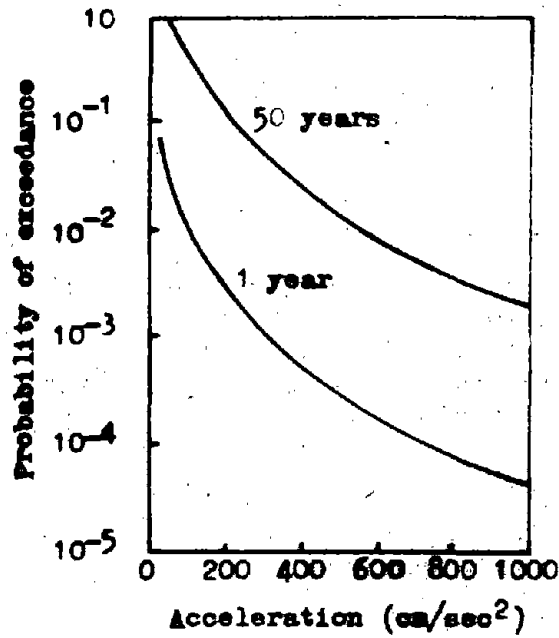


Fig.7 Seismic hazard curve for Beijing

EARTHQUAKE RESISTANT RELIABILITY OF
BRICK RESIDENTIAL BUILDINGS

Huo Zizheng (1)

ABSTRACT

In this paper, the earthquake response deformations of multistory brick residential buildings built nowadays are determined by the series model of multiple degree of freedom and 40 seismic waves on the basis of test data of wall fragments, and the probability distribution of the above-mentioned deformations and the values of deformation of wall fragments by tests are examined.

Besides, the probability of failure of multistory brick residential buildings are calculated by the linear-second moment check point method on the basis of the statistic probability parameters obtained, and the quantitative relationship between the probability of failure and the number of stories of brick residential buildings and that between the latter and earthquake intensities are discussed.

(1) Engineer. Shaanxi Research Institute of Building and Construction. the People's Republic of China.

The mathematical calculations involved herein are carried out with the help of Engineers Wang Wenguang, Zhang Luo, Lan Jie, Zhang Yao and Zhai Houqin.

1 CALCULATION OF EARTHQUAKE RESISTANT RELIABILITY OF STRUCTURES BY LINEAR-SECOND MOMENT CHECK POINT METHOD

The "Uniform Standard on Structural Design of Buildings" of the People's Republic of China states that the limit design of a structure must meet the following requirement:

$$g(S, R) = R - S \geq 0 \quad (1)$$

in which

S = effect of action of load on structure

R = resistance of structure

Of course this fundamental requirement also applies to seismic design.

It is generally accepted that the design criterion of buildings in seismic areas is that "they shouldn't fail under small earthquakes or collapse under violent earthquakes" and the quantitative standard is deformation. When the response deformation of a masonry structure under earthquake action exceeds its allowable deformation, it means that the structure fails. In fact the seismic response deformation of a structure and the allowable deformation of a structural wall determined by test are all random variables, that is to say, the deformations of a structure under different earthquake actions, even if the peak values of acceleration being equal, are not always the same, they all obey certain probability distribution, and so does the allowable deformation of a structural wall determined by tests. Therefore, the problem of reliability of a masonry structure under earthquake action is actually a problem of quantitative determination based upon the fundamental variables mentioned above.

According to the linear-second moment limit state design method, when the two fundamental variables are of normal distribution, the index of reliability may be determined by the following formula:

$$\beta = \frac{\mu_R - \mu_S}{\sqrt{\sigma_R^2 + \sigma_S^2}} \quad (2)$$

in which

β = index of reliability

μ_S, σ_S = the average value and standard deviation of the effect of action of load (which is referred to as the seismic response deformation in this paper).

μ_{X_1}, σ_{X_1} = the average value and standard deviation of resistance (which is referred to as the allowable deformation of structural wall in this paper).

Since the response and the allowable deformation do not always obey normal distribution, the statistical parameters in the formula for calculating reliability should undergo a process of equivalent normalization, and their expressions are:

$$\mu_{X_1}' = X_1^* - \Phi^{-1} [F_{X_1} (X_1^*)] \sigma_{X_1}' \quad (3)$$

$$\sigma_{X_1}' = \sigma_{X_1} \{ \Phi^{-1} [F_{X_1} (X_1^*)] \} / f_{X_1} (X_1^*) \quad (4)$$

in which

$\Phi(\cdot)$ = normalized normal function of density

$\Phi^{-1}(\cdot)$ = inverse function of normalized normal function

$F(\cdot)$ = probability function

$f(\cdot)$ = probability function of density

X_1^* = assumed coordinate of check point

$\mu_{X_1}', \sigma_{X_1}'$ = equivalently normalized average value and standard deviation

The state of distribution of random variables is determined by K-S examination, and the index of reliability is calculated by equivalent normalization of parameters $\mu_{X_1}', \sigma_{X_1}'$, and thus the probability of failure P_f is determined as:

$$P_f = \Phi(-\beta) \quad (5)$$

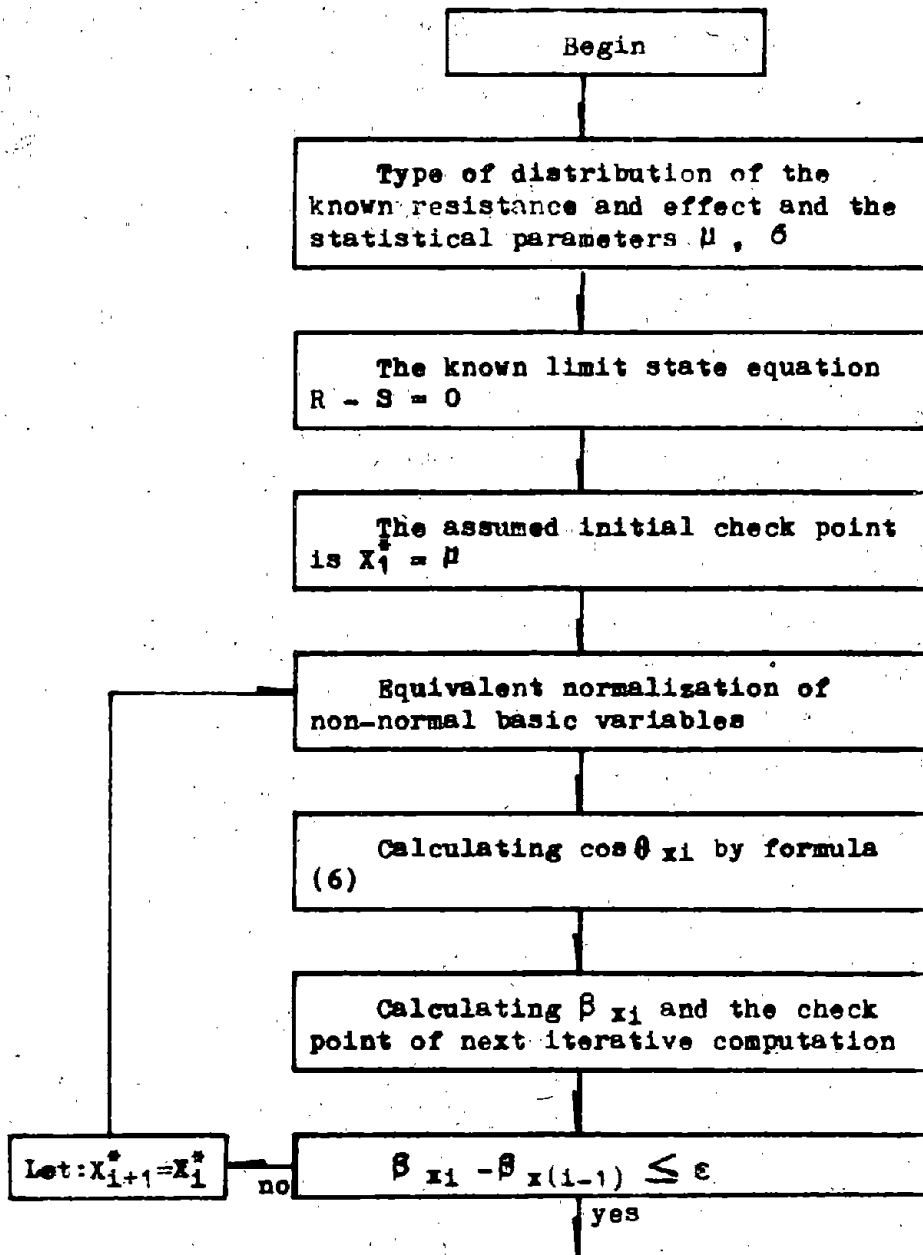
actually, the values of β and P_f may be determined by successive iteration of formula (2), (3) and (4). Assign the initial value of X_1^* first, then the check point of resistance and effect for the next step are calculated by the following formulas respectively:

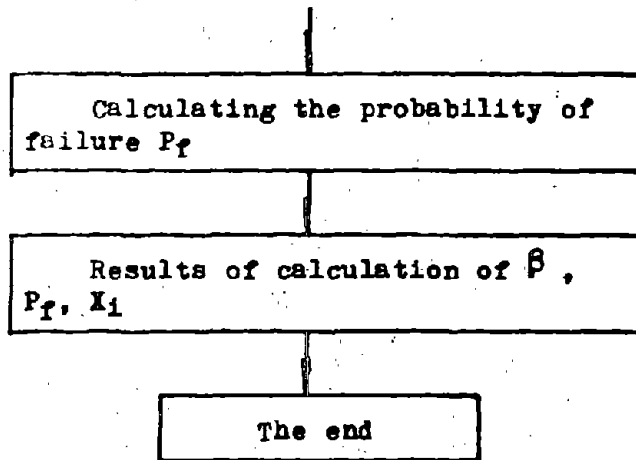
$$X_1^* = \mu_{X_1} + \sigma_{X_1} \cos \theta_{X_1} \quad (6)$$

$$\cos \theta_{X_1} = \frac{- \frac{\partial g}{\partial X_1} \Big|_{P^*} \cdot \sigma_{X_1}}{\left[\sum_{i=1}^n \left(\frac{\partial g}{\partial X_i} \Big|_{P^*} \cdot \sigma_{X_i} \right)^2 \right]^{1/2}}$$

and thus go on with cyclic iterative method. When

it is considered that the index of reliability is obtained. The block diagram of calculation is as follows:

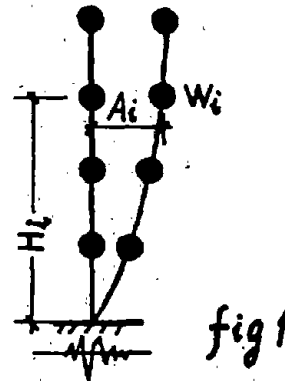




II DEFORMATION RESPONSE OF BRICK BUILDINGS AND RESISTANCE OF BRICK WALL

It is considered till now that the direct dynamic method of solving the differential equation of motion (7) by inputting the seismic waves is a reasonable method for solving earthquake response. A brick residential building can be simplified as a series system of multiple degree of freedom (fig 1).

If the mass of point mass, story rigidity of each story, story strength and "the mode of restoring force" characterizing the whole process of the relationship between force and deformation are known, the story response deformation can then be determined by inputting any seismic wave at the base of foundation and substituting equation (7) in:



$$[M]\{\ddot{Y}\} + [C]\{\dot{Y}\} + [K]\{Y\} = -[M]\{\ddot{Y}_g\} \quad (7)$$

in which

$[M]$ = mass matrix of mass point

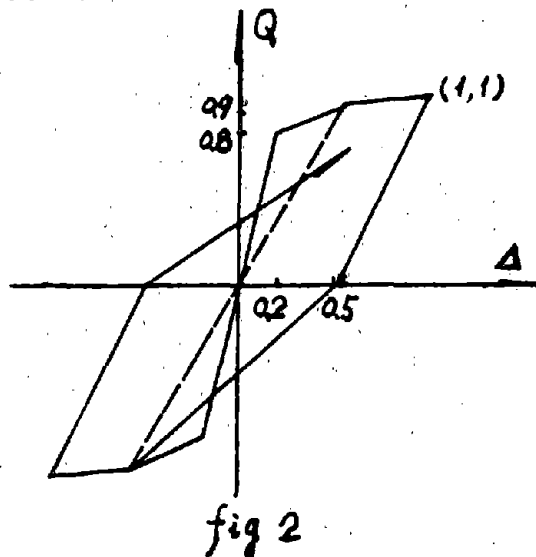
$[K], [C]$ = story rigidity and damping matrixes

$\{Y\}, \{\dot{Y}\}, \{\ddot{Y}\}$ = story displacement, velocity and acceleration column matrixes

$\{\ddot{Y}_g\}$ = acceleration of seismic wave column matrixes

In fact, the values of story mass (weight), story rigidity and

story strength of brick residential buildings are within certain limits, i.e. the story weight is about 11—18 KN/m², the story rigidity is about 200—250 KN/cm·m² and the story strength is about 20—70 KN/m² when calculated according to the floor area of a building, and they are smaller for upper stories and larger for lower stories. Reference (2) gives their average values for a series of existing buildings from statistical estimation, as shown in table 1, and also the non-dimensional mode of restoring force based upon the test results of side thrust tests of 68 brick wall fragments as shown in fig 2 (taking limit load as unity).



Calculated structural parameters from statistics for multistory brick structures

table 1

NO. of stories	Weight(KN/m ²)	Rigidity(KN/cm·m ²)	Load carrying ability(KN /m ²)
10	11.5	227.1	30.1
9	12.0	227.1	33.3
8	13.0	227.1	36.2
7	14.0	258.8	42.5
6	14.0	266.5	46.1
5	16.0	334.5	63.5
4	16.0	374.0	67.2
3	17.0	414.9	70.8
2	17.0	455.2	74.5
1	18.0	495.4	78.1

Note: The calculated load carrying capacity against lateral force per unit area of a building

Substituting the above parameters in equation(7), inputting 40 seismic waves and adjusting the peak value of acceleration of each seismic wave to the same value, determine the deformation response. It is shown from calculation that the deformation response is different for different seismic waves. Taking eight story building as an example, when a seismic wave having its peak acceleration of 0.4g is inputted and the deformation response of each story being of lognormal distribution, the probability parameters are as shown in table 2.

Probability parameters for an eight story building when the peak acceleration of seismic wave is 0.2g table 2

Story	Average value	Mean square deviation
1st	0.12786	0.04541
2nd	0.12534	0.04651
3rd	0.12004	0.04483
4th	0.16417	0.08292
5th	0.13567	0.04817
6th	0.12392	0.04023
7th	0.09253	0.02828
8th	0.05221	0.01524

Note: the data listed above are calculated on the basis that the story limit deformation in unity.

Besides, the mode shown in fig 2 is only an average, but it obeys actually certain type of distribution. The probability parameters of initial crack and failure (both of them are lognormal distribution) are shown in table 3.

Probability parameters of structural resistance table 3

	Initial crack	Failure
Average value	0.21048	1.00
Mean square deviation	0.08904	0.87

III EARTHQUAKE RESISTANT RELIABILITY OF BRICK RESIDENTIAL BUILDINGS

In fact, the deformation parameters shown in table 2 for brick residential buildings of various number of stories can be obtained when inputting seismic waves of different peak accelerations. And the earthquake resistant reliability and probability of failure of each story of a building can be obtained by using the linear-second moment method and the parameters shown in table 3. Since maximum deformation always occur in the weakest story of a building, the maximum probability of failure must occur in the same story. We consider that the probability of failure of the story in which the maximum probability of failure occurs represents the probability of failure of the building. Table 4 shows the probability of failure of an eight story residential building when the peak acceleration is 0.2g. It is seen from the table that the weakest story is the fourth one, the probability of initial crack is 32.7% and that of failure is 3.2%.

The probability of failure of an eight story residential building %

Table 4

Story	Initial crack	Failure
1st	18.6	1.3
2nd	17.8	1.2
3rd	15.8	1.1
4th	32.7	3.2
5th	21.7	1.5
6th	16.7	1.1
7th	6.0	0.4
8th	0.3	0.05

The probability of failure for buildings of various number of stories can be calculated by inputting seismic waves of different peak acceleration. Table 5 shows the probability of failure of buildings of different number of stories for reference. It is seen from the table that the greater the number of stories and the larger the peak acceleration, the greater the probability of failure.

Results of calculation of probability of failure of brick residential buildings (%)

Table 5

Peak of acceleration	State of failure	0.1g		0.2g		0.4g	
		Initial crack	Failure	Initial crack	Failure	Initial crack	Failure
No of stories	10	6.6	0.5	38.9	4.6		
	8			35.7	4.0	88.0	33.9
	6					77.4	23.7
	4					57.8	6.8

Reference

- 1 "Uniform Standard on Structural Design of Buildings" of the People's Republic of China.
- 2 Huo Zizheng, Wang Wenguang, Zhang Luo, Lan Jie, Zhang Yao: "Limit Value of Number of Stories of Brick Residential Building in Earthquake Area" Research report of Shaanxi Research Institute of Building and Construction. 1985

COMPARISON OF U.S. AND CHINESE METHODOLOGIES
FOR THE SEISMIC EVALUATION AND STRENGTHENING
OF EXISTING UNREINFORCED MASONRY STRUCTURES

Neil M. Hawkins¹, F. Chou² and X. Yin³

SUMMARY

A comparison is made of the separately developed and tested U.S. and Chinese methodologies for the seismic evaluation and strengthening of existing unreinforced multistory masonry buildings. It is shown that the methodologies of both countries work reasonably well for the type of unreinforced masonry building encountered in that country. However, neither is appropriate for the building type commonly encountered in the other country. There are major differences in the dynamic models assumed in the two methodologies, in the assumed increase in shear strength with axial load, and in the significance attached to the diaphragm's role.

INTRODUCTION

One of the most pressing earthquake hazard mitigation issues is how best to proceed with the seismic evaluation of an existing structure and, if necessary, its strengthening. In the USA and China seismic evaluations of existing structures have been carried on for many years with the resultant accumulation of considerable theoretical and practical experience. However, the record shows that in the USA there is no unanimity of opinion as to the appropriate procedures for such evaluations and any necessary subsequent strengthening. What is clear is that a structure's total dynamic response must be considered. If a building is strengthened inappropriately, from a dynamic response viewpoint, its seismic resistance for subsequent earthquakes can be lowered to less than that extant before strengthening (1,2). It is better, and undoubtedly more cost effective, to work with the building's existing structural system than to superimpose another system on the existing system, and to trust that both systems will work satisfactorily together (3,4).

This paper forms part of a research study of the "Seismic Strengthening of Unreinforced Masonry and Inadequate Strength Concrete Frame Buildings." That research was sponsored by the US National Science Foundation under grant CEE-8212079 and was a joint activity of the Department of Civil Engineering, University of Washington, and the Institute of Earthquake Engineering, China Academy of Building Research.

1 Professor and Chairman; 2, 3 Research Assistants, Civil Engineering, University of Washington, Seattle, WA 98195.

AMERICAN URM BUILDINGS AND EVALUATION PROCEDURE (7)

Characteristics of American URM Building

Shown in Fig. 1 is the floor plan and elevation of a Seattle URM building that has characteristics typical of American URM buildings. Surveys (7,8) have shown that American URM buildings generally have the following characteristics:

- (1) In their unstrengthened state, they are not engineered for either vertical or lateral loads. They were constructed at the turn of the century and were proportioned by rules of thumb.
- (2) The URM walls are bearing walls located on the building's perimeter. Typically their height-to-thickness ratios are between 10 and 20. The interior of the building is spacious.
- (3) The roof and floor systems are timber.
- (4) Ties connect the exterior masonry walls to the floors and roofs. However, the spacing and size of those ties are arbitrary and their strength usually inadequate for severe excitations.
- (5) The thick walls make the building's weight significant. Consequently, subsoil conditions have little influence on the building's response unless it is located on fill.
- (6) There are many large openings in the exterior walls, especially in the first story.
- (7) There are often ornaments on the building's facades and parapets, gables and chimneys on its roof.
- (8) Several buildings with abutting walls often constitute a city block. In an earthquake those buildings respond as a single unit rather than as individual units.

URM buildings have suffered badly in US earthquakes with the degree of damage being almost directly dependent on the intensity of the ground motion. For strong motions in 0.2G regions, damage has been due primarily to the breaking away of inadequately anchored parapets, cornices, etc., and the collapse of inadequately tied URM walls under out-of-plane bending actions. Only for base motions of 0.2G or greater have diagonal cracks due to in-plane shearing actions been observed in walls. Collapse of walls under in-plane actions has generally not been observed until base motions of about 0.4G (6).

American Evaluation Procedure

The most widely accepted American methodology, the ABK methodology (7) recognizes that appropriate evaluation procedures differ according to the EPA Zone, 0.1G, 0.2G or 0.4G in which the building is located. A shortened flow chart for a URM building in an EPA Zone of 0.4G is shown in Fig. 2. The methodology has essentially three parts: (1) a field survey of the existing building; (2) a seismic evaluation based on the results of the field survey; and (3) design of the required retrofit.

The seismic evaluation has three major phases involving examination of: (1) the adequacy of the anchorages connecting the walls to the roof and floors; (2) the dynamic stability of the walls for out-of-plane loading; and (3) the adequacy of the vertical load-carrying system for seismic excitations. In accordance with observed behavior, the methodology assumes that ground motions are transmitted upward without magnification by the walls in the direction of the motion responding essentially as rigid bodies. Those walls excite the ends of the diaphragms which can amplify the earthquake motions and drive the response of the out-of-plane walls. Thus, adequate ties between the out-of-plane walls and the diaphragms are essential to the stability of the out-of-plane walls. Further, for severe excitations the diaphragms can yield, limiting the inertial forces applied by the diaphragms to the in-plane walls, and therefore reducing the probability of cracking in those walls as compared to a building with non-yielding diaphragms. Only when ground accelerations become large is cracking of the in-plane walls likely, and then two modes of failure are possible: (1) collapse of the piers between doors and windows in combined axial loading and shear; and (2) concentration of damage at one floor level due to an inadequate lateral load restoring capacity for the given displacement.

For combined axial load and shear, the maximum shear force, V_N , that can be carried by a given pier is taken as $2/3 v_a$ times the net area of the pier. The allowable bed-joint shear, v_a , is determined from in-place shear tests on individual bricks and is taken as:

$$v_a = A(Bv_t + \sigma_o) \quad (1)$$

where A = a constant to adjust for workmanship and taken as 0.75;
 B = reduction factor to adjust test values for probable bonding of collar joint and taken as 0.75;
 v_t = basic bed-joint shear stress equal to stress for which 20 percent of test values are less, when test values are adjusted to value for zero axial stress on bed-joint; and
 σ_o = axial stress normal to bed-joint.

For a wall with frequent openings, lateral displacements are likely to cause cracking through the depth of the ends of the piers as shown in Fig. 3. Experiments (7) have demonstrated that the maximum lateral load restoring shear resistance, V_R , for that situation is effectively:

$$V_R = 0.9 PD/H \quad (2)$$

where P is the axial force on the pier; D its depth in the direction of motion and H its height.

CHINESE URM BUILDINGS AND EVALUATION PROCEDURE (5,10)

China has unique field experience on the performance of masonry buildings as a result of the 1975 Haicheng and 1976 Tangshan earthquakes. China

has learned that buildings up to six stories in height, when evaluated, and if necessary strengthened according to the procedures described in References 5 and 10 can resist intense ground shaking with only limited damage and without collapse.

Characteristics of Chinese URM Buildings

Chinese URM buildings (10) usually have the following features:

- (1) They were built to a design that did not include seismic considerations;
- (2) Height to thickness ratios are typically 20 to 40 for perimeter walls and 30 to 60 for partition walls. Brick grades are between 700 and 1,000 psi and mortar grades between 150 and 300 psi. Those ratios and material strengths are considerably greater than for the older US URM buildings;
- (3) Roof and floor systems are cast-in-place or precast, made monolithic, reinforced concrete slabs. Corridor floors are short span, topped but not made monolithic, precast slabs, and sometimes the roof is wooden;
- (4) Original architectural and structural documents are still available;
- (5) Rooms are not spacious and are created by multiple URM cross-walls;
- (6) Walls are arranged symmetrically throughout the building's plan and are continuous over its height;
- (7) The fraction of the perimeter wall area punctured by holes is considerably less than for an American Building.

The earthquake performance of non-strengthened Chinese buildings has depended more on the total structural concept for the building, and the faithfulness with which that concept was executed, than the adequacy of the individual structural components. The poorest performance has been for buildings for which the framing was essentially longitudinal load-bearing walls, with few transverse walls, and the diaphragms were precast concrete. The performance for buildings with both longitudinal and transverse load-bearing walls and cast-in-place floors was strikingly better. The characteristics of a building's elevation have had more effect on its performance than the characteristics of its plan. For buildings of irregular plan or elevation, or differing cross-wall framing systems, damage has decreased as deformation differences for the brick walls either on the same floor or in the same vertical plane, has decreased. This observation demonstrated the desirability of tying the building together, provided that tying resulted in reduced relative deformations; the desirability of having equal door and window spacings so that the rigidities of intervening piers were approximately the same; and the desirability of keeping vertical openings for refuse chutes, drains, etc., out of areas, such as connections, that are vital to the structural integrity of the building.

Chinese Evaluation Procedure

The Chinese seismic evaluation procedure, Fig. 5, has four parts: (1) A survey of the building's existing condition; (2) Determination of the intensity (Chinese scale) for the evaluation; (3) Assessment of the significance of any building irregularities and the potential for secondary damage (gas explosions, fire, etc.) following an earthquake; and (4) Evaluation of the building's seismic resistance. That last step has both

analytical and empirical components. In the analytical component, calculated wall-to-floor area ratios are compared to permissible minimum values. Those minimums are based on a mathematical model which assumes that the building deforms primarily in shear, has six stories or less of equal height and weight, has a uniformly distributed mass and stiffness and has a capacity limited by the principal tensile strength of the wall. The empirical component includes consideration of the building's height, the dimensioning of its brick piers, the adequacy of the concrete ring beam surrounding each diaphragm and the adequacy of the connections between ring beams and walls and roof.

The shear resistance, V_N , of a wall is based on the formula:

$$V_N/A_e = \zeta v_t \sqrt{(1 + \sigma_o/v_t)/K} \quad (3)$$

where K = factor of safety, taken for load-bearing walls, as 2.0 for design intensity 7 (EPA of 0.1G), and 1.4 for intensities 8 and 9 (EPA's of 0.2 and 0.4G) and reduced by 25% for non-load-bearing walls.

ζ = coefficient for non-uniform distribution of shear stress and equal to 1.2 for a rectangular cross-section.

v_t = tensile strength of wall. Value is related directly to mortar strength and equals 2 kg/cm^2 for 25 kg/cm^2 mortar.

σ_o = average compressive stress on wall.

A_e = effective cross-sectional area of wall. Equal to thickness times effective length at mid-height. If height to thickness of pier exceeds 5.0, its A_e is taken as zero.

For buildings with rigid diaphragms, calculations for wall-to-floor area ratios utilize the A_e values for all walls parallel to the seismic loading direction. For flexible diaphragms, separate calculations are made for each wall. For buildings with precast reinforced concrete diaphragms, wall-to-floor area ratios are computed using the average of the ratios for a stiff and a flexible diaphragm.

COMPARISON OF AMERICAN AND CHINESE EVALUATION PROCEDURES

The philosophies of the American and Chinese procedures differ. The American procedure is closely tied to dynamic responses observed in laboratory tests on elements. The Chinese procedure is tied to what has proven effective for their buildings in severe earthquakes. Obviously, each procedure is effective for the given country's construction. Both procedures presume that the walls in the direction of the motion respond essentially in shear and that ties between out-of-plane walls and diaphragms are critical to effective performance. Differences result primarily from the diaphragm's assumed response and the nature of the interior gravity load-carrying system. A flexible wooden diaphragm is the norm in an American building and a rigid diaphragm the norm in a Chinese building. Further, wall-to-floor and roof ties are more frequent and more reliable in their characteristics for Chinese than American construction. Interior partition

walls in China are usually masonry, and therefore the effective uniformly distributed weight of the structure is usually greater in China than the USA. Since Chinese construction is recent, mortar and brick strengths are greater and wall height-to-thickness ratios are also greater for Chinese than American buildings. Finally, in China ventilation ducts and refuse chutes are often buried in the wall reducing their effective thickness, while in the USA the walls at the lowest floor level are often punctured by large openings for store fronts and doors. Thus, in-plane wall failures in shear are consistent with Chinese construction and out-of-plane wall failures for the upper floors are consistent with the inadequate ties and softer lower stories of USA buildings.

The Chinese and American procedures were used to evaluate the building whose plan and elevation are shown in Fig. 1. That evaluation was made for EPA Zones of both 0.2 and 0.4G (Chinese intensities of 8 and 9). The vertical load-carrying system for the building was interior timber columns, timber diaphragms and URM clay brick lime mortar walls. Consistent with results for in-situ tests on buildings of similar age in the same area of Seattle, the compressive strength of the mortar and brick were taken as 300 and 1,000 psi, respectively. Since both the Chinese and US procedures yielded almost the same base shear for low-level excitations, direct numerical comparisons between the two procedures were possible. Only differences in the predicted in-plane capacities of the walls are examined in this discussion.

Shown in Table 1 are the predicted locations of the weakest story in each wall and the ratio of the strength provided at that level to the strength predicted as necessary for intensities 8 and 9, respectively. For the Chinese procedure, the building was weakest at the second floor on wall line A (Fig. 1). With the 1.4 factor of safety for the Chinese procedure neglected, that wall had only 66 and 33% of the strength predicted as necessary for intensities of 8 and 9, respectively. For the American procedure with restoring capacity issues ignored, the building was predicted as weakest on wall line A, but at the fifth-floor level. Further, the strength was inadequate only for an EPA Zone of 0.4G.

That building withstood the 1965 Seattle earthquake without damage. Maximum ground accelerations in the N-S and E-W directions were almost equal at about 0.085G. Thus, the response of the building in the 1965 quake was consistent with the predictions of both procedures. However, according to the Chinese procedure, wall A would have collapsed if the E-W acceleration had reached 0.13G. Differences in the predictions of the American and Chinese procedures were primarily the result of differences in the predicted increase in shear strength with axial stress and differences in the mathematical models used for determining the building's seismic response.

Increase in Shear Strength with Axial Stress

Shown in Fig. 6 are the predicted increases in wall shear strength with axial stress according to Eqs. (1) and (3). For the Chinese procedure,

the wall's shear resistance for zero axial load, v_t , was taken as the principal tensile strength of the wall, R_j (5). Also shown in Fig. 6 are expressions recommended in Reference (12) and (13) for a wall's shear strength based on the results of US and Chinese racking tests. Unbroken lines indicate the range over which test data were obtained. For all four expressions shown in Fig. 6, correction factors for workmanship, safety, and non-uniform shear distribution were neglected. Shown to scale at the top of Fig. 6 are the σ_0/v_t ratios acting on the east-west walls at 0.4G for the American procedure. Ratios of the strengths predicted by Eq. (1) to those predicted by Eq. (3) vary from 1.04 to 2.33 for wall A. Obviously strength predictions for that wall will vary widely depending on whether Eq. (1) or (3) is used.

Listed in Table 1, as the predictions of the American (modified) procedure, are the strengths obtained when Eq. (3) is used as the limiting shear capacity in the American procedure. With that substitution, differences between the predictions of the American and Chinese procedures are sharply reduced. In addition for the Chinese procedure, σ_0 values were calculated using the recommended "more exact" expression. Resulting values were between 97 and 192% of the corresponding σ_0 values for the American procedure. When σ_0 values for the Chinese procedure were taken as those calculated by American procedures, the Chinese (modified) strengths of Table 1 were obtained. That adjustment further reduced differences in strengths predicted by the two methods. The proper strength comparison is that of the American (modified) and the Chinese (modified) procedure and for that comparison the average strength for the north-south walls (walls 1, 3 and 6) is the same for both procedures, while the average strength for the east-west walls is considerably less for the Chinese than American procedure.

Influence of Diaphragm Action on Mathematical Model

The loading paths and deformations assumed in the Chinese and US response models are shown in Figs. 7 and 8, respectively. In both figures the deformed building is shown on the left and the undeformed building on the right. For the Chinese model the building deforms as a single unit in shear. Consequently for a ground displacement Δ_G , the displacement at the center of the roof, Δ_D , exceeds Δ_G even though no amplification of Δ_G by diaphragm deformations is recognized. Limitations on the maximum spacing for cross-walls reinforce that deformation pattern. Effectively for a building located in an EPA Zone of 0.4G, the in-plane end wall must be designed for the base shear, V , shown on Fig. 7.

For the American procedure it is assumed that the in-plane wall translates primarily as a rigid body and that it is the diaphragm's amplification of that end motions that result in roof displacements Δ_D exceeding Δ_G . Thus, for low-level excitations the in-plane end wall must be designed for the same shear as for the Chinese procedure. However, for high-level excitations the American procedure recognizes that the diaphragm can yield so that a limitation must be placed on V as shown in Fig. 8. Since the yield capacity of the usual American wood diaphragm is relatively low, the upper bound shown in Fig. 8 usually determines the design shear, V .

Recognition that the diaphragms can yield is the prime reason the American (modified) procedure (Table 1), predicts a building with strengths equal in the N-S direction, but greater in the E-W direction, than the strengths predicted by the Chinese (modified) procedure. For the E-W direction and a 0.4G ground motion, the American procedure predicted shear yield of the wood diaphragms at values between one-half and one-eighth the shear predicted for the Chinese model. For the N-S direction, however, the American procedure predicted that the diaphragms between walls 1 and 3 remained elastic at the second, third and fourth floor for the same intensity of ground motion.

Influence of Openings

The walls of American buildings are usually perforated at frequent intervals by windows and doors resulting in piers between openings that can be slender and, on any given line, variable in width. The opening of flexural cracks at the ends of such piers, Fig. 3, raises the possibility of the structure falling sideways due to cumulative racking deformations or the failure of the piers in combined flexure and shear. For a wall with K piers at the given level, the American procedure predicts satisfactory performance only if the restoring shear resistance for the wall as a whole, $\sum V_R$, exceeds the restoring shear force, $\sum V_P$. The quantity $\sum V_P$ is taken as half the shear V on the wall at the given level for V calculated as shown in Fig. 8. The quantity V_R is calculated from Eq. (2). If $\sum V_R$ is less than $\sum V_P$ but for all piers $V_R < V_N$ (where V_N is calculated from Eq. 1), then satisfactory racking performance can be obtained by adding materials so that $\sum V_P \leq \sum V_R$. If, however, for any pier $V_R > V_N$, then shear failure of the piers is probable and the capacity of the stiffest element must be checked. The shear V is distributed to piers according to their stiffness D/H . If the shear stress, v , on the stiffest pier exceeds the allowable bed-joint shear, v_a , (Eq. 1), then that individual pier must be strengthened until $v < v_a$.

The walls of Chinese buildings contain fewer openings than American buildings, and the Chinese procedure stipulates certain minimum lengths for intermediate and end piers. Thus, the possibility of racking failures is less for Chinese than American buildings. The Handbook (10) suggests that an opening has no effect until the H/D ratio exceeds 0.8. Then for increasing H/D values the shear capacity should be gradually reduced to zero for H/D values greater than 4.

The requirement of the American procedure that $\sum V_P < \sum V_R$ and that $V = 2 \sum V_P$ can be written as:

$$V \leq \sum \eta v_a A_k / 1.5 \quad (4)$$

where η is a coefficient for the effect of flexure on shear strength and equal to $1.8 (D_k/H_k)(\sigma_o/v_a)$. For the Chinese procedure one logical method for accounting for the influence of flexure on shear strength is to take the shear capacity of pier k as (K_{bs}/K_s) times V_N , where K_{bs} is the shear

stiffness of the pier and K_{bs} is the stiffness in combined bending and shear of the pier. Then for a rectangular pier:

$$\phi = K_{bs}/K_s = \frac{1}{\left(\frac{H_k}{2D_k}\right)^2 + 1} \quad (5)$$

Shown in Fig. 4 is the relation between ϕ , η , and H_k/D_k for σ_o/v_a values of 0.5 and 1.0. The Chinese Handbook recommendation, indicated by broken lines, is close to the American requirement, indicated by solid lines when σ_o/v_a is 0.5, and considerably more stringent when σ_o/v_a is greater than that value. Shown in Table 2 are σ_o/v_a values (for σ_o from the American procedure) for typical piers at different levels and in all four exterior walls of the building of Fig. 1. Column (4) lists the H/D ratio for that typical pier and column (5) the H/D ratio at which flexural effects, according to the scheme of Fig. 4, first become felt. Obviously, restoring force effects are not significant except where there are very slender piers.

AMERICAN AND CHINESE STRENGTHENING MEASURES

The American procedure requires that new materials added to a building provide additional capacity and not replace the capacity of existing materials. Thus, all supplemental materials are designed at their yield capacities. All new masonry is to be reinforced masonry and all new concrete frames to be ductile moment resistant. Chinese strengthening procedures are described in References 9 and 11. Because of considerable US interest in strengthening provided by additional concrete columns and tie rods, an evaluation of the applicability of that method to US buildings was made. While the strengthening elements of this basketing method can often be arranged so that they have an aesthetic, as well as a structural value, this Chinese system is not likely to be useful for US buildings. The older US building often represents an important cultural and economic resource, especially for small towns with economies largely dependent on tourism (8). Alteration of the facade of such buildings is likely to impact tourism and, therefore, be unacceptable to the property owner, the town, and the historic preservationist. There are also strong structural reasons for the non-applicability of basketing. In the US buildings there are few interior masonry cross-walls, and any retrofitted walls are likely to be gypsum or plywood over lightgauge metal or wood framing and not suitable for strengthening. The exterior walls in US buildings are generally thicker than their Chinese counterparts, and the buildings are often open-fronted with slender piers. Thus, methods for extrapolating basketing principles to those situations would have to be developed for US applications. Further, the Chinese building is tied together more firmly in its initial conceptual design than the American building. Basketing reinforces the original Chinese concept. If, however, the US building were stiffened by basketing, more of the inertial effects of the out-of-plane walls would be transferred to the in-plane walls and the basketing would work against the preferred load path for severe excitations.

CONCLUSIONS

Based on the studies reported here, it is concluded that:

- (1) There are considerable differences in the architectural and structural characteristics of existing American and Chinese URM buildings, in the type of damage those buildings have suffered in past earthquakes, and in the procedures used to construct those buildings.
- (2) The American and Chinese seismic evaluation procedures utilize different mathematical models for the building's response, different allowable shear stresses for the masonry, and account for wall openings in different ways. However, both evaluation procedures have yielded convincing results for the existing buildings of the country in which they were developed.
- (3) Proper idealization of the likely dynamic response of the horizontal diaphragms is crucial to the construction of a realistic response model for a URM building.
- (4) The restoring shear capacity concept of the US methodology is a refinement that need not be checked for buildings of the proportions used in China.
- (5) The assumption in the US methodology that it is not necessary to check the in-plane shear resistance of walls in buildings located in an EPA Zone of 0.2G is not consistent with the findings of this paper.
- (6) Strengthening, as used in China, with additional reinforced concrete columns, ring beams and steel tie rods is not appropriate for US buildings.

REFERENCES

- (1) Gallegos, H. and Rios, R., "Earthquake-Repair-Earthquake," SP-53, Reinforced Concrete Structures in Seismic Zones, American Concrete Institute, Detroit, MI, 1977.
- (2) Wei, L. and Zhong, Y., "Seismic Evaluation Procedure for Existing Reinforced Concrete Building Frames," Institute of Earthquake Engineering, China Academy of Building Research, Beijing, Aug. 1984.
- (3) Hawkins, N.M. and Stanton, J.F., "Building Rehabilitation Strategies in Seattle, Washington," Proceedings, PRC-USA Joint Workshop on Earthquake Disaster Mitigation through Architecture, Urban Planning and Engineering, Beijing, 1981.
- (4) Tomazevich, M., Sheppard, P. and Zarnich, R., "Experimental Studies of Methods and Techniques for Repair and Strengthening of Historic Buildings in Old Urban and Rural Nuclei," US-Yugoslavia Joint Workshop on Protection of Historic Structures and Town Centers in Seismic Regions, June, 1985.
- (5) China Academy of Building Research, "Chinese Aseismic Criterion for Evaluation of Industrial and Civil Buildings (TJ 23-77)," Chinese Building Industrial Publishing House, Beijing, 1977. English translation by F. Chou, Department of Civil Engineering, University of Washington, September, 1984.

- (6) Jennings, P.C. and Housner, G.W., "The San Fernando, California, Earthquake of February 9, 1971." Proceedings, Fifth World Conference on Earthquake Engineering, Rome, 1974, Vol. VI, pp. 16.
- (7) ABK "Methodology for Mitigation of Seismic Hazards in Existing Unreinforced Masonry Building: The Methodology," Topical Report 08, Agabian Associates, El Segundo, CA, January 1984.
- (8) Hawkins, N.M. and Burke, P., "Seismic Hazards in Unreinforced Masonry Buildings in Small Towns in the Pacific Northwest," SM 85-1, Dept. of Civil Engineering, University of Washington, Seattle, WA, Apr., 1985.
- (9) Editorial Group, "Regulations for Aseismic Strengthening Design and Construction of Multistoried Brick Buildings with Additional Reinforced Concrete Column," Institute of Earthquake Engineering, China Academy of Building Research, 1984.
- (10) Editorial Group, "Chinese Aseismic Design Handbook for Industrial and Civil Buildings," Research Institute of Aseismic Engineering, China Academy of Building Research, Beijing, 1982.
- (11) Niu, Z., "Calculating Methods of Strengthened and Repaired Brick Masonry Structures for Earthquake Resistance," Proceeding, PRC-USA Joint Workshop on Earthquake Disaster Mitigation through Architecture, Urban Planning and Engineering, Beijing, 1981.
- (12) Fattal, S.G. and Cattaneo, L.E., "Evaluation of Structural Properties of Masonry in Existing Buildings," NBS Building Science Series, No. 62, US Government Printing Office, Washington D.C., 1977.
- (13) Zhu, B., Wu, M. and Jiang, E., "Experimental Study on Basic Behavior of Brick Masonry under Reversed Loading," Journal of Tongji University, No. 21, 1980.

TABLE 1 - COMPARISON OF STRENGTHS PREDICTED BY CHINESE AND AMERICAN PROCEDURES

Procedure	Wall					
	A	K	1	3	6	1
Chinese	Weakest Story					
	I of Required Strength	66	79	226	107	147
	Intensity 8	33	39	113	54	73
American	Weakest Story					
	I of Required Strength	5	3	1	4	5
	0.2G	163	174	246	217	202
American (modified) *	Weakest Story					
	I of Required Strength	81	87	123	108	101
	0.4G	1	1	1	2	1
Chinese (modified) **	Weakest Story					
	I of Required Strength	89	121	167	159	95
	Intensity 8	45	60	83	79	47
Chinese (modified) **	Weakest Story					
	I of Required Strength	2	3	1	4	1
	Intensity 9	60	74	205	107	126
Chinese (modified) **	Weakest Story					
	I of Required Strength	30	37	102	54	63
Chinese (modified) **	Weakest Story					
	I of Required Strength	30	37	102	54	63

* Modified so that v_x relationship for American procedure is that of Chinese procedure.

** Modified so that σ_o value is that of American procedure.

TABLE 2 - EFFECT OF OPENINGS

Wall	Level	σ_o/v_x	H_x/D_x	Critical H_x/D_x
A	1	1.91	4.3	3.4
	4	0.87	2.0	1.6
	5	0.46	1.0	0.8
K	1	1.22	2.0	2.2
	5	0.33	1.2	0.6
1	1	1.70	1.2	2.2
	5	0.45	1.2	0.8
6	1	2.07	4.3	3.7
	4	0.88	2.0	1.6
	5	0.56	1.0	2.0

σ_o from American Procedure; v_x from Chinese Procedure.

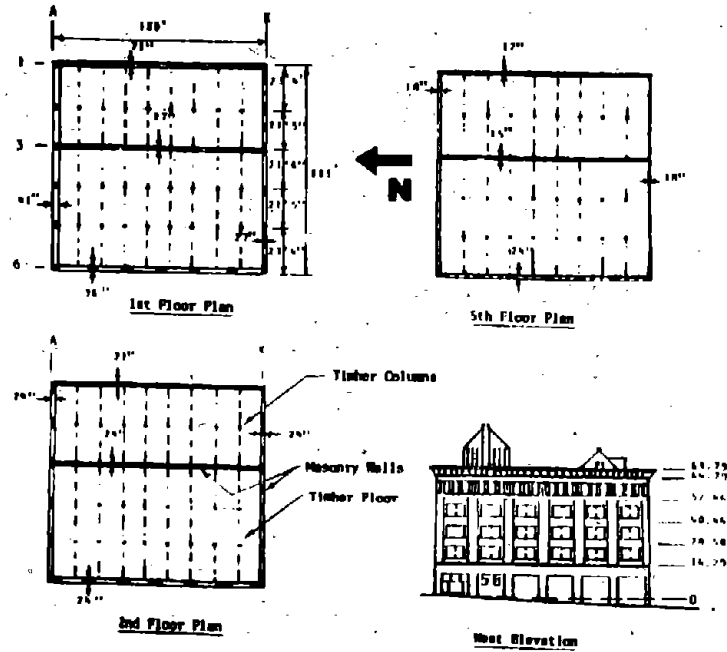


FIG. 1 TYPICAL FLOOR PLAN AND ELEVATION FOR US-URM BUILDING

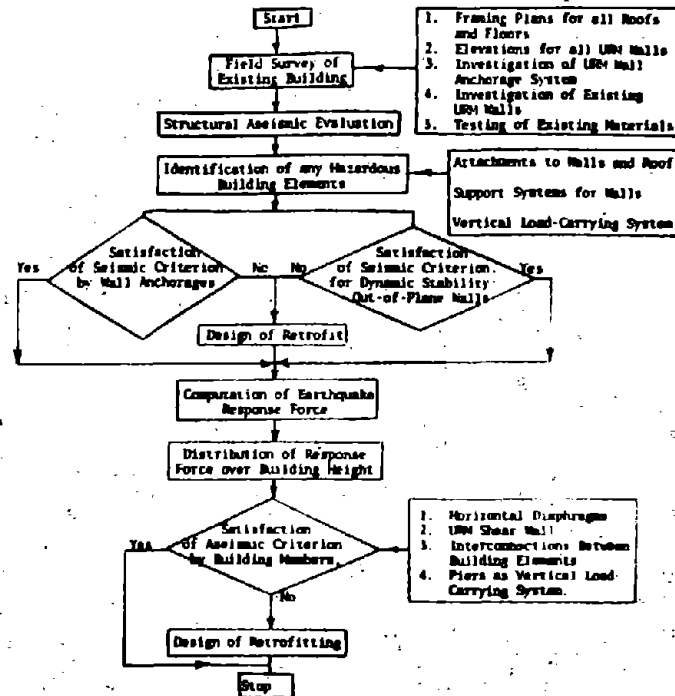
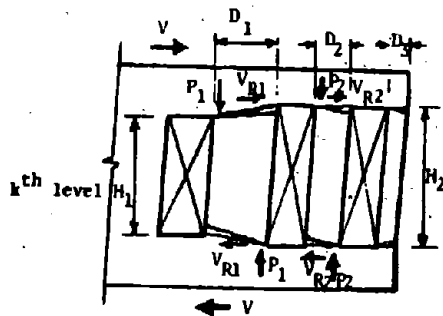


FIG. 2 AMERICAN SEISMIC PROCEDURE FOR BUILDING IN 0.4G KPA ZONE



$$V_{R1} = P_1 D_1 / H_1 \text{ and } V_{R2} = P_2 D_2 / H_2$$

1) If $\frac{1}{2} V_R < V/2$ and $V_R < V_N$ for all piers

Add Materials so that $V/2 \leq \frac{1}{2} V_R$

2) If $V_R > V_N$ Any Pier

Distribute Shears V to Piers According to Shear Stiffness

Strengthen so that $V < V_N$

Influence Coefficient n, β

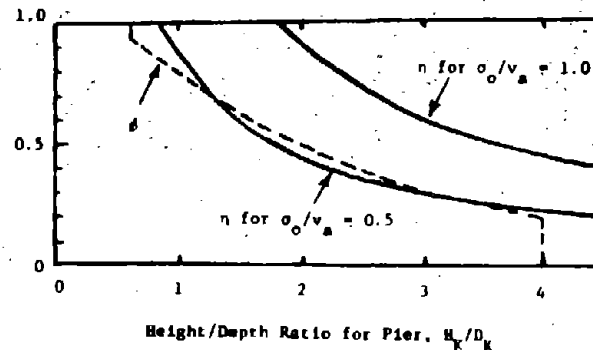


FIG. 3 EFFECT OF OPENINGS FOR US PROCEDURE

FIG. 4 EFFECT OF AXIAL FORCE AND FLEXURE ON SHEAR CAPACITY OF PIERS

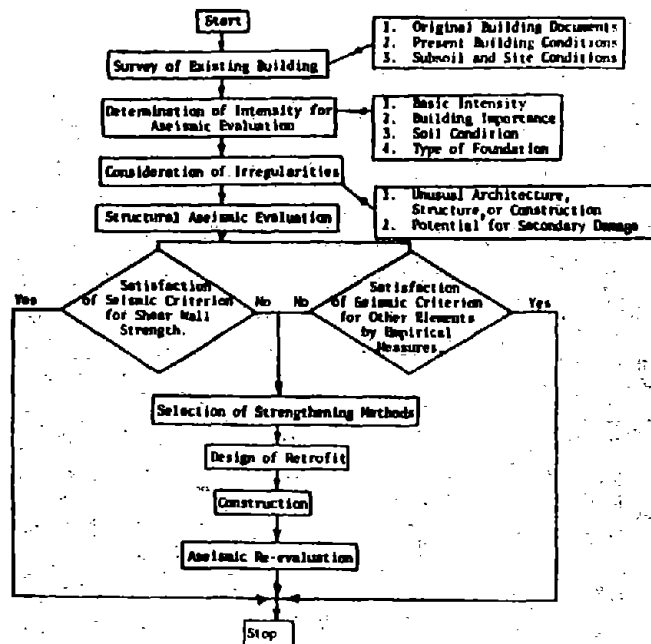


FIG. 5 CHINESE SEISMIC EVALUATION PROCEDURE

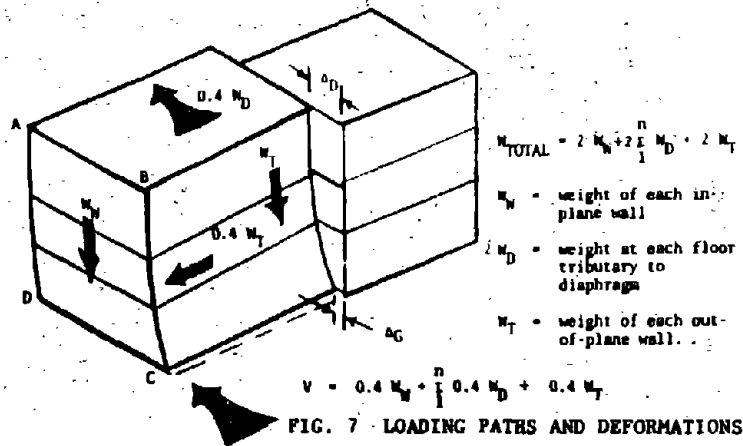


FIG. 7 LOADING PATHS AND DEFORMATIONS FOR PRC PROCEDURE FOR INTENSITY 9 ZONE

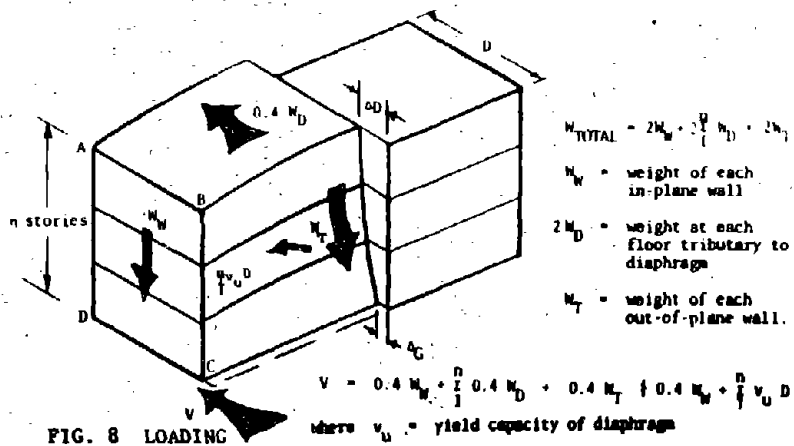


FIG. 8 LOADING PATHS AND DEFORMATIONS FOR US PROCEDURE FOR 0.4G EPA ZONE

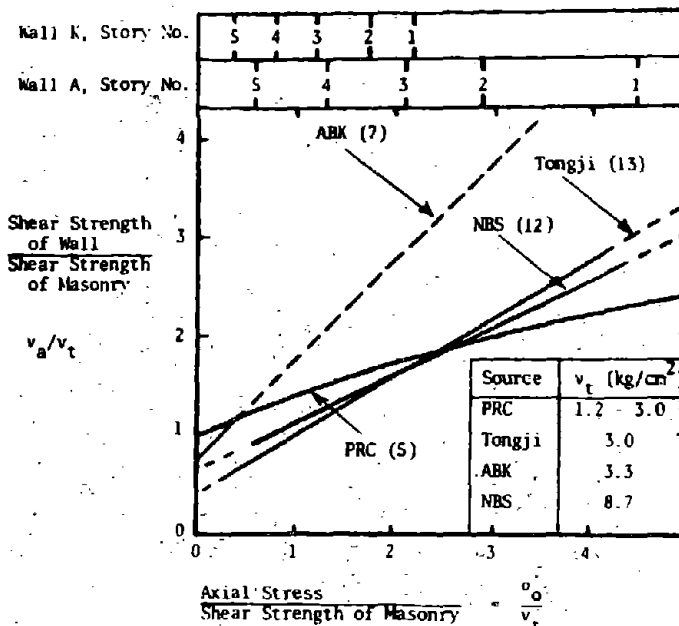


FIG. 6 INCREASE IN WALL SHEAR STRENGTH WITH AXIAL STRESS

SEISMIC COMPUTATION OF STRENGTHENED BRICK STRUCTURES

Niu Zezhen¹

SUMMARY

The methods of calculating strengthened brick masonry walls and columns are presented in this paper. The strengthening technologies of cement mortar coating and reinforced cement mortar coating attached to the wall surfaces are used to strengthen brick walls and columns, and reinforced concrete columns with tie beams are used to strengthen brick buildings. The computation methods are based on testing data obtained by institutions concerned in the recent years. The paper shows that the results calculated by the methods described in this paper are in good agreement with those obtained from experiments. The methods developed in this paper have been adopted in "The Seismic Strengthening Measures for Civil and Industrial Buildings".

INTRODUCTION

The 1976 Tangshan earthquake is one of the catastrophic events in China. One of the important lessons learned from the quake is that strengthening and/or upgrading existing hazardous buildings situated in the areas where a destructive earthquake might occur in the near future are an effective measures for earthquake disaster mitigation. Satisfying with the requirements of large scale seismic strengthening work soon after the Tangshan event, the "Seismic Strengthening Measures for Civil Brick Buildings" and the "Reference Drawings for Seismic Strengthening" are published based on the research works conducted in the institutions concerned. In 1980, the author developed some methods for calculating strengthened brick masonry structures for seismic hazard applications. All of the methods described in the above mentioned references can be used only for solid brick walls.

Since the earthquake resistant capacity for cavity walls and hollow-brick walls is much less than those for solid brick walls, it is in urgent need to develop seismic calculating methods and strengthening technologies for cavity and hollow-brick walls. According to the results obtained from experiments conducted in the recent years, some methods for calculating strengthened brick columns and brick walls including cavity brick walls and hollow-brick walls are described in this paper.

¹ Structural Research Engineer and Head of Fifth Research Section, Institute of Earthquake Engineering, Chinese Academy of Building Research, Beijing, China

The results obtained from the methods presented in this paper are consistent with those from experiments. The following three strengthening technologies are discussed in this paper:

- Using cement mortar coating or reinforced cement mortar coating attached to the surfaces to strengthen brick walls including solid, cavity, and hollow-brick walls
- Using additional reinforced concrete columns with tie beams to strengthen brick buildings
- Using reinforced cement mortar coating or reinforced concrete coating to strengthen brick columns

For regular brick buildings, the calculating tables are provided for simplifying computation process.

USING CEMENT OR REINFORCED CEMENT MORTAR COATINGS TO STRENGTHEN BRICK WALLS

The cement mortar coating or reinforced cement mortar coating can be used to strengthen solid brick wall, cavity brick wall and hollow-brick wall when their earthquake resistance are not satisfied with the requirements specified in the current seismic evaluation criterion. In this case, the lateral stiffness and lateral loading capacity of the strengthened walls can be calculated by following formulae:

$$D = \frac{G_z (A_m + A_s)}{1.2h} \quad (1)$$

$$P = \frac{(R_z j + 0.7\sigma_0)}{1.9} A_m \quad (2)$$

Where

G_z -- Shear modulus of strengthened masonry, $G_z = 0.43E_z$
 E_z -- Modulus of elasticity for strengthened masonry,

$$E_z = (E_m A_m + E_s A_s) / (A_m + A_s)$$

A_m -- Net cross section area of the wall at the middle of the story height before strengthening

A_s -- Net cross section area of the coating at the middle height of the story considered

E_m -- Modulus of elasticity of the unstrengthened brick masonry specified in the current "Design Code for Brick and Stone structures"

- E_s -- Modulus of elasticity of coating mortar specified in Table 1
 h -- Story height
 R_{zj} -- Shear strength converting the strengthened wall to the original wall, for which the greater value obtained from the following formulae can be taken:

$$R_{zj} = \frac{nt_s}{t_m} R_{sj} + \frac{2}{3} R_{mj} + \frac{0.03nA_g}{\sqrt{s} t_m} R_g$$

(Controlled by strength of cement mortar coating)

$$R_{zj} = \frac{0.4nt_s}{t_m} R_{sj} + 0.26R_{mj} + \frac{0.35nA_g}{\sqrt{s} t_m} R_g$$

(Controlled by strength of steel bars in the coatings)

- R_{sj} -- Shear strength of coating mortar specified in Table 1
 R_{mj} -- Shear strength along the horizontal joints of brick masonry specified in the current "Design Code for Brick and Stone Structures", and it can be taken as the half of the code value for the cavity brick masonry wall
 R_g -- Design tension strength of steel bar specified in the current "Design Code for Reinforced Concrete Structures"
 t_m -- Thickness of brick wall including the cavity part
 t_s -- Thickness of mortar coating
 n -- Number of coating layers, $n=1$ for single layer of coating, and $n=2$ for double layers of coatings
 S -- Spacing of reinforcements in reinforced cement coating (cm), and the unit of spacing still keep on cm for its square root
 A_g -- Cross section area for single steel bar
 σ_0 -- Average compression stress at the cross section of brick wall at the level of middle story height

The comparison between testing and calculating results of lateral loading capacity for the sandwichlike strengthened brick wall are listed in Table 2. It shows that the testing values are always greater than that of calculating values. Therefore, the calculating values are of conservative.

For brick buildings up to six stories, if the weight and stiffness are uniformly distributed, the method of minimum ratio of wall cross section area to floor area can be used to check earthquake resistance of strengthened wall. Let α_d (see Table 3) and α_p (see Table 4) are raise coefficients of lateral rigidity and lateral loading capacity for strengthened sandwichlike brick walls respectively:

$$\alpha_d = 1 + \frac{E_s A_s}{E_m A_m} \quad (3)$$

$$\alpha_p = \frac{0.63(R_{zj} + 0.7\bar{\sigma})}{R_r} \quad (4)$$

then, the ratio of seismically strengthened wall cross section area to floor area can be checked by following formulae:

For longitudinal wall and transversal wall with rigid floor diaphragm

$$\frac{\alpha_{pk}}{\alpha_{dk} F} \geq \left[\frac{A}{F} \right]_{\min} \cdot a \quad (5)$$

$$\sum_{i=1}^n \alpha_{di} A_{mi}$$

For transversal wall with flexible diaphragm

$$\frac{\alpha_{pk} A_{mk}}{F_k} \geq \left[\frac{A}{F} \right]_{\min} \cdot a \quad (6)$$

For transversal wall with moderate rigidity diaphragm, such as prefabricated reinforced concrete diaphragm

$$\frac{2\alpha_{pk} A_{mk}}{\alpha_{dk} A_{mk} + \sum_{i=1}^n \alpha_{di} A_{mi} F + F_k} \geq \left[\frac{A}{F} \right]_{\min} \cdot a \quad (7)$$

Where

$\left[\frac{A}{F} \right]_{\min}$ -- Minimum earthquake resistant wall-to-floor area ratio, for solid and cavity brick walls, the $\left[\frac{A}{F} \right]_{\min}$ values in Table 4 of "Seismic Evaluation Criterion for Civil and Industrial Buildings" shall be used; for load bearing cavity brick wall, the $\left[\frac{A}{F} \right]_{\min}$ values in the Table shall be multiplied by the coefficient of 1.27; for non-load-bearing cavity brick wall, the $\left[\frac{A}{F} \right]_{\min}$ values in the Table shall be multiplied by the coefficient of 1.55; and when buildings with cavity brick walls and with average weight of story unit area "W" differed much from 1000kg/m², the $\left[\frac{A}{F} \right]_{\min}$ values calculated by the above mentioned method shall be multiplied by the coefficient W/1000.

a -- Adjustment coefficient, for solid brick wall and hollow-brick wall, "a" in Table 5 of Criterion shall be used, for

cavity brick walls, when the seismic evaluation and strengthening intensity is 7, $a=1.0$ and when the intensity is 8, $a=1.6$

- α_{pk} -- Raise coefficient of lateral loading capacity for kth strengthened wall in the story concerned
- α_{dk} -- Raise coefficient of lateral rigidity for kth strengthened wall in the story concerned
- F -- Story's building floor area
- F_k -- One half of the building area between the two neighboring seismic resistant walls of the Kth earthquake resistant wall
- R_τ -- Shear strength of brick masonry while checking earthquake resistance

$$R_\tau = R_j \sqrt{1 + \sigma_o/R_j}$$

- R_j -- Tension strength of brick masonry, for solid brick wall and hollow-brick wall, it can be taken as the shear strength along the stepped cross section of brick masonry specified in the current "Design Code for Brick and Stone Structures"; for cavity brick wall, one half of the " R_j " values obtained for solid wall shall be used

USING ADDITIONAL REINFORCED CONCRETE COLUMNS TO STRENGTHEN BRICK BUILDINGS

For a multistory brick building, when the lateral loading capacities of most of the transversal walls are less than those calculated by the requirements of "Seismic Evaluation Criterion for Civil and Industrial Buildings" and the difference between them is about 20%, the additional reinforced concrete columns with tie beams can be used to strengthen it. However, in case its total height is greater than limiting height in Table 2 of the Evaluation Criterion in 3m, the placement of the additional R/C columns shall be satisfied the requirements set forth in Table 5.

For the story's transversal brick wall strengthened by R/C columns at both sides and tie beam or tie rod at the wall top, the lateral rigidity (D) and the lateral loading capacity (P) of the strengthened wall can be calculated by following formulae:

$$D = \eta \frac{G_m A_z}{1.2h} \quad (8)$$

$$P = \beta \left[R_\tau A_m + (1 + \alpha_g) R_1 A_c + 0.4 R_{g1} A_{g1} \right] \quad (9)$$

Where

η -- Opening-related coefficient of the wall, $\eta = 1 - 1.2p$

- p -- Opening ratio of the strengthened wall, $p = 1 - A_d/A_z$
 A_d -- Cross section area of the openings
 A_z -- Converting cross section area of strengthened wall

$$A_z = A_m + A_d + 2\eta_g A_c E_c / E_m$$

- A_m -- Net cross section area of brick wall, the cross section area contributed by wall pier with ratio of height to width greater than 4 shall not be considered
 η_g -- Coefficient considering nonuniform distribution of shear stresses, when $h/b \geq 0.5$, $\eta_g = 0.22$ and when $h/b < 0.5$, $\eta_g = 0.20$
 b -- Width of the brick wall of spacing of additional R/C columns
 E_c -- Modulus of elasticity of concrete specified in the current "Design Code for Reinforced Concrete Structures"
 β -- Brick wall type-related coefficient, for solid brick wall and hollow-brick wall, $\beta = 1$ and for cavity wall, $\beta = 0.75$
 γ -- Shear strength-related coefficient of the brick wall, when $h/b \geq 0.5$, $\gamma = 0.7$; when $h/b \leq 0.25$, $\gamma = 0.75$ when $0.25 < h/b < 0.5$, calculating by interpolation
 A_c -- Cross section area of an additional R/C column
 α_g -- Longitudinal reinforcement-related coefficient of additional R/C columns, $\alpha_g = 0.4R_g A_g / R_1 A_c$
 A_g -- Total cross section area of longitudinal reinforcements in an additional R/C column
 R_1 -- Concrete tension strength of additional R/C columns set forth in the current "Design Code for Reinforced Concrete Structures"
 R_{g1} -- Design tension strength of steel rod
 A_{g1} -- Total net cross section area of steel rods of strengthened wall

The strength of the steel tie rod shall conform with the following requirement:

$$R_{g1} A_{g1} \leq (1 + \alpha_g) R_1 A_c \quad (10)$$

When $\beta(\gamma R_1 A_m + (1 + \alpha_g) R_1 A_c + 0.4 R_{g1} A_{g1}) < R_1 A_m / 1.2$, it is necessary to redesign by changing cross section area of additional R/C columns and reinforcement content.

The comparison between testing data and calculating results by formula (9) for the brick walls strengthened by reinforced concrete columns and tie beam or tie rod is shown in Table 6.

For the brick building up to six stories with regular configuration both in plan and elevation, when its seismic transversal walls are uniformly distributed and lacking in earthquake resistance and it is strengthened by additional reinforced concrete columns and tie rods with uniform placement of columns, the seismic shear Q_{zk} subjected by R/C columns and tie rods of story's K th transversal wall can be calculated based on the results obtained from seismic evaluation computation. After that, the cross section and reinforcement content of

R/C columns and diameter of steel tie rods can be selected by Table 7.

For the transversal wall with rigid floor slab:

$$Q_{zk} = \left(\frac{(A/F)_{\min} \cdot a}{1.2A_m/F} - \gamma_m \right) R_r A_{mk} \quad (11)$$

For the transversal wall with flexible floor slab:

$$Q_{zk} = \left(\frac{(A/F)_{\min} \cdot a}{1.2A_{mk}/F_k} - \gamma_m \right) R_r A_{mk} \quad (12)$$

For the transversal wall with moderate rigidity floor slab:

$$Q_{zk} = \left(\frac{(A/F)_{\min} \cdot a}{\frac{2.4A_{mk}}{\frac{F A_{mk}}{A_m} + F_k}} - \gamma_m \right) R_r A_{mk} \quad (13)$$

USING REINFORCED CEMENT MORTAR COATING OR REINFORCED CONCRETE COATINGS TO STRENGTHEN BRICK COLUMNS

Checking earthquake resistance of composite brick column strengthened by reinforced cement mortar coating or by reinforced concrete coating is in a similar way to check eccentric compression strength of composite masonry elements set forth in the "Design Code for Brick and Stone Structures" (GBJ 3-73).

Computation of Fundamental Period of Composite Brick Column

Considering the rigidity of the coating the lateral displacement under the action of lateral unit load at the top of the column can be calculated as follows:

In case of using reinforced concrete coating

$$\delta = \frac{H^3}{3 (E_m I_m + E_c I_c + E_g I_g)} \quad (14)$$

In case of using reinforced cement mortar coating, in equation (14), the $E_s I_s$ shall be used instead of $E_c I_c$. Where the sign δ denotes the lateral displacement under the action of lateral unit load at the top of the column; H, height of composite column; E_c , E_s , E_g , modulus

of elasticity for coating's concrete, coating's cement mortar, and longitudinal steel bars respectively; I_m , I_c , I_s , I_r , the moment of inertia about the centroid axis of converting cross section area of composite brick column for brick masonry cross section area, concrete coating cross section area, cement mortar coating cross section area, and for cross section area of longitudinal reinforcements respectively. When calculating the value of " I_m " the cross section area of flange is neglected.

The fundamental period of composite brick column can be calculated by the following formula:

$$T_1 = 2\pi \sqrt{\frac{(W_1 + W_2/4) \delta}{g}} \cdot \nu \quad (15)$$

Where, T_1 denotes the fundamental period of composite column; W_1 , part of roof weight subjected by one brick column; W_2 , self-weight of one brick column; g , acceleration of gravity; and ν , modified coefficient considering the effect of flange of T-cross section column and the effect of fixed action between truss and columns. The values of ν are listed in Table 8.

Identification of Eccentricity

According to the longitudinal force and seismic moment at the cross section considered, the height of compression zone can be calculated by the following formula:

When using reinforced concrete coating

$$1.05R_m S_{mn} + 1.85R_a S_{cn} \pm 1.2R_s A_s e' + 1.2R_g A_g e = 0 \quad (16)$$

When using reinforced cement mortar coating

$$1.05R_m S_{mn} + 1.85R_s S_{sn} \pm 1.08R_s A_s e' + 1.2R_g A_g e = 0 \quad (17)$$

In case the longitudinal force N is applied on the outside of both centres of gravity of compression steel bars (A_s') and of tension steel bars (A_s), the positive sign shall be taken for the third term in left-hand member of the equations of (16) and (17), otherwise the negative sign shall be taken. The eccentricity can be identified by the ratio between the converting moment of cross section area of composite brick column (S_z) and of compression zone area of composite brick column (S_{z_a}) about the centre of gravity of steel bars subjected to less compression or tension. In case of $S_{z_a}/S_z < 0.8$, the great eccentricity shall be identified; while in case of $S_{z_a}/S_z \geq 0.8$, the small eccentricity shall be recognized. In equations of 16 and 17, N denotes longitudinal force applied to composite brick column; R_m , R_a , and R_s , axial compression

ssion strengths of brick masonry, coating concrete, and coating cement mortar respectively; R and R' , tension and compression strengths of design of reinforcements respectively; S_{mm} , S_{cn} , and S_{sn} , moment of compression zone area of cross section of brick masonry, coating concrete, and coating cement mortar about applied point of vertical axial force respectively; A_g and A'_g , cross section of tension and compression reinforcements respectively; and e and e' , distance between applied point of longitudinal force and centres of gravity of A_g and A'_g respectively.

Formulae for Checking Earthquake Resistance

Great Eccentricity in Compression

Using reinforced concrete coating:

$$KN \leq \phi_z (1.05R_m A_{ma} + 1.85R_a A_{ca} + 1.2R'_g A'_g - 1.2R_g A_g) \quad (18)$$

Using reinforced cement mortar coating:

$$KN \leq \phi_z (1.05R_m A_{ma} + 1.85R_s A_{sa} + 1.08R'_g A'_g - 1.2R_g A_g) \quad (19)$$

Small Eccentricity in Compression

Using reinforced concrete coating:

$$KN \leq \phi_z \{ 0.85R_m S_m + 1.5R_a S_c + 1.2R'_g A'_g (h_o - a'_g) \} / e \quad (20)$$

Using reinforced cement mortar coating:

$$KN \leq \phi_z \{ 0.85R_m S_m + 1.5R_s S_s + 1.08R'_g A'_g (h_o - a'_g) \} / e \quad (21)$$

Where,

- K -- Design strength safety factor of composite column, for intensity 7, $K=1.7$; for intensity 8 and 9, $K=1.5$
- A_{ma} , A_{ca} , A_{sa} -- Compression zone area of cross section of brick masonry, coating concrete, and coating cement mortar respectively
- h_o -- Effective height of cross section of composite column
- a'_g -- Distance between centre of gravity of A_g and the nearest side of cross section
- ϕ_z -- Longitudinal buckling coefficient of composite column
 $\phi_z = 1 / [1 + 1.5(R_z/E_z)(H_o/h)^2]$
- R_z , E_z -- Converting strengthen and modulus of elasticity of cross section of composite brick column respectively
- H_o -- Computation height of composite brick column, and
- h -- Cross section height parallel to the direction of seismic load for composite brick column

The comparison of N values between testing and calculating results for composite brick column is shown in Table 9. It shows that the calculating results are in good agreement with testing one.

ACKNOWLEDGMENTS

The author is indebted to Mr. Lou Yonglin, Mr. Bai Aodong, and Mr. Cui Jianyou for the data they provided and information they collected to make this paper possible.

Table 1 MECHANICAL PROPERTIES OF CEMENT MORTAR(kg/cm²)

grade of mortar	axial compression strength (R _s)	shear strength (R _{sj})	modulus of elasticity
75	38	12	5.9×10 ⁴
100	50	14	7.4×10 ⁴
150	77	17	9.6×10 ⁴

Table 2 COMPARISON OF LATERAL LOADING CAPACITY BETWEEN TESTING AND CALCULATING VALUES FOR STRENGTHENED SANDWICHLIKE WALLS

type of wall	thickness of wall (mm)	number of specimens	testing/calculating			data prov. by
			average	standard deviation	variat. coeff.	
solid	240	21	1.007	0.129	0.128	(1)
solid	180	4	1.340	---	---	(2)
hollow-brick	180	13	1.215	0.107	0.088	(3)
cavity	240	27	1.639	0.230	0.140	(4)

Note: (1) Building Research Institute of Liaoning Province
 (2) Building Research Institute of Yunnan Province
 (3) Building Research Institute of Sichuan Province
 (4) Building Research Institute of Jiangsu Province

Table 8 MODIFIED COEFFICIENT OF FUNDAMENTAL PERIOD FOR COMPOSITE BRICK COLUMN

type of roof truss	$\frac{\text{flange width of brick column}}{\text{web width of brick column}}$	modified coeffic.
R/C	≥ 5	0.8
	< 5	0.9
wooden, steel and wooden, light steel	≥ 5	0.9
	< 5	1.0

TABLE 3 ENHANCEMENT COEFFICIENT OF LATERAL STIFFNESS OF STRENGTHENED SANDWICHLIKE BRICK WALLS (α_d)

number of coatings		single			double		
thickness of coating(mm)	grade of coating mortar	4	10	25	4	10	25
20	100	1.39	1.12	--	2.71	1.98	1.70
	150	1.58	1.13	--	3.22	2.27	1.91
30	100	1.71	1.30	1.15	3.57	2.47	2.06
	150	2.00	1.46	1.26	4.33	2.90	2.37
40	100	2.03	1.49	1.29	4.43	2.96	2.41
	150	2.43	1.70	1.44	5.44	3.54	2.83

Note: The values in the Table shall be used for solid and hollow-brick walls with thickness of 24cm. In case its thickness is t_m , α_d in the Table shall be corrected. When using double coatings, $\alpha_{dt} = 24d_d/t_m - (24/t_m - 1)$; and when using single coating, $\alpha_{dt} = 24d_d/t_m - 0.75(24/t_m - 1)$. For cavity brick wall, $\alpha_d' = 1.67 (\alpha_d - 0.4)$

TABLE 5 INSTALLATION OF ADDITIONAL COLUMNS FOR BUILDING WITH HEIGHT EXCEEDANCE

spacing between transverse walls(L)	intensity	
	7	8 and 9
$L < 4.5m$	Intersection of interior and exterior walls at every other bay, intersection of interior and exterior walls of staircase and quoin of exterior walls	Intersection of interior and exterior walls at each bay and quoin of exterior walls
$L \geq 4.5m$	each bay along exterior longitudinal walls and quoin of exterior walls	

TABLE 9 COMPARISON BETWEEN TESTING AND CALCULATING VALUES FOR AXIAL FORCE (N) OF COMPOSITE BRICK COLUMNS

strengthening measure	eccentricity	specimen number	testing/calculating			data prov. by
			average	standard deviation	variat. coeff.	
R/C coating	great	3	0.909	0.108	0.119	(3)
	small	6	1.293	0.268	0.207	
reinforced cement mortar coating	great	2	1.021	0.163	0.160	(5)
	small	3				
		6	1.300	0.249	0.192	(3)

Note: The name of (3), see Table 2; and (5), see Table 6

TABLE 4 ENHANCEMENT COEFFICIENT OF LATERAL LOADING CAPACITY OF STRENGTHENED SANDWICHLIKE BRICK WALL (d_p)

thickness of walls (mm)	number of coating	grade of masonry mortar		L							LO					25					
		thickness of coating (mm)	grade of coat. mortar	spacing of steel bars (mm)							spacing of steel bars (mm)					spacing of steel bars (mm)					
				150	200	300	400	500	no	150	200	300	400	500	no	150	200	300	400	500	no
240	single	20	100	--	--	--	--	--	1.46	--	--	--	--	--	1.04	--	--	--	--	--	--
			150	--	--	--	--	--	1.63	--	--	--	--	--	1.24	--	--	--	--	--	--
		30	100	2.37	2.23	2.06	1.93	1.86	1.80	1.60	1.50	1.35	1.33	1.32	1.27	1.15	1.07	--	--	--	--
			150	2.43	2.29	2.12	2.06	2.05	1.99	1.64	1.54	1.45	1.44	1.43	1.40	1.19	1.12	1.11	1.11	1.10	1.08
		40	100	2.46	2.33	2.16	2.14	2.14	--	1.66	1.57	1.51	1.51	1.50	--	1.21	1.17	1.16	1.16	1.16	--
			150	2.53	2.41	2.37	2.36	2.35	--	1.72	1.67	1.66	1.65	1.64	--	1.30	1.29	1.28	1.27	1.26	--
	double	20	100	--	--	--	--	--	2.08	--	--	--	--	--	1.46	--	--	--	--	--	1.13
			150	--	--	--	--	--	2.31	--	--	--	--	--	1.62	--	--	--	--	--	1.25
		30	100	3.42	3.22	2.97	2.81	2.70	2.55	2.35	2.22	2.05	1.94	1.85	1.72	1.77	1.66	1.52	1.43	1.43	1.38
			150	3.49	3.31	3.07	2.91	2.89	2.81	2.42	2.29	2.11	2.05	2.04	1.98	1.82	1.71	1.59	1.58	1.57	1.53
		40	100	3.53	3.36	3.12	3.02	3.01	--	2.45	2.32	2.15	2.14	2.13	--	1.84	1.74	1.65	1.65	1.64	--
			150	3.64	3.46	3.32	3.31	3.30	--	2.52	2.39	2.34	2.34	2.33	--	1.90	1.81	1.80	1.80	1.79	--
360	single	20	100	--	--	--	--	--	1.22	--	--	--	--	--	--	--	--	--	--	--	
			150	--	--	--	--	--	1.33	--	--	--	--	--	--	--	--	--	--	--	
		30	100	1.88	1.77	1.63	1.53	1.51	1.47	1.24	1.16	1.16	1.15	1.15	1.12	--	--	--	--	--	
			150	1.94	1.82	1.69	1.68	1.67	1.64	1.28	1.19	1.18	1.18	1.17	1.16	--	--	--	--	--	
		40	100	1.96	1.85	1.75	1.74	1.74	--	1.24	1.24	1.23	1.22	1.22	--	--	--	--	--	--	
			150	2.03	1.94	1.93	1.92	1.91	--	1.37	1.36	1.36	1.35	1.35	--	1.06	1.06	1.05	1.04	1.04	--
	double	20	100	--	--	--	--	--	1.71	--	--	--	--	--	1.20	--	--	--	--	--	
			150	--	--	--	--	--	1.89	--	--	--	--	--	1.33	--	--	--	--	--	
		30	100	2.76	2.60	2.40	2.27	2.17	2.09	1.88	1.77	1.62	1.53	1.51	1.47	1.39	1.30	1.18	1.17	1.17	1.14
			150	2.83	2.67	2.47	2.37	2.36	2.32	1.94	1.82	1.68	1.67	1.66	1.63	1.43	1.34	1.29	1.29	1.28	1.26
		40	100	2.86	2.71	2.51	2.47	2.46	--	1.96	1.85	1.75	1.74	1.74	--	1.45	1.36	1.35	1.34	1.34	--
			150	2.95	2.80	2.73	2.72	2.71	--	2.03	1.94	1.93	1.92	1.91	--	1.50	1.49	1.49	1.48	1.48	--

- Note: 1. "no" denotes that there are no steel bars in coatings.
 2. The diameter of steel bars in the Table is $\phi 6$, and $R_g = 2400 \text{ kg/cm}^2$.
 3. For cavity brick wall, the grade of masonry mortar shall be decreased in one grade.

TABLE 6 COMPARISON BETWEEN TESTING AND CALCULATING VALUES OF LATERAL LOADING CAPACITY OF BRICK WALL STRENGTHENED BY ADDITIONAL REINFORCED CONCRETE COLUMNS

type of brick wall	opening	number of specimen	testing/calculating			data prov. by
			average	standard deviation	variat. coeff.	
solid brick wall	no	12	0.991	0.136	0.138	(5)
		9				(6)
		3				(7)
		2				(3)
		4				(8)
1/4 scale solid wall	no	6	1.161	0.108	0.093	(9)
	opening	5	1.138	0.191	0.167	(10)
		14				
cavity brick wall	no	12	1.191	0.136	0.114	(4)

Note: (3) and (4) see Table 2;

(5)-- Institute of Earthquake Engineering, China Academy of Building Research

(6)-- Dali Polytechnical Institute

(7)-- Institute of Structural Theory, Tongji University

(8)-- Building Research Institute of Ganshu Province

(9)-- Building Research Institute of Shandong Province

(10)- Building Research Institute, Beijing Design Institute

TABLE 7 SELECTION OF CROSS SECTION AND REINFORCEMENTS FOR ADDITIONAL COLUMNS AND OF STEEL TIE RODS

NO.	$Q_{2k}(t)$	cross section of columns (mm by mm)	longitudinal reinforcements	steel tie rods	remark
1	12	250×150	4Φ12	2Φ16	mark of concrete is 200
2	13	240×200	4Φ12	2Φ16	
3	14	250×200	4Φ12	2Φ16	
4	15	240×240	4Φ12	2Φ18	grade of steel is I
5	16	300×200	4Φ12	2Φ18	
6	16	250×250	4Φ12	2Φ18	
7	17	300×240	4Φ12	2Φ18	is I
8	18	300×240	4Φ12	2Φ20	
9	20	300×250	4Φ14	2Φ20	
10	20	300×240	4Φ14	2Φ20	
11	22	360×240	4Φ14	2Φ20	
12	24	360×240	4Φ16	2Φ22	
13	26	350×250	4Φ18	2Φ22	
14	19	120×500	6Φ12	2Φ20	
15	24	120×700	8Φ12	2Φ20	
16	29	"L" 120×600	8Φ12	1Φ24	

REPAIR AND STRENGTHENING OF REINFORCED CONCRETE COLUMNS

Zhong Yichun¹, Ren Fudong², Tian Jiahua³

INTRODUCTION

Reinforced concrete frame is one of the most common structural types in industrial and civil buildings in China, there are large quantities of existing R/C frames without having seismic design. During the 1976 Tangshan Earthquake, many of them suffered serious damages or even fell down. The main problem of the buildings are the lacking of requisite strength and adequate ductility of columns.

This paper presents the experimental results of the R/C columns repaired and strengthened by steel angles at the four corners, and puts forward the calculation methods of their stiffness and strength.

EXPERIMENTAL PROGRAM

To evaluate effectiveness of column repaired and strengthened by steel angles, we carried out three sets of tests for column. Each set includes original column, repaired and strengthened ones. In addition, a set of columns only strengthened by flat bar hoops was tested.

The dimensions, axial force ratio and steel ratio of eleven specimens are shown in Table 1 and Fig. 1. Table 2 summarizes the material properties.

A photograph of the test set up is shown in Fig. 2. Each specimen was loaded laterally with two antisymmetric forces applied through the two beam-column joints and a constant axial load was applied at the top of column.

After testing specimens YZ 83-1 and YZ 83-3, the column ends near the joints were considerably damaged, and then repaired by high-strength

¹ Section Chief, Institute of Earthquake Engineering, China Academy of Building Research, Beijing.

² Engineer, Beijing Building Institute, China.

³ Senior Research Engineer, Beijing Polytechnical University, China.

concrete. The binding material used between steel angles and concrete column faces is cement mortar added 5% vinyl-acetic ester.

OBSERVED BEHAVIOURS

During the tests, the main behaviours of the repaired and/or strengthened columns are as follows:

1. Due to the tensile effect of the steel angles, the cracking load of the specimens can be substantially increased even for the large eccentrically loaded columns. In general, the first flexural crack of concrete occurred at about 70-80% maximum load.

2. Before the maximum load, the steel angles can work as an integral whole with the concrete column. After the maximum load, the bond slip between the steel angles and concrete faces gradually occurred, but the additional tensile force of the flat bar hoops, caused the different vertical displacements at its ends, would also increase the frictional force of the contacting faces, the load carrying capacity of the column didn't speedily decrease, and the steel angles could carry load untill the severe damage of the compression zone. The typical hysteresis curves of the specimens are shown in Fig. 3.

3. The final failures of all specimens were the concrete crushing at the "plastic hinge" in the vicinity of the critical section. Then because the compression zone of the column was enclosed by closely spaced flat bar hoops, the crushing concrete was hardly broken down. Fig.4 shows the obvious difference between the repaired and ordinary columns after the tests.

4. The deformation of ordinary column concentrated at the "plastic hinge" zone, and the rest part of column shaft almost remained its original shape. The deformation of the repaired and/or strengthened columns distributed along the column shaft comparatively uniform, and the damaged specimen obviously appeared the antisymmetric flexure as showed in Fig. 5.

CALCULATING METHODS OF STIFFNESS AND STRENGTH

One of the most important behaviours obtained from the test is that the steel angle can combined action with the concrete column, so that the calculations of stiffness and strength can use the similar method for reinforced concrete column.

The following formula for calculation of stiffness is proposed

$$EI = \alpha E_c I_c + E_a I_a \quad (1)$$

in which

- EI — the elastic stiffness of repaired and/or strengthened columns;
- $E_c I_c$ — the elastic stiffness of original column;
- $E_a I_a$ — the elastic stiffness of steel angles;
- α — a reduction coefficient of stiffness reflecting the damage degree of original column
when undamaged $\alpha = 1.0$;
when severely damaged $\alpha = 0.4$.

The results obtained from the calculations and experiments are listed in Table 3. It is seen that the proposed formula is acceptable.

Fig. 6 shows the strain distributions of the steel angles at the critical section of the columns. It can be clearly seen that most part of the steel angle section, especially the compressive steel angle, had reached the yield strength under specified axial compression ratio ($\frac{N}{bdf_c} \leq 0.5$).

The following expression is recommended for the calculation of the yield strength.

$$M_y = \beta M_{oy} + A_a f_{ay} \cdot h \quad (2)$$

in which

- M_y — the yield moment of repaired and/or strengthened columns;
- M_{oy} — the yield moment of original column;
- A_a — the sectional area of steel angles at one side of the column;
- f_{ay} — the yield strength of steel angle;
- h — the distance between the centre lines of steel angles at two sides of the column;
- β — a reduction coefficient of the strength reflecting the damage degree of original column,
when undamaged $\beta = 1.0$;
when severely damaged $\beta = 0.6$.

Table 4 lists the calculated results. Evidently, good agreement between experimental and calculated values was obtained.

OTHER BEHAVIOURS OBTAINED FROM TESTS

During the tests, a number of the other behaviours obtained from the test data can be summarized as follows:

1. Underreversal loading, the repaired and/or strengthened columns had good loading reproducibility (see Fig. 7).

2. Fig. 8 shows that the hysteresis energy dissipations (W) and the equivalent visous damping coefficients (h_e) of all columns strengthened by steel angles were larger than that of the ordinary columns.

3. The external hoops of flat bar can work well with the concrete column untill the final failure of the specimens, and enlarge the plastic hinge region (see Fig. 9). If the column was only strengthened by the external hoops, especially the space of flat bar hoops was not close, the strength, ductility and hysteresis energy were not obviously improved.

CONCLUSION

1. The concrete column repaired and/or strengthened by steel angles at the corners can obviously enhance the strength and improve the ductility of the R/C frame, but almost has no effect on the stiffness of structure and the function of building.

2. The proposed calculation methods of stiffness and strength for repaired and/or strengthened columns were simple and practical.

REFERENCE

- (1) Wei Lian et al, Aseismic Strengthening of Existing Reinforced concrete Frames, Journal of Building Structures, 1982, No. 3.
- (2) Zhong Yicun et al, An Experimental Study on the Elasto-Plastic Behaviour of Two-Bay Two-Storey Reinforced Concrete Frames, Journal of Building Structures, 1981, No. 3.

Table 1

Set No.	Specimen No.	Axial Compression ratio	Longitudinal reinforcement		Transversal reinforcement			
			bar	Angle	Middle			
					Bar	Flat bar	Bar	Flat bar
I	YZ 83-1	0.52	4Ø18	4<25×3	Ø6.5@100		Ø6.5@100	
	YZ 83-1J					3×12@100		3×12@200
	JZ 83-1	0.31	4Ø12		Ø6.5@200	3×16@50	Ø6.5@200	3×16@200
II	YZ 83-2	0.18	4Ø14	4<25×3	Ø6.5@100		Ø6.5@100	
	YZ 83-2J					3×12@100		3×12@200
	JZ 83-2		4Ø8		Ø6.5@200		Ø6.5@200	
III	YZ 83-3	0.47	4Ø18	4<25×3	Ø6.5@100		Ø6.5@100	
	YZ 83-3J					3×12@50		3×12@200
	JZ 83-3				Ø6.5@200		Ø6.5@200	
IV	JZ 83-4	0.47	4Ø18		Ø6.5@100	3×12@50	Ø6.5@200	3×12@200
	JZ 83-5					3×12@100		

Table 2

Set No.	Concrete (kg/cm ²)		Steel (kg/cm ²)		
	R	E (10 ⁵)	f _y	f _{su}	
I	192		Ø6	2680	4310
II	282	2.96	Ø8	2430	3820
III	318		Ø12	2570	3620
IV	268		Ø14	2900	4600
			Ø18	2950	4100
			3×12	2600	3800
			3×16	3140	3890
			*425×3	3000	4100
		<25×3	3400	4560	

* Only used in specimens JZ 83-1 and JZ 83-3.

R — cube compressive strength of concrete (15×15×15);

f_y — yield tensile strength of steel;

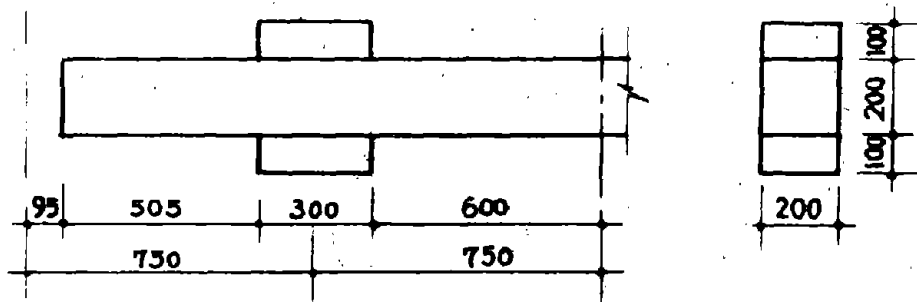
f_{su} — ultimate tensile strength of steel.

Table 3

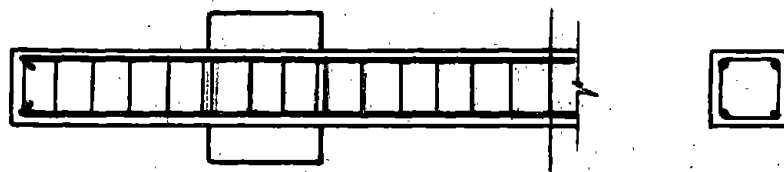
Set No.	Specimen No.	Experiment (EI) _E (t·m ²)	Calculation (EI) _C (t·m ²)	$\frac{(EI)_E}{(EI)_C}$
I	YZ 83-1	422	406	0.92
	YZ 83-1J	281	305	0.92
	JZ 83-1	454	522	0.87
II	YZ 83-2	508	471	1.08
	YZ 83-2J	301	309	0.97
	JZ 83-2	603	548	1.10
III	YZ 83-3	527	522	1.01
	YZ 83-3J	325	330	0.98
	JZ 83-3	603	640	0.94

Table 4

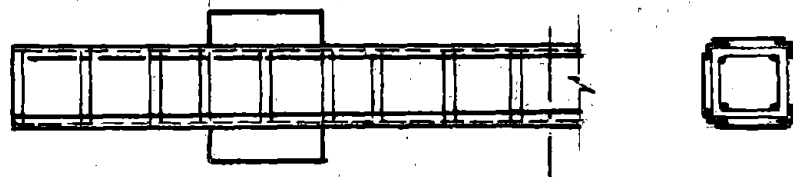
Set No.	Specimen No.	Experiment P _E (t)			Calculation P _C (t)	$\frac{\bar{P}_E}{P_C}$
		Positive	Negative	Average		
I	YZ 83-1	9.59	8.23	8.91	10.96	0.81
	YZ 83-1J	12.50	9.50	11.00	13.06	0.84
	JZ 83-1	14.50	15.00	14.75	12.62	1.17
II	YZ 83-2	9.37	8.54	8.96	8.80	1.02
	YZ 83-2J	11.79	13.27	12.53	11.76	1.07
	JZ 83-2	11.95	11.80	11.88	12.03	0.99
III	YZ 83-3	13.04	13.02	13.03	14.05	0.86
	YZ 83-3J	14.81	14.61	14.71	15.18	0.97
	JZ 83-3	20.03	—	20.03	20.98	0.95
IV	JZ 84-4	13.58	12.09	12.84	12.94	0.99
	JZ 84-5	11.45	11.16	11.31	12.94	0.87



A. specimen dimension



B. reinforcing bar



C. strengthening angle steel

Fig. 1 Dimensions and reinforcements of the specimens

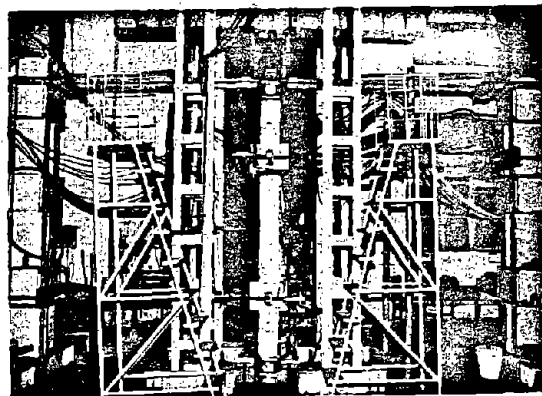


Fig. 2 Test set up

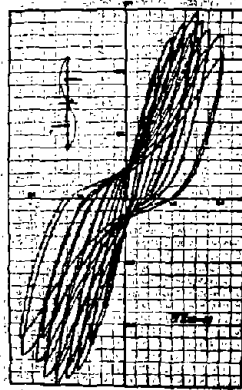
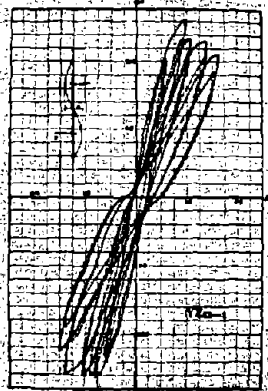
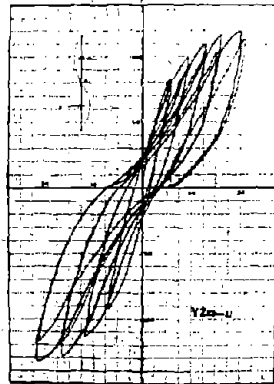
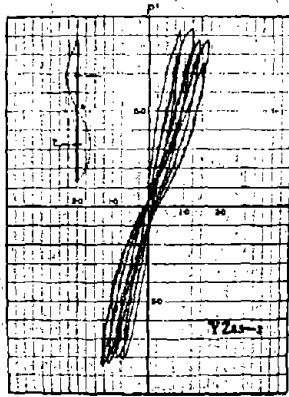
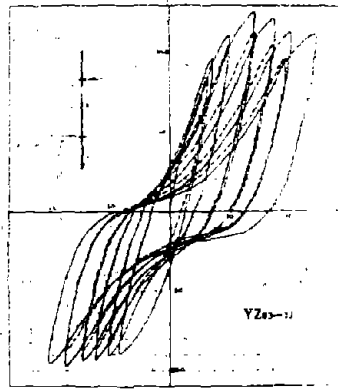
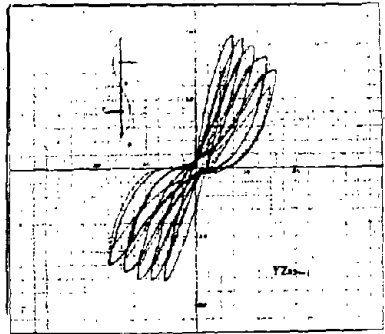


Fig. 3 Hysteresis curves of the specimens

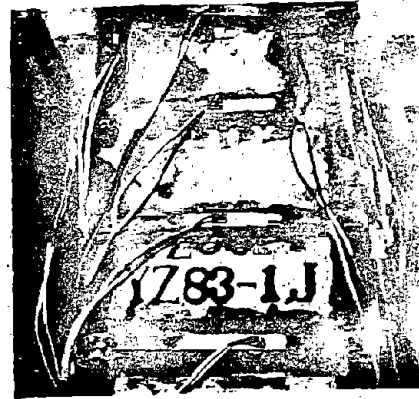
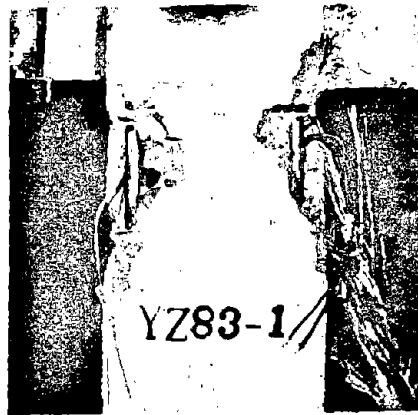


Fig. 4 Specimens YZ 83-1 and YZ 83-1J after test

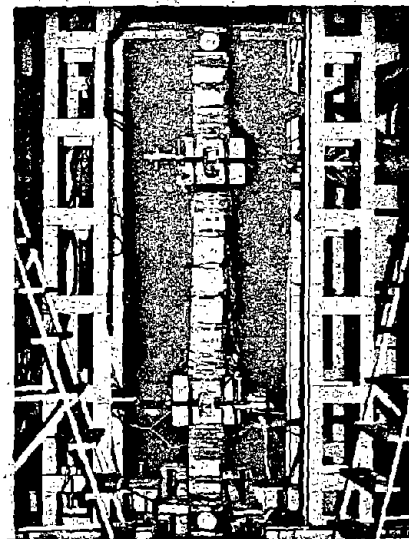
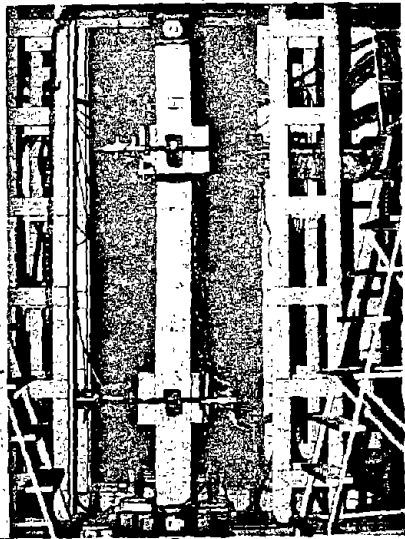


Fig. 5 Deformation of the specimens YZ 83-3 and YZ 83-2J after test

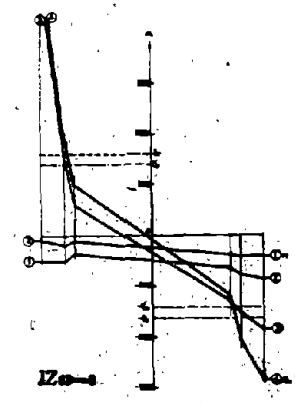
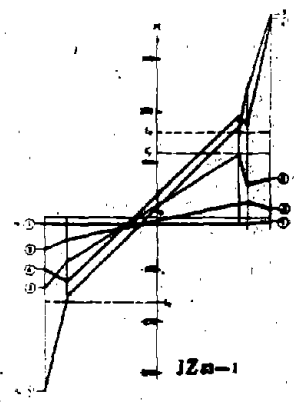
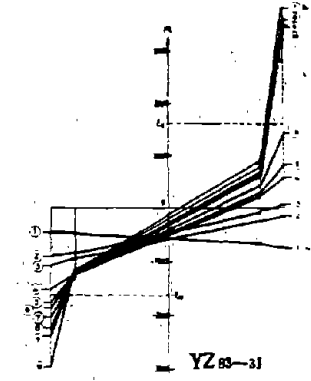
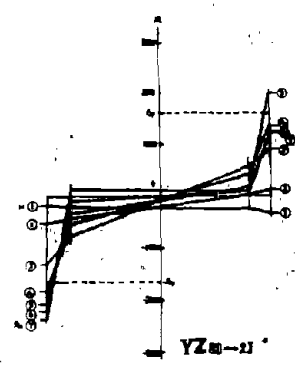
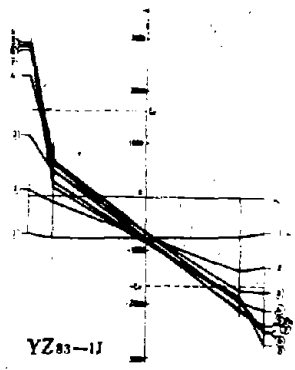


Fig. 6 Angle strains

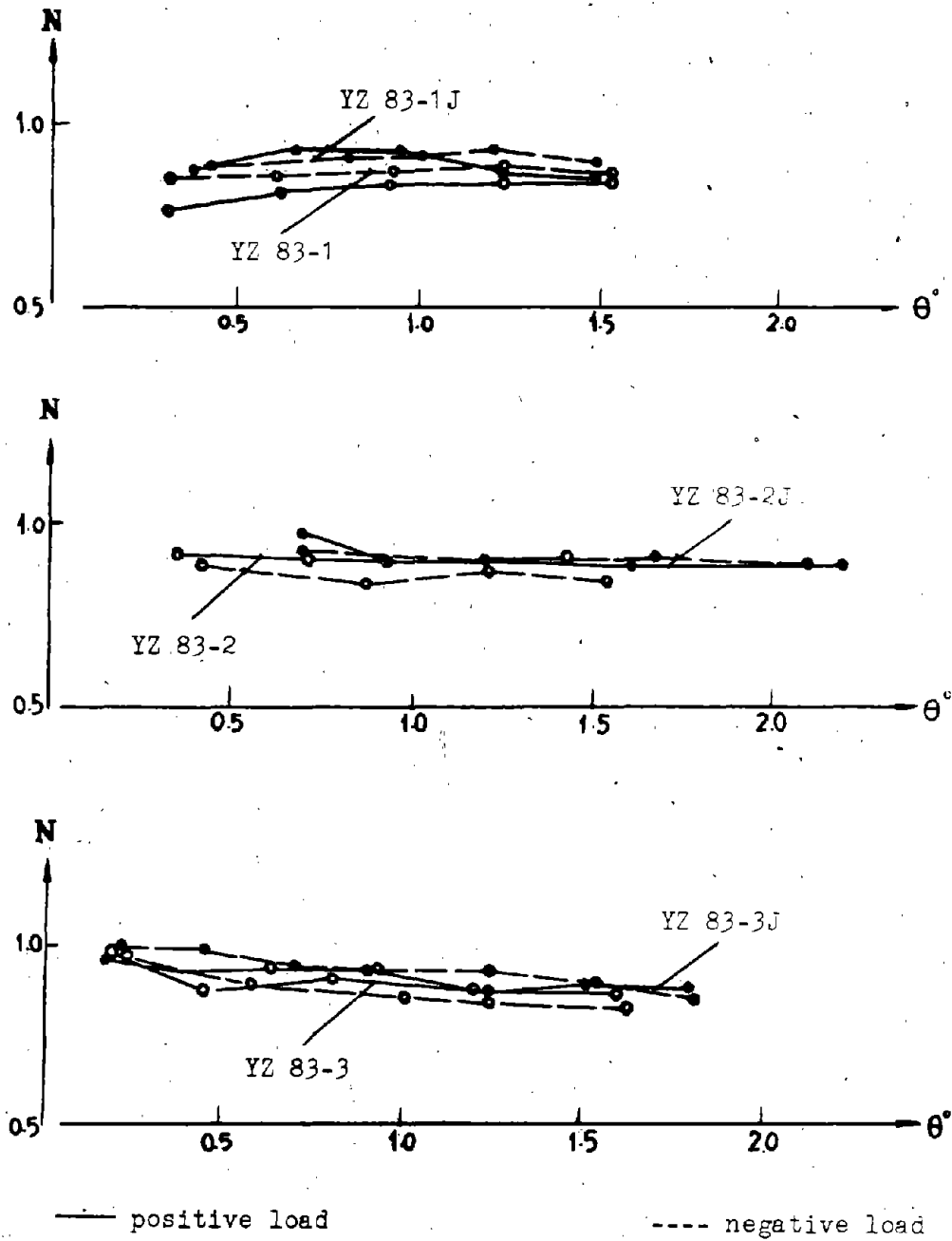


Fig. 7 Load decreased ratio

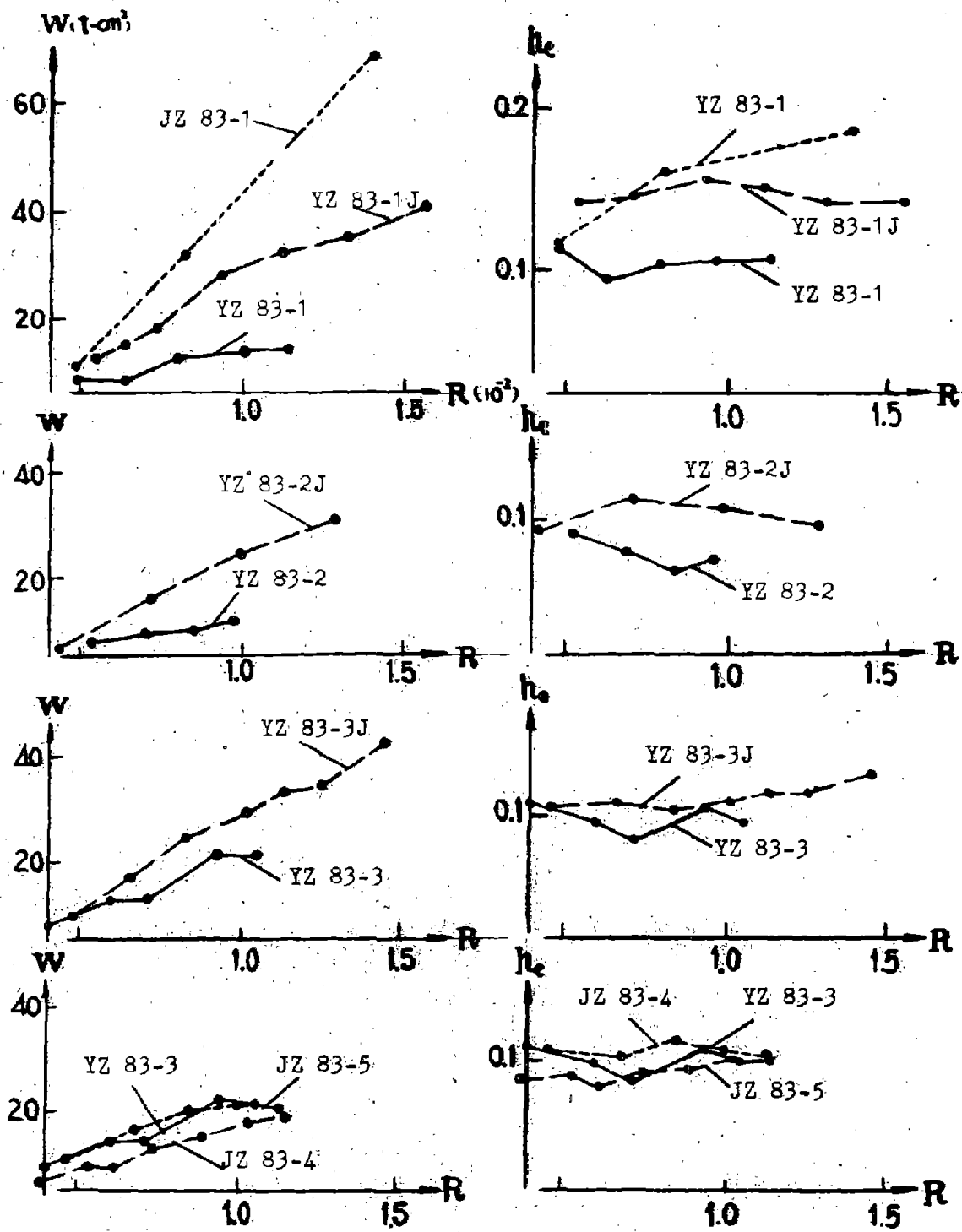
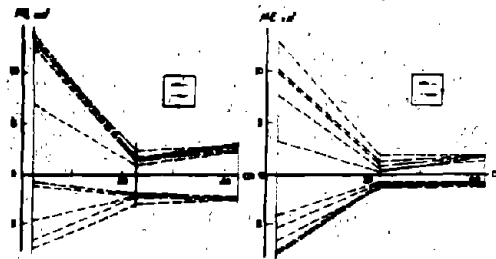
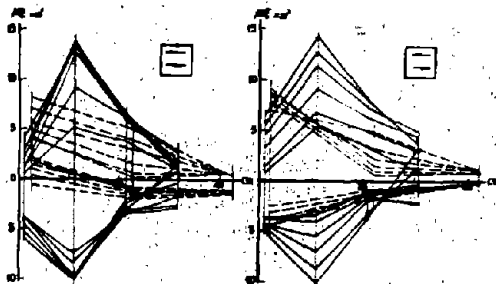


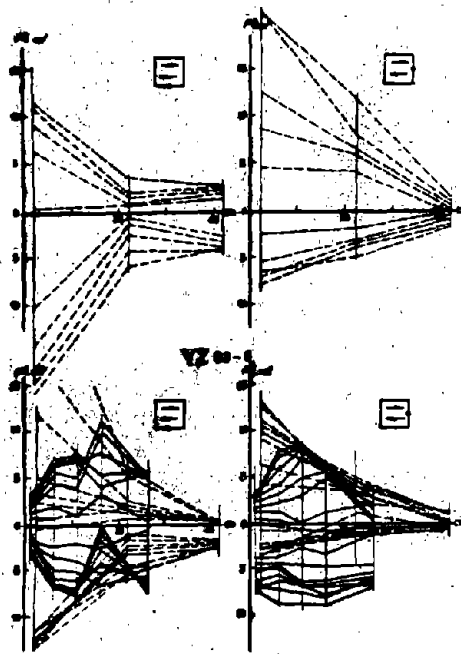
Fig. 8 Hysteresis energy



YZ 62-1



YZ 62-12



YZ 62-13

— flat bar hoop - - - - - general bar hoop

Fig. 9 Stirrup strains

SHAKING TABLE STUDY OF A FIVE-STORY UNREINFORCED
BLOCK MASONRY MODEL BUILDING STRENGTHENED WITH
REINFORCED CONCRETE COLUMNS AND TIE BARS

Zhu Bolong¹

Wu Mingshun²

Zhou Deyuan³

SUMMARY

A five-story unreinforced concrete block masonry model building strengthened with reinforced concrete columns and tie bars was tested on shaking table in Tongji University. From the test results, it can be found that the failure mechanism and aseismic capacity of strengthened building are quite different from that of unstrengthened one. Just as it is shown in authors' previous paper⁽¹⁾, the pseudo-static test can not show the actual collapse phenomenon of the strengthened building. On the basis of shaking table test results, all above-mentioned problems are discussed in this paper.

INTRODUCTION

During Tangshan Earthquake of July 28, 1976, one building with internal reinforced concrete frame and external bearing brick wall strengthened with reinforced columns has experienced the strong ground motion without collapse. Since then, using reinforced concrete columns and tie bars to strengthen unreinforced brick or concrete block buildings is widely adopted in seismic area in China. In the past eight years a number of pseudo-static tests of masonry walls strengthened with reinforced concrete columns have performed in many universities and research institutes. The general conclusions can be summarized as follows:

- (1) The columns contribute to shearing capacity only at the limit state as well as at descending branch of skeleton curve of masonry wall.
- (2) Owing to the fact that the section area of column compared with masonry wall is very small, the static tests show that the shearing capacity of strengthened wall is only 20% larger than that of unstreng-

¹ Prof. of Civil Engineering, Tongji University, Shanghai, China

² Assoc. Prof. Tongji University, Shanghai, China

³ Master of Structure Engineering, Tongji University, Shanghai, China

thened one.

(3) Because the masonry wall is confined by reinforced columns, the deformability of masonry wall is greatly improved.

It should be pointed out that the static test can not explain the following phenomenon: during Tangshan Earthquake the strengthened masonry wall could resist strong ground motion or two times more than that of unstrengthened one. Besides, the static test also cannot show how the strengthened building is collapsed. It is necessary to carry out a model-strengthened block building test on shaking table to study the failure procedure during "earthquake". The test results of the first strengthened concrete block model building is presented in this paper.

OUT-LINE OF THE TEST MODEL BUILDING AND INPUT DATA

The geometry of the strengthened model building is the same as the unstrengthened one which was tested on $4 \times 4\text{m}$ shaking table at Tongji University in 1984⁽²⁾. The scale of the model building is 1:4, and it satisfied with the similitude requirements of the prototype block masonry building⁽²⁾.

The model building was strengthened by reinforced columns having $6 \times 5\text{cm}$ section and $2 \phi 6$ steel tie bars to connect two columns in the transversal direction, besides, in the longitudinal direction of every floor the columns were connected by reinforced concrete lintel bands with $6 \times 5\text{cm}$ section, as shown in Fig. 1.

The strength of the mortar was 2.14 MPa and the strength of concrete block was 15 MPa; besides, all the concrete of columns and lintel bands had a strength of 15 MPa.

The model building was built on reinforced concrete crisscross beams as a foundation. In order to increase the normal pressure on the masonry walls, the additional mass was fixed on every floor of the model building, and then the total weight of the model building with foundation is about 11 tons. When the model building was craned on the shaking table, the crisscross beams were fixed with a set of bolts.

During dynamic test 15 accelerometers were arranged on every floor as well as on the crisscross beams and roof. Besides, 2 strain gages were glued to the surface of every tie bar to measure its strain response, and 44 strain gages were glued to the surface of main bars of reinforced concrete columns to measure the deformation of steel.

An artificial earthquake accelerogram corresponding to the third category of soil condition of Chinese "Aseismic Design Code for Industrial and Civil Buildings"⁽³⁾ was used as an input data. According to the similitude requirements, because the ratio between the natural frequencies of model and prototype building is equal to 3.448, the time of

duration 12 sec. should be compressed to 3.48 sec.

The schedule of peak value of input data during the test is shown in Table 1.

Peak Value of Accelerogram

Table 1.

Direction	Input No.						
	1	2	3	4	5	6	7
X	0.18g	0.38g	0.7g	1.15g	1.5g	2g	2g
Y	0	0	0	0	0	0.79g	0.85g

RESULTS OF SHAKING TABLE TEST

When the strengthened model building was excited at peak acceleration of 0.18g, the response of the model was elastic, and the deformation of that was very small. The peak value of the acceleration response at roof was about 0.4g. The story-displacement of the top floor was only 0.77mm, and the stress of the steel in reinforced column was under 250 kg/cm². When the strengthened model building was excited at peak acceleration of 0.38g, the small cracks appeared in the lateral wall of the building's ground floor. At that moment, the maximum acceleration at the roof was up to 0.95g. The story-displacement of the top floor had increased to 1.54mm, and the stress in the steel of reinforced concrete column also had increased to 900kg/cm². The earthquake response of strengthened building at roof level is shown in Fig. 2.

When the input peak acceleration was increased to 0.7g, the cracks became larger and longer in the lateral walls of the ground floor, and some local horizontal micro-cracks appeared in the longitudinal walls of the second floor. The peak value of acceleration response at the roof was up to 1.3g. Besides, the cracks also appeared in the reinforced concrete columns, and the stress of steel was increased to 1700kg/cm² at crack section.

The comparison of test results between the strengthened and the unstrengthened⁽²⁾ model buildings shows that because the cross section of reinforced concrete column is much smaller than that of masonry wall, the damages of the two buildings are very similar. It means that when the strengthened prototype building meets an earthquake corresponding to Intensity 8, which was estimated by the input peak value of accelerogram according to similitude relationship, the contribution of reinforced concrete columns is relatively small.

When the strengthened model building was excited at the peak value of 1.15g, the horizontal cracks in the wall of ground floor connected each other, to form a stepped diagonal crack with a width of 2 ~ 3 mm (see Fig. 3). Besides, the stress of the bars in reinforced concrete

columns on the ground floor reached yielding point. The time history of roof acceleration is shown in Fig. 4. It can be found that because of the decreasing in stiffness of the wall at ground floor, the maximum acceleration at the roof only reached 1.4g. The maximum roof displacement was equal to 4.81mm ($H/790$, H — the height of model building).

From the comparison of test results between strengthened and un-strengthened⁽²⁾ model buildings it can be found that the damages are quite different: When the unstrengthened model building was excited at the peak value of 1.2g, partial masonry of the external lateral wall crushed at first story (Fig. 5), and the drift of roof was equal to 1/46 of the height of model building. Because the masonry walls are confined by the reinforced concrete columns, the damages of strengthened model building is much lighter than that of unstrengthened one. It means that after the formation of stepped cracks in the walls, the contribution of reinforced concrete columns is evident.

It should be mentioned that the unstrengthened model building was only excited in one direction, and it was collapsed at fifth run of repeated excitations with a peak value of 1.2g. Just as shown in Table 1, when the peak value of excitation was increased to 2g in X-direction, another excitation in Y-direction was inputed to the building simultaneously, and the strengthened building was collapsed during the repeated excitation at that peak level.

During the first two-way excitations the damages of strengthened model building in the walls of ground floor were serious: some concrete blocks near the opening in the lateral walls of ground floor fell down, and partial concrete blocks in the longitudinal walls moved out-plane about 4 ~ 5cm and even fell down too (Fig. 6). At that moment the steel strain in reinforced column at the ground floor reached 4390 $\mu\epsilon$. The seriously deformed columns even were separated from the masonry (Fig. 7). It should be pointed out that the damages on the second and upper floors were much lighter than those on the ground floor.

From the time history of acceleration (Fig. 8), it can be found that the maximum response of acceleration is 0.8g, which is smaller than the input peak value. It means that the input energy was dissipated by the cracking walls.

It should be noted that the confined effect by the reinforced concrete columns results in the fact that the openings in masonry wall became smaller and smaller. It means that during earthquake the doors and windows of strengthened building maybe could not be opened, if their frames were not strengthened.

When the strengthened model building was excited at peak value of 2g in X-direction and 0.85g in Y-direction, the first story was collapsed but the upper four stories did not collapse and stood on the

ruins (Fig. 9). The damages in the upper four stories were minor. This phenomenon also can be illustrated by the strain responses of steel in reinforced concrete columns at the ground floor (Fig. 10) and the third floor (Fig. 11).

According to the similitude relationship the estimated peak acceleration of the strengthened prototype building can be calculated from the test results of the model. Table 2 shows the estimated peak value A_p of strengthened prototype building. In order to compare the aseismic capacity with unstrengthened building, its test results are also listed in Table 2.

Estimated Peak Value A_p Table 2.

Unstrengthened Building		Strengthened Building	
A_m (g)	A_p (g)	A_m (g)	A_p (g)
0.2 g	0.065	0.18g	0.051g
0.56g	0.183	0.38g	0.109g
0.72g	0.237	0.7 g	0.200g
1.22g	0.402	1.15g	0.327g
		1.5 g	0.471g
		2 g	0.580g

DISCUSSION

Effect of Reinforced Concrete Columns for Strengthened Building

The Test results of strengthened and unstrengthened⁽²⁾ model buildings show that when the strengthened model building was excited with a peak value of acceleration less than 0.7g corresponding to Intensity 8 for prototype building, the effect of reinforced concrete columns is not very evident; but when the peak value increased to 1.15 ~ 1.22g the damages of the two buildings were quite different. The damages of unstrengthened building is more serious than that of strengthened one. The displacement of strengthened building due to the confined action of reinforced concrete columns and tie bar system is much less than that of unstrengthened.

Aseismic Capacity of Strengthened Building

Because the strengthened model building collapsed under the two-way excitation, it can be estimated that if the unstrengthened model building was also excited under two-way excitation, the peak value of acceleration in main direction may be much less than 1.22g. It means that the aseismic capacity of strengthened building may be about one time larger than that of the unstrengthened one. The convincing estimation may be given by the next test of unstrengthened building excited by two-way input in Tongji University.

Different Collapse Patterns

From Fig. 12 it can be found that the unstrengthened model building completely collapsed, but the Fig. 9 shows that the upper four stories of strengthened building stood on the ruins. It means that the 80% inhabitants may be survived in the strengthened building compared with in the unstrengthened one during strong earthquake.

Improvement of Aseismic Capacity for Strengthened Building

It is evident that the weak point of strengthened model building is the openings. Because the openings did not strengthen, the concrete blocks easily moved to the openings. If all the openings were strengthened by reinforced concrete frames, it can be believed that the damages of strengthened building may be lighter; and the building can resist stronger earthquake.

REFERENCES

- (1) Zhu Bolong, Jiang Zhixian, Wu Mingshun, "A Study on Aseismic Capacity of Brick Masonry Buildings Strengthened with Reinforced Concrete Columns and Tie Bars", Proc. of US-PRC Bilateral Workshop on Earthquake Engineering, Aug. 1982, Harbin, China.
- (2) Zhu Bolong, Li Xilin, "Shaking Table Study of a Five-Story Unreinforced Concrete Block Masonry Model Building", Proc. of International Workshop on Earthquake Engineering, March, 1984, Shanghai, China.
- (3) State Capital Construction Commission of PRC", Aseismic Design Code for Industrial and Civil Buildings (TJ-11-78)" (in Chinese), Beijing.

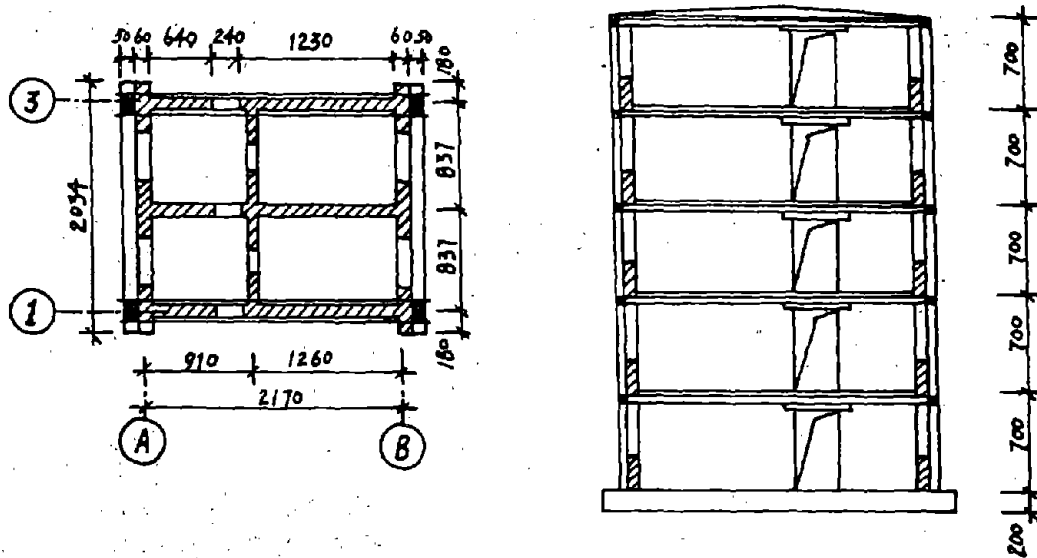


Fig. 1

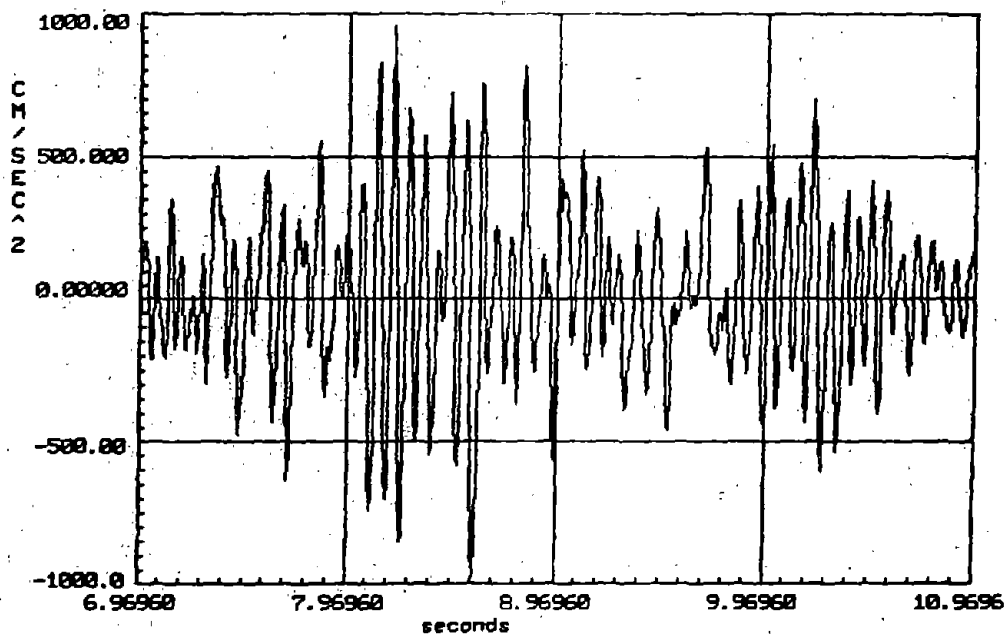


Fig. 2

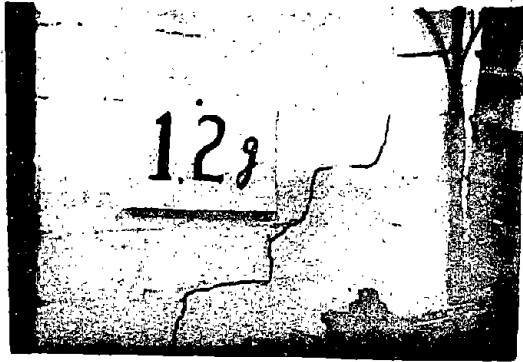


Fig. 3

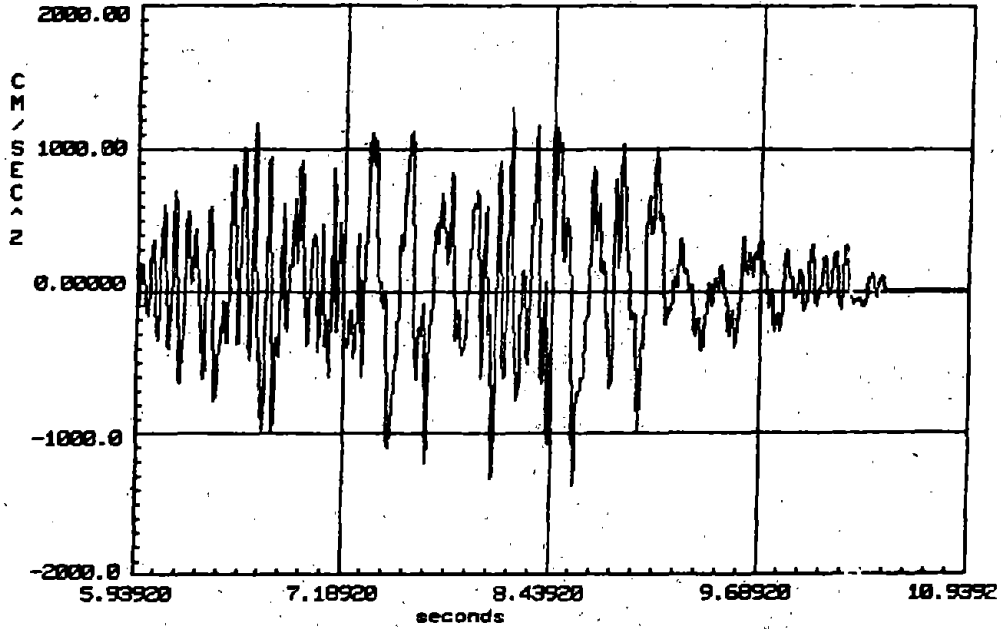


Fig. 4

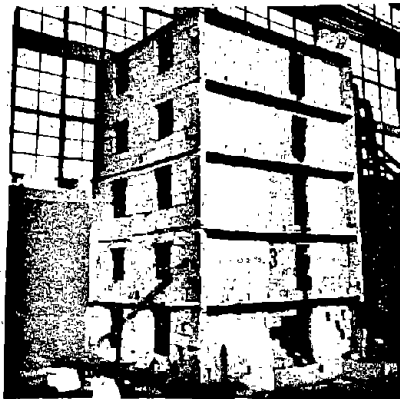


Fig. 5

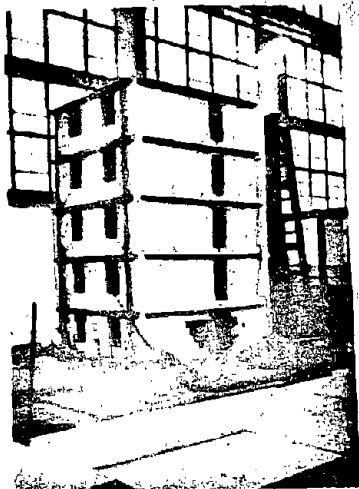


Fig. 6

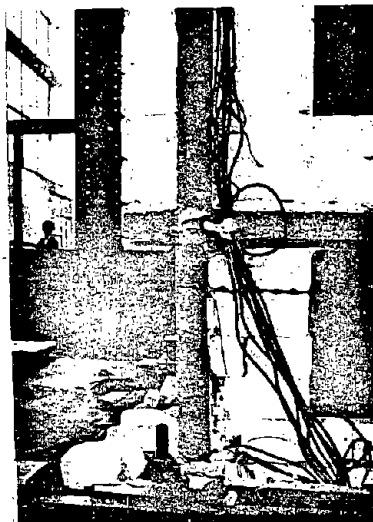


Fig. 7

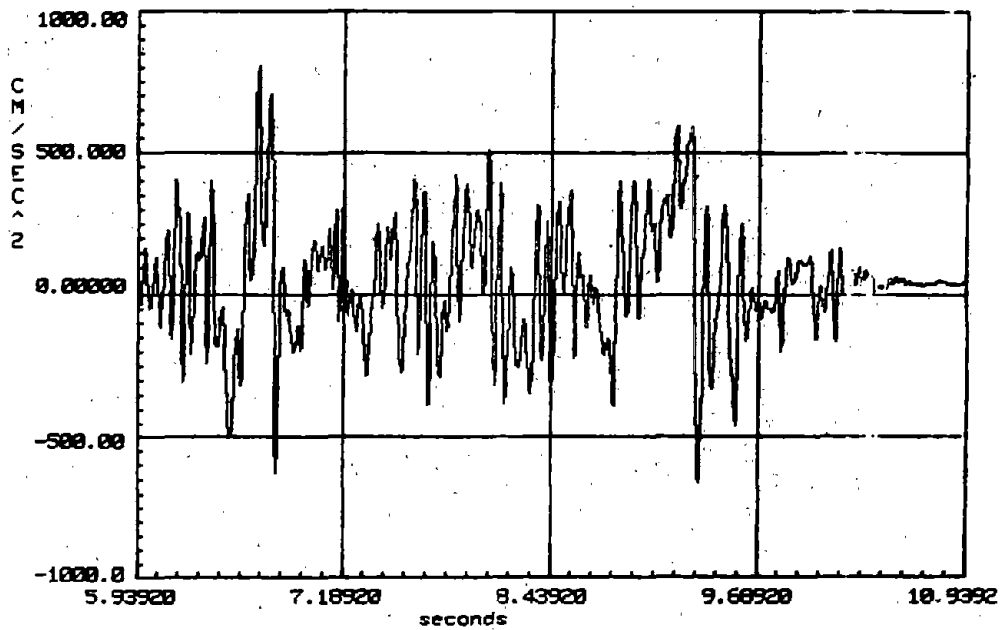


Fig. 8

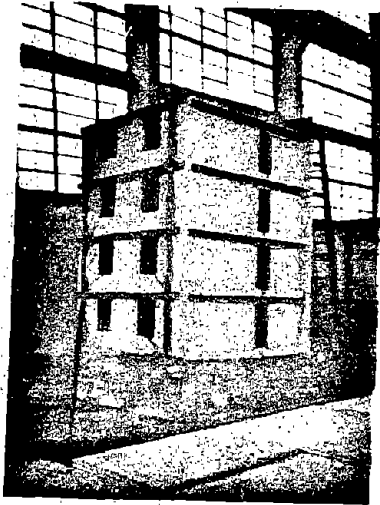


Fig. 9

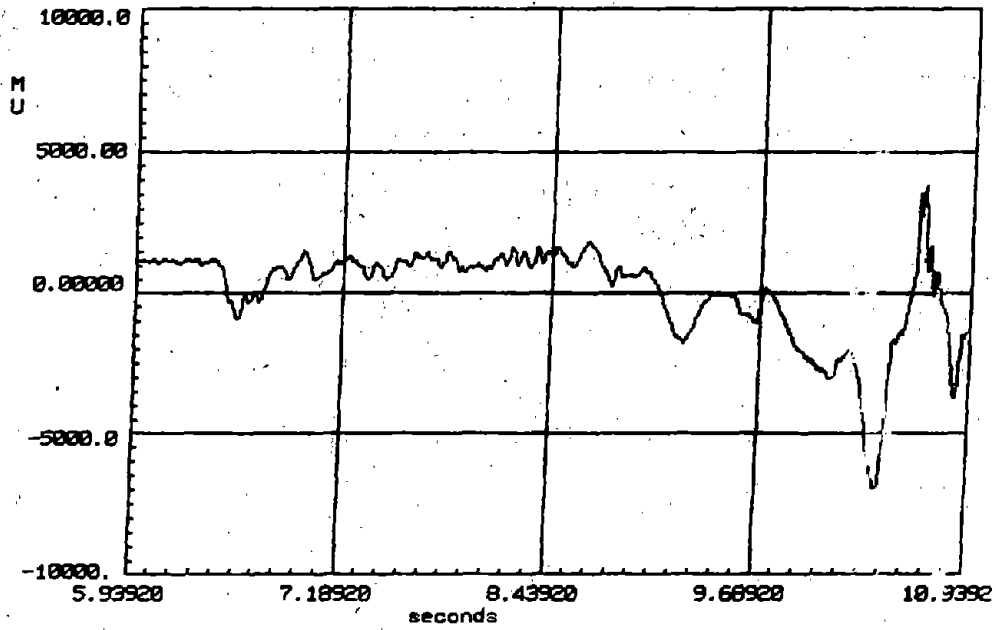


Fig. 10

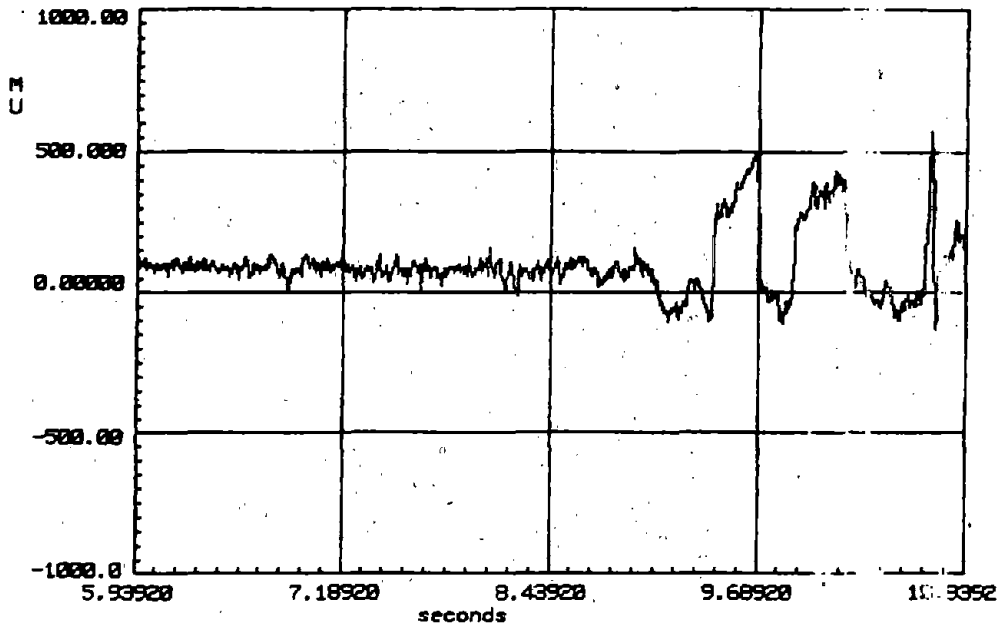


Fig. 11



Fig. 12

Errata

The following correction should be made to the original papers:

Page II-4-2, line 3, the 8th word: Should read Sinha instead of inha.

Page II-4-2, line 15, the 2nd word: Should read stress σ_0 instead of stress.

Page II-4-7, Eq. (9), the left hand: Should read $\frac{\partial Q}{\partial \alpha}$ instead of —.

Page II-4-8, Table 2, the forth row of the last cloumn: Should read
 $C_v = 0.143$ instead of $C_v = 0.43$

Page IV-2-11, line 7 and 8, the last words: Should read Fig. 5 and Fig. 6
instead of Fig. 3 and Fig. 4 respectively.

Page IV-6-7, Eq. 30, the numerator of right hand: Should read
 $(0.77+0.23 \sigma) E_b$ instead of $(0.77 + 0.23) E_b$

Page IV-7-6, line 3 from bottom, the 3rd word: Should read 0.2g instead
of 0.4g

Supplement to Seismic Reliability Analysis of Multi-Story Brick Buildings

Jinren Jiang and Feng Hong

ACKNOWLEDGMENTS

This report is one of the research works conducted at the Institute of Engineering Mechanics under the US-PRC Cooperative Research in Earthquake Engineering supported by State Seismological Bureau and National Science Foundation. Under this project, the direction of Professor HU, Yuxian and the cooperation of Professor ANG, A. H-S. during the course of the study are appreciated.

ADDENDUM

to

COMPARISON OF U.S. AND CHINESE METHODOLOGIES
OR THE SEISMIC EVALUATION AND STRENGTHENING
OF EXISTING UNREINFORCED MASONRY STRUCTURES

Neil M. Hawkins, F. Chou, and X. Yin

This paper compares the U.S. and Chinese procedures only in those aspects where such comparisons have some validity; namely, the mathematical models used to characterize the building's response, calculations for the in-plane shear strength of walls, and the need to consider openings. Complete calculations with either procedure predict lower strengths and different relative values to those shown in Table 1. For example, from Table 2 it is clear that for the U.S. procedure for walls A and 6 at floors 1 through 4, the restoring shear characteristics of the piers rather than their direct shear strength controls the in-plane shear strength. Similarly, the building's pier proportions do not meet the empirical requirements of the Chinese procedure. Further, it should be recognized that in Fig. 6, the NBS and Tongji relationships are curves representing test results for which the shear strength of the wall is taken as the test strength and the shear strength of the masonry as v_t times the wall's cross-sectional area. The ABK and PRC curves, however, are the design recommendations of Eqs. (1) and (3) expressed in terms of stress. If those recommendations are expressed as forces and account taken of the correction factors in Eqs. (1) and (3) for workmanship, safety, and non-uniform distribution of shear stress, then the relative positions of the four expressions become as shown in Fig. 9.

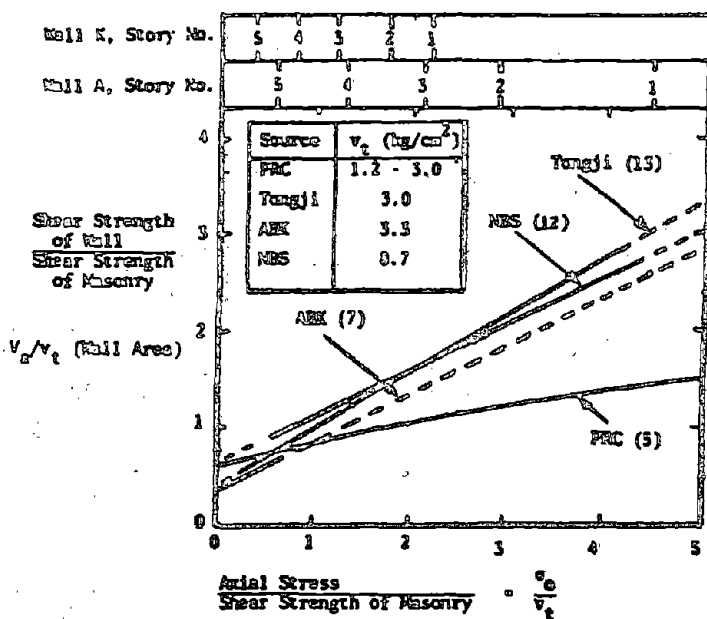


FIG. 9 INCREASE IN WALL SHEAR STRENGTH WITH AXIAL STRESS